THE POLYMETAMORPHIC SEQUENCE IN THE PALEOZOIC ROCKS OF NORTHERN VERMONT: A NEW APPROACH USING METAMORPHIC VEINS AS PETROLOGIC AND STRUCTURAL MARKERS

Thesis by

James Rodney Anderson

In Partial Fulfillment of the Requirements

for the Degree of

Doctor of Philosophy

California Institute of Technology

Pasadena, California

1977

(Submitted September 23, 1976)

ACKNOWLEDGEMENTS

I would like to thank Professor Arden L. Albee for supporting this work, for posing questions that have helped to focus the thesis, and for providing the opportunity for me to independently pursue the study and determine its goals. Art Chodos has helped me in learning the techniques and sorcery of the electron microprobe. I am grateful to Dr. Charles G. Doll for his assistance in obtaining access to restricted highway roadcuts. I have benefitted from many discussions with Jo Laird, who has generously shared her ideas on the metamorphic history of Vermont as recorded in amphibolites. I also had several very helpful discussions with Professor James B. Thompson, Jr. of Harvard University. Professors Robert P. Sharp and Samuel Epstein provided much needed encouragement.

This study was supported by the National Science Foundation, grants DES75-03416 and GA-12867. A portion of the field work was supported by the Geological Society of America, Penrose Bequest grants 1745-73 and 1852-74. During my stay at Caltech, I have received financial assistance from the Tyng Foundation of Williams College, the A.R.C.S. Foundation, and as an Earle C. Anthony Fellow, a Graduate Research Assistant, and a Graduate Teaching

Assistant.

I am grateful to my parents for their early encouragement of my interest in geology. My wife, Pat, has helped greatly in the preparation of this thesis, did much of the drafting, and has aided in many other ways. We were both helped by our three little assistants, Jennifer, Craig, and Meredith.

ABSTRACT

The sequence of metamorphic events that have affected the lower and middle Paleozoic rocks of northern Vermont has been defined in this study. The use of metamorphic veins as structural and petrologic markers has helped to establish the correspondence between deformational and mineral growth features. The effects of the major metamorphic events have been followed through the area along several traverses, the longest of which is 50 miles in length. The study combines detailed analysis of the sequence of structural elements with electron microprobe and petrographic analysis of the mineral growth in the metamorphic veins and host rock.

Much of the history of the chemical path of the vein and host rock systems is preserved in zoned grains and grains included in other minerals. The zoning trends in certain key minerals such as plagioclase, amphibole, muscovite, and coexisting calcite and ankerite indicate that the grade of each rock system was changing with time. The path of the systems can be followed in considerable detail. Not only are the effects of changing grade during a single event typically preserved, but also the effects of several superimposed mineral growth events can be preserved in a sample.

Five major metamorphic events and several minor events have occurred in northern Vermont. The two oldest events affected only the Cambrian and Ordovician rocks; these events are designated O_a and O_b. Event O_a involved widespread biotite grade mineral growth and the formation of a secondary bedding schistosity. O_b is the most prominent of the pre-Silurian events and is Late Ordovician in age. It produced high grade mineral growth in the Green Mountains and in the Worcester Mountains; in the latter area staurolite-kyanite grade assemblages occur. There was also widespread formation of small scale isoclinal folds with east-west axial trends during O_b. Major east-west trending folds of the same generation occur locally.

Three events affected both the pre-Silurian rocks and the Silurian and Devonian rocks. These events are Middle to Late Devonian in age. D_a is the oldest of the three and produced biotite to garnet grade or higher mineral growth over the entire study area. D_a was also a significant deformational event, responsible for the formation of major and minor north-south trending folds. Event D_b mainly involved deformation, but biotite grade mineral growth occurred in rocks where the axial plane foliation associated with D_b was developed. Folds formed during D_b have north-south trends and are most prominent in the

eastern part of the area. The last major event, D_c, was a period of mineral growth without associated deformation and was widespread in extent. The highest grade mineral growth of D_c, up to staurolite-andalusite and sillimanite grades, has a close spatial relationship to the intrusive bodies of the New Hampshire plutonic series. In areas far from such plutons, this mineral growth is biotite grade or absent.

Metamorphic veins are associated with each of the major events except D_b. The veins are discontinuous and have a general chemical correspondence to mineral growth of the same generation in the adjacent host rock. Differences in the relative timing of growth in the veins and host rocks occur in some instances, so that the correspondence is fairly complicated. The veins appear to have formed during the metamorphic events from material derived locally in the host rocks.

TABLE OF CONTENTS

LIST OF FIGURES

CHAPTER III

LIST OF TABLES

CHAPTER I. INTRODUCTION

A. Purpose of study

The purpose of this study is to determine in detail the history of polymetamorphism in northern Vermont. Polymetamorphism is manifested by both deformational features and mineral growth generations. In order to have a reasonably complete metamorphic history, both the deformation and mineral growth sequences must be understood and correlated.

Most previous studies in northern Vermont have combined structural and petrologic techniques, although to varying extents. One problem that has remained is that of correlating structural elements with mineral growth generations. Microtextural approaches, correlating microstructures and minerals in thin section, are useful but often ambiguous due to the near parallelism of structural elements of different events and other problems. Previous methods did not appear to offer unambiguous answers, so a new approach seemed necessary.

Another difficulty, one specifically in northern Vermont, was a lack of structural correlation from east to west across the area. This was partly due to the nature of most of the previous work, largely mapping projects of fifteen minute quadrangles, but primarily due to a lack of outcrop in critical places. The construction of Interstate Highway I89 has provided good roadcuts which have allowed

such a structural correlation.

This study differs from previous work in several important aspects. Metamorphic veins are used in making the correlation between mineral growth and structure and the study has been made within a large, continuous area which consists primarily of seven adjoining fifteen minute quadrangles, plus nine other quadrangles in which limited data and samples were collected. The only previous study made in an area of comparable size is White and Jahns (1950). The other difference between this and previous studies is the extensive use of electron microprobe analysis to separate the various mineral growth generations and to study each generation in detail with regard to the major element chemistry of most of the phases.

B. Regional geologic setting

The study area is in the northern part of the Appalachian Mountain belt. The rocks consist of metamorphosed lower and middle Paleozoic units of sedimentary and volcanic origin which overlay a crystalline Precambrian basement. These and other relationships which follow are shown on the geologic map of Vermont (Doll, Cady, Thompson, and Billings, 1961). The principal intrusive rocks are a number of Ordovician ultramafic bodies in the central part of the area and the Devonian New Hampshire plutonic series in the east. Figure 1 shows the general distribution of the rock units.

Figure 1 Map of northern Vermont showing general distribution of rock units and major structures (modified after Doll and others, 1961). Also shown are the traverses and sample locations of this study.

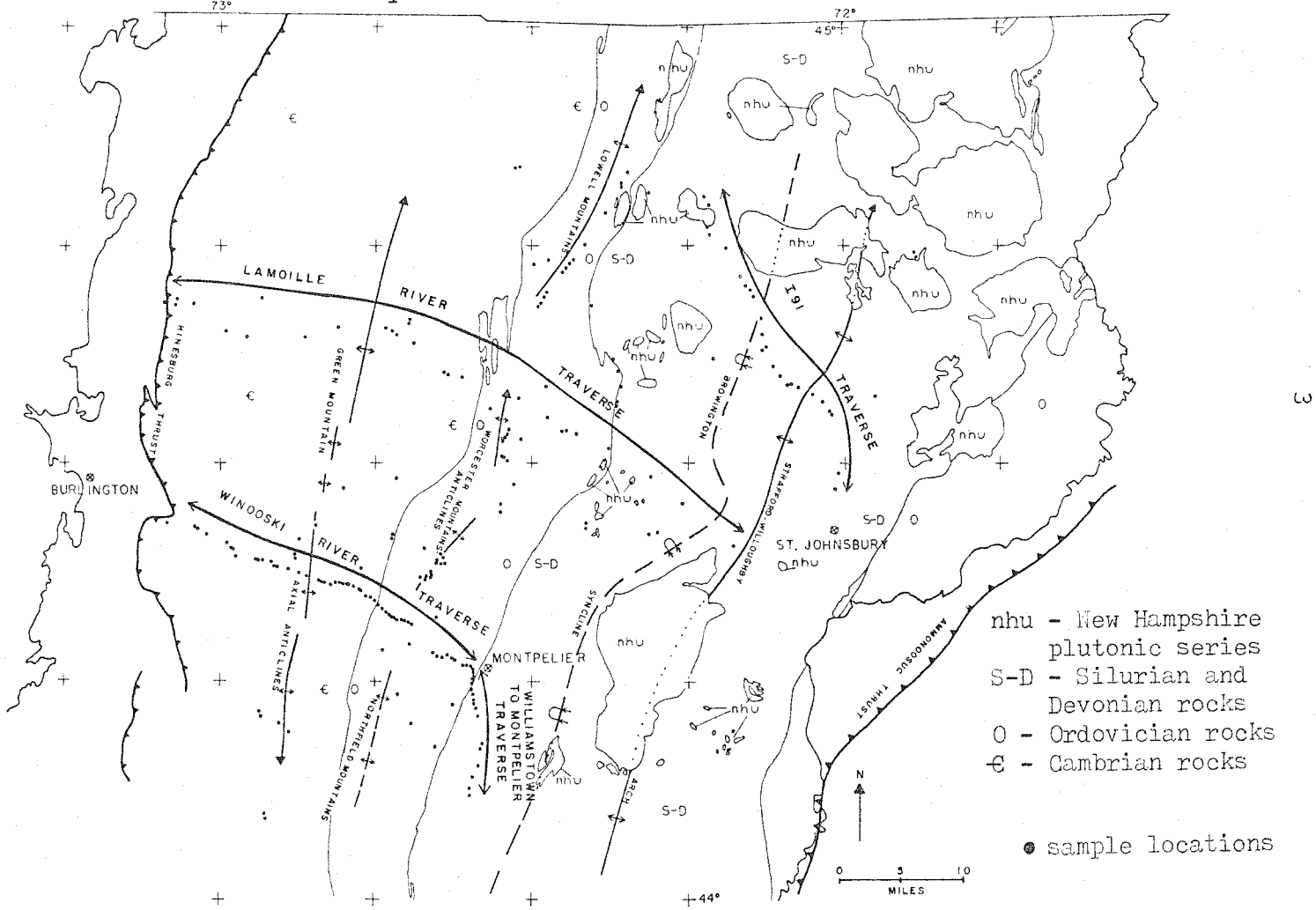

The study area is bounded on the west by the Hinesburg thrust. There has apparently been substantial displacement on this thrust fault. The correlation of structural elements across the fault has not been attempted in this study. Another major fault, the Ammonoosuc thrust, bounds the east side of the area.

The Precambrian basement crops out to the south of the study area and will not be described. The lower Paleozoic rocks consist of Lower Cambrian through Middle Ordovician units. There also are late Precambrian rocks which conformably underlie the Lower Cambrian units. The rocks are mostly eugeosynclinal in character, consisting primarily of interlayered pelite, greywacke, quartzite, and basaltic volcanic rocks. The metamorphic grade of pelitic rocks ranges from biotite to staurolite grade.

The lower and middle Paleozoic strata are separated by a pronounced erosional unconformity. The middle Paleozoic units are comprised of Silurian through Middle Devonian eugeosynclinal sedimentary and volcanic rocks which have been metamorphosed to biotite through sillimanite grades in pelitic rocks. The original rock types were primarily impure carbonate, pelite, quartzite, and both felsic and basaltic volcanic layers.

Except for minor faults with small offsets, the area between the Hinesburg and Ammonoosuc thrusts is undisturbed

by faulting. Structural features which are present include several generations of folds and various small scale planar and linear features which are described in the structure chapter. The major mapping folds trend NNE. The most important of these large folds are the axial anticlines of the Green Mountain anticlinorium, the Northfield Mountains - Worcester Mountains - Lowell Mountains anticlines, the Brownington syncline and the Strafford - Willoughby arch. These are shown on Figure 1.

C. Previous work

There has been extensive previous work in northern Vermont. A number of these studies bear directly on the problems with which this thesis is concerned and these are described below. A discussion of the other work and an extensive bibliography is in Cady (1969).

The geology of most of the area has been mapped on fifteen minute, 1:62,500 quadrangles. The samples and structural data in this study come from 16 different quadrangles. The locations of these quadrangles and references to the authors who mapped them are shown in Figure 2. These studies plus some reconnaissance mapping have been compiled into the geologic map of Vermont (Doll and others, 1961). The quadrangle maps and the state map provide an essential base for a study such as this.

White and Jahns (1950) made an important study of

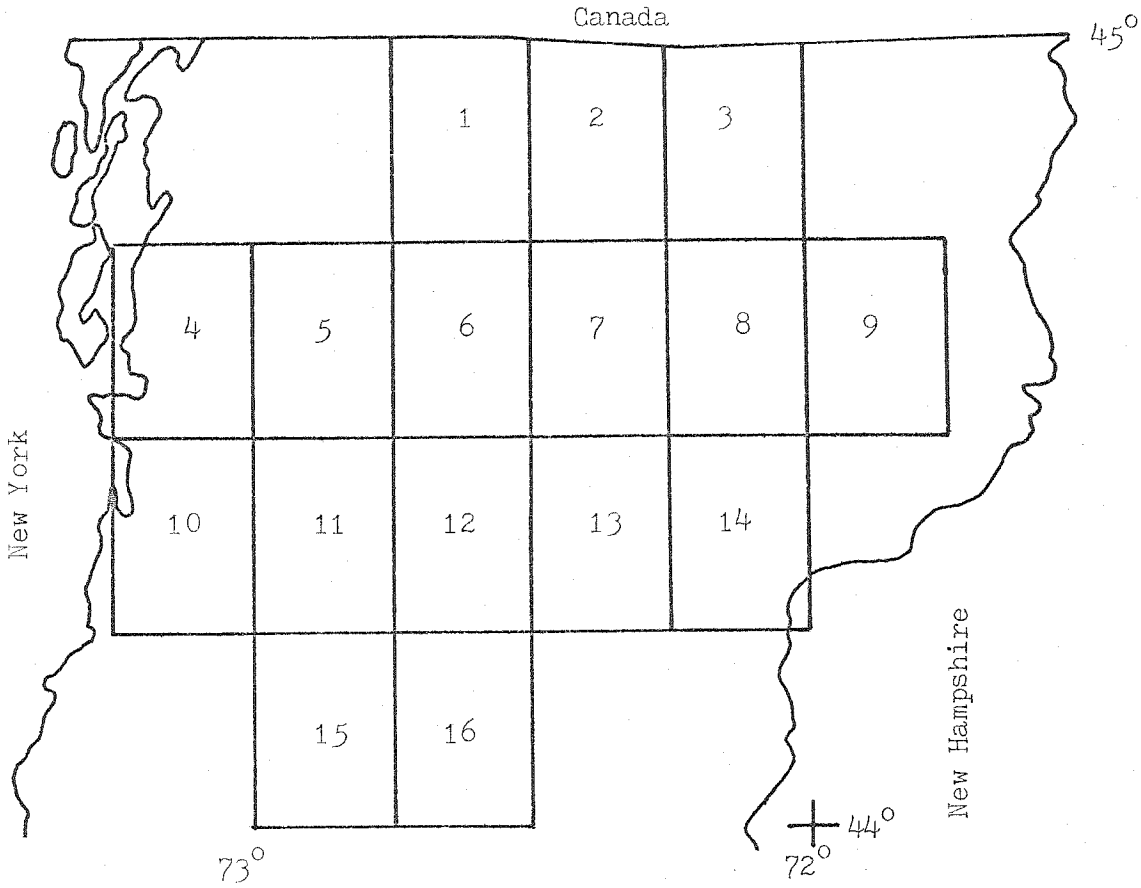

Figure 2 Index map to quadrangles in study area

1. Jay Peak, eastern part, Cady, Albee and Chidester (1963)
2. Irasburg, Cady, Albee and Chidester (1963)
3. Memphremagog, Doll (1951)
4. Milton, Stone and Dennis (1964)
5. Mt. Mansfield, Christman (1959)
6. Hyde Park, Albee (1957a and b)
7. Hardwick, Konig and Dennis (1964)
8. Lyndonville, Dennis (1956)
9. Burke, Woodland (1965)
10. Burlington, eastern part, Doll and others (1961)
11. Camels Hump, Christman and Secor (1961)
12. Montpelier, Cady (1956)
13. Plainfield, Konig (1961)
14. St. Johnsbury, Hall (1959)
15. Lincoln Mountain, Cady, Albee and Murphy (1962)
16. Barre, White and Jahns (1950)

deformational polymetamorphism in central and east-central Vermont. They defined two major stages of deformation which affected Cambrian through Devonian units. They also recognized more than one mineral generation based upon the relationships of mineral grains and small scale structures.

White and Jahns (1950) and almost all other workers up to and including Cady (1969) thought that the structural features and mineral generations of the Cambrian and Ordovician units were identical to those of the Silurian and Devonian rocks. These elements were thought to have all formed in the Acadian Orogeny of Devonian age. Isoclinal folds with E-W axes which are observed only in pre-Silurian rocks were thought to be cross-folds associated with the earliest Devonian folds with N-S axial trends (Cady, 1969). Significant metamorphism of Ordovician age, associated with the Taconic Orogeny, was not thought to be present in Vermont.

Evidence for significant metamorphism in the Ordovician was first presented by Harper (1968), based on K-Ar dating, although these results were not given much attention. Albee (1968) also suggested major Ordovician metamorphism and deformation based on field and petrologic relationships and also on interpretation of previous isotopic age data. Zen (1969 and 1972) proposed widespread regional metamorphism of Late Ordovician or Early Silurian age throughout the

western part of the northern Appalachians. Lanphere and Albee (1974) provided further isotopic age data which confirmed that significant high grade metamorphism of Ordovician age occurred in northern Vermont.

Albee (1972a) made a correlation of some of the structural elements from east to west across several quadrangles. This was done along a traverse roughly parallel to the Lamoille River, like one of the traverses in this study. The correlation of structural elements in the Cambrian and Ordovician units with structural elements in the Silurian and Devonian units was not made because of the difficulties encountered in the Hardwick quadrangle. I attempted such a correlation through the Hardwick quadrangle and had similar problems. The correlation of structure across the unconformity that separates Ordovician and Silurian rocks is easier to make along a traverse parallel to the Winooski River, about 25 miles south of the Lamoille River.

D. Method of study

Field work was conducted during May-June, 1973, and July-August, 1974. Sampling was done along several long traverses and at other locations thought to be important. A traverse in this study is essentially a linear sequence of locations along which I have attempted to follow the structural elements. The locations of the traverses are shown on Figure 1. More detailed sketch maps of the trav-

erses are shown in Figure 3.

There are three main traverses in this study. The longest traverse is parallel to Highway I89. It consists of roadcuts on I89 and U.S. Route 2, plus some nearby natural exposures. The traverse extends from the Williamstown exit on I89 in the Barre quadrangle to the town of Williston in the Burlington quadrangle, a distance of about 50 miles. In the discussion of the structural elements, this traverse has been divided into two smaller traverses. The longest of these is called the Winooski River traverse and extends from location JR-108, south of Montpelier west to JR-149, near Williston (see Figure 3a). Unnumbered locations indicate those which are nearby but not on the traverse. The Winooski River traverse has been divided into five segments to help in describing the correlation of structural elements from east to west.

The smaller subdivision of the traverse along I89 is called the Williamstown to Montpelier traverse. This includes locations JR-203 through JR-108 which are shown in Figure 3b. The I89 traverse is divided at the unconformity between Ordovician and Silurian rocks at JR-108.

A traverse in the eastern part of the area is parallel to Highway I91. It extends from location JR-10, north of St. Johnsbury, northwest to JR-34, near the town of Orleans. The locations are roadcuts along I91 and U.S. Route 5, plus

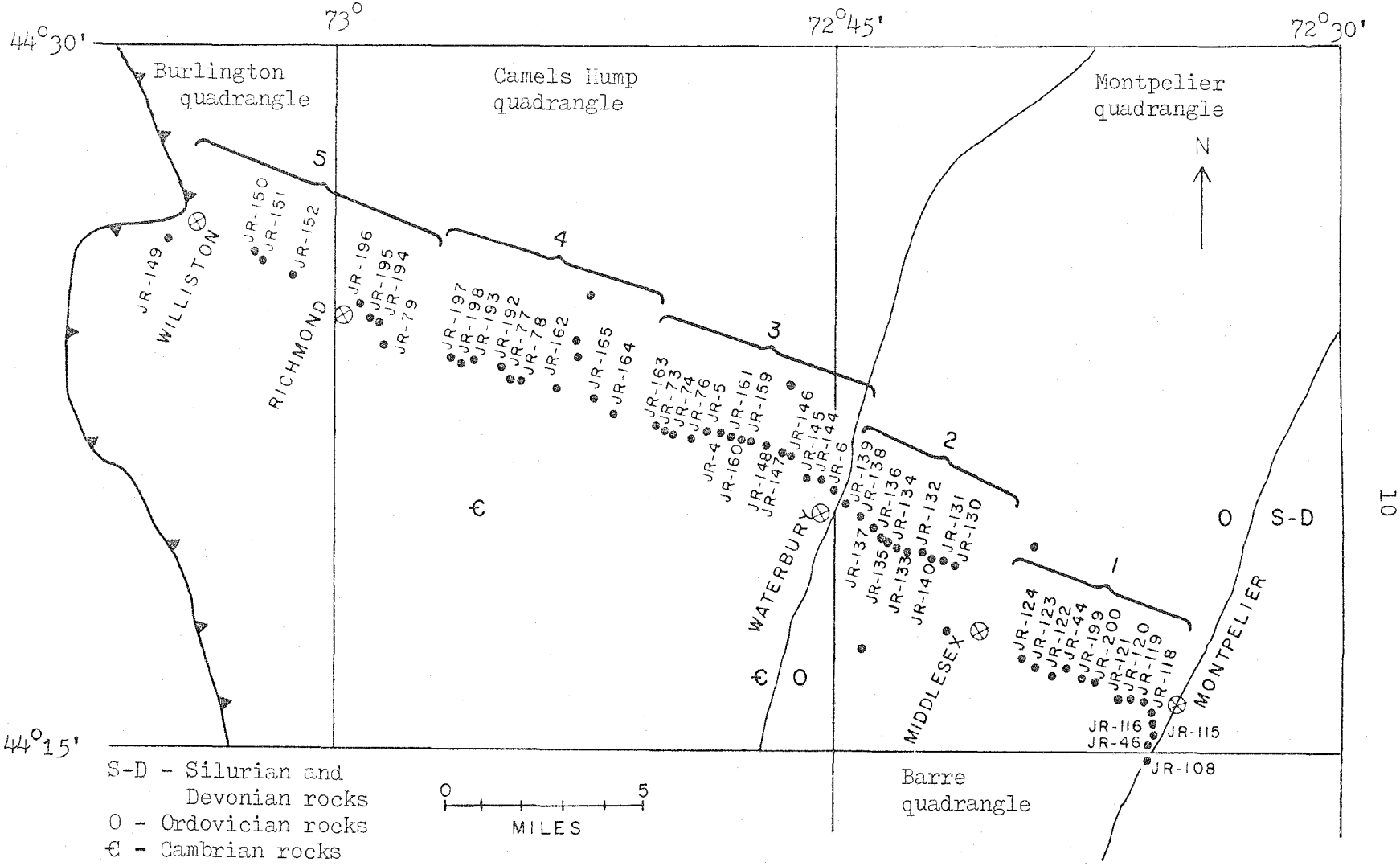

Figure 3a Map of Winooski River traverse, Barre through Burlington quadrangles. Brackets indicate traverse segments.

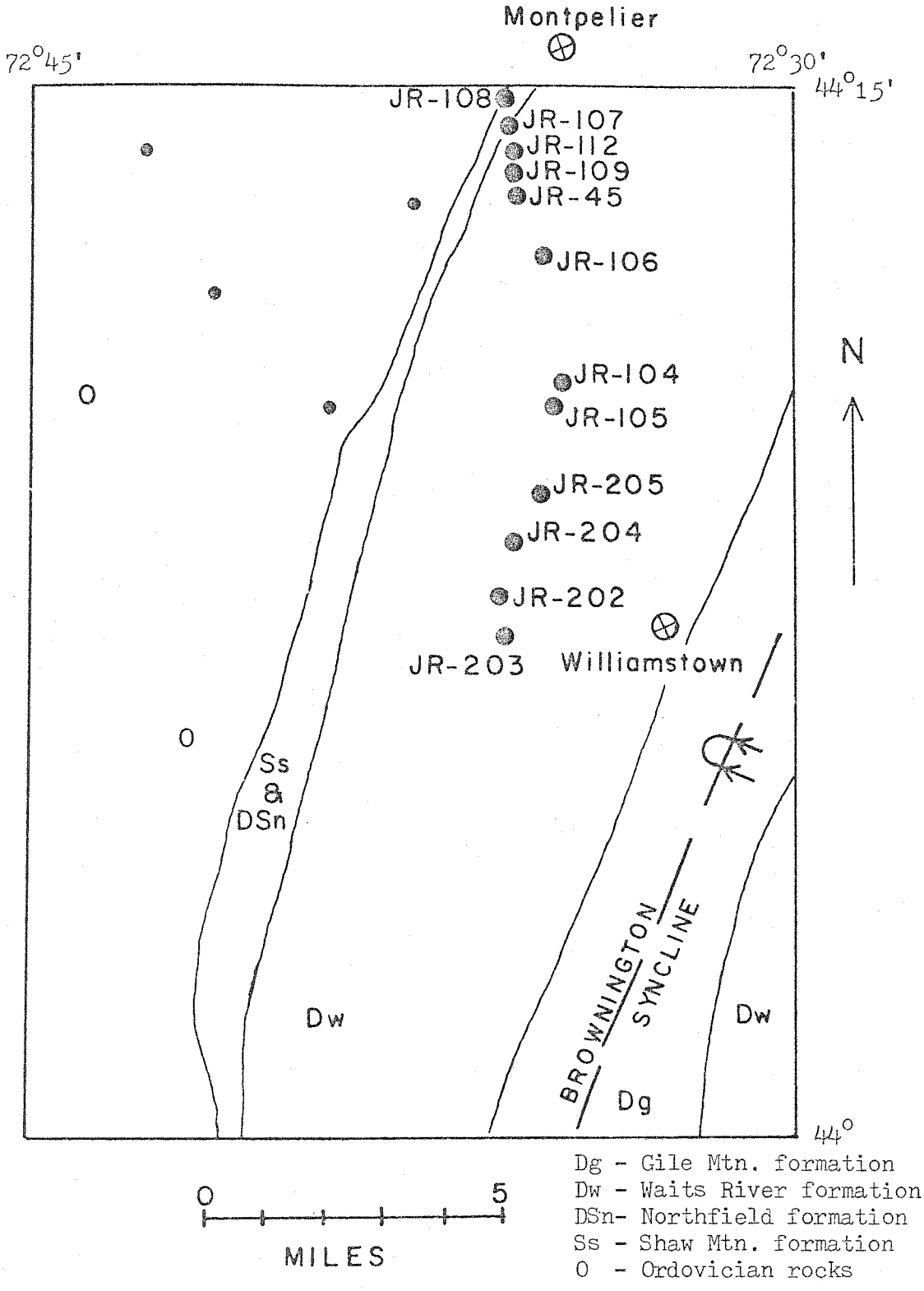

Figure 3b Map of Williamstown to Montpelier traverse, Barre quadrangle.

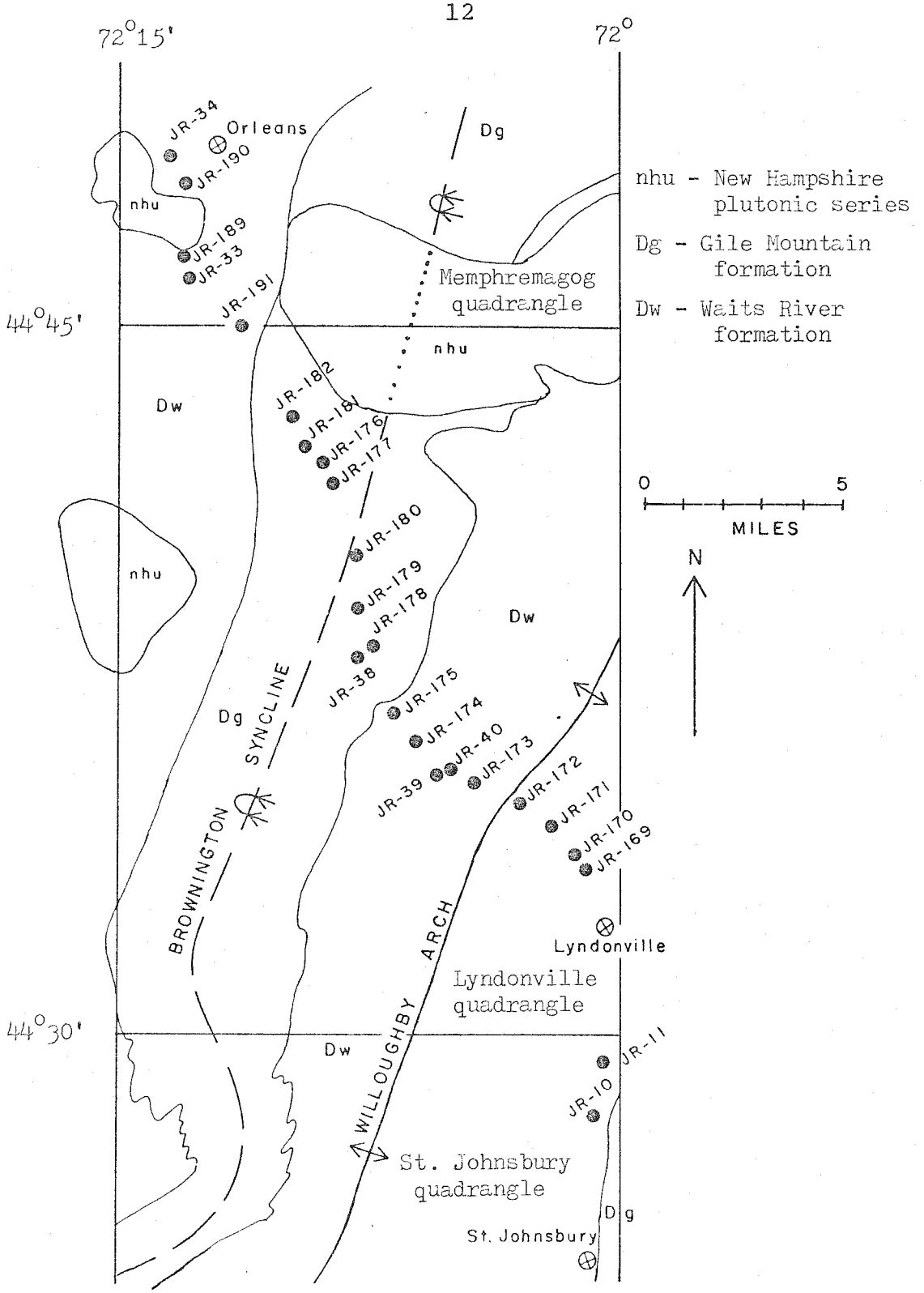

Figure 3c Map of I91 traverse, St. Johnsbury, Lyndonville, and Memphremagog quadrangles.

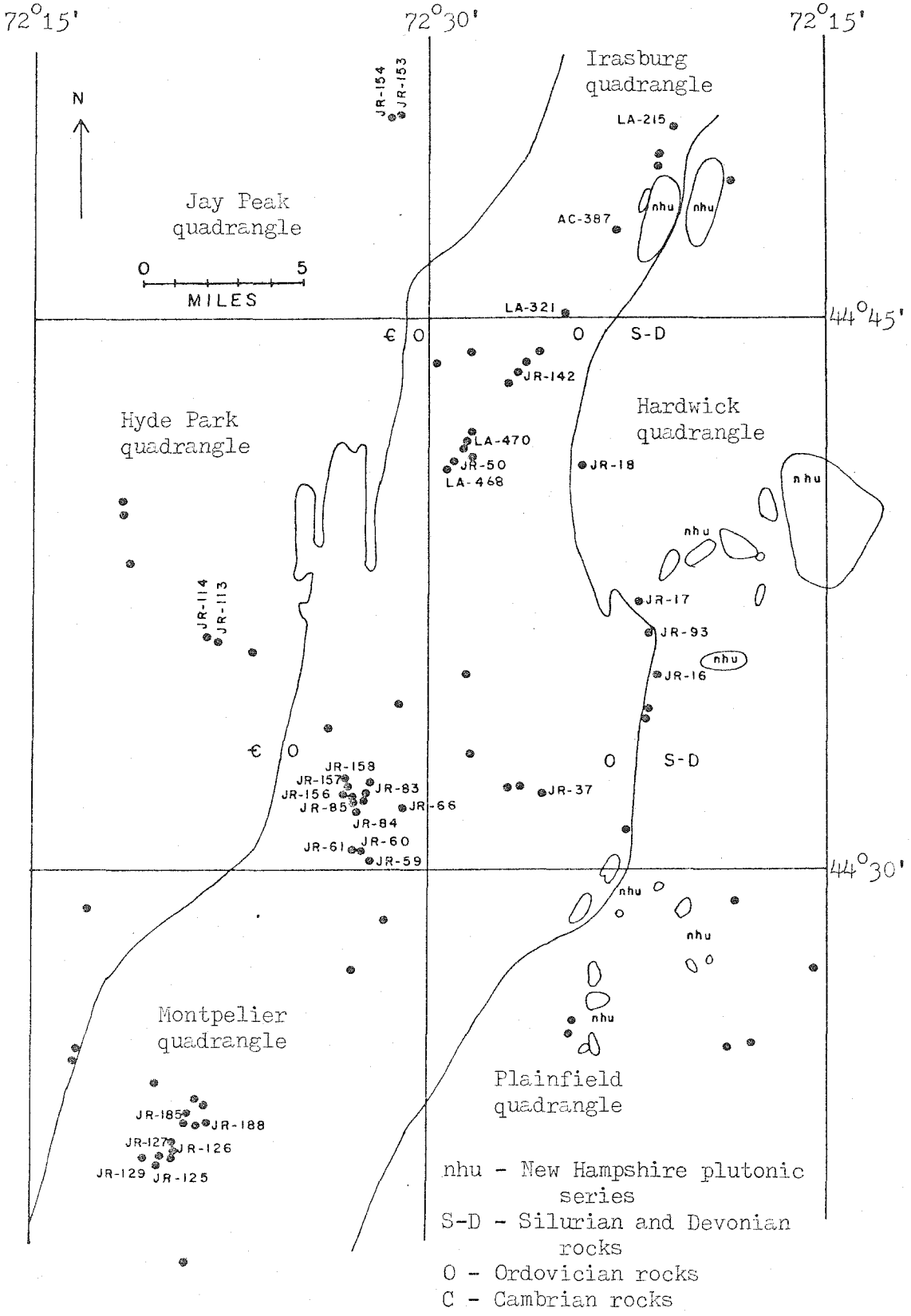

Figure 3d Map of cited locations not along traverses.

natural exposures close to I91. The traverse is shown in Figure 3c.

The other major traverse is generally east-west, parallel to the Lamoille River. This is about 25 miles north of the Winooski River traverse. The Lamoille River traverse includes location JR-9, near the town of Danville in the St. Johnsbury quadrangle, through the Hardwick, Hyde Park, and Mt. Mansfield quadrangles, to location JR-20, near the town of East Georgia in the Milton quadrangle. Data from this traverse are not discussed in detail.

There are a number of locations which are not along the traverses shown in Figures 3a, 3b, and 3c, but which are discussed in the text. These include locations in the Worcester Mountains, the Lowell Mountains, and a few locations along the Lamoille River traverse and are shown in Figure 3d. Location numbers preceded by "LA" are sample locations of A. Albee. One location in the Lowell Mountains is AC-387, a sample location of A. Chidester. Location descriptions for all outcrops described in detail in the text are given in Appendix 1.

Phase relationships and microtextural features were studied in thin sections made from many of the samples. About 40 of these samples were then chosen for detailed electron microprobe analysis. Complete microprobe analyses were made on 100 to 200 points per sample so as to ascertain

the degree and pattern of zoning in all the major phases. Analytical procedures are described in Chapter III.

There are many obvious disadvantages to covering such a large area as northern Vermont with only widely separated traverses. In particular, the lack of a high density of structural coverage presents problems in some areas. The correlation of small scale features with large scale regional structures suffers because of this. However, there is no single quadrangle, or even two quadrangles, in which all of the details of the metamorphic history shown in this study can be unambiguously demonstrated. Features which are prominent and straightforward in one area are often subtle and ambiguous in another. Knowledge of the features where they are clearcut eliminates many of the problems in areas where the features are not so distinct.

The purpose of studying the small scale structural elements of the area was to determine the correspondence between deformational events and mineral growth and to provide a basis for identifying metamorphic vein generations. Small scale structural features were studied in detail and an attempt was made to identify all small fold, S-surface and vein generations. However, this work is not intended to be an exhaustive study of the structural history of northern Vermont, particularly not in terms of mechanisms, stress orientations and so on.

CHAPTER II. STRUCTURAL ELEMENTS

A. Summary of structural elements in northern Vermont

The Silurian and Devonian strata of northern Vermont have been deformed by two prominent, generally north-south trending fold generations. Widely developed, but often difficult to observe, is another north-south trending set of folds which represents the youngest recognized deformational feature of regional significance in the eastern part of the study area. A fourth set of folds with general east-west trends is developed in some areas, but seems to be of minor importance. Associated with each fold generation are transverse features such as schistosity, slip cleavage or fracture cleavage. These planar features are generally parallel to the axial planes of the cogenetic small folds.

These same structural elements can be followed into the Ordovician and Cambrian units, although their style and intensity can be radically different from their expression in the Devonian and Silurian rocks. Some of the elements tend to diminish in intensity, or disappear entirely, westward from the unconformity that separates Ordovician and Silurian units. Uniquely developed in the pre-Silurian units are east-west trending isoclinal folds which are the oldest folds observed and do not extend across the unconformity into the Silurian rocks. Muscovite from a metamorphic vein which is undeformed by these folds gives a K-Ar age of 439

m.y. (Lanphere and Albee, 1974). For these reasons, the east-west isoclinal folds are assigned a Late Ordovician age. Developed with the isoclinal folds is a prominent axial plane schistosity or slip cleavage. Also developed in the Cambrian and Ordovician units is an older bedding schistosity. The pre-Silurian portion of the structural sequence is truncated at the unconformity between the Ordovician and Silurian rocks.

This study is also concerned with another type of structural feature, metamorphic veins. These veins provide the basis for correlating mineral growth generations with structural events. There are a number of different vein generations and several different types of veins. Some of the veins are associated with deformational events which produced folding and others were formed between folding events. The veins seem to be a result of brittle failure of their host rock brought about by localized extension. Commonly individual veins are visibly discontinuous within an average sized outcrop. Vein generations not associated with clearly defined deformational events do show a consistency of orientation that requires a fairly uniform regional stress field for each generation, as is the case for veins associated with folding; the localized extension is brought about as a response of an anisotropic medium to a fairly uniform regional stress field. The regional stress fields for the

various structural events in most, if not all, cases involve compression.

The metamorphic veins are not to be confused with typical hydrothermal veins of the type which are sometimes ore bearing and often have reaction sheaths in the host rock around them. The metamorphic veins in northern Vermont seem to be in chemical equilibrium with their host rocks in the sense that simultaneous growth in the vein and adjacent host rock results in nearly identical chemical compositions in any given phase. The source of the vein material is apparently a volume of the adjacent host rock.

Lineations are widely developed and commonly observed as crenulations on prominent s-surfaces and as intersections of a prominent s-surface set with another s-surface set. The crenulations essentially appear as microfolds with wavelengths of a few millimeters or more and are best developed in phyllite and mica-rich schist. Crenulation lineations are usually parallel to the axes of observable small folds in the outcrop. As a number of different s-surfaces are in the area, there are many possible lineations produced by s-surface intersections. These can be coincident with crenulations if the latter of the two s-surfaces is related to folding. In this study, lineations have not been treated extensively and have only been used with regard to the gentle east-west trending folds in Silurian and Devonian

rocks.

Therefore, the three major types of structural elements that are treated in this study are folds which occur on an outcrop scale, s-surfaces and metamorphic veins. In general, the sequence of folds and s-surfaces is used to establish the sequence of vein generations. However, in some problem areas a well-established vein generation sequence is used to help in identifying part of the fold and s-surface sequence.

B. Nomenclature of structural element generations

For the purpose of this study a system of nomenclature is needed that is flexible enough to apply throughout the area. The following letters are used to denote structural elements and mineral phase generations:

F - folds

L - lineations

M - mineral growth generations

S - planar structures such as bedding, schistosity and cleavage

V - metamorphic veins

Elements that occur only in the Cambrian and Ordovician units are prefixed by the letter "O" and elements that occur in Silurian and Devonian units and therefore can occur also in the older units are prefixed by "D". Elements associated with major metamorphic events are subscripted by small case

letters, beginning with "a" for the oldest event within each of the two major periods denoted by "O" and "D". For instance, OS_a would designate the oldest pre-Silurian schistosity, while DS_a would denote the oldest prominent schistosity developed in the Silurian and Devonian units and the correlative feature in the pre-Silurian rocks. Minor features which formed between major events are subscripted by a letter plus a number, so that OV_{a+1} denotes the oldest metamorphic vein to form between event O_a and event O_b. Elements which have identical prefixes and subscripts are cogenetic, so that OF_b, OV_b and OS_b would all have formed in the same event, O_b. S_o is used to denote bedding. All features which are prefixed by "D" are not necessarily Devonian in age, but may be younger. Some features which are prefixed by "O" are not necessarily Ordovician, but may be Cambrian or Early Silurian. The probable age of the events will be discussed later.

C. Definitions of structural terms

Some of the terms in this chapter have been used with somewhat different connotations by various authors. Also, there is some terminology employed that is not in common usage. In order to clarify the meanings of these terms as they are applied in this study, the definitions are given below.

Schistosity

Schistosity is a secondary foliation defined by the parallel preferred orientation of mineral grains. There are not discrete spacings between planes of schistosity. Rather, schistosity is an s-surface that completely pervades the rock.

Slip cleavage

Slip cleavage is a distinctly spaced foliation defined by mineral grains with preferred orientations within planar zones. Typically slip cleavage has been formed by microfolding of a pre-existing s-surface. Grains with preferred orientation parallel to the older s-surface have been rotated by microfolding into near-parallelism with the axial planes of the microfolds. In addition, some mineral grains with preferred orientation that help to define the slip cleavage were probably formed by primary mineral growth. The typical spacing between the planes is 1-5 millimeters. "Slip cleavage" in this study is used to describe any spaced foliation defined by grains with preferred orientation, regardless of whether it is formed by rotation or growth.

Fracture cleavage

In this study, fracture cleavage refers to a set of closely spaced fractures that does not involve any preferred orientation of grains. The distance between the fractures

is less than about one or two centimeters. Fractures with larger spacings are called fracture sets or joints.

Right-handed and left-handed fold patterns

Most of the small folds observed are asymmetric in cross section. The patterns of small folds have been used by previous workers in the area of attempting to determine the character of the major folds. White and Jahns (1950) defined the terms "dextral" and "sinistral" to describe the patterns of asymmetric folds in plan view. The terms refer to the apparent relative offset of the long limbs by the short limbs. Many of the outcrops in this study are essentially vertical roadcuts, so that it is more convenient to describe the fold patterns as seen in cross section rather than in plan view. The terms "right-handed" and "left-handed" are used in a similar manner to "dextral" and "sinistral" except that the fold patterns are viewed in a reference plane perpendicular to the fold axis. The direction toward which the observer was facing is always specified.

Intensity of deformation

There is reference made in the text to the relative intensity of deformation from place to place. This describes the degree to which the structural elements are developed and the degree to which earlier structural elements are obliterated. A well-developed schistosity is taken to indi-

cate a greater intensity of deformation than a well-spaced slip cleavage. Tight, prominent folds indicate more intense deformation than gentle, open folds. The most intense deformation involves the obliteration of older elements by mechanical processes and/or recrystallization.

D. Criteria for the identification and correlation of structural elements

The determination of the structural sequence, and its regional correlation, is based upon the recognition of the elements in the field. Graphical treatment of structural data using stereonet diagrams is useful, both in the field and in the laboratory, given a number of measurements of a properly identified element. However there are many nearly parallel structural features of different generations and any artificial treatment cannot unambiguously separate an unidentified individual element from other nearly parallel elements of other generations.

The structural sequence is established by observing the superposition of younger elements upon older elements. Typical superposition relationships are folded s-surfaces, folded veins, folded folds, folds cut by s-surfaces, folds cut by veins, s-surfaces cut by veins, veins cutting other veins, s-surfaces cutting other s-surfaces and so on. Metamorphic veins which cut older folds but which are folded by younger folds were found to be especially useful in identi-

fying late folds in highly deformed rocks. Locally the superposition relationships are ambiguous such as with two intersecting, unfolded s-surfaces which don't show any displacement or two open fold sets with axes at 90^{o} to each other. The ambiguity can be resolved if other types of elements are present. The structural relationship of veins to other elements is generally unambiguous.

The correlation of structural elements involves following the continuity of an element along a traverse and, more importantly, following the entire sequence of elements. At each location an attempt has been made to identify all the elements in the sequence, but a complete sequence is rarely found. There is generally enough of the sequence so that all of the structural features present can be identified. The traversesin this study involve the correlation of the structural sequence across the area, from which the correlation of single elements immediately follows. The "key" outcrops are those in which a fairly complete structural sequence is present and clearcut.

Correlations of individual elements based on features such as fold style, vein style and so on can lead to difficulties as rapid changes in style from one lithologic type to another are possible. Style, size, wavelength and other characteristics are useful in the correlation as long as the possibility of abrupt changes is considered and the entire

sequence of elements is used as the primary correlation criterion.

One textural feature of the quartz-rich metamorphic veins is used as an additional criterion in determining relative age relationships. This is the comparative degree of granulation of two different vein generations in the same host rock. Vein quartz is typically very coarse-grained. However, many highly deformed veins consist of fine-grained quartz which has a "sugary," granular texture. Fragments of coarser quartz or other minerals may be surrounded by the fine-grained quartz. In some samples, the quartz appears to be granulated and fine-grained in hand specimen, but the apparent grain boundaries of the original coarse-grained quartz can be observed in thin section. Such quartz is highly strained and typically fractured in thin section. Quartz in relatively undeformed veins never has a fine-grained, granular texture either in hand sample or thin section. This indicates that the granulation is produced by deformation. Granulation may also affect the host rock, but it is difficult to demonstrate that a fine-grained host rock was originally coarse-grained. Given the same type of host rock in the same outcrop, a generation of consistently granulated veins is considered to be older than a generation of consistently ungranulated veins. The contrast in textures in the two generations indicates intervening deformation. The textural comparison of veins is useful where crosscutting relationships

are not found. However, clearly demonstrated superposition is always the primary criterion for establishing the relative ages of two structural elements.

Table 1 shows the sequence of deformational and mineral growth events in northern Vermont. Most of the remaining pages in Chapter II are devoted to developing this sequence and showing how the elements are manifested in the area. The most important aspect of the regional correlation is the recognition of the oldest Devonian elements within the Cambrian and Ordovician units; any deformational element which is deformed by these must be no younger than Early Silurian. The structural features least important to the regional correlation are the minor vein generations.

E. Deformation in Silurian and Devonian units

The Lower Devonian Waits River formation and Gile Mountain formation (Doll and others, 1961) have been deformed by four generations of folds which are therefore Lower Devonian or younger in age. Of course, these folds can also affect the older units. The two most prominent fold generations generally trend north-south and are the same fold generation observed by White and Jahns (1950) in the Silurian and Devonian rocks and subsequently observed by other workers (for instance, Dennis, 1956; Murthy, 1957; Hall, 1959; and Konig and Dennis, 1964). Konig and Dennis (1964) recognized a slip cleavage (their s_3) which is axial planar to the

Table 1 Structural and metamorphic mineral growth sequence in northern Vermont

Major event	Folds	S-surfaces	Veins	Mineral growth
		OS_o		
O_a	none	OS_a	OV_a	OM_a
			OV_{a+1}	
O_b	OF_b	OS_b	OV_b	OM_b
			OV_{b+1}	
			OV_{b+2}	
			OV_{b+3}	
Major Unconformity				
		DS_o		
		DS_{a-1}	DV_{a-1}	
D_a	DF_a	DS_a	DV_a	DM_a
			DV_{a+1}	
			DV_{a+2}	
			DV_{a+3}	
D_b	DF_b	DS_b	none	DM_b
	DF_{b+1}	DS_{b+1}		
			DV_{b+2}	
D_c	none	none	DV_c	DM_c
(D_d)	DF_d	DS_d	none	?
(D_e)	none	none	none	DM_e
			DV_{d+}	

third set of north-south trending folds.

Konig and Dennis (1964) also attempted to correlate the structural elements across the unconformity between the Silurian and Ordovician units. They equated their s_3 with the prominent north-south striking slip cleavage found to the west in the pre-Silurian rocks. It appears that this prominent slip cleavage in the pre-Silurian rocks, called "Green Mountain" slip cleavage by Konig and Dennis (1964) and other workers in northern Vermont, is equivalent to s_1 of Konig and Dennis; in this study it is called DS_a. Konig and Dennis based their correlation on the relationships between garnet porphyroblasts and the two slip cleavages, their s_3 in the Hardwick quadrangle and the "Green Mountain" slip cleavage. However, they did not consider that the garnet porphyroblasts could be of more than one generation. As demonstrated in the next chapter, much of the growth of high-grade minerals, such as garnet, in the pre-Silurian rocks took place during Ordovician times while the garnet growth in Silurian and Devonian rocks is of necessity much younger.

This study presents the first correlation of the structural elements across the unconformity firmly based on the structural elements alone, rather than relying on mineral growth generations. The basic approach is that structural sequence is used to identify mineral growth generations rather than the reverse. The elements will first be estab-

lished for the Silurian and Devonian rocks.

Two locations in the Barre quadrangle serve to show the method by which the sequence is established and individual elements identified. They also provide examples of the structural sequence observed in the Silurian and Devonian rocks. The two outcrops are JR-107 and JR-112; these are shown in Figure 3b in Chapter I.

JR-107

Location JR-107 is a large roadcut along Highway I89. Bedding, designated DS_o, is shown by contrasting rock types. DS_o is folded by large, north-south trending, asymmetric folds. The wavelengths of these folds vary from 5 to 40 meters and the amplitudes are of similar dimensions. Axial planar to these folds is a well-developed schistosity which is parallel to DS_o on the long limbs of the folds and which crosscuts DS_o on short limbs and fold noses. Parallel to this axial plane schistosity are metamorphic veins. The folds do not appear to deform any earlier, well-developed schistosity or any metamorphic veins, although a vague schistosity parallel to DS_o is visible on short limbs. The veins, axial plane schistosity, and folds are themselves folded by a set of generally north-south trending, asymmetric folds which vary from open to nearly isoclinal. The wavelengths of the smallest folds of this set are much smaller than the wavelengths of the older folds. Axial planar to the later

set of folds is another s-surface, a well-developed slip cleavage. The slip cleavage cross-cuts the deformed earlier axial plane schistosity and associated veins. No veins are observed which are parallel to the slip cleavage. On exposed surfaces of the early schistosity, two sets of crenulation lineations can be observed. One set is parallel to the axes of the later north-south folds and the other set trends generally east-west and is associated with a set of open, east-west trending folds which deform the early schistosity. The time relationship between the east-west folds and the later set of north-south folds is not clear. These two sets are essentially perpendicular to each other and in such cases time relationships can be ambiguous. The late slip cleavage appears to be gently warped by a third possible set of north-south trending folds.

This is a typical sequence in the Silurian and Devonian rocks and given the above relationships, it is possible to identify the individual elements. The earliest folds are DF_a with associated axial planar DS_a and DV_a veins. The vague schistosity folded by DF_a is DS_{a-1}. The north-south trending folds which deform DS_a, DV_a, and DF_a are DF_b folds and have axial plane DS_b slip cleavage. The east-west folds with the associated lineation are DF_{b+1} and these clearly deform DS_a but have an ambiguous relationship to DF_b (elsewhere it appears that DF_{b+1} may be younger than DF_b). DS_b

slip cleavage is gently warped by the third set of north-south trending folds, DF_d. The refolding of DF_a folds by DF_b can be easily seen, but the DF_d folds are so gentle that they can really only be demonstrated as warps of DS_b slip cleavage. This is not the entire sequence shown in Table 1, but there is enough of the sequence to identify the individual elements with reasonable confidence.

JR-112

Location JR-112 is also a roadcut along Highway I89. It is about 0.5 miles to the south of JR-107. DF_a folds were not observed at JR-112, perhaps due to the size of the exposed outcrop. The height of the roadcut at JR-112 is small compared with the amplitudes of the DF_a folds at JR-107. Other elements are present, however.

The oldest prominent secondary foliation is a well-developed schistosity which is identical to DS_a at JR-107. Parallel to DS_a are metamorphic veins, DV_a. DS_a and DV_a are folded by a set of north-south trending folds, DF_b, associated with which is a poorly developed axial plane slip cleavage, DS_b. There is a set of east-west trending open folds, DF_{b+1}, which interfere with DF_b and deform DS_a. Undeformed by and crosscutting DF_b and DF_{b+1} folds is a north striking vein which is gently warped by north-south trending folds, DF_d. The vein is probably a DV_c vein, although the identification of DV_c veins is not as clearcut in

the Barre quadrangle as it is to the north, in the Lyndonville quadrangle for instance, where DV_c veins are associated with high-grade mineral growth in the host rock. Regardless of the specific generation of this vein, it clearly crosscuts DF_b folds and is folded by a younger set of north-south trending folds. The use of veins, regardless of generation, as structural markers in this fashion provides in many cases the least ambiguous evidence regarding the number and relative age relationships of fold sets in an outcrop.

Well demonstrated at JR-112 are three fold sets which deform the oldest prominent schistosity, DS_a. At JR-107, DS_a is seen to be parallel to the axial planes of a fourth, oldest fold set. There is evidence of the other three fold generations at JR-107, but the two youngest sets, DF_{b+1} and DF_d, are best demonstrated at JR-112. Developed within these two outcrops are all the major structural elements of Silurian and Devonian rocks. There are four fold sets, DF_a, DF_b, DF_{b+1}, and DF_d. Two s-surface sets which are parallel to the axial planes of folds are found: DS_a and DS_b. DV_a veins are prominently developed in both exposures. There is one possible DV_c vein at JR-112. The DV_c vein crosscuts DF_b and DF_{b+1} folds, but is folded by DF_d folds.

General description of the structural elements

There is a great deal of variation in the style and intensity of the structural elements in the Silurian and Devo-

nian rocks. The two examples just described are typical of a portion of the Barre quadrangle, but are not necessarily typical of other parts of the study area. Each structural element will be discussed in general by comparing and contrasting the elements along two traverses: the Williamstown to Montpelier traverse along I89 in the Barre quadrangle and the I91 traverse in the Lyndonville quadrangle. A few specific examples are cited from other locations.

DS_o and early secondary bedding schistosity (DS_{a-1})

Bedding surfaces, DS_o, are often observed as the contacts between layers of contrasting lithologic type and as banding within a single layer. However, care must be exercised in exposures where contrasting lithologic types are not present. A well developed secondary foliation can closely imitate bedding surfaces and yet be at a significant angle to the original bedding. A weakly developed schistosity, apparently due to growth of mica grains at low metamorphic grade, is observed which is always parallel to DS_o. This schistosity is called DS_{a-1}, as the first prominent schistosity, DS_a, is usually the oldest s-surface of metamorphic origin that can be found. The difficulty in observing DS_{a-1} is brought about by a combination of weak development and strong overprint by later events. In a few locations, for example JR-181 in the Lyndonville quadrangle,

thin veins are observed to be parallel to DS_o and truncated by DV_a veins which are parallel to DS_a. These small veins, called DV_{a-1}, are not necessarily veins in the sense used in this study. The veins are never more than 1 cm wide, generally occur in closely spaced sets, and do not show the internal textural features observed in other veins. The DV_{a-1} veins consist of quartz and/or calcite. In any event, the mineral growth associated with DS_{a-1} and DV_{a-1} is of no great significance in terms of the metamorphic history of the area. Presumably DS_{a-1} was formed during diagenesis and pre-deformation, low-grade metamorphism.

Elements of event D_a

A prominent schistosity, DS_a, is associated with the first major deformational event in the Silurian and Devonian rocks. This schistosity is often observed to be parallel to bedding, DS_o, but in many places DS_a is at an angle to DS_o. In sufficiently large outcrops (for instance, JR-107), DS_a can be seen to be axial planar to asymmetric, tight folds which have varying amplitudes and wavelengths, but are typically not smaller than 6 to 10 meters in wavelength with similar amplitudes. Some observed folds of this generation, DF_a, are much larger, but DF_a folds with wavelengths of a few meters or less have been only rarely observed in the Silurian and Devonian units. Because of the typical size of DF_a folds, they are not often observed except in the

largest outcrops. This situation, if not recognized, can introduce error in the structural interpretation of the area.

In the Barre quadrangle DF_a folds are prominently developed and exposed in the large outcrops of Highway I89. The largest observed DF_a folds are exposed at JR-107, but these folds can also be seen at JR-106, JR-202 and other locations. Here the long limbs of the asymmetric DF_a folds are parallel to the axial plane DS_a and therefore DS_a and DS_o are parallel on the long limbs. On the short limbs DS_a and DS_o can be at angles of 20^o or 30^o or more to each other. In tighter folds the angle is less. At the fold noses, of course, the angle between DS_a and DS_o becomes very large. In an area with only small outcrops, DF_a folds can be exceedingly difficult to find and DS_a can be mistaken as a bedding schistosity on exposed long limbs. The Barre quadrangle is an area in which White and Jahns (1950) worked and DF_a in this study corresponds to their earliest major generation of folds. The two most prominent sets of north-south trending folds found in this study in the Silurian and Devonian rocks correspond exactly to the two major fold sets first defined by White and Jahns.

Examples of the relationship between DS_a and DF_a are shown in Figures 1 and 2, both from locations in the Barre quadrangle. Figure 1 shows a DF_a fold with a smaller than typical wavelength that folds the contact between phyllite

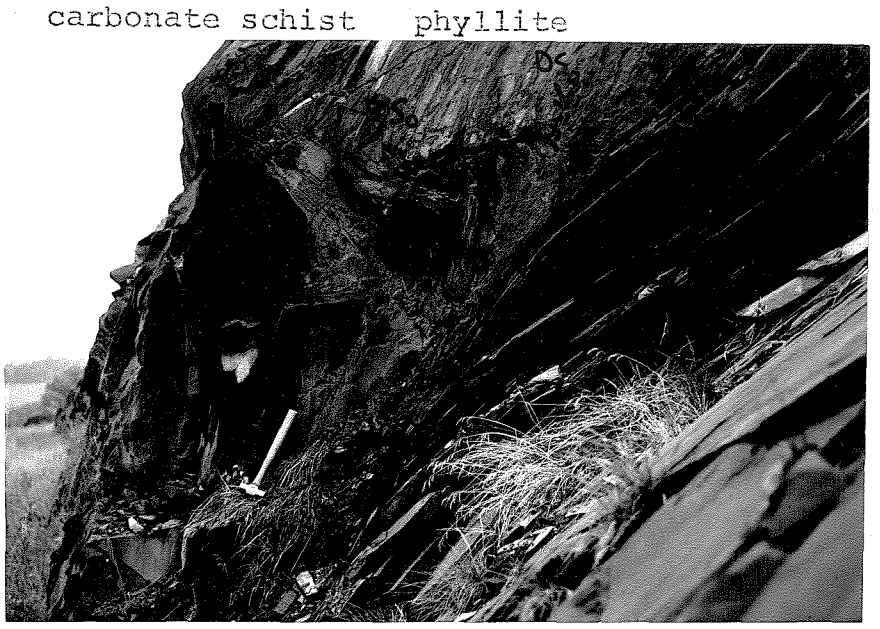

Figure 1 DF$_a$ fold at location JR-103, Barre quadrangle. DS$_o$ and DS$_a$ are outlined in black. DS$_o$ is a contact between phyllite and carbonate schist. Axial plane schistosity DS$_a$ is parallel to long limbs of fold.

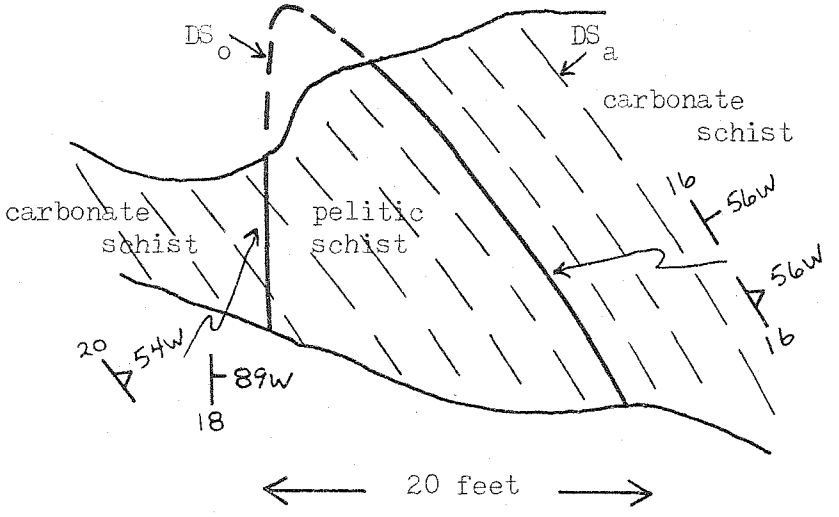

Figure 2 DF$_a$ fold at location JR-202, Barre quadrangle. DS$_a$ schistosity is parallel to long limb. Sketch is from a polaroid photograph.

to the right side of the photograph and carbonate schist to the left. DS_a schistosity is axial planar to the DF_a fold and roughly parallel to the long limb. Figure 2 is a sketch from a polaroid photograph of a somewhat larger DF_a fold at another location, JR-202, with similar relationships. DF_a folds are observed in the Silurian and Devonian rocks in the Hardwick and Lyndonville quadrangles, although DF_a fold noses are more difficult to find. Figure 3 shows a DF_a fold in metavolcanic rocks of the Gile Mountain formation in the Lyndonville quadrangle. As is true in this case, DF_a folds sometimes have an axial plane DS_a surface which is parallel to neither limb.

Parallel or closely subparallel to DS_a, and therefore not necessarily parallel to DS_o, are metamorphic veins which are abundantly developed throughout the Silurian and Devonian metamorphic rocks. These veins are called DV_a and are described in more detail later. The mineral assemblages in the veins are comprised of minerals also found in the adjacent host rock, although vein assemblages tend to be simpler than host rock assemblages. Quartz, calcite, and/or plagioclase are typically the predominant vein minerals. For a given mineral, for instance chlorite or muscovite, there is a general compositional correspondence between mineral growth in the DV_a vein and host rock mineral growth of the same generation. One type of evidence used to show that

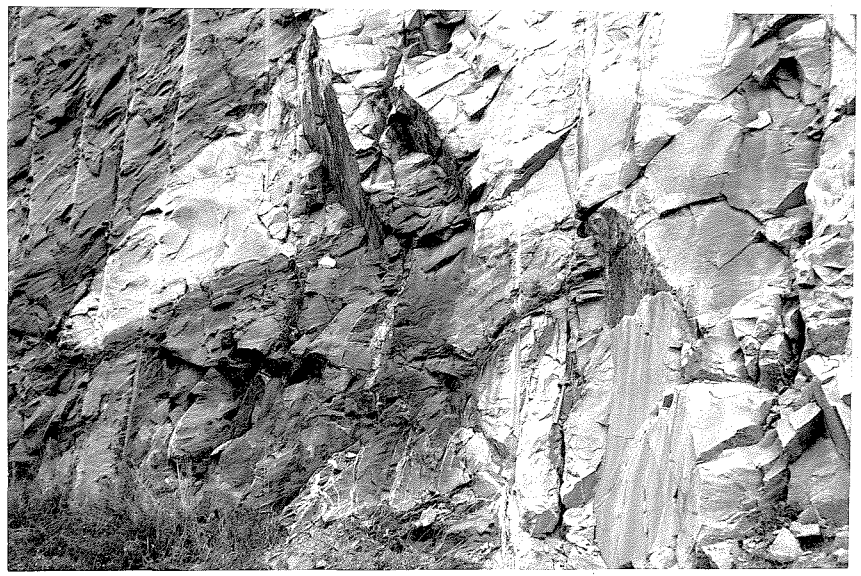

Figure 3 DF_a fold at location JR-178, Lyndonville quadrangle. Rocks are metavolcanic layers of the Gile Mountain formation. DS_a is parallel to neither limb.

host rock mineral growth formed during event D_a is preferred orientation of grains parallel to DS_a. Electron microprobe analysis shows that the compositions of DV_a vein chlorite and muscovite are about the same as the compositions of host rock chlorite and muscovite grains with preferred orientation parallel to DS_a. There is a significant variation within single grains of minerals such as chlorite and muscovite, however. Establishing the chemical correspondence of vein and host rock mineral growth is fairly complicated in general. The compositional variation trends are established for DM_a mineral growth in the DV_a veins and in the adjacent host rock. Compositional correspondence is shown by demonstrating overlapping portions of the variation trends of a given mineral in the vein and host rock. Specific cases are discussed in detail in Chapter III. In general for a given mineral growth generation, in this case generation DM_a, the microprobe data show that host rock mineral growth began first, then vein growth began with host growth sometimes continuing, and finally the last mineral growth was in the vein only.

DV_a veins are very useful in identifying structural elements. They provide highly visible markers of DS_a and aid in differentiating DF_a folds from the prominent refold set, DF_b. They are abundantly developed throughout the Silurian and Devonian metamorphic rocks and also are found

in the pre-Silurian rocks. DV_a veins are a key element in the correlation of structures across the unconformity between Silurian and Ordovician units.

Figure 4 shows stereonet plots of DF_a axes and poles to DS_a observed along a traverse from Williamstown to Montpelier in the Barre quadrangle. The axes of DF_a in this area trend NNE-SSW with generally steep plunges. The small number of axes plotted reflects the difficulty in finding DF_a fold noses. DF_a folds are refolded by DF_b, but the variance in plunge of DF_a folds is probably not entirely produced by refolding. The refold axes are nearly parallel to the DF_a axes so that the variance in plunge may reflect the noncylindrical nature of DF_a folding, that is, the variance in plunge is a primary feature of DF_a folding. DF_a folds may be predominantly shear folds in character, although flexure folding could have been the mechanism of initial deformation. Shear folds, also called passive folds (Donath and Parker, 1964), are the result of movements within or parallel to an s-surface set such as DS_a which is in general non-parallel to bedding surfaces, at least at fold noses. Flexure folding involves movement parallel to the bedding planes as layers are warped. Actual folding may involve a combination of mechanisms during the deformational event. The prominence of the DS_a schistosity suggests that shear folding occurred. Shear folds are often observed to be noncylindri-

Figure 4a

Stereonet plot of DF_a axes at locations along the Williamstown to Montpelier traverse. (All stereonets are lower hemisphere projections.)

Figure 4b

Stereonet plot of poles to DS_a at locations along the Williamstown to Montpelier traverse.

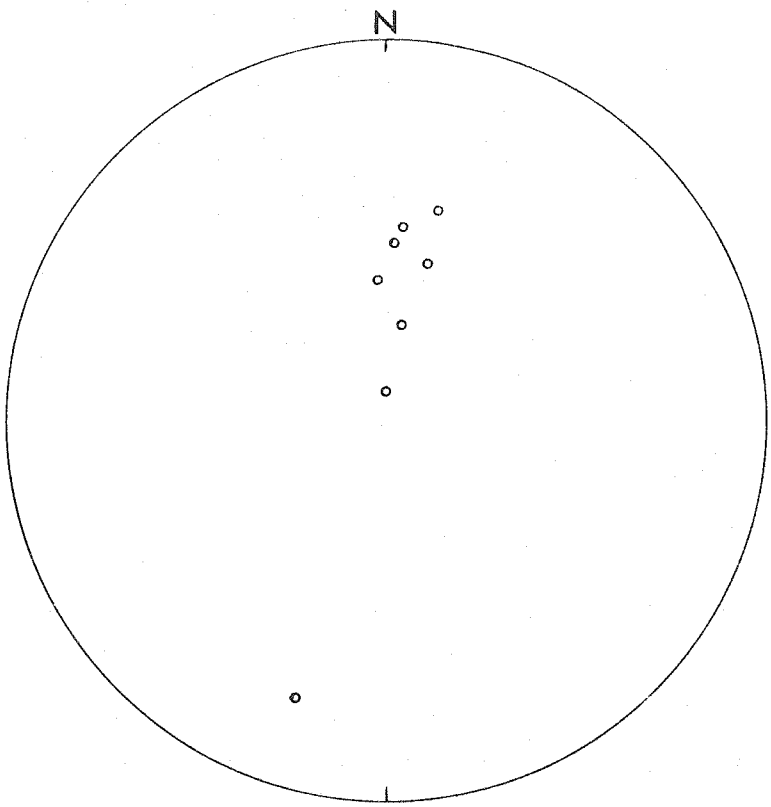

Figure 4a

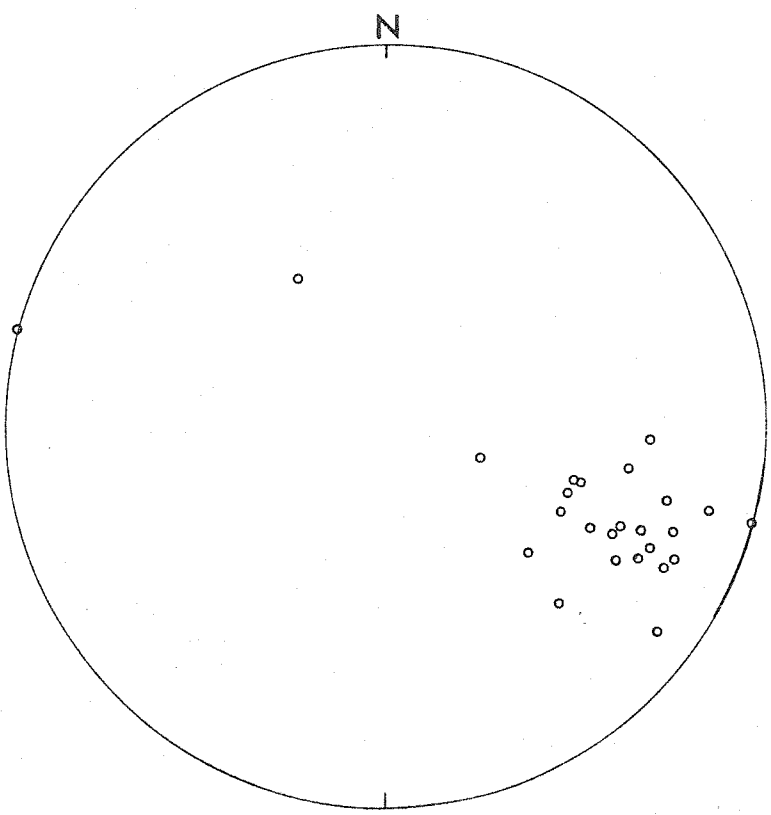

Figure 4b

cal and have axes which plot along a great circle of stereographic projection rather than at a maximum (Donath and Parker, 1964, p.56). This great circle represents the axial plane of the folds. The physical meaning of the measured axis of a shear fold is that it represents the intersection of the axial plane surface, to which DS_a is parallel in this case, with some other pre-existing surface such as a bedding plane, DS_o for DF_a folds. If the axial plane surface has a constant orientation and the orientation of the pre-existing surface varies from fold to fold or from one part of a single fold to another, then the locus of intersections coincides with the great circle which the axial plane surface defines. The variation in the attitude of the pre-existing surface may be brought about because of pre-existing deformation, early flexure folding resulting from the same event that caused the shear folding, or changes in the style of folding which are most often due to changes in rock type. The attitude of the axial plane may change due to local variations in the stress field.

DS_a in the Silurian and Devonian units is generally a well developed schistosity, especially in mica-rich rocks. In some of the more massive carbonate rocks and sometimes in metavolcanic rocks such as those in Figure 3, DS_a is poorly developed. DS_a is defined by grains with preferred orientation of white mica (typically muscovite), chlorite, and/or biotite, plus amphibole, tourmaline, ilmentite and others if

they are present. Elongation of quartz grains parallel to DS_a is often observed. The only pre-existing schistosity observed is the vague DS_{a-1} surface which is parallel to DS_o and which in many cases cannot be seen at all. It seems reasonable that DS_a formed as a result of simple metamorphic mineral growth parallel to the axial planes of DF_a folds and therefore parallel to the plane of maximum flattening and perhaps parallel to the plane of dominant movement if shear folding occurred. Although the plane of maximum flattening should be a plane of zero shear stress, both flattening and shearing along DS_a appear to have occurred in observed samples. This contradiction has been the subject of considerable debate in the past.

Poles to DS_a surfaces measured along the traverse from Williamstown to Montpelier are shown in Figure 4b. DS_a is typically deformed by DF_b folds so that significant dispersion of DS_a is to be expected. The measurements in Figure 4b were made only on the limbs of DF_b folds so that the dispersion of the attitudes of DS_a seen at the noses of DF_b folds is not represented. DS_a and parallel DV_a generally strike NNE with varying dips to the WNW. Due to the complications of refolding, there is not a great deal of information that can be obtained from plots of DS_a and DV_a attitudes. Examples of highly deformed DV_a veins and DS_a are shown in Figures 5 and 6, from the Lyndonville and Barre quadrangles

Figure 5 Disharmonic DF_b folds at location JR-170, Lyndonville quadrangle. Folds deform quartz-rich DV_a veins and carbonate host rock of Waits River formation.

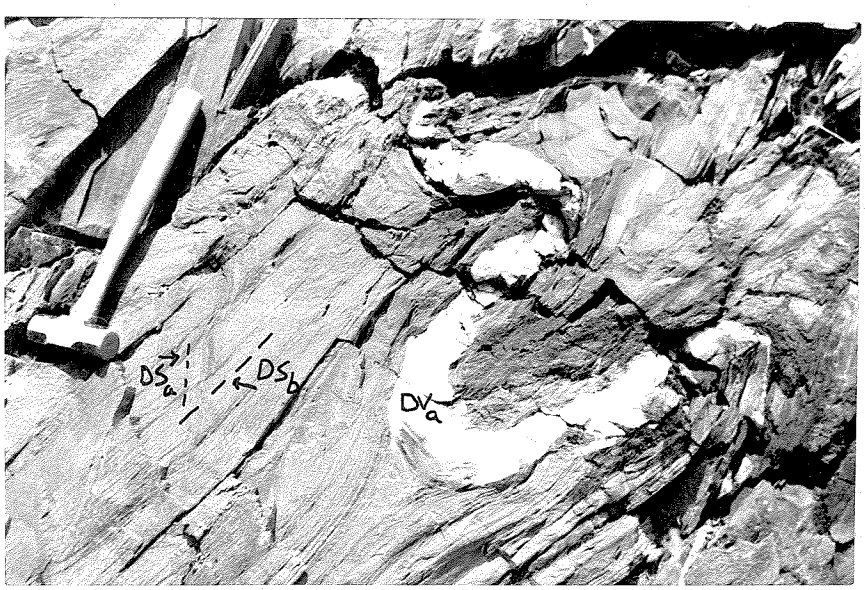

Figure 6 DF_b folds at location JR-108, Barre quadrangle. Folds deform DV_a vein and Northfield phyllite. DS_a is crosscut by DS_b schistosity.

respectively. In the Barre quadrangle the deformation of DS_a and DV_a is commonly observed to be less intense than that shown in these two photographs.

Elements of event D_b

The features of event D_a are deformed by the most prominent folds in the Silurian and Devonian rocks, DF_b. These folds are recognized on the same basis as all the other elements; DF_b folds have a particular position in the sequence of elements defined at each location, such as the sequences earlier described for locations JR-107 and JR-112. DF_b folds correspond to the later generation of major folding described by White and Jahns (1950). The fold axes generally trend from N to NNE and plunge from 0^o to 45^o both north and south. Fold style varies from tight asymmetric and isoclinal folds to fairly gentle, asymmetric open folds. The tightness of folding varies both regionally in all rock types and locally from one rock type to another. Regionally, the DF_b folds generally become more open as the unconformity between the Silurian and Ordovician rocks is approached from the east. DF_b folds west of the unconformity in the Ordovician rocks are open and gentle. Disharmonic forms such as the small scale ptygmatic folds shown in Figure 5 are not uncommon, especially when the folding involves quartz-rich metamorphic veins together with carbonate

or pelitic host rocks. Small scale DF_b folds typically have wavelengths of a few meters or less.

These folds are easily observed almost everywhere in the Silurian and Devonian rocks. Often two orders, in terms of size, of DF_b folds can be recognized in an outcrop with, for instance, wavelengths of perhaps 0.5 - 1 meter and 6 - 10 meters or more. There is probably a heirarchy of fold orders ranging up to folds of regional extent with wavelengths on the order of kilometers. The same is probably true for DF_a, but the wavelength of the average smallest DF_a fold is much greater than the wavelength of the average smallest DF_b fold. This makes DF_b appear more prominent to the field observer. For instance, the smallest DF_a folds at JR-107 have much larger wavelengths and amplitudes than the prominent small DF_b folds there.

Parallel to the axial planes of DF_b folds is a foliation surface, DS_b. DS_b varies in intensity from a pervasive schistosity to a spaced slip cleavage to virtually absent. In pelitic schists, phyllites, and carbonate schists, DS_b can be the dominant schistosity with DS_a being largely obliterated by the overprint. Figure 6 shows a good example of DS_b schistosity which is axial planar to DF_b folds of a DV_a vein and parallel DS_a. DS_a is heavily overprinted in this example and DS_b is a pervasive schistosity. Note the influence of the difference in mechanical properties between

the vein and host phyllite on DS_b, in particular the deflection of DS_b around the vein at the nose of the most prominent synform in the photograph. DS_a is best preserved at this same fold nose. Figure 6 is a photograph of phyllite in the Northfield formation from location JR-108, an exposure of both the Northfield rocks of Silurian age and the Moretown member of the Mississquoi formation of Ordovician age. The unconformity between these two units is well exposed in this outcrop.

The DF_b folds in Figure 6 show evidence of shear folding; just to the right of the hammer, DS_a surfaces are offset along DS_b planes. There is also evidence that plastic flow of the vein material and perhaps some flow of the host rock occurred. Veins do not normally show such rapid changes in thickness unless they are deformed and the deformation of the vein in Figure 6 cannot be explained by shear folding alone. It appears that the plastic flow took place parallel to DS_a and therefore flexural flow folding is also involved. Some DF_b folds may be flexural folds without plastic flow.

Figure 7a is a stereonet plot of measured DF_b axes along the I91 traverse. In the southeast, the traverse starts on the east limb of the Willoughby arch, goes northwest across the crest, then down the west limb and into the Brownington syncline.

In the Waits River formation along the axis of the

Figure 7a

Stereonet plot of DF_b axes at locations along the I91 traverse.

Figure 7b

Stereonet plot of poles to DS_b at locations along the I91 traverse.

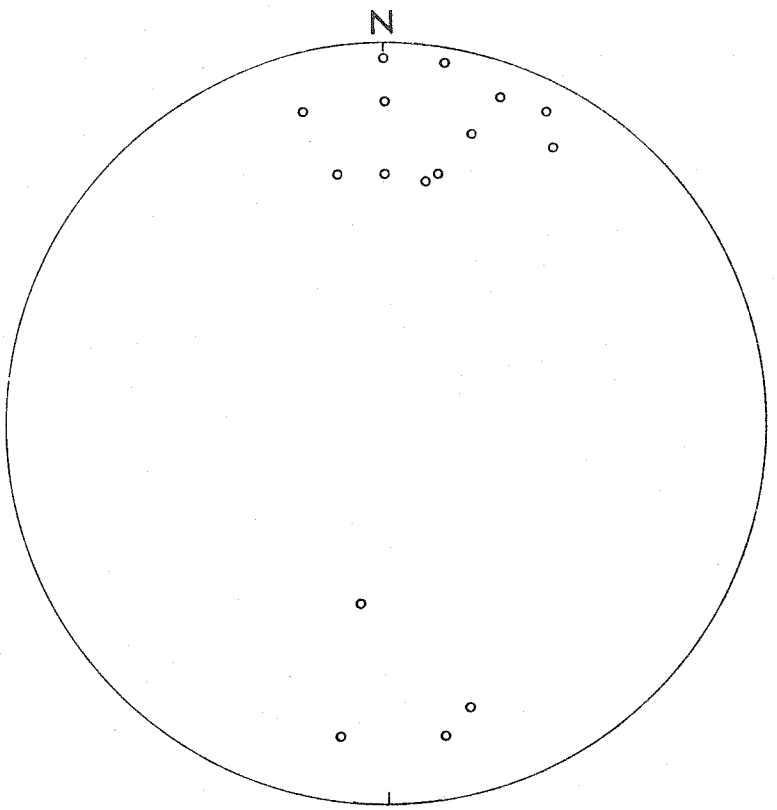

Figure 7a

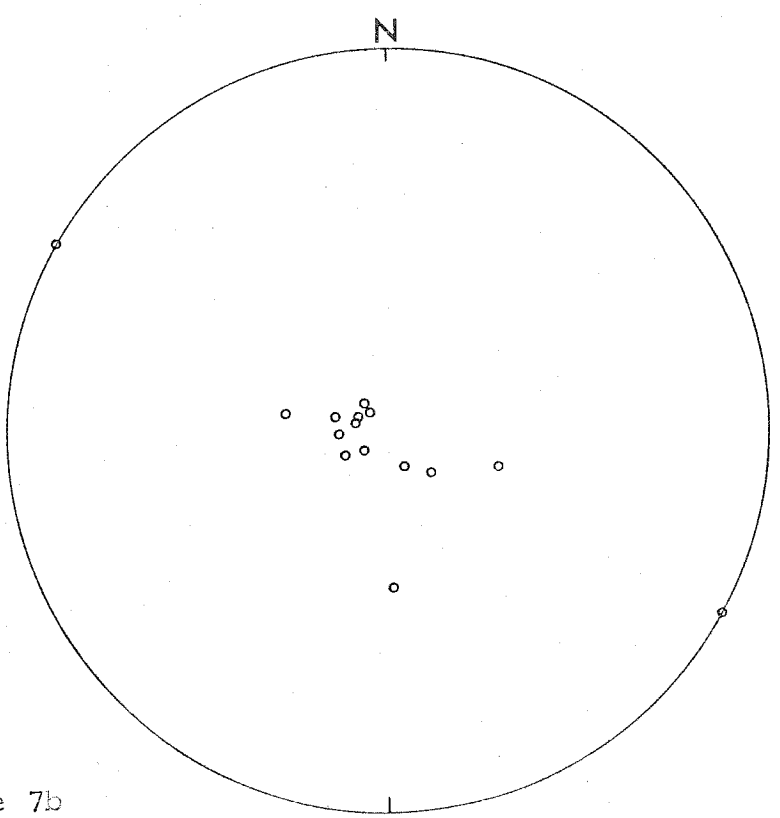

Figure 7b

Willoughby arch, DF_b folds are very tight and have shallow plunges north and south. To the northwest in the Gile Mountain formation and at JR-191 in the eastern exposure of the Waits River formation, these folds become more open and in general have slightly steeper plunges. The relationship of the small folds to the major structures will be discussed later.

The increase in openness of DF_b folds along this traverse also coincides with a decrease in the intensity of DS_b. Figure 7b shows a stereonet plot of poles to DS_b planes measured along the traverse. Most of these measurements are from where there are tight DF_b folds. DS_b surfaces generally have NNE strikes and shallow dips. The steeper dips are associated with the more open folds. DS_b is weakly developed to absent in the Gile Mountain formation rocks along the northwest portion of the traverse. Where DS_b is not developed, the axial planes of DF_b folds tend to have moderate to steep dips. Only measurements of actual DS_b foliation are shown in Figure 7b.

Figure 8 shows DF_b axes and poles to DS_b measured at outcrops along the traverse from Williamstown to Montpelier in the Barre quadrangle. The traverse is within the Waits River and Northfield formations on the west limb of the Browning syncline about 45 miles southwest of the I91 traverse. The entire traverse is no more than 5 miles east of

Figure 8a

Stereonet plot of DF_b axes at locations along the Williamstown to Montpelier traverse.

Figure 8b

Stereonet plot of poles to DS_b at locations along the Williamstown to Montpelier traverse.

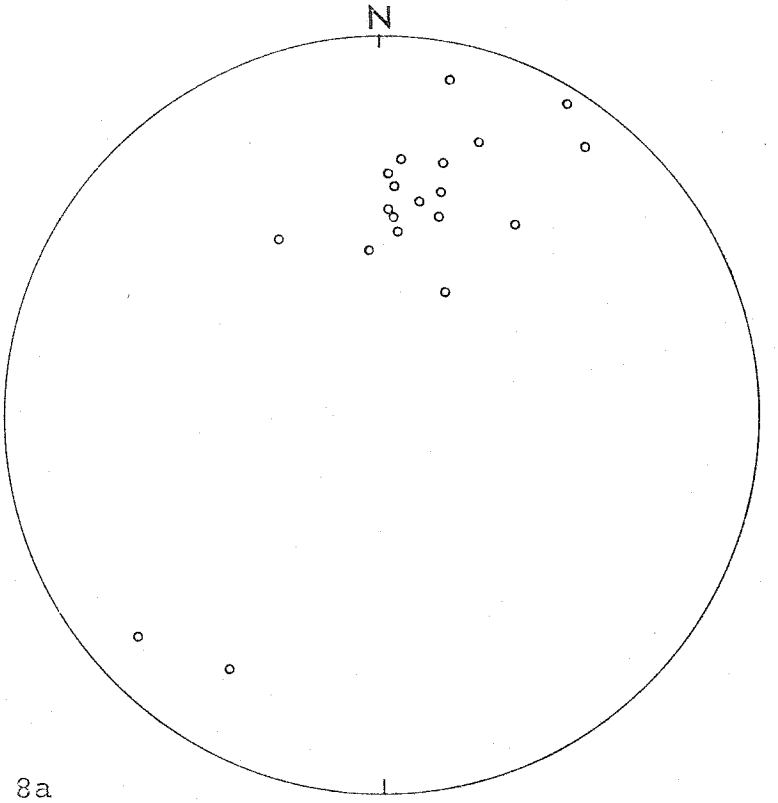

Figure 8a

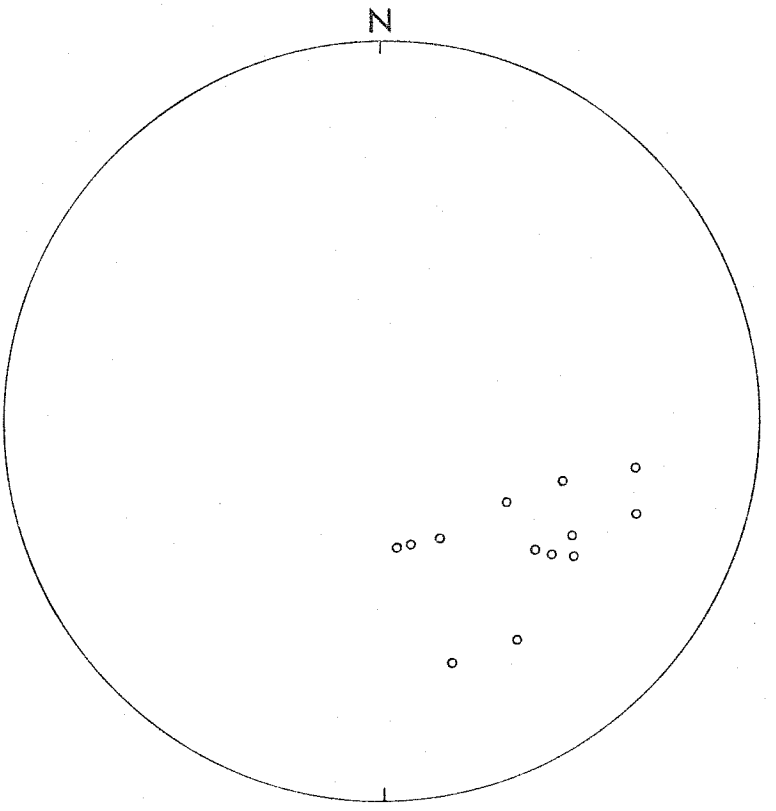

Figure 8b

the unconformity between the Silurian and Ordovician rocks. The style of folding varies greatly from isoclinal folds to gentle open folds. A few small chevron folds have also been observed. These DF_b folds are on the average more open than the DF_b folds near the crest of the Willoughby arch. DS_b ranges from a well developed schistosity, such as shown in Figure 6, to a well spaced slip cleavage to a poorly developed cleavage or absent. Figure 8b shows that DS_b surfaces here have much steeper dips than in the Lyndonville quadrangle. DS_b is folded by the later DF_d folds and possibly by the east-west trending DF_{b+1} folds; location JR-107 shows good examples of this. The pattern of DS_b may reflect dispersion due to this later deformation. Observations in the Hardwick quadrangle, due west of the Lyndonville quadrangle, also indicate that DF_b in the Silurian and Devonian rocks near the unconformity are more open and have more steeply dipping axial planes than DF_b folds along the Willoughby arch.

No metamorphic veins have been observed which are associated with the D_b event. This is important in the establishment of the structural sequence. In over 200 outcrops throughout northern Vermont, only one vein was observed which might be associated with D_b, and even this one is doubtful. The lack of vein formation does not mean that significant mineral growth did not occur during D_b. In rocks in which

Figure 9 Interfering DF_b and DF_{b+1} folds at JR-106, Barre quadrangle. Folded surface is DS_a. Fold axes are shown by tape "x"; DF_b axes are nearly horizontal and DF_{b+1} axes are nearly vertical in photograph. The interference produces basin and dome structures on DS_a.

DS_b is a well developed schistosity or slip cleavage, mica grains which grew with preferred orientation parallel to DS_b are commonly observed. However, this generation of mineral growth, DM_b, is apparently absent from large portions of the study area. In particular DM_b is not observed in most of the Ordovician and Silurian rocks and is lacking in the Silurian and Devonian rocks where DS_b is poorly developed or absent. No high-grade mineral growth (garnet grade or higher) of DM_b has been observed in the study area.

DF_{b+1} folds

In the Barre quadrangle (locations JR-106, JR-107, and JR-112 for instance) and in a few places in the Hardwick quadrangle (locations JR-16 and JR-93) a set of open folds with WNW trending axes was observed. These form well developed basin and dome interference structures with open DF_b folds on exposed DS_a surfaces at some locations such as JR-106, from which Figure 9 is taken. The axes of the east-west folds, DF_{b+1}, trend nearly vertically across the photograph and the trend of the DF_b folds is at 90° to these. It might be argued that the east-west folds represent locallized plastic flow in the rock in response to DF_b, but there is a remarkable consistency of trend of measured DF_{b+1} folds from the Barre quadrangle as shown in Figure 10; the variation in plunge is of course due to the interference of DF_b folds.

Figure 10

Stereonet plot of DF_{b+1} axes at locations along the Williamstown to Montpelier traverse.

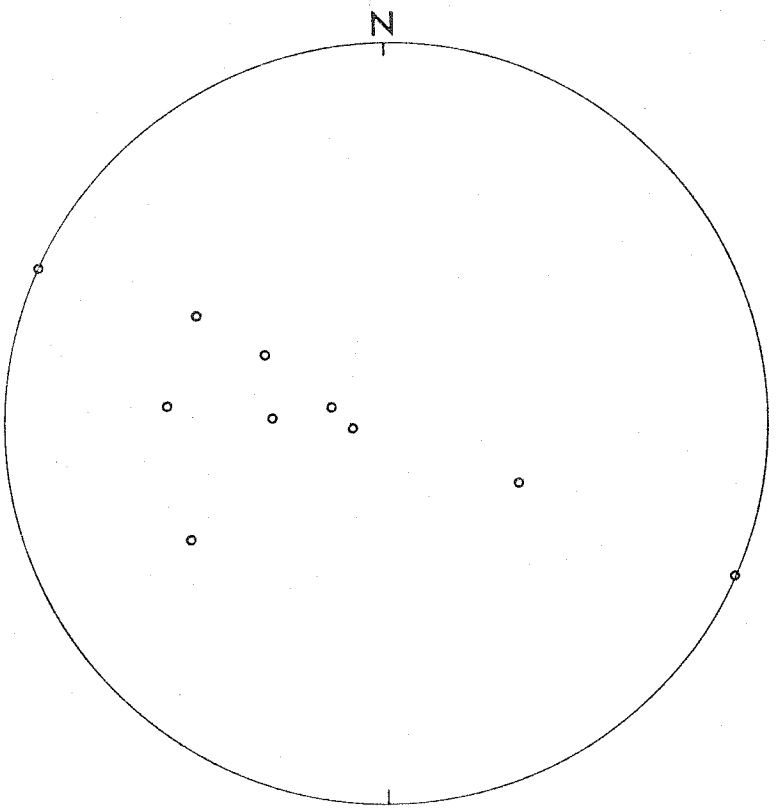

Figure 10

Furthermore, a crenulation lineation which is parallel to DF_{b+1} axes is present in many locations along the traverse in the Barre quadrangle. DF_{b+1} folds are therefore a distinct fold set.

A poorly developed spaced slip cleavage or fracture cleavage was observed to be axial planar to DF_{b+1} folds at location JR-16 in the Hardwick quadrangle. These DS_{b+1} surfaces have a WNW strike and dip steeply to the northeast. At this location it appeared as if DS_{b+1} and DF_{b+1} deformed DS_b although this relationship is not without some ambiguity. Such a demonstration of the apparent age relationships is fortunate, since graphical methods could not resolve the problem. However, this evidence is not conclusive and in any event it cannot be demonstrated that DF_b and DF_{b+1} must be significantly separated in time. One of the criteria for showing separations in time between two structural elements, fold sets for instance, is the presence of an intervening vein generation which is deformed by one element but which cross-cuts the other element. No such intervening vein generation was found for DF_b and DF_{b+1}.

DF_{b+1} have in every instance been observed to be gentle, open folds with wavelengths of only a meter or less. They are often difficult to recognize in many localities within their range of occurrence. DF_{b+1} folds have not been observed in the Silurian and Devonian rocks in the Lyndonville

quadrangle or throughout most of the area of exposed Ordovician and Cambrian rocks.

Event D_c

DS_b s-surfaces are deformed by a fourth generation of folds, DF_d. However, between the two deformational events, D_b and D_d, there was a significant period of mineral growth. This intervening event, D_c, produced non-preferentially oriented porphyroblasts of various minerals in the Silurian and Devonian rocks in much of the eastern part of the study area. This growth is particularly well developed in the Lyndonville and Memphremagog quadrangles in the vicinity of the larger intrusive bodies of the New Hampshire plutonic series. Associated with the DM_c mineral growth is a set of metamorphic veins which consist of minerals also found in the host rock, including those which form the porphyroblasts such as biotite, muscovite, and chlorite. Some of the minerals in these DV_c veins are not seen as porphyroblasts in the host rock; quartz, plagioclase and calcite are examples. However, DM_c growth in the host rock doesn't seem to have been limited to porphyroblast formation.

DV_c and DM_c formation do not seem to be related to any folding or formation of an s-surface. In some cases DM_c biotite porphyroblasts appear roughly oriented, but this is a mimetic texture brought about by the nucleation of biotite

on pre-existing ilmenite grains that had a preferred orientation parallel to DS_a. It must be stressed that all porphyroblasts found in the Silurian and Devonian rocks are not necessarily of this generation. In particular, garnet porphyroblasts which are DM_a in generation are found in several areas described in the next chapter. The assumption that all porphyroblastic growth is of the same generation will lead to misinterpretations of the metamorphic history. DV_c veins are further discussed later in this chapter and DM_c mineral growth is discussed in Chapter III.

The DV_c veins occupy a distinct position in the structural sequence. The veins crosscut D_b elements and also DF_{b+1} folds. DV_c veins are folded by DF_b folds. However, there are also some relatively rare minor vein generations which are in the same position between D_b and D_d in the sequence. The minor generation veins do not appear to be related to any significant mineral growth in adjacent host rock. Therefore, both the structural position and the relationship to host rock mineral growth are criteria for identifying DV_c veins.

DF_d folds

The fourth generation of folds, DF_d, occurs throughout the Silurian and Devonian rocks in the study area. These are gentle, open asymmetric folds which trend N to NNE and

generally plunge gently to the north or south. DF_d folds have been observed in a few places to have a poorly developed axial plane cleavage, although in general this planar feature, DS_d, is absent.

As with DF_{b+1} folds, DF_d folds are often difficult to recognize because of their openness and the intensity of the prior deformation. DF_d folds can be seen as warps of DS_b, as described for location JR-107. These relationships can only be observed if the outcrops where DF_b folds are developed are carefully examined. However, DF_d are most easily seen as folds of veins which are younger than and therefore cross-cut DF_b and DS_b such as the DV_c vein at JR-112. Another example of DF_d folds deforming a DV_c vein is shown in Figure 11, a photograph taken at location JR-173 in the Lyndonville quadrangle.

As DV_c veins are most abundant in the Lyndonville quadrangle, this relationship of DF_d folding DV_c is observed in many locations along the I91 traverse. Figure 12 shows a stereonet plot of DF_d axes observed along that traverse. DV_c veins are not so abundant in the Barre quadrangle, but where DS_b is well developed, DF_b folds can often be observed. Figure 13 shows DF_d axes from the traverse from Williamstown to Montpelier in the Barre quadrangle. The axes from both areas are essentially the same with N to NNE trends and shallow plunges generally to the north. The only possible

Figure 11 DV_c vein folded by DF_d at location JR-173, Lyndonville quadrangle. DV_c vein crosscuts DF_b folds of DV_a veins and host rock.

Figure 12

Stereonet plot of DF_d axes at locations along the I91 traverse.

Figure 13

Stereonet plot of DF_d axes at locations along the Williamstown to Montpelier traverse.

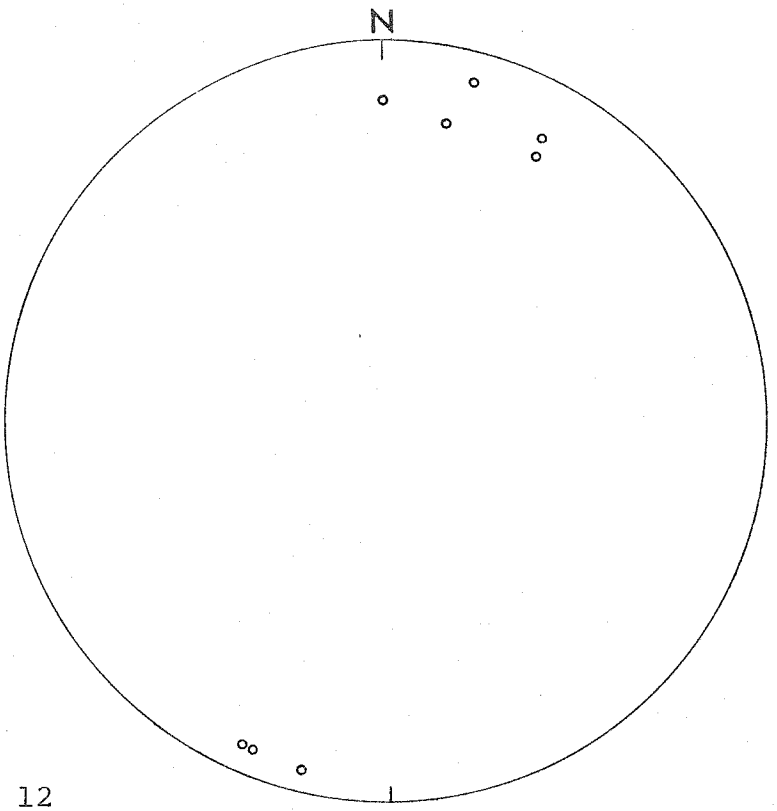

Figure 12

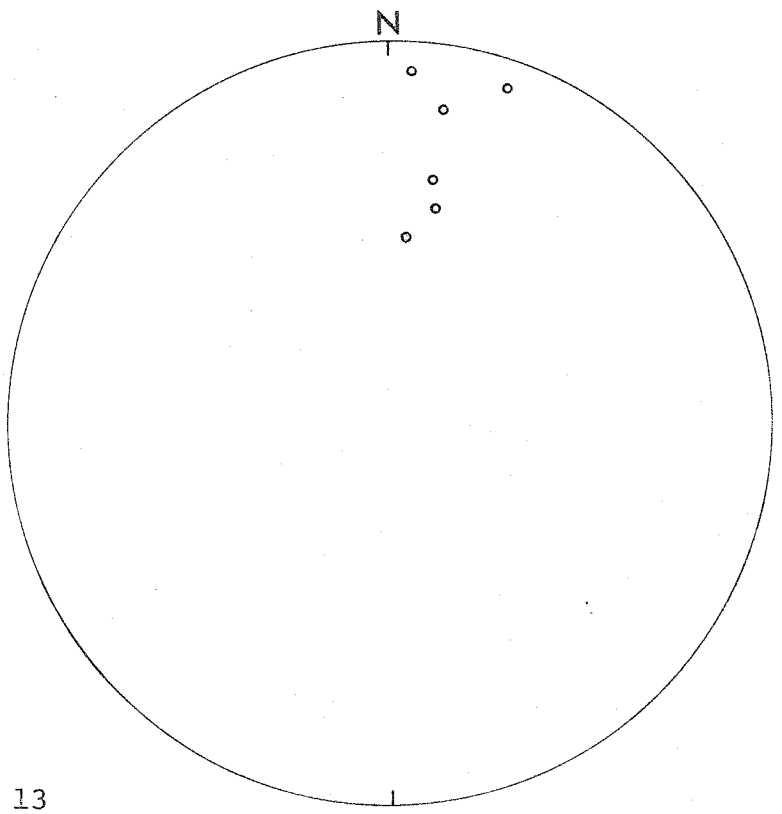

Figure 13

difference is that some DF_d folds in the Barre quadrangle have slightly steeper plunges. The small number of measurements reflects the difficulty in finding DF_d folds.

DS_d cleavage is observed at location JR-17 in the Hardwick quadrangle. It appears that DS_d, with an attitude of about 10° 85°E here, is equivalent to s_3 of Konig and Dennis (1964) which they observed in the same part of the Hardwick quadrangle. They also observed what they felt was an older surface, related to the formation of the Willoughby arch, which they called s_2. This would be equivalent to DS_b of this study. DS_{b+1} is also locally present in the Hardwick quadrangle, but Konig and Dennis seem to have not found it. DS_{b+1} is not a particularly prominent and well-developed s-surface. In any case, they postulate that s_3 in the Silurian and Devonian rocks is equivalent to the prominent "Green Mountain" slip cleavage found to the west in the pre-Silurian rocks and which in particular is well developed along the axis of the Green Mountain anticlinorium. None of the three youngest s-surfaces, DS_b, DS_{b+1}, or DS_d is well developed along the Green Mountain axis in the study area. As is discussed in the following section, the "Green Mountain" cleavage is equivalent to DS_a, or s_1 of Konig and Dennis (1964), found in the Silurian and Devonian rocks.

No metamorphic veins have been observed which are associated with DF_d folds. There are several other vein genera-

tions which occur in the structural sequence, but these do not appear to be related to events that produced folding. The minor veins are useful as structural markers if they formed between two folding events. A detailed analysis of minor vein generations is not essential to establishing the sequence of major elements. They may be useful in adding detail to the tectonic history of the area, but this aspect has not been pursued in this study. The detailed description of the various vein generations, both major and minor, is given in a later section.

F. Deformation in the Cambrian and Ordovician units

The deformational elements in the Silurian and Devonian rocks can be traced across the unconformity into the Ordovician and Cambrian rocks. This is most easily accomplished along the traverse on Highway I89 where the unconformity is well exposed south of Montpelier at location JR-108. There are also a number of good exposures of the rocks on either side of the unconformity. The elements can then be followed to the west along the Winooski River traverse through the Montpelier and Camels Hump quadrangles to Williston in the Burlington quadrangle.

A similar attempt was made to follow the structural elements in the Silurian and Devonian units from Hardwick to the west along Lamoille River traverse. The correlation

of elements directly across the unconformity can be made here and elsewhere in the Hardwick and Barre quadrangles, but significant problems are encountered in trying to follow the structural sequence through the Ordovician Missisquoi formation. A nearly complete structural sequence could rarely be found in the Missisquoi formation rocks along the Lamoille River traverse and in many cases it appeared that older features were obliterated by younger deformation. Large outcrops are scarce and, taken together, the problems were such that a correlation could be made but only with a great deal of ambiguity.

The correlation of the sequence into the units older than the Missisquoi formation along the Lamoille River traverse was accomplished by following the sequence north from the Winooski River traverse along the Worcester Mountains and Green Mountains. The correlation that results is essentially the same as that resulting from trying to follow the sequence along the Lamoille River traverse through the Missisquoi formation, but with less uncertainty. There remain problem outcrops in the Missisquoi formation along the northern traverse where it is difficult to identify with confidence the fold generations and s-surfaces.

There are some striking differences between the structural sequence in the Silurian and Devonian rocks and the structural sequence in the Cambrian and Ordovician rocks.

Two examples illustrate the structural elements typically observed in the Cambrian rocks of the Green Mountain area. The structural elements are identified in the descriptions of these locations, but the proof of the identifications remains for the later discussion of the Winooski River traverse.

JR-113 and JR-114

The first example is two adjacent outcrops, JR-113 and JR-114, near Ithiel Falls in the Hyde Park quadrangle. Exposed at these locations are interlayered pelitic schist and quartzite of the Hazens Notch formation. Bedding planes, OS_o, are well shown by the contrasting rock types. Parallel to OS_o is a well-developed schistosity. The schistosity does not appear to be related to any folds. Parallel to OS_o are also a number of small metamorphic veins which consist primarily of quartz. The veins are generally only a few centimeters wide and 0.5 meters or less in length. These may not be the original dimensions as the veins are highly deformed.

OS_o, the secondary bedding schistosity, and the small veins parallel to OS_o are folded by isoclinal folds with axial trends from E to ESE and generally moderate plunges to the east. The isoclinal folds are best shown by the folded quartzite layers, as illustrated in Figure 14. The small veins in the pelitic schist are highly deformed by isoclinal folds which are smaller than those shown in the figure. Parallel to the axial planes of the folds is an

Figure 14 Isoclinal OF_b folds refolded by DF_a at JR-113, Hyde Park quadrangle. Rocks are interlayered quartzite and pelitic schist of the Hazens Notch formation. A sketch of the elements is shown below.

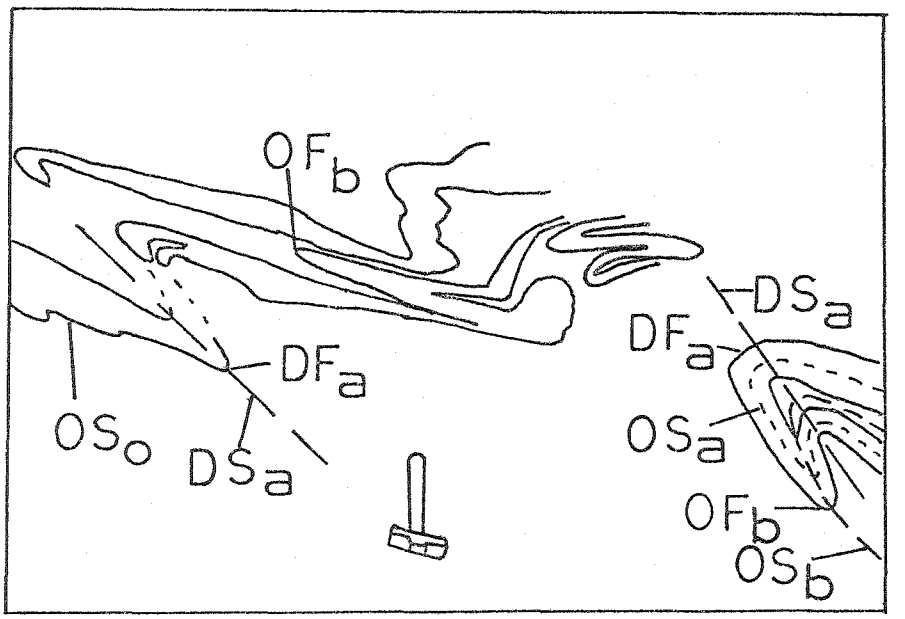

s-surface which ranges from a pervasive schistosity to a slip cleavage. Except at the noses of isoclinal folds, the secondary bedding schistosity and this axial plane schistosity are difficult to distinguish. Also parallel to the axial planes of the isoclinal folds is a second generation of metamorphic veins. These are generally larger than the older veins; they are typically 15 to 20 centimeters wide and several meters in exposed length.

All of the above structural elements are deformed by N to NNE trending asymmetric folds. Both north and south plunging folds of this generation are observed. The plunge angle is typically less than 20^{o} although steeper plunges are also seen. Parallel to the axial planes of the north trending folds are a slip cleavage and a set of metamorphic veins. The slip cleavage planes generally strike N to NNE and have steep dips either to the east or west. The veins parallel to the slip cleavage range in exposed size from 1.2 meters wide and at least 7 meters long to 10 centimeters wide and 1 meter long. The smaller veins are roughly lens-shaped in exposed section. The larger veins have indeterminate shapes as the terminations are not exposed. The north trending folds are also shown in Figure 14.

In places, the slip cleavage and the veins parallel to the slip cleavage appear to be gently warped by open folds which have axial trends to the north and near horizontal

plunges. No other structural elements were observed at these outcrops. There are three sets of secondary s-surfaces. Parallel to each s-surface is a set of metamorphic veins. The first fold set has east-west axial trends. The two younger fold sets have north-south trends. In the Silurian and Devonian rocks, there is only one set of metamorphic veins which is parallel to an s-surface set; these are the DV_a veins. The oldest folds in the Silurian and Devonian rocks trend generally north-south and there are no folds which seem to correspond to the east-west trending isoclinal folds.

The most prominent and oldest set of north-south trending folds has been identified as DF_a. The axial-plane slip cleavage is DS_a and the parallel set of veins is DV_a. The gentle folds of DS_a and DV_a are probably DF_b folds, although it is not obvious at these outcrops whether the folds are DF_b or DF_d. The D_a features and DF_b form an incomplete sequence which is compatible with the structural sequence in the Devonian and Silurian rocks; the other elements at JR-113 and JR-114 are not compatible with this sequence. The incompatible elements are pre-D_a. As D_a appears to be the oldest metamorphic event to have affected the Silurian and Devonian rocks, the pre-D_a elements also are pre-Silurian. The proof of this is the subject of considerable discussion in following pages.

The oldest metamorphic feature is the secondary bedding schistosity. This is designated OS_a. The veins which are parallel to OS_a are OV_a. OS_a, OV_a, and OS_o are deformed by east-west trending isoclinal folds which are called OF_b. The schistosity parallel to the axial planes of OF_b folds is OS_b. Also parallel to the axial planes of OF_b folds are metamorphic veins, OV_b.

The events which are demonstrated at these outcrops are O_a, O_b, D_a, and D_b. The elements of the three oldest events are typically well developed in the locations in the Green Mountain area. DF_b folds are always observed to be gentle and may be absent at some locations. DS_b is typically absent.

JR-163

The second example is location JR-163, an exposure of the Underhill formation along the Winooski River traverse in the Camels Hump quadrangle. Except for the lack of prominent OF_b folds, the structural sequence is unusually complete here. The oldest secondary foliation present is OS_a. There are also small, quartz-rich OV_a veins. OS_a and OV_a are highly deformed by small isoclinal folds similar to the small OF_b folds at JR-113 and JR-114. Parallel to the axial planes of the isoclinal folds is a well developed schistosity, OS_b. Because of the pervasive presence of these very

tight, small OF_b folds, there is really no clear distinction between OS_a and OS_b. The OV_a veins are the only good markers that allow OS_a to be distinguished from OS_b. The predominant schistosity at the outcrop must be referred to as OS_a/OS_b.

The OV_a veins are highly granulated. The veins are in general no more than a few centimeters wide and a meter long. The high degree of deformation may have substantially changed the veins from their original sizes. These veins are in contrast to the somewhat larger OV_b veins which are parallel to OS_a/OS_b but are not deformed by the small isoclinal OF_b folds. The OV_b veins are ungranulated and appear to preserve the primary coarse-grained texture. OV_b veins range in width from 3 to 15 centimeters and have lengths up to about 2 meters in exposed section.

The OV_b veins are folded by asymmetric folds which trend generally north-south and plunge gently in either direction. These folds have an associated axial plane slip cleavage. Parallel to the slip cleavage are coarse-grained veins that are similar in size to the OV_b veins. Both these veins and the OV_b veins are quartz-rich. The north-south trending folds appear to be DF_a folds. The associated slip cleavage is DS_a and the veins parallel to the slip cleavage are DV_a veins.

DS_a and DV_a veins are folded by open north-south trending asymmetric folds. These open folds are crosscut by a 2

centimeter wide and at least 8 meters long albite-rich vein. Mineral growth in the vein is related to biotite grade mineral growth in the host rock which overprints a garnet grade assemblage. A sample from this vein, JR-163-A, is discussed in the next chapter. The vein is warped by very gentle north-south trending folds which are out of phase and gentler than the open post-DV_a folds which the vein crosscuts. This youngest set of folds is very difficult to see through the older deformation except with the aid of the young vein.

Using the structural sequence observed in the Silurian and Devonian rocks, these younger structural elements at JR-163 can be identified. There are two north-south trending sets of folds that are younger than DF_a. These are DF_b and DF_d. The vein which formed between DF_b and DF_d is related to mineral growth in the host rock. This is therefore a DV_c vein. Elements of all of the major events which have affected the Silurian and Devonian rocks are present at this outcrop. There are three sets of north-south trending folds, DF_a, DF_b, and DF_d. Associated with the oldest of these fold sets is a set of veins, DV_a. Only one other set of veins associated with a major event is found in the Silurian and Devonian rocks, the DV_c set. The portion of the structural sequence at JR-163 that consists of the post-O_b elements matches exactly the sequence of elements in the Silurian and Devonian rocks. The only important element missing is

DS_b.

Winooski River traverse

The structural sequence will be described as seen along the Winooski River traverse from location JR-188, south of Montpelier, to JR-149, near Williston. The traverse has been divided into five segments of roughly equal length. The Winooski River traverse shares one location in common with the Williamstown to Montpelier traverse through the Silurian and Devonian rocks in the Barre quadrangle: location JR-108, an exposure of the unconformity between the Ordovician and Silurian rocks. The structural elements at JR-108 on either side of the unconformity will first be described. The descriptions of the structural sequence observed within each traverse segment then follow, starting with the easternmost segment.

JR-108

By describing the structural sequence on each side of the unconformity exposed at location JR-108 and then comparing the two sequences, the correspondence of elements can be established. The unconformity as exposed here is the contact between grey, graphitic phyllite of the Northfield formation and light green and grey, granular textured schist of the Moretown member of the Mississquoi formation. The Northfield rocks at JR-108 are all similar in lithologic

type, but the Moretown rocks range from the granular schist to fine-grained green and grey phyllite. Also there are layers of dark green, granular, fine-grained epidote-chlorite schist that may be metabasalts. The contact itself is not knife-sharp but rather is a zone, up to perhaps 30 cm wide, of mixing of Northfield phyllite and Moretown schist. The mixed zone seems to have resulted from shearing and the rocks within it have a fine-grained cataclastic texture. The contact is roughly parallel, although not in detail, to the schistosity seen in the rocks on either side immediately adjacent to the contact zone.

The Northfield formation is not always the Silurian unit present at the unconformity, as the Shaw Mountain formation is locally in contact with the Moretown member. For instance, to the north of JR-108 along the unconformity, Cady (1956) has mapped discontinuous exposures of the Shaw Mountain formation. The Shaw Mountain rocks include a locally present, distinctive quartz-pebble conglomerate that is found in contact with the Moretown rocks. Cady has demonstrated that either the Northfield or Shaw Mountain rocks can be along the unconformity. This is a consistent relationship over the entire length of the state, as shown by Doll and others (1961). The consistency over such large distances and the local presence of conglomerate were important pieces of evidence that led to the conclusion that

contact between Ordovician and Silurian rocks is an unconformity.

The contact and surrounding rocks are strongly deformed and therefore the predeformational nature of the contact surface cannot be established in this outcrop. There is evidence that there was no significant displacement along the contact after the formation of DV_a veins; a DV_a vein occurs in the shear zone and, although it is highly deformed, it has branches which extend into the Moretown schist and Northfield phyllite on either side. The deformation of the DV_a vein and the formation of the mixed contact zone appear to have accompanied DF_b and DS_b formation.

On the east side of the contact in the Northfield rocks, the structural sequence is essentially the same as that previously described for location JR-107, which is about .6 miles to the southeast of JR-108. There is an early schistosity, DS_a, and a parallel set of metamorphic veins, DV_a. Clearcut bedding surfaces are not always easy to find, but DS_a seems to be parallel to DS_o in some places and non-parallel elsewhere. No DF_a folds are observed. The portion of the outcrop which consists of Northfield rocks is small compared to the size of the very large DF_a folds seen at JR-107. DS_a and DV_a are strongly deformed by DF_b folds with NNE axial trends which plunge from 10° south to 30° north. When viewed in cross-section, looking to the north, DF_b

folds are asymmetric and are consistently left-handed in pattern. Parallel to the axial planes of DF_b folds is a generally well developed DS_b schistosity which strikes NNE and dips consistently to the northwest. The magnitude of the dip varies from 40^o to 70^o. DS_b schistosity and highly deformed DS_a and a DV_a vein from JR-108 are shown in Figure 6. Open, east-west trending folds, DF_{b+1}, are also present and there may be a very gentle warping of DS_b by north-south trending DF_d folds. All metamorphic veins are parallel to DS_a and are deformed by DS_b. Although the deformation is fairly intense, the veins are all coarse-grained and appear to be typical DV_a veins.

To summarize the sequence on the east side of the contact, the exposed Northfield rocks have only one generation of veins, DV_a, two generations of deformational s-surfaces, DS_a and DS_b, one set of prominent folds, DF_b, and two sets of open, gentle folds, DF_{b+1} and possibly DF_d. DF_b folds are left-handed in cross-sectional pattern when the oberver is looking north, with NNE axial trends and shallow to moderate plunges. DS_b surfaces strike NNE and have consistent dips to the northwest.

The structural sequence in the Moretown rocks is not identical to that of the Northfield phyllite. There are not less than four generations of veins and three deformational s-surfaces. The correspondence between the two sequences must

be established by finding the elements which are common to both.

The oldest observed metamorphic s-surface in the Moretown rocks is a partly obliterated schistosity which is generally parallel to the compositional layering. Parallel to this oldest schistosity are highly deformed metamorphic veins with fine-grained, granular textures. Apparently crosscutting the schistosity are two sets of small lens-shaped en echelon veins. That there are two sets is established by what appear to be cross-cutting relationships of one vein set upon the other. Veins of the two sets are not always seen together. The three granular-textured vein generations and the old schistosity are cross-cut by a second schistosity; this s-surface is best developed in the most mica-rich layers and in some of the more massive quartz-rich rocks it is apparently not developed. In the least competent layers the second schistosity is in some places observed to be essentially parallel to the older schistosity. Figure 15 is a photograph of the Moretown showing the early schistosity, labeled OS_a/OS_b, a granulated vein, labeled OV_b, parallel to this s-surface, and the second schistosity, DS_a. Also shown are one of the sets of small, granulated, lens-shaped veins, labeled as OV_{b+2}. The identification of the minor vein generations is discussed in a later section. The second schistosity is not developed in the massive layer in

Figure 15 Structural elements in Moretown formation at JR-108, Barre quadrangle. Elements present are OS_a/OS_b, OV_b, OV_{b+2}, and DS_a. These are shown in sketch below.

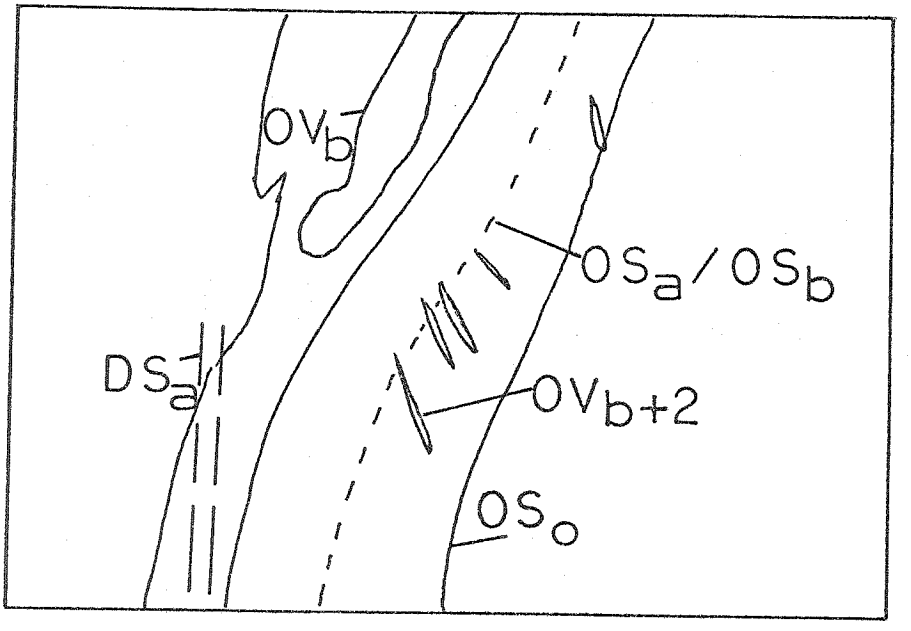

which the en echelon veins are present, but is well developed in the layer to the left and here it is non-parallel to the early schistosity.

Parallel to the second metamorphic schistosity are coarse-grained veins which do not show the granular texture of the other vein generations. These appear to be identical to the DV_a vein which is in the contact zone. The veins and the parallel s-surface are deformed by folds with similar attitudes of axes and axial planes and the same sense as shown by DF_b folds in the Northfield. Parallel to the axial planes of these folds is a locally developed slip cleavage which cross-cuts the second schistosity. These folds are left-handed when viewed looking north with NNE axial trends and moderate plunges to the north. The axial planes strike NNE and have consistent steep dips to the northwest. No folds with east-west axial trends are observed and no other north-south folds can be demonstrated.

There is a possiblity of other vein generations being present. There are ungranulated coarse-grained veins which are deformed by the folds which fold the second schistosity and which may be separate in generation from the veins parallel to the second schistosity. These veins, however, are not in a cross-cutting relationship with the other ungranulated veins and are developed where the second schistosity is absent. These are probably the same generation as the other

ungranulated veins. Another possible vein generation is a highly deformed set of veins which appear to be older than the granulated veins parallel to the early schistosity. These are smeared out parallel to the first schistosity and seem more deformed than the other granulated veins. This deformation may involve small scale isoclinal folding of this possible early vein generation, with the axial planes of the isoclinal folds being parallel to the first schistosity. The overprint by later elements is such that these are only suggested relationships.

Several of the described elements in the Moretown are closely similar to those in the Northfield. The coarse-grained, ungranulated veins parallel to the second schistosity in the Moretown appear to be DV_a veins parallel to DS_a. That they are DV_a veins is further supported by the vein present in the contact zone. The apparent DV_a veins and DS_a schistosity are folded by folds very similar to DF_b in the Northfield. This similarity includes axial and axial plane attitudes and fold pattern. The axial plane slip cleavage would then be equivalent to the axial plane DS_b schistosity in the Northfield. The similarity of these individual elements to elements in the Northfield and the similarity of the sequence that they define to the sequence in the Northfield strongly suggests the above correlations.

The two structural sequences are compared in Table 2.

Table 2 Comparison of the structural elements in the Moretown and Northfield rocks exposed at JR-108

Moretown formation	Northfield formation
OV_a?? - possible smeared out, isoclinally folded granulated veins	
OF_b?? - possible small isoclinal folds of OV_a?	
OS_b - oldest demonstrated schistosity	(not present)
OV_b - fine-grained, granulated veins parallel to OS_b	
OV_{b+1}, OV_{b+2} - minor generations. Veins are fine-grained and granulated	
DS_a - second schistosity	DS_a - oldest prominent schistosity
DV_a - coarse-grained, ungranulated veins parallel to DS_a	DV_a - coarse-grained, ungranulated veins parallel to DS_a
DF_b - north-south trending folds that deform DS_a and DV_a	DF_b - north-south trending folds that deform DS_a and DV_a
DS_b - slip cleavage parallel to the axial planes of DF_b folds	DS_b - schistosity parallel to the axial planes of DF_b folds
	DF_{b+1} - open east-west trending folds of DS_a
	DF_d - very gentle north-south trending warps of DS_b

The possible smeared out veins in the Moretown are shown as OV_a (??). The possible isoclinal folds of these veins are OF_b (??). There are three other generations of highly granulated veins in the Moretown rocks that do not have corresponding veins in the Northfield. The sequence of elements of D_a and D_b in both the Northfield and Moretown rocks are in exact agreement. The only elements found in the Northfield that are not in the Moretown are the very gentle DF_{b+1} and DF_d folds. If the later elements in the Moretown are equivalent to the sequence in the Northfield, then the oldest schistosity and the granulated veins are all pre-D_a and necessarily pre-Northfield. There are no pre-D_a features in the Silurian and Devonian rocks that correspond to this well-developed metamorphic schistosity and the three or four vein generations. This relationship establishes the contact as a surface intermediate in age between two structural sequences; one sequence is pre-Northfield and the other is post-Northfield.

One thing that does vary within this sequence when comparing the Northfield and the Moretown at JR-108 is the character and/or intensity of the elements. In particular, DF_b folds are much less intense in the Moretown than in the Northfield. Some DF_b folds in the Northfield are nearly isoclinal, but DF_b folds in the Moretown are much more open (although not nearly as open as DF_d folds in the Northfield).

DS_b is a pervasive schistosity in most of this exposure of the Northfield, but DS_b is only a localized slip cleavage in the Moretown. Also, DS_a in the Moretown is not so all-pervasive as it is in the younger rocks. This is not surprising, however, as the Moretown in general consists of more competent rock types compared to the graphitic phyllite of the Northfield.

A feature of the oldest three or four vein generations in the Moretown is their high degree of granulation. Undeformed or only moderately deformed veins are never observed to be fine-grained and granular in texture. It appears very likely that the granulation is a deformational feature rather than a primary feature of vein growth. Granulated veins are common in large areas of the pre-Silurian rocks, but fine-grained, extensively granulated veins were not observed in the Silurian and Devonian rocks, even given veins in rock types similar to some of the rock types in which granulated veins in the pre-Silurian occur. Highly granulated veins are a feature of pre-Silurian rocks, and this helps to further support the correlation of elements across the unconformity.

Within the Moretown are small epidote pods which are generally parallel to OS_a/OS_b. The pods are deformed by DS_a and the minerals within the pod, particularly epidote, are highly granulated. There are masses of micron-sized

grains of epidote and within these masses are larger grains of extensively altered actinolite and also plagioclase, some of which appears to be zoned and have exsolution lamellae. Within the granulated OV_b veins are grains of optically zoned albite with apparent exsolution lamellae of more calcic plagioclase (found with EBS pictures on the microprobe). These grains are surrounded by much finer-grained, granulated quartz. The epidote and actinolite in the pods and the plagioclase in the pods and OV_b veins appear to be pre-Northfield.

The presence of deformational and metamorphic mineral growth features in the Moretown rocks that are not present in the Northfield at JR-108, or anywhere else in the Silurian and Devonian rocks, indicates that the Moretown rocks were subjected to significant metamorphism before the deposition of the Silurian and Devonian strata. The estimated maximum metamorphic grade of Ordovician mineral growth in Moretown is biotite to low garnet grade. If the unconformity is not a tectonic contact, then considerable uplift and erosion of the Moretown must have preceded the beginning of deposition of the Northfield. The presence of probable pre-Silurian metamorphic elements in the Ordovician rocks adjacent to the unconformity is not restricted to this location but is observed elsewhere in the Barre and Hardwick quadrangles.

Segment 1

The first segment extends from location JR-108, where the unconformity between the Silurian and Ordovician strata is exposed, to location JR-124, just east of the town of Middlesex. The segment is largely within the Moretown member of the Missisquoi formation, of Ordovician age. A principal rock type of the Moretown is the "pinstripe granulite," a granular, fine-grained quartz-albite schist with thin, chlorite- and muscovite-rich layers which are spaced a few millimeters or more apart and thereby produce the "pinstriping." Also exposed along this segment are layers of granular quartzite, chlorite-epidote greenstones, chlorite schist, and graphitic, sulfide-rich phyllite. To a great extent, the style and intensity of the various structural elements depend upon the rock type in which they occur.

Most of the pre-Silurian elements present along this traverse segment have been described for location JR-108. In general it is difficult to distinguish OS_a from OS_b and OV_a from OV_b, due in part to the overprint of event D_a. The pinstripe foliation offers a good example. The pinstripe foliation is a pre-Silurian feature as shown by the fact that it is folded by DF_a and cross-cut by DS_a and DV_a. At some locations, such as JR-115, two pinstripe foliations can be observed. It appears that there is an older pinstripe foliation parallel to OS_o and a younger set, not as well devel-

oped at JR-115, which cross-cuts the other set at a small angle. Both sets are folded by DF_a and each has an associated set of granulated veins. There seem to be two pinstripe foliations at location JR-124 also, but the set non-parallel to bedding planes is most prominent and this younger pinstripe schistosity appears to be related to isoclinal folds, probably OF_b folds. At some locations, granulated veins which appear to be parallel to OS_o are cut by a single pinstripe foliation; elsewhere the dominant pinstripe foliation is parallel to OS_o and a set of granulated veins.

The oldest of the pinstripe surfaces, parallel to OS_o, appears to be OS_a with the associated vein set, OV_a. The younger set is seen in some instances to be non-parallel to OS_o and probably related to fairly tight to isoclinal folds at JR-124, JR-115, and possibly JR-108. This second set is therefore probably OS_b which is associated with OF_b folds and OV_b veins. Most OV_b veins are highly granulated, but at one location, JR-199, OV_b veins were observed to be only partly granulated. Which of the two pinstripe foliations is predominent seems to vary from place to place. Also present are several generations of granulated veins that cross-cut OV_b and OV_a. These are treated as minor generations and discussed later.

It must be stressed that these relationships between the pre-Silurian elements are not really straightforward in

most exposures. In general only one pinstripe is apparent and this must be called OS_a/OS_b. It is often difficult to tell OV_a and OV_b apart. OF_b folds are very rarely observed and those found were somewhat obscured by later deformation.

The elements of event D_a--DF_a, DS_a, and DV_a--are very important as they define the boundary between the pre-Silurian and post-Silurian structural sequences. DF_a folds and associated DS_a are present at every location along this segment. Within mica-rich schists and phyllites near the unconformity, DS_a is the dominant schistosity. It can be either parallel to the earlier OS_a/OS_b schistosity or it can crosscut OS_a/OS_b. The pervasiveness of DS_a generally decreases to the west, although there can be significant variation in the nature of DS_a even within a given rock type at a single outcrop. The nature of DS_a also typically depends upon the rock type. In the less competent chlorite schist and particularly in the graphitic phyllite, DS_a is either a well developed schistosity or a strong slip cleavage, even at the western end of the segment. In the granular quartz-albite schist and quartzite, DS_a is usually observed to be a slip cleavage but may be absent. Adjacent layers of different competencies show abrupt changes in the character of DS_a. At locations such as JR-199, DS_a is parallel to the axial planes of asymmetric tight DF_a folds. DS_a is parallel to the long limbs of these folds, and therefore parallel to

OS_a/OS_b, but DS_a is non-parallel to the short limbs.

DF_a folds range from tight, asymmetric and rarely isoclinal folds, most common near the unconformity, to much more open, asymmetric folds. The tighter forms are generally associated with the more pervasive DS_a seen in the less competent mica-rich rocks. In the "pinstripe granulite," DF_a small folds are often in discrete harmonic kink bands with rounded hinges, such as schematically shown in Figure 16, drawn from field notes taken at location JR-118. In this case DS_a is present as a slip cleavage only within the kink bands. These small folds are on the limbs of folds with wavelengths of a meter or more and small folds of opposing senses can be seen on opposite limbs, still maintaining essentially parallel slip cleavage planes. DF_a folds are observed to have a hierarchy of fold size orders, ranging from a set of folds with wavelengths of a few centimeters to a set of folds with wavelengths comparable to the size of the outcrop.

Figure 17 shows the attitudes of DF_a fold axes and poles to DS_a along this segment. DF_a fold axes trend consistently NNE with a great range in plunges both north and south; the steeper plunges are generally, but not strictly, associated with the tighter folds. This dispersion of plunge seems to reflect the noncylindrical character of the folding as there is no later set of folds which could

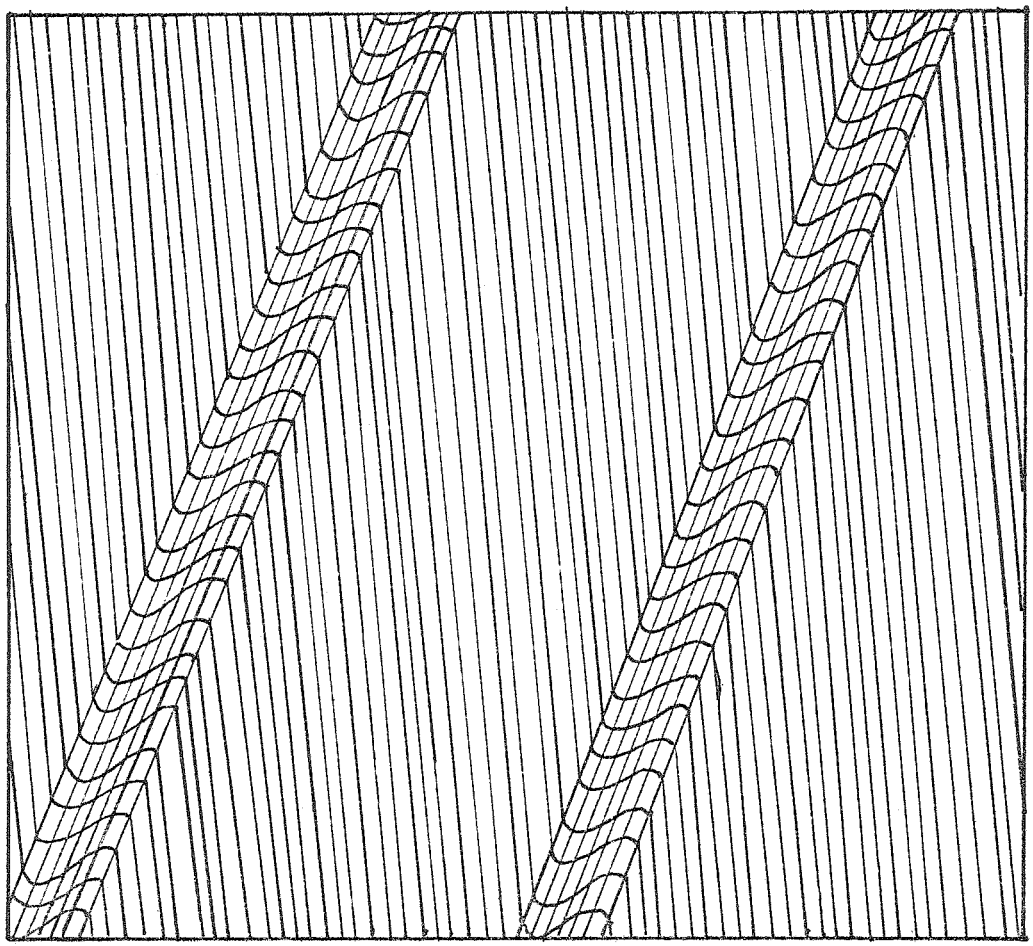

Figure 16 Sketch of harmonic DF_a folds forming kink bands with rounded hinges at JR-118, Montpelier quadrangle. Folds are in "pinstripe granulite" of the Moretown member. DS_a slip cleavage is only developed within kink bands. Attitudes are: DF_a, 18° trend, 37° plunge; DS_a, 23° strike, 78° NW dip. Sketch approximately to scale.

Figure 17a

Stereonet plot of DF_a axes at locations along the first segment of the Winooski River traverse.

Figure 17b

Stereonet plot of poles to DS_a and DV_a at locations along the first segment of the Winooski River traverse.

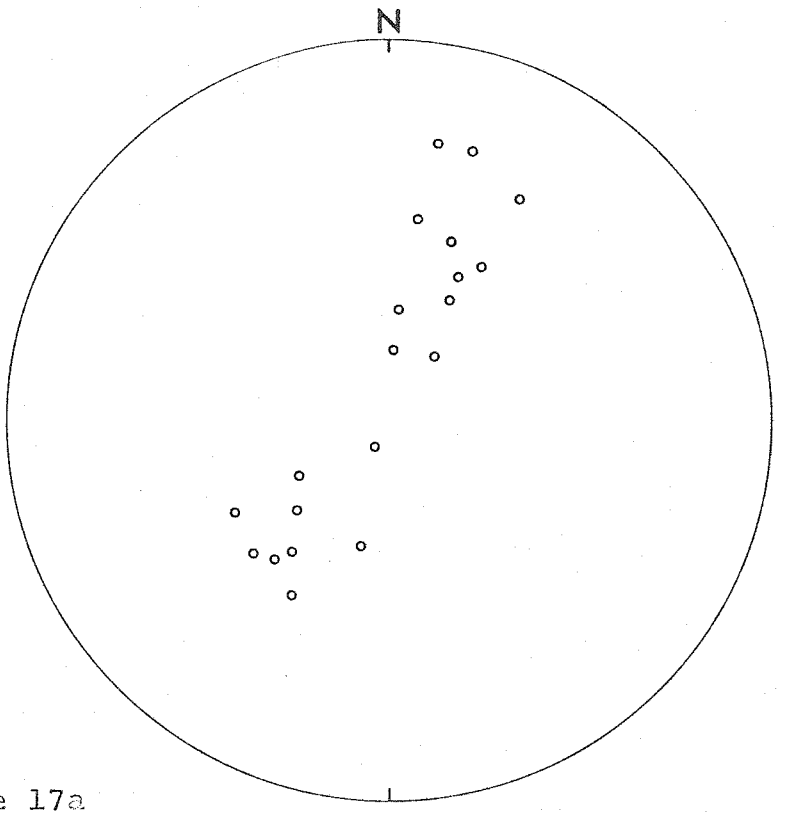

Figure 17a

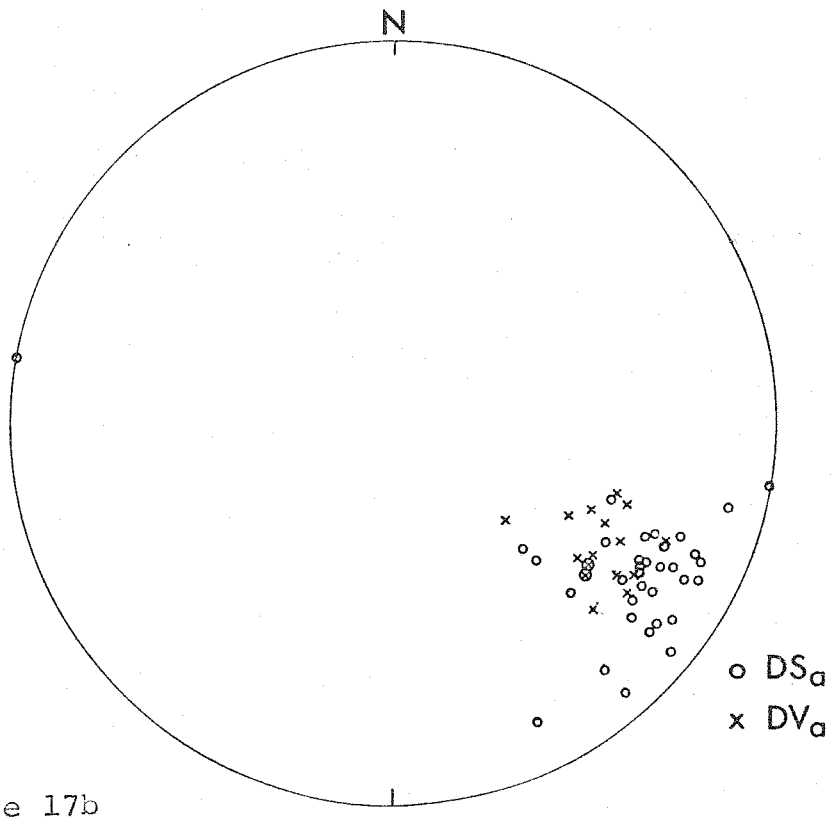

Figure 17b

Figure 17c

Stereonet plot of DF_a axes at location JR-116.

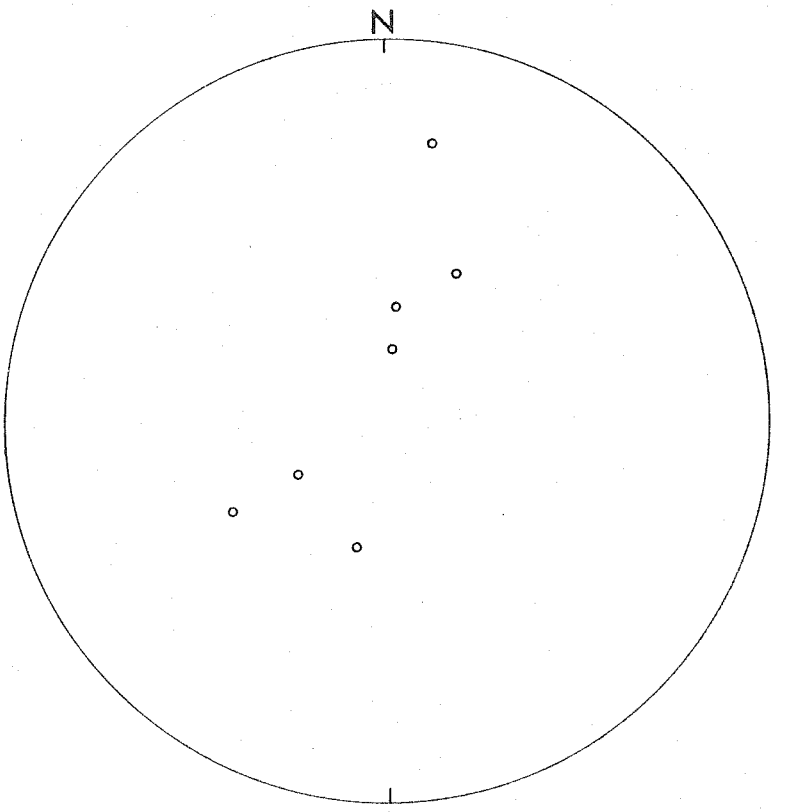

Figure 17c

be responsible (a refold set of tight folds with axes close to 90° to DF_a axes is needed to produce this dispersion if DF_a folding is statistically cylindrical over the domain in which the dispersion is seen). Strong dispersion of plunges is seen within single outcrops, such as shown in Figure 17c for location JR-116. The only east-west trending folds seen at JR-116 are very gentle DF_{b+1} folds which are clearly not responsible for the dispersion. In addition, JR-116 is the only location along this segment in which DF_{b+1} folds were observed.

DS_a surfaces have consistent NNE strikes with steep dips to the northwest. Also shown in Figure 17b are poles to DV_a veins which have strikes similar to DS_a but in general their dips are less steep. In fact, DV_a veins are not always strictly parallel to DS_a and are seen in some places to cut DS_a at small angles. The steeper DS_a surfaces are mostly found on the long limbs of DF_a folds where DS_a is parallel to OS_a/OS_b. The orientation of DS_a on these long limbs may be affected by the anisotropy produced by OS_a/OS_b and may not be in the orientation that they would have assumed in an isotropic medium given the same stress field. DV_a veins, and also OV_b veins, are shown to have formed perhaps somewhat later than the associated s-surface; the evidence is based upon the composition of vein minerals compared to host minerals of the same generation and is discussed in

Chapter III. DV_a veins are seen to be most often non-parallel to DS_a where DS_a is parallel to OS_a/OS_b. An explanation may be that the earlier formed DS_a is affected by the pre-existing planar anisotropy while the later formed veins are not and only reflect the stress field as if the anisotropy did not exist.

Even with the complications of noncylindrical folding, anisotropy of the rock, and extreme differences in rock types, the attitudes of DS_a surfaces show relatively little dispersion. The dispersion of DF_a and DS_a that is observed can be explained without calling upon any later refold events. Field observations show that only DF_b folds have produced any significant refolding.

DF_b folds along this segment are very open, asymmetric flexures of DS_a and DV_a which tend to die out in intensity towards the west. Near Middlesex, DF_b folds are barely discernible flexures of DS_a. The strongest DF_b folds are found near the unconformity, location JR-108 for instance. Figure 18a shows the attitudes of DF_b folds in this area. DF_b axes have N to NNE trends and plunges which range from shallow to steep both north and south. The pattern shown in Figure 18a is very similar to the pattern of DF_b axes in the Barre quadrangle shown in Figure 8a.

DS_b slip cleavage parallel to the axial planes of DF_b folds is developed at only two outcrops along this segment:

Figure 18a

Stereonet plot of DF_b axes at locations along the first segment of the Winooski River traverse.

Figure 18b

Stereonet plot of poles to DS_b at locations along the first segment of the Winooski River traverse.

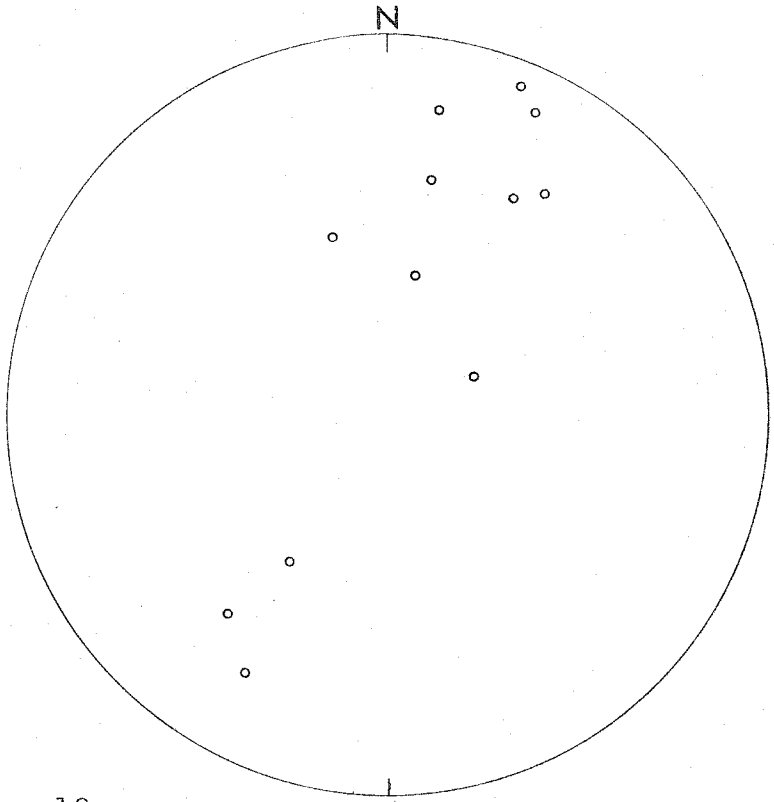

Figure 18a

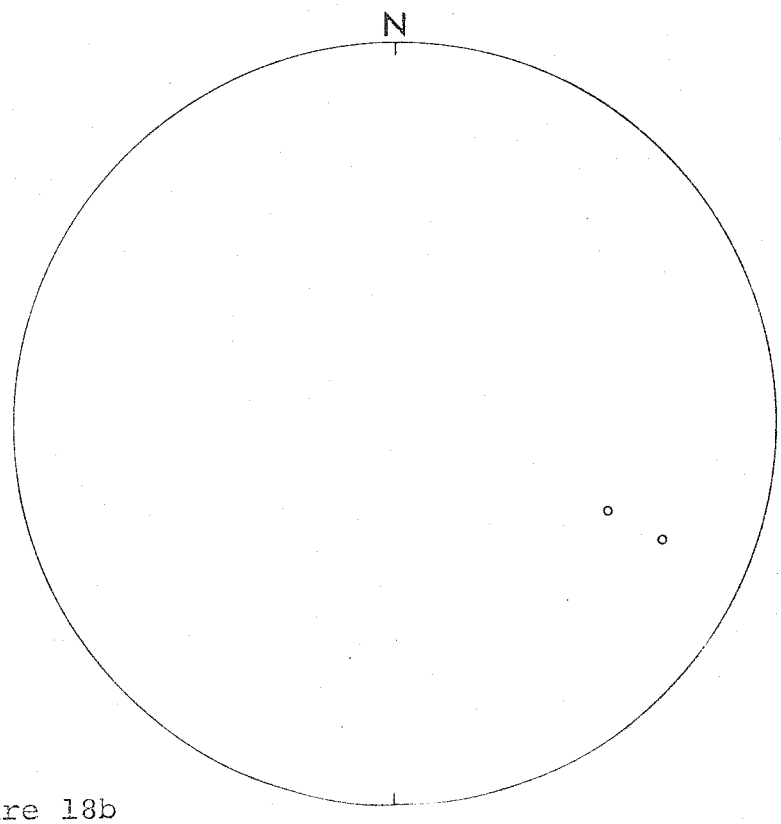

Figure 18b

JR-108, at the unconformity, and JR-120. At these two locations DS_b has an orientation similar to DS_b in the Northfield formation on the east side of the unconformity. Figure 18b shows the poles to measured DS_b. The change in the character of DS_b across the unconformity is dramatic and can only be explained by the sudden change in rock type.

No DV_c veins were observed along the segment and neither were any DF_d folds. As the marker surfaces for DF_d folds, DS_b and DV_c, are poorly developed or absent, DF_d folds may be present but not observed. In any event, DF_d folds cannot be prominent features, because the few occurrences of DS_b show no folding by DF_d. The only other elements observed are minor vein generations which formed between D_a and D_b.

Segment 2

The second traverse segment extends from JR-130 and JR-201 near Middlesex to JR-139, just east of Waterbury within the Montpelier quadrangle. All of the locations are exposures of the Stowe formation, Ordovician in age, which consists largely of relatively incompetent muscovite-chlorite schist and graphitic schist interbedded with more competent chlorite-epidote and actinolite-chlorite-epidote greenstone. The contrast of interlayered greenstone and schist produces sharp contrasts in the character of the deformational elements.

The pre-Silurian elements found along the first segment are also observed here. One difference is that both O_b deformation and D_a deformation were very intense in the incompetent schist so that the prior elements were strongly obscured in most places. Typically observed is what appears to be a single pre-Silurian schistosity and parallel to this are granulated to partly granulated veins. These veins range in size up to 15 centimeters wide and 2 to 6 meters long. Within the same host rock are small smeared-out quartz "stringers" and pods that typically are a centimeter or two wide and perhaps a few centimeters long, although some are larger. These appear to be granulated fragments of veins which were deformed before DF_a. The larger granulated veins do not reflect this deformation. It is probable that the older vein fragments are OV_a and that the larger, younger granulated veins are OV_b. The intense pre-D_a deformation appears to be the result of the formation of a pervasive transposition schistosity, OS_b, which has destroyed most of the evidence of OS_a. Demonstrable OF_b folds are not found except as tiny isoclinal folds of the OV_a veins, and even these are rare. Similar relationships are found in the Stowe to the north in the Worcester Mountains, for instance at location JR-125 and JR-129 on the west slope of Densmore Mountain, four miles to the north of the traverse segment. Small OF_b folds, while not completely straightforward, can

be demonstrated here as can the presence of two generations of granulated veins parallel to OS_a/OS_b. Both of these generations are clearly deformed by DF_a and the oldest generation is also deformed by O_b elements.

If compared in similar rock types, DF_a folds found at locations on this segment differ very little in character from DF_a folds observed on the first segment. DF_a axial trends are N to NNE with essentially the entire range of possible plunges north and south as shown in Figure 19a. An extreme range in plunges can be seen in a single outcrop such as shown in Figure 19b from location JR-131. This is a further indication of the noncylindrical nature of DF_b folds.

DS_a is present at all locations and is typically observed to be a strong slip cleavage. In the less competent layers, DS_a is parallel to the long limbs of asymmetric DF_a folds and therefore parallel to OS_a/OS_b. The abundance of mica-rich rock types results in DS_a being coincident with OS_a/OS_b in a higher percentage of the exposed rock than observed to the east. Within the massive greenstone layers, DS_a is typically a weak slip cleavage or absent so that strong contrasts in the nature of DS_a are seen at many locations.

DS_a surfaces have consistent N to NNE strikes with steep dips both east and west, as shown in Figure 19c. DV_a

Figure 19a

Stereonet plot of DF_a axes from locations along the second segment of the Winooski River traverse.

Figure 19b

Stereonet plot of DF_a axes from location JR-131.

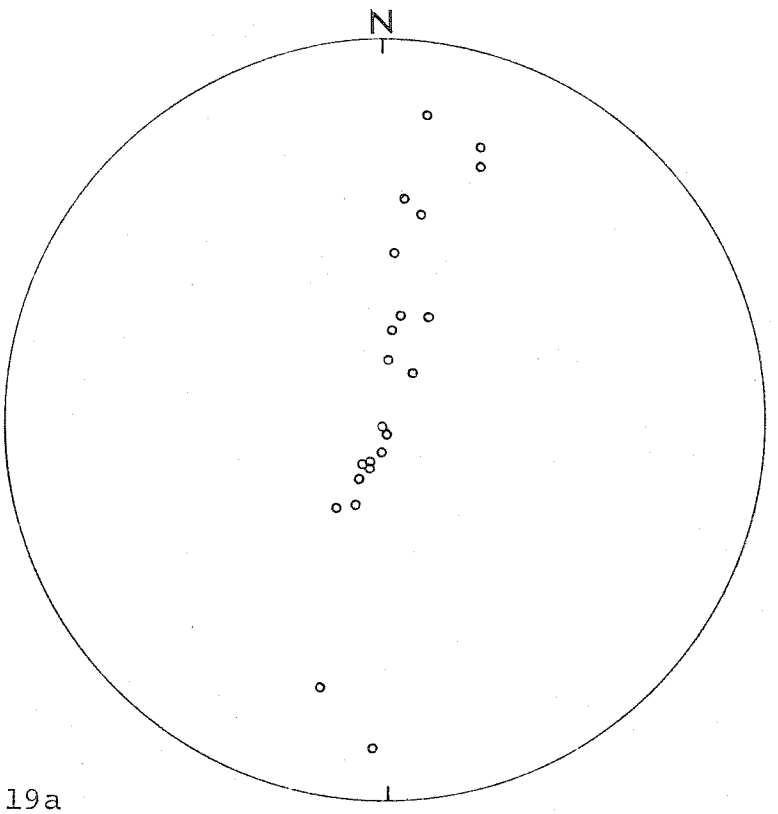

Figure 19a

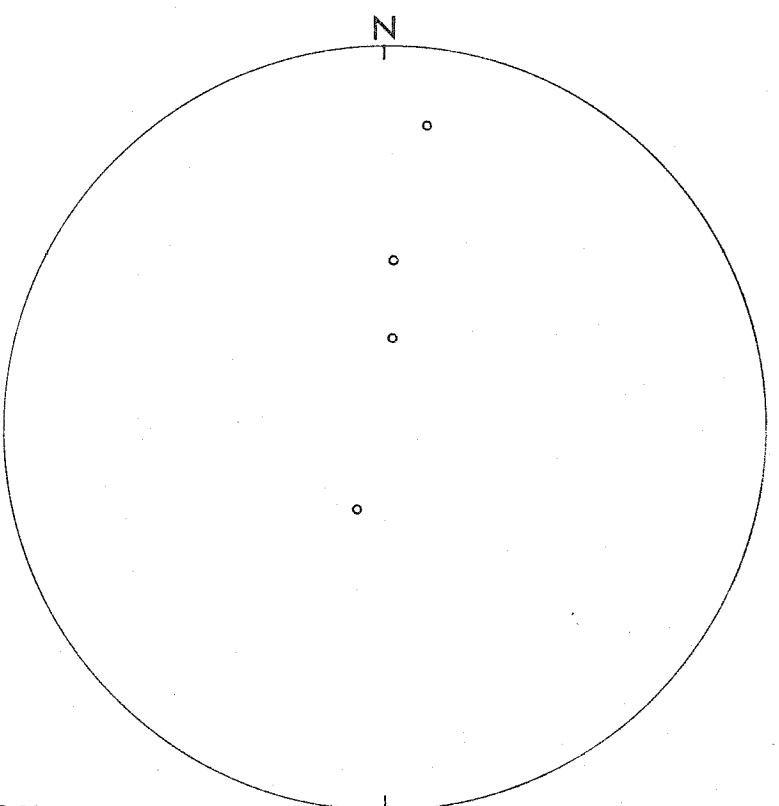

Figure 19b

Figure 19c

Stereonet plot of poles to DS_a at locations along the second segment of the Winooski River traverse.

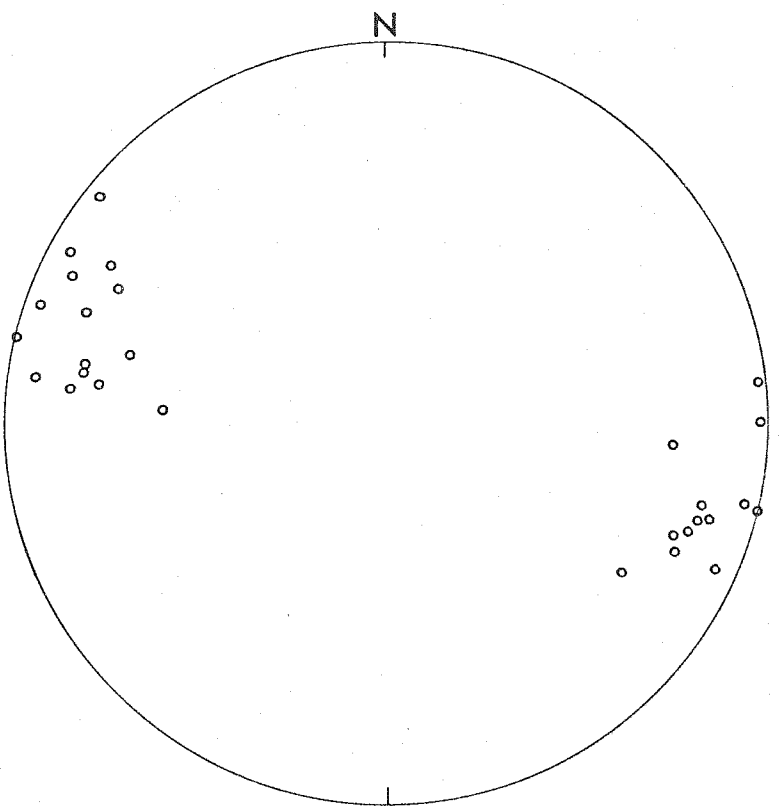

Figure 19c

veins are commonly observed and are generally parallel to DS_a, although DV_a veins may be at a small angle to DS_a. This is observed in situations similar to those described for the first segment where DS_a is parallel to OS_a/OS_b and DV_a veins are crosscutting at a small angle. DV_a veins are uniformly ungranulated and in general are undeformed or only slightly deformed by DF_b.

DF_b folds with wavelengths greater than a few feet are rarely observed. In the typical Stowe schist, DF_a folds have axial planes which are parallel to the long limbs and non-parallel to the short limbs. The amplitude, wavelength and style of small DF_a folds seems to depend upon the specific makeup of the rock. The smallest, tight folds with the most intense transposition schistosity are found in the least competent sulfide-rich graphitic schist. Schist which has a higher percentage of non-micaceous minerals may have DS_a slip cleavage which is not parallel to either limb of DF_a folds.

There seems to be very little dispersion of the trends of DF_a folds. The dispersion of plunges can be accounted for with noncylindrical folding, typical of DF_a throughout the study area. DS_a shows very little dispersion and a refold event is not demonstrated by the pattern of DS_a poles in Figure 19c. In fact, DF_b folds are extremely gentle flexures to essentially absent except at location JR-139,

which is at the western end of the segment.

DF_b folds observed are very open asymmetric folds with axes that trend NNE and plunge 30^o or less to the north and south. At JR-139, DF_b folds are much tighter and have a fairly well developed DS_b slip cleavage that cuts DS_a slip cleavage. DS_b surfaces strike NNE with steep dips consistently to the northwest. DS_b is not developed at other locations but the axial planes of DF_b folds have similar orientations to that shown by DS_b at JR-139. JR-139 is an important outcrop because the relationships between the elements of D_a and D_b are well demonstrated here. Except for minor vein generations, other post-Silurian structural elements are not observed.

Segment 3

The third traverse segment is from location JR-6, near Waterbury, to location JR-163 and is within the Camels Hump quadrangle. The exposed units are the Ottauquechee, Hazens Notch and Underhill formations, all of Cambrian age. The western end of the segment is just east of the main axis of the Green Mountain anticlinorium as mapped by Christman and Secor (1961) so that these locations are all on the east limb of the anticlinorium. There is some variation in rock type, from the fine-grained graphitic and non-graphitic mica-rich schist typical of the Ottauquechee to medium-grained

pelitic schist with plagioclase and garnet porphyroblasts towards the west in the Underhill. Layers of quartzite occur in the Underhill and Hazens Notch and serve to show prominent OF_b folds. The contrast in competencies of the rock types observed in single outcrops is not as strong as observed at locations along the previous traverse segment.

This segment is important because there is a significant transition in the intensity and style of DF_a and DS_a across the east limb of the Green Mountain anticlinorium. As the D_a elements change, the ease with which pre-D_a elements can be recognized also changes. The pre-Silurian elements found here are the same as found to the east and as previously described for location JR-163 at the western end of the segment. At JR-163, DS_a is a slip cleavage which is not parallel to OS_a/OS_b on either limb of moderately tight to open DF_a folds. OV_a and OV_b veins are easily distinguished from each other and from DV_a veins parallel to the DS_a slip cleavage. In the eastern part of the segment, DS_a is commonly parallel to OS_a/OS_b on either the long or short limbs of fairly tight, typically steeply plunging DF_a folds. Where DS_a represents renewed deformation along the older s-surfaces, the distinction between OV_a and OV_b veins tends to become less clear. OF_b folds can be hard to find where they are intermixed with small, tight, steeply plunging DF_a folds. The transition in the character of the D_a elements coincides

with an apparent increase in metamorphic grade to the west. Both OM_b and DM_a mineral growth seem to show this grade increase, as discussed in the next chapter.

The two easternmost locations, JR-6 and JR-144, are exposures of the Ottauquechee formation. The most prominent structural elements present at these locations are asymmetric DF_a folds and well developed DS_a slip cleavage. The slip cleavage typically has a distinct spacing, at least 1-3 millimeters. The pre-Silurian elements are highly deformed, but can be found. There are highly granulated, highly deformed veins which appear to be the oldest element that can be demonstrated. The veins are folded by small, tight isoclinal folds. Many of the folds are rootless, as the veins have been pinched out and fragmented. These folds form nice transposition structures. The old veins and the apparent s-surface to which they are parallel have been rotated into parallelism with the axial plane schistosity of the isoclinal folds. The composite s-surface is OS_a/OS_b. The highly granulated veins are OV_a veins folded by small, isoclinal OF_b folds. The OF_b folds can only be demonstrated where D_a deformation is the least intense. Parallel to OS_a/OS_b are partly granulated veins which are not affected by the small isoclinal folds. These are OV_b veins. The degree of granulation of OV_b veins varies somewhat within the two locations. Some granulation is always present and the OV_b

veins are always less granulated than the OV_a veins.

OV_b veins and OS_a/OS_b are in turn deformed by generally steeply plunging DF_a folds. The measured DF_a folds at JR-6 plunge 45°-65° to the south. At JR-144, the plunges range from 15° south through vertical to 35° north. The trends are roughly north-south. One measured OF_b fold had an attitude of 143° trend, 63° plunge. Because both generations are steeply plunging, they are difficult to sort out.

Parallel to the axial planes of the DF_a folds is DS_a slip cleavage. Typically OS_a/OS_b has been rotated into parallelism with the DF_a axial planes. Where such transposition structures are developed, OS_a, OS_b, and DS_a are all parallel. Ungranulated DV_a veins are parallel to DS_a. These are best developed at JR-144. Some DV_a veins are gently warped by north-south trending folds, apparently DF_b.

The coincidence of OS_a, OS_b, and DS_a makes it difficult to sort out the structural elements. However, the veins are very helpful for this purpose. Highly granulated OV_a veins are folded by small, typically rootless OF_b isoclinal folds. These do not deform OV_b veins, which are partly granulated. Both OV_a and OV_b veins are folded by DF_a folds. Where DS_a and OS_a/OS_b are not parallel, the relationships are a little easier to demonstrate. Where DS_a is most prominently developed, it can be impossible to

distinguish the pre-D_a elements from each other.

The next outcrop to the west of JR-144 is JR-145, an exposure of interbedded schist and massive quartzite of the Hazens Notch formation. Here the relationships between the elements of O_a, O_b, and D_a are clear. Well demonstrated isoclinal OF_b folds of the quartzite have an associated axial plane schistosity, OS_b, which crosscuts OS_o and OS_a at fold noses. The wavelengths of the OF_b folds are about 1-2 meters. The isoclinal folds are refolded by fairly open, steeply plunging, asymmetric DF_a folds. DS_a slip cleavage is weakly developed. Attitudes of two OF_b folds are 110° trend, 55° plunge and 125° trend, 41° plunge. The DF_a folds which refold these two folds have an attitude of 184° trend, 60° plunge.

In the schist away from the quartzite layers at JR-145, the D_a deformation is similar to that seen at JR-6 and JR-144. OF_b folds are seen as very small, commonly rootless isoclinal folds of granulated OV_a veins. The OV_b veins are partly granulated. To the west the granulation of OV_b veins dies out. Granulation of OV_a veins is ubiquitous.

Westward from the Ottauquechee, D_a elements don't change very much in the Hazens Notch formation to about location JR-161. At location JR-4, just west of JR-161, DF_a folds with DS_a slip cleavage parallel to the short

limb or neither limb become predominant. An example of a DF_a fold at JR-4 is shown in Figure 20. This continues for about a half mile to the west and then from location JR-76 to the Green Mountain axis, DS_a is not parallel to either limb of DF_a folds and is therefore not parallel to OS_a/OS_b. In the western part of the segment, DS_a is either seen as a well spaced slip cleavage or it is absent.

As observed elsewhere, there is a variation in the intensity and style of DF_a and DS_a with differences in lithologic type. The transition described above is not a function of changing rock type as can be demonstrated by comparing the features in similar rocks across the traverse segment. Most of the transition takes place within a single unit, the Hazens Notch formation. This change in style of D_a deformation is an important tectonic feature. While there is considerable change from location JR-161 to location JR-4, the transition is really not that sharp and the changes can be followed in detail. The evidence tends to rule out the possibility of this change being brought about by bringing two distinctly different structural domains into juxtaposition along a fault surface.

Several orders of DF_a folds are present in this area. Larger folds with wavelengths of 7 meters or more are easier to see when DS_a is not parallel to OS_a/OS_b, but even in locations such as JR-6 in the Ottauquechee, large

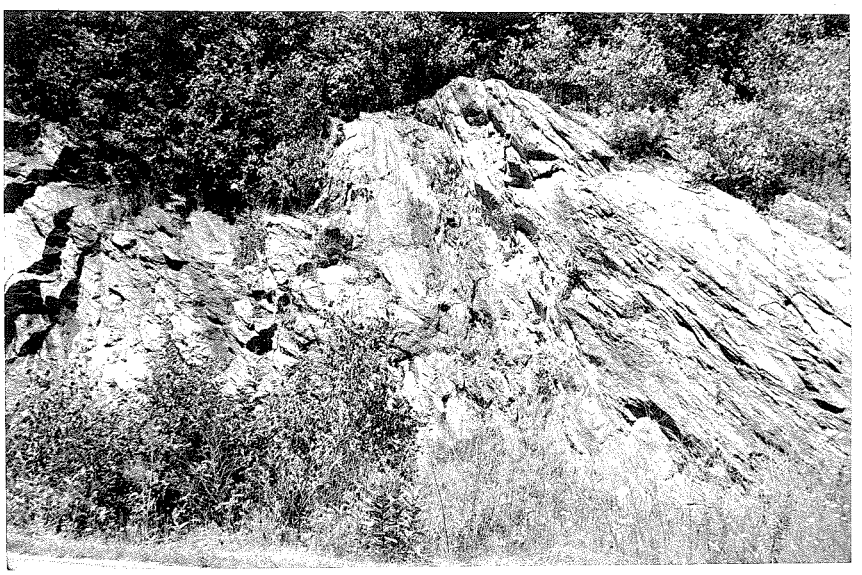

Figure 20 DF_a fold in Hazens Notch schist at JR-4, Camels Hump quadrangle. DS_a slip cleavage is parallel to short limbs of fold.

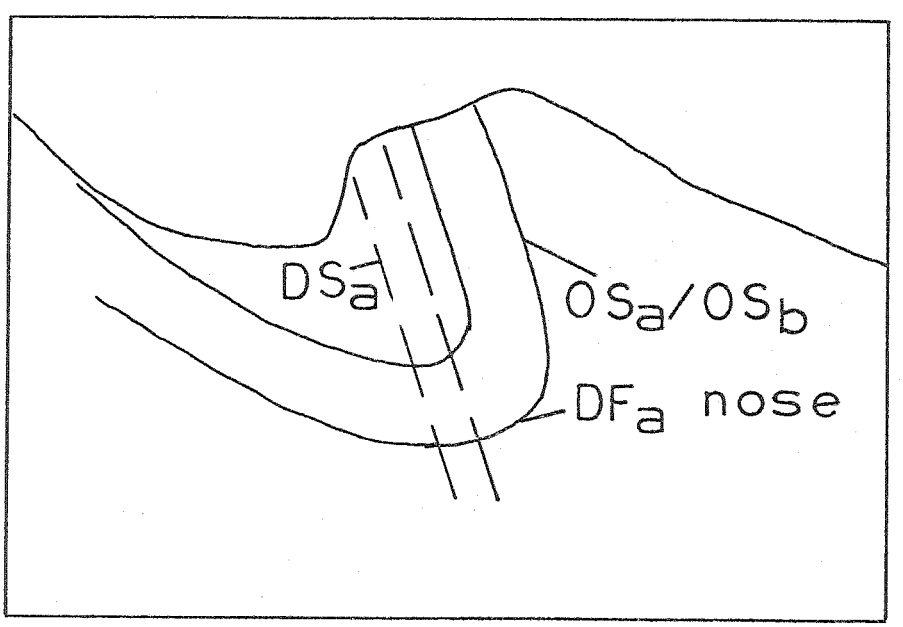

DF_a folds can be observed which have the same geometry as the smaller orders. Much larger DF_a folds may be present in the area but of course they cannot be directly observed.

The attitudes of DF_a axes along the traverse segment from Waterbury to the Green Mountain axis are shown in Figure 21a. The axes trend on the average north-south but there is a small but significant dispersion of axial trends. The plunges are north and south over the entire 180° range that is possible. The segment can be divided according to the transition in D_a structures just described and thereby produce two separate DF_a patterns. Along the eastern half from JR-6 to JR-161, where DS_a is commonly parallel to OS_a/OS_b, DF_a axes have plunges which range over the entire possible 180° as shown in Figure 21b. From JR-4 to JR-163, DF_a axes do not have plunges steeper than 50° and plunges greater than 10° are all to the south. This is shown in Figure 21c. There is no change in the trend of DF_a axes over the segment. As was observed along the traverse segments to the east of this one, there is no refold generation present that is sufficient to disperse DF_a axes over this range of plunges. Within a single outcrop the range in plunge of DF_a can be nearly as great as shown by all DF_a folds along the segment. An example is location JR-161 for which the attitudes of DF_a axes is shown in Figure 21d. As before, DF_a folds appear to be strongly noncylindrical.

Figure 21a

Stereonet plot of DF_a axes at locations along the third segment of the Winooski River traverse.

Figure 21b

Stereonet plot of DF_a axes at locations JR-6 through JR-161.

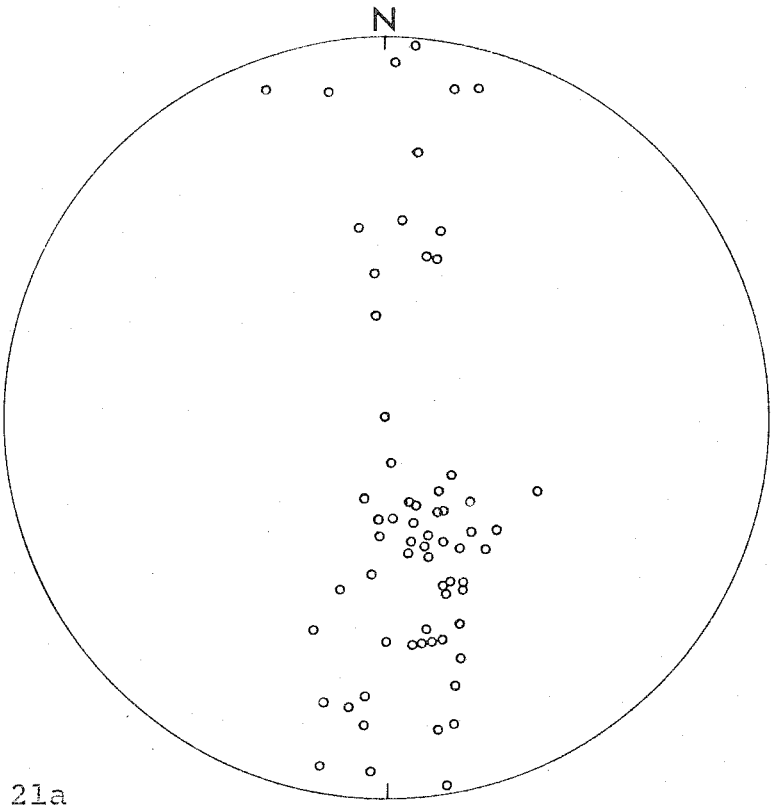

Figure 21a

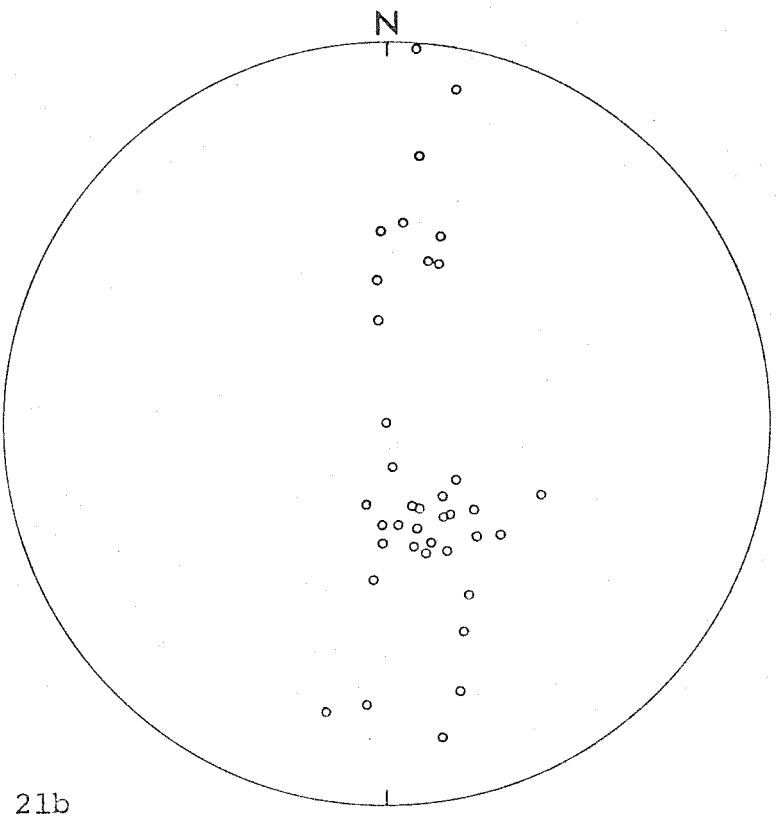

Figure 21b

Figure 21c

Stereonet plot of DF_a axes at locations JR-4 through JR-163.

Figure 21d

Stereonet plot of DF_a axes at location JR-161.

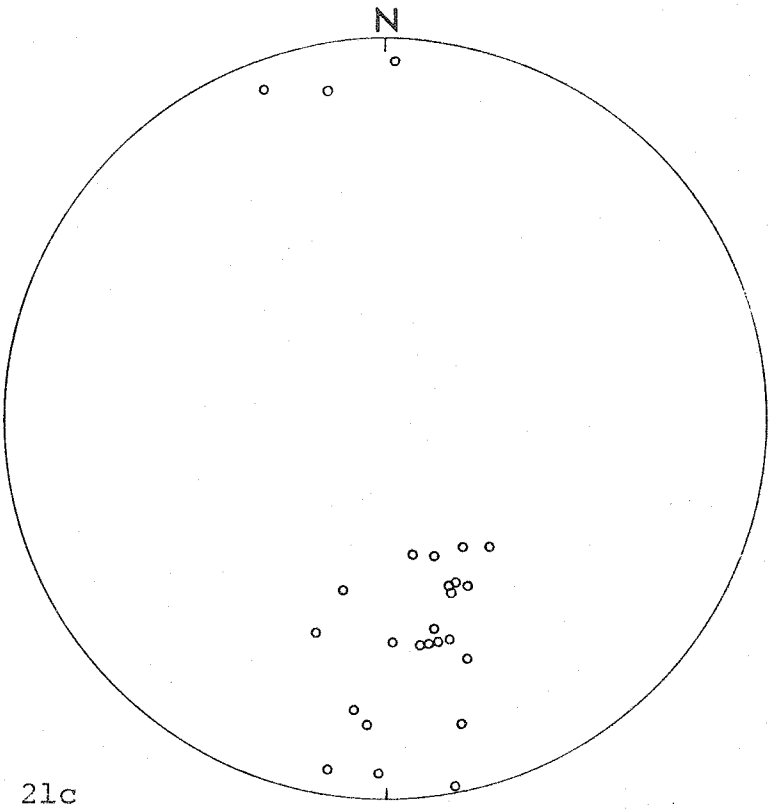

Figure 21c

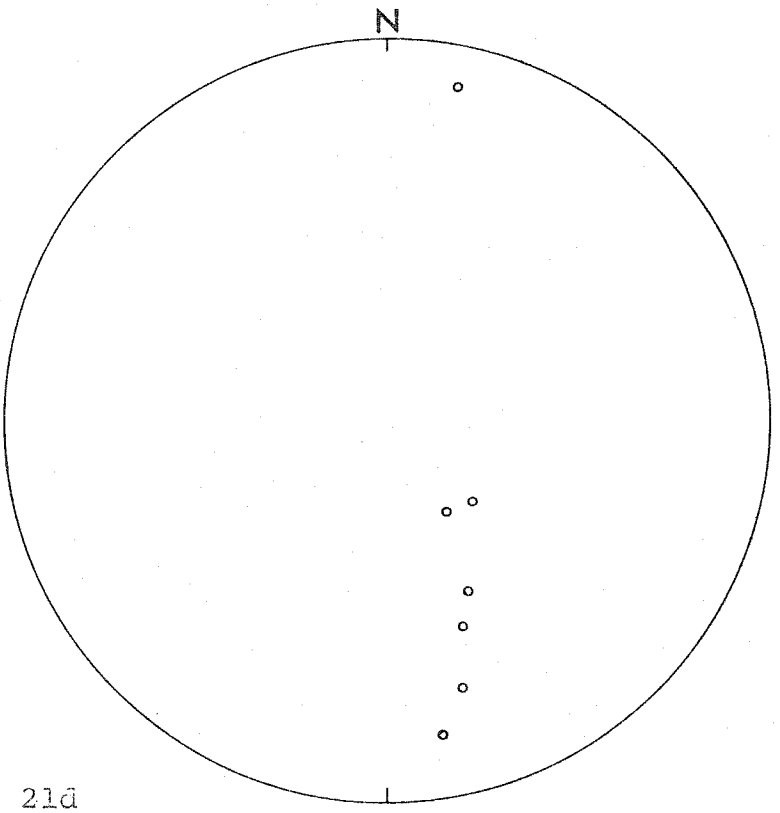

Figure 21d

Figure 21e

Stereonet plot of poles to DS_a at locations along the third segment of the Winooski River traverse.

Figure 21f

Stereonet plot of poles to OS_a/OS_b at locations along the third segment of the Winooski River traverse.

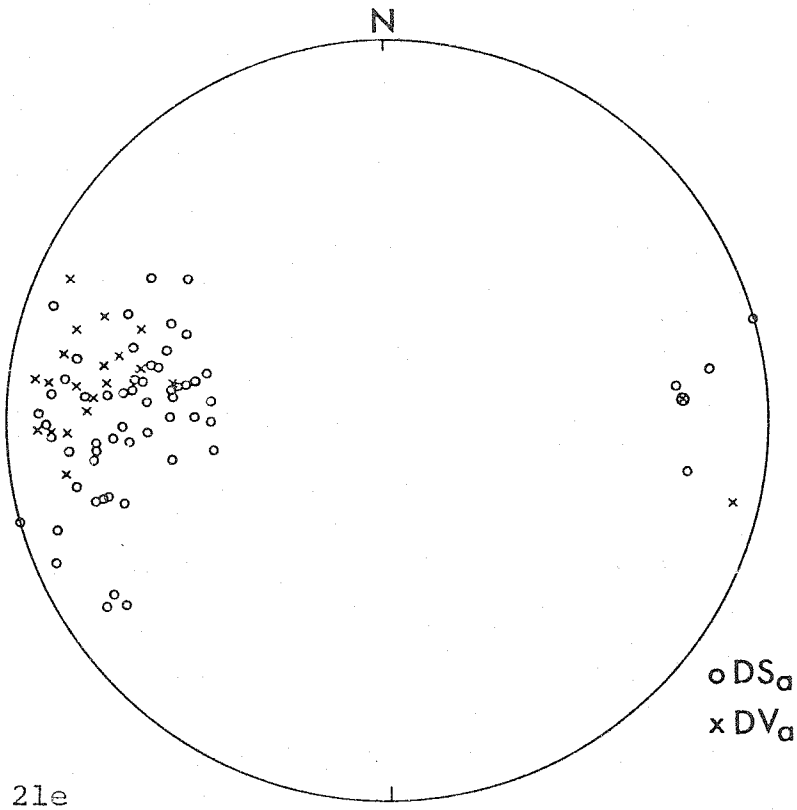

Figure 21e

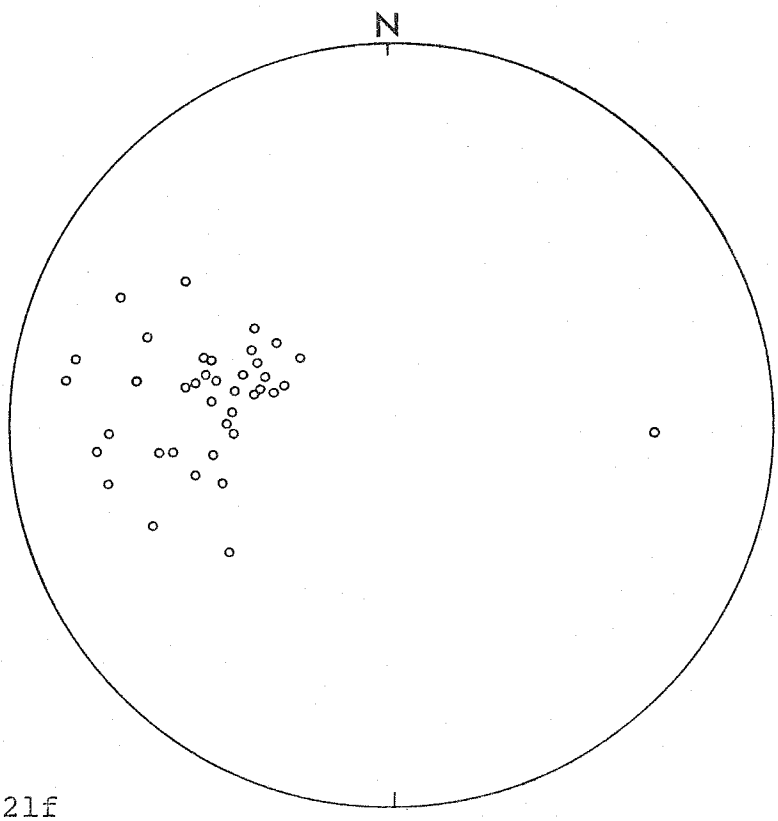

Figure 21f

Figure 21g

Stereonet plot of poles to DS_a and OS_a/OS_b at location JR-161.

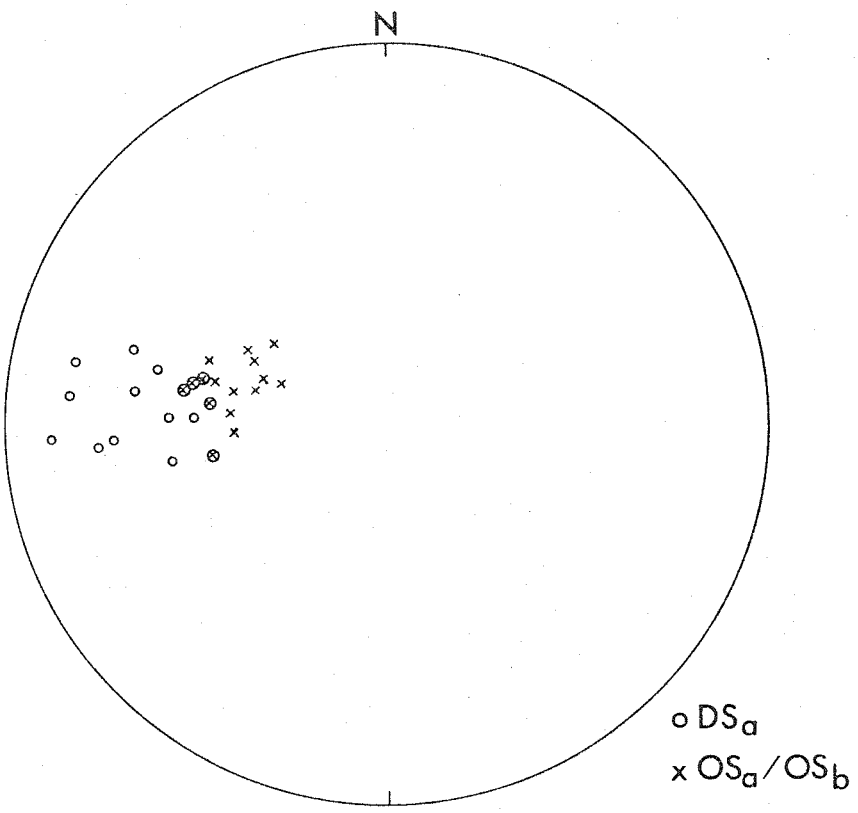

Figure 21g

The small dispersion of DF_a trends can be accounted for by DF_b refolding.

Figure 21e shows a plot of DS_a and DV_a poles along this same segment. DS_a surfaces strike NNE to NNW with generally steep dips to the east although a few dips are steep to the west. If the same division of the segment is made as above, DS_a poles also form two distinct patterns. DS_a in the western half from JR-4 to JR-163 never are seen to dip less than 70°. Along the eastern half DS_a surfaces have dips from 50° to vertical. The dips between 50° and 70° are usually seen where DS_a is parallel to the long limbs of DF_a folds and therefore is accommodated along the pre-existing OS_a/OS_b surface. Figure 21f is a plot of poles to a few OS_a/OS_b surfaces measured along the segment. OS_a/OS_b surfaces have the same general trend as DS_a but have generally less steep dips to the east. Figure 21g shows a plot of poles to DS_a and OS_a/OS_b at a single location, JR-161. DS_a surfaces that are less steep and overlap with the attitudes of OS_a/OS_b are in fact coincident with OS_a/OS_b. The steeper DS_a surfaces are not parallel to limbs of DF_a folds. It appears that if the planar anisotropy OS_a/OS_b were not present, then DS_a would everywhere dip from 70° to 90°.

DF_b folds are present as gentle, asymmetric flexures of DS_a with wavelengths usually not less than about 2 meters.

While DF_b folds can be seen at most outcrops, it is generally very difficult to get a reasonable measurement of a DF_b fold axis. Only four DF_b folds were measured with any certainty along this traverse segment and these are shown in Figure 22. There is a larger error associated with these measurements than with measurements of DF_a. The folds are clearly present, however, and are not the result of an originally curviplanar DS_a. On the east limb of the anticlinorium, DF_b folds have N to NNE trends with very shallow plunges to the north. No axial plane DS_b foliation of any sort was observed.

The effect of DF_b folding can perhaps be seen in the dispersion of trends of DF_a axes. Unrefolded, noncylindrical DF_a folds should fall along a great circle that represents their axial surface. This assumes that the axial surface is planar and that it had an originally constant orientation over the domain being considered.

Along the traverse segment from Middlesex to Waterbury, DF_a axes fall between two great circles which strike 10° and dip 80° east and west. In effect, the average axial plane of DF_a folds at locations between Middlesex and Waterbury is a plane which strikes 10° and has a vertical dip. DF_b folds are rarely observed along this segment, except at JR-139, so that it is not surprising that there appears to be little or no dispersion of DF_a trends by

Figure 22

Stereonet plot of DF_b axes at locations along the third segment of the Winooski River traverse.

Figure 23

Stereonet plot of DF_a axes at locations along the third segment of the Winooski River traverse. A DF_b refold axis of 20° trend, 0° plunge and possible resultant small circles of rotation of DF_a axes are shown.

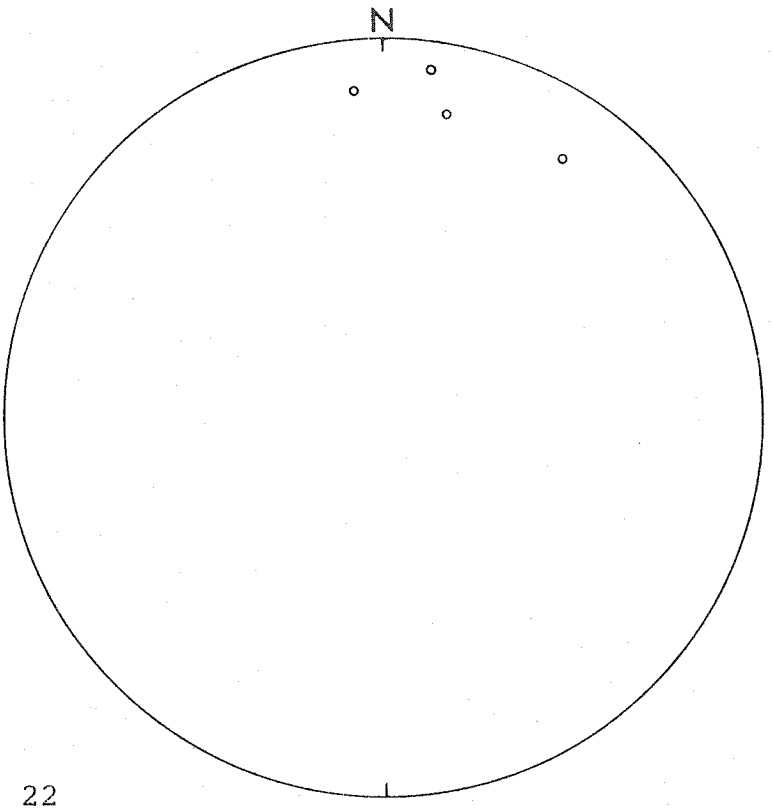

Figure 22

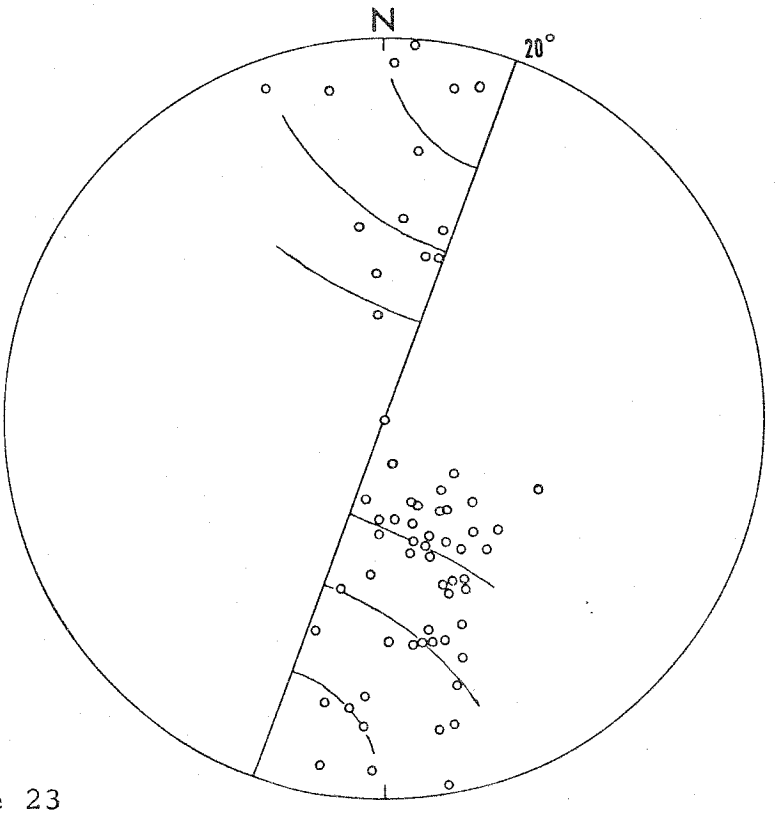

Figure 23

north-south refolding. It appears that the axial planes of DF_a folds have a fairly constant orientation over this segment.

The measured trends of DF_b folds in the area between Middlesex and the Green Mountain axis have a range of values which average about 20^o with a shallow plunge to the north. More error is associated with the measurement of DF_b fold axes than of DF_a axes because of the openness of DF_b folds. If DF_a axes which fell along an axial plane with 10^o strike and vertical dip were refolded by an open flexural fold system that had an axial trend of 20^o with a shallow or horizontal plunge, the dispersion pattern shown in Figure 23 would result. DF_b with an average axial trend of 10^o would work just as well. Flexural folding of linear elements such as DF_a axes produces small circle rotations of the linear elements.(1) The sense of rotation is determined by the relative positions of the pre-existing linear elements and the refold axis. The sense of rotation shown in Figure 23 is correct for DF_a axes which are along an axial plane that strikes more to the northwest than the trend of DF_b folds (the strike of the axial plane of DF_a is at a small angle counterclockwise from the trend of DF_b).

(1) The geometry of folded linear elements is discussed in Ramsay (1967) and Turner and Weiss (1963).

If the positions were reversed, then the rotation would be in the opposite sense. The assumption that DF_b folds are flexural in nature is reasonable, as DF_b folds are gentle and have no association axial plane foliation along this segment.

Of course, such a solution is not unique. Even if the assumptions about the nature of DF_a folds are correct, the axes were originally dispersed along a great circle so that rotations other than small circle rotations could have produced the present pattern. Other fold mechanisms which are not purely flexural will produce rotations that are not along small circles, but the net effect of gentle DF_b folds of any mechanism will produce roughly the same pattern as flexural DF_b folds.

Two other post-Silurian elements are seen along the traverse from Waterbury to the Green Mountain axis. Possible DV_c veins are present at JR-163 and JR-76. These seem to be related to biotite grade mineral growth in the host rock. There is not a great deal of textural evidence of such mineral growth, DM_c in generation, but microprobe data on sample JR-163-D indicate its presence. There is also evidence of possible DM_c grown in other samples from the traverse segment. Chapter III contains a discussion of the mineral growth along this segment and the next segment to the west.

Due to the lack of DS_b foliation and the small number of veins, or other post-DF_b veins, DF_d folds would be hard to find even if they are present. The only folds observed which are probably DF_d in generation are the very gentle folds of the DV_c vein at JR-163. These folds have a north-south trend and a roughly horizontal plunge.

Segment 4

Continuing to the west along the Winooski River traverse, the next segment extends from the Green Mountain axis to location JR-197, just past the village of Jonesville. The small scale structures remain virtually the same in style and orientation as those in the immediately adjacent traverse segment to the east. The pre-Silurian elements OS_a, OS_b, OV_a, OV_b, and OF_b are present as are the post-Silurian elements DS_a, DV_a, DF_a, and DF_b. Locations JR-193, JR-197, and JR-198, all near Jonesville, are in the Pinnacle formation and the other locations are within the Underhill formation.

The pattern of DF_a fold axes is similar to that seen just to the east and is shown in Figure 24a. The average trend of DF_a folds is north-south and the plunges range from 0° to 50° north and south. There is perhaps moderate dispersion of DF_a trends by the gentle DF_b folds. The attitudes of DS_a and DV_a show an average strike of about

Figure 24a

Stereonet plot of DF_a axes at locations along the fourth segment of the Winooski River traverse.

Figure 24b

Stereonet plot of poles to DS_a and DV_a at locations along the fourth segment of the Winooski River traverse.

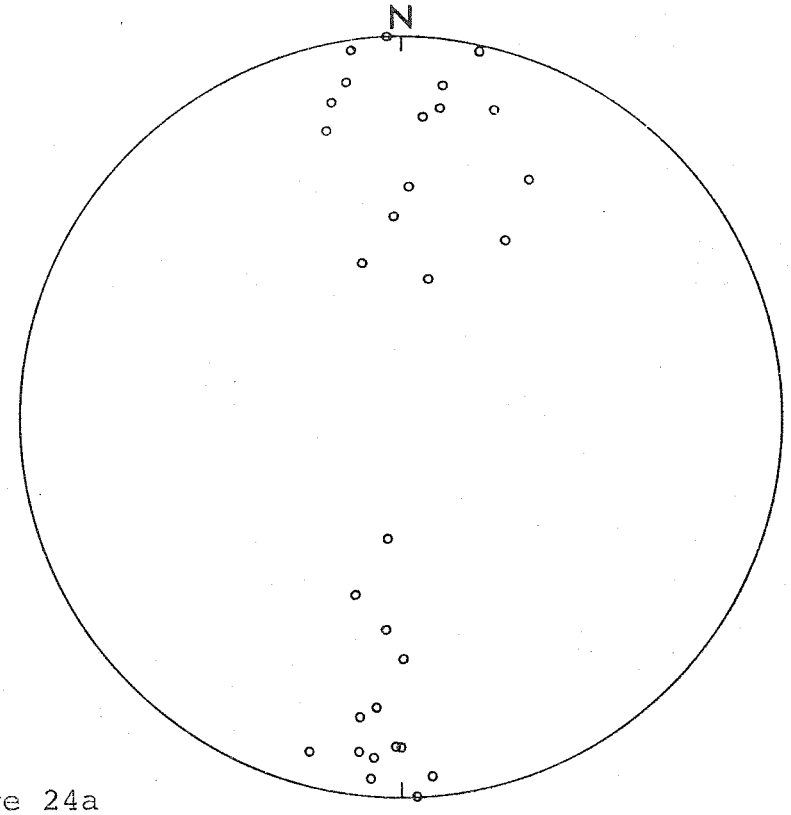

Figure 24a

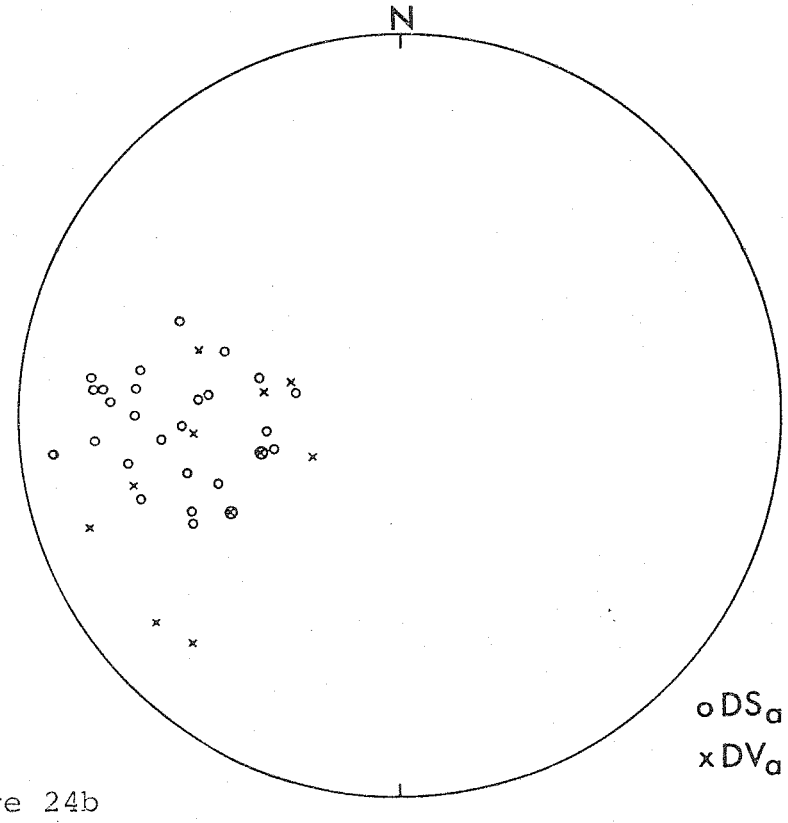

Figure 24b

0^{o} and steep to moderate dips consistently to the east. Poles to DS_a and DV_a are shown in Figure 24b.

DF_b folds are open folds which trend about 10^{o} and have nearly horizontal plunges. These folds tend to be a little more noticeable than the DF_b folds on the eastern limb of the anticlinorium. No DS_b foliation is developed but the axial planes of DF_b folds dip consistently to the west.

All of the above elements can be observed at location JR-198. Figure 25 is a photograph from JR-198 which shows OS_a, the early schistosity, with parallel OV_a veins folded by nearly isoclinal OF_b folds. The OF_b folds are refolded by DF_a folds and crosscut by DS_a slip cleavage. OV_b, OS_b, and DV_a are also seen at the outcrop, as are gentle DF_b folds of DS_a. Another location where all of the elements can be observed is JR-162.

Segment 5

The last portion of the traverse is from location JR-79 to location JR-149, near the Hinesburg thrust at the western edge of the study area. The exposures are within the Underhill and Pinnacle formations. In the Underhill relatively incompetent rock types, such as fine-grained chlorite-muscovite schist, are more abundant as compared to the Green Mountain axial region. The exposures of Pinnacle formation

Figure 25 OF_b fold refolded by DF_a at location JR-198, Camels Hump quadrangle. Folds deform rocks of the Pinnacle formation. Elements are shown in sketch below.

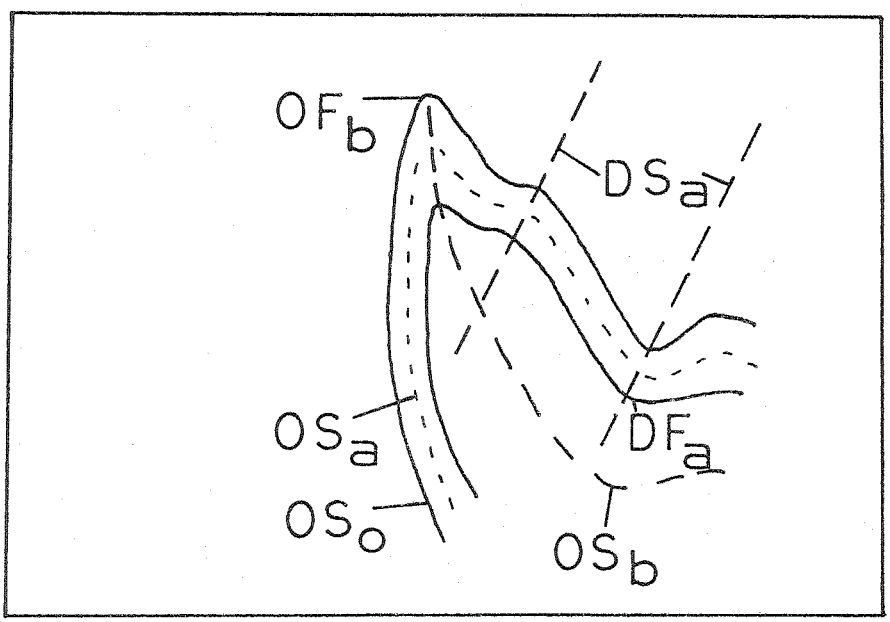

consist largely of metagreywacke, which tends to be in massive layers. The main difference between these rocks and those just to the east is that along this segment the rocks have been metamorphosed to a lower grade, biotite grade here as opposed to garnet grade near the Green Mountain axis (for OM_b mineral growth only). This traverse segment is characterized by changes in the style and intensity of DF_b folds and the appearance of a significant fold set which may be equivalent to DF_d.

DF_a and DS_a also tend to change in character west of Jonesville. DS_a is in most cases seen to be well developed and in more mica-rich layers can be parallel to OS_a/OS_b on one limb of tighter DF_a folds. The general trend of DF_a axes and the large variation in plunges remains the same as that seen to the east.

DF_b folds are generally fairly tight and often are observed to have an axial plane slip cleavage, DS_b (examples can be seen at locations JR-194, JR-195, and JR-152). DF_b axes trend about 0° on the average and have near horizontal plunges. This is an apparent change in trend from DF_b to the east and the angular relationship of DF_b and DF_a axes is reversed. As expected, the dispersion of DF_a axes seems to reflect rotation in the opposite sense from that observed near the Green Mountain axis.

Also developed in this westernmost segment is a fourth

generation of folds which deforms DS_b slip cleavage. These folds are fairly open, asymmetric folds which have axial trends of NNW and plunges of about 40^o to the south. Although these folds are in the same position in the structural sequence as DF_d folds, found to the east in the Silurian and Devonian rocks, there is of course no continuity of DF_d across most of the Ordovician and Silurian rocks. The only other possible occurrence of DF_d folds is at JR-163 where the folds have axial attitudes very similar to the DF_d folds east of the unconformity. The fourth generation of folds along this westernmost segment (seen at locations such as JR-152 and JR-149) have significantly different attitudes. At the present time it is impossible to decide if these folds are DF_d or not. For simplicity, these folds in the western segment will be called $DF_d(?)$. Possibly associated with $DF_d(?)$ folds is a poorly developed s-surface observed at location JR-194. At this location, OS_o, OS_a/OS_b, DS_a,DS_b, and this surface, $DS_d(?)$, can be seen to all be superimposed on each other within the same rock volume.

Another feature observed near Jonesville and to the west are OF_b folds which have axial trends that are more nearly north-south with steep to shallow plunges. These folds are clearly deformed by DF_a and they deform OV_a veins. OV_b veins are not deformed by the OF_b folds and are parallel

to the axial planes of the folds. The apparent change in the orientation of OF_b folds may be the result of several stages of refolding, as there are three refold sets in the area. Another possibility is that the change in attitude reflects a change in the stress field that formed OF_b folds. The third and obvious possibility is that they are another fold generation.

Thresher (1972) worked in this area and found eight folds which seem to be the equivalent of OF_b folds in this study and these had generally north-south trending axes. Thresher's s_2 seems to be DS_a of this study, so that his s_1 and associated folds would be OS_b and OF_b. Thresher's other structural elements seem to correspond to DF_a, DF_b, DS_b, and DF_d(?).

Lamoille River traverse

The other major traverse in Cambrian and Ordovician rocks in this study was parallel to the Lamoille River, 20 to 25 miles north of the Winooski River. The structural sequence and the elements of the sequence found along the Lamoille River traverse are identical to the sequence of elements already described. In a very general way, the variation from east to west in style and intensity of the individual elements is similar for both traverses. OS_a, OV_a, OS_b, and OV_b are commonly observed and OF_b folds are seen

in some outcrops. DF_a, DS_a, and DV_a are present and well developed along the traverse. There is considerable local variation in the intensity of DF_b, but near the Green Mountain axis along the Lamoille River traverse DF_b folds are gentle, asymmetric flexures of DS_a usually without an associated axial plane DS_b. The features found at location JR-113 and JR-114 have been previously described and these are typical of locations near the Green Mountain axis. The structural sequence can be easily followed along the Green Mountain axis as there is essentially no change in the style of elements and the sequence in which they occur.

Previous studies within the present area in which the various small-scale structural elements were distinguished in detail are by Albee (1957a & b and 1972a). This work concerns the geology of the Hyde Park quadrangle and along a traverse like the Lamoille River traverse of this study. The structural sequence presented in the present study generally agrees with that of Albee (1957a & b). A possible exception is that Albee's $L_3(?)$ and $S_5(?)$ are similar to features thought to be DF_a and DS_a in this study. L_2 and S_4 also appear to correspond to DF_a and DS_a. As I did not visit these outcrops at which Albee found $L_3(?)$ and $S_5(?)$, the correspondence of these two elements to elements of this study remains unresolved. The interpreted correspondence of elements of both studies is shown in

Table 3. Albee's elements $L_3(?)$ and $S_5(?)$ were found in the Moretown member and from their description these features seem to be equivalent to the kink bands with rounded hinges and associated slip cleavage bands shown in Figure 16. These are thought to be DF_a folds and associated DS_a.

The main area of disagreement between this study and the work of Albee (1957a & b) involves the differentiation of OF_b and DF_a in the difficult central part of the Hyde Park quadrangle within the Ottauquechee formation and eastern part of the Hazens Notch formation. Albee interpreted most of the steep plunging folds with general north-south trends in this area as being rotated L_1 folds (OF_b). The folding relationships of OV_a, OV_b, and DV_a veins were used in this study to separate OF_b and DF_a folds. Based on this and by following the structural sequence as a whole, most of the steep folds examined were found to be DF_a, although there are steep plunging OF_b folds which appear in fact to have been rotated by D_a deformation. The steep folds are therefore probably a mixture of OF_b and DF_a folds, but when OF_b and DF_a are differentiated, most of the prominent north-south trending, steeply plunging folds are DF_a. The relationships are not as obscure to the south along the Winooski River traverse, to a great extent due to the better exposures in the roadcuts of Highway I89. In the area along the Green Mountain axis, the work of Albee

Table 3 Correspondence of structural elements

This study	Albee (1957a & b)
OS_o	S_1
OS_a	S_2
OF_b (& OL_b)	L_1
OS_b	S_3
DF_a (& DL_a)	L_2
DS_a	S_4
possibly DF_a	L_3 (?)
possibly DS_a	S_5 (?)

(1957a & b) and this study are in agreement.

Structural elements in the Worcester Mountains

The Worcester Mountains are a NNE trending range between the Winooski and Lamoille Rivers. Exposed here are Stowe formation rocks which have been metamorphosed to garnet and kyanite grades. The area was originally studied by Cady (1956) and Albee (1957a & b) and discussed in a later paper by Albee (1968). The mineral growth in the rocks of the Worcester Mountains is described in the next chapter.

Locations in the Worcester Mountains are concentrated in two areas. One area is in the central part of the Montpelier quadrangle between Densmore Mountain and Mt. Hunger, just north of the second segment of the Winooski River traverse. The other area is in the southeastern part of the Hyde Park quadrangle near Elmore Mountain, just south of the Lamoille River traverse. At the locations in the Montpelier quadrangle, the same elements present along the Winooski River traverse are found, although they are somewhat different in character. Part of the difference lies in the coarses-grained nature of the high grade rocks in the Worcester Mountains. Bedding surfaces are well demonstrated generally only as contacts between pelitic schist and massive amphibolite, the two major rock types present.

In the schist, highly granulated OV_a veins have been deformed by small, isoclinal OF_b folds. OV_a and OS_a have been rotated into parallelism with the axial planar OS_b schistosity. Where present, kyanite blades in the schist have preferred orientations parallel to OS_b. Also parallel to OS_b are granulated OV_b veins. At some locations such as JR-129, OV_b veins have kyanite and/or garnet within them. There is hornblende within OV_b veins in amphibolite.

The granulated OV_b veins are highly deformed by generally north-south trending DF_a folds. These plunge either north or south from 0^o to 75^o. Parallel to the axial planes of DF_a folds is DS_a slip cleavage. Locally DS_a is parallel to the long limbs of DF_a folds, but not in general. DS_a tends to be a well developed slip cleavage in the schist, but only a poorly developed fracture cleavage or absent in the amphibolite. A DV_a vein parallel to DS_a in pelitic schist is found at location JR-127. The vein is folded by open north-south trending folds, probably DF_b. DV_a veins have not been found at the other locations. With two exceptions, the outcrops are very small compared to the roadcuts along the Winooski River traverse; the apparent scarcity of DV_a veins may in part be due to this.

To the north in the Elmore Mountain area, the structural elements are similar. There is an important location

on the west slope of Elmore Mountain, JR-158. The contact surface between schist and amphibolite is folded by east-west trending isoclinal folds with wavelengths on the order of 1-2 meters. At the noses of these folds, the principal schistosity of the schist is parallel to the axial planes of the folds and it crosscuts the bedding surface. There are smaller, nonisoclinal folds with similar axial trends in the nearby amphibolite. A crenulation lineation which is parallel to the fold axes is developed on the contact surface. One measured isoclinal fold had an axis of 260° trend, 26° plunge. The folds appear to be OF_b folds with axial plane OS_b schistosity. The folds and the schistosity are themselves folded by north-south trending, asymmetric DF_a folds. One DF_a fold had an axial attitude of 353° trend, 37° plunge. DS_a slip cleavage is developed in the schist and crosscuts OS_b. A set of crenulation lineations similar to that at JR-158 is found at JR-157 on a contact surface between schist and amphibolite. The lineations had an attitude of 84° trend, 26° plunge. The lineations are folded by DF_a folds, one of which had an axial attitude of 1° trend, 3° plunge. At both locations DS_a slip cleavage dips steeply either east or west. DV_a veins are found in amphibolite host rock at locations JR-66 and JR-86.

As to the south, high grade minerals such as garnet and kyanite are locally found in OV_b veins. Kyanite blades

in the schist have preferred orientations parallel to OS_a/OS_b. As discussed in the next chapter, all of the high grade mineral growth in the Worcester Mountains appears to be OM_b.

Albee (1968) has suggested that some of the major north-south structures in the Worcester Mountains may be Ordovician in age. In this study only two sets of small scale north-south trending folds were found in the range. These are the prominent DF_a folds and the much less prominent, open DF_b folds. The structural sequence is fairly complete and agrees with the sequences found along the Lamoille River and Winooski River traverses. The possibility of north-south trending major folds of Ordovician age cannot be ruled out, but there are apparently no small folds which provide evidence of such features.

General description of the elements in the pre-Silurian rocks

All of the important structural elements in the pre-Silurian rocks have been described in the preceding discussion. It is useful to briefly consider the elements in general and as they are seen in other areas of the exposed pre-Silurian rocks.

Events O_a and O_b

Everywhere that OS_o and OS_a can be well demonstrated,

they are observed to be parallel. Nowhere has OS_a been found to be related to folds. OV_a veins are parallel to OS_a and are found throughout the pre-Silurian rocks. They are typically abundant in pelitic schist.

In pelitic rocks, OF_b folds of OS_o and OS_a are generally present as small isoclinal folds with wavelengths of a few centimeters or less. Larger OF_b folds are rare except at exposures of pelitic rocks interbedded with massive quartzite or amphibolite. A few fairly open OF_b folds have been found, but the folds are typically isoclinal. The trends of OF_b folds are roughly east-west. There is variance in the trend and particularly in the plunge due to the folding by DF_a folds. Figure 26 shows the attitudes of isoclinal OF_b folds observed along the east limb of the Green Mountain anticlinorium from the Winooski River north to Hazens Notch in the Jay Peak quadrangle.

In the area near Hazens Notch, Cady, Albee, and Chidester (1963) have mapped large scale folds with east-west axes. In cross section, the structures are shown as tight, nonisoclinal folds. The large folds appear to be related to small east-west trending OF_b folds which occur in the area. If the major folds are OF_b, then they are the only recognized pre-Silurian large scale folds in northern Vermont.

Figure 26

Stereonet plot of OF_b axes at locations along the east limb of the Green Mountain anticlinorium. The locations are between the Winooski River in the Camels Hump quadrangle and Hazens Notch in the Jay Peak quadrangle.

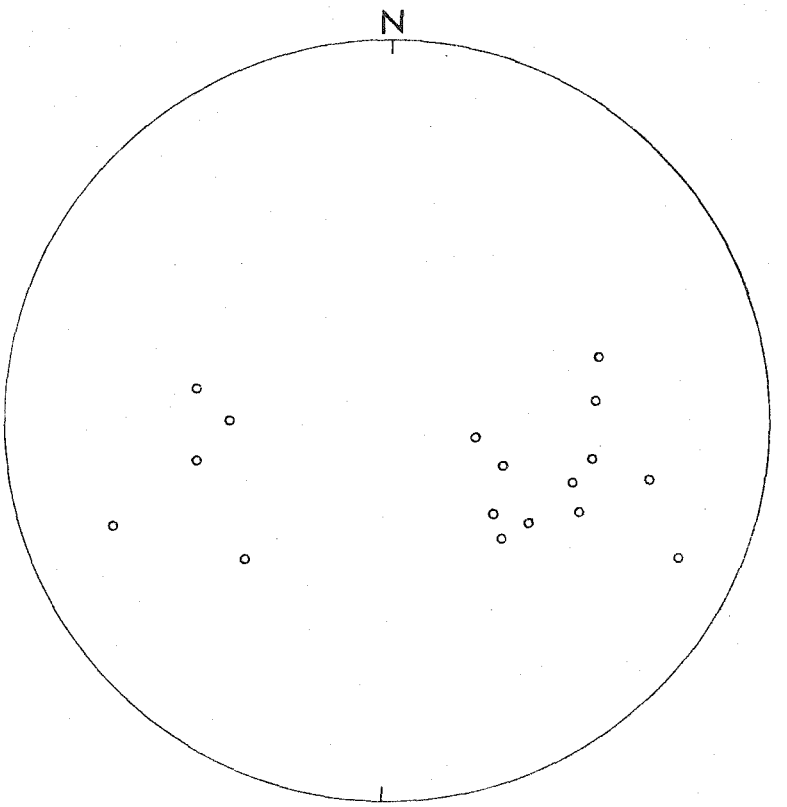

Figure 26

OS_b is developed throughout the pre-Silurian rocks and is parallel to the axial planes of OF_b folds. OS_b is a pervasive schistosity or locally a slip cleavage. OS_a is rotated into parallelism with OS_b on the limbs of isoclinal OF_b folds. The two surfaces generally cannot be distinguished on such fold limbs. In some pelitic rocks with well developed plagioclase porphyroblasts, OS_b appears to have a discrete spacing between planes with the spacing determined by size of the porphyroblasts. The porphyroblasts commonly show evidence of rotation by movement along OS_b. Where OF_b folds are not strictly isoclinal, OS_a and OS_b can be at an angle to each other on one or both limbs. Of course, OS_a and OS_b are not parallel at the noses of OF_b folds.

OV_b veins parallel to OS_b are well developed in the Cambrian and Ordovician rocks. Most OV_a and OV_b veins are easily distinguished by the deformation of OV_a veins by small OF_b folds and the lack of such deformation of OV_b veins. Also, within an outcrop OV_a veins may be granulated whereas OV_b veins are not. This is a common relationship near the Green Mountain axis along the Winooski River traverse.

OS_a and OS_b generally strike north-south with dips controlled by the later DF_a and DF_b folding. All of the

major north-south trending structures in the Green Mountain anticlinorium in northern Vermont are probably either DF_a or DF_b in generation and these are responsible for the prominent regional trend shown on geologic maps of the area. It is difficult to assess the situation which existed before the Devonian folding.

There are several vein generations which are younger than OV_b veins and are deformed by DF_a, thereby making these veins pre-Silurian in age. None of these vein generations seem to be associated with either folding or significant mineral growth of regional extent. These are treated as minor vein generations and are described in a later section.

Event D_a

Generally the most prominent fold in the Cambrian and Ordovician rocks are the asymmetric, generally north-south trending DF_a folds. Unlike DF_a folds in the Silurian and Devonian rocks, these DF_a folds are typically characterized by the presence of small folds with wavelengths of several centimeters or so, along with other orders of larger folds. Axial plane DS_a ranges from a dominant schistosity to a slip cleavage to completely absent. DS_a is typically seen as a slip cleavage with spacings of 1-3 mm. The style of

DS_a, and also of DF_a, varies both regionally and, within a small area, with differing rock types. DS_a is most likely to be a strong schistosity within graphitic phyllite or other mica-rich rock whereas it is commonly absent from a massive amphibolite layer, or at most a spaced fracture cleavage. DF_a folds are often observed to be tighter and more prominent where DS_a is well developed and more open in more competent layers where DS_a is absent or weakly developed. DV_a veins are well developed throughout the area west of the unconformity.

Post-D_a elements

DF_b folds in the pre-Silurian rocks tend to be open, gentle folds most easily observed as flexures of DS_a and DV_a. These north-south trending folds are apparently absent at many locations. DS_b slip cleavage is only locally developed. No veins associated with DF_b folds have been found. East-west trending DF_{b+1} folds have only been found at one location.

A few DV_c veins have been found to the west of the unconformity. These are related to biotite grade mineral growth in the adjacent host rock. Only a few DF_d folds have been demonstrated in the Cambrian and Ordovician rocks. As DV_c veins and DS_b are the markers for DF_d folds, the

apparent scarcity of these gentle north-south trending folds may be due to the scarcity of the markers. Wherever the markers are present and both DF_b and DF_d folds are found, DF_b folds are more prominent and less gentle than DF_d folds at the same outcrop. Fairly well developed folds of DS_b are found near Richmond and to the west in exposed Cambrian rocks. These have somewhat different axial trends than DF_d folds to the east. They are in an equivalent position in the structural sequence to DF_d and for simplicity these are designated $DF_d(?)$.

G. Metamorphic veins

The original purpose of studying the structural sequence was to be able to identify the various vein generations throughout the area. The veins are an important part of the sequence and have been used in its definition. The most important use of veins is as markers of fold generations. To an extent, the use of veins in this manner does not depend on the specific generations involved, but only upon the relative time relationships of their formation and the folding. The establishment of the structural sequence does not rely upon the correct identification of the vein generations; rather, the identification of the veins depends upon their position in the entire structural

sequence. Identifying factors such as vein style are regarded as ambiguous and are used only to help distinguish the minor vein generations in cases where more than one generation formed between two major events and the evidence of structural superposition is insufficient.

Major generations

There are four major vein generations found in northern Vermont and these correspond to four major mineral growth generations in the host rock as shown by petrographic and electron microprobe examination. Two of the generations occur only in the Cambrian and Ordovician rocks and two generations occur in Silurian and Devonian rocks as well as in the pre-Silurian strata. The four generations are OV_a, OV_b, DV_a, and DV_c; these are described below, starting with the oldest, OV_a. The minor vein generations, of which there are several, are described later as these do not relate to regionally significant mineral growth.

OV_a

OV_a veins are parallel to the early secondary bedding schistosity in the Cambrian and Ordovician rocks, OS_a. The occurrence of these veins is strictly confined to pre-Silurian strata. As OV_a veins are almost always strongly deformed, it is difficult to ascertain their original shape

and dimensions. Where OV_a veins are least deformed, they are seen to be sheet-like structures, typically 2-10 centimeters wide with extents of up to a few meters in the other two directions. In small outcrops, weakly deformed OV_a veins may not have their terminating ends exposed, but in larger outcrops the veins are always seen to be discontinuous. It appears that these veins were originally thin, discontinuous planar features with their greatest dimension less than 10 meters. Typical, highly deformed OV_a veins show boudinage, pinch and swell structures, and thinning on fold limbs; the terminations of these veins often appear to be caused by deformation. In some instances where the subsequent deformation has been very intense, features which appear to be OV_a cannot be clearly distinguished as metamorphic veins; these possible OV_a veins are seen as quartz stringers and pods. Where the post-DV_a deformation is not so intense, OV_a have the textural features associated with veins and are more clearly the result of metamorphic vein growth.(2)

(2) These textural features are discussed in Chapter III. Some of the vein growth features are the presence of border zones rich in iron-magnesium-aluminosilicates and/or other minerals, the presence of coarse grained mineral growth without preferred orientation (except in some border zones), and the absence of certain minerals, zircon for instance, which are seen in the surrounding host rock but not in veins except when clearly within an inclusion of broken-off host rock. Border zones are not always present and deformation can cause a vein to be fine-grained, but in general if the subsequent deformation is not too intense, it is not difficult to distinguish a vein from the host rock.

OV_a veins in pelitic rocks typically are predominently comprised of quartz with minor amounts of other minerals such as calcite, plagioclase, chlorite, biotite, sulfides, and muscovite. The carbonate and sulfide content seems to vary with the composition of the host rock and only phases occurring in the host rock occur in the veins. In epidote-rich host rocks OV_a veins can contain significant amounts of epidote. Where least deformed, the veins are coarse-grained, but typically the strong deformation by O_b and D_a has granulated the mineral grains, particularly grains of quartz, so that the present texture is fine-grained and granular.

An example of an OV_a vein is shown in Figure 27. This is from location JR-4 in the Hazens Notch formation along the Winooski River traverse. The vein is folded by a small, isoclinal OF_b fold and there is strong thinning of the vein on the fold limbs. At the fold nose the vein is cut by OS_b schistosity. This vein is typical of OV_a veins as seen in the Underhill and Hazens Notch formations on the limbs of the Green Mountain anticlinorium.

$\underline{OV_b}$

Parallel to OS_b and the axial planes of OF_b folds are the OV_b veins. In most cases, the only observable OF_b

Figure 27 OV_a vein deformed by small OF_b isoclinal fold at location JR-4, Camels Hump quadrangle.

folds are the small isoclinal folds which clearly deform OV_a veins but do not deform OV_b veins. Being parallel to the axial planes of OF_b folds does not uniquely relate OV_b to the OF_b-forming event; the correspondence was shown by comparing the compositions of vein phases and host phases with preferred orientation parallel to OS_b. Even without electron microprobe data, petrographic evidence is sufficient to establish the correspondence in cases such as JR-129 where a key, high-grade phase, kyanite, occurs in the host rock with preferred orientation parallel to OS_b and in the vein border zone without preferred orientation. Microprobe data from the host rock and OV_b vein have been obtained from samples JR-5-A and JR-5-B as well as samples from other locations. The OV_b vein at JR-5 from which the samples were taken is shown in Figure 28. The data are discussed in Chapter III.

In general, OV_b veins are similar in shape to OV_a veins; they are thin, discontinuous, planar sheets that have subsequently been deformed. OV_b veins are typically larger than OV_a veins with widths that average 5-15 centimeters but in some instances exceed 30 centimeters. Their planar extent is usually hard to determine, but it appears that their largest dimension is generally less than 15 meters. In small outcrops, it may not be possible to find

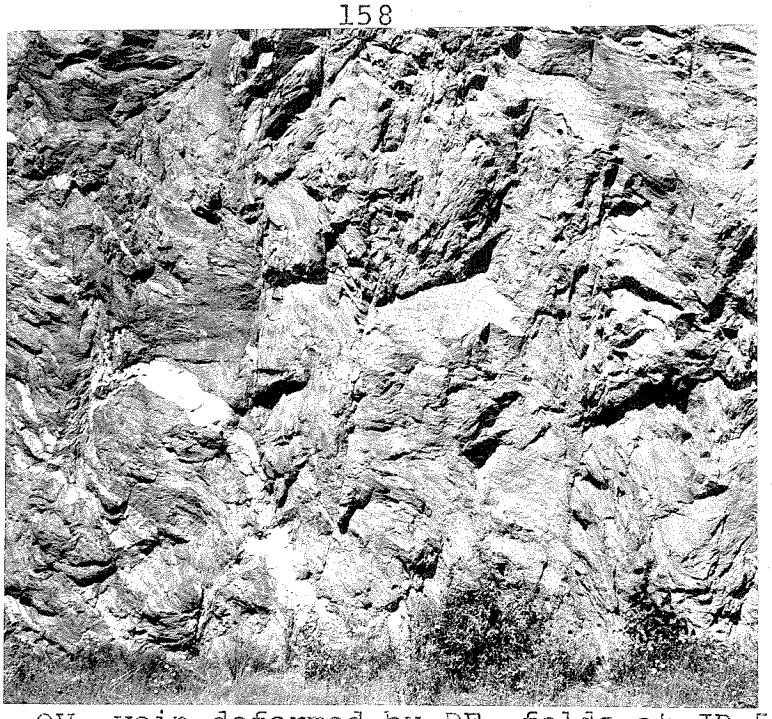

Figure 28 OV_b vein deformed by DF_a folds at JR-5, Camels Hump quadrangle. OV_b vein is largest vein in photograph, smaller veins are OV_a. Host rock is typical schist of Hazens Notch formation.

the vein terminations exposed. As is the case for OV_a veins and other generations, the two-dimensional exposure in outcrops prevents the determination of the exact dimensions and shape of OV_b veins.

Because OF_b folding does not affect OV_b veins, these veins are not as highly deformed as OV_a. However, they are always observed to be deformed by DF_a and DS_a so that pinch and swell structures and thinning of the veins are common. Many of the exposed terminations are perhaps due to pinching out by deformation rather than a primary feature, but in such cases more of the same OF_b vein can be found by following OS_b. In areas where D_a deformation is most intense, it can be difficult to distinguish OV_b veins from OV_a and other pre-Silurian veins.

The mineral assemblages in OV_b veins tend to be a little more complex than those in OV_a veins, especially in the areas of high-grade OM_b mineral growth, garnet grade or higher. While quartz is a constituent of almost all OV_b veins, many have significant amounts of plagioclase and other aluminosilicates. Calcite and ankerite as well as sulfides such as pyrite, pyrrhotite, and chalcopyrite are common constituents. Kyanite is locally found in OV_b veins in the Stowe formation in the Worcester Mountains and in the Umbrella Hill member of the Missisquoi formation in the

Lowell Mountains. Examples are described in the next chapter. Only those minerals which are in the host rock are in the veins with minor exceptions.

OV_b veins are very coarse-grained except in instances in which they have been highly granulated by D_a. Individual grains of subhedral to euhedral plagioclase can have dimensions on the order of 1-2 centimeters or more and masses of sulfide can be fist-sized. Vein mineral grains do not show preferred orientation with the exception that there is some preferred orientation of mineral grains in the border zones apparently due to the effects of nucleation and growth along the host rock wall. This is discussed further in the next chapter.

DV_a

DV_a veins are the oldest generation of major veins in the Silurian and Devonian rocks. They are also abundantly developed in the pre-Silurian strata and are an element of a metamorphic event that can be followed throughout the 1500 square mile study area. DV_a veins show the greatest degree of variation in vein style of any of the vein generations in northern Vermont. The style of DV_a veins changes with the style and intensity of DF_a and DS_a. Because of this, DV_a veins must be identified only on the basis of

structural position and never on the basis of style.

In general DV_a veins are parallel to DS_a or the axial planes of DF_a folds in cases where a distinct DS_a surface is not developed. Mineral growth in the veins has been shown to be related to DM_a host rock mineral growth in samples such as JR-5-G, JR-18-B, and others. At some locations in the pre-Silurian rocks, such as JR-199 and JR-122 from the Winooski River traverse, DV_a veins crosscut DS_a at small angles. This is mostly observed where DS_a is parallel to one limb of DF_a folds and therefore the orientation of DS_a may have been affected by the presence of the pre-existing planar anisotropy, OS_a/OS_b; the DV_a veins are oriented parallel to the DS_a surfaces which do not coincide with OS_a/OS_b in the same outcrops.

Within the Silurian and Devonian strata, DV_a veins share similarities with the OV_a and OV_b veins in the older rocks. DV_a veins are parallel to the oldest metamorphic schistosity, DS_a, which is everywhere well developed. They are discontinuous planar bodies. The veins typically consist of coarse-grained quartz and/or other minerals, with the complexity of the vein assemblage apparently dependent upon the local grade of DM_a mineral growth in the host rock. Deformation, by D_b, is in many places intense enough to obscure the original extent of the veins. An example of a

highly deformed DV_a vein is shown in Figure 29.

DV_a veins can be much larger than the largest observed pre-Silurian veins; in particular, they tend to be wider with widths up to 2 meters or more. The veins are not observed to be continuous in their planar dimensions on a scale greater than perhaps 50 meters in the larger outcrops. In small outcrops, terminations often cannot be found. Where the terminations of the wider veins are exposed, such as at JR-4, the wide vein is seen to finger into a number of smaller veins parallel to DS_a and then these smaller veins pinch out.

While the DV_a veins in the Silurian and Devonian rocks are all similar in style, there are several different styles within the Cambrian and Ordovician rocks. Discontinuous veins with blunt ends such as shown in Figure 30, are characteristic of much of the eastern part of the exposed pre-Silurian strata, especially the Missisquoi formation. These are often observed where DS_a is parallel to OS_a/OS_b and the veins are not necessarily strictly parallel to this DS_a. The veins appear to be fillings of openings developed by extension within the plane of DS_a or nearly within the plane of DS_a where DS_a is parallel to OS_a/OS_b. Smaller veins of this type could be called boudin fillings and the mechanism for vein formation and formation of nor-

Figure 29 DV_a veins strongly deformed by DF_b folds at JR-177, Lyndonville quadrangle. Host rock is schist of the Gile Mountain formation.

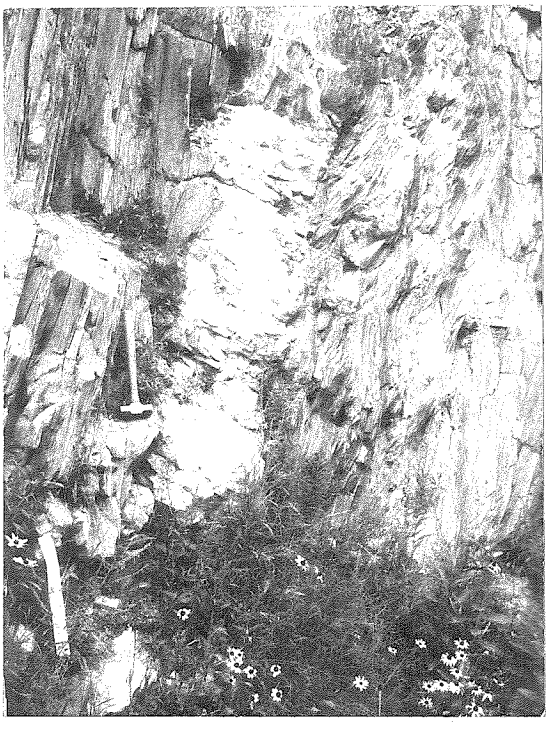

Figure 30 DV_a vein with blunt ends in Moretown member at location JR-122, Montpelier quadrangle.

mal boudins is perhaps the same except that vein growth occurred rather than plastic flow of surrounding host material. The veins can be up to 30 centimeters or so wide and have unequal planar dimensions. The planar dimension perpendicular to the average DF_a axial trend is considerably smaller than the planar dimension parallel to these axes. Therefore such veins have the general shape of a long parallelopiped.

Another style common in pre-Silurian rocks is shown in Figure 31. These veins are usually closely parallel to DS_a slip cleavage and have ends which pinch out as the width decreases. Except for the pinching out, their shape is similar to the above blunt-ended veins with their planar dimensions being unequal; the dimension parallel to DF_a axes is the longest. Such relationships are seen in roadcuts where a single vein is exposed on the face of the roadcut and on the top. DV_a veins of this style are developed where DS_a is not parallel to OS_a/OS_b but is a well developed slip cleavage. The veins are typically near the axial region of DF_a folds and may be produced by local extension perpendicular to the axial plane associated with the folding. The vein from location JR-5 in Figure 31 is in the axial region of a small DF_a synform. This style is common in the Underhill and Hazens Notch formations on the

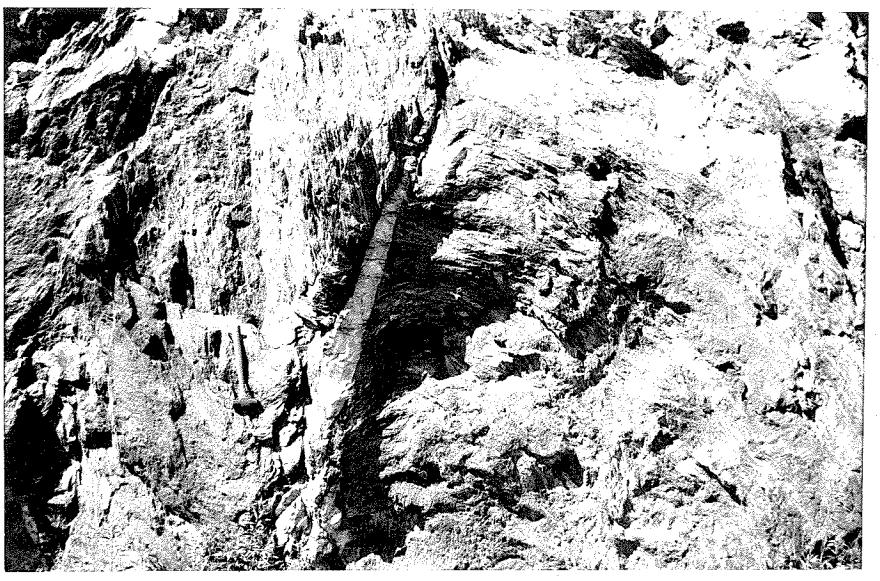

Figure 31 DV_a vein parallel to DS_a slip cleavage at JR-5, Camels Hump quadrangle. Vein is in axial region of a DF_a synform.

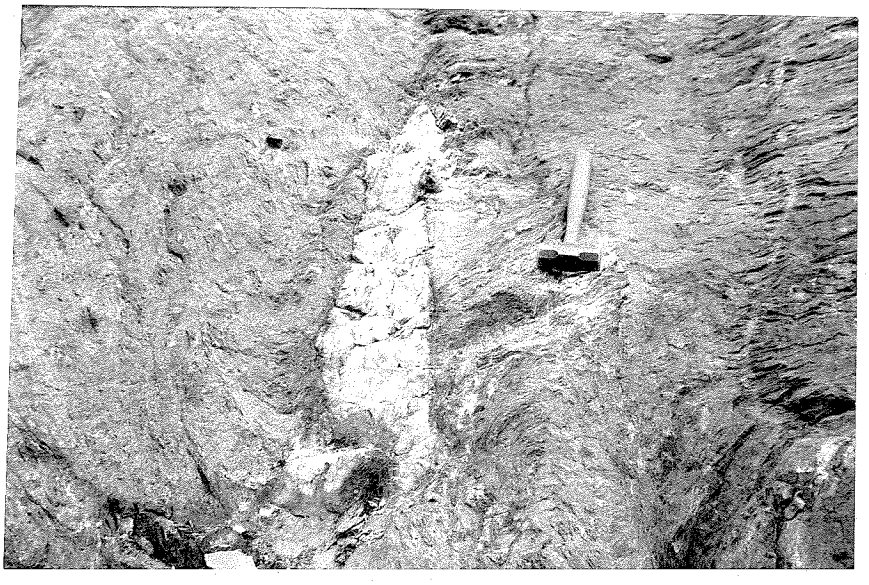

Figure 32 DV_a vein at location JR-163, Camels Hump quadrangle. Vein is hybrid type and is generally parallel to DS_a slip cleavage in Underhill schist.

limbs of the Green Mountain anticlinorium.

Some DV_a veins have one end that pinches out and one end that is blunt, as shown in Figure 32. These have features of both the blunt-ended boudin-filling veins and the lens-shaped axial-region veins. Perhaps a combination of the two mechanisms is involved. "Hybrid" veins such as these and axial-region veins can have widths of up to 2 meters or more in the widest part of the vein, but are more typically 7-15 centimeters at maximum width. Their extent within DS_a perpendicular to DF_a axes may be 2 or 3 meters, but this varies greatly. Their other dimension, where observed, is generally larger but probably not more than 10-15 meters. Very small veins of these types, one being an axial-region vein and the other perhaps a "hybrid" vein, are shown in Figure 33.

The last common type of DV_a vein is usually found in pre-Silurian amphibolites where DS_a is no more than a weak fracture cleavage. In these cases the veins are thin, fracture fillings such as shown in Figure 34. The veins are discontinuous and have dimensions typically smaller than the other styles. The veins terminate by pinching out.

As for other vein generations, DV_a veins can consist of a variety of minerals, with the specific assemblages determined by the host rock composition and the grade of

Figure 33 Small DV_a veins at JR-162, Camels Hump quadrangle. Host rock is Underhill schist.

Figure 34 DV_a veins parallel to DS_a fracture cleavage in Stowe amphibolite at location JR-155, Hyde Park quadrangle.

DM_a mineral growth. Most veins in host rocks which are quartz-bearing have a high proportion of quartz. Veins in amphibolite may be predominantly plagioclase, as is the case for the veins in Figure 34. All DV_a veins, except where intensely deformed, are coarse-grained.

DV_c

Unlike the other major vein generations, DV_c veins are not parallel to a well developed s-surface, nor are these veins related to any fold generation. DV_c veins are associated with a major mineral growth generation in their host rocks so that the event in which DV_c veins were formed involves only mineral growth of regional significance, an unusual metamorphic event. DV_c veins crosscut DF_b and DS_b and are deformed by DF_d folds, where they are developed. As there are minor vein generations which occupy this same position between DF_b and DF_d, another criterion for the identification of DV_c veins is that they are related to mineral growth in the host rock.

Most DV_c veins are thin, sheetlike bodies which have greater planar extents than the other vein generations. The veins terminate by pinching out. It appears that they are discontinuous although they are observed to be up to 50 meters or more in greatest exposed dimension. The width

varies from 2 to 15 centimeters. Because of their size, the terminations of DV_c veins are not always observed even in the larger outcrops so that it cannot be proven that all DV_c veins are discontinuous. However, a number of DV_c veins which are clearly discontinuous have been observed. Another style of DV_c veins appears as short lenses in one cross-section with a third, much larger dimension so that they are shaped like a long ruler with tapered edges. A number of the lens shaped veins may occur together in an en echelon arrangement or they may occur alone. Examples of both types of DV_c veins are shown in Figure 11 and Figures 35 and 36. Both types are not found together but are both apparently related to the same generation of mineral growth in the host rock.

At location JR-191 in the Lyndonville quadrangle, a DV_c vein crosscuts a semi-concordant granitic intrusive sheet, apparently related to the New Hampshire plutonic series. There is no reason to suppose that the DV_c veins are younger than all of the bodies of this igneous series but at least the phase represented by this intrusive sheet had time to intrude and completely solidify before the formation of the DV_c vein. Actually there is a close spatial relationship between the intrusive bodies of the New Hampshire series and the mineral growth in the host rocks

Figure 35 DV_c vein in Waits River formation at location JR-175, Lyndonville quadrangle. Vein has typical sheet-like form.

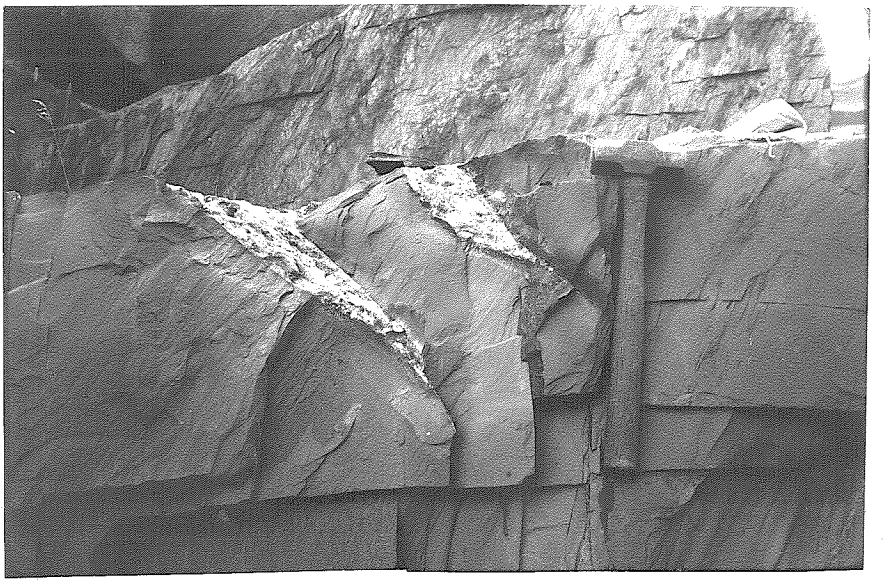

Figure 36 Lens-shaped DV_c veins in Waits River formation at location JR-189, Memphremagog quadrangle. Veins are roughly cut in half in this exposure.

with which DV_c veins are related. The grade of this mineral growth generation, DM_c, generally increases toward the larger bodies, particularly in the Lyndonville, Memphremagog, and Burke quadrangles within the study area. This is well shown on the isograd map of Doll and others (1961). The abundance of DV_c veins is regionally related to the granitic intrusives as the veins are most abundant in the above three quadrangles, but within these quadrangles the abundance of DV_c veins seems to be independent of proximity to an exposed pluton.

DV_c veins have also been observed far away from any exposed intrusives in the Cambrian and Ordovician rocks, although they are scarce in this area. Figure 37 shows the distribution of locations at which one or more DV_c veins have been observed. Even where the veins are most abundant, most of the outcrops have no more than one or two DV_c veins. There may be as many as 100 or more DV_a veins in the same outcrops. In the areas of least abundance, finding a DV_c vein is largely a matter of chance. The mineral growth generation is found throughout the area except for the far west and apparently DV_c veins can be found wherever DM_c growth is present in the host rock.

That the veins are related to DM_c growth has been shown by petrographic observations of many samples and

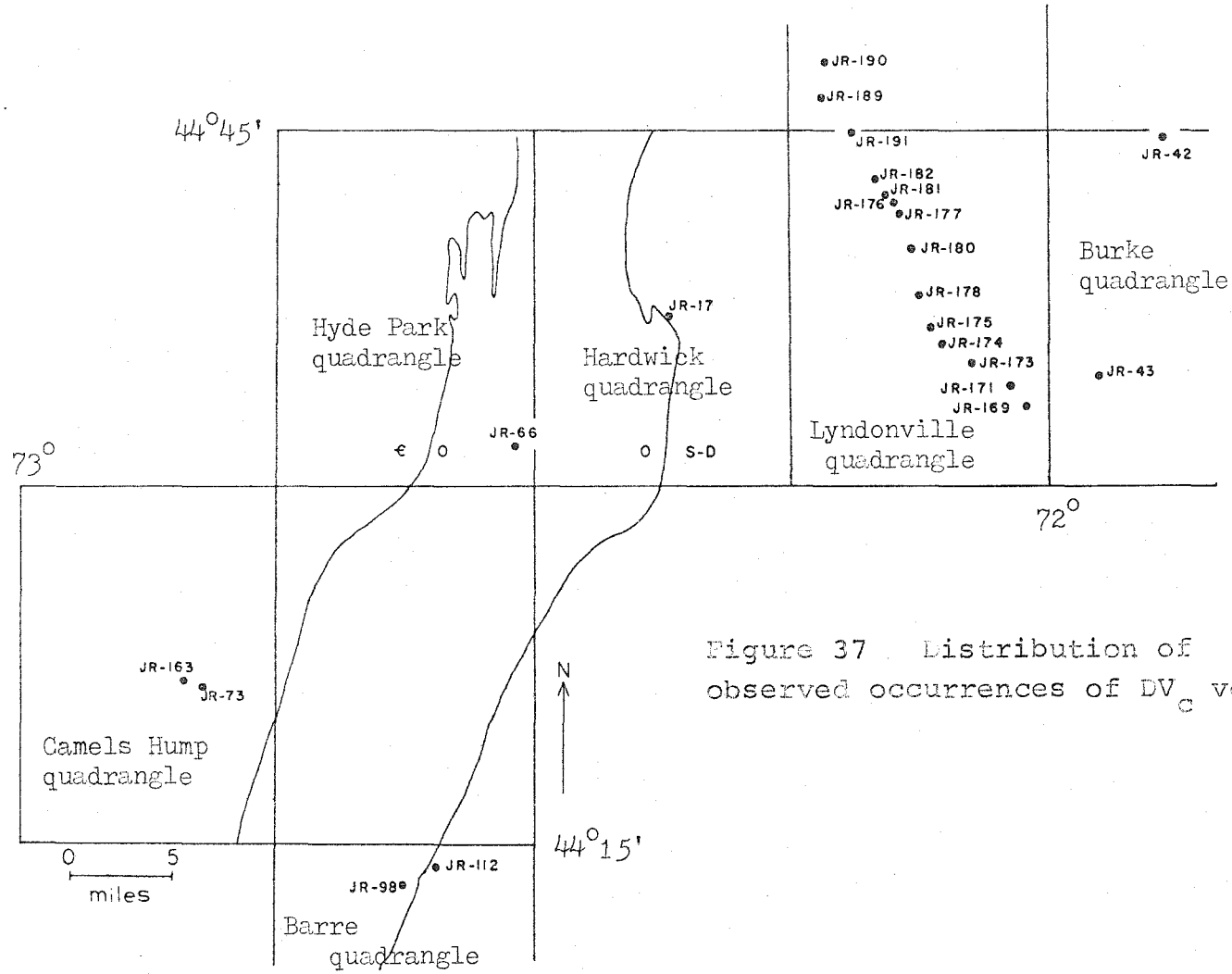

Figure 37 Distribution of observed occurrences of DV_c veins.

electron microprobe analyses of one sample, JR-190-A. In the northeast part of the area, near the plutons, DM_c mineral growth in the host rocks is characterized by porphyroblasts of various minerals such as biotite, muscovite, garnet, cummingtonite, and others which show no preferred orientation and are superimposed upon DS_a and DS_b (where present). These same minerals can be found in the DV_c veins as well as minerals such as calcite, sulfides, quartz, and plagioclase which are in the host rock but not as porphyroblasts. The vein textures are typically coarse-grained and are pegmatitic in the high-grade areas in the northeast. These veins may have been mistaken for pegmatites of igneous origin by some previous workers, but the mineral assemblages in the veins clearly rule out an igneous origin; some veins are 90% quartz, others may be mostly plagioclase, significant amount of chlorite and calcite can be present, and in most cases potassium feldspar is absent. The only reaction rinds observed to have formed around a DV_c vein are seen within the crosscut granitic sheet at JR-191.

Although DV_c veins have no apparent relationship to any small scale folds or s-surfaces, their orientation is not random. Most DV_c veins have attitudes which fall within the girdle shown in Figure 38, with an average strike of

Figure 38

Stereonet plot of poles to DV_c veins at all locations in the study area. Except for DV_c veins at locations near to the Willoughby pluton in the Lyndonville and Memphremagog quadrangles, all DV_c veins have poles that fall within the girdle shown.

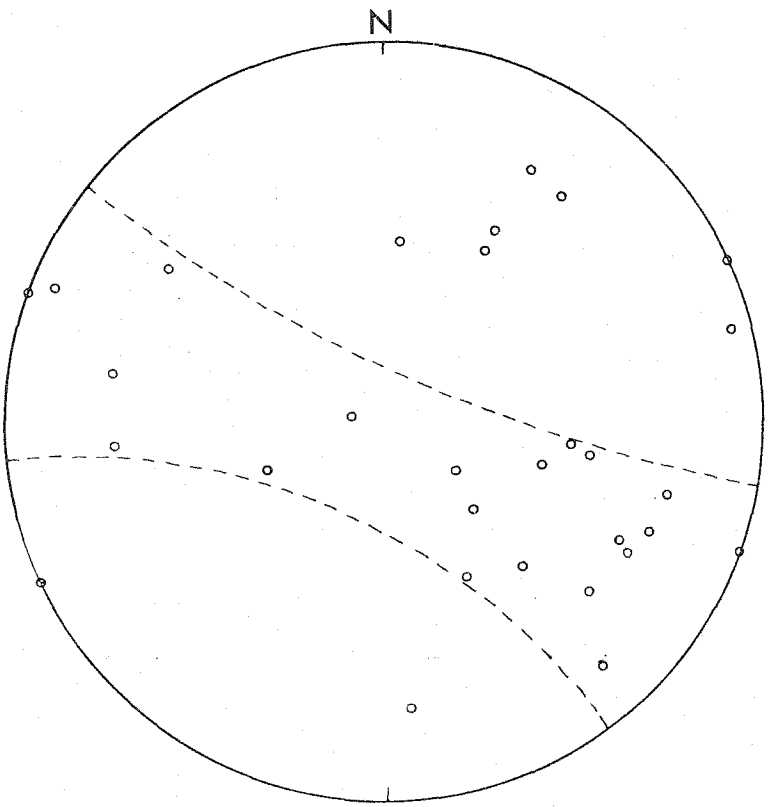

Figure 38

NNE. In part, the girdle is the dispersion pattern of DF_d folds; however, if the effects of folding were removed, the attitudes would probably not fall at a maximum. Those veins which do not lie within this girdle are all found at the locations nearest the Willoughby pluton in the Lyndonville and Memphremagog quadrangles. There are at least two possible explanations for this shift in orientation. One possibility is that forceful emplacement of at least the last phases of the plutonic series caused local deformation that produced this rotation after the veins were formed. The other is that perhaps the stress field, regional in extent as shown by the consistency of DV_c attitudes, was locally affected by the plutons, either as solid bodies or during their emplacement. The regular orientation of most DV_c veins argues against the stress field which produced the veins being a product of pluton emplacement. DV_c vein formation and the emplacement of some of the plutons may or may not have been roughly syncronous; they may be elements of a single event. The veins do not, however, seem to be directly produced by effects on the country rocks of the emplacement of New Hampshire series plutons.

Minor vein generations

In many locations there are vein generations which formed between the major deformational and mineral growth events. Minor vein generations are not related to any observed folds or s-surfaces and are not seen to be associated with mineral growth of regional extent. However, veins of a single minor generation can occur over a large area with perhaps a systematic orientation so that they are related to events of regional scale. The tectonic significance of minor veins is not treated in any detail in this thesis, as this would require a good deal of further work. These veins were studied in enough detail to roughly assign generations and show their time relationships to the major structural elements. The descriptions of the minor veins are included here because they may be of use in future investigations in northern Vermont.

The abundance of the veins of the minor generations is very small compared to the major generations such as OV_a, OV_b, and DV_a. Because of this, there is very little continuity of observation of a minor generation throughout an area. Veins of a generation may be found at an outcrop and the nearest outcrop at which that generation is also observed may be several miles or more away. Because of the low abundance, the identification of the minor veins is

based upon several factors including orientation and style, unlike the major generations. The most important factor in identification is the position of a vein in the structural sequence; the position is considered with regard first to the major elements and then to the other minor veins. Several minor vein generations may occur between two major events. If all of these minor generations are present at an outcrop, then the superposition relationships determine to which generation they belong. In many cases only one of the possible generations of minor veins is present in the position between elements of two major events at an outcrop so that superposition of minor veins cannot be used. In such a case, the orientation and, to a lesser extent, the vein style are used to identify the vein.

The identification of the major vein generations is fairly straightforward, but there is unavoidable ambiguity in the identification of the minor veins. The simplest possible sequence of minor vein generations has been used. The generations described below are the smallest possible number of generations as shown by crosscutting relationships and differences in structural position shown by the minor veins. For instance, three minor generations are defined between two major events if an outcrop is found in which three vein generations in that structural position

are present. The minor generations are defined only as required by the evidence from structural position, but given the defined generations, then identification of veins at outcrops where all of the minor generations are not present may rely upon the other factors.

The generations which have been defined are consistent with all field observations so that a vein of one generation is never seen to crosscut a vein assigned to a younger generation. Given only veins from locations at which there are superposition relationships among the minor generations, there seem to be consistent regional orientations of veins within each generation; as some of the other veins may have been assigned to a generation based in part upon orientation, these veins cannot then be used to make the argument that there is a consistent regional orientation. The ambiguity associated with the minor vein generations is of no consequence to the other aspects of this study.

OV_{a+} veins (OV_{a+1})

Throughout most of the Cambrian and Ordovician rocks, deformation by OF_b folding is very intense. If more than one pre-OF_b vein generation were present, they would be very difficult to distinguish. Where OS_b is a pervasive

transposition schistosity, only fragments of apparent veins are present. Where pre-OF_b veins are not so highly deformed, almost all appear to be OV_a veins. However, within the Moretown member there are a few highly granulated veins which have been found which crosscut OS_a, parallel to OS_o, and seem to be crosscut by OS_b, non-parallel to OS_o. These veins are small, lens-shaped veins which consist largely of fine-grained, granular quartz. The veins are called OV_{a+1}, but it must be stressed that the subsequent deformation has made the relationships somewhat less than straightforward.

OV_{b+} veins

There are at least three generations of veins which crosscut OF_b, OS_b, and OV_b but are deformed by DF_a and DS_a. The veins are found in the Moretown member of the Missisquoi formation near the unconformity and are observed to be highly granulated. Two, and possibly three, of these generations are present at the exposure of the unconformity already described, JR-108, in the Moretown and these veins are clearly pre-Northfield. These veins typically consist primarily of fine-grained, granular quartz with only small amounts of other minerals.

$\underline{OV_{b+1}}$

Developed within the eastern part of the exposed Cambrian and Ordovician strata is a generation of small veins, generally lens-shaped in cross-section. These typically occur in the more quartz-rich layers and are always observed to be highly granulated by subsequent deformation. These veins generally have ENE strikes and steep dips as shown in Figure 39.

OV_{b+1} veins are typically 1-2 centimeters wide and 15-30 centimeters long in cross-section. The other dimension is probably larger. Often they are developed with another set of veins of similar form which cross OV_{b+1} at varying angles. In a few locations it appears that this crossing set is younger than OV_{b+1}; however, the cross-cutting relationships of highly granulated quartz veins are rarely straightforward except when an offset of the older vein can be observed. Offsets of OV_b veins by OV_{b+1} veins and by OV_{b+2} veins are observed and, more rarely, small offsets of OV_{b+1} by OV_{b+2} are also seen.

$\underline{OV_{b+2}}$

Most OV_{b+2} veins are small lense-shaped veins similar to OV_{b+1}, with which they often occur. They are found

Figure 39

Stereonet plot of poles to OV_{b+1} veins at all locations.

Figure 40

Stereonet plot of poles to OV_{b+2} veins at all locations.

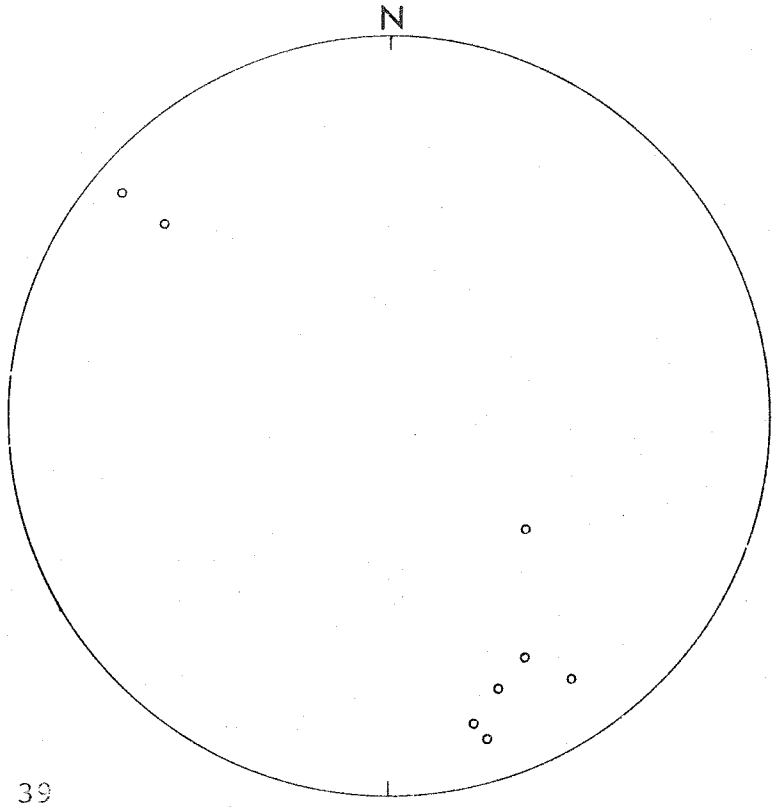

Figure 39

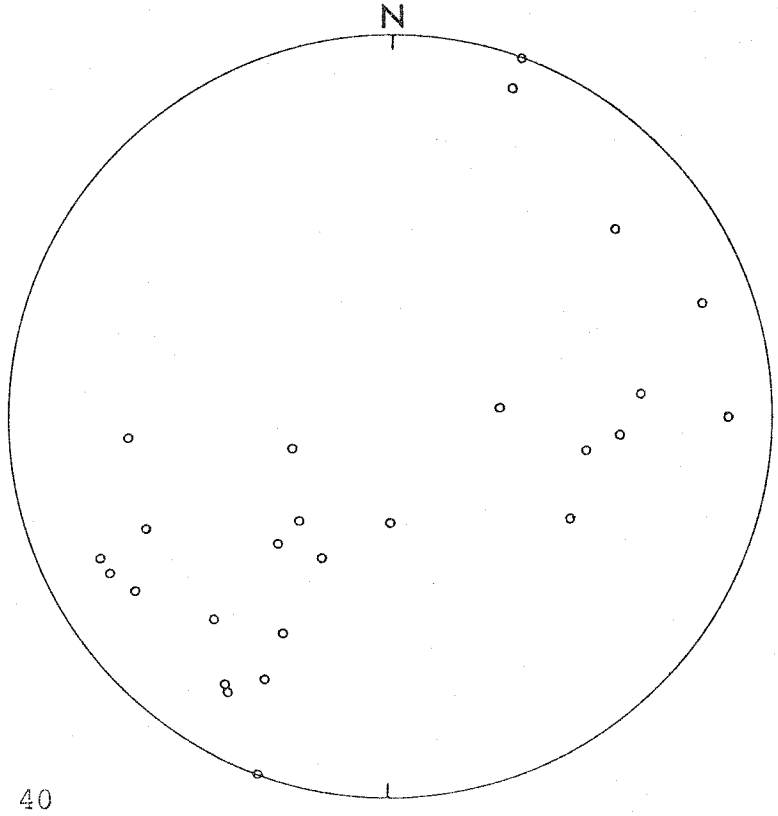

Figure 40

primarily within the Ordovician units, but a few veins in the Cambrian strata have been tentatively indentified as OV_{b+2}. Those in the Cambrian are more planar in form. Attitudes of OV_{b+2} veins are shown in Figure 40. As mentioned already, these veins may crosscut OV_{b+1} veins. However, there is no way to establish that there is any significant difference in the time of formation of the two generations.

A common style for OV_{b+2} veins is to form as extension fractures at a large angle, often 90^{o}, to OS_{o}. An example from location JR-115 is shown in Figure 41. Very different from this style are thin planar veins which are also tentatively assigned to OV_{b+2}. OV_{b+2} may well represent more than one generation, but there is no evidence of superposition.

$\underline{OV_{b+3}}$

A few discontinuous planar veins have been locally seen to crosscut OV_{b+2} veins. These veins are typically several centimeters wide and have exposed planar extents of a meter or so. The veins terminate by pinching out. The attitudes of OV_{b+3} veins are shown in Figure 42. These and the other OV_{b+} veins are of course deformed by DF_{a} and DS_{a}.

Figure 41 OV_{b+2} veins in Moretown member at JR-115, Montpelier quadrangle.

Figure 42

Stereonet plot of OV_{b+3} veins at all locations.

Figure 43

Stereonet plot of DV_{a+1} veins at all locations.

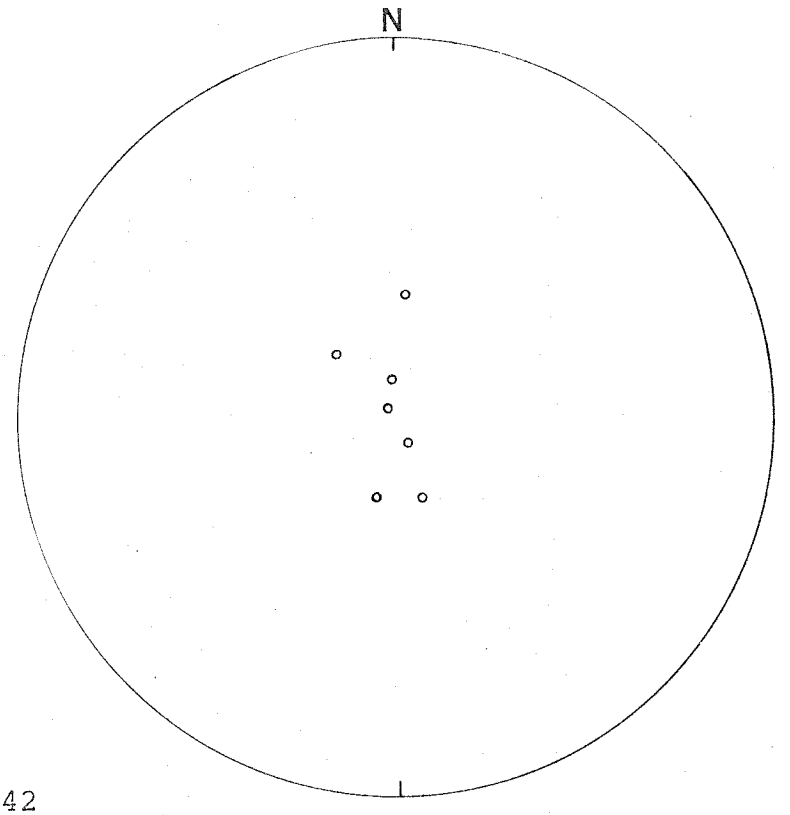

Figure 42

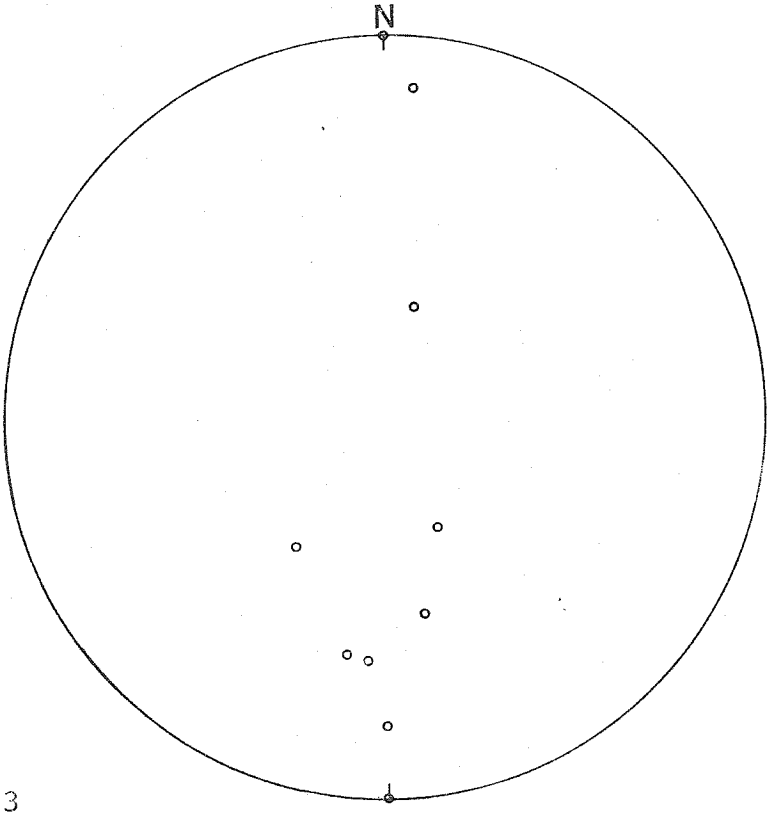

Figure 43

DV_{a+} veins

There are several generations of veins which crosscut D_a structures but are deformed by DF_b and DS_a. There are clearly at least three such generations, as at a few locations three distinct DV_{a+} sets can be observed. There may be more than three generations, but the assignment of all DV_{a+} veins to three generations does not produce any inconsistencies. The veins are characterized by simple mineral assemblages, typically quartz and/or calcite, plus occasionally observed minor amounts of plagioclase, chlorite, or sulfides.

DV_{a+1}

These veins range in width from 0.5 to 15 centimeters and in length from 15 centimeters to 10 meters or more. Their general form is planar, although the shorter ones are more lense-shaped in cross-section. DV_{a+1} veins are found in sets or singly and have been most often observed in competent rock types such as greenstone and amphibolite. They have general east-west strikes with varying dips as shown in Figure 43. As with the other DV_{a+} veins, DV_{a+1} veins are rarely observed in the Silurian and Devonian rocks, perhaps due to the lack of adequate field coverage.

DV_{a+2}

DV_{a+2} are planar veins with average widths from 0.5 to 2.5 centimeters and lengths of 5 to 10 meters on exposed surfaces. Typically only one or two of these veins are seen in an outcrop and they occur in many different types of host rock. The orientations of observed DV_{a+2} veins are shown in Figure 44.

DV_{a+3}

DV_{a+3} veins clearly crosscut DV_{a+2} veins at several locations and are not observed to be crosscut by any other DV_{a+} veins. They are typically 2 to 25 centimeters long and 0.5 to 8 centimeters wide in exposed outcrop surfaces. Attitudes of these veins are shown in Figure 45. DV_{a+3} veins are not very abundant.

DV_{b+} veins (DV_{b+2})

At five locations, veins have been observed which crosscut DF_b and DS_b but are deformed by DF_d. Where DV_c veins are present, DV_{b+} veins are crosscut by DV_c. The veins are also younger than DF_{b+1} folds. Although there may be more than one generation of these veins, they are all lumped into one general generation, DV_{b+2}. The veins are discontinuous planar veins with exposed widths of 0.5

Figure 44

Stereonet plot of poles to DV_{a+2} veins at all locations.

Figure 45

Stereonet plot of poles to DV_{a+3} veins at all locations.

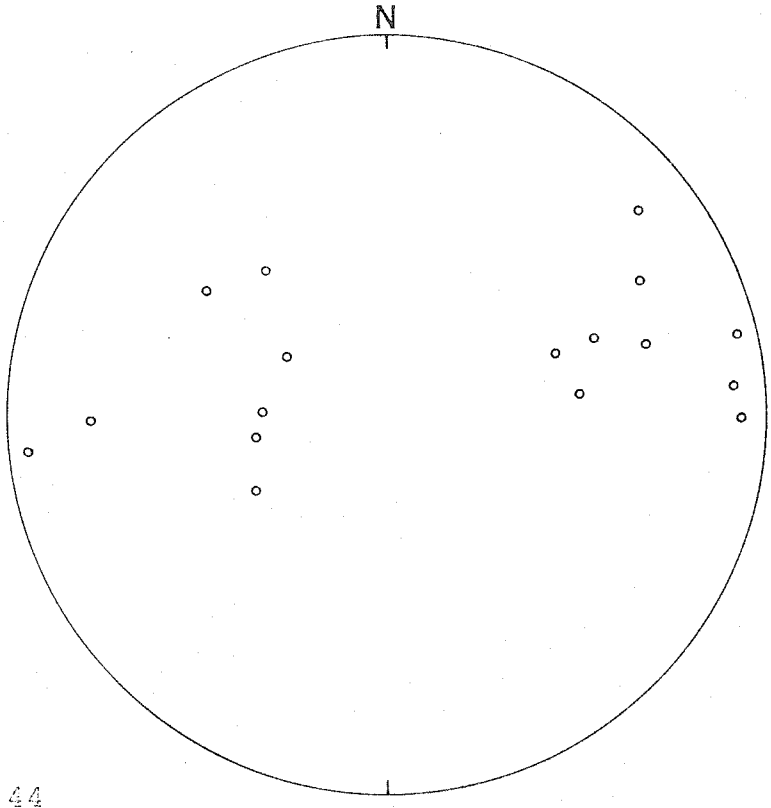

Figure 44

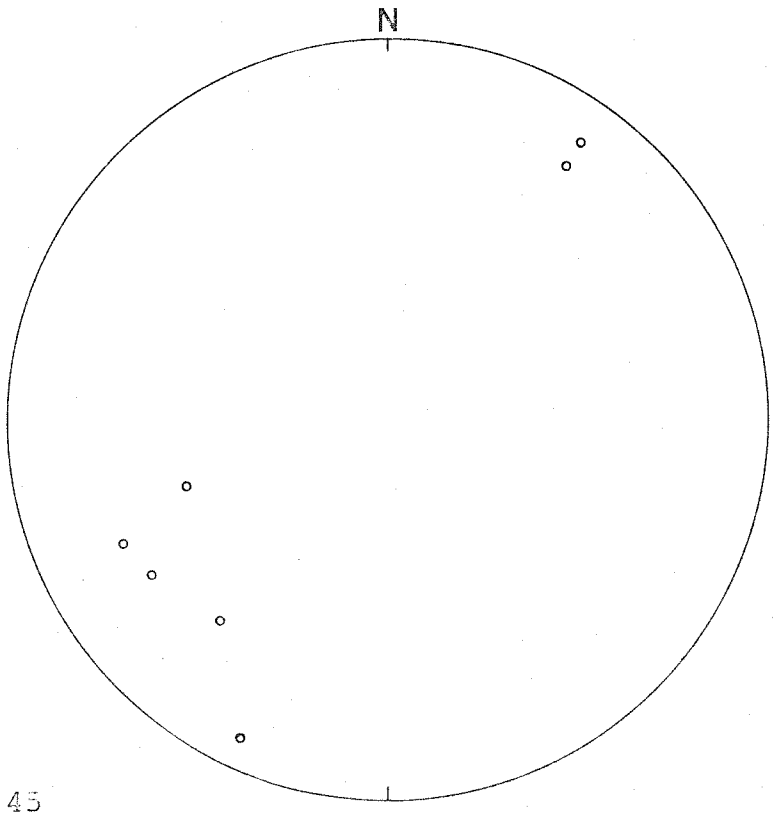

Figure 45

to 5 centimeters and lengths of 1.5 meters or more. Attitudes of observed veins are shown in Figure 46.

DV_{d+} veins

There are also veins in northern Vermont which cross-cut all known folds and penetrative s-surfaces. These veins appear as fillings of joints and/or small shear zones. The number of generations cannot be determined and they have not been treated in detail. The simple mineralogy, typically only quartz and/or carbonate, of these veins and their relationship to late, possibly post-metamorphic, structures indicates that they probably have no real significance to a study of the metamorphic history of the area.

H. Relationships between small scale and major folds

Two generations of large scale folding have been recognized by previous workers in the Silurian and Devonian strata of northern Vermont. These fold generations correspond to DF_a and DF_b in this study and are generally referred to as "early" and "late" folds. These were first recognized by White and Jahns (1950) and White and Billings (1951) and have been described by a number of subsequent workers. A good example of an area where the two generations of major and minor folds have been recognized is the

Figure 46

Stereonet plot of poles to DV_{b+2} veins at all locations.

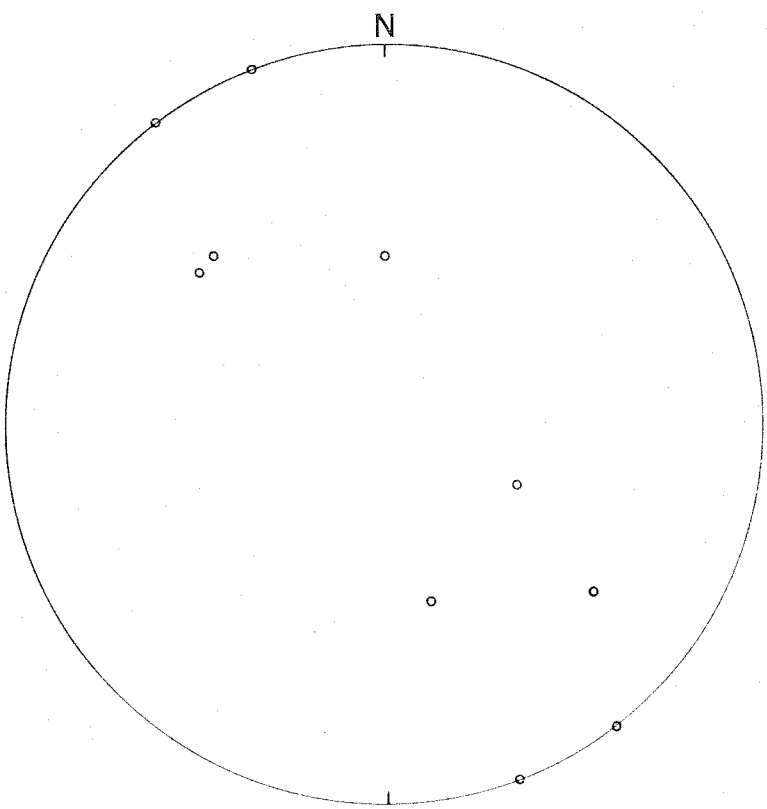

Figure 46

St. Johnsbury quadrangle where Hall (1959) mapped ten major folds. Five of these folds, including the Brownington syncline, were thought to be early folds with associated small folds; the Strafford-Willoughby arch plus four other major folds and associated minor folds were thought to be late folds. Dennis (1956) made a similar assignment of generations to the Brownington syncline (early) and the Strafford-Willoughby arch (late) in the Lyndonville quadrangle. There has been some dispute about the nature of the Brownington syncline (Murthy, 1957; Goodwin, 1963; Woodland, 1965 and in press) but in general this structure has been thought to be related to the early (DF_a) folding event.

In the pre-Silurian strata in the western part of the area the major folds of the north-south trending Green Mountain anticlinorium have been regarded as being related to the generation of prominent north-south small folds, recognized as DF_a in this study. Albee (1957) and Christman and Secor (1961), for instance, postulated the correspondence of these small folds and all of the major north-south folds were thought to be Devonian, although a firm correlation of these structures to a specific fold generation, early or late, in the east had not been made. Later, Albee (1968) suggested that some of the major north-south structures in the Worcester Mountain and Green Mountain

anticlinoria might be of Ordovician age. This was based in part on the structural relationships and the retrogradation of high grade assemblages observed in the vicinity of Elmore Mountain in the Worcester range. As previously discussed, results of this study indicate that all of the small scale folds with north-south trends in the Worcester Mountains are probably DF_a and younger generations. The pre-Silurian small folds present have the typical east-west axial trends of OF_b. The higher grade minerals such as kyanite are related to the axial plane schistosity OS_b. Garnet and kyanite are found in OV_b veins on Elmore Mountain and at locations to the south in the Worcester Mountains. The possibility of large pre-Silurian north-south folds cannot be ruled out, but there seems to be no evidence in the form of small scale folds.

Although gentle DF_b folds and perhaps very gentle DF_d folds are found in the Green Mountain and Worcester Mountain anticlinoria, the results of this study essentially verify the early work for, excepting the far western part of the area, only one generation of prominent north-south trending small folds are found; it seems reasonable to postulate that these small folds, now known to correspond to DF_a folds in the east, are related to the major north-south trending folds.

The only other generation of major structures recognized in the study area are the isolated east-west trending folds in the Jay peak and Irasburg quadrangles, first demonstrated by Cady, Albee, and Chidester (1963). These structures include a syncline known as the "trilobite" in which J. Laird (pers. comm.) has found the only known occurrence of glaucophane in New England. The large east-west folds seem to be related to abundant small, isoclinal OF_b folds. At least some of the glaucophane grains appear to have a preferred orientation parallel to an s-surface (perhaps OS_a) which is folded by small OF_b folds. These large east-west folds are the only documented features of this orientation and, if indeed they are OF_b folds, the only recognized pre-Silurian major folds in northern Vermont.

As folds with wavelengths on the order of 10 meters or less are the only folds typically exposed in an area such as northern Vermont, the evidence for larger folds is necessarily indirect. The largest folds have been mapped on the basis of stratigraphic pattern and changes in the dip of bedding. Another type of data used extensively in the eastern part of the area is the sense of the pattern of small asymmetric folds as observed in plan view, described by White and Jahns (1950). The small folds were assumed to

be secondary or "drag" folds which could be related to the geometry of the larger folds.

When used with caution, the sense of small folds should be useful in the study of the large structures. In some instances, the small folds were used, beyond their reliability perhaps, to make major hypotheses about regional structure and, as a consequence, about relative stratigraphic ages. The problem in the use of small folds lies in the fact that the observable folds are not secondary to the major folds but are secondary to folds of smaller wavelength than the major folds. In the larger outcrops of northern Vermont, particularly the extensive roadcuts along Highway I89, as many as four orders of folds can be observed. The folds of the size typically observed in smaller outcrops are usually second or third largest in the large outcrops. Between the largest folds observed in the largest outcrops and the major folds that have been mapped there may be several orders of fold sizes of a single fold generation. The sense of the typically observed folds therefore reflect upon the geometry of folds that are many orders smaller than the major folds. In an area with a generation of highly asymmetric folds, statistically more of the outcrop should be on the long limbs of the various orders of folds. If the sampling size is large enough, the

statistically predominant sense of small folds should indicate the geometry of the major folds. However, in a case such as DF_a folds in the Silurian and Devonian rocks a small sample size can lead to major errors.

The recognition of the importance of DF_b folds in the Cambrian and Ordovician strata brings up the question of major folds of the same generation in the area of the Green Mountain anticlinorium. DF_b here is manifested both as small open folds observed in outcrops and as dispersion of DF_a and DS_a attitudes. As is found to the east in the area near the Willoughby arch, there well may be broad major DF_b structures superimposed on the earlier DF_a folds. The data from this study are insufficient to determine which, if any, of the major folds in the pre-Silurian rocks may be DF_b folds. Reversals of sense of small DF_b folds, the criterion described above that has been used to identify fold axes in some previous studies, occur in several places along the Winooski River traverse of this study. By chance or not, these reversals coincide with such major fold axes as the main axis of the Green Mountain anticlinorium, the Worcester Mountain anticline and the syncline that occurs between these two. The small folds are in the sense reversed of that which would be expected for these structures. While there is less consistency, perhaps due to more meas-

urements, small DF_b folds also show reversals in sense that coincide with the axes of major folds to the west of the Green Mountain main axis. DF_a folds show patterns with the normal sense expected for small folds on these large folds as they are mapped. In a more complete study of a single quadrangle along the Green Mountain axis, Christman and Secor (1961) in their study of the Camels Hump quadrangle were unable to find any consistent relationship between the sense of small DF_a folds and the major folds that they mapped. Christman (1959) describes a similar situation in the Mt. Mansfield quadrangle.

If major DF_b folds are present in the Cambrian and Ordovician section, such folds might be expected to be much more open than the major DF_a folds, assuming that the small folds reflect the geometry of the large folds. The use of the sense of DF_b small folds must be approached with caution, even if they do reflect on the major structures, as they are thought to be consistently reversed in sense in eastern DF_b structures such as the Willoughby arch (Dennis, 1956; Hall, 1959). This effect has been postulated to be due to vertical uplift rather than lateral compression being the mechanism for arching and doming. Data collected on DF_b folds across the Willoughby arch in the Lyndonville quadrangle are in complete disagreement with the reported re-

versal in sense, but data from a single traverse are insufficient to disprove earlier observations. It may depend upon where the data are collected along the axis of this structure.

As DF_b small folds are more intense and prominently developed in the western part of the Camels Hump quadrangle, and the eastern part of the Burlington quadrangle, this may be the most likely area in the pre-Silurian strata to look for major DF_b folds. At present, it appears probable that at least most of the major north-south trending folds that have been mapped within the Green Mountain anticlinorium and elsewhere in the pre-Silurian rocks are DF_a in generation. Finding gentle folds superimposed on the more intense and prominent DF_a folds will probably be very difficult.

Another generation of generally north-south trending folds that have not been widely recognized before are the very gentle DF_d folds which are best developed in the Lyndonville quadrangle. There is no evidence that these are associated with any major folds, but the possibility exists. The previous workers who did not recognize the small DF_d folds certainly did not consider the possibility of major DF_d structures. One point that clearly emerges from the observation of three fold sets with essentially parallel

axial trends is that the parallelism of minor fold axes to major fold axes is only a permissive criterion in determining the correspondence of minor and major structures.

The other major structural elements of northern Vermont are the plutons of the New Hampshire plutonic series. Except for thin, semi-concordant granitic sheets, there were no field observations in this study of the contacts between such intrusives and their host rock. All of the contacts that I attempted to investigate were covered by surficial deposits. The few observations in this study indicate that the semiconcordant sheets were emplaced after DF_b folding and before DV_c vein formation. Any analysis of the structural relationships of the larger bodies must rely on previous work.

In all of the previous studies in northeastern Vermont, it has been pointed out that the actual contact surfaces between plutons and host rock are rarely observed. Woodland (1965), in the Burke quadrangle, found a few good exposures of the contact between granitic bodies and host rock; he observed that the emplacement occurred after the formation of the early schistosity (DS_a) and the late cleavage (DS_b). In the St. Johnsbury quadrangle Hall (1959) observed that the earlier folds (DF_a) were clearly truncated by pluton emplacement, but as an actual contact surface was

never found, the relationship to the later D_b structures was not clear. Konig (1961) suggested that the emplacement of the Knox Mountain pluton in the Plainfield quadrangle was associated with the formation of later folds (presumably DF_b). Thus in one case, emplacement of a pluton of the New Hampshire series may be clearly later than DF_a folding but perhaps synchronous with DF_b folding. There is no reason to suppose that emplacement of the various plutons of the series could not have occurred over a reasonably long period of time so that the relationship between DF_b folding and emplacement could vary. However, the widespread occurrence of DF_b folds and the limited extent of New Hampshire series plutons is convincing evidence that DF_b folding is not a direct result of igneous intrusion.

One other line of evidence is the relationship between DV_c veins and DM_c mineral growth in the host rock. DM_c growth seems to have resulted from a thermal event spatially related to the plutons. DM_c porphyroblasts and DV_c veins are clearly younger than DF_b folds and DS_b foliation at the locations studied. If the emplacement of most of the plutons is roughly synchronous with DM_c growth (it may not be), then DF_b folding is older than the New Hampshire series granitic bodies.

I. Timing of structural events

The relative structural ages of the various elements have been extensively discussed in the preceding sections. Further control on the ages of structural elements can be obtained by using the stratigraphic control provided by the units which are affected or not affected by a given element and also by using isotopic age determinations. For the pre-Silurian elements there is good stratigraphic control. Those elements which occur in the Silurian and Devonian rocks have an upper age limit established by stratigraphy, but no practical stratigraphic lower limit. The discussion of stratigraphic age limits uses the ages of the various formations given by Doll and others (1961).

All of the elements observed in the Ordovician and Cambrian rocks can be found in the youngest unit, the Missisquoi formation, which is thought to be Middle Ordovician in age. The pre-Silurian elements are all truncated by the unconformity on which the Shaw Mountain and Northfield formations were deposited. The beginning of deposition of these units is thought to have occurred in the Lower to Middle Silurian. If these stratigraphic ages are correct, then there is very good control on the stratigraphic age of the pre-Silurian structural elements; they must be Middle Ordovician or younger, but no younger than

Lower to Middle Silurian. This is a relatively small span of time, perhaps 20-30 m.y. or a little longer.

The post-Silurian structural elements affect the Lower Devonian strata of the Waits River and Gile Mountain formations, thereby limiting their age to Lower Devonian or younger. Except for surficial deposits, there are no strata younger than Lower Devonian exposed in northern Vermont. Isotopic evidence must be used to further define the age of these structures.

The isotopic data available can be considered to be of two types: direct and indirect. Direct determinations are isotopic ages obtained on primary mineral grains which occur within a structural element such as a plutonic body or a metamorphic vein. Indirect isotopic ages are those determined on mineral grains in the host rock which are interpreted to be of a particular mineral growth generation.

Direct ages are much more satisfactory for determining the timing of structural events. If there are no effects of overprinting by later thermal events, the age obtained is a direct age of the formation or cooling of the structural element. All elements which are structurally older must also be older in terms of absolute age. The use of direct age determinations requires far less interpretation than the use of indirect ages.

The use of metamorphic veins in this study has allowed the correlation of mineral growth generations and structural elements. If mineral grains of a particular growth generation are isotopically dated then this is an indirect age determination of the structures related to that generation. Even more interpretive is the use of isotopic data to date the youngest major thermal overprint event. Mineral grains which appear to be of Ordovician age based on structure may have Devonian K-Ar ages due to the thermal overprint of a Devonian thermal event. If there is evidence from the veins of such a high grade thermal overprint, for instance the presence of high grade minerals in DV_a veins, then the isotopic data may be interpreted as reflecting this overprint. Because of the great uncertainty of the interpretation of indirect ages, such ages will be shown with a question mark when they refer to a specific structural event.

There is only one available direct age of a pre-Silurian vein. This is the 439±9 m.y. age obtained by Lanphere and Albee (1974) on coarse muscovite from an OV_b vein in the Worcester Mountains (location LA-384 of Albee, location JR-129 in this study). Lanphere and Albee also obtained a date on hornblende in the Worcester Mountains of 457±26 m.y. Both ages were determined with the $^{40}Ar/^{39}Ar$ method. The hornblende is from Albee's location LA-385, equivalent to location JR-89 in this study. Based on the vein rela-

tionships, I interpret the hornblende to be OM_b in generation. Within the error the two ages are equivalent, but the direct determination on the OV_b vein requires less interpretation and is used as the minimum age of event O_b.

Unpublished conventional K-Ar and $^{40}Ar/^{39}Ar$ ages have been measured by M. Lanphere for host rock muscovite and biotite separates from samples of pre-Silurian rocks collected by A. Albee from Mt. Grant in the Lincoln Mountain quadrangle. There are several consistent ages which indicate a significant thermal event at around 375 m.y. Work in this study has been done to the north and to the south of Mt. Grant, but not in the Mt. Grant area itself. At these locations there is evidence of the presence of both OM_b and DM_a growth. There is no evidence of DM_b or DM_c growth. I cannot establish whether the ages reflect a thermal overprint on OM_b growth resulting in argon loss or are ages of argon retention in primary DM_a growth. In either event, it seems reasonable that the ages reflect the timing of event D_a. Obviously this interpretation is highly speculative.

There are also isotopic data available on samples from plutons of the New Hampshire plutonic series. Muscovite and biotite from three plutons in northeastern Vermont have been dated by Naylor (1971) using Rb/Sr. For the muscovite

samples the ages range from 380 to 344 m.y., with concordant results from the biotite. However, Naylor (1971) chose to discard those ages younger than 380 m.y. because microcline and plagioclase in those samples from which the younger ages were obtained appeared to be altered by a younger event. While I have no data on trace element compositions, it is not uncommon for the major element compositions of muscovite to appear to be unchanged in samples in which the feldspar is highly altered. This is true of muscovite in the DV_c sample JR-190-A, which is from the Lyndonville quadrangle in an area where the alternation of feldspar in both granitic intrusive rocks and DV_c veins is commonly observed. It may be that Naylor observed good evidence that the muscovite and biotite in these samples were disturbed, but if the textural evidence of overprint was clearcut the age determinations presumably would not have been made on these samples. In any event, Naylor's data seem to be the best available for intrusives in northeastern Vermont and an age span of 380-344 m.y. is not unreasonable for the emplacemant of the intrusive series.

Lanphere and Albee (1974) also obtained a $^{40}Ar/^{39}Ar$ age on fine-grained muscovite, pseudomorphic after kyanite (the kyanite is OM_b in generation), of 358 ± 4 m.y. There appear to be two post-OM_b generations of mineral growth,

both of which are characterized by the retrogradation of the garnet and kyanite grade OM_b assemblages. The oldest generation is generally medium- to fine-grained in texture and is probably DM_a. Superimposed on both the OM_b and DM_a growth is a very fine-grained mineral growth, thought to be DM_c. In general it is impossible to separate the effects of DM_a and DM_c. The fine-grained muscovite is clearly post-OM_b, but could be either DM_a or DM_c. The 358 m.y. age corresponds to the later stages of intrusion of the New Hampshire series. DM_a growth is structurally older than the intrusives, but DM_c growth may be closely related in time. For these reasons, the age is thought to reflect DM_c mineral growth. This isotopic age cannot really be used in determining the timing of event D_c because of difficulties in the interpretation.

There are no data which reflect upon the age of DF_d folding other than it is post-DM_c and probably post-New Hampshire plutonic series. DF_d folds are therefore younger than about 350 m.y. Zartman and others (1970) present evidence of a possible Permian thermal disturbance that affected the Paleozoic rocks of New Hampshire and perhaps southeastern Vermont. This event has an age of 260-200 m.y. There is a late alteration of DM_c mineral growth, which is called DM_e in this study, that could conceivably represent

this event. This is only a speculative suggestion, however.

Table 4 shows the major events and their stratigraphic and isotopic ages. The events are listed in relative structural age with the oldest at the top. Some ambiguity may always remain, however, as it cannot be assumed that a structural element was formed throughout a large area such as this at the same time at every place.

Table 4 Age relationships in northern Vermont

Event	Stratigraphic age (1)	Isotopic age
End of deposition of Missisquoi formation	Middle Ordovician	
O_a (OS_a, OM_a, OV_a)		
O_b (OF_b, OS_b, OM_b, OV_b)		439 ± 9 m.y. (2)
Major erosional unconformity		
Beginning of deposition of Shaw Mountain and Northfield formations	Lower to Middle Silurian	
End of deposition of Waits River and Gile Mountain formations	Lower Devonian	
D_a (DF_a, DS_a, DM_a, DV_a)		~375 m.y. ? (3)
D_b (DF_b, DS_b, DM_b)		
New Hampshire plutonic series (may in part be synchronous with D_b)		380-344 m.y. (4)
D_c (DM_c, DV_c) (may be roughly synchronous with some plutons of the New Hampshire series)		(358 ± 4 m.y. ??) (2)
D_d (DF_d, DS_d)		
(DM_e)		(260-200 m.y. ??) (5)

(1) Doll and others, 1960

(2) Lanphere and Albee, 1974

(3) Unpublished data of Albee and Lanphere

(4) Naylor, 1970

(5) Zartman and others, 1970

CHAPTER III. GENERATIONS AND CHARACTER OF MINERAL GROWTH IN METAMORPHIC VEINS AND HOST ROCKS

A. Summary of mineral growth generations in northern Vermont

Five major mineral growth generations occur in northern Vermont; four of these occur much more widely than the fifth. A sixth mineral growth generation has only been tentatively demonstrated. Two major generations affect only the pre-Silurian rocks and are designated OM_a and OM_b. Two major generations, DM_a and DM_c, affect large areas of both pre-Silurian and Silurian and Devonian rocks. DM_b is generally low grade mineral growth occurring in rocks in which the axial plane foliation DS_b is well developed. Superimposed upon the youngest major generation, DM_c, is retrogradation of minerals such as garnet and plagioclase. There may also be some post-DM_c growth of porphyroblasts of low grade minerals such as chlorite. This may represent a late stage in DM_c growth or may be a separate generation. This mineral growth is tentatively called DM_e, although it cannot be clearly demonstrated as a separate generation with the type of structural evidence that establishes the other generations.

The grade of metamorphism reached in each mineral growth event varies over the area in such a way that the

inferred isograd surfaces of the various generations do not coincide nor in general do they approach parallelism. This produces a very complicated, hybrid isograd map pattern when only one generation of isograd surfaces is assumed. Three generations, OM_b, DM_a, and DM_c, attained garnet grade or higher in wide-spread areas of northern Vermont, as discussed in later sections of this chapter.

$\underline{OM_a}$

OM_a mineral growth, restricted to pre-Silurian rocks, is seen as growth in OV_a veins and growth in the host rock of grains parallel to the bedding schistosity OS_a. In general, the overprint of the later events, both in terms of deformation and apparent recrystallization, is very intense; OM_a is often present as apparently no more than a structural element whose minerals have chemically changed from their original state. This can be seen in samples from locations JR-4 and JR-5 where OS_a can be observed; there is chemical evidence of only limited survival of OM_a minerals in the samples analyzed with the microprobe. Throughout most of the area of exposed pre-Silurian rocks, the highest grade attained during OM_a growth appears to have been biotite grade. Some garnet grade growth may have occurred in limited areas, but the later overprint makes the interpretation

of such samples difficult. Biotite grade OM_a growth was clearly widespread and it seems unlikely that there was any OM_a growth of any grade higher than garnet grade.

$\underline{OM_b}$

OM_b mineral growth is very prominent in samples from throughout the exposed pre-Silurian rocks in the study area. OM_b growth is seen both in OV_b veins and in the host rocks. Minerals which tend to show preferred orientations are oriented parallel to the axial plane schistosity OS_b in the host rock. The same minerals occur in OV_b veins but without preferred orientation. Although OM_b growth is biotite grade through much of the area of exposed pre-Silurian strata, two important areas are garnet grade and kyanite grade. The largest high grade area is within the Green Mountain anticlinorium, extending from the southern limit of the study area, north at least to the Lamoille River and perhaps continuously to the northern limit in the Jay Peak quadrangle where OM_b garnet occurs in the vicinity of Hazens Notch (location JR-154). The other main area of high grade OM_b mineral growth is in the Worcester Mountains, where garnet and kyanite grade assemblages occur. Albee (1968) shows the two main areas of high grade OM_b growth as the Worcester Mountain higher-grade zone and the Green Mountain

higher-grade zone in his Figure 25-1. Albee (1968) reports staurolite in the kyanite grade assemblages from both areas (locations 1, 30, and 31 in his Figure 25-1). OM_b assemblages with kyanite, but no garnet, are found in the host rock and OV_b veins in the Umbrella Hill member of the Missisquoi formation in the Lowell Mountains. The Lowell Mountains are essentially the northern extension of the Worcester Mountains. The Umbrella Hill rocks have unusual compositions, very aluminous, high in Fe^{3+} and low in Fe^{2+}, which probably excludes the formation of garnet. Other areas of high grade OM_b growth may be obscured by later overprint.

$\underline{DM_a}$

DM_a is a major mineral growth generation which has significantly affected virtually the entire study area. In the Silurian and Devonian rocks DM_a growth represents the first major metamorphic mineral growth in the rocks and is also seen in DV_a veins. Muscovite, biotite, chlorite, and some other minerals have preferred orientations parallel to the axial plane schistosity DS_a. In the pre-Silurian rocks, DM_a growth is superimposed upon the earlier assemblages, with grains of minerals such as chlorite and muscovite commonly showing preferred orientation parallel

to DS_a slip cleavage or schistosity. DV_a veins are also abundantly developed in the pre-Silurian rocks. DM_a is always observed to be either biotite grade or garnet grade where it can be detected; it is inferred to be biotite or lower grade elsewhere. It is sometimes difficult to interpret the grade of DM_a in an area due to the overprint of DM_c in the Silurian and Devonian rocks and the intermixing of OM_b and DM_a assemblages in the pre-Silurian rocks, but its grade can be well established in several areas. In the vicinity of Eligo Pond in the Hardwick quadrangle (locations JR-16, JR-17) there is garnet grade DM_a growth and garnet grade DM_a assemblages are also observed at location JR-37 in the Hardwick quadrangle. Garnet grade DM_a growth is observed in the central part of the Barre quadrangle along I89 (JR-203) as well as at locations in the St. Johnsbury and Lyndonville quadrangles which are discussed later. The coverage is not sufficient to delimit the areas of DM_a garnet grade growth, but it is certainly not uncommon. Along the Winooski River traverse in the Green Mountain axial region, DM_a growth does not seem to attain garnet grade, but in pelitic rocks there is DM_a oligoclase and andesine plagioclase. In the Worcester Mountains, DM_a growth appears to be biotite grade.

DM_b

DM_b is commonly observed as the growth of chlorite, biotite, and/or muscovite grains parallel to DS_b and cross-cutting DS_a. As DS_b is not developed in large areas of northern Vermont, particularly in most of the pre-Silurian rocks, DM_b growth is apparently absent in a significant proportion of the rocks. Where DF_b folding is intense but DS_b is not prominent, microprobe analysis may provide chemical evidence of possible DM_b growth; an example is sample JR-11-D from the St. Johnsbury quadrangle. In general it seems that where DS_b is not well developed, DM_b growth is either minor or absent. DM_b growth was not observed to be higher in grade than biotite grade. The D_b event appears to be largely a deformational event. In the vicinity of the Athens and Chester domes in southern Vermont, Rosenfeld (1968) has observed garnet growth that appears to correlate with DM_b. The garnet porphyroblasts studied by Rosenfeld seem to record growth during rotation that accompanied late folding associated with doming; these late folds are probably equivalent to DF_b. Nothing comparable to this DM_b garnet growth has been found in the present study area.

DM_c

Of the various mineral growth generations, DM_c has the

widest variation in grade and prominence. In northeastern Vermont, DM_c growth can be seen as porphyroblasts of minerals such as garnet, biotite, muscovite, staurolite, cummingtonite, hornblende and others which show no preferred orientation. There is some apparent preferred orientation of biotite which nucleated on DM_a ilmentite grains, but the ilmenite cores are generally preserved so that the mimetic relationship is not obscured. In the pre-Silurian rocks, DM_c growth is not so prominent. It is characterized as retrograde alteration of pre-existing DM_a and OM_b minerals. In some areas of the exposed pre-Silurian rocks there is little or no evidence of DM_c growth. DM_c growth is also found in DV_c veins which are most abundant in the northeast, but a few can be found in the pre-Silurian rocks, such as at locations JR-66 and JR-163. In the northeast near the plutons of the New Hampshire plutonic series, DM_c growth attained sillimanite grade. Garnet and staurolite grades are more typical in the northeast and there are large areas of biotite grade DM_c growth. In the pre-Silurian rocks it appears that DM_c is nowhere higher than biotite grade. The high grade DM_c growth seems to have a close spatial relationship to the plutons of the New Hampshire series, although the regional extent of DM_c rules out a direct contact metamorphic origin for DM_c. The grade of DM_c growth

generally decreases with increasing distance from the nearest pluton.

B. The intergranular fluid phase--assumptions and evidence

Implied in the discussion which follows is the presence of an intergranular fluid phase through which diffusion of dissolved chemical species can occur. Such a fluid is expected to consist predominantly of H_2O, CO_2, and related species plus lesser amounts of S species. These are the volatile constituents that are present within the mineral phases and there must be a finite vapor pressure of these various species in equilibrium with the minerals. The fluid appears to be able to move from the host rock into discontinuous fractures which become filled with vein material. Even when the fluid is static it appears that transport by diffusion of dissolved species can occur. Knowledge of the specific composition and quantitative thermodynamic properties of the fluid are not necessary for this study.

One line of evidence that bears upon the presence of a fluid phase is the type and degree of equilibrium achieved on several scales. The common preservation of major element zoning is evidence that diffusion within single grains is restricted relative to the time scale involved and that equilibrium in the solid state is not achieved in general.

In a particular sample, grains of a given mineral type and mineral growth generation display similar zoning patterns. In many samples studied, the chemical zoning relationships suggest that there may have been a systematic compositional variation trend. A single grain does not in general preserve the entire compositional path of growth for that mineral type, exceptions being minerals such as garnet that tend to form a small number of large porphyroblasts. The similarity of zoning patterns indicates that the activities of the major chemical species were relatively uniform within the system; this apparently leads to a fairly close approach to equilibrium between simultaneously growing grain surfaces. The equilibrium between grain surfaces must be explained by some mechanism other than solid state diffusion, for such diffusion is clearly restricted. Therefore a non-solid diffusion medium must be present, such as the intergranular fluid which is indicated by the presence of volatile constituents in the mineral phases.

Samples of this fluid are preserved as inclusions in veins and are commonly observed in vein minerals such as quartz, apatite, and calcite. The vein samples from the study area typically have fluid inclusions which range in diameter from 1 to 15 microns. No attempt was made to observe smaller inclusions. The inclusions contain either two

or three separate fluid phases. Inclusions in veins granulated by deformation tend to be smaller and less abundant than inclusions in less deformed veins.

Fluid inclusions are also observed in host rock minerals although the inclusions tend to be smaller and less abundant than vein inclusions. Where fluid inclusions are present in both the host rock and vein minerals, the presence of an intergranular fluid is well documented by the preserved fluid samples. However, the lack of observed fluid inclusions in some host rock samples does not necessarily lead to the conclusion that there was no intergranular fluid. Host rock samples without observable fluid inclusions occur in the Moretown at location JR-108. These rocks have been highly deformed and are very fine-grained, finer-grained than the associated granulated veins which do have some fluid inclusions. The fluid in the veins must have come from host rock, as the veins are discontinuous in nature throughout the study area. Evidence from the size and abundance of inclusions in deformed and undeformed veins suggests that deformation eliminates or reduces in size the inclusions which formed during vein growth. Host rocks may inherently contain fewer and smaller fluid inclusions due to the non-hydrostatic stress environment, which may involve active shearing, in which host grains grow.

During active growth veins seem to have been essentially hydrostatic stress environments. Given these factors, the lack of inclusions in a host rock may only indicate that it was more difficult to form and preserve inclusions in the host rock grains.

Even without samples of the intergranular fluid preserved as inclusions in grains, the presence of a fluid with a pressure comparable to the confining pressure is demanded by the presence of the tension fractures which are hosts for the vein formation. The structural settings of many veins strongly suggest that tensile failure is involved; veins occur as boudin fillings, discontinuous fracture fillings in the axial planes of folds, fillings of en echelon fractures apparently related to shear couples acting on competent layers, and fillings of apparent extension fractures which are perpendicular to the bedding surfaces of thin, competent layers. Veins related to the major mineral growth events, such as the kyanite-bearing OV_b veins at JR-129, were necessarily formed under high confining pressures. Tension fractures could not occur under such conditions because of the high compressive stresses unless there was a fluid phase present. The law of effective stress has been shown by Brace (1968) to hold for crystalline rocks of low porosity. Because of the law of effective stress, the

effective principal stresses are equal to the principal stresses minus the pressure of the fluid. For a system with a confining pressure of 5 kb and a fluid pressure of 4.5 kb, the effective confining pressure is 0.5 kb. This has a dramatic effect upon the differential stress necessary for failure, either by shearing or tensile failure. The fluid pressure is the effective zero normal stress.

To get an idea of the order of magnitude of the maximum allowable difference between the maximum compressive stress and the fluid pressure for tensile failure, the work of Phillips (1972) can be used. Phillips uses a composite failure envelope which utilizes the Griffith theory in the tensile region and the Mohr-Coulomb theory in the compressive region, as shown in Figure 1. The failure envelope intersects the normal stress axis at -T, where T is the tensile strength of the rock. Tensile failure can only occur if the differential stress is less than or equal to 4T and the minimum principal stress is equal to -T; the difference between the maximum compressive stress and the pore fluid can be no greater than 3T. If the differential stress is greater than 4T then only failure by shearing can occur. Handin (1966) lists the cohesive strengths of a variety of materials, and the cohesive strengths of various metamorphic rocks are all less than 200 bars. In this for-

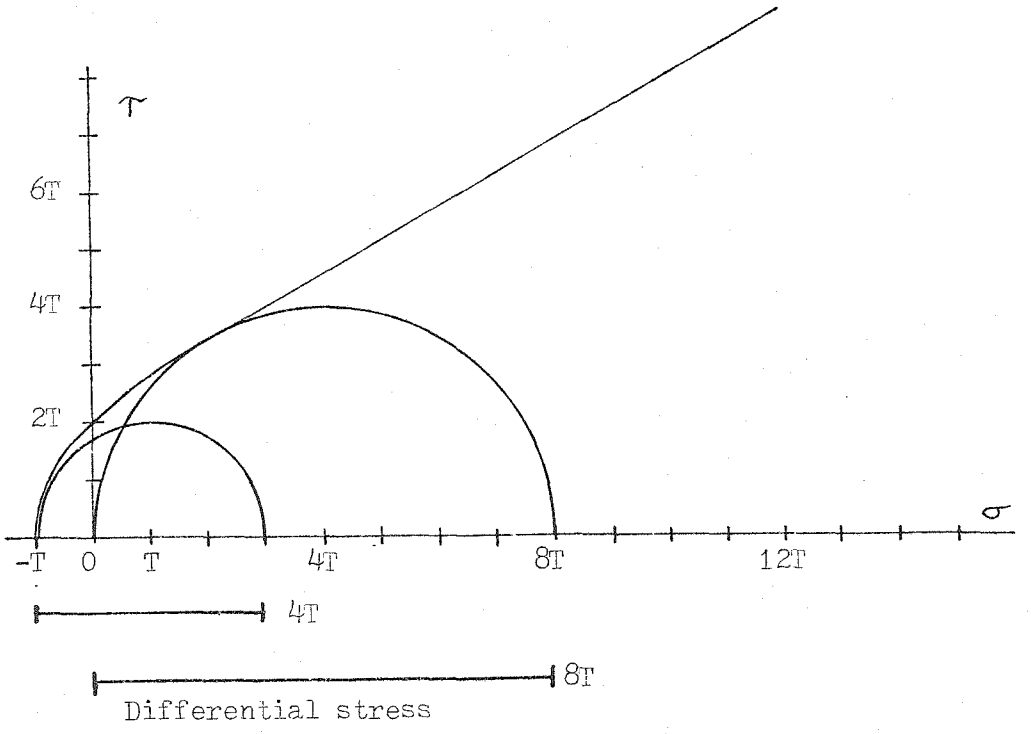

Figure 1 Stress diagram showing maximum differential stress at which tensile failure can occur (4T). Shear failure occurs for greater differential stress, such as shown for 8T. From Phillips (1972).

mulation, the cohesive strength is equal to 2T, so that T is estimated to be less than 100 bars. Therefore, as a rough approximation it seems that tensile failure, and consequent vein formation, cannot occur if the difference between the maximum compressive stress and the fluid pressure exceeds some value which is less than 300 bars. Despite the inexactness of this analysis, it seems clear that in order to form metamorphic veins of the type observed in northern Vermont, the difference between the fluid pressure and the confining pressure must be small relative to the absolute value of the confining pressure, which is less than or equal to the maximum compressive stress by definition.

Metamorphic veins are closely associated with the four most important generations of metamorphic mineral growth, OV_a, OV_b, DM_a, and DM_c. Only generation DM_b is not associated with the growth of veins and the above discussion may provide a partial explanation; perhaps fluid pressures during event D_b were too low to facilitate tensile failure. DM_b growth is always low grade in northern Vermont and may involve either hydration or only recrystallization of hydrous minerals. Although the complete explanation is undoubtedly more complex, hydration may tend to lower the fluid pressure and thereby prevent vein formation.

The above evidence suggests that an intergranular fluid is present, that during events in which veins form the fluid pressure must be close to the confining pressure, and that diffusion of chemical species through the fluid can occur. One other property of interest is whether the fluid itself can move. As there is evidence of the intergranular fluid in veins, the fluid must have moved from the host rock to the vein fracture. The volume of fluid does not have to be large and there is no requirement for the fluid to circulate once it is in the vein. The veins are discontinuous which rules out fluid moving in from other sources or locally derived vein fluid moving out of the system. While some mobility of the fluid is required by vein formation, it appears that during most of the time an essentially static fluid can account for the observed effects. Only the free movement of the vein-forming components by diffusion through the fluid is required; these components include species of F, Na, Mg, Al, Si, P, S, Cl, K, Ca, Ti, Mn, Fe^{2+}, and Fe^{3+}.

C. General characteristics of mineral growth

As many as four mineral growth generations have been observed in single thin sections of host rock samples from the Cambrian and Ordovician units. An example is JR-4-M, a

host rock sample from the Hazens Notch formation. In general, only two or three generations can be documented, but host rock samples with evidence for only one generation are relatively rare. In the Silurian and Devonian rocks, three major generations may be present and two generations are typically observed. There are areas where only one generation may be observed in host rock samples. Veins differ from host rocks in that they can have no record of the events which occurred before their formation. Also veins in general are less affected by moderate overprint than is the average host rock.

Partial to complete chemical reconstitution of pre-existing minerals due to an overprinting event can be shown with the microprobe data from some samples, such as JR-163-D. The extent of this effect seems to depend upon the grade, duration, and associated mechanical deformation of the superimposed event. Within a single event, there may also be a tendency for early formed compositions to re-equilibrate, particularly at high metamorphic grade. In most cases, the exact causes of such effects cannot always be sorted out from the various possibilities.

Where one mineral generation has heavily overprinted another, evidence of the oldest mineral growth generation is best preserved in relatively isolated environments such

as coarse-grained metamorphic veins and as inclusions in certain host minerals. Chlorite, biotite, and muscovite are often well preserved as inclusions in quartz or plagioclase grains in host rocks and veins. JR-4-M is a very good example of this and is discussed later. Garnet can be preserved as included grains in plagioclase. Plagioclase in quartz-rich metamorphic veins can survive subsequent high grade events without compositional change, but low grade sericitization is more destructive to vein plagioclase than is higher grade overprint. Minerals such as chloritoid, chlorite, ilmenite, plagioclase, and others can be preserved as inclusions within garnet porphyroblasts; in the case of JR-73-A, the only chloritoid in the sample is preserved as inclusions in garnet. In many cases a significant number of grains survive relatively unchanged through superimposed metamorphism even when they are not inclusions in other phases or otherwise isolated. Metamorphic veins are likely to have a large percentage of unchanged grains of its original mineral growth generation, given only moderate overprint. Amphibolite commonly shows good preservation of older generations, but most other host rock types do not generally show as high a degree of preservation.

Mineral grains are in general zoned with respect to

major elements, given that zoning is possible. The chemical path of a mineral of a single generation can usually be shown by analyzing the zoned grains. Typically the zoned grains define a single chemical variation trend and each grain represents growth along part or all of that trend. The compositional variation of a mineral defined in such a manner may be only a general trend or it may be a trend which is followed in detail by the zoning in every grain. The effects of overprint are a problem that cannot always be satisfactorily resolved. In some cases there is evidence of a lack of equilibrium between growing grain surfaces on the scale of a thin section, but grain surface equilibrium is always approached more closely than solid state equilibrium within single grains.

Minerals such as garnet, plagioclase, chloritoid, amphibole, and staurolite may show the entire compositional trend of a generation within single grains. The trend is preserved in general by concentric zoning apparently due to concentric growth. Amphibole and plagioclase in some of the samples studied show the compositional variation history for two or more generations within a single grain. Less frequently, a single grain of chlorite, muscovite, calcite, ankerite, sphene, or some other mineral may show the entire compositional path of a single generation of

mineral growth. Biotite, chlorite, and muscovite are more apt to show only a portion of the compositional trend within a single grain so that many grains must be analyzed to determine the entire path.

Biotite and, to a lesser extent, chlorite tend to have reequilibrated if they were overprinted by a relatively high temperature event. Biotite commonly does not preserve zoning and the compositional path of a generation of biotite may only be preserved in grains included within a plagioclase. With increasing grade of the overprinting event, the various minerals begin to reequilibrate, destroying the original zoning, In the rocks studied it is unusual to find uniform compositions in most minerals and it is clear that only partial reequilibration has taken place. For minerals other than biotite, the grade at which significant reequilibration begins to occur seems to be roughly "middle" garnet grade or higher, depending upon the mineral. Discontinuous reactions seem to be much more efficient in eliminating evidence of a mineral growth generation even at fairly low grades; the discussion in this section largely concerns minerals which do not become unstable because of such a reaction. When a mineral is removed by reaction, grains of that mineral may be only preserved as inclusions in a nonreactive mineral.

Concentric growth tends to armor older compositions in minerals such as plagioclase, chloritoid, garnet, amphibole, and others. If the armoring rims were removed the core compositions might not survive when exposed to the rest of the system. In fact in many samples there are no grains found which have unarmored core compositions. Miscibility gaps and other discontinuities, such as generation growth boundaries, can also be preserved in single grains which are concentrically zoned.

The degree of chemical reconstitution caused by an overprinting event depends upon the basic kinetic parameters; time, temperature, and activation energy. An important process is the mechanical grinding of grains that can accompany the formation of an s-surface or more generalized granulation. The increased surface area produced by mechanical grinding reduces the activation energy barrier and can also expose grain interiors armored by concentric growth or by inclusion in another mineral. Such mechanical deformation acting along a distinct s-surface set or restricted zones in a rock can be a selective process that affects only a portion of the grains in a sample; this allows the preservation of some grains of the older mineral growth generations while providing material for new mineral growth.

The kinetic barriers to equilibrium combined with the overprint processes such as deformation and reaction of

older grains allows the effective bulk composition of the system to change with time. The volume of material in the interiors of zoned grains and included in other minerals is effectively removed from the system. When there is a strong partition of an element into one phase, such as Mn in garnet, significant depletion zoning can occur; this effectively removes most of that element from the system. Strong overprinting by deformation or mineral reactions can restore some or all of the material to the effective bulk composition. Although some minerals such as garnet tend to preserve zoning better than others, the presence of major element zoning in all the minerals in which zoning is possible in a system indicates that only a small volume of material, the rims of grains, is an active part of the system at a given time.

Apparent nonequilibrium is present to some extent in all of the samples studied with the electron microprobe. The scale and nature of the nonequilibrium are not always easy to determine, but must be understood if the treatment of a metamorphic system depends upon the assumption of equilibrium. If disequilibrium is only present in the solid state, present methods of treating metamorphic systems should be valid if care is taken to determine which compositions of the various minerals grew simultaneously. An assumption implicit in many previous studies is that most of the mineral growth in a sample grew

at the peak of an event and that the temperature and pressure were effectively constant for the growth which is now seen in the sample. This assumption does not apply to any of the 40 samples studied with the microprobe in this study.

D. Previous ideas in northern Vermont

The presence of two mineral growth generations, corresponding to DM_a and DM_c, was recognized in Silurian and Devonian rocks by White and Jahns (1950). White and Billings (1951) recognized mineral growth in the rocks of the Woodsville quadrangle which is equivalent to generation DM_b. The generations were not precisely defined, however, and it was not known whether the different generations represented growth in separate events or growth in different stages of a single continuous event. Albee (1968) suggested that the high grade assemblages in the Worcester Mountains and the Green Mountains were of Ordovician age and that there was a superimposed Devonian retrograde event. Lanphere and Albee (1974) confirmed this for the Worcester Mountains by isotopic age determinations on minerals formed in each event. The high grade Ordovician event corresponds to OM_b of this study and the dated retrograde event in the Worcester Mountains is perhaps DM_c. The fifth major generation, OM_a, has never been discussed as a separate mineral generation but

was recognized as a structural entity by Albee (1957a & b). Although the various major generations were recognized individually by different authors in different parts of the area, the entire sequence had not been previously defined nor had the detailed correlation of these generations been accomplished throughout northern Vermont. Also, by using the veins and the structural sequence, the various generations can be established as the results of separate events even though some of the events are closely related in time.

Because of the relatively recent development of the electron microprobe, there are only two previous studies of northern Vermont which made substantial use of microprobe data; both are by Albee (1968 and 1972b). Compositional variation within minerals in a single sample can only be observed with microanalysis. Wet chemical analyses of mineral separates always represent some sort of average composition. The average may be weighted by the mineral separation process because grains which are included in other minerals and a disproportionate amount of rim material of matrix grains are likely to be excluded from the mineral separate.

Albee (1968 and 1972b) observed compositional zoning in grains of garnet, chloritoid, and staurolite, but indicated that chlorite and biotite were essentially homogeneous.

There are probably two factors to account for not finding significant compositional variation in chlorite and biotite. The most important factor perhaps is the limitations of the manually operated microprobe, used by Albee in these studies. The present automated microprobe system gathers data much faster than a manual system and the analytical error is much less because analysis of all the desired elements is accomplished simultaneously and spots do not have to be relocated. Given the severe time limitations of the manual microprobe system, the second factor follows directly; the points to be analyzed are carefully selected to maximize the chance that they represent equilibrium compositions as only a few analyses of each mineral type could be made in a reasonable time. This selection excluded grains that were in isolated environments, were not in contact or near other grains to be analyzed, or that showed any textural peculiarities. Thus the grains most likely to preserve the history of multiple generations and compositional variation within these generations were avoided.

Compositional variation with time of minerals in a rock is not in conflict with previously held views. Pelitic rocks, with muscovite and quartz present, are often described in terms of the condensed system K_2O - Al_2O_3 - FeO - MgO using the projection of Thompson (1957). Even in an

"invariant" three phase assemblage on this projection, compositional variation will occur if P, T, and other parameters such as $a_{(H_2O)}$ are varied. If the simplified four component system does not adequately describe the rocks, then the variance can be increased even more.

Most of the systematic treatment of metamorphic rocks in New England has involved pelitic rocks because they are widespread in occurrence, they can be described in terms of fewer components than other rock types, and they can contain a variety of index minerals which indicate the relative grade attained. Most of the pelitic samples in this study don't violate the predictions of the four component system if the different mineral generations are separated, but there are exceptions. Garnet in analyzed samples contains significant Ca and the data suggest that Ca should be considered in the treatment of such samples, as is discussed later. One assumption of most previous treatments of pelitic rocks is that there is a relatively simple equilibrium among grains. In a number of samples in this study, two adjacent grains of the same mineral have been found to have significantly different rim compositions. The close approach to equilibrium that would make the graphical treatment of the condensed four component system most useful seems to be the exception rather than the rule.

The structural setting and petrology of the metamorphic veins has not been previously studied in northern Vermont. Studies of veins in other areas have generally focused on vein formation or some particular aspect of the veins. The first treatment of metamorphic veins in this general area was by Chapman (1950) in west-central New Hampshire. Fluid inclusions in veins in central Vermont were studied by Rich (1973 and 1975). Vidale (1974) tried to use the basic vein assemblages in the metamorphic rocks in Dutchess County, New York, as indicators of metamorphic grade. Veins have not been previously used as an integral part of the metamorphic sequence which provide the means for directly correlating deformational elements with mineral growth generations.

E. Relationship between host and vein mineral growth

As mentioned in the previous chapter on structure, the genetic relationship between vein minerals and host minerals of the same generation can be shown by chemical comparison. In the case of a vein which is parallel to an s-surface, the vein minerals are similar in composition to host rock minerals that have preferred orientations parallel to the s-surface. For host minerals which tend to have no preferred orientation, the correspondence is shown by

compositional and textural features other than orientation, such as overgrowth and crosscutting relationships, inclusion relationships, and reaction textures. If the s-surface set is a well spaced slip cleavage, minerals such as chlorite and muscovite may have preferred orientations within and immediately adjacent to the slip cleavage planes, but may have no preferred orientation between planes. For veins which are not parallel to an s-surface, host minerals of that generation generally show no preferred orientation. No detailed set of rules applies to all samples. Typically, however, within a host rock there are two or more texturally distinct mineral growth generations and the vein minerals chemically correspond to only one generation. Where the textural evidence is ambiguous or lacking, the correspondence of compositions is used alone to separate the generations.

In the majority of samples studied, mineral types in major vein generations have corresponding minerals of the same generation in the adjacent host rock. In some instances, vein minerals of low abundance cannot be found in thin sections of the adjacent host, but this could easily be a sampling problem. Exceptions are also found in the case of veins formed during retrograde events; an example is JR-66-F, a DV_a vein that formed during the retro-

grade alteration of the host amphibolite. Retrograde products such as potassium feldspar and biotite are concentrated in the vein, although very small amounts can be found in the host if it is carefully examined. In any event, vein minerals are never seen to be incompatible with the host minerals of the same generation. The general situation is that the host assemblage is more complicated than the vein assemblage; minerals which can be in the host rock but are typically absent from the vein are tourmaline, zircon, garnet, and others depending upon the rock type. In many pelitic rocks, the host rock assemblage contains epidote and sphene, but neither of these is in the veins. Veins in amphibolitic host rock may contain abundant epidote and sphene.

For a single mineral growth generation in a sample of a vein and adjacent host rock, comparison of the compositional trends in the vein and host minerals indicates that in general there is an overlap in the time period of mineral growth in each. The overlap may not be extensive. The time periods can, but do not generally coincide exactly. It appears that mineral growth in veins can continue after mineral growth in the host rock has ceased. Growth in the host may begin before growth in the vein. No sample has been observed in which vein mineral growth can be docu-

mented to have started before growth of the same generation in the host rock.

An example of the timing of mineral growth can be seen in samples from JR-5, described in detail later. OM_b plagioclase grains in the host are zoned from albite in the cores to andesine at the rims. Plagioclase grains in an OV_b vein are zoned from andesine in the cores to albite at the rims. The host rock plagioclase appears to have been rotated by movements along OS_b during growth, but the vein shows no effects from shearing or other deformation related to O_b. This evidence and the compositional trends indicate that the host rock plagioclase grew first, then there may have been a brief period in which both the vein and the host rock plagioclase grew, and finally there was growth in the vein only. The chlorite compositional trends seem to indicate a similar growth history, although the clorite trends are not as well established as the plagioclase trends. If the compositions of plagioclase and muscovite can be used as indications of relative grade, as discussed later, then the compositional trends in these samples suggest that grade was increasing during host rock mineral growth and decreasing during vein mineral growth. Apparent down-grade zoning patterns in vein minerals are common, but not always present. Host rock compositional trends gener-

ally indicate increasing grade with time.

F. Metamorphic vein formation--general chemical and morphologic evidence

There is a great deal of variation in the external morphology of veins, internal vein structures, details of compositional variation of minerals, and overall makeup of veins with respect to mineral assemblage and bulk chemical composition. A few generalizations are possible and these are important to consider.

Metamorphic veins in northern Vermont appear to occupy discontinuous fracture openings which have been filled by vein mineral growth. The structural setting of most of these fractures indicates that they are due to tensile failure. The contacts between veins and their host rock are very sharp and distinct. The formation of such tensile fractures requires that a fluid phase be present and that the fluid pressure be close to the confining pressure, as discussed earlier. Samples of the fluid are preserved as inclusions in the veins and commonly in the host rock. This fluid phase provided a medium through which diffusion of vein mineral components could occur and thus facilitated the growth of the fracture-filling minerals. There are apparently no sources for vein material other than the surrounding host rock.

The discontinuous nature of metamorphic veins in northern Vermont suggests that the vein-forming material was derived locally. The discontinuity of the veins eliminates the possibility of a circulating fluid that brought in dissolved species from some external source. The only other way to bring in material is by diffusion through some medium in the host rock, since the host rock completely surrounds the veins. The logical diffusion medium is the fluid phase which is required by other evidence. Given a difference in the chemical potential of some component between the host and the vein and given that the difference favors diffusion into the vein, material is most likely to come from an adjacent volume of the host rock in which the chemical potential gradient is steepest.

The bulk composition of veins, including their border zones, is typically vastly different than the bulk composition of the enclosing host rock. Actual determinations of the bulk chemical compositions are not necessary for this observation; the difference in bulk chemistry can be easily shown by considering the relative abundances of the minerals in vein and host. This contrast is so great that it eliminates the possibility that the veins formed by recrystallization of the host rock.

There are many veins which do not contain minerals

such as zircon, tourmaline, and garnet, even though these minerals may be abundant in the host rock. Zircon in particular is typically not in the vein but present in the host rock; an exception is the zircon-rich metagreywackes of the Pinnacle formation in which veins are observed that contain zircon. Zircon can also be found in host rock fragments which have apparently been ripped off the host rock wall of the vein and are now included in the normal vein material. Because of the lack of these minerals in the vein and because of the relative lack of Al in many veins relative to the host, replacement of host rock does not appear to be a mechanism by which the veins could form; the elements that would have to be removed from the veins are generally regarded as the least soluble. The textural evidence also tends to rule out replacement.

However, the minerals present in the veins and their relative abundance do seem to depend upon the host rock composition and the metamorphic grade. The major vein-forming minerals in northern Vermont are quartz, plagioclase, K-feldspar, calcite, and ankerite. Epidote can be important in veins in fairly low grade greenstone host rocks. In pelitic rocks, quartz is by far the predominant vein-forming mineral. Quartz can also be the predominant vein mineral in other host rock types. Plagioclase is

commonly a major constituent in veins in amphibolite and moderate to high grade pelitic rocks. K-feldspar is a common vein mineral in the K-rich, low grade rocks of the Pinnacle formation. Carbonate minerals are most abundant in veins within carbonate-rich host rocks. These minerals probably constitute over 90% of the combined volume of the metamorphic veins in northern Vermont.

In general the veins have more Si and significantly less Mg, Al, Ti, Mn, and Fe (except sometimes as sulfide) than the host rock. There is a wide range in the relative abundance of elements such as Ca, S, and P; these depend upon the abundance of carbonates, sulfides, and apatite. The Na and K contents of a vein depend upon the abundance of Al-rich minerals which contain these; for veins in pelitic rocks the abundance of Al, and therefore of Na and K, tends to increase with increasing grade. The abundance of the minor elements such as Zn, V, and Nb depend upon the amount of the minerals in which they are generally present as minor constituents. Zr, Y, and REE are typically in very low abundance or essentially absent in the vein relative to the host rock. The relative Cu and B contents of the vein depend upon the relative amounts of chalcopyrite and tourmaline, respectively.

The host rocks adjacent to veins are in general not

significantly different from rocks of a similar lithologic type which are far away from any veins. Localized zones which have been depleted of the vein-forming minerals are not apparent in the host rocks. This is difficult to test quantitatively as there is no firm control on the composition of the host rock. Reaction zones are not observed in the host rock adjacent to veins except where DV_c veins cross-cut thin, semiconcordant granitic sheets; in such a case the reaction zone is confined entirely to the igneous rock and does not extend into the adjacent metamorphic rock. The only type of feature in the host rock observed adjacent to veins are thin zones, typically not more than a few millimeters wide, in which the host minerals are coarser than normal. These are most often observed next to DV_c veins and are relatively uncommon. Because of the lack of strong depletion effects, there must be a relatively small amount of depletion over a fairly large volume of host rock. Depending upon the size of the vein, this volume could consist of the host rock within a few meters or less of the vein margin and still account for the apparent lack of depletion. There does not appear to be any requirement for vein material to diffuse over any distance greater than this.

Veins commonly have a thin border zone which consists of a concentration of certain vein minerals. The composi-

tionsof these minerals indicate that they are vein minerals rather than part of the host rock. There is also textural evidence that the border zone is a feature of vein growth rather than depletion or some other mechanism; this is described below. Rarely are the border zones uniformly developed on the entire host rock wall of the vein and many veins have no discernable border zones. Border zones vary in width from a few millimeters or less to a few centimeters; the width apparently depends on a number of factors including the overall width of the vein and the minerals in the border zone. Border zones which consist primarily of minerals such as chlorite, biotite, muscovite, or chloritoid tend to be thin relative to border zones which consist of plagioclase. Most of the Mg, Ti, Mn, and Fe of the vein may be concentrated in the border zone. Al may or may not be concentrated in the border zone. Fe can also be abundant in the interior of the vein as sulfide. Sulfides are not a common constituent of border zones.

Preferred orientation of grains may be shown by some minerals in the border zone. Grains in the vein interior are typically without preferred orientation. However, the preferred orientation in the border zone differs from that in the host rock; the preferred orientation of grains in the border zone seems to reflect the effects of the host rock

wall on nucleation and growth of border zone minerals. Elongate grains of minerals such as amphibole and sphene can have their longest dimension oriented perpendicular to the host rock wall. Platy minerals such as chlorite and muscovite can be oriented with their basal planes parallel to the host rock wall. Feathery aggregates of stilpnomelane and elongate plates and planar aggregates of minerals such as ilmenite and hematite can be oriented with their planar faces perpendicular to the host rock wall. Grains of the same minerals with random orientations are in many instances intimately associated with the grains with preferred orientation.

Compositional variation in the border zone minerals seems to indicate that in general border zone growth begins at the host rock wall and continues progressively away from the wall, thereby gradually increasing the width of the border zone. A few border zones also show segregation of minerals into generalized bands which contain mostly one mineral type and are parallel to the host rock wall. There are several possible explanations of this including progressive introduction and removal of mineral types in the border zone with time, activity gradients across the border zone, or some nucleation or other kinetic effect. The irregularity of development of border zones and the lack

of border zones along large areas of the host rock wall tend to rule out activity gradients. Other considerations such as the zoning patterns and the invariably present intermixing of minerals even in the best developed segregation bands also suggest that the bands are not the result of activity gradients. Both of the other two mechanisms, together or alone, seem to be responsible for the observed banding. The structure and compositional variation relationships shown by border zones are not so regular that the above generalizations can be assumed for all samples.

A limited amount of replacement or "digestion" of small fragments of host rock did occur. Apparently these fragments were broken off the host rock wall as the veins were forming. The process of digestion is characterized by grain size coarsening of the minerals in the inclusions. However, there are unrecrystallized residual grains of minerals such as zircon, tourmaline, REE-rich epidote or allanite, and others which do not otherwise occur in the vein. The outline of such a fragment is typically easy to observe even where the digestion has been extreme. Various stages of this process have been observed and most host rock fragments do not show very strong effects of recrystallization. Host rock fragments are never seen to account for a significant volume of the vein and in most cases are absent.

Fluid inclusions in vein minerals are generally larger than fluid inclusions in corresponding host minerals. There are open cavities, up to a few centimeters in diameter, in some veins and these have euhedral crystals growing into the opening. A good example is the DV_c vein at JR-66 which has euhedral plagioclase and ilmenite grains growing into a network of open cavities. Such openings with euhedral grains at the margins are relatively rare in northern Vermont. Cavities in veins not lined with euhedral grains are commonly observed; these appear to be the result of the weathering out of minerals such as calcite and ankerite. The presence of abundant fluid inclusions, of less abundant open cavities, and the coarse-grained minerals which do not show preferred orientation due to directed stress all suggest that actively growing veins were fluid-rich, hydrostatic environments.

There is evidence that the opening of vein fractures was gradual rather than instantaneous. The fluid-filled voids are generally not very large. The largest fluid inclusions in a vein are typically 10-20 microns in diameter. Open cavities are relatively rare. The fluid-filled openings were never large enough to allow the settling of vein crystals to the lowest part of the vein. There are a few cases in which it appears that coherent mineral growth

"bridged" a vein and became attached to the opposite border zone. As the opening of the vein continued, the border zone pulled away from the host rock wall and deformed in a manner suggesting simple extensional fracture opening. A thin border zone, apparently formed after the old border zone was removed, is present in the place of the old border zone material. A good example of this is shown in an OV_b vein at location JR-5. This also seems to be the mechanism by which host rock fragments were broken off and included in the veins. If a border zone is present on a host rock fragment, it appears that the growth of the border zone stopped after it was broken off and there was border zone growth on the newly exposed host rock wall. Border zones developed on the host rock wall where a fragment has been removed tend to be thinner than the border zone elsewhere.

G. Minerals and mineral compositions as indicators of grade

Increasing grade in a metamorphic terrain involves progressive devolatilization reactions which change the mineral assemblages within the rock and the compositions of the minerals in the assemblages. The major volatile components are H_2O and CO_2, in as much as hydrous and carbonate minerals are abundant constituents in unmetamorphosed and low grade rocks from which the higher grade

rocks are produced. S_2, H_2S, or other sulfur species are also products derived from devolatilization reactions in sulfide-bearing systems.

For a rock of sedimentary or volcanic origin which is initially subjected to metamorphism, increasing grade necessarily implies increasing temperature. In regional metamorphism increasing pressure, which tends to oppose the effects of temperature, is also involved. A system already at metamorphic P and T conditions can undergo changes in grade due to changes in the partial pressures of the volatile components without any changes in P and T (P is always meant to be P_{total} unless otherwise stated). For instance, dehydration reactions can be caused by decreasing $a_{(H_2O)}$, everything else being equal.

Changes in the total fluid pressure are possible in rocks which are being deformed. Dilatancy resulting in decreased pore fluid pressure has been shown experimentally to accompany strain induced by compressive stress in crystalline rocks at confining pressures similar to metamorphic conditions (Brace, 1968). The difference in temperature between the experimental and metamorphic conditions may affect the extent of the dilatancy because of the temperature-dependency of the mechanical properties of rock. The opening of tension fractures in which veins form is also a

dilatant effect and some drop in the pore fluid pressure might be expected. However, the magnitude of the fluid pressure drop cannot be very great in systems in which veins are forming, as discussed earlier. Even after the vein fractures are initiated, the fluid pressure cannot fall below the minimum compressive stress; if this occurred there would be no effective tensile stress and the vein fractures would not open any further. Total fluid pressure changes in systems in which metamorphic veins are forming probably cannot be great enough in magnitude to cause significant apparent changes in grade in the host rock or vein assemblages. There are no such constraints in systems in which veins are not forming; significant changes in the total fluid pressure are possible and such effects are difficult to distinguish from the effects of P and T. If the total fluid pressure is constant, changes in the partial pressure of a volatile component can occur if compensated by opposing changes in the partial pressures of the other components.

The devolatilization reactions themselves also affect the fluid pressure. If the response of the fairly low porosity rocks is such that volatile reactions products cannot be removed from the system quickly, then an increase in the fluid pressure might be expected. Increased porosity due

to dilatancy may facilitate the flow of volatile components from the system. It may be that the effects of devolatilization are to a great degree offset by the opposing effects of dilatancy during progressive metamorphism which is accompanied by deformation. The abundance of metamorphic veins in northern Vermont suggests that fluid pressures were typically close to the confining pressures.

In general, it is impossible to sort out the specific causes of changes in grade; the concept of grade is therefore used without regard to the variables which affect it. There are two types of indicators of grade used in this study. When comparing the rocks in one outcrop or small area with those in another, the presence of specific mineral types or distinct compositions of a mineral type are used. These are the conventional grade indicators. The other type of grade indicator is used only to determine the relative path with respect to grade of a particular mineral growth generation within a single sample; for this, the compositional variation in specific indicator minerals of that generation is used. This relies on much more subtle variations than the first type and it is generally not possible to compare different samples in the detail in which the path a single sample can be determined.

Within a given chemical system, such as a pelitic

rock, there is a typical sequence of mineral assemblages which indicates increasing grade. For instance, garnet can be used as a grade indicator because it forms as a product of devolatilization reactions involving reactants such as chlorite, biotite, calcite, and others. The conventional indicators of increasing grade in pelitic rocks are the appearance of biotite, garnet, staurolite, kyanite or andalusite, and others which are all products of dehydration reactions. The distribution of these key minerals has been investigated by virtually all of the previous investigators in the area who have already been cited. The latest compilation of this data is shown by Albee (1968).

In carbonate-bearing rocks, decarbonation reactions can be important; significant amounts of carbonate minerals are not restricted to rocks such as the metalimestones of the Waits River formation but can be also present in pelitic rocks. Decarbonation reactions in pelitic rocks can be involved in the formation of the Ca component in garnet and the anorthite component in plagioclase. In plagioclase-bearing pelitic rocks of garnet or high biotite grade, progressive decarbonation seems to be responsible for the typical plagioclase zoning pattern: albite cores to oligoclase or andesine rims. In many of these rocks there is not enough epidote, other than epidote rich in REE, to account for the

zoning in a large volume of plagioclase. In epidote-rich rocks, such zoning can indicate progressive dehydration. Typical plagioclase-bearing rocks in pelitic rocks in this study have both calcite and epidote so that the reactions are not necessarily simple.

Compositional trends in minerals other than plagioclase can also indicate changes in grade within a mineral growth generation. Two minerals used in this study are Ca-amphibole and muscovite. The compositional zoning of these minerals within single samples has been used to interpret the relative path of the system with respect to grade. Also, the specific compositional types within the Ca-amphiboles such as actinolite and hornblende are used as more general indicators.

Ernst (1968) has reviewed the experimental data and field occurrences of the calcic amphiboles. In regional metamorphic terrains a typical up-grade sequence in metabasaltic rocks is actinolite→hornblende, which involves a decrease in the formula proportions of Si. The work of J. Laird in this area (Ph.D. thesis in preparation) has shown that within a given assemblage and for a similar metamorphic gradient, there is a progressive decrease in the formula proportions of Si in the actinolite to hornblende transition with increasing grade. Within a single genera-

tion in a sample, zoning with respect to Si can be used to indicate the path of that generation with respect to relative grade. However, two different rocks cannot be compared in the same kind of detail.

There are three common substitutions which can occur in muscovite. The ferrimuscovite ($Fe^{3+VI} \leftrightarrow Al^{VI}$) substitution and the phengite ($Fm^{2+VI}Si^{IV} \leftrightarrow Al^{VI}Al^{IV}$) substitution are described by Ernst (1963). The muscovite-paragonite solvus and the limits of Na$\leftrightarrow$K substitution in each mineral are discussed by Eugster and others (1972). The solvus and the phengite substitution are both applicable to the determination of grade of a system. The ferrimuscovite substitution cannot be used in this regard. In practice, the muscovite-paragonite solvus can rarely be used because of the lack of paragonite coexisting with muscovite of the same generation in the samples of this study. Much of the paragonite observed appears to be a low grade alteration product of plagioclase, especially common in metamorphic veins. Paragonite is also found as a primary mineral of the major growth generations. Such paragonite is typically found to be finely intergrown with muscovite so that the analysis of pure paragonite is difficult.

In samples with zoned muscovite and zoned plagioclase, it has been observed that there is a consistent relation-

ship between the zoning patterns of these two minerals for a given mineral growth generation. For instance, if the plagioclase shows increasing anorthite component from core to rim (typically albite→andesine), then the associated muscovite will usually show zoning with decreasing phengite component (and therefore decreasing Si) from core to rim. Exceptions are in cases in which strong overprint has occurred. This observation is in accordance in general with the experimental work of Velde (1965, 1967) which indicates that the maximum possible phengite substitution is dependent upon P and T. The amount of phengite substitution decreases with increasing T and increases with increasing P ($P_{H_2O}=P_{total}$).

Given an assemblage that buffers the phengite substitution, such as quartz-muscovite-biotite-microcline or quartz-muscovite-biotite-chlorite, the amount of phengite substitution in the muscovite may provide a means of comparing relative grade from sample to sample, keeping in mind the strong dependence on P. Even without the buffering assemblages listed above, the muscovite zoning consistently indicates the same relative grade path as does the zoning in plagioclase. For instance, phengite substitution decreases from core to rim as anorthite substitution in plagioclase increases from core to rim. Therefore it

seems that in the typical pelitic assemblages in the samples studied, the zoning in muscovite reflects the relative path with respect to grade of that generation. In practice, I have only used the muscovite substitution within single samples and have not compared from sample to sample even with buffered assemblages. The data of Velde (1965,1967) suggest that the comparison from one sample to another or one generation to another is not a simple thing if there are differences in the relative P/T gradients from place to place or with time. In this study the data from samples with buffering assemblages do not agree with the numerical values given by Velde; generally the phengite substitution is less than expected for the estimated maximum temperature of the rock. This can be shown by comparing Velde's data with compositions of analyzed muscovite from garnet and biotite grade assemblages which are presented in later sections.

Desulfurization reactions involving the breakdown of pyrite or pyrrhotite can be important in the sulfide-rich systems in the area. The local occurrence of clusters of chlorite or biotite around remnant sulfide cores suggests such desulfurization. The breakdown of pyrrhotite may be responsible for Fe-enrichment trends in minerals such as chlorite in some of the samples in this study. The produc-

tion of volatile sulfur species can result from the reaction of pyrite to pyrrhotite, but Thompson (1972) has shown that desulfurization is not necessarily always involved. The pyrite to pyrrhotite reaction has been used as an indicator of grade in other metamorphic terrains, for example Carpenter (1974).

There are two other minerals which commonly occur and can have zoning that indicates the relative path of the system with respect to grade. Calcite is typically zoned with respect to the substitution of Fe, Mg, and Mn for Ca. Ankerite also is typically zoned with respect to the substitution of Ca for Fe, Mg, and Mn. Ankerite is not nearly so widespread in occurrence as calcite, but is in a number of samples and is always with calcite. The Fm (Fe+Mg+Mn) substitution in calcite tends to change in the same direction as the anorthite component in plagioclase of the same generation, even when the substitution is not buffered by the presence of ankerite. In samples with calcite and ankerite of the same generation the Fm and Ca substitutions, respectively, increase or decrease together. The limits of substitution in coexisting calcite and ankerite have not been experimentally determined, but the calcite-dolomite system has been investigated (for instance, Goldsmith and Newton, 1969). The addition of Fe and Mg into

the system should not change the general relationships. At a given P, the substitution of Fm in calcite and the substitution of Ca in ankerite should increase with increasing T. In the calcite-dolomite system, there is a pressure dependency of the degree of solid solution at a given T. However the effect of temperature is much stronger than the effect of pressure. If it can be assumed that there were not significant changes in the total pressure on the order of several kilobars or more, significant zoning in calcite and ankerite can be used as an indicator of the path of the system with respect to temperature. The path of total pressure may in fact involve significant changes, so that calcite and ankerite zoning must be used with this in mind.

H. Analytical procedures

In this study extensive use has been made of electron microprobe data from metamorphic vein and host rock samples. Each microprobe sample is a standard-sized thin section. The analytical procedures and error need to be discussed before the presentation of data in the later sections of this chapter.

Data collection

Electron microprobe analyses were made on an automated

MAC-5-SA3 microprobe using the programs ULTIMATE and ULTIMATE II (Chodos and others, 1973), which employ the correction techniques of Bence and Albee (1968) and Albee and Ray (1970). Almost all of the data were collected using wavelength-dispersive spectrometers; normal conditions were 15 KV accelerating voltage, .05 microamps sample current on brass, and electron beam diameters of 10-15 microns on most minerals and 15-20 microns on albite, muscovite, paragonite, biotite, potassium feldspar, stilpnomelane and carbonates. In some runs a sample current of .01 microamps on brass and 10 micron spots were used for the alkali-rich minerals and carbonates. Some data were collected using an energy-dispersive, solid-state x-ray detector with the output processed by an NS-880 multi-channel analyzer. Normal conditions for EDA work were a sample current of .005 microamps on brass, electron beam diameter of 1-5 microns, and an accelerating voltage of 15 KV. Caltech standard mount #1 or #1A was used for all runs.

The standard electron microprobe operating conditions represent a compromise between several opposing factors. The sample current of .05 microamps on brass is a compromise between good counting statistics in a reasonable time, obtained with high beam currents, and avoiding the loss of volatile components, favored by low beam currents. Electron

beam diameters of 15-20 microns were used on minerals with volatile components in order to minimize this loss. However, increasing the beam size sacrifices the spatial resolution which can be important in compositionally zoned grains. Beam diameters of 10 microns typically were used on most minerals, although in some instance 1-5 micron diameters were used. There is more of a tendency for carbon deposits to build up at the analyzed spot when the smaller beam diameters are used and this may have some small effect on the results.

The counting times for the elements are determined by the ULTIMATE program during computer operation of the electron microprobe. For most of the analyses in this study, the program required counting times which were sufficiently long to obtain relative standard deviations of 1% or less for those elements abundant enough such that their peak-to-background ratios were 5 or greater, a concentration of about 1 weight percent for most elements. The peaks and backgrounds were counted for equal times. The minimum counting time was 15 seconds and the maximum was 120 seconds. Three elements were run at a time and if the computer determined that it was necessary to count longer than 15 seconds for one element, it also counted longer for the other two elements of the triad. In general,

relative standard deviations of less than 1% were commonly obtained for major constituent elements. While the peaks were being counted, the beam current was constantly being sampled at the upper aperture. The peak and background intensities were normalized by dividing by the average beam current and the live-time. This normalizes the data to a constant flux of electrons.

Spatial resolution

The limits of x-ray spatial resolution are determined by the accelerating voltage and the material being analyzed. For 15 KV and typical silicate materials, the spatial resolution is about 1 micron for an infinitely small beam. Reed (1975) has a discussion of the x-ray resolution and the factors that affect it. The smallest beam diameter used in this study was 1 micron, so that 2 microns is the best spatial resolution achieved.

The analysis of a 10 micron diameter spot on the surface of a grain represents an averaging of the composition of a volume about 11 microns in diameter and 1 micron deep. Significant compositional differences may exist within such a volume. The worst case is where the analyzed spot includes material on either side of a chemical discontinuity, such as a solvus or generation growth boundary. The anal-

ysis obtained may be a composition which is not actually present in the analyzed volume.

A problem which is generally minor, but which can be significant in analyzing small grains and grain rims, is secondary fluorescence in adjacent phases. This effect depends upon the element being analyzed and the composition of adjacent phases. An example is the secondary fluorescence of Fe in Fe-rich phases adjacent to plagioclase, as discussed by Longhi and others (1976). They give an empirical relationship that indicates, for instance, that about 0.2% FeO (uncorrected) would be seen in the analysis of Fe-free plagioclase if the analyzed spot was 10 microns from a mineral with about 30% FeO. Secondary fluorescence in adjacent phases is more of a problem for Fe than for other major elements typically analyzed. For distances greater than about 10 microns, such secondary fluorescence effects can generally be ignored.

Analyses from grain rims in this study were 5-10 microns or more within the grain. Besides secondary fluorescence in adjacent minerals, there are several other problems. Very thin edges sometimes occur on grain rims; an analysis of such a rim can be contaminated by the mineral directly underneath the thin edge. Another problem that occurred occasionally was drift in the location of the beam

on the sample. The beam never drifted more than a few microns, but is another factor in considering spatial resolution. The 5-10 micron margin was used to avoid these various problems in analyzing grain rims.

The above problems are most important when analyzing very small grains, such as grains included in other minerals. Included grains are important in this study as they are generally thought to be the most likely material to have preserved original compositions. The inclusions analyzed were typically 50 microns or larger in diameter, and the 5-10 micron margin from the rims was used. Included grains smaller than 20 microns were avoided unless larger grains did not occur. As most of the included grains analyzed in this study were within host plagioclase, the strong secondary fluorescence of Fe in the host mineral was not a factor.

Normalization of data

The normalization of electron microprobe data to formula proportions requires that an ideal formula and normalization procedure be selected for each mineral type. The ideal formulas used in this study are shown in Table 1. For minerals such as stilpnomelane with no specific ideal formula, only ratios of atom percents are used. The use of

Table 1 Ideal formulas used in mineral normalizations

Mineral	Formula
Ca-amphibole	$(Na,K)_{0-1}(Ca,Na)_2(Mg,Fe^{2+},Fe^{3+},Al)_5[Si_{6-8}Al_{2-0}O_{22}](OH,F)_4$
apatite	$Ca_5(PO_4)_3(OH,F,Cl)$
biotite	$K(Mg,Fe^{2+})_{3-2}(Fe^{3+},Al,Ti)_{0-1}[Si_{3-2.5}Al_{1-1.5}O_{10}](OH,F)_4$
calcite	$CaCO_3$
ankerite	$(Ca,Mg,Mn,Fe)_2(CO_3)_2$
chlorite	$(Mg,Fe^{2+},Fe^{3+},Al)_6[Si_{2-3.5}Al_{2-0.5}O_{10}](OH)_8$
chloritoid	$(Fe^{2+},Mg,Mn)_2(Al,Fe^{3+})Al_3O_2[SiO_4]_2(OH)_4$
epidote group	$Ca_2(Al,Fe^{3+})Al_2O\cdot OH[Si_2O_7][SiO_4]$
allanite	$(Ca,REE)_2(Al,Fe^{2+},Fe^{3+})Al_2O\cdot OH[Si_2O_7][SiO_4]$
feldspar	$Na_{1-0}Ca_{0-1}[Al_{1-2}Si_{3-2}O_8] - (K,Na)[AlSi_3O_8]$
garnet	$(Mg,Mn,Fe^{2+})_3Al_2Si_3O_{12} - Ca_3(Al,Fe^{3+},Cr)_2Si_3O_{12}$
kyanite	Al_2SiO_5
muscovite	$(K,Na)(Al,Fe^{3+},Fe^{2+},Mg)_2[Si_{3-3.5}Al_{1-0.5}](OH,F)_2$
paragonite	$(Na,K)Al_2[Si_3AlO_{10}](OH)_2$
pyrophyllite	$Al_2[Si_4O_{10}](OH)_2$
sphene	$CaTi[SiO_4](O,OH,F)$
staurolite	$(Fe^{2+},Mg)_2(Al,Fe^{3+})_9O_6[SiO_4]_4(O,OH)_2$
hematite	Fe_2O_3
ilmenite	$FeTiO_3$
magnetite	$Fe^{2+}Fe^{3+}O_3$
rutile	TiO_2

ratios eliminates many of the problems caused by normalization for any mineral type.

Table 2 shows the elements normally analyzed for each mineral type using the programs ULTIMATE and ULTIMATE II. Some of these elements are not commonly found in the mineral type for which they are determined; they are used to detect contamination by other minerals. For example, Na in chlorite would indicate contamination by plagioclase or Na-rich mica. The normalization procedures are also shown in Table 2. In general an analysis is normalized to the total number of cations in the ideal formula. Amphibole, biotite, chlorite, and white mica are exceptions to this and the normalizations are made to the total cations minus Na, K, and Ca. It is assumed that there are no vacancies in sites other than those specifically excluded from the normalization. Of course, there may in fact be some vacancies. The normalization of amphibole analyses is covered in detail by Laird (in preparation). All of the Ca-amphibole analyses in this study are normalized by setting the total cations minus Na+K+Ca equal to 13. This assumes that no Fe is in the Ca site. Other normalization procedures are generally less satisfactory.

The microprobe does not discriminate between Fe^{2+} and Fe^{3+} so that only a value for total Fe is obtained. In the

Table 2 Elements analyzed and normalization factors for microprobe analyses

Mineral	Elements analyzed	Normalization
Ca-amphibole	Na,Mg,Al,Si,K,Ca,Ti,Cr,Mn,Fe,F,Cl	total cations - (Na+K+Ca) = 13
apatite	Na,Mg,Al,Si,Ca,Fe,P,Ce,F,Cl,Y,La,Nd	total cations = 8
biotite	Na,Mg,Al,Si,K,Ca,Ti,Mn,Fe,Zn,F,Cl	total cations - (Na+K+Ca) = 7
calcite	Mg,Ca,Mn,Fe	total cations = 1
ankerite	Mg,Ca,Mn,Fe,Ba	total cations = 2
chlorite	Na,Mg,Al,Si,Ca,Ti,Cr,Mn,Fe,Zn,F,Cl	total cations - (Na+Ca) = 10
chloritoid	Mg,Al,Si,Ca,Ti,Mn,Fe,Zn,F	total cations = 8
epidote	Mg,Al,Si,Ca,Ti,Mn,Fe,Ce,F	total cations = 8
allanite	Mg,Al,Si,Ca,Ti,Mn,Fe,Ce,F,Y,La,Nd	total cations = 8
feldspar	Na,Mg,Al,Si,K,Ca,Ti,Fe,Ba	total cations = 5
garnet	Mg,Al,Si,Ca,Ti,Cr,Mn,Fe	total cations = 8
kyanite	Na,Al,Si,K,Ti,Fe	total cations = 3
muscovite, paragonite, & pyrophyllite	Na,Al,Si,K,Ca,Ti,Mn,Fe,Zn or Ba,F,Cl	total cations - (Na+K+Ca) = 6
sphene	Ma,Al,Si,Ca,Ti,Mn,Fe,Ce,F	total cations = 3
staurolite	Mg,Al,Si,Ca,Ti,Mn,Fe,Zn,F	total cations = 15
stilpnomelane	Na,Mg,Al,Si,K,Ca,Ti,Mn,Fe,Ba,F,Cl	only ratios used
Fe, Ti oxides and zircon	Mg,Al,Si,Ti,Cr,Mn,Fe,Zr,V or Zn,Nb	total cations = 1, 2, or 3
tourmaline and others	Na,Mg,Al,Si,K,Ca,Ti,Cr,Mn,Fe,F,Cl	only ratios used

discussion in later sections, only total Fe is considered for most minerals. However, Fe^{3+} is important for minerals such as amphibole and garnet and needs to be calculated based on some set of assumptions. Wherever Fe^{2+} or Fe^{3+} are discussed in the text, they are specifically noted. Fe always refers to total Fe.

Assuming that the normalizations are correct and that there are no vacancies or impurities, Fe^{3+} can be calculated in one of two ways: by charge balance or by full occupancy of specific sites. The total charge of an analysis is calculated arbitrarily assuming that all Fe is Fe^{2+}. Each mineral type has an ideal total charge for the elements considered in the normalization. A deficiency in the calculated total charge relative to ideal total charge can be used to calculate Fe^{3+}. In addition to assuming no vacancies, this assumes no substitution of $O^{=}$ for OH^{-} in hydrous minerals and full occupancy of the OH site by OH, F, and Cl. This type of calculation is used for minerals such as amphibole, chlorite, and chloritoid. For amphibole analyses from some samples, for example JR-66-F, Fe^{3+} commonly constitutes more than half of the total $Al^{VI}+Fe^{3+}+Ti+Cr$. The calculated Fe^{3+} in minerals such as chlorite and biotite is typically less than 1% of the total Fe.

For garnet, any deficiency in the Al site not occupied

by Ti or Cr is assumed to be Fe^{3+}. The Fe^{3+} in garnet is small compared to the total Fe, but may account for up to 5% of the total Al site occupancy. There is no calculated Fe^{3+} in many garnet analyses.

Obviously, the calculation of Fe^{3+} is subject to considerable error. There is no way to calculate the degree of paired $Fe^{2+} \leftrightarrow Fe^{3+}$, $OH^- \leftrightarrow O^=$ substitution. The calculated Fe^{3+} is strongly dependent on the normalization procedure. However, the presence of small amounts of Fe^{3+} should not greatly influence the general relationships that are described later. Even in the discussion of amphibole, different compositional groups generally can be differentiated on some basis which does not depend on Fe^{3+}.

Analytical error

Microprobe analyses are subject to both random and systematic error from a number of sources. Some of the systematic error can be reduced by data handling procedures, but random error is always present. This random error is due to the variations of x-ray peak and background intensities about mean values. The relative standard deviation of an analyzed element depends upon the number of counts at the peak and the peak-to-background ratio (P/B); increasing either of the parameters results in a lower

standard deviation.

Counting error is present in both standard analyses and sample analyses. Random error in the standard values becomes a systematic error in the sample analyses. Standards were run at the beginning of each run, and the counting times were sufficiently long to achieve a relative standard deviation of less than 1%. Each standard was run at least twice to obtain two values within less than 1% relative to each other. The standard values were also compared to previous values to insure that there were no unusual changes in the values. For a single run, this error does not need to be considered when comparing sample analyses. As previously discussed, the microprobe operating program determines the counting time for the samples so that relative standard deviations of 1% or better are achieved for elements with a P/B of 5 or more.

In addition to the error in the standard values there are several sources of systematic error which affect the data. Some systematic error is due to the gradual build-up of carbon and hydrocarbons on the upper aperture. The beam current is measured here and build-up affects the measurement. Over the course of a 10-12 hour run, the standard values can effectively change 1% because of this drift. An experienced operator does not allow the drift

to be more than 1% before correcting it and the drift only affects the weight percent values. The error introduced is a constant factor which is eliminated when the data are normalized to formula proportions.

Other sources of error are sample roughness, variations in the inclination of the sample relative to the beam, and poor focus. To the extent that these factors affect all of the analyzed elements similarly, part of the error is eliminated by the normalization. There are many other minor sources of error which need not be discussed here.

From the above discussion, it can be seen that there is the least relative error when treating formula proportions of analyses collected with the same standard values. Typically traverses of points across single grains in the samples of this study meet these conditions. However, each sample was commonly run on 2-4 different days, so that the error in the standard values is also of concern.

Two reference samples of known composition, garnet and sanidine, were analyzed at the beginning of each sample run and in the middle of long runs to provide a check on the standard values. Analyses of these reference samples run by various microprobe operators have been statistically analyzed by Champion, Albee, and Chodos (1975). The reproducibility for these analyses is about 1½ to 3 times the

error from counting statistics for the elements concerned. However, only weight percent values were used; it would be expected that the reproducibility for formula proportion values would be better than for weight percentages because systematic errors which affect all of the elements by a constant factor are eliminated in the normalization. Another possible source of error could be slight inhomogeneities in the reference samples, but this is clearly not a major problem because of the good reproducibility of the analyses. Also, the Si value in the garnet, which might not be expected to vary much in this sample, has roughly the same reproducibility as the other elements.

The error shown in the diagrams in later sections are calculated from the sample counting statistics only. Ratios and formula proportions (which are ratios in a closed array) are used so that some of the systematic error is eliminated. From the discussion of Champion and others (1975), and taking into consideration the differences between weight percent data and formula proportions, the reproducibility when comparing analyses from two different runs is estimated to be up to two times the error shown. For example, the formula proportions of Si in the reference garnet sample for 76 analyses have a relative standard

deviation of 0.5%. This compares to the relative standard deviation of 0.3% calculated from sample counting statistics alone. The 76 analyses represent data collected over a period of about a year.

The standard deviations for ratios or formula proportions involving volatile elements, such as Na and K, and calculated Fe^{3+} and Fe^{2+}, are not shown on the diagrams. The only exceptions are on a few K-feldspar diagrams and also on garnet diagrams where error for total Fe is shown. The possible loss of volatile components under the electron beam introduces a systematic error that is hard to evaluate for each analysis. The calculated Fe^{3+} and Fe^{2+} are so dependent upon the assumptions that there is no realistic way to determine the error.

Many of the standard deviations of the ratios shown on the diagrams are very small, in some cases smaller than the standard deviations of the single elements. This is the result of the type of ratio used; all of the ratios are of the type X/X+Y where Y may be the sum of a number of elements. Formula proportions are ratios of this type where Y equals the sum of all the elements other than X. The normalization procedure adds a constant factor that

affects both X and Y. For ratios of the type X/Y, the standard deviation of the ratio is always larger than the individual standard deviations, as the relative standard deviation of the ratio is equal to the square root of the sum of the squares of the individual relative standard deviations. However, this relationship does not hold for ratios of the type X/X+Y. X does not vary independently of X+Y, only independently of Y. As X becomes large relative to Y, the relative error of the ratio decreases. The standard deviations were calculated by first calculating the standard deviation values of the X/Y ratios and then converting these to X/X+Y ratios.

Composition diagrams

Several features of the composition diagrams need to be explained. In a number of diagrams, thin lines connect dots and there are arrows on the lines. The lines connect adjacent analyzed points in a single grain and the arrows indicate the core-to-rim direction. The lines connecting adjacent points are not shown in every diagram, but are useful in considering the zoning trends.

Thicker arrows which do not connect points indicate inferred zoning trends. The arrows are dashed or question marks are added to indicate how well the trends are established. The trends are based on the individual zoning patterns and the textural relationships of grains and points within individual grains. The trends have no statistical basis; there are too many subjective factors to consider in establishing compositional trends.

Five-digit identification numbers are shown next to some points in the diagrams. These are code numbers assigned to the points during analysis. The first digit indicates the area; an area is typically 4-8 square millimeters, but may be 1-24 square millimeters. The second digit indicates the sub-area, the third and fourth digits indicate the grain and the last digit indicates the point number of the analysis. Single grains may have more than one grain number if there are more than 9 analyzed points. The electron microprobe analysis data are available upon request.

I. Several general examples of samples analyzed with the electron microprobe

The following sections of this chapter deal with samples that have been analyzed with the electron microprobe. Although all are not presented in detail, forty samples have been analyzed and the data from these are comprised of about 5000 complete analyses of 1-20 micron diameter spots on mineral grains in these samples, supplemented by other data such as semiquantitative wavelength scan analyses and qualitative electron beam scanning pictures (EBS). It is useful to first consider a few examples with regard to the analytical approach and the types of relationships observed. Each sample is different in some way from the others but a general method was used for all of the samples; involved in this method of approach are certain assumptions and generalized observations.

These assumptions are concerned with the way in which mineral growth in metamorphic veins and host rock occurs. For a compositionally zoned grain, the trend of zoning with respect to time is of critical importance. If a grain is concentrically zoned as shown by a sufficient number of analyses, the core is assumed to have formed before the rim. Such a grain would have grown by progressively adding new material to the outside surface.

In a few cases such as the host rock chlorite grains

in sample JR-163-D, it appears that diffusion in the solid state could have produced the observed zoning patterns. This is in contrast to zoning produced by compositional variation as the grains grew which has been preserved. The chlorite compositions in the strongly zoned grains in JR-163-D are essentially linear combinations of the core and rim compositions, although the relationship is not simple because there are not single end-member compositions. The zoning is largely with respect to Mg and Fe; it can be accounted for by diffusion of Fe in toward the core and diffusion of Mg out toward the rim. The chemical reconstitution would have involved a simple Mg-Fe exchange. One distinct feature of these chlorite grains in JR-163-D is that there are significant compositional changes over distances of a only a few microns. The compositional variation is much greater than typically observed. In samples such as this one, it cannot be clearly demonstrated that diffusion really occurred, but there is permissive evidence of diffusion. There is also textural evidence to support such a conclusion for this sample as is discussed in detail later.

The chemical zoning in minerals in many samples seems to reflect changing compositions with time as these grew. An example which is discussed later in this section is the

chlorite in sample JR-73-A. In a general way, the zoning pattern can be reproduced in grains of the same generation. The compositional trend is more complex than could be produced by linear combination of two end members. The complexity of the trend is perhaps a good test of whether zoning is produced by diffusion and exchange or by the preservation of compositional variation as the grains grew. If the compositional trend is not complex, then several criteria might be used to determine the nature of the zoning: reproducibility of the zoning pattern; the similarity of the compositions and zoning patterns between grains in the matrix and grains which are included in other minerals and therefore relatively isolated from the rest of the system; and the lack of apparent overprint textures, such as irregular optical zoning. It is not always easy to separate the effects of growth zoning and diffusion zoning.

There are odd grain geometries, such as grains with reentrants, that could produce apparent concentric zoning patterns for which the simple assumptions of the time relationship between core and rim and intermediate material do not hold in detail. Such geometries are much less likely than simple ones if the present grain shapes are an indication of the typical situation. Because of the possibility of odd geometries and because of the criteria for establish-

ing the type of zoning present, at least several grains of each mineral type must be analyzed.

It is common for single grains of a mineral to preserve only a portion of the compositional variation trend of that generation. Because of this a number of grains must be analyzed, regardless of the problems of grain geometry. It is assumed in such a case that the overall trend is defined by grains which have overlapping portions of the trend. Depending upon the complexity of the compositional trend and the amount of overlap from grain to grain, this procedure for establishing the trend can become very complicated and at times ambiguous.

Grains of one mineral can be included in a grain of another, a common example being grains of chlorite and biotite included in plagioclase. If there are a number of included grains in a single host grain, a concentric pattern of compositions of the inclusions may be found which is similar to the concentric zoning of single grains. If such a concentric composition pattern of included grains exists, then the inner grains are assumed to have grown before the outer grains. Such an assumption is sometimes reinforced by the zoning patterns of single included grains which can have overlapping portions of the same overall trend.

Not all compositional zoning is concentric. There are

grains in which there is no apparent closure of the bands of uniform composition. If the zoning is nonconcentric then the time relationships of compositional variation are ambiguous. It is possible to establish the entire compositional trend of a mineral but not know the time direction of the trend. In most cases there is evidence to establish the time relationship.

It is assumed that for a given mineral two points with identical compositions along the same portion of the compositional trend in two grains represents simultaneous growth. Showing the correspondence in time between compositions of two different mineral types is a much more difficult problem. In a number of samples two adjacent grains of a single mineral have been observed which have different rim compositions. Using the above assumption, these two rims should have formed at different times. If this can be true for a single mineral, then it is possible for the rims of adjacent grains of two different minerals to have grown at different times. The situation is even worse for the cores of the grains as there is even less control. Apparently the best control on the compositional correspondence between two minerals is obtained when small grains of the minerals are included within some host mineral, such as the grains of chlorite and biotite in plagioclase in sample

JR-4-M. The compositional pairs obtained from the rims of adjacent included grains in the plagioclase may be a reasonable approach to simultaneously grown pairs, although there are still problems.

The compositional variation trends of minerals are often very complex and difficult to interpret. For those cases in which a well defined trend can be reproduced in a number of grains, the detailed trends are shown in the diagrams that follow in this chapter. In many cases the trends are not well established because of the small number of points or the complexity of the compositional variation; only a general trend can be shown for these. In all samples the actual trends are probably more complicated than shown and the defined trends are at least partially incomplete. To establish the compositional trends in detail would require many hundreds of analyses per mineral in each sample; it is not clear at this point how useful such information in general would be. The trends shown on the compositional diagrams that follow are based upon the available data and the assumption that the variation may have been systematic. Such trends may have never actually been experienced by the samples.

The examples that follow illustrate the general approach of this study in using microprobe analysis and the

petrographic analysis of textures in determining the mineral growth history of a sample. Two samples from JR-66 are good examples of the use of metamorphic veins in separating the effects of different mineral growth generations. The other example is from JR-73 and serves to show the textural and chemical features of polymetamorphism that can be observed in pelitic host rock.

JR-66

Location JR-66 provides a good example of the use of metamorphic veins. The location is a small outcrop of Stowe amphibolite at the southeast end of Elmore Pond in the Hyde Park quadrangle and is within the garnet isograd as mapped by Albee (1957a & b). JR-66 is about one mile east of Elmore Mountain at the northern end of the Worcester Mountains. The amphibolite host rock has been overprinted by retrograde events as evidenced by the partial alteration of hornblende to actinolite and other reaction products. In some samples, up to 50% of the hornblende has been altered. The retrograde reaction products are also found as primary minerals in two structurally distinct vein generations, DV_a and DV_c. The two generations of reaction products in the veins are compositionally similar. Without the veins, there would be no reason to

suppose that both DM_a and DM_c retrogradation had occurred. Even with the knowledge that DM_a and DM_c are present, it is essentially impossible to separate their effects in the amphibolite. In the host rock there is also chemical and textural evidence of a third event, pre-D_a, that involved the retrogradation of hornblende. The hornblende-bearing assemblage is thought to be OM_b.

The small scale structural features present at JR-66 are primary layering, OS_o, a schistosity parallel to OS_o, OS_a/OS_b, two generations of metamorphic veins which crosscut OS_a/OS_b, moderately well developed fracture cleavage, and a set of irregular, poorly developed fractures which crosscut the fracture cleavage. OS_a/OS_b is fairly well developed in chlorite-rich layers and poorly developed in the more massive amphibolite layers. The fracture cleavage which crosscuts OS_a/OS_b has a strike of 355^o and a nearly vertical dip; it appears to be essentially parallel to DS_a slip cleavage in the nearby pelitic schist of the Stowe formation. For example, the DS_a slip cleavage in schist at location JR-83 on Elmore Mountain strikes 7^o and dips 74^o west. There is only one prominent slip cleavage set in the schist, so that it seems likely that the fracture cleavage is also DS_a.

Parallel to the fracture cleavage is the oldest vein.

It primarily consists of slightly granulated quartz. The vein is pod shaped, about 30 centimeters long and 10 centimeters wide at its widest point. If the fracture cleavage is DS_a, then this vein is DV_a in generation. The vein is slightly deformed as indicated by the weak granulation of vein quartz and by small displacements along a few irregular fractures which crosscut the fracture cleavage.

About 10 meters away from the DV_a vein, a set of younger veins crosscut the fracture cleavage and appear to be undeformed. These may or may not be related to fracture surfaces which crosscut the DV_a vein. The younger veins strike 35^o and dip 25^o northwest. The veins are discontinuous in the outcrop with the largest being about 2-3 centimeters wide and a meter long. One vein of this set has open cavities into which protrude euhedral crystals of plagioclase and ilmenite. The vein minerals appear to be related to the retrogradation of the host amphibolite. Based on the superposition on DS_a and DV_a and the correspondence of the vein minerals to mineral growth in the host rock, the vein is thought to be DV_c in generation. The orientation of these veins is similar to the orientation of DV_c veins elsewhere in the study area.

There is good structural evidence on Elmore Mountain that high grade, pre-DV_a mineral growth is OM_b. Kyanite

and garnet are found as primary minerals in OV_b veins in pelitic host rock. In the schist, blades of kyanite have preferred orientations parallel to OS_a/OS_b. There is no evidence of any other generations of garnet or kyanite grade mineral growth. It appears that the hornblende in the amphibolite is also OM_b. The mineral growth generations on Elmore Mountain and to the south in another part of the Worcester Mountains are discussed later in this chapter.

The host amphibolite consists largely of partly altered hornblende, epidote, magnetite partly altered to hematite, plagioclase, and the hornblende retrograde products, actinolite and chlorite. Quartz is present in some layers. Hornblende is rimmed by actinolite. Aggregates of chlorite grains without preferred orientation are spatially associated with the actinolite. Chlorite and actinolite also occur along abundant fractures in the remnant hornblende cores. Some amphibole grains appear to have two different zones within the actinolite rims. The inner zone is slightly darker in color than the outer zone. The boundary between the two zones is sharp, which suggests perhaps two separate retrograde events were responsible. The microprobe data indicate that the inner actinolite may predate DM_a. There is no textural evidence in the host

rock that allows the separation of the retrograde effects of D_a and D_c, but the two structurally distinct vein generations indicate that both events affected the amphibolite.

The veins of both the DV_a and DV_c generations contain the following minerals: plagioclase, calcite, actinolite, K-feldspar, chlorite, biotite, sphene, epidote, and apatite. The DV_a vein is predominantly quartz and also contains hematite. The DV_c veins are largely plagioclase and calcite and contain no quartz. Magnetite with hematite intergrowth or alteration and ilmenite are also present in the DV_c veins.

Two samples from this location have been analyzed with the microprobe, JR-66-C and JR-66-F. JR-66-F is a sample of the DV_a vein and the adjacent amphibolite. JR-66-C is from the largest DV_c vein and the adjacent amphibolite. The data from these two samples are discussed together so that the textural and compositional features can be compared.

Although the DV_a vein of sample JR-66-F is largely quartz, developed along perhaps half the area of the host rock wall is a 1-2 millimeters wide border zone. The border zone consists primarily of chlorite, biotite, actinolite, hematite, and plagioclase, plus minor sphene, K-feldspar, and calcite. There is a general layering within

the border zone involving chlorite, biotite, and hematite. For example, in one small area of the sample the border zone is about 1.5 millimeters wide. This area is shown in Figure 2. Adjacent to the host rock wall is a layer of chlorite which is about 1.0 millimeter wide. Next is a 0.2 to 0.4 millimeter wide layer of intergrown chlorite and biotite. Closer to the vein interior is a sometimes absent layer of biotite that does not exceed 0.1 millimeter in width. Adjacent to the quartz in the vein interior is a 0.1 to 0.2 millimeter wide band of hematite. Actinolite, plagioclase, and sphene are distributed throughout most of the border zone, but are not found in the monomineralic hematite layer. The chlorite layer is always present in the border zone, but one or more of the other three layers may be absent. The relative order of the layers is always the same.

The chlorite and biotite grains of the border zone generally show preferred orientation with their basal planes parallel to the host rock wall. Many actinolite grains have preferred orientation with their longest dimension roughly perpendicular to the host rock wall, as can be seen in Figure 2. However, there are a number of smaller actinolite grains which do not have preferred orientation. In typical amphibolite, preferentially oriented grains of

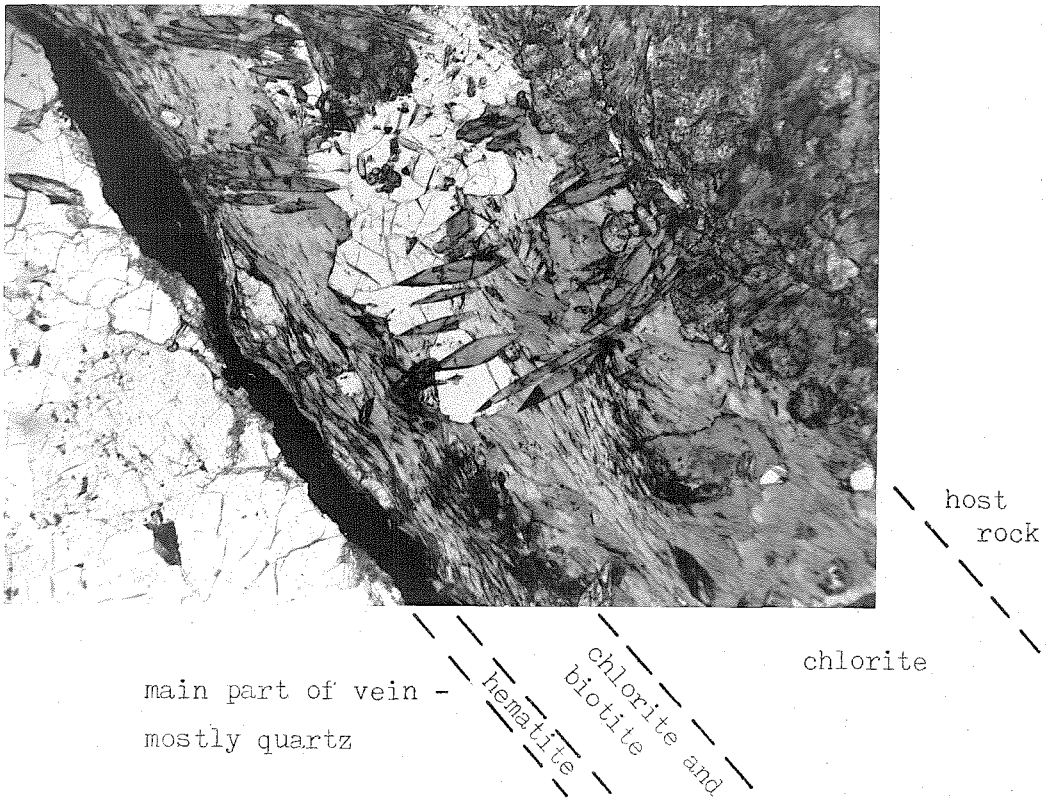

Figure 2 Border zone of DV_a vein in JR-66-F. 3 mm field of view, plane polarized light.

chlorite and actinolite of the same generation tend to be parallel. The preferred orientation directions of chlorite and actinolite in this border zone are roughly perpendicular. This suggests that the preferred orientations in the border zone are features of vein growth in a relatively hydrostatic environment, rather than growth in a directed stress field. The first chlorite grains to nucleate in the border zone may have been influenced by the host rock wall, so that the chlorite basal planes were parallel to this planar surface. Further growth of the border zone would have continued layer by layer in toward the vein interior. Actinolite grains that were oriented perpendicular to the chlorite basal planes may have been able to grow faster or continue growth for a longer period of time than grains with other orientations.

Developed at irregular intervals in the outermost biotite or chlorite-biotite layer are small (1 mm or less) pods of K-feldspar. An example is shown in Figure 3a. Seemingly continuous platy grains, partly included in the pods, are biotite outside the pods and chlorite inside the pods. This may indicate that a reaction of biotite to chlorite occurred only within the pods. Both chlorite and biotite seem to have been stable outside of the K-feldspar. One interesting feature of the pods is that the larger ones,

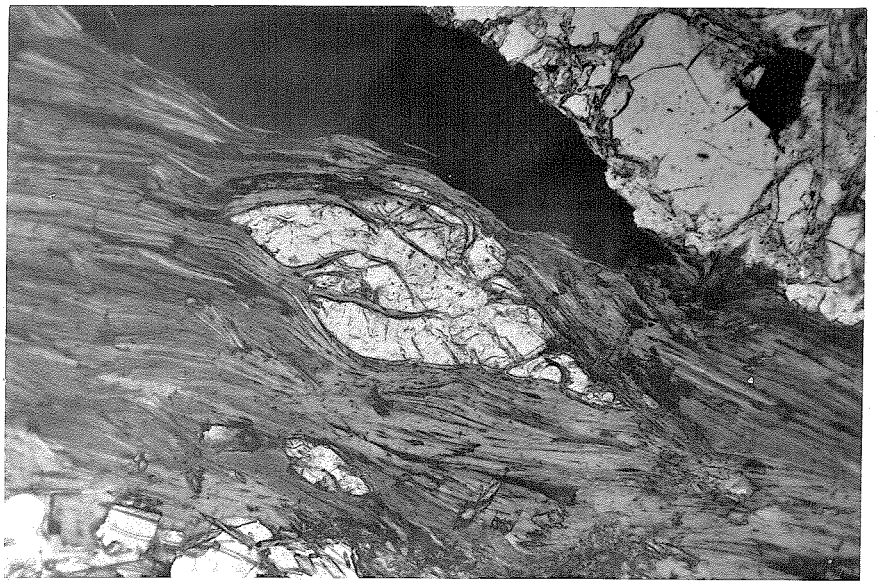

Figure 3a K-feldspar pod in border zone of DV_a vein, JR-66-F. The opaque mineral is hematite. Above and to the right of the hematite is the interior portion of the vein. 1.2 mm field of view, plane polarized light.

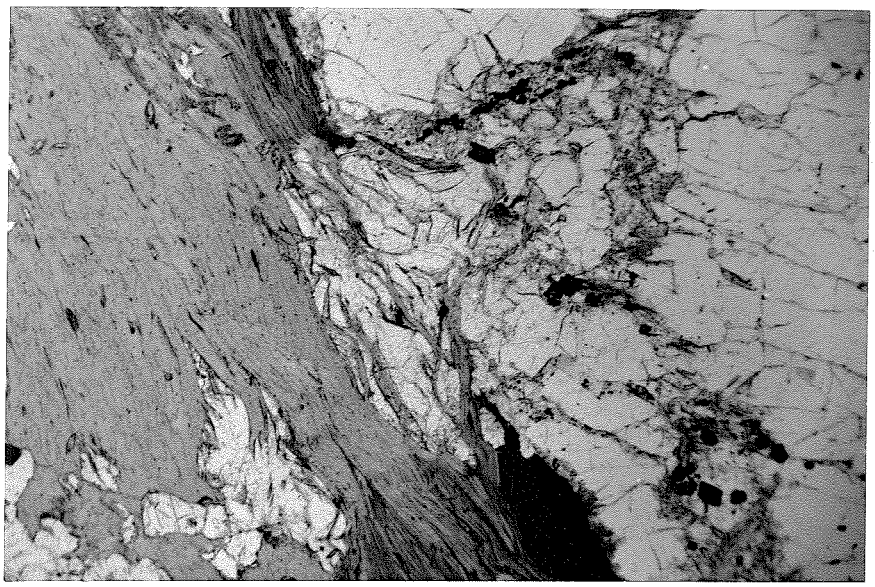

Figure 3b K-feldspar pod in border zone of DV_a vein, JR-66-F. Pod has "popped" out into vein. 3 mm field of view, plane polarized light.

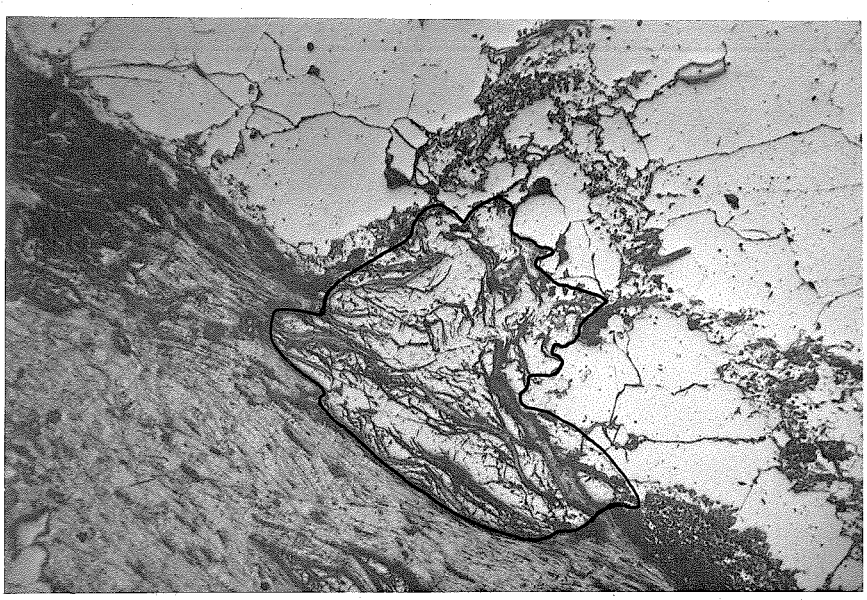

Figure 3c Same as Figure 3b, but in reflected light. Pod is outlined in black.

such as that shown in Figures 3b, have "popped" out of the border zone and grown into the main part of the vein. The included chlorite grains and surrounding chlorite and biotite grains appear to have been deformed by the K-feldspar growth out into the vein interior. Figure 3c, a reflected light photograph of the same pod in Figure 3b, serves to show the deformed platy grains. Chlorite and biotite grains on the host rock wall side of the pods may be slightly deformed, but the "popping" and accompanying strong deformation occurred toward the vein interior only.

The K-feldspar in the pods is compositionally zoned; the part of the pods nearest the vein interior is different in composition from the part nearest to the host rock wall. The "popping" seems to have been caused by growth of K-feldspar which could exert enough pressure to deform thin sheets of chlorite. The border zone behind the pod on the host wall side was apparently relatively firm and significant deformation could not occur. The vein interior must have been less resistant to the growth and deformation so that the pod pushed out into the vein as growth continued. This suggests that that quartz grains in the vein interior were not firmly interlocked and that they could be moved out of the way by the growing pod fairly easily. This may be a general property of most quartz veins. The rela-

tive infrequence of observed deformation of border zones or plucking off of host rock fragments due to continued extension and growth of the veins suggests that the interiors of most veins were not firmly attached to the host rock wall or border zone. The behavior of border zones in general suggests that they were firmly attached to the host rock wall.

One interesting problem is the origin of the banded structure in the DV_a border zone of JR-66-F. The border zone seems likely to be a feature that first nucleated at the host rock wall and grew inward toward the interior of the vein. This could account for the preferred orientation of the chlorite and biotite. If this is correct the banding may represent a sequence of minerals which grew in the vein. Chlorite grew first, then chlorite and biotite, and then perhaps biotite grew alone. The potassium-feldspar pods appear to be a late feature as they deform sheets of biotite and have "popped" out into the vein interior. The innermost band of hematite is a problem to a certain extent. It seems unlikely hematite alone grew after the growth of chlorite and biotite stopped. The hematite layer is monomineralic. It may be that the hematite grew at the same time as chlorite and biotite, but nucleated and grew at the interface between the growing border zone and the vein interior.

If a sequence of appearance of minerals accounts for the layered structure in the border zone, then there was no K-rich mineral that grew in the early stages of vein formation. The actinolite has less K than the hornblende from which it is formed, so that if no K-mineral was forming, the K^+ content of the intergranular fluid must have been gradually increasing with time. At some point the activity of K^+ in the fluid must have become great enough for biotite to appear.

Beyond the border zone in the interior part of the DV_a vein is coarse-grained quartz with a small amount of calcite, a few percent or less of the volume. Also present are minor amounts of plagioclase, hematite, magnetite, chlorite, and actinolite. The vein interior is unstructured and none of the minerals show preferred orientation. Most of the aluminum-rich minerals are concentrated in the border zone.

The DV_c vein in sample JR-66-C is in sharp contrast to the DV_a vein just described. There is no well developed border zone in the DV_c vein, nor are there any features such as banding or preferred orientation of grains. Although plagioclase is a major DV_c mineral in general, this sample is from a part of the vein that is comprised mostly of calcite. There is no quartz in the vein. K-feldspar is

present, but there are no pods such as those in JR-66-F. The aluminum-rich minerals are distributed throughout vein interior.

The amphibolite host rock samples adjacent to the veins of the two generations are very similar. Grains of dark blue-green hornblende have been partially retrograded to actinolite and chlorite. The remnant hornblende grains are irregular and fractured. The retrograde products show no preferred orientation. Small amounts of sphene, biotite, and K-feldspar are in the host rock. Epidote grains with irregular optical zoning are abundant. Quartz is present in the host rock adjacent to the DV_a vein, but is not present in the host rock adjacent to the DV_c vein. Plagioclase is present in all samples of amphibolite from this outcrop, but the plagioclase abundance varies greatly from layer to layer. The only striking difference between the assemblages in the two host rock samples is that JR-66-F contains quartz and JR-66-C does not.

Figures 4a and 4b show plots of $Al^{VI}+Fe^{3+}+Ti$ vs. Si and Na+K vs. Si for analyzed amphibole points in the DV_a vein and host rock of JR-66-F. There are three compositional groups in this sample. Group I amphibole is the remnant OM_b hornblende grains in the host rock. Group II amphibole analyses are from the distinct innner actinolite

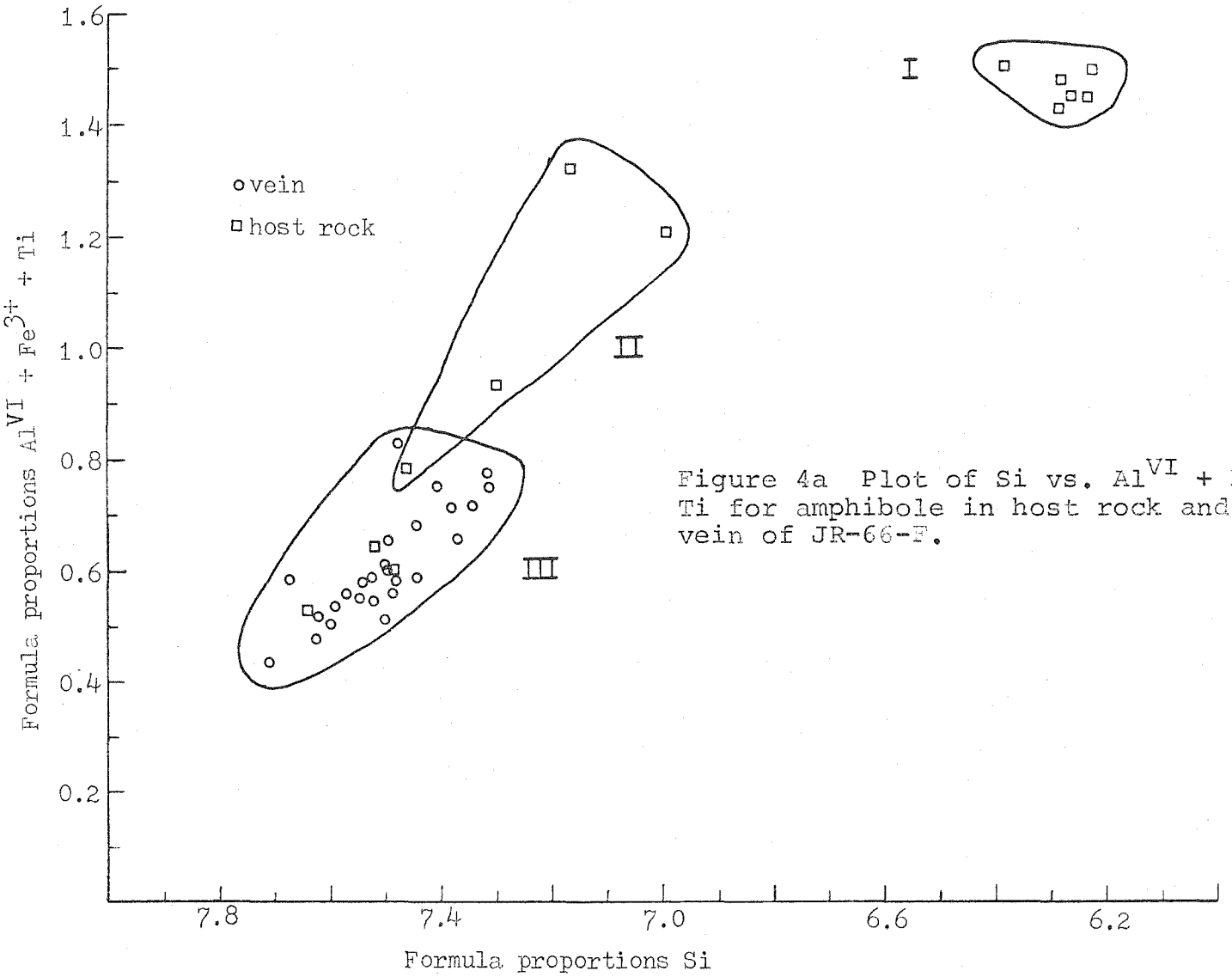

Figure 4a Plot of Si vs. $Al^{VI} + Fe^{3+} + Ti$ for amphibole in host rock and DV_a vein of JR-66-F.

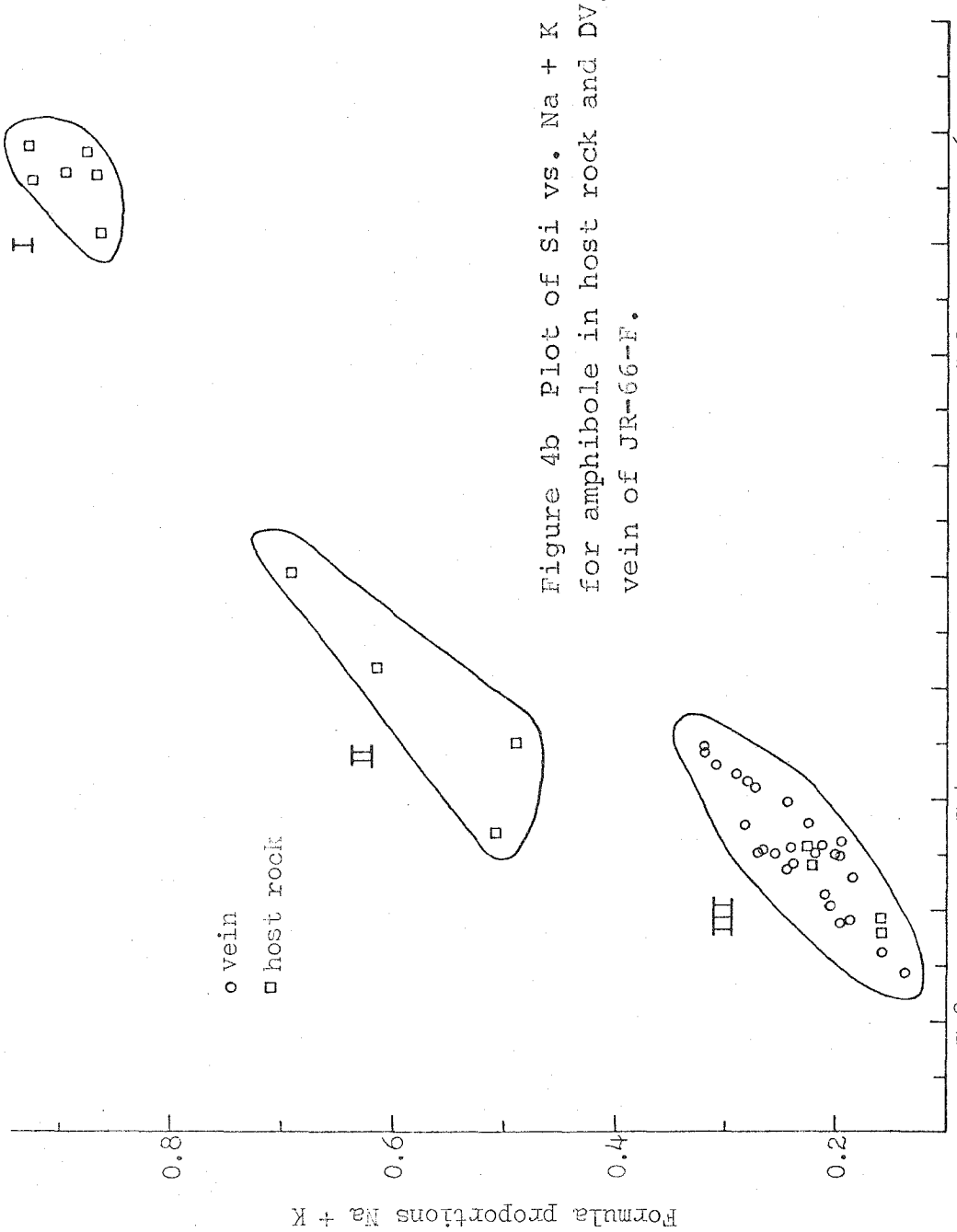

Figure 4b Plot of Si vs. Na + K for amphibole in host rock and DV_a vein of JR-66-F.

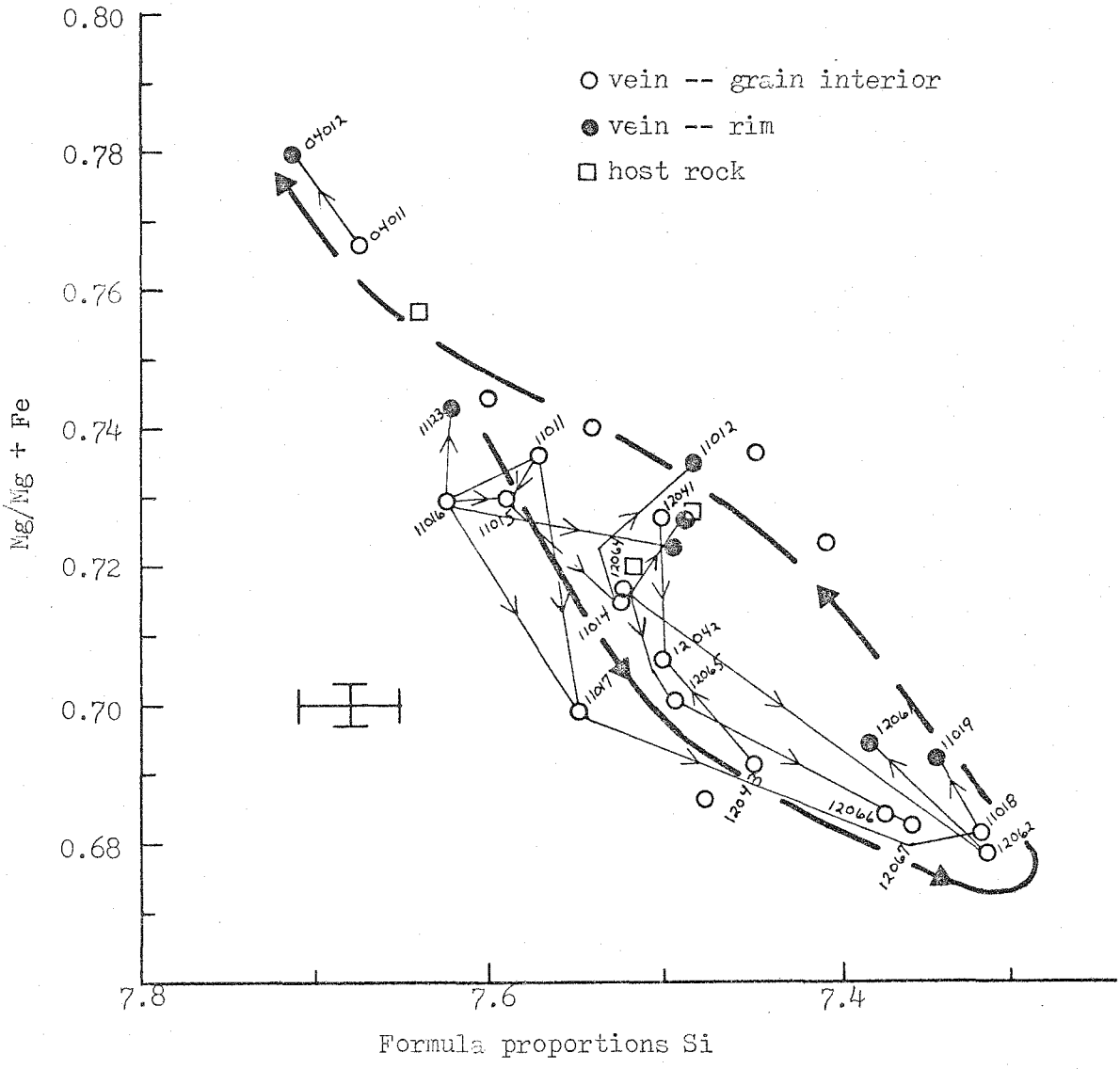

Figure 4c Plot of Si vs. Mg/Mg+Fe for DV_a vein actinolite in JR-66-F. Also shown are analyses from Group III actinolite in host rock.

rims that are lighter in color than the hornblende, but slightly darker than the outer actinolite rims and actinolite in the fractures in hornblende. Group III amphibole consists of two textural types; DV_a vein actinolite and the light colored actinolite in the host rock that rims Group II actinolite and is in the fractures in hornblende. There is no amphibole in either vein that corresponds to Group II.

Although there are not many analyses of Group II amphibole, Figure 4b shows that Group II is distinct from Group I. In thin section there are sharp boundaries between the three compositional groups in the host rock. Group II points have increased Na+K substitution relative to the other groups and somewhat more $Al^{VI}+Fe^{3+}+Ti$. Group II and Group III taken together have a considerable range of Si values and they are very different from Group I amphibole.

The compositional correspondence between DV_a vein actinolite and the light colored actinolite in the host rock suggests that this host rock actinolite may be DM_a. There is a distinct compositional difference between DV_a actinolite and Group II amphibole. Group II is apparently older than the DM_a actinolite in the vein and host rock. Group II may represent a late stage in OM_b growth or a minor event between O_b and D_a.

Figure 4c is a plot of Si vs. Mg/Mg+Fe for DV_a vein actinolite in JR-66-F. Also shown are analyses from Group III actinolite in the host rock. There appears to be a fairly systematic compositional trend for the vein actinolite as indicated by the heavy arrow in the diagram. The early part of the trend involves decreasing Si (and therefore decreasing actinolite component) and decreasing Mg/Mg+Fe. Apparently the compositions along this early part of the trend represent most of the volume of actinolite in the vein. The trend reaches a minimum value of Si and then there is a reversal; the later part of the trend involves increasing Si and Mg/Mg+Fe. The early part of the trend is well established by microprobe traverses across several grains. The outermost rims on these grains are compositions along the later part of the trend. The three analyses of Group III actinolite from the host rock fall within the range of compositions of the DV_a vein actinolite.

The trend of the DV_a vein actinolite has two interesting points. First, if the trend is correct it seems to rule out the possibility that Group II amphibole represents early growth in the host rock of the same generation. The trend starts at a high Si value, goes through a minimum and then increases again. The Group II analyses have generally lower Si contents and to fit the trend, the trend

would have to be much more complicated and involve another reversal; there is no evidence for this. That Group II is earlier than Group III is demonstrated by the textural relationships in the host rock. The other feature of the trend is that apparently during the vein forming event there was initially increasing grade, indicated by decreasing Si, and then a peak in grade was reached and growth continued as the grade decreased.

For comparison, the amphibole in the DV_c vein and adjacent host rock of JR-66-C will be discussed. Figures 5a and 5b are plots of Si vs. $Al^{VI}+Fe^{3+}+Ti$ and Si vs. Na+K for both the vein and host rock amphibole. The compositions fall into two groups which correspond to Group I and Group III of JR-66-F. Group I compositions are from remnant hornblende cores in the host rock. Group III in JR-66-C are from actinolite in the host rock and DV_c vein. For these two plots, the actinolite in the DV_a vein and the actinolite in the DV_c vein are essentially indistinguishable based only on composition. This brings up a problem in interpreting to which generation the host rock actinolite belongs. There is no analyzed amphibole in the host rock of JR-66-C which corresponds to Group II of JR-66-F.

Figure 5c is a plot of Si vs. Mg/Mg+Fe for Group III actinolite in JR-66-C. There are not enough analyses to

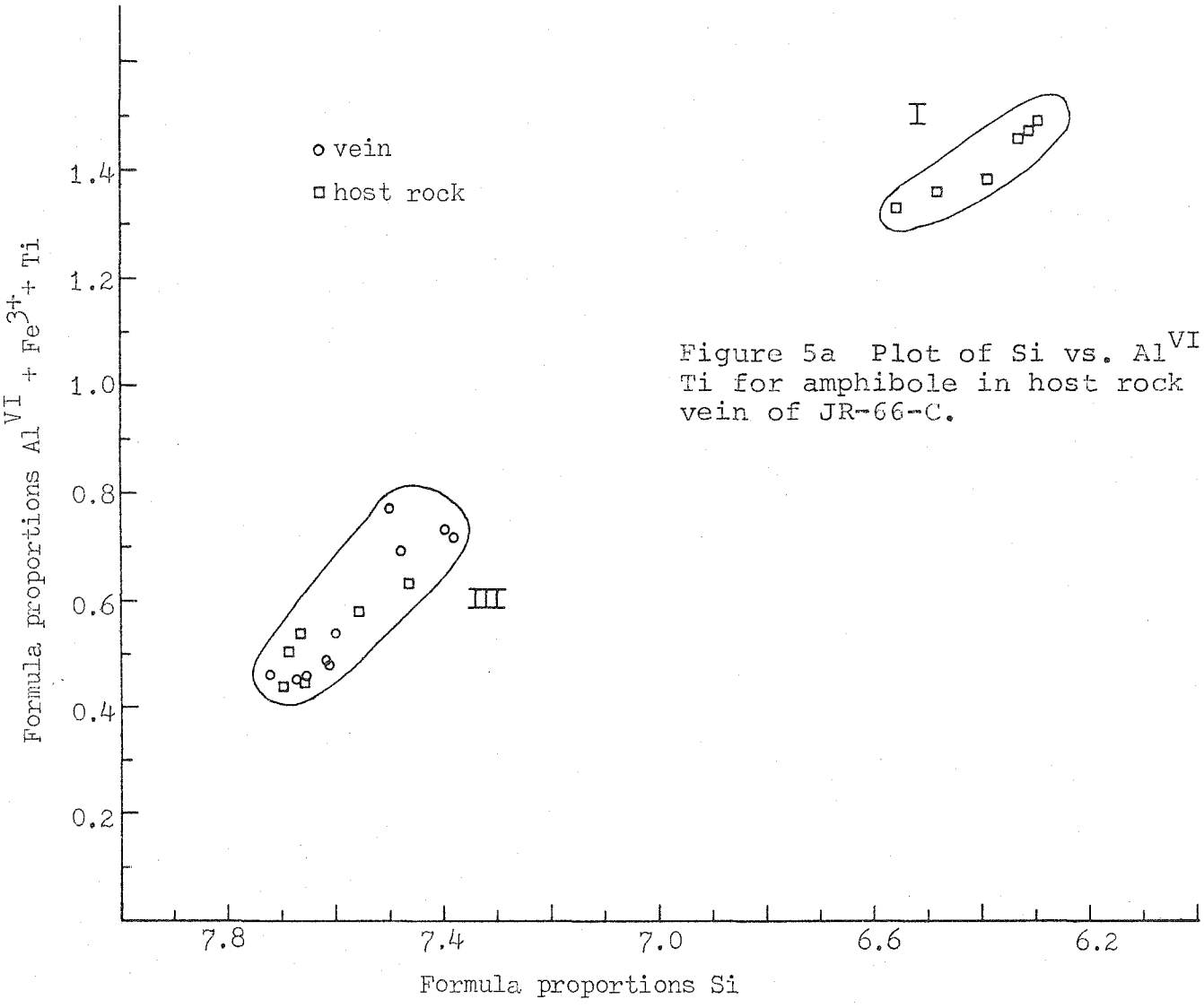

Figure 5a Plot of Si vs. $Al^{VI} + Fe^{3+} + Ti$ for amphibole in host rock and DV_c vein of JR-66-C.

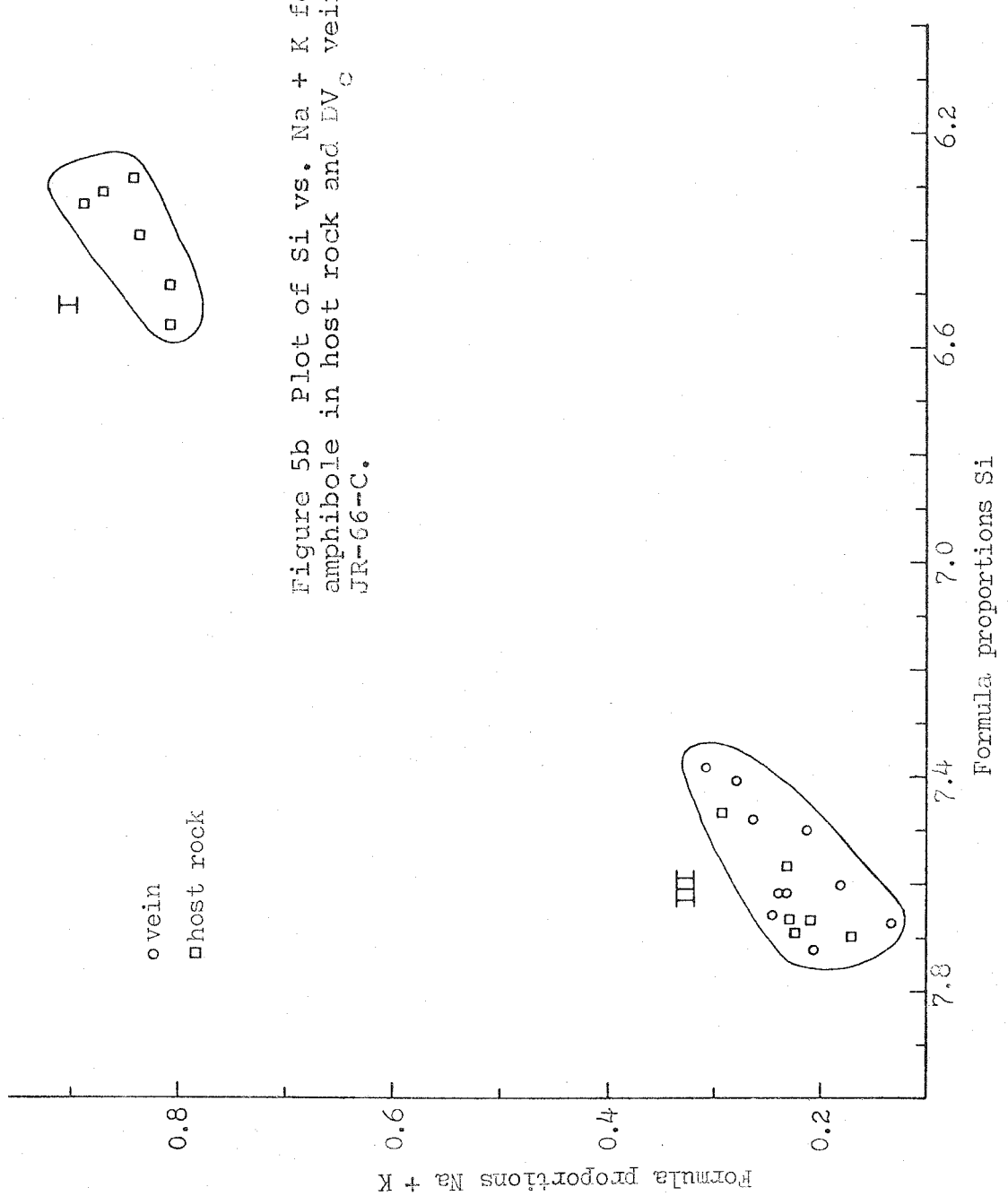

Figure 5b Plot of Si vs. Na + K for amphibole in host rock and DV_C vein of JR-66-C.

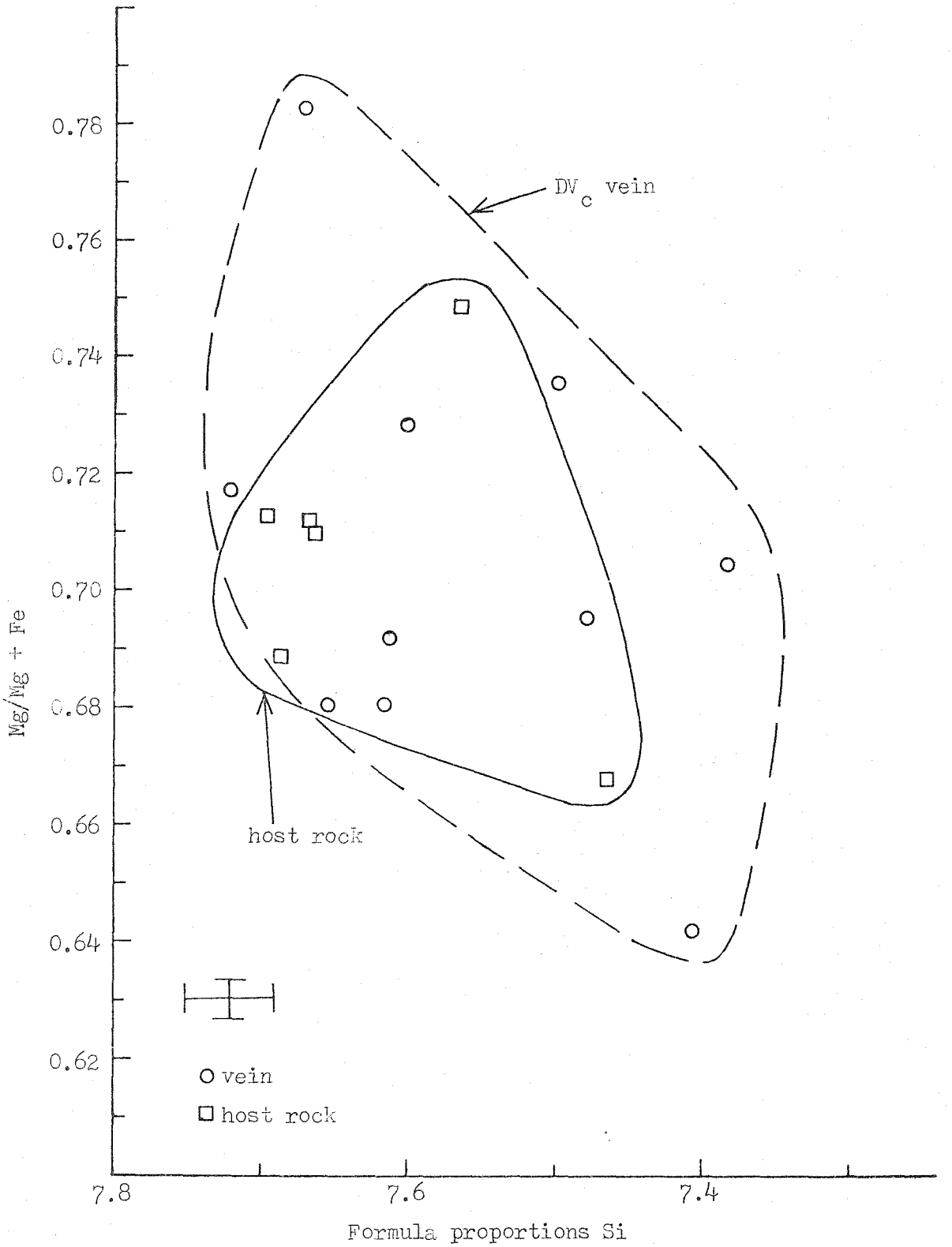

Figure 5c Plot of Si vs. Mg/Mg+Fe for DV$_c$ vein actinolite in JR-66-C.

Figure 5d Plot of Si vs. Mg/Mg+Fe for hornblende in host rocks of JR-66-F and JR-66-C.

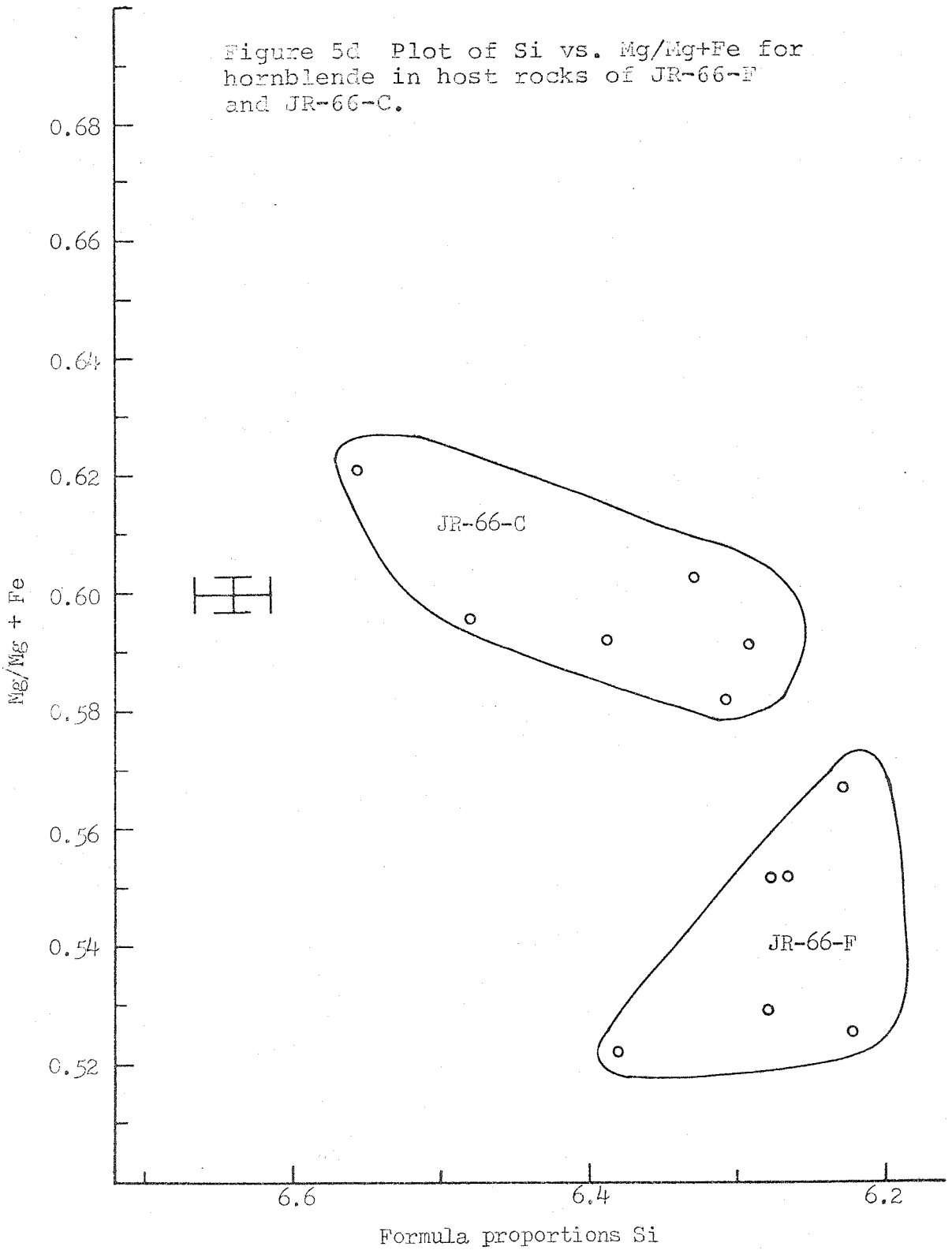

establish the compositional trends. The range of values for DV_c vein actinolite on both plots is close to the range of compositions for DV_a actinolite, although there are differences between the two. The fact that the two assemblages are different must be kept in mind when making comparisons, however. There are six analyses of actinolite from the host rock in JR-66-C and these all fall within the range of compositions of DV_c vein actinolite; they could well be DM_c in generation. Some of the host compositions also fall within the range of compositions of DV_a vein actinolite in JR-66-F. There seems to be no unambiguous solution for determining the generation of the host rock actinolite, given the lack of textural information.

Figure 5d shows host rock hornblende compositions from JR-66-C and JR-66-F on a plot of Si vs. Mg/Mg+Fe. The analyses from these two samples are not coincident. It may be that there is considerable compositional variation within this generation, OM_b, and that not enough analyses have been obtained to show the actual correspondence. The other possibility is that the difference in assemblages, with quartz in JR-66-F but not in JR-66-C, accounts for these not being coincident. There are not enough analyses in either sample to establish compositional trends.

Chlorite also occurs in both veins and host rocks. Most or all of the host rock chlorite appears to be produced by the alteration of hornblende; chlorite grains show no preferred orientation and are closely associated with actinolite in fractures within altered hornblende and in irregular masses outside the hornblende. The major compositional variables in chlorite are Al, Si, Mg, and Fe. There is some variation in the Mn content but the variation is only slightly greater than the analytical error in these two samples.

Figure 6 is a plot of Al vs. Mg/Mg+Fe for chlorite in the DV_a vein and host rock of JR-66-F. The detailed compositional trend has not been established. The general trend in the vein chlorite, suggested by the core to rim zoning in a few grains, seems to be increasing Al and roughly constant Mg/Mg+Fe. Most of the analyses of host rock chlorite in JR-66-F fall within the range of the vein chlorite, although two analyses from the cores of host rock grains do not. These two may represent early DM_a growth or they could be associated with the pre-DM_a group II actinolite. Other than these two, the chemical correspondence suggests that the host rock chlorite could be DM_a.

Figure 7 is a similar plot of Al vs. Mg/Mg+Fe for chlorite in the DV_c vein and host rock of sample JR-66-C.

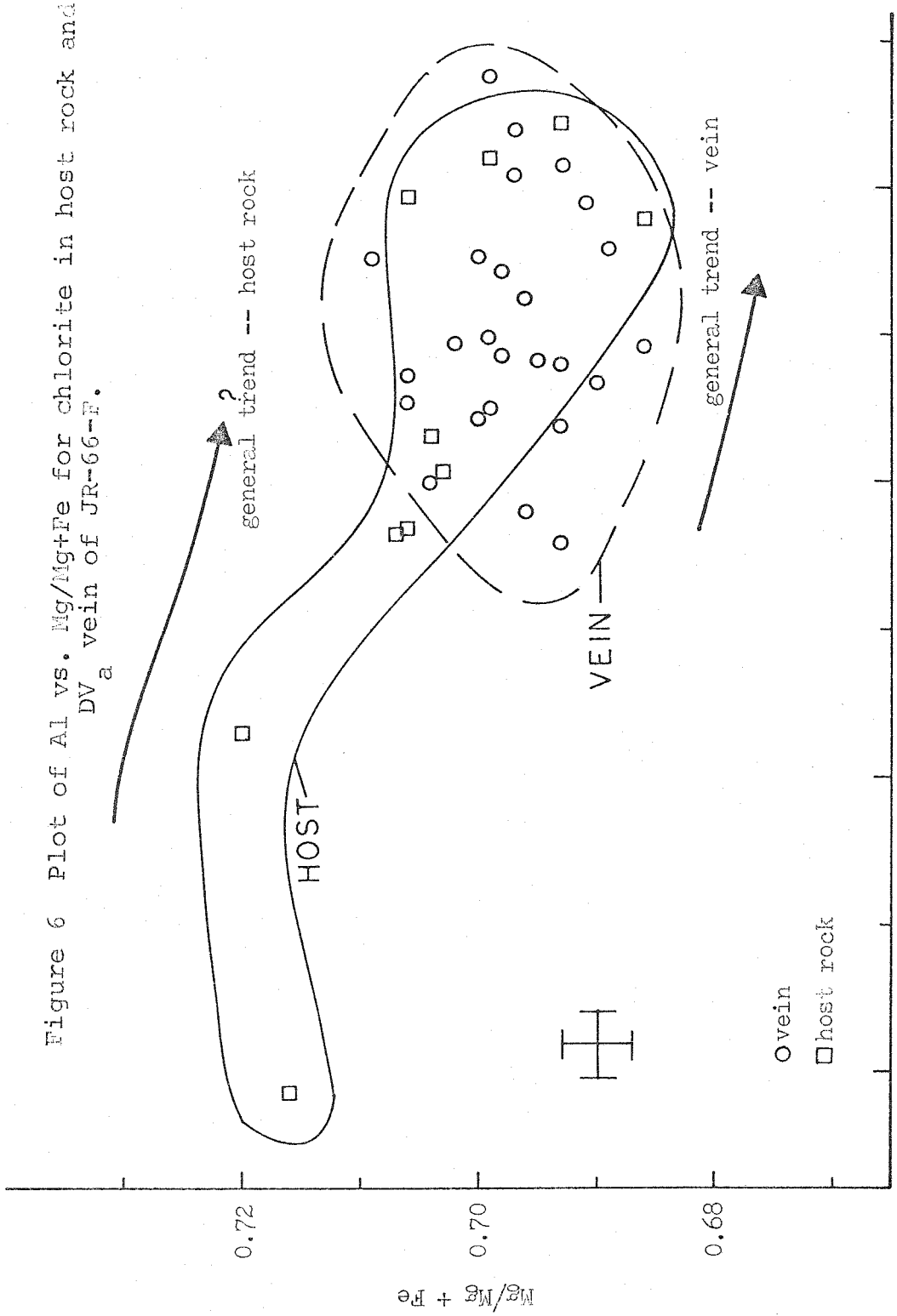

Figure 6 Plot of Al vs. Mg/Mg+Fe for chlorite in host rock and DV_a vein of JR-66-F.

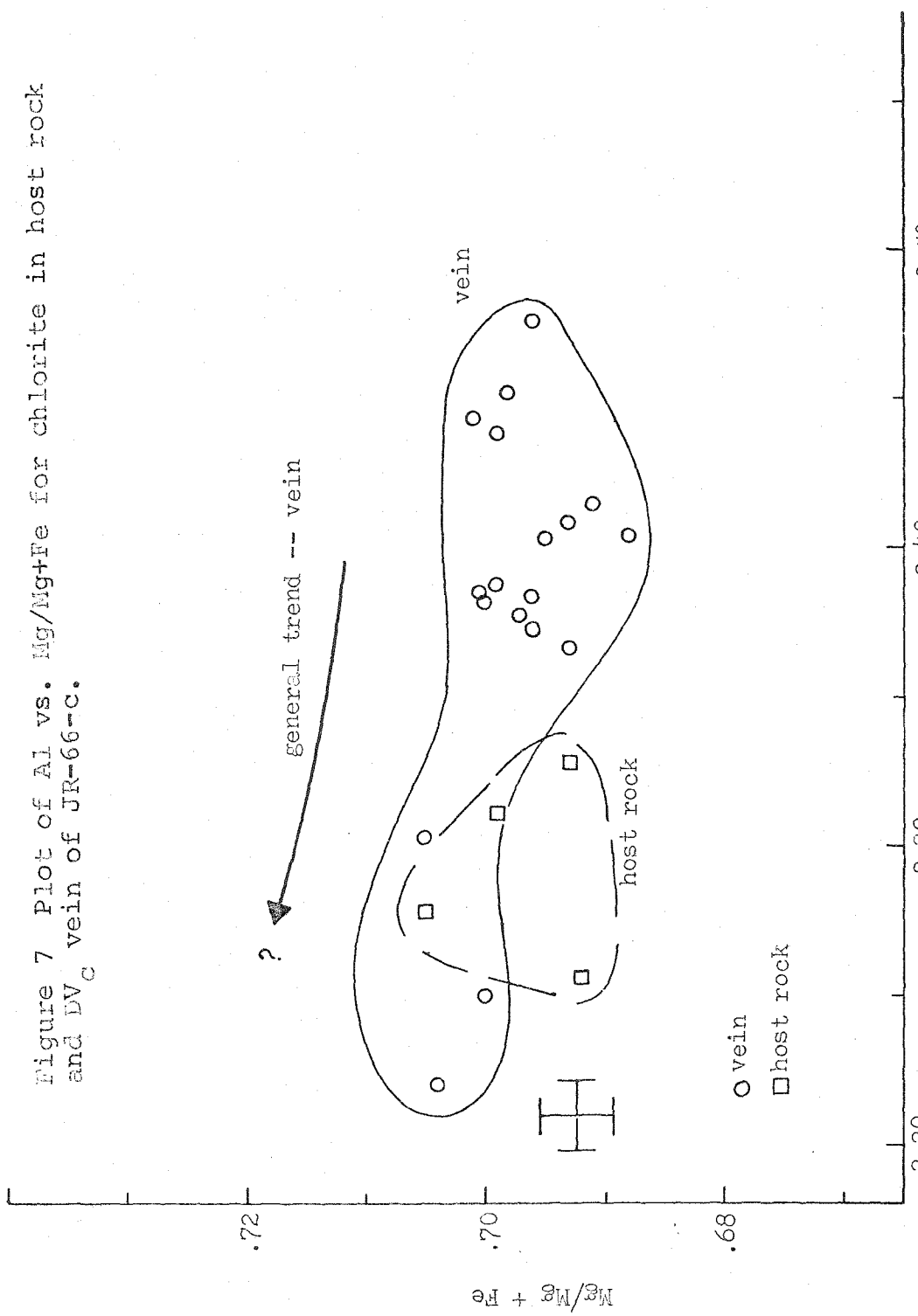

Figure 7 Plot of Al vs. Mg/Mg+Fe for chlorite in host rock and DV_c vein of JR-66-c.

The general trend for DV_c vein chlorite may be decreasing Al and relatively constant Mg/Mg+Fe. Of the four analyses of host rock chlorite, two may be outside the range of DV_c vein chlorite.

DV_c vein chlorite and DV_a vein chlorite have similar compositional ranges, although they do not exactly coincide. The host chlorite analyses from JR-66-C which do not fall within the range of DV_c vein chlorite do fall within the range of DV_a vein chlorite in JR-66-F, suggesting perhaps that these are DM_a growth. The two analyses of host chlorite in JR-66-F that fall outside the range of DV_a chlorite do not fall within the range of DV_c vein chlorite, although other analyses of host chlorite do. As is the case for host rock actinolite it is very difficult to determine the generation to which the host chlorite grains belong. For both minerals, it may be that there is a mixture of the two generations in the host rock which I have not been able to distinguish, either chemically or texturally. Only the structural relationships of the veins establish the generations.

The compositional variation of DV_a vein plagioclase in sample JR-66-F is shown in Figure 8a. The trend in most of the plagioclase in the border zone is decreasing anorthite component from core to rim. Within the vein, two

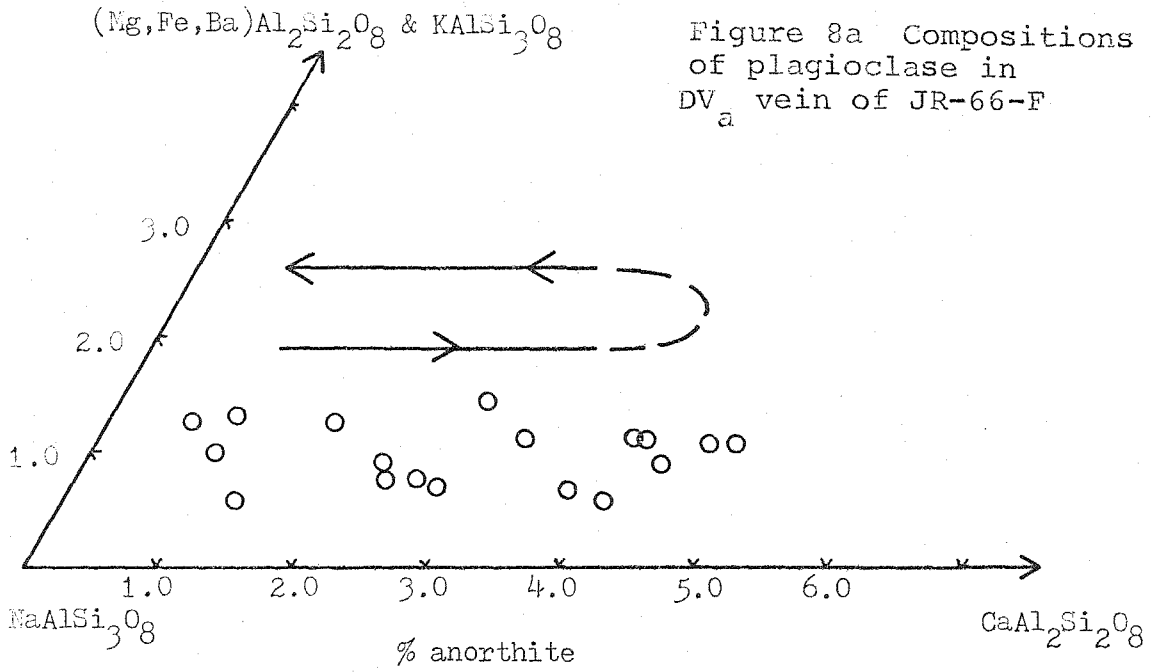

Figure 8a Compositions of plagioclase in DV_a vein of JR-66-F

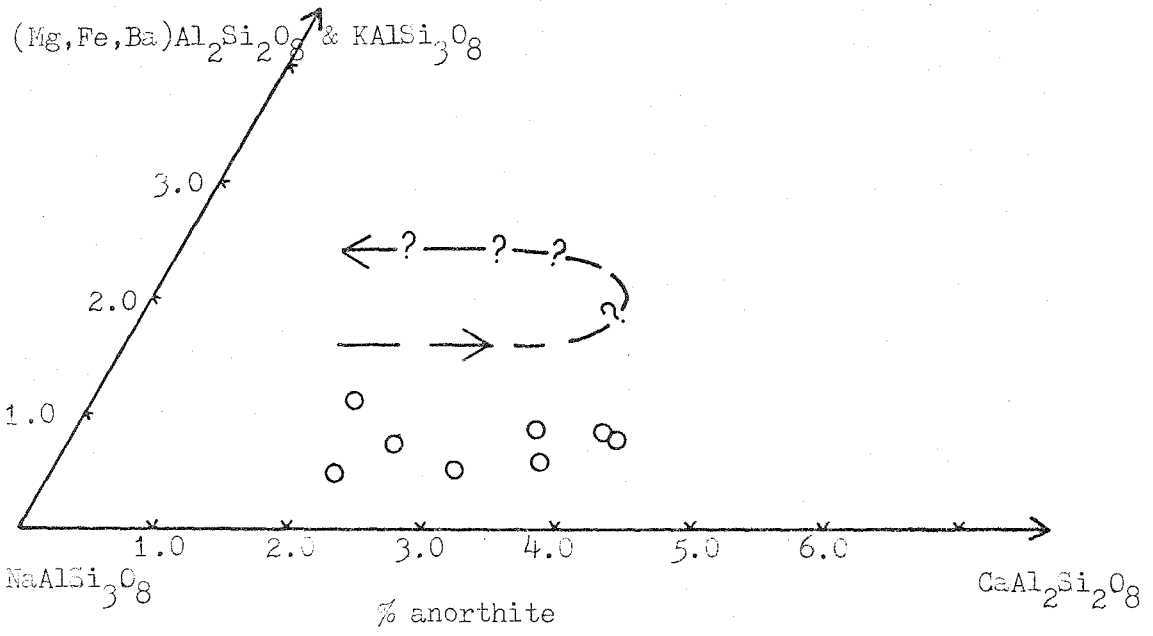

Figure 8b Compositions of plagioclase in host rock of JR-66-F.

grains show increasing anorthite component from core to rim. The low-An rims in the border zone seem to be related to the late, high-Si rims on the actinolite, so that it seems reasonable that the overall trend is initially increasing An content and then decreasing An content. The reversal in trend of the plagioclase probably does not coincide with the reversal in trend of the actinolite. The late, increasing-Si part of the actinolite trend represents only a small proportion of the total actinolite volume while plagioclase with decreasing An content seems to be predominant. Another possibility is that the initial part of the plagioclase trend is decreasing An content and that the reversal occurs in the less calcic albite compositions. In either case, the apparent trends in grade shown by the compositional trends of vein plagioclase and vein actinolite do not seem to coincide. The trend shown by the actinolite is probably more reliable as small changes in the calcium content of plagioclase may be due to minor changes in $a_{(CO_2)}$. In other samples in which plagioclase is used as an apparent indicator of grade, the relative change in composition is on the order of 20-30% in An content, much larger than the 4% change in this sample.

The compositions of host rock plagioclase in JR-66-F are shown in Figure 8b. The range in compositions is some-

what less than in the DV_a vein plagioclase, but these compositions fall entirely within the vein plagioclase range. The overall trend is not well established but may be similar to the vein plagioclase trend.

In sample JR-66-C there is not much plagioclase in the DV_c vein, but the analyzed vein plagioclase is similar in composition to the DV_a vein plagioclase. The compositional trend of the DV_c vein plagioclase seems to be increasing An content from core to rim. The range of the host rock plagioclase in JR-66-C is also similar to that in JR-66-F. One host rock grain shows textural evidence of two generations of growth; a photograph of this grain is shown in Figure 9a.

The grain in Figure 9a is a few millimeters away from the DV_c vein. There is a rounded, oblong, cloudy core surrounded by a clear rim with euhedral external boundaries. The analyzed points in this grain and their compositions are shown on the sketch in Figure 9b. The compositions are shown plotted in Figure 9c. The cloudy core is zoned from $An_{2.8}$ at the center out to $An_{1.2}$ at the boundary between the core and the clear rim. The overgrowth plagioclase is zoned from $An_{2.3}$ at the boundary between core and rim to $An_{4.2}$ at the outside rim. The earlier core perhaps has a trend of decreasing An content similar to the dominant trend of DV_a vein plagioclase; the cloudy core may be DM_a

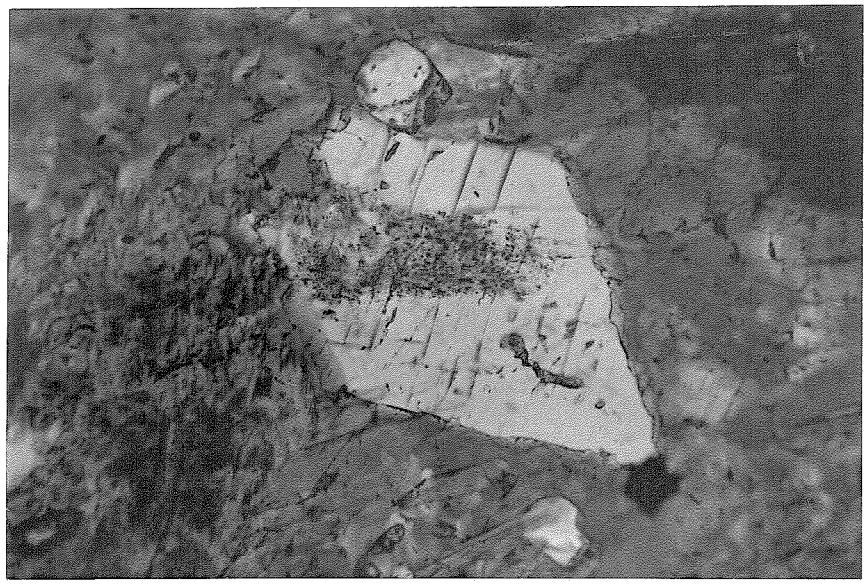

Figure 9a Plagioclase grain in amphibolite, JR-66-C. Grain appears to have two generations of mineral growth; the oldest is the cloudy core (DM_a?) and the youngest is the clear rim (DM_c?). 1.5 mm field of view, plane polarized light.

Figure 9b Sketch of plagioclase grain in Figure 9a. Numbers indicate percent anorthite content of analyzed points.

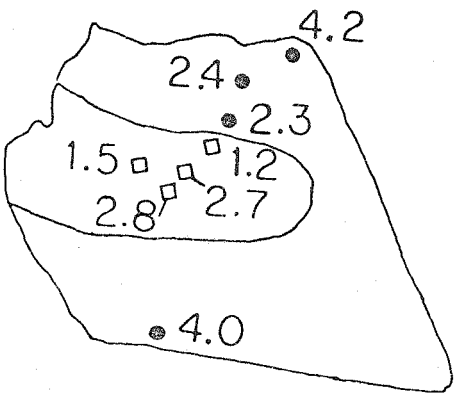

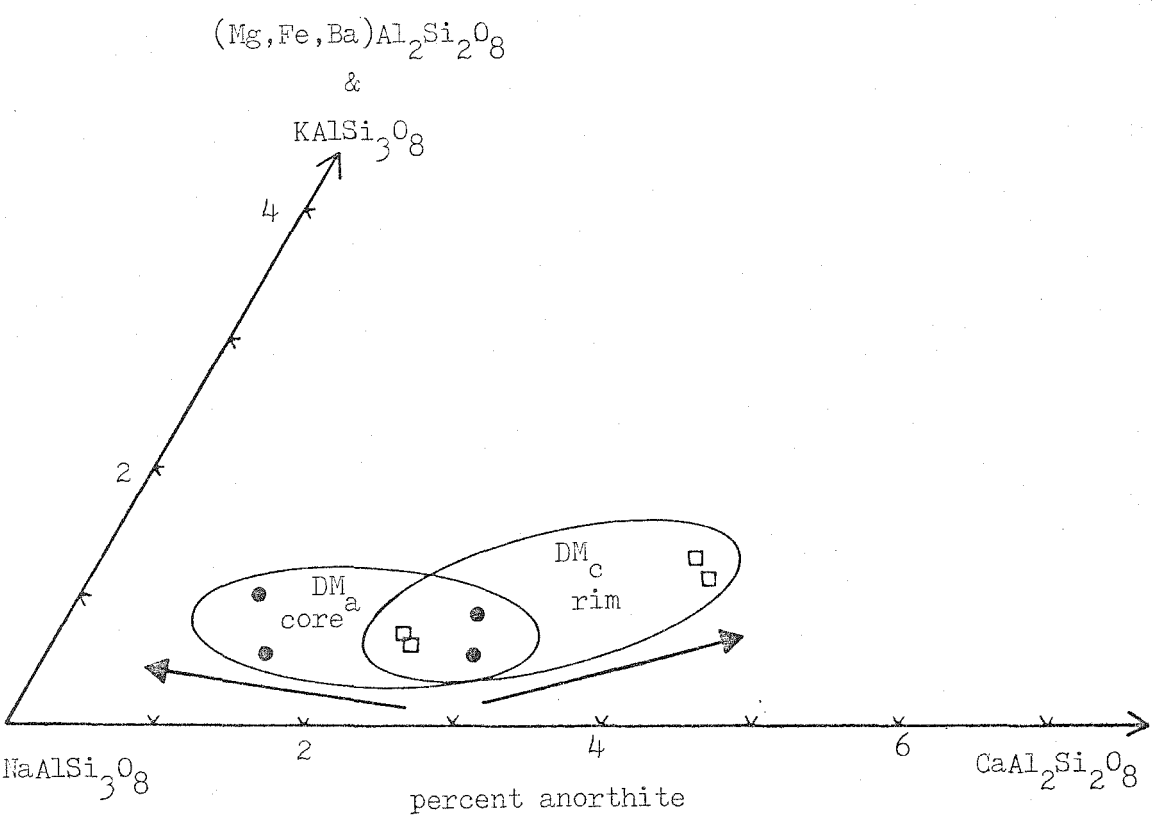

Figure 9c Compositions of plagioclase grain in Figure 9a. From host rock of JR-66-c.

in generation. The rim plagioclase has a trend similar to the DV_c plagioclase trend and may be DM_c in generation.

Figure 10 shows the compositional variation for the K-feldspar in the pods of the DV_a vein border zone in JR-66-F. The compositions are shown on triangular plots of K-feldspar vs. albite vs. Fe+Mg+Ba feldspar. There is no significant Ca in the K-feldspar of either sample. The diagram shown has an expanded scale; the variation is not great although it appears to be systematic. Figure 11 shows the compositional variation for K-feldspar in the DV_c vein of sample JR-66-C. The range of compositions is similar to that shown in Figure 10, but the trend is reversed. These trends are reasonably well established. There is very little K-feldspar in the host amphibolite of either sample.

Calcite is a major constituent of the DV_c vein. Figure 12 shows the compositional variation for vein calcite in sample JR-66-C. Also plotted are two analyses from small grains in the host rock. The vein calcite has up to 3.2% substitution of Mg, Fe, and Mn. The trend from core to rim is increasing Fe and Mg substitution and roughly constant, perhaps slightly increasing Mn. There is a late reversal in trend involving decreasing substitution of Fe and Mg.

Another mineral in the DV_c vein sample that shows

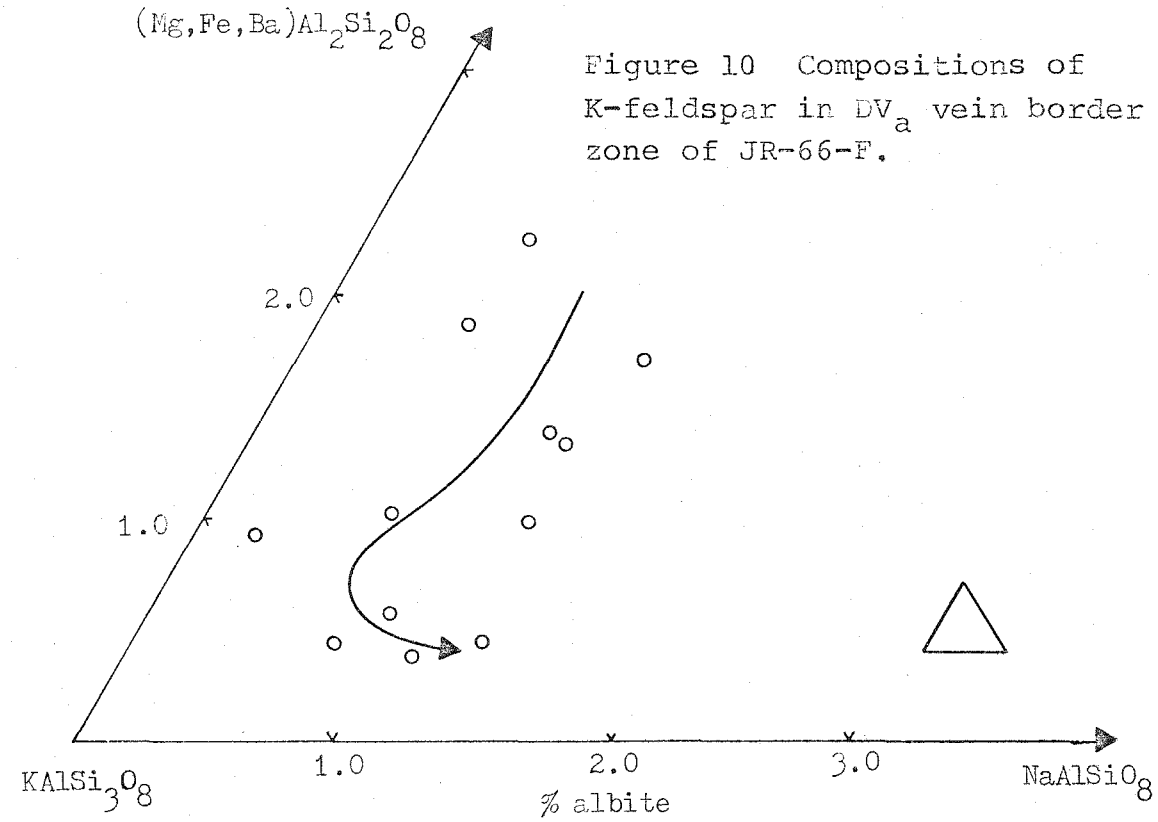

Figure 10 Compositions of K-feldspar in DV_a vein border zone of JR-66-F.

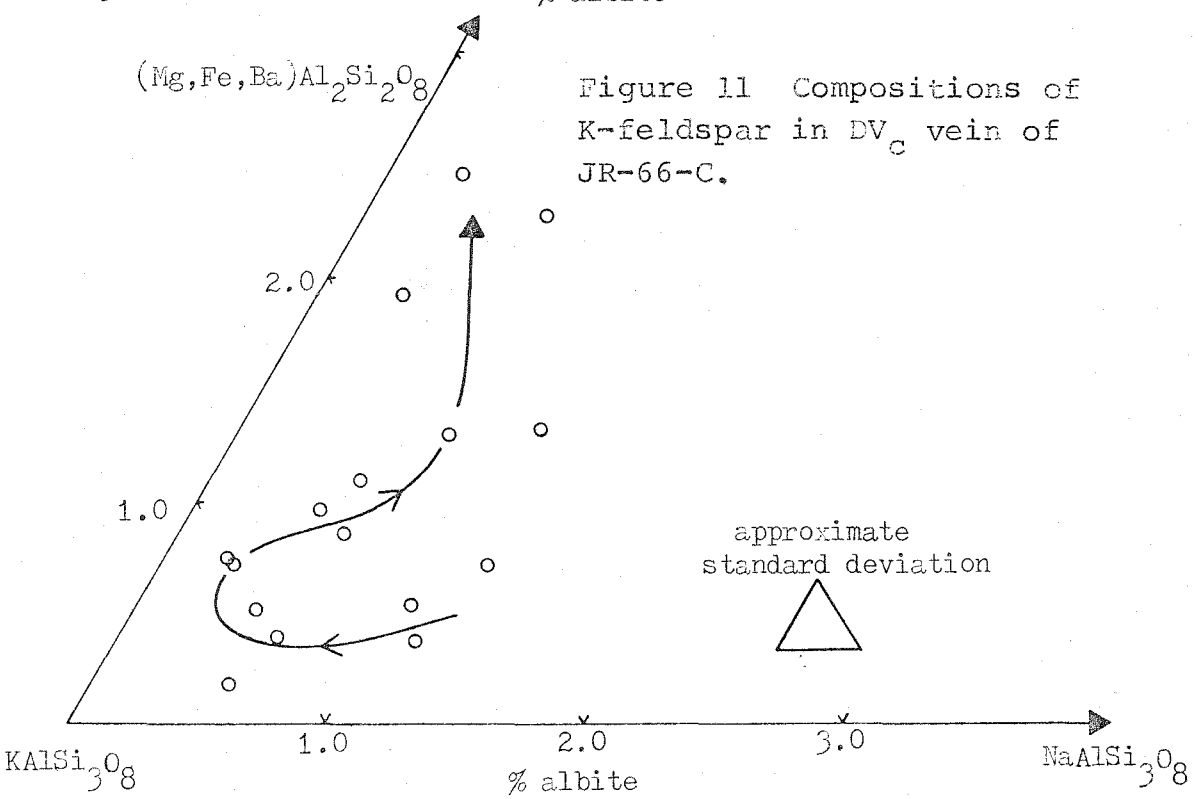

Figure 11 Compositions of K-feldspar in DV_c vein of JR-66-C.

Figure 12 Compositions of calcite in DV_c vein of JR-66-C. Also shown are two host rock calcite analyses.

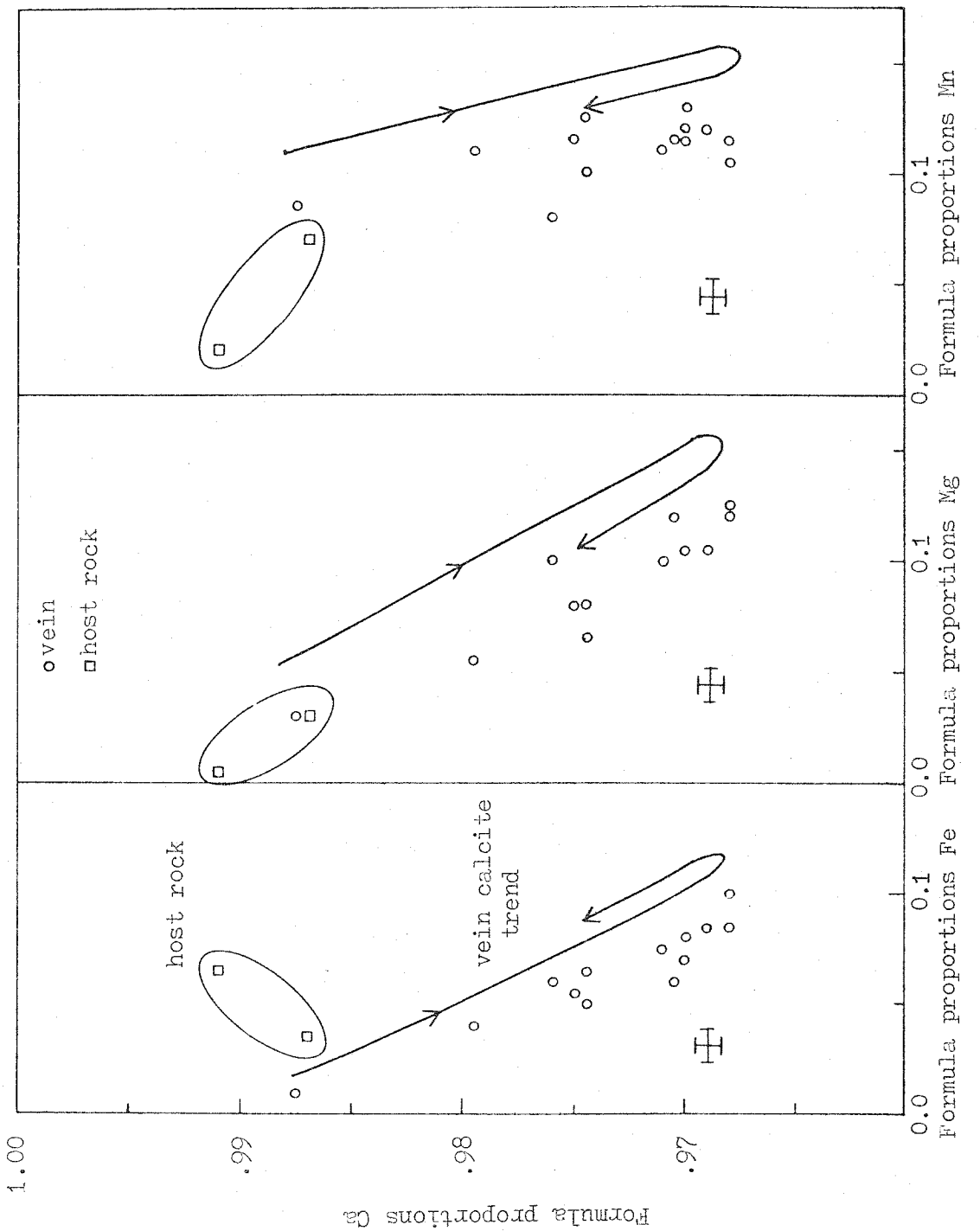
1.00
.99
.98
.97
Formula proportions Ca
host rock
vein calcite trend
vein
host rock
0.0
0.1
Formula proportions Fe
0.0
0.1
Formula proportions Mg
0.0
0.1
Formula proportions Mn

systematic compositional variation is sphene. The compositional variation for sphene in JR-66-C is plotted in Figure 13; this shows the variation in the titanium site which can also be occupied by Al and Fe. Within the limits of error, Ca and Si for these analyses have the ideal formula proportions of 1.0. Ce and Mg are not present above the limits of detection and Mn is just about at that limit in some samples with concentrations of 0.1% by weight MnO. The compositional variation trend has been established in concentrically zoned grains and involves decreasing Ti content with initially increasing Al content and constant Fe content and then apparently increasing Fe content with constant Al. Two analyses from host rock grains fall close to this trend. Apparently the substitution mechanism is the paired substitution of Ti^{4+} plus O^{2-} for Al^{3+} or Fe^{3+} plus OH^{-}, as the occupancy of the other two sites remains constant and there is not sufficient variation in the F content.

Biotite occurs in both veins, but only as minute, rare grains in the amphibolite. Figure 14 shows the range of analyzed biotite compositions from the DV_c vein and Figure 15 shows the range for biotite from the DV_a vein. Most of the biotite in the DV_a border zone is finely intergrown with chlorite and it is difficult to get an uncontaminated

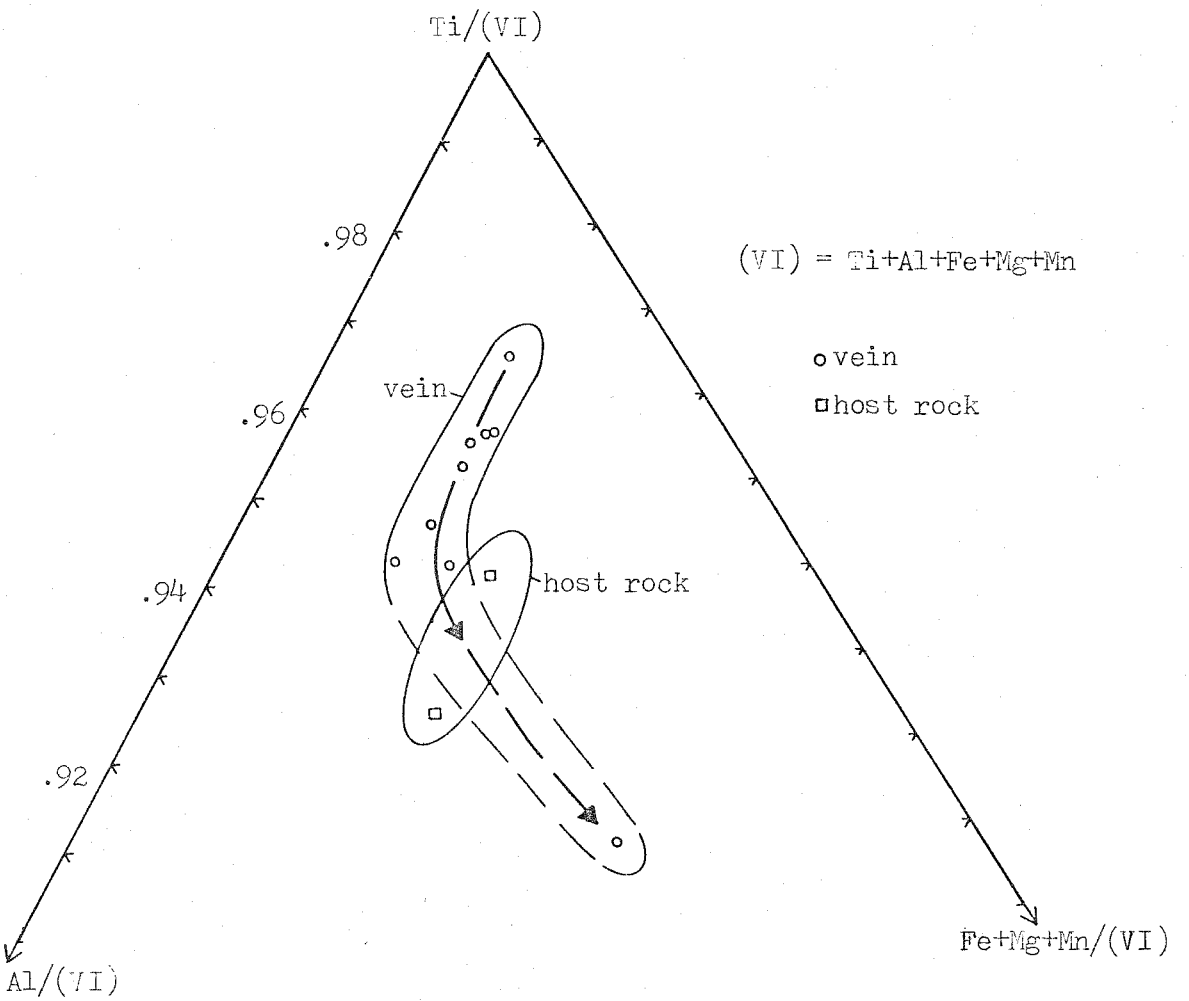

Figure 13 Compositions of sphene in DV_C vein and host rock of JR-66-C.

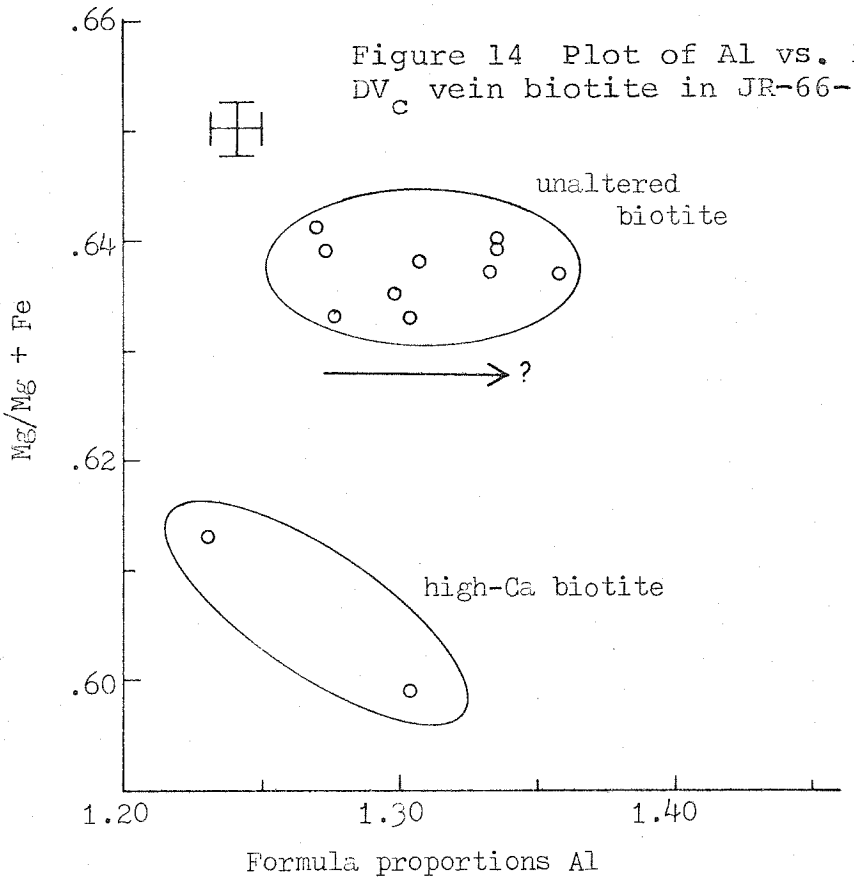

Figure 14 Plot of Al vs. Mg/Mg+Fe for DV_c vein biotite in JR-66-C.

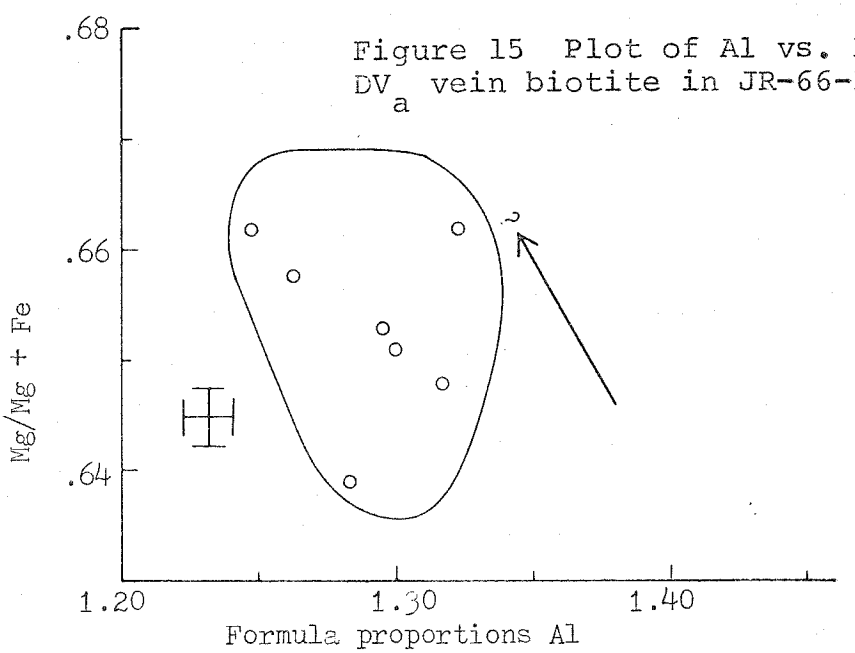

Figure 15 Plot of Al vs. Mg/Mg+Fe for DV_a vein biotite in JR-66-F.

analysis so that the vein border analyses are from the border zone band with only biotite. The suggested general trends are shown in the diagrams, but these are not well established.

Two of the DV_c vein biotite analyses shown on Figure 14 have high Ca contents. It appears that these represent interlaminated biotite and clintonite. The two analyses have 26% and 34% clintonite component. This appears texturally to be a late alteration of originally low-calcium vein biotite. This alteration may be a late stage of DM_c growth or may be younger.

One other major mineral in the host amphibolite is epidote. This shows variation in the $Al \leftrightarrow Fe^{3+}$ substitution. Host epidote grains are irregularly and nonconcentrically zoned, so that no systematic trend can be established. The only systematic feature of the zoning is that the more Fe^{3+}-rich epidote seems to be closely associated with the retrograde products such as actinolite and chlorite. Other minerals show minor compositional variation; hematite has minor variation in the Ti and V contents and apatite varies in the Ce content from 0.0 to 0.3 weight percent.

Taken together, the data from these two samples show that there is variation preserved in all of the major minerals except quartz. Given sufficient numbers of analyses,

there seem to be systematic variations in at least several of the minerals such as actinolite, plagioclase, K-feldspar, sphene, calcite, and perhaps chlorite. Only epidote appears to have nonsystematic compositional variation as shown by zoning patterns in grains. In several cases no systematic trend has been established because of insufficient numbers of analyses, but these are not shown to be unsystematic either.

Preservation of systematic trends, whether detailed or general, suggests that the zoning is a growth feature. Despite the number of events that have affected these rocks, it appears that a great deal of the mineral growth history is preserved within the veins and the host rock. The data from these two samples, about 300 microprobe analyses, provide a general understanding of what happened in these events. To obtain a more detailed account of the mineral growth history would require much more data.

The presence of zoned grains of the reactants and products makes it impossible to write a reaction with fixed proportions even if other problems were not present. It is not possible to unambiguously match the corresponding compositions of the different product minerals and there is no way to determine the average composition of the reactants at any one time. Even the reversals in trend of the product

minerals may not coincide, as seems to be the case for DV_a vein plagioclase actinolite.

The general reactions can be considered, however. If it is assumed that the layering in the DV_a border zone represents a sequence of growing assemblages, the initial DM_a retrograde reaction is:

hornblende + Al-rich epidote + plagioclase (?) +magnetite→actinolite + chlorite + albite + calcite + hematite + sphene + Fe^{3+}-rich epidote + K^+

Later biotite and then K-feldspar would appear. Quartz is present in both the reactant and product assemblages. The retrogradation represents the formation of minerals which contain more H_2O and CO_2 than the reactants. The reaction for the formation of DM_c minerals is essentially the same except that quartz is not present and hematite may or may not be involved. Also, there is no evidence that DV_c veins biotite and K-feldspar were not always part of the DM_c assemblage.

Only a small proportion of the volume of the two veins seems to be provided by the retrograde reactions. The DV_a vein is predominantly quartz. The quartz must be removed from the host rock by some mechanism other than a retrograde reaction. A possible mechanism is a small pressure difference between the confining pressure in the host rock

and the fluid pressure in the vein. The DV_c veins are mostly calcite and plagioclase. A similar pressure gradient mechanism may have been responsible; however, a reaction involving the breakdown of more calcic plagioclase and the formation of albite and calcite is possible.

The structural positions of the two generations of veins establishes that there were at least two generations of amphibolite retrogradation; these generations are DM_a and DM_c. The high grade hornblende is probably OM_b in generation, as the high grade assemblages in the nearby pelitic rocks have been shown to be OM_b. Similar hornblende found further to the south in the Worcester Mountains was dated by Lanphere and Albee (1974) as late Ordovician and unpublished dates on hornblende from Elmore Mountain indicate a similar age. The only unidentified generation is that to which the Group II amphibole in JR-66-F belongs. There may be chlorite and perhaps other minerals associated with this pre-DM_a generation. One possibility is this represents a late stage in OM_b growth and another is that it is a separate generation between OM_b and DM_a. Such a generation has been found at location JR-24 near Fairfax Falls in an outcrop of the Pinnacle formation; there mineral growth in the host rock is related to the growth of veins identified as OV_{b+3}. The OV_{b+3} assemblage at JR-24 includes

stilpnomelane, K-feldspar, calcite, and the rare mineral crichtonite; this mineral growth represents a retrograde overprint on a biotite-bearing OM_b assemblage. JR-24 is far from JR-66 but at least there is a suggestion that there may be a mineral growth event of perhaps minor importance which is widespread and occurs between O_b and D_a.

It is not possible to determine which of the two Devonian retrograde events, D_a and D_c, is most important in terms of the volume of amphibolite that was affected. There is too much ambiguity because of the overlap of compositions. Only much more detailed microprobe work could possibly separate these two in the host rock and it may be that even then ambiguity would remain. There is no reason to suppose that the effects of an event are uniform throughout a volume of rock even on an outcrop scale. Data from location JR-5 to the west of Waterbury indicate that the effects of DM_a overprint in the host schist are not uniform throughout the outcrop. In any event, the veins serve to show that the two generations are present, something which detailed microtextural analyses or microprobe work in the host amphibolite might not establish.

JR-73-A

Sample JR-73-A is a good example of multiple genera-

tions within a pelitic host rock. The sample is comprised mainly of OM_b minerals, including muscovite, chlorite, garnet, and plagioclase. The zoning in plagioclase and muscovite indicates that grade was progressively increasing during OM_b growth. The OM_b assemblage has been overprinted by limited DM_a growth of clorite, mucovite, and perhaps others. Some DM_a chlorite and muscovite grains have preferred orientation parallel to DS_a slip cleavage. Other grains have no preferred orientation. DS_a is largely defined by OM_b grains which have been rotated on the limbs of DF_a microfolds.

Location JR-73 is along the Winooski River traverse on the east limb of the Green Mountain anticlinorium in the Camels Hump quadrangle. The mineral growth along the portion of the traverse across the Green Mountain axis is described in detail in the next section. JR-73 is an outcrop of the Underhill formation. Sample JR-73-A is a fairly typical silver-green schist with porphyroblasts of garnet, magnetite, and plagioclase surrounded by a matrix of quartz, chlorite, muscovite, and minor amounts of other minerals. The entire assemblage, regardless of generation, is quartz-muscovite-chlorite-garnet-chloritoid-magnetite-ilmenite-epidote+allanite-tourmaline-apatite-zircon. All of the chloritoid is present as included grains in garnet porphyroblasts.

The location is a small outcrop and all of the structural elements found in the area are not present at JR-73. A prominent schistosity, OS_a/OS_b, is everywhere present and defined by the preferred orientation of chlorite and muscovite grains. Parallel to this schistosity are OV_b veins, which are rich in plagioclase and have euhedral garnet grains at the vein margins. The vein plagioclase is zoned with oligoclase cores overgrown by thin albite rims; between the two compositional zones is a sharp optical discontinuity which apparently represents the peristerite gap. This is a typical zoning pattern in OV_b vein plagioclase in the immediate area and has been documented with microprobe analyses at locations JR-5 and JR-4. The schistosity and the OV_b veins are folded by asymmetric moderately tight DF_a folds which have an associated slip cleavage, DS_a, only locally present. DS_a is not a pervasive, well-developed feature in general. It seems to be largely the result of rotation of muscovite and chlorite grains along the short limbs of DF_a microfolds so that OM_b minerals in general define DS_a. However, observed in thin section is some growth of chlorite and muscovite grains which clearly crosscut OM_b grains and are oriented parallel to DS_a where OM_b grains are not; this is therefore DM_a growth. It appears from the thin sections observed and from field observations of the

nature of DS_a that DM_a growth is probably limited in extent. Except for some small OF_b folds, these are the only structural elements present at JR-73.

Sample JR-73-A reflects the same elements and structural style which are seen in the entire outcrop. There is a well developed schistosity, OS_a/OS_b, and the most of the matrix chlorite and muscovite grains have preferred orientations parallel to this. The schistosity is folded by tight, asymmetric DF_a microfolds. The average grain size is a few tenths of a millimeter or less in largest dimension, but also present are abundant porphyroblasts of garnet, plagioclase, and magnetite that average about 1-4 millimeters in diameter. In the vicinity of these porphyroblasts, the DF_a microfolds tend to assume styles and orientations which are different from typical DF_a folds away from the porphyroblasts; isoclinal and box microfolds are only observed near to the porphyroblasts. DS_a is largely defined by bands of rotated muscovite and chlorite grains along the short limbs of the microfolds. The average wavelength of DF_a microfolds is 0.5 - 1.0 centimeters. A few grains of chlorite and muscovite have preferred orientations parallel to DS_a and appear to crosscut grains oriented parallel to OS_a/OS_b. This is illustrated in Figures 16a and 16b. There are also areas in the sample in which mus-

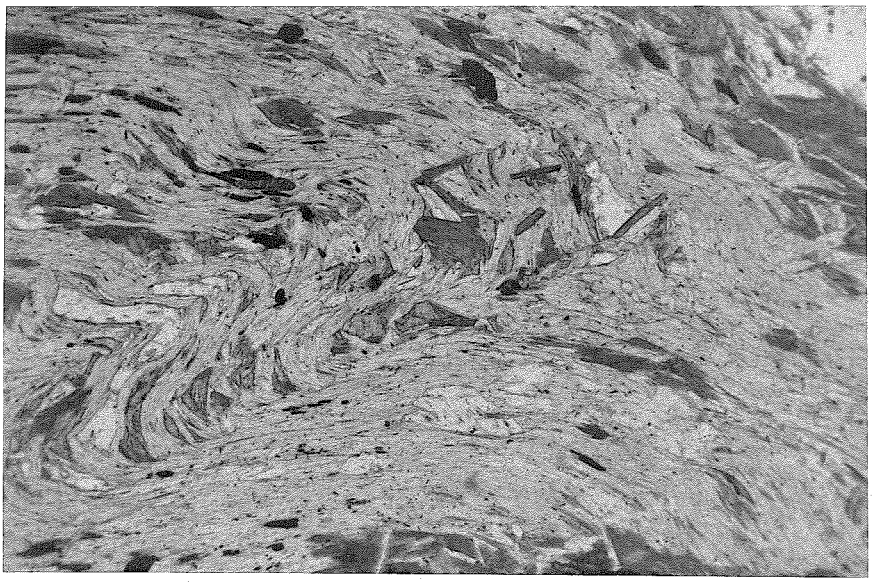

Figure 16a DF_a microfold in JR-73-A. Folds deform OS_a/OS_b, defined by parallel preferred orientation of muscovite and some chlorite. DS_a is weakly defined by rotated OM_b muscovite on limbs. 3 mm field of view, plane polarized light.

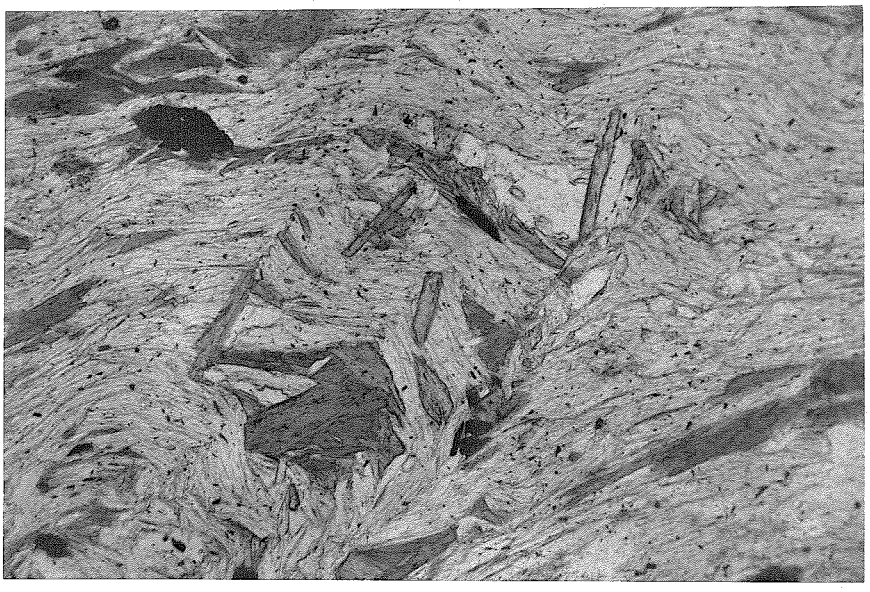

Figure 16b Blow-up of central portion of Figure 16a. Photograph shows primary DM_a chlorite grains which cross-cut OS_a/OS_b and are parallel to DS_a. 1.5 mm field of view, plane polarized light.

covite and chlorite grains show no preferred orientation but appear to represent growth later than the formation of OS_a/OS_b. Some of the chlorite without preferred orientation is in contact with magnetite and garnet porphyroblasts.

In Figure 16a, muscovite grains with preferred orientation parallel to OS_a/OS_b have been rotated by DF_a microfolds so that they define DS_a slip cleavage. There is only a limited amount of growth of chlorite and muscovite grains parallel to DS_a. This area of the sample is not really representative because there is even less growth of DM_a chlorite and muscovite with preferred orientation parallel to DS_a throughout most of the thin section. One feature of interest is the lopolith-shaped chlorite grains in the axial region of the DF_a fold in the photograph. These may also be DM_a growth, but there are no analyses of these grains to verify it.

Garnet grains tend to be euhedral, although there is textural evidence of resorption of a few of the garnet grains; these few have irregular boundaries and are generally surrounded by grains of other minerals which have no preferred orientation. Garnet grains show sector twinning and are biaxial; these are probably strain induced phenomena as there are no compositional peculiarities which could explain them. The garnet growth is probably all OM_b in

generation based upon garnet in the OV_b vein in sample JR-73-B and upon observations at locations in the immediate area. At nearby locations, DM_a growth is seen to represent retrogradation of preexisting garnet. No DM_a garnet growth has been observed along the Winooski River traverse.

The plagioclase porphyroblasts are elongate parallel to OS_a/OS_b and appear to be deformed by DF_a microfolds. The plagioclase is probably OM_b in generation. Plagioclase grains are optically zoned and each has a close elliptical optical discontinuity, observed with crossed nicols; this appears to represent the peristerite gap and is the boundary between oligoclase in the core and albite in the rim. The peristerite gap is a break between albite and oligoclase in the mostly continuous solid solution series in the plagioclase feldspars at low to moderate metamorphic temperatures. A recent discussion can be found in Orville (1974).

Samples at nearby location JR-5 show good evidence of overgrowth of DM_a plagioclase on OM_b plagioclase. This is discussed in the next section. There is no such evidence in JR-73-A, although very thin rims which occur on some of the plagioclase grains are possibly DM_a growth. In general, the plagioclase and other minerals do not show the evidence of overprint that can be found in some samples from nearby locations.

Chloritoid is found only as grains included in garnet porphyroblasts. Chloritoid inclusions generally occur within the inner two-thirds of the porphyroblasts. There are inclusions of other minerals in the outer portions of the garnet grains, but not chloritoid. This textural evidence suggests that the chloritoid is OM_b in generation, that chloritoid growth stopped before garnet growth stopped, and that matrix chloritoid was all removed by reaction, perhaps during late OM_b growth.

Significant variation is found in the compositions of plagioclase, garnet, chlorite, muscovite, and chloritoid. These, along with magnetite, which shows no significant compositional variation, and quartz make up the bulk of the sample. There appear to be two generations of chlorite and muscovite: OM_b and DM_a. There is no textural or chemical evidence for any other mineral growth generation with the possible exception of remnant OM_a cores or inclusions in OM_b garnet.

Figure 17a is a photograph of a typical plagioclase porphyroblast in JR-73-A. Microprobe data from several grains are shown in Figure 17b. Cores have albitic compositions zoned from An_3 in the inner cores to about $An_{6.5}$ near the optical discontinuity between cores and rims. Compositions immediately across the discontinuity on the

Figure 17a Plagioclase porphyroblast in JR-73-A. The core is albite and the rim is oligoclase. The optical discontinuity between core and rim probably represents the peristerite gap. 3 mm field of view, crossed nicols.

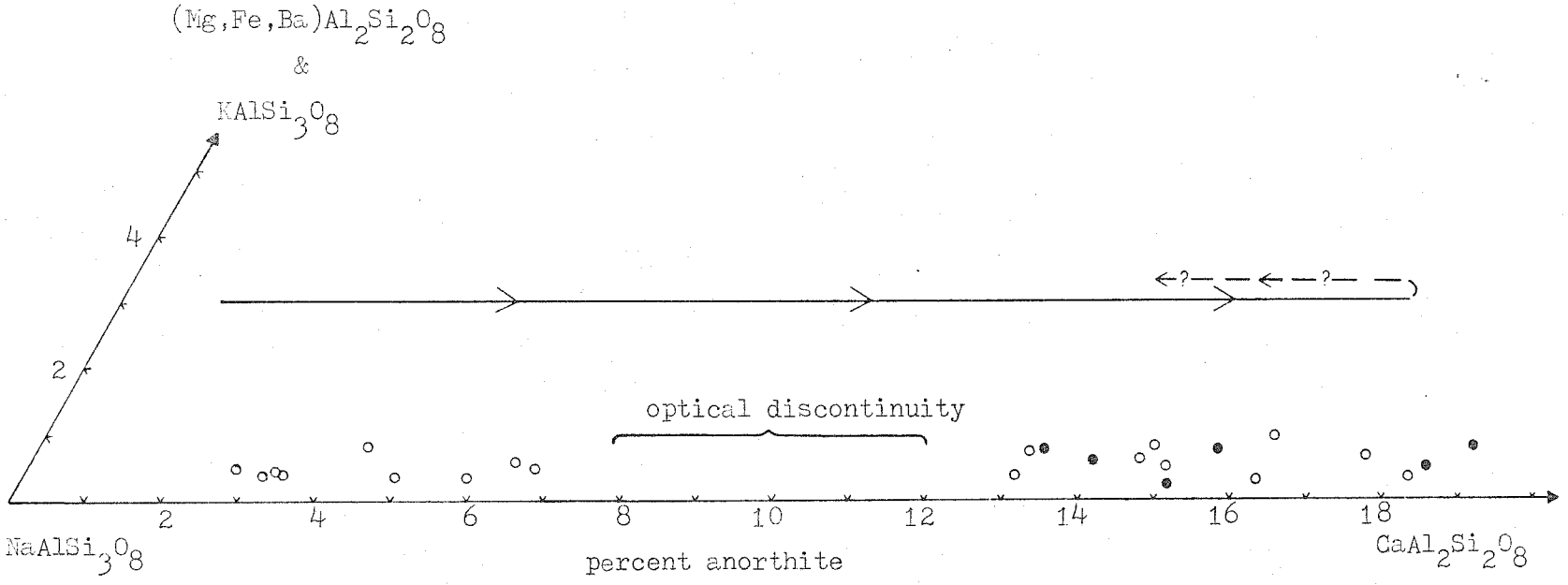

Figure 17b Compositions of plagioclase in JR-73-A. Location of optical discontinuity, probably representing the peristerite gap encountered during growth, is shown with brackets. Filled circles on diagram are rim analyses.

other side are about An_{13}, and the outer portions are zoned from An_{13} to almost An_{19} at the outermost rims. Therefore, the zoning pattern indicates increasing grade as the plagioclase grew during event O_b. The plagioclase-forming reaction in this case was perhaps a dehydration reaction involving epidote as there is no calcite in the sample. This is a zoning pattern typical of OM_b plagioclase along this segment of the Winooski River traverse regardless of the calcium mineral present, calcite and/or epidote. There is evidence of a zoning reversal in one plagioclase grain involving a very thin portion of the outermost rim. The reversal is from An_{19} to about $An_{14.5}$ and may represent either late, down-grade OM_b growth or limited DM_a overgrowth.

Garnet compositions are shown in Figure 18a. Garnet grains are fairly consistently zoned with decreasing Mn from core to rim, so that Fe^{2+}, Ca, and Mg are shown plotted against Mn. The data are from traverses in four grains. The plot of Mn vs. Mg defines a smooth curve with gradually increasing Mg as Mn decreases. This apparent systematic relationship between Mn and Mg is seen in garnet from other samples in portions of the grains in which there is no reversal of Mn, although the value of Mg that corresponds to a given value of Mn differs from sample to sample. In con-

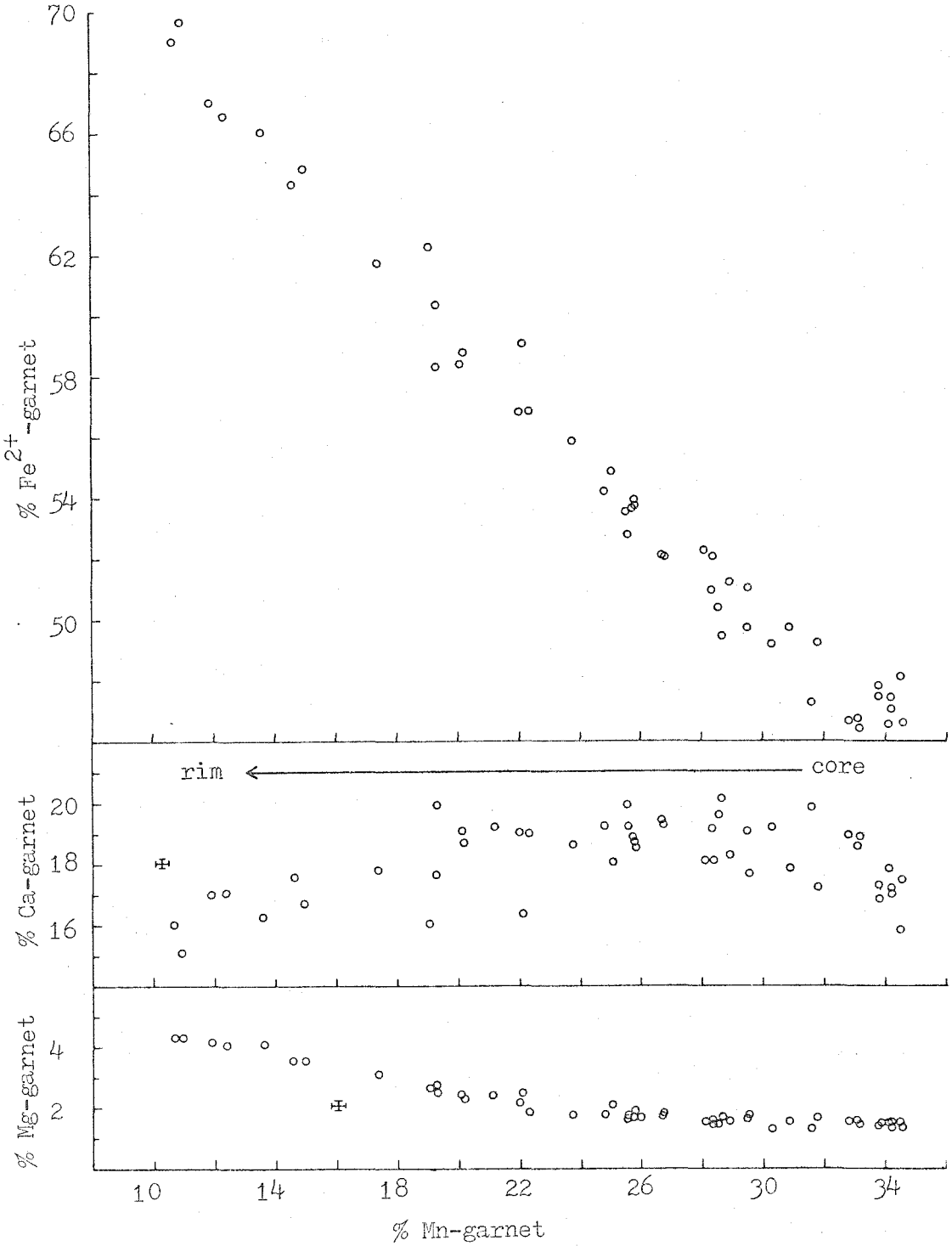

Figure 18a Compositions of garnet in JR-73-A.

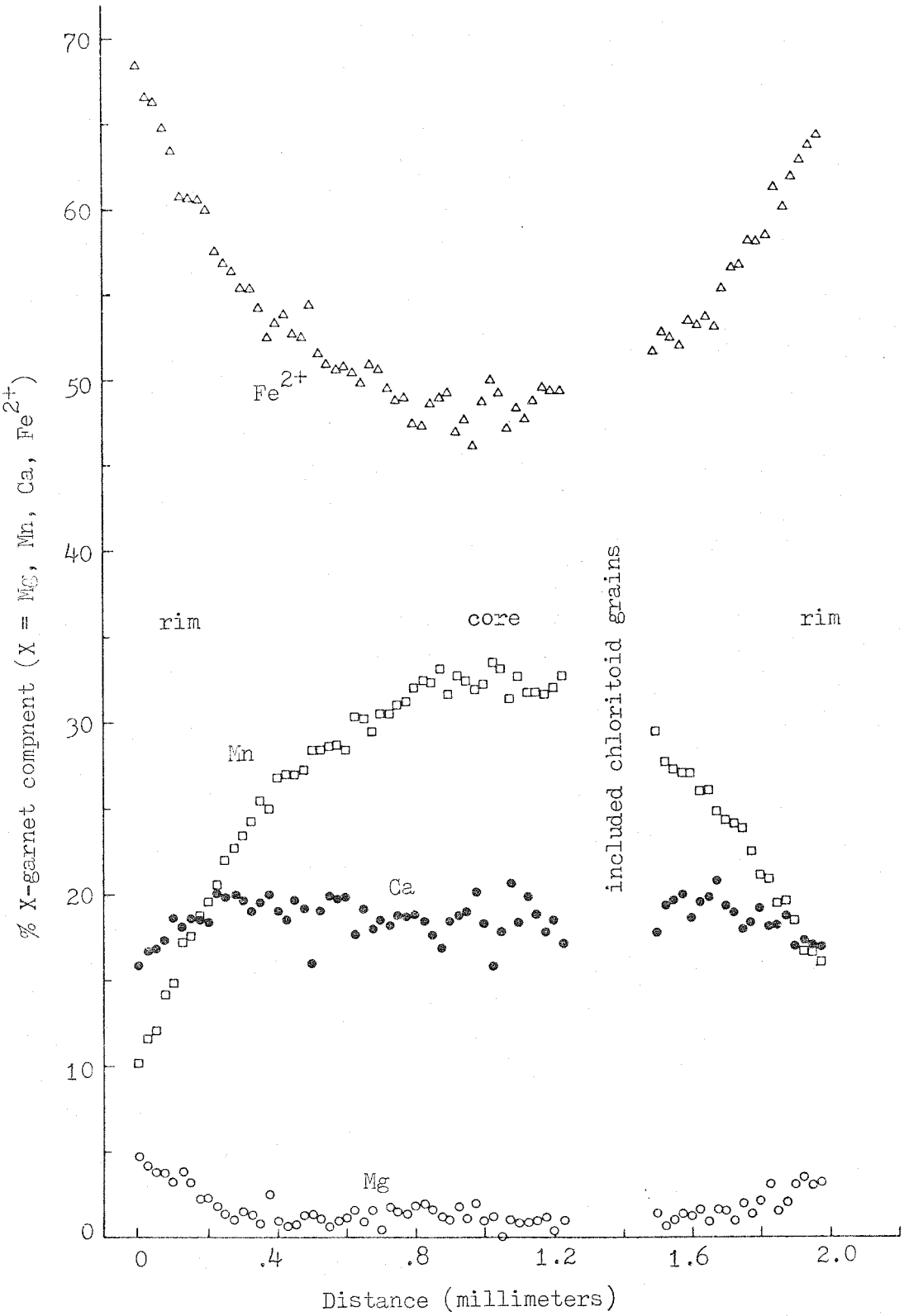

Figure 18b EDA traverse across 2mm garnet grain in JR-73-A.

trast, there is not a smooth relationship between Mn and Ca. Sharp changes of several percent Ca-garnet component occur within single traverses, such that the Ca content oscillates about a long range trend of increasing, then gradually decreasing Ca content from core to rim. The overall trend of Fe^{2+} is increasing content from core to rim. However, superimposed on the long range variation are short range variations similar to those of Ca. The short range Fe^{2+} variations are opposite to the changes in Ca content and therefore the changes in one compensate for the changes in the other. As Mn decreases fairly consistently from core to rim and there is a smooth relationship between Mn and Mg, the short range variations in Fe^{2+} and Ca would seem to be necessarily antithetic.

In order to test this, a traverse was made across one grain using energy dispersive analysis (EDA). EDA was used because it takes perhaps a fourth of the time required to make a similar traverse using wavelength dispersive analysis. The traverse consists of 65 points, 1 micron in diameter, spaced 25 microns apart across a 2 millimeter grain. The results are shown in Figure 18b. There is a 260 micron gap in the traverse because of the presence of included grains. The Mn content decreases from core to rim, with the exception that there may be some small reversals

near the core. The Mg content generally increases from core to rim, but the Mg zoning is not as smooth as shown by the data in Figure 18a. This is probably due to error in the analyses, as the relative error for EDA analyses of small amounts of light elements seems to be large. The smooth Mg zoning relationship is well established by the wavelength dispersive analyses. Ca and Fe^{2+} behave as was indicated for the data in Figure 18a. There are sharp changes in Ca, up to 5% Ca-garnet component(about 20% relative to the total Ca content). The Fe^{2+} trend is generally increasing content from core to rim, with superimposed short range irregularities. These sharp changes in Fe^{2+} coincide with and partially compensate for the changes in Ca. There is some suggestion in the data that there may be some short range changes in Mn content that also coincide with the Ca variations.

Both the wavelength dispersive and EDA data suggest that there are short range changes in Ca and Fe^{2+} that are relatively independent of Mg and, to a lesser extent, Mn. Considering only the long range variation, there are no peculiarities in the garnet zoning, such as pronounced reversals in Mn. The compositional range, from $Fe^{2+}_{46}Mg_{1}Mn_{34}Ca_{16}$ (subscripts indicate percent of the component) in the core to $Fe^{2+}_{70}Mg_{4}Mn_{11}Ca_{16}$ at the rim, is fairly typical of

OM_b garnet. There is no obvious explanation of the short range variation of Fe^{2+} and Ca. Other minerals in the sample do not seem to have corresponding compositional oscillations.

One interesting point in Figure 18b is that the opposite rims have different compositions. It appears that growth continued on one side of the garnet after growth had stopped on the other side. Limited resorption on one side of the grain may also explain the difference.

A question that remains unanswered is whether the short range zoning trends can be reproduced from grain to grain. This would require several more detailed traverses. If both the short range and long range zoning patterns are nearly identical from grain to grain, then it would seem likely that there was a very close approach to equilibrium among the growing grain surfaces.

Chlorite in JR-73-A can be divided into two textural and compositional groups. The first group consists of chlorite grains which have preferred orientation parallel to OS_a/OS_b plus compositionally similar grains included in OM_b plagioclase or garnet. This group appears to represent OM_b growth. The second group consists of grains with preferred orientation parallel to DS_a, but crosscutting OS_a/OS_b and compositionally similar grains without preferred

orientation. The second group represents DM_a growth. There is no evidence of any other generation of chlorite growth.

The compositions of these two groups of chlorite are shown in Figures 19a and 19b. A fairly systematic trend for OM_b chlorite is indicated on Figure 19a. No systematic trend has been defined for DM_a chlorite; in any event, there is not a great deal of compositional variation for this generation. The envelope that encloses all OM_b points is included in Figure 19b and this shows that DM_a chlorite must be separated from OM_b based upon textural relationships, because grains which fall within the compositional range of DM_a may belong to either generation.

Chlorite in this sample can be used as an example of the manner in which compositional trends are defined. Figures 19c, 19d, 19e, 19f, and 19g are plots for individual grains or groups of grains separated by areas in the thin section for OM_b chlorite only. The arrows from point to point indicate the core-to-rim direction. The trend shown in Figure 19a is established by taking into account the zoning shown by all such grains. Many of the grains do not have most of the trend preserved within them, so that the entire trend is established by using grains which have overlapping portions of the trend. The trend that is de-

Figure 19a Plot of Al vs. Mg/Mg+Fe for OM_b chlorite in JR-73-A.

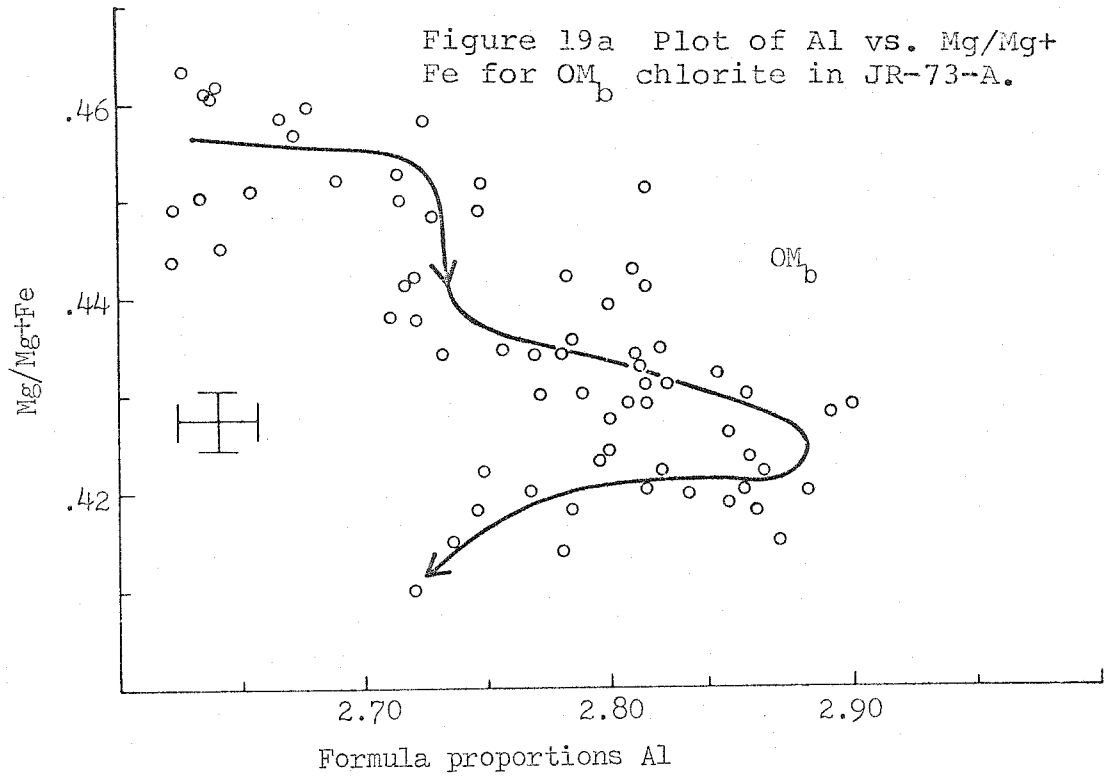

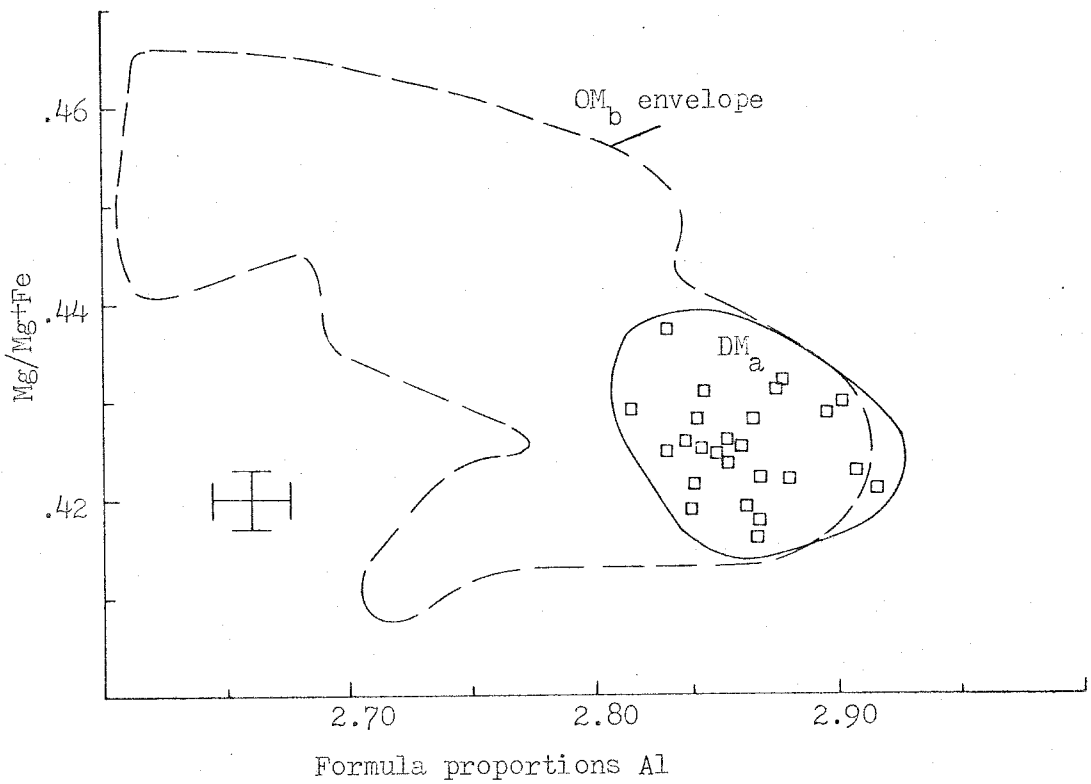

Figure 19b Plot of Al vs. Mg/Mg+Fe for DM_a chlorite in JR-73-A. OM_b chlorite envelope is shown for comparison.

Figure 19c Plot of Al vs. Mg/Mg+Fe for single chlorite grain in area 8-1.

Figure 19d Plot of Al vs. Mg/Mg+Fe for single chlorite grain in area 8-1.

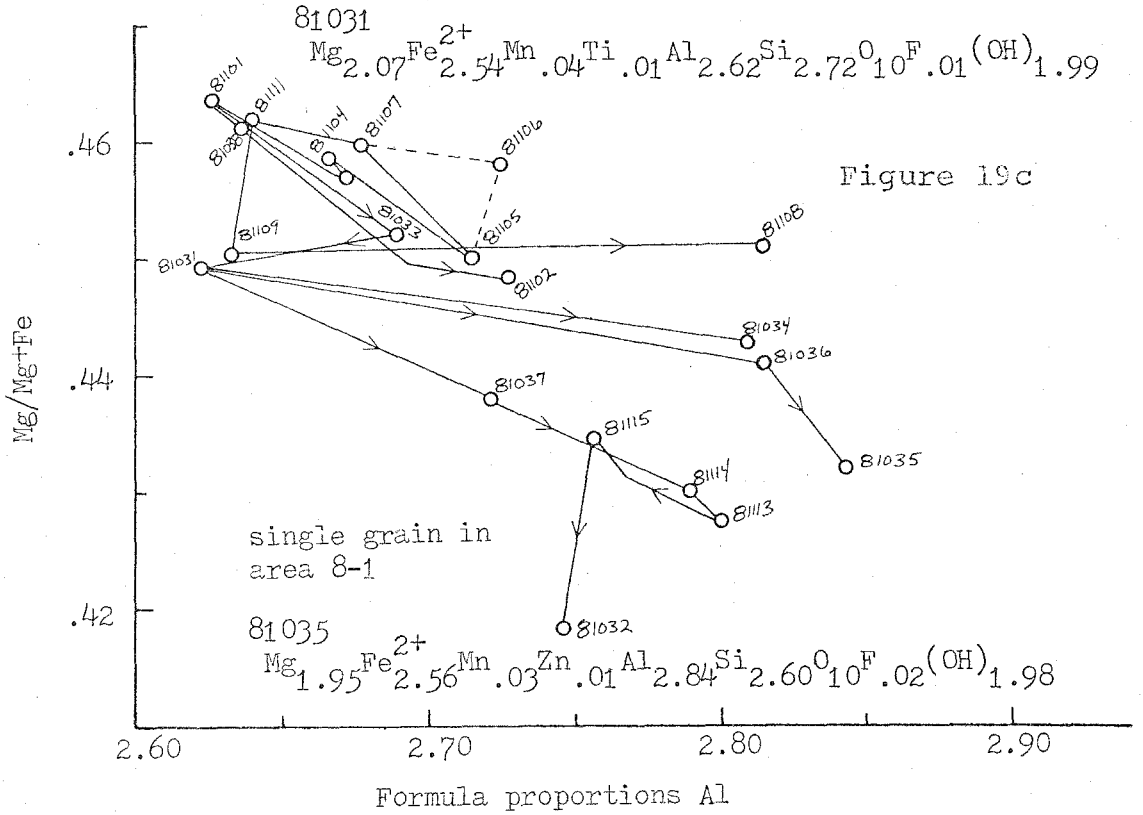

Figure 19c

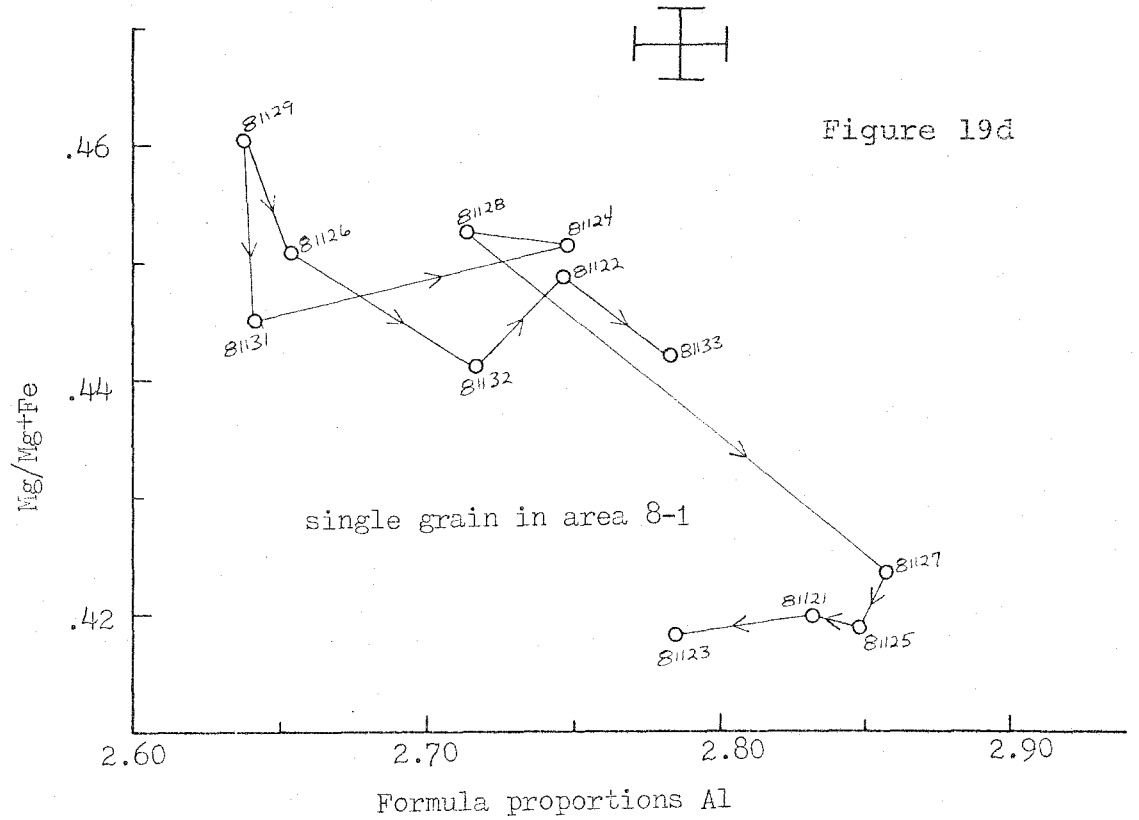

Figure 19d

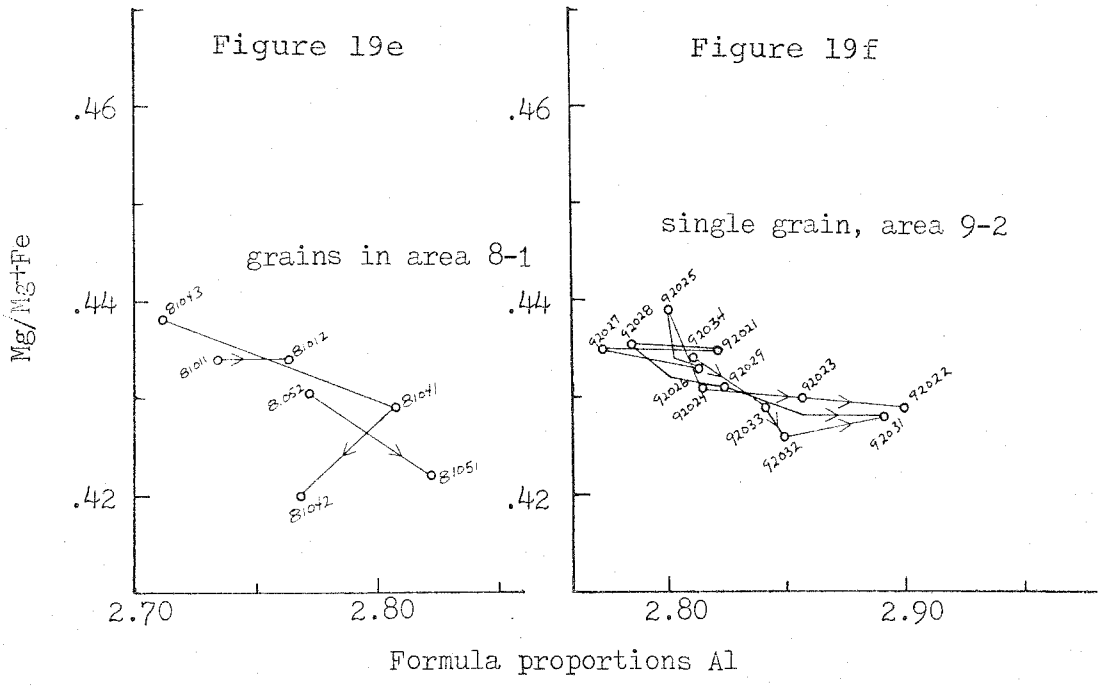

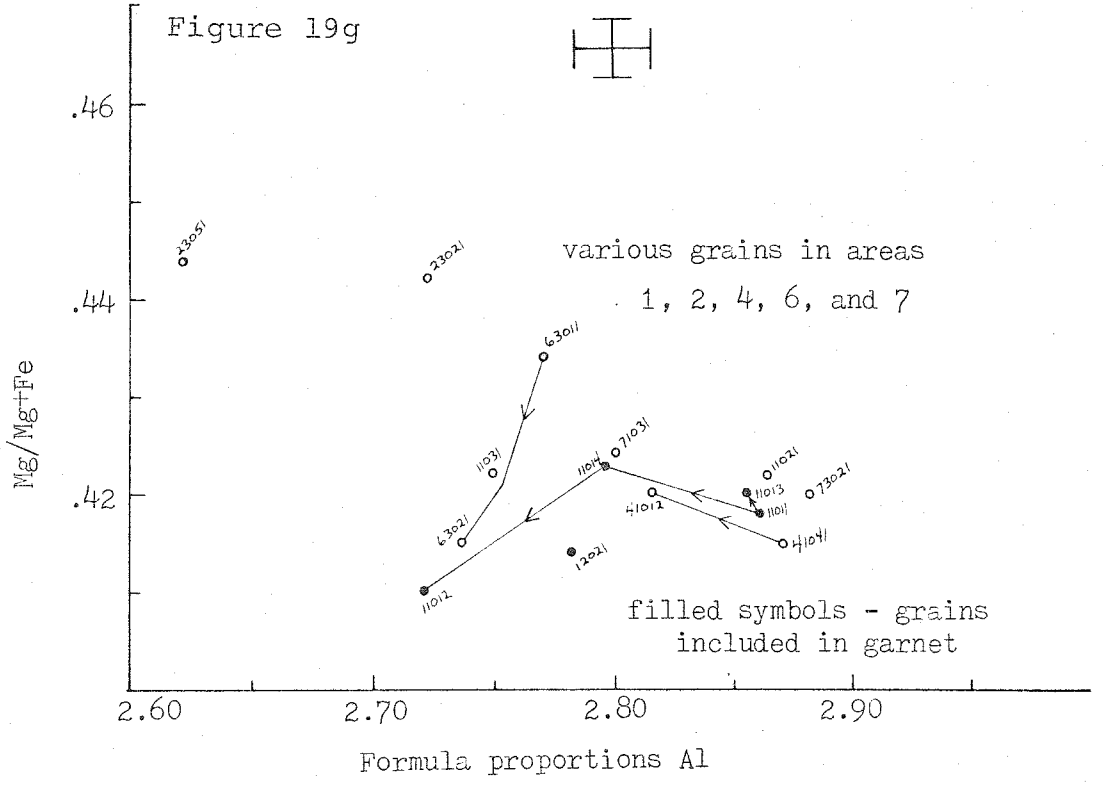

Figures 19e, f, g Plots of Al vs. Mg/Mg+Fe for chlorite grains in various areas of JR-73-A.

fined is consistent with all of the zoning patterns shown by the grains. The defined trend is somewhat more general than the actual trends in the grains. The data indicate that a more complicated compositional trend is probably present, but the trend shown is perhaps the most complicated trend that can be justified given the analytical error. Complete compositions of two points are shown in Figure 19c. There is no Fe^{3+} in these as determined by the total charge calculation.

Another element of interest in chlorite is Mn, especially for chlorite in an assemblage with garnet. Figure 20a is a plot of Mn/(total Fm) vs. Al for OM_b garnet in areas 8 and 9 of the thin section. "Fm" is the sum of Mg+Mn+Fe+Zn. Within the error, there is no variation in Mn/Fm in area 8 chlorite. Just at the limits of the error is a possible trend of increasing, then decreasing Mn/Fm for the single grain in area 9. Figure 20b shows all chlorite analyses of both generations on a plot similar to 20a. Any possible variation is within the limits of error and, in any event, the points do not define a systematic trend. The two generations are similar to each other in Mn/Fm. The OM_b chlorite grains presumably grew at the same time as OM_b garnet, which is strongly zoned with respect to Mn. DM_a chlorite seems to be associated with the limited resorption of Mn-

Figure 20a Plot of Al vs. Mn/Fm for grains in areas 8 and 9 of JR-73-A.

Figure 20b Plot of Al vs. Mn/Fm for all chlorite analyses in JR-73-A. Circles are OM_b and squares are DM_a.

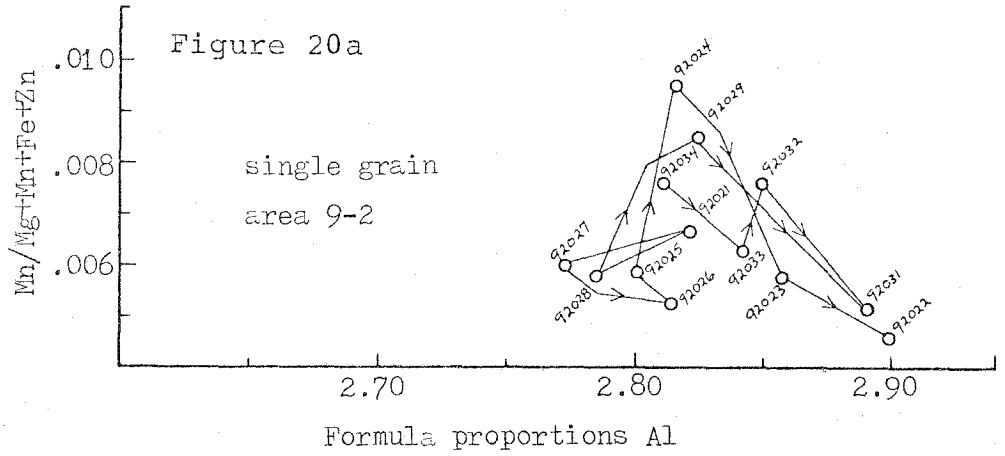
Figure 20a
single grain
area 9-2
Mn/Mg+Mn+Fe+Zn
.010
.008
.006
2.70
2.80
2.90
Formula proportions Al

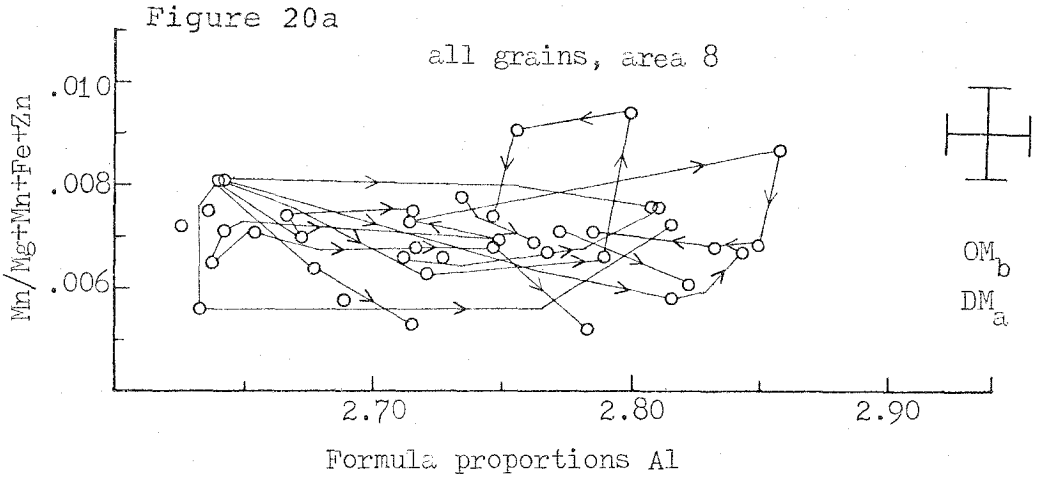
Figure 20a
all grains, area 8
Mn/Mg+Mn+Fe+Zn
.010
.008
.006
OMb
DMa
2.70
2.80
2.90
Formula proportions Al

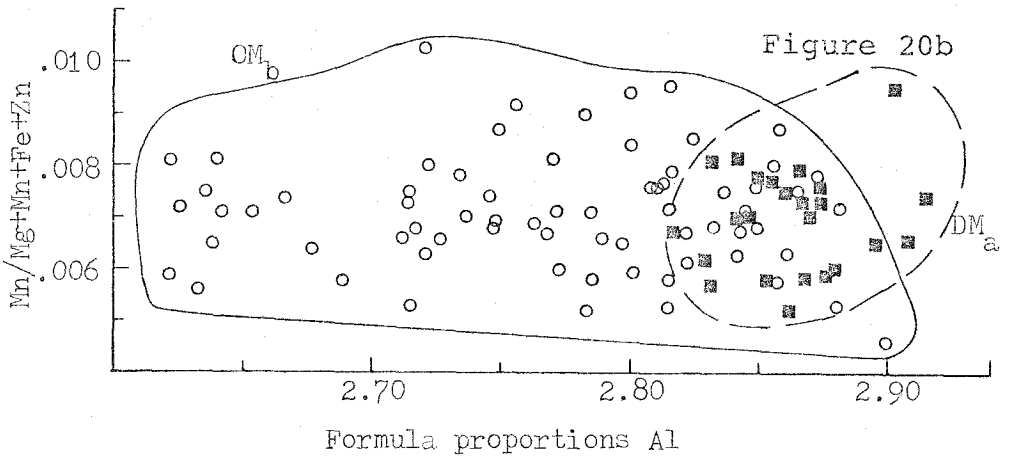
Figure 20b
OMb
DMa
Mn/Mg+Mn+Fe+Zn
.010
.008
.006
2.70
2.80
2.90
Formula proportions Al

rich OM_b garnet. It seems unreasonable that the chlorite grains would preserve significant compositional zoning with respect to Mg, Fe, Al, and Si, but not preserve Mn zoning. The lack of Mn variation in both OM_b and DM_a chlorite is probably a primary feature of the original chlorite growth.

The consequences of strong Mn variation in the garnet and the lack of Mn variation in chlorite of the same generation are significant. If there was a regular fractionation of Mn and Fe between simultaneously growing garnet and chlorite, then the partition coefficient for the Mn-Fe equilibrium must have been continually changing. If the partition coefficient was changing, then T would probably have to have been continually changing. Whatever the case, the lack of Mn variation in zoned chlorite grains leaves the problem of the source of Mn for the growing garnet grains. Typically the most Mn-rich minerals other than garnet in these rocks are ilmenite and calcite (plus ankerite and chloritoid if they are present). There is ilmenite in this rock, but no calcite has been observed. There may well have been calcite at one time in the rock and the breakdown of calcite may have provided the Ca for the plagioclase growth and the Ca and Mn for the garnet growth. Calcite is common in nearby rocks which are otherwise similar to JR-73-A. An obvious source in this sample is chloritoid;

the chloritoid grains included in garnet provide good evidence that there was chloritoid in the assemblage at one time, but was removed by reaction sometime before OM_b growth stopped.

Muscovite grains in JR-73-A are texturally similar to chlorite. There appear to be two groups, identical to the OM_b and DM_a chlorite groups distinguished by texture. OM_b muscovite analyses are shown in Figure 21a, a plot of Mg/Mg+Fe vs. Si. The core-to-rim direction from point to point is shown for each pair with an arrow. The overall trend is decreasing Mg/Mg+Fe and decreasing Si. The trend indicates continually increasing grade, which was also indicated by the plagioclase compositional trend. The variation in the formula proportions of Si from 3.31 to 3.04 is very significant in terms of the total phengite substitution variation observed in all samples, which is from 3.00 to 3.45.

Compositions of DM_a muscovite are shown in Figure 21b. There is not nearly as much variation as seen in OM_b muscovite and no systematic trend has been defined. If more data were available, a systematic trend might be observed. As is the case for DM_a chlorite which overlaps compositionally with OM_b chlorite, the compositional range of DM_a muscovite is entirely within the range of OM_b muscovite given

Figure 21a Plot of Si vs. Mg/Mg+Fe for OM_b muscovite in JR-73-A.

Figure 21b Plot of Si vs. Mg/Mg+Fe for DM_a muscovite in JR-73A. OM_b envelope is shown for comparison.

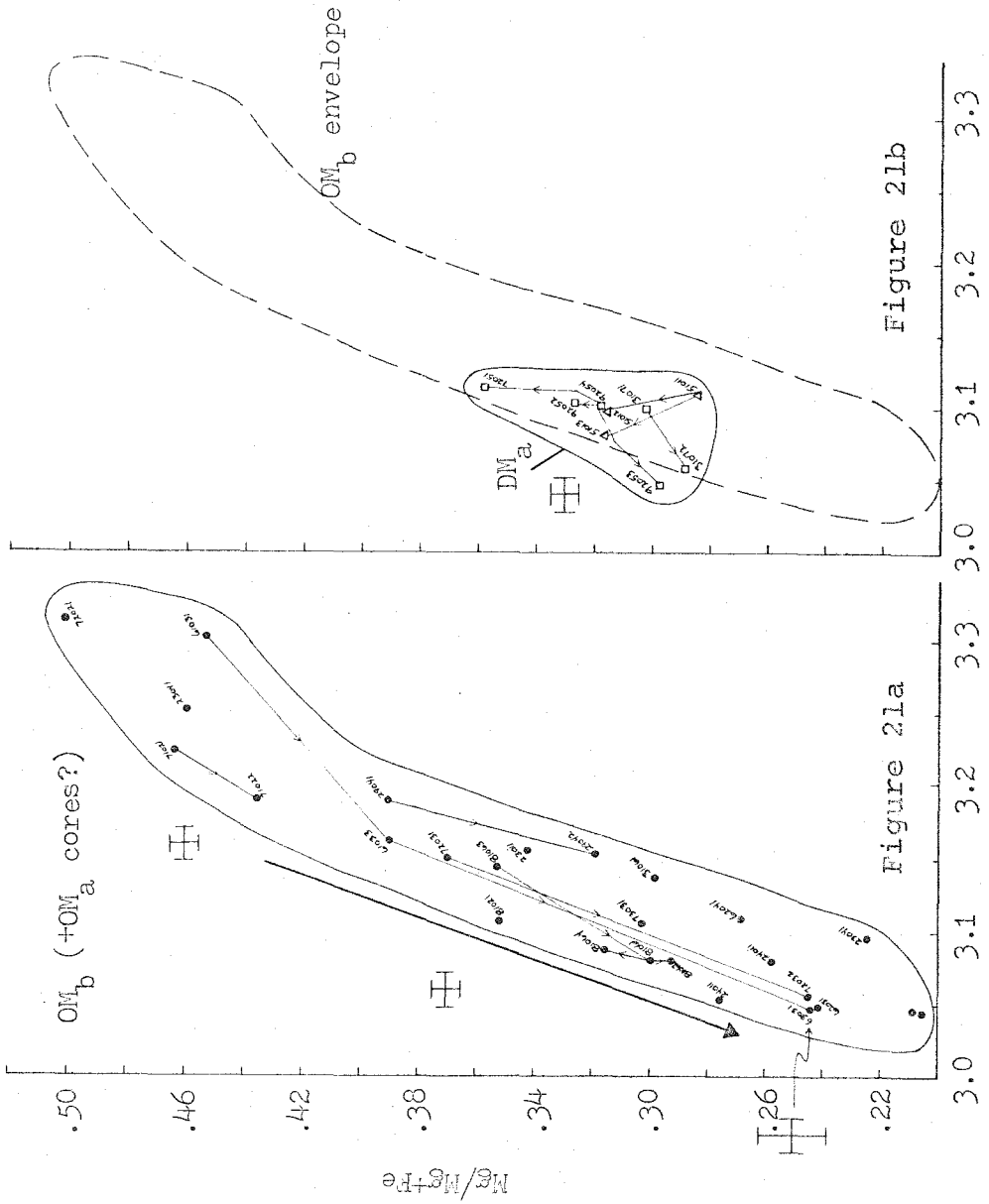
OM_b envelope
DM_a
Figure 21b
OM_b (+OM_a cores?)
Figure 21a
$Mg/Mg+Fe$
.50
.46
.42
.38
.34
.30
.26
.22
3.0
3.1
3.2
3.3
3.0
3.1
3.2
3.3
Formula proportions Si

the analytical error.

The last mineral in JR-73-A to be discussed is chloritoid. All of the chloritoid appears to have formed before the OM_b garnet stopped growing and any chloritoid not included in garnet grains appears to have been removed from the system by reaction. The compositional variation in chloritoid is smaller than that in other OM_b minerals discussed, but still statistically significant. A compositional variation trend is shown in Figure 22; however, this trend has not been well established and must be viewed more as a suggestion than a documented path of variation. The trend is decreasing, then increasing Al. Mg/Mg+Fe doesn't vary greatly, perhaps decreasing somewhat. Also shown in Figure 22 is a plot of Mn/Mg+Fe+Mn+Ca vs. Al. There is statistically significant variation in the Mn content, but a systematic trend could not be defined.

Sample JR-73-A is typical in that it is very difficult to establish the compositions of two different minerals which formed simultaneously. In the matrix there is really no hope of finding compositional pairs which can be demonstrated to have formed simultaneously. Grains of a single mineral type, chlorite for instance, which are of different generations can be found together. One possibility for finding cogenetic pairs is to look at the rims of chloritoid

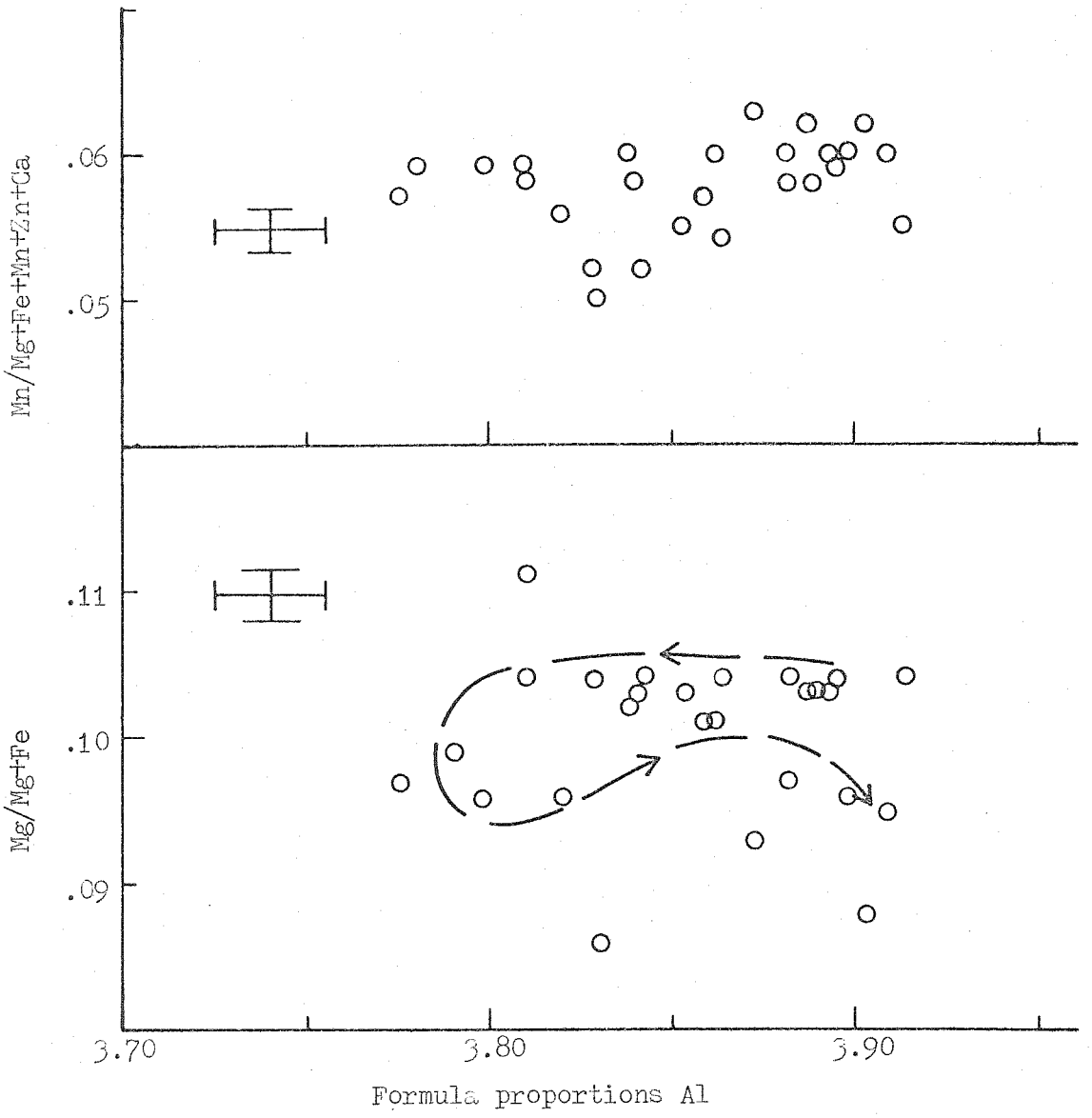

Figure 22 Plots of Al vs. Mg/Mg+Fe and Al vs. Mn/Mg+Fe+Zn+Ca for chloritoid in JR-73-A.

grains and the enclosing garnet that is immediately adjacent to the rims. Six pairs of adjacent chloritoid-garnet pairs are shown in Figure 23, logarithmic plots of Mg/Fe^{2+} and Mn/Fe^{2+}. Fe^{2+} can be reasonably calculated for garnet and chloritoid and Fe^{3+} is always small and consistent for both minerals in JR-73-A.

Lines of equal length between pairs on a diagram such as Figure 23 represent equal partition coefficients, assuming that the pairs were formed at the same time. For the Mg/Fe^{2+} pairs there is noticeable variation in the apparent partition coefficients. The Mn/Fe^{2+} pairs seem to be a little more consistent, but there is some variation. Pairs 1, 2, and 3 come from two adjacent chloritoid grains and the surrounding garnet. The variation in apparent partition coefficients shown by three pairs which are spatially so closely related suggests that the use of included grains and the adjacent host minerals is not really a satisfactory method to determine partition coefficients. For rocks such as these, there seems to be no satisfactory method to determine partition coefficients in enough detail to document the path of the system. The data could be averaged but it is not clear that an average K_D is of any particular use for detailed considerations of the metamorphic history. If a systematic variation in a particular K_D in a sample could

Figure 23 Logarithmic plots of Mg/Fe^{2+} and Mn/Fe^{2+} for adjacent chloritoid and garnet. Also shown are the K_D values. The relative standard deviations for K_D values are about 8% for Mg/Fe^{2+} and 2.5% for Mn/Fe^{2+}.

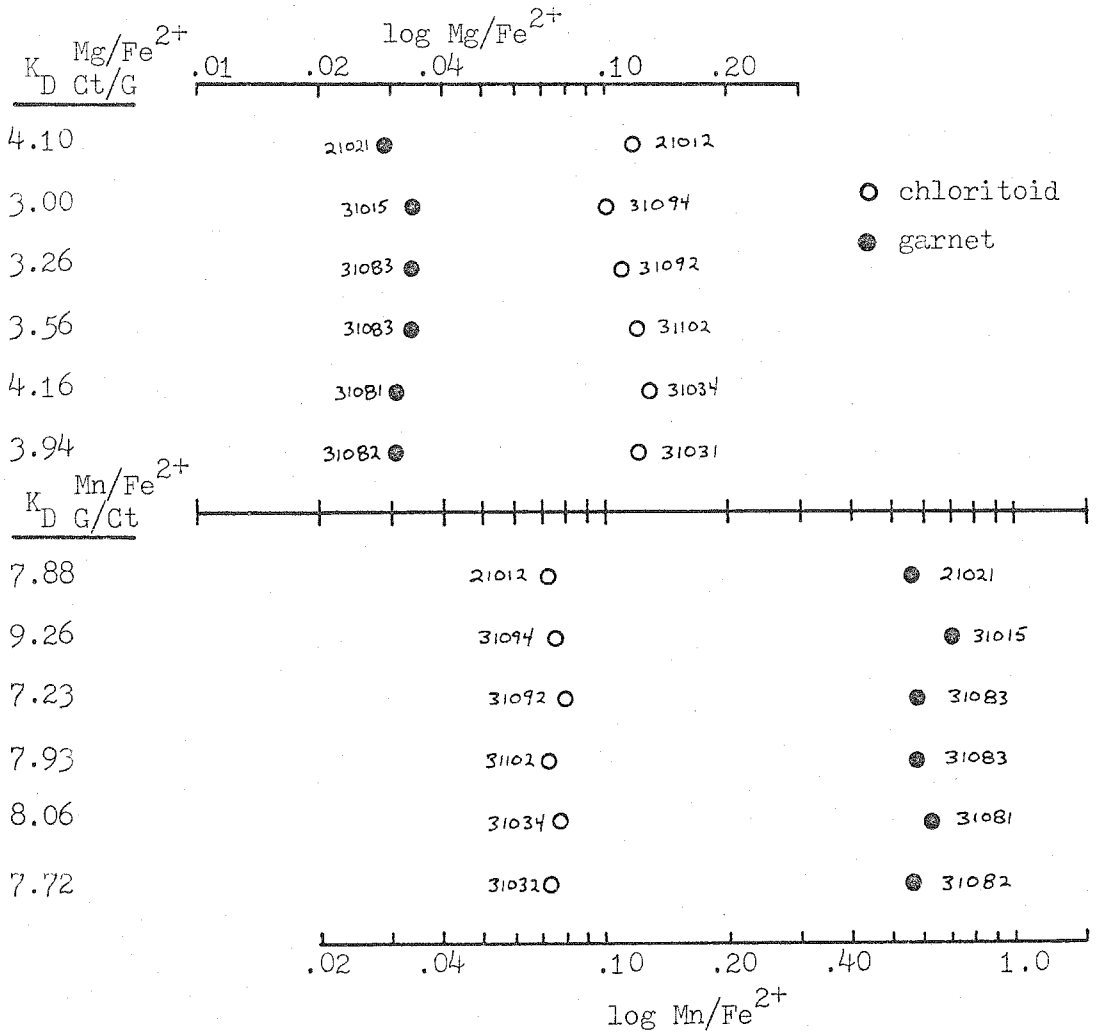
log Mg/Fe2+
.01
.02
.04
.10
.20
K D Mg/Fe2+ Ct/G
4.10
3.00
3.26
3.56
4.16
3.94
21021
21012
31015
31094
31083
31092
31083
31102
31081
31034
31082
31031
chloritoid
garnet
K D Mn/Fe2+ G/Ct
7.88
9.26
7.23
7.93
8.06
7.72
21012
21021
31094
31015
31092
31083
31102
31083
31034
31081
31032
31082
.02
.04
.10
.20
.40
1.0
log Mn/Fe2+

be documented, then a great deal of information about the path of the system would be available.

A fairly detailed history of the rock has been determined just by using the zoning patterns and the textural relationships in JR-73-A. The oldest documented mineral growth generation is OM_b and the bulk of the rock is comprised of OM_b minerals. The compositional variation of plagioclase and muscovite indicate that grade was progressively increasing during OM_b growth. It is not clear when garnet first appeared, but after garnet began to form the assemblage included quartz-muscovite-clorite-garnet-chloritoid-plagioclase. Later, growth of chloritoid stopped while OM_b garnet growth continued. Matrix chloritoid was apparently removed by reaction near the peak of the OM_b event. The OM_b minerals were later deformed by DF_a microfolds and there was limited recrystallization resulting in the formation of DM_a chlorite, muscovite, and perhaps a small amount of plagioclase. Limited resorption of a few garnet porphyroblasts seems to have accompanied DM_a growth.

J. Characterization of the mineral growth generations in the vicinity of the Green Mountain axis along the Winooski River traverse

The samples described in this section are from locations along the Winooski River traverse in the Camels Hump

quadrangle. Samples from which microprobe data have been obtained are confined to the portion of the traverse between JR-4 and JR-77. These locations are in the Underhill and Hazens Notch formations and lie within the garnet isograd which was mapped by Christman and Secor (1961) on the basis of the presence or absence of garnet without regard to multiple mineral growth generations. Therefore the isograd could represent a hybrid isograd of more than one period of garnet growth and/or it could represent the limits of preserved garnet growth that has been overprinted by retrograde events. The main axis of the Green Mountain anticlinorium trends north-south and is about midway between the traces of the garnet isograd surface. Samples analyzed with the electron microprobe will first be described. The assemblage data from these samples and from petrographic examination of other samples will then be shown by mineral growth generation on sketch maps of the area, such as the one in Figure 24.

Most of the structural elements of the deformational sequence are well developed along this traverse segment. Isoclinal OF_b folds with east-west trending axes deform bedding planes, OS_o, and the secondary bedding schistosity, OS_a. Also deformed are abundant OV_a veins which are

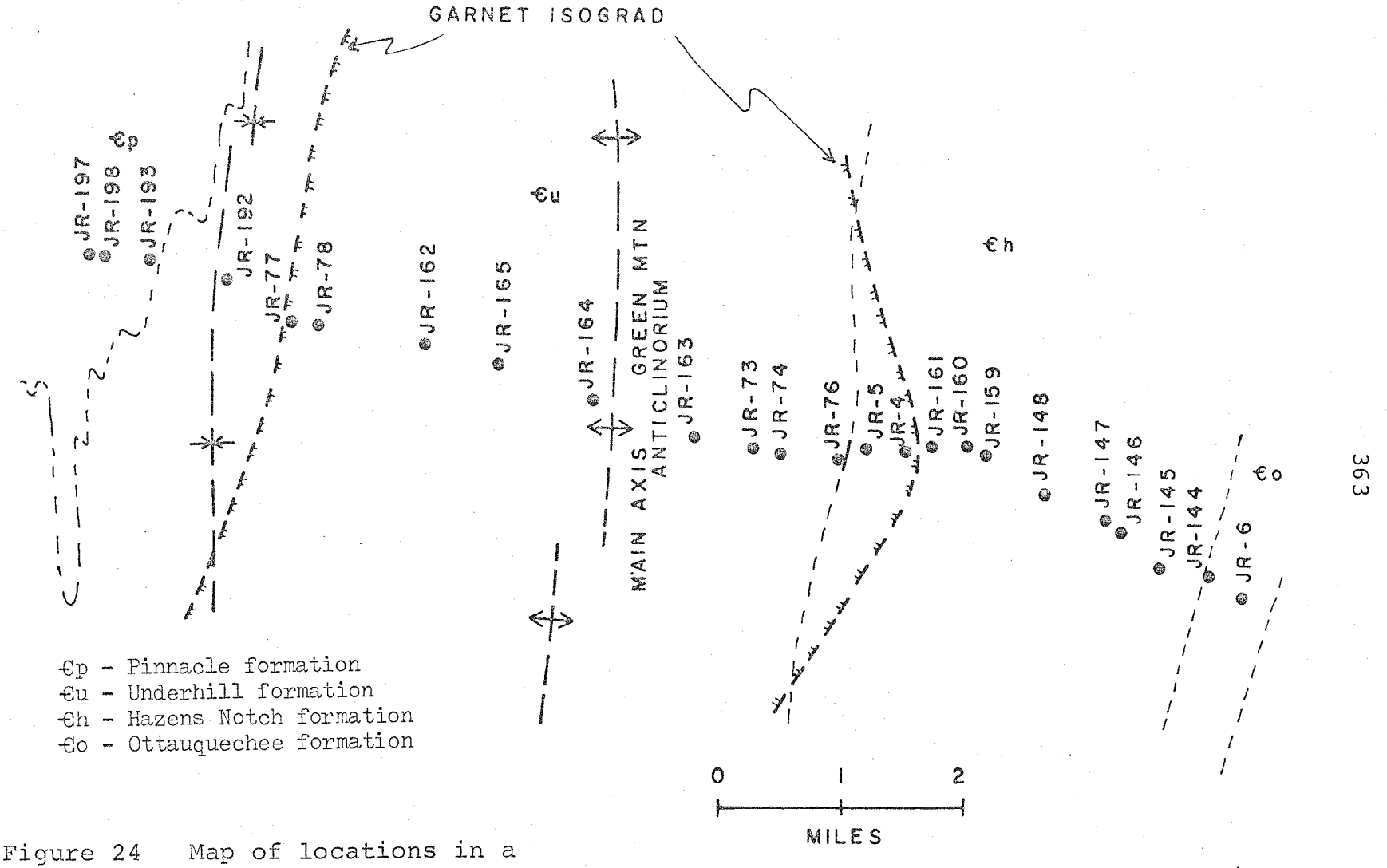

Figure 24 Map of locations in a portion of the Camels Hump quadrangle along the Winooski River traverse. Stratigraphy, fold axes, and garnet isograd were mapped by Christman and Secor (1961).

parallel to OS_a. Axial planar to the OF_b folds are the well-developed schistosity OS_b and associated OV_b veins. These pre-Silurian structures have been folded by very prominent, generally north-south trending DF_a folds. DF_a folds are asymmetric and have an associated slip cleavage, DS_a, which is parallel to the DF_a axial planes. DS_a planes are typically spaced 1-3 millimeters apart, but in some places DS_a appears to be absent. Abrupt changes in the character and development of DS_a can occur within a single outcrop. DS_a is typically not parallel to OS_a/OS_b to the west of location JR-161 along this traverse segment. The garnet isograd mapped between JR-4 and JR-161 coincides with a change in the character of DS_a and D_a deformation in general. To the east of JR-161 DS_a is commonly parallel to OS_a/OS_b on one of the limbs of DF_a folds and DF_a folds tend to be tighter. Parallel to DS_a is a well developed set of veins, DV_a, observed at most outcrops along this traverse segment. DS_a and DV_a can be seen in places to be gently flexed by north-south trending asymmetric DF_b folds. Cross-cutting DS_a slip cleavage and DF_b folds are rare DV_c veins. The DV_c veins may be very gently folded by DF_d folds. Some of the minor vein generations are also present in this area.

Location JR-5

Of the thirteen samples from this segment analyzed

with the microprobe, five are from location JR-5. The analyzed samples from JR-5 are as follows:

JR-5-A OV_b vein and adjacent host schist

JR-5-B OV_b vein (same vein as JR-5-A, but 15 cm away)

JR-5-D schist 15 cm away from OV_b vein (JR-5-A)

JR-5-G DV_a vein and adjacent host schist (10 m from JR-5-A)

JR-5-I schist 1 meter from JR-5-G and 30 cm away from any vein

These samples represent the most extensive sampling of an outcrop in this study with regard to microprobe analysis.

The rock exposed at JR-5 is a medium-grained quartz-muscovite-chlorite-plagioclase schist with porphyroblasts of plagioclase ranging from 1 to 3 centimeters. The rock is typical of much of the Hazens Notch formation which has attained garnet grade. Garnet porphyroblasts occur in some layers and some of the garnet grains show evidence of extensive resorption and/or retrograde reaction. The assemblage observed in the schist is quartz-muscovite-chlorite-plagioclase-calcite-epidote + allanite-ilmenite-pyrrhotite-apatite, plus or minus garnet, tourmaline, zircon, pyrite, and chalcopyrite. Most or all of the pyrite seems to be a product of the alteration of pyrrhotite rather than primary grains. The OV_b vein studied has the assemblage quartz-muscovite

-chlorite-plagioclase-calcite-ilmenite-pyrrhotite-chalcopyrite-pyrite (after pyrrhotite). The assemblage in the DV_a vein from which JR-5-G is taken is quartz-muscovite-plagioclase-calcite-pyrrhotite with very minor amounts of chlorite at the vein margin.

The veins establish the presence of the OM_a, OM_b, and DM_a mineral growth generations. These generations can then be identified in the host rock, although perhaps not as unambiguously as in the veins. Generation OM_a is the hardest to find as it has been heavily overprinted by OM_b and DM_a growth. Very little of the OM_a growth seems to be preserved in the host rocks and even the OV_a veins are largely recrystallized.

JR-5-A & JR-5-B

JR-5-A and JR-5-B are samples from an OV_b vein and the immediately adjacent schist. This vein is shown in Figure 28 in Chapter II. The minor structural elements in the host rock are typical of this region except that DS_a slip cleavage is not well developed. Tight, isoclinal OF_b microfolds of OS_a can be observed in thin section. Axial planar to the OF_b microfolds is OS_b schistosity. In sample JR-5-A the OS_b planes have discrete spacings of 0.1 to 0.5 millimeters apart. The spacing reflects the size of plagi-

oclase porphyroblasts which are between OS_b planes. These porphyroblasts have apparently been rotated during OF_b folding by movements along OS_b. This is indicated by the sigmoidal pattern of inclusion trails within OM_b plagioclase.

The OV_b vein is coarse-grained and consists largely of plagioclase and quartz. Between the vein and the host rock is a very sharp contact which is parallel to OS_b. There is a band of plagioclase and lesser amounts of other minerals which is generally about 1 centimeter wide; this constitutes the border zone. At the vein margin along the host rock wall is some growth of chlorite and muscovite which may involve vein mineral growth on grains which were originally part of the host rock. There is chemical evidence for this in the chlorite grains. The central part of the OV_b vein is comprised mostly of quartz, plagioclase, calcite, and masses of pyrrhotite up to several centimeters or larger in diameter. Most of the muscovite and chlorite in the vein is within the border zone. The border zone does not have any regular structuring.

Figure 25 shows the compositions of analyzed points of plagioclase in the host schist of JR-5-A. These compositions can be divided into two groups based upon the position of the analyzed point within the grains. Host plagioclase grains have an inner core of albite in which the inclusion

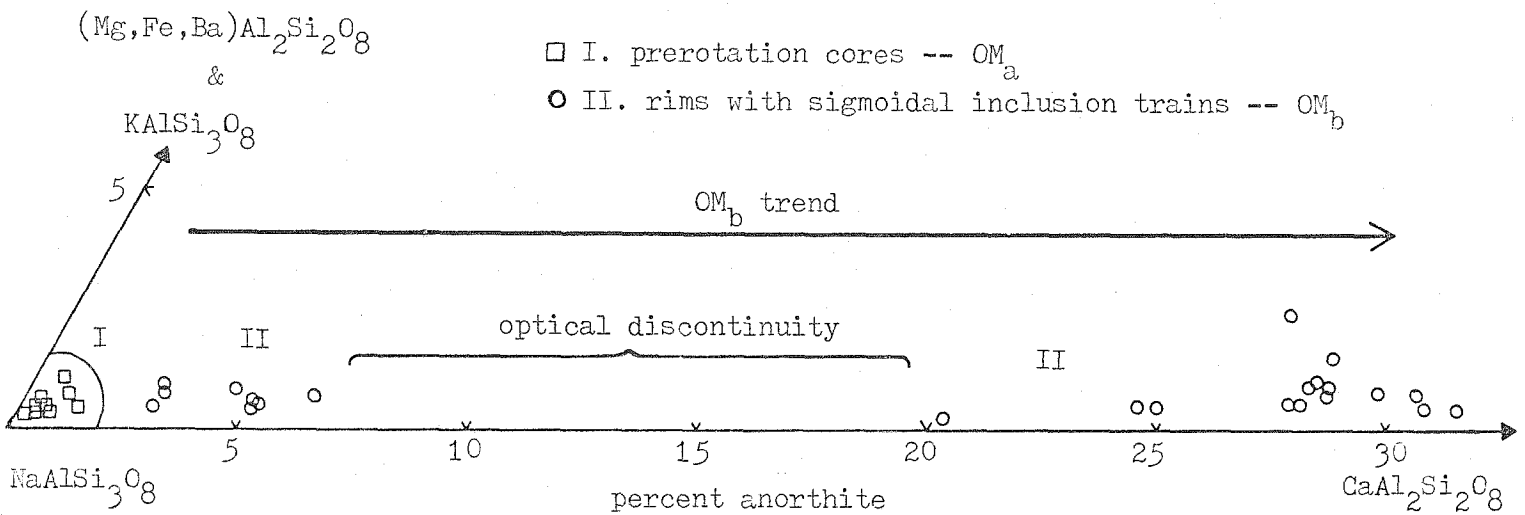

Figure 25 Compositions of plagioclase in the host schist of JR-5-A.

trains are straight and do not form a sigmoidal pattern. Overgrown on these cores are rims of albite and more calcic plagioclase which have sigmoidal inclusion trains. Within this second zone are closed optical discontinuities that appear to represent the peristerite gap. The prerotation cores with straight inclusion trains are shown as Group I in Figure 25. All of the points have compositions between $An_{0.2}$ and $An_{1.3}$. The rims which appear to have formed as the grains were rotated by movements along OS_b are shown as Group II in Figure 25. These points have compositions from $An_{2.8}$ and $An_{31.3}$. The optical discontinuity corresponds to a compositional discontinuity in Group II analyses between $An_{6.3}$ and $An_{20.2}$. The zoning pattern of Group II plagioclase is in every case increasing An content towards the rim. A typical plagioclase grain with a prerotation core and overgrowth of Group II material is shown in Figure 26.

Group II plagioclase appears to be OM_b in generation. The sigmoidal inclusion trains are compatible with OF_b microfolding and accompanying movement along OS_b planes. OS_b spacing seems to be defined by the plagioclase grains. There is a compositional relationship between Group II plagioclase and OV_b plagioclase, as will be further discussed. Another line of evidence is the compositions of included chlorite grains; this is discussed later. The

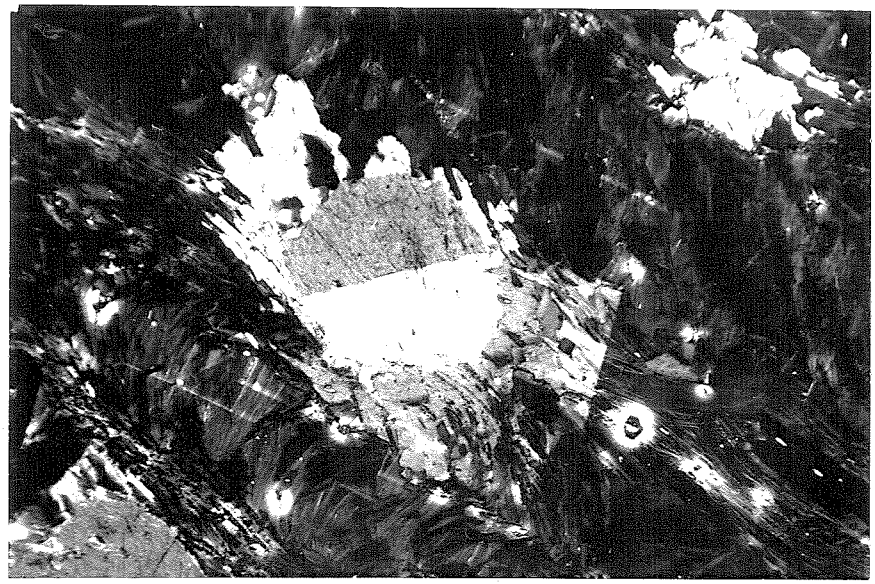

Figure 26 Plagioclase grain in host rock of JR-5-A. Core is albite and rim is oligoclase. Faint inclusion trains have a sigmoidal pattern through most of grain, but are straight in central part of albite core. 1.6 mm field of view, crossed nicols.

Figure 27 Euhedral plagioclase grain in OV_b vein of JR-5-A. Core is andesine to oligoclase, thin rim to right is albite. Opaque mineral is pyrrhotite. 3.2 mm field of view, crossed nicols.

generation of the prerotation albite cores is not so easy to determine. If the cores are pre-OM_b then they are OM_a mineral growth. However, they could represent early OM_b growth. Based upon the differences in the compositions of chlorite included in the cores and chlorite in the matrix and included in Group II plagioclase, the Group I cores are thought to be OM_a.

A small, but otherwise typical grain of OV_b plagioclase is shown in Figure 27. Vein plagioclase grains tend to be euhedral to subhedral. The compositions of analyzed points from OV_b vein plagioclase are shown in Figures 28a and 28b, which are for JR-5-A and JR-5-B respectively. The zoning pattern involves decreasing An content from core to rim. The range of compositions is from an An_{34} to An_{15}. The grain shown in Figure 27 also has a thin rim of plagioclase which is albite in composition. There may be a small reversal in trend in the early part of OV_b vein plagioclase growth. This involves decreasing An content from An_{34} to An_{29}, then increasing to An_{32} and finally consistently decreasing to An_{15}. Most of the grains show a consistent zoning pattern of decreasing An content from core to rim. The albite rim of the grain in Figure 27 has a high Fe content which is as much as 1.8% FeO. The points are within a few tens of microns of a grain of pyrrhotite, so that the Fe may

Figure 28a Compositions of plagioclase in OV_b vein of JR-5-A.

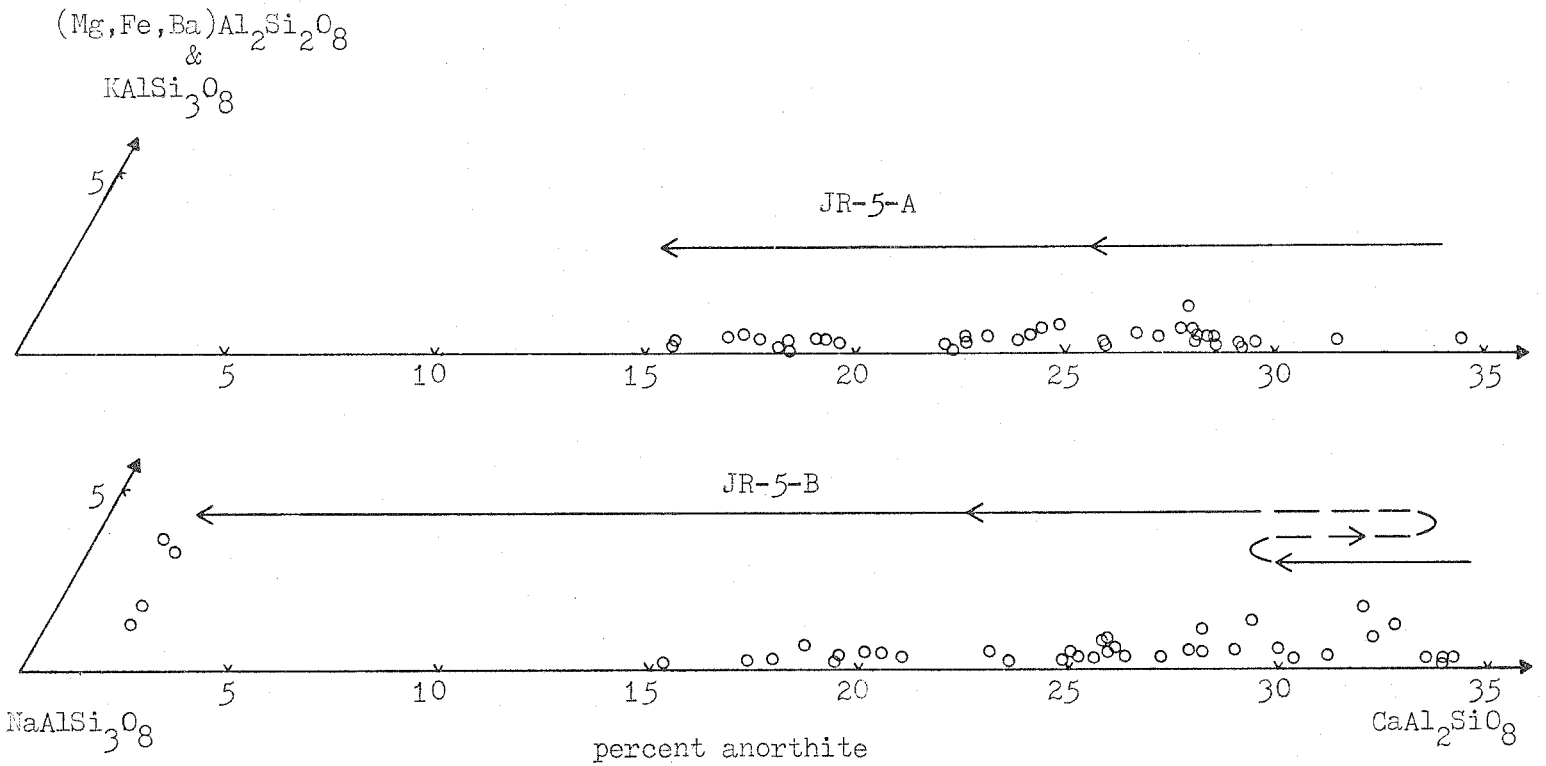

Figure 28b Compositions of plagioclase in OV_b vein of JR-5-B.

be due to this.

The zoning patterns observed in host OM_b plagioclase and vein OM_b plagioclase are directly opposite to each other. The only apparent overlap in compositional range involves the most calcic compositions represented by vein plagioclase cores and host plagioclase outer rims. The albite rims on vein plagioclase cannot correspond to the host albite cores because OV_b veins are unaffected by OF_b folding and movements along OS_b which caused host plagioclase rotation. The host zoning pattern indicates growth during progressively increasing grade and the zoning pattern of vein plagioclase indicates decreasing grade. During the growth of the earliest vein plagioclase, grade may have not been strictly decreasing as indicated by the small reversal. There is no evidence of any overprinting by DM_a plagioclase growth in either the vein or host rock.

Figure 29a shows the compositions of host rock chlorite in JR-5-A. The compositions are divided into two groups which are interpreted to be OM_a and OM_b chlorite growth. OM_a chlorite compositions are from grains which are included in prerotation albite cores in the host plagioclase grains. Two of the OM_a points are from the core of a large host matrix chlorite grain. OM_b chlorite compositions are from host matrix grains and grains included in OM_b plagio-

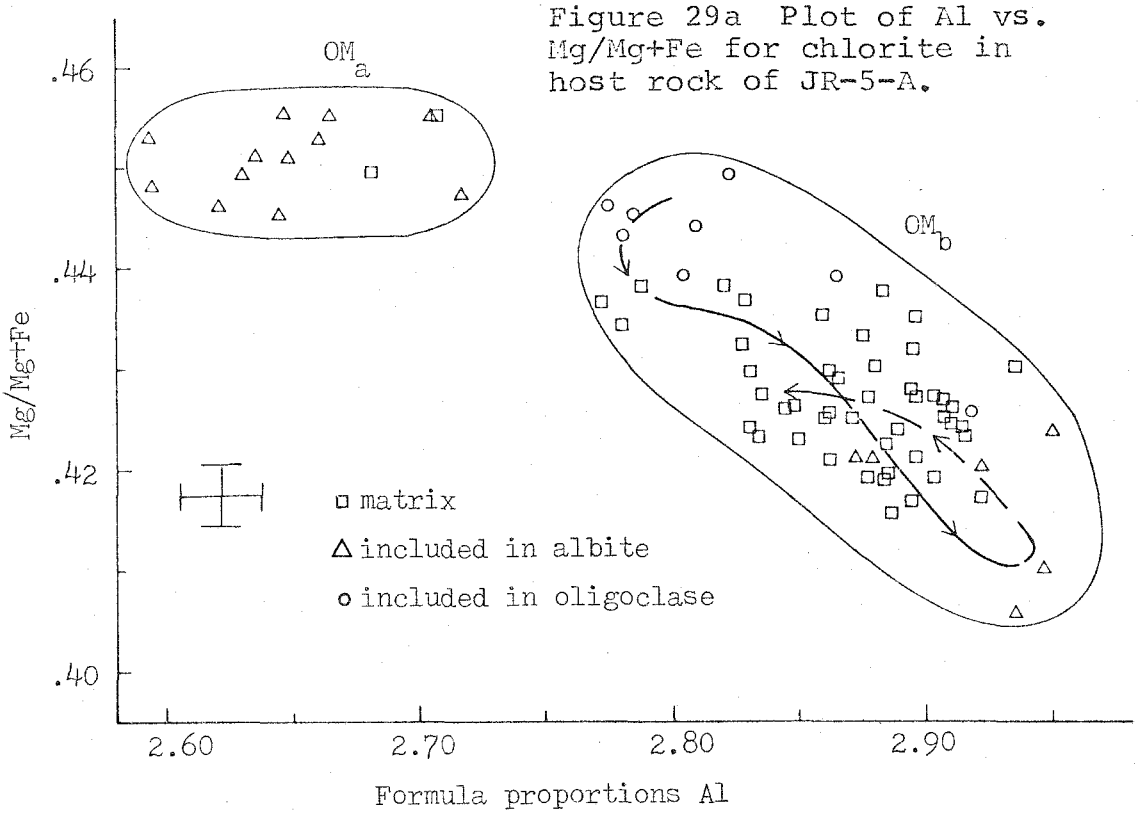

Figure 29a Plot of Al vs. Mg/Mg+Fe for chlorite in host rock of JR-5-A.

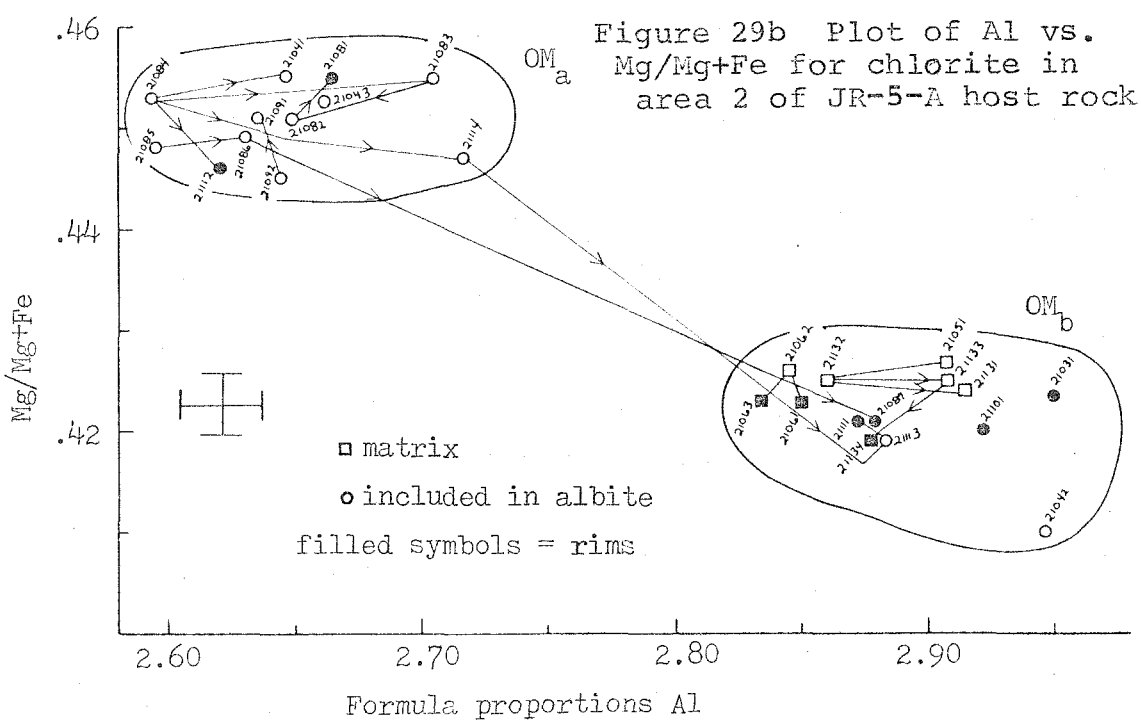

Figure 29b Plot of Al vs. Mg/Mg+Fe for chlorite in area 2 of JR-5-A host rock.

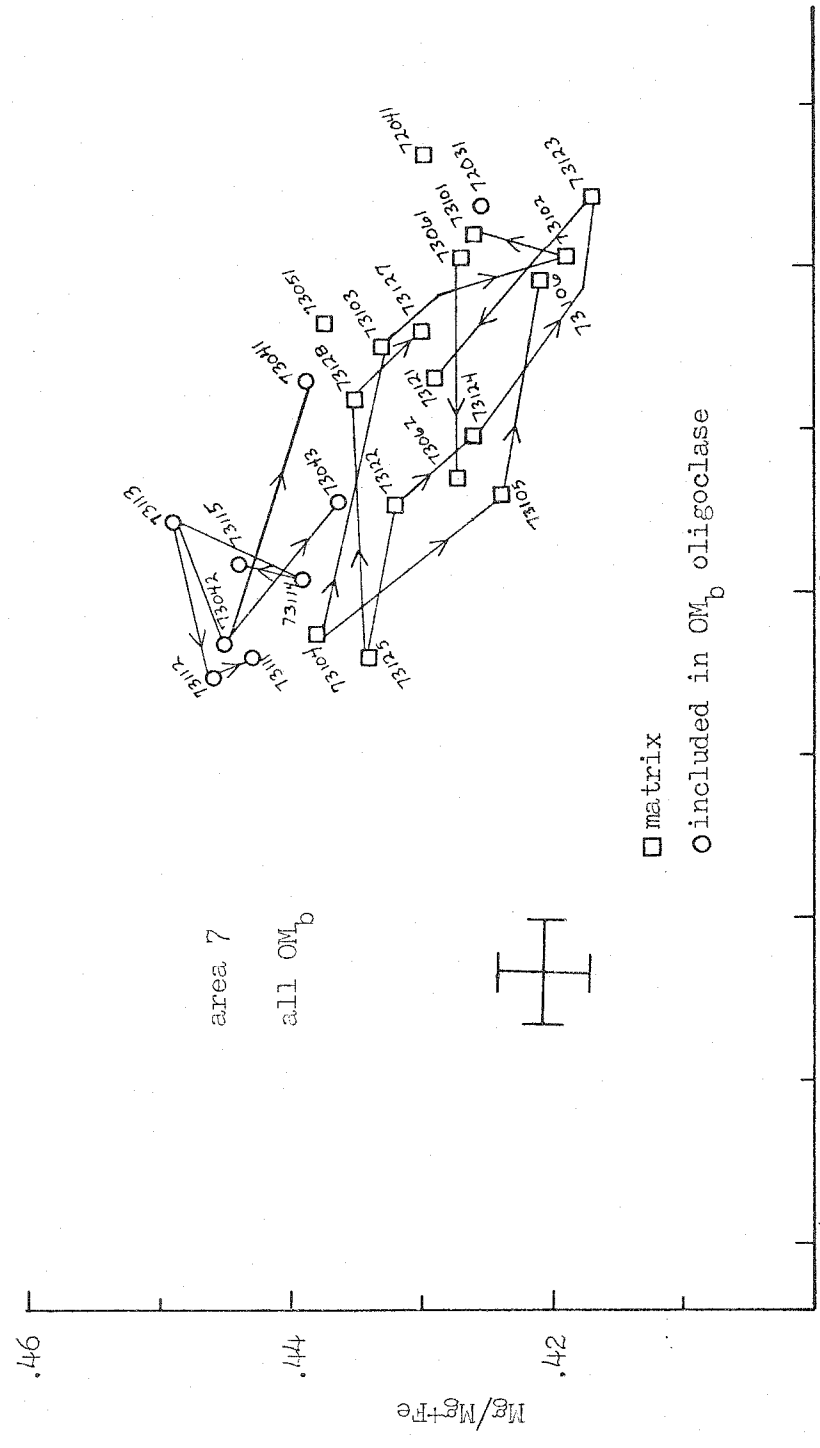

Figure 29c Plot of Al vs. Mg/Mg+Fe for chlorite in area 7 of JR-5-A host rock.

clase. A few of the OM_b points are from thin rims on grains included in OM_a plagioclase. These thin rims seem to represent some limited overgrowth on the included grains during OM_b overprint. There seem to also be some small, irregular areas of OM_b plagioclase growth in the OM_a albite near these chlorite grains. Figure 29b shows compositions from one area of the host rock in the thin section and illustrates the dichotomy of these two chlorite groups. There does not appear to be a continuous compositional variation from OM_a to OM_b chlorite, even in the included OM_a grains which have OM_b rims. This sharp compositional distinction in this area of the thin section is part of the reason for interpreting the prerotation albite cores and included chlorite grains as OM_a. Figure 29c shows compositions of matrix grains and grains included in OM_b plagioclase from another area in the host rock of JR-5-A. The zoning patterns in the grains shown in Figures 29b and 29c plus data from grains in other areas define the fairly complex compositional trend of OM_b host rock chlorite shown in Figure 29a. The possible late reversal of the compositional trend creates problems in comparing the host and vein chlorite.

The compositions of analyzed points in OV_b vein chlorite are shown in Figure 30a. There is less variation than

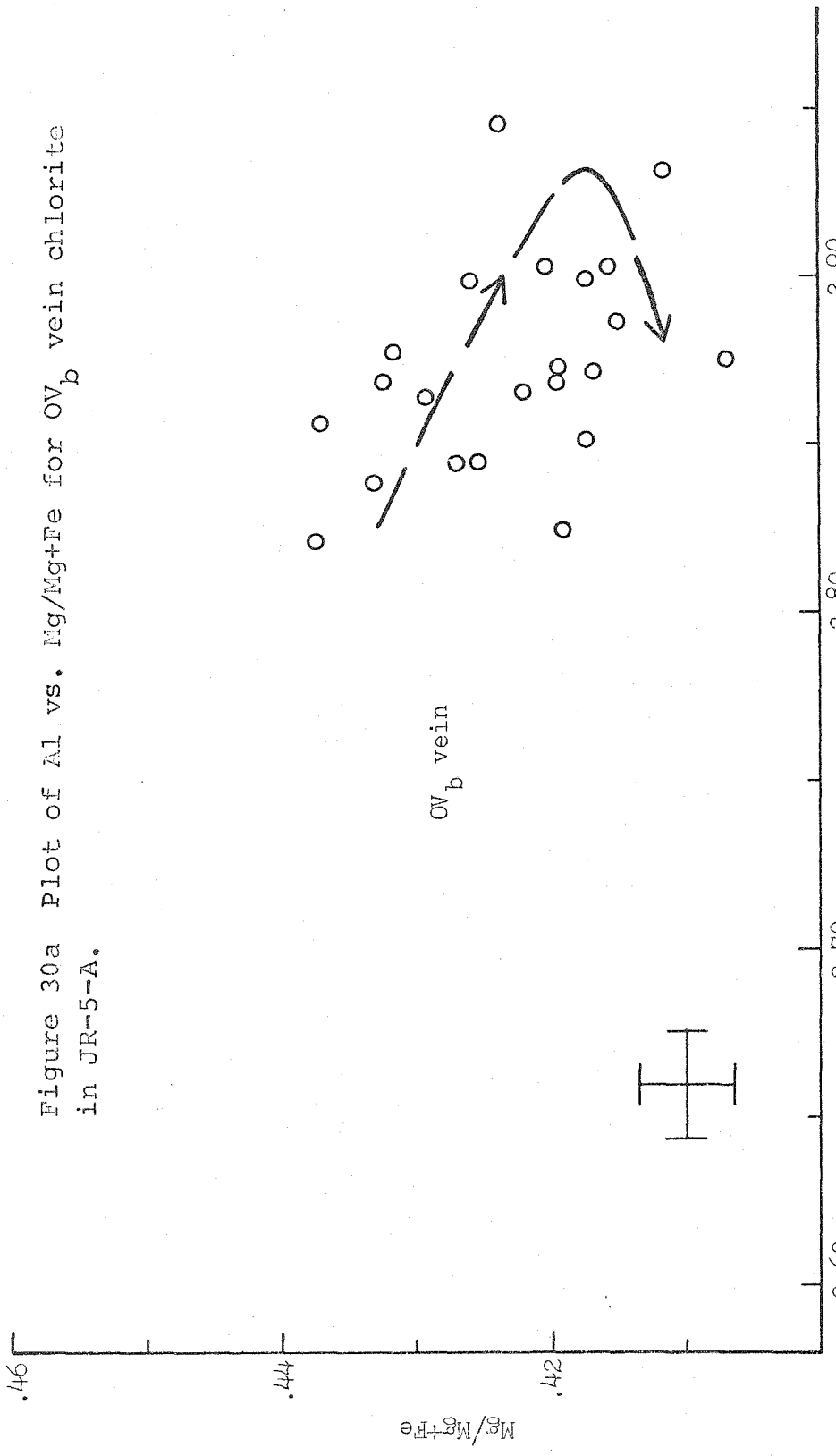

Figure 30a Plot of Al vs. Mg/Mg+Fe for OV$_b$ vein chlorite in JR-5-A.

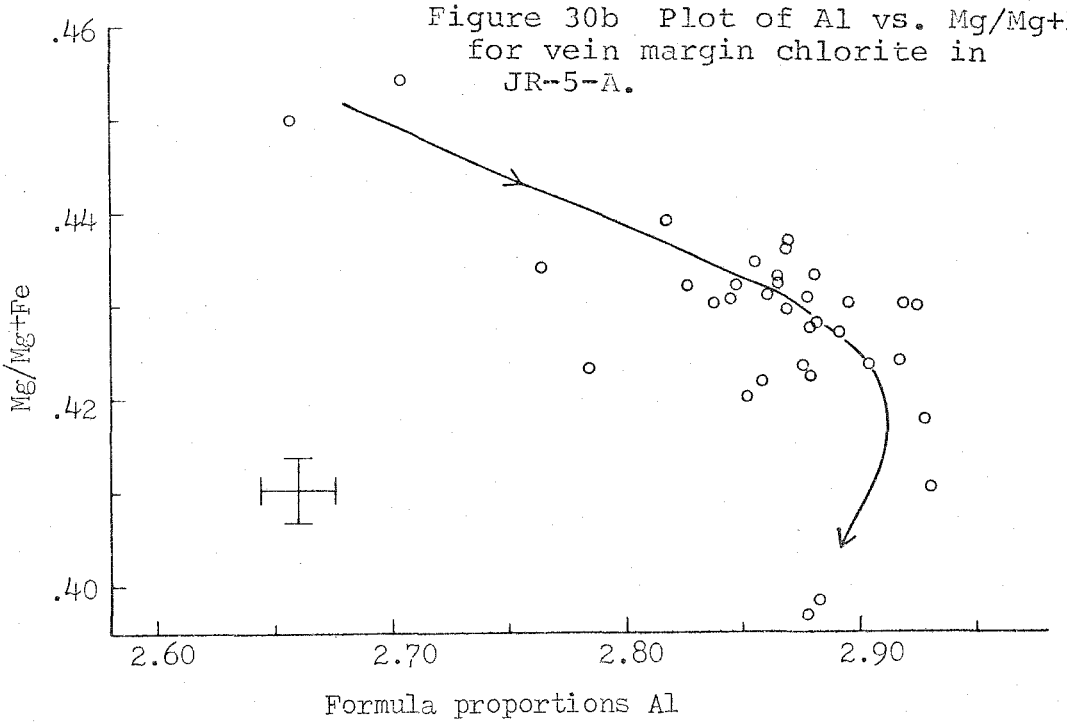

Figure 30b Plot of Al vs. Mg/Mg+Fe for vein margin chlorite in JR-5-A.

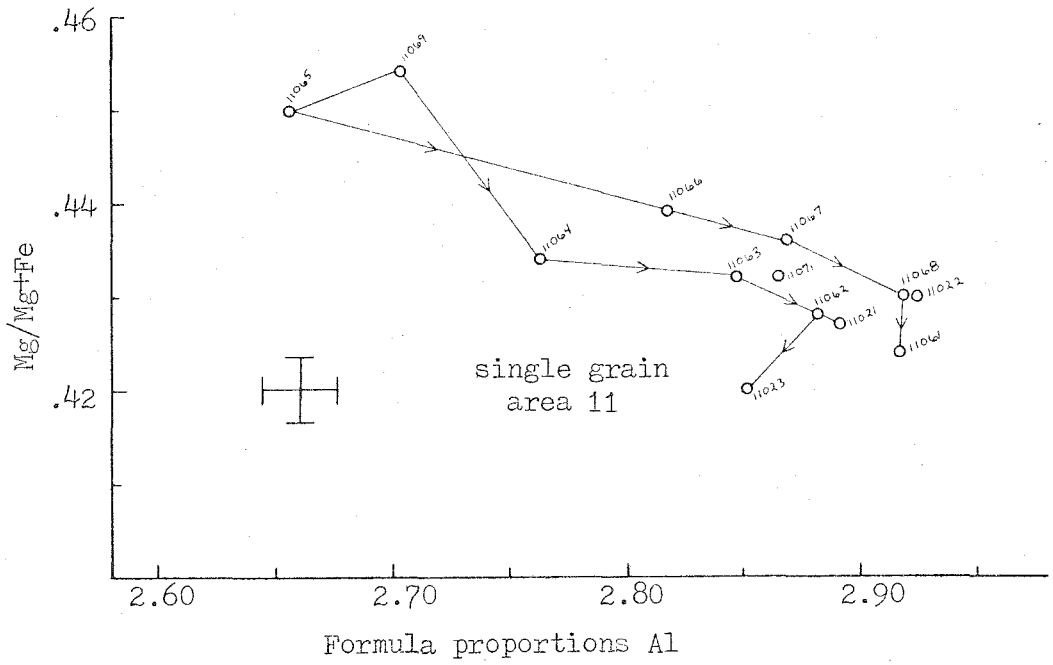

Figure 30c Plot of Al vs. Mg/Mg+Fe for single grain in area 11 of JR-5-A vein margin.

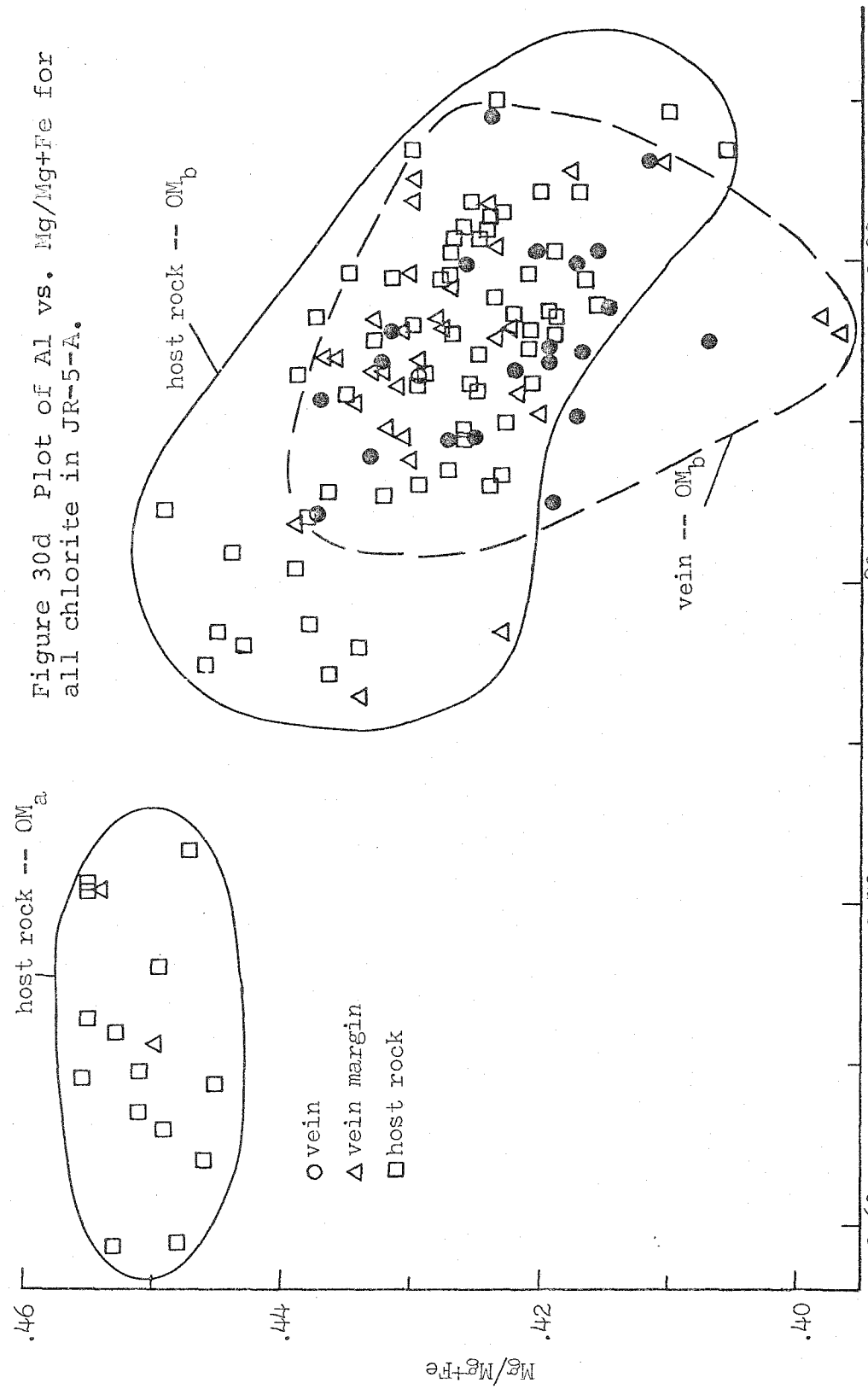

Figure 30d Plot of Al vs. Mg/Mg+Fe for all chlorite in JR-5-A.

seen in host chlorite compositions, but the variation seems to be systematic and is shown on the diagram. Significant overlap occurs in the compositions of vein and host chlorite. If the compositional variation trends are correct as shown, the only true overlap in the vein and host chlorite growth would seem to be with the last host rock chlorite growth and the first vein chlorite growth. This is much like the relationship between host rock and vein plagioclase compositional trends. In any event, the compositional evidence from the chlorite suggests that OM_b host rock and OM_b vein chlorite was formed in the same continuous event, although perhaps in different parts of that event.

Figure 30b shows compositions from chlorite grains along the vein margin at the host rock wall. Grains in the vein margin appear to be part of the host rock but there is also evidence of growth during vein formation. A small amount of chlorite and muscovite growth appears to be border zone growth somewhat like that observed in the DV_a vein of JR-66-F. The distribution of points and the general trend indicated seems to confirm the observation that both host rock and vein chlorite growth is involved. Two points in the core of one grain seem to be preserved OM_a host growth. Figure 30c shows the points in a traverse across this grain. All of the complexities of the composi-

tional trend of the host rock chlorite do not appear, but this could be a sampling problem. Because of the overlap of the compositional ranges of host rock and vein chlorite, it is difficult to determine exactly how much of the vein margin chlorite growth is associated with either group.

Figure 30d shows the compositions of all analyzed chlorite on one diagram. The envelopes drawn on this diagram include analyses from the vein margin which have been arbitrarily assigned to each group. The overlap between host rock OM_b chlorite compositions and OM_b vein chlorite compositions is considerable. There is no significant variation in the Mn or Zn contents of chlorite in this sample.

The compositions of analyzed muscovite in the host rock and OV_b vein of JR-5-A are shown respectively in Figures 31a and 31b. Fewer muscovite analyses have been obtained than for chlorite and therefore, the trends are not well defined. Vein muscovite seems to have increasing Si from core to rim, indicating decreasing grade such as shown by the vein plagioclase zoning. For both types of muscovite there isn't much variation in Si content when compared to the variation of phengite substitution observed in the OM_b muscovite of sample JR-73-A. The vein and host rock muscovite compositions are very similar to each other. No muscovite in the host rock can be shown to be OM_a.

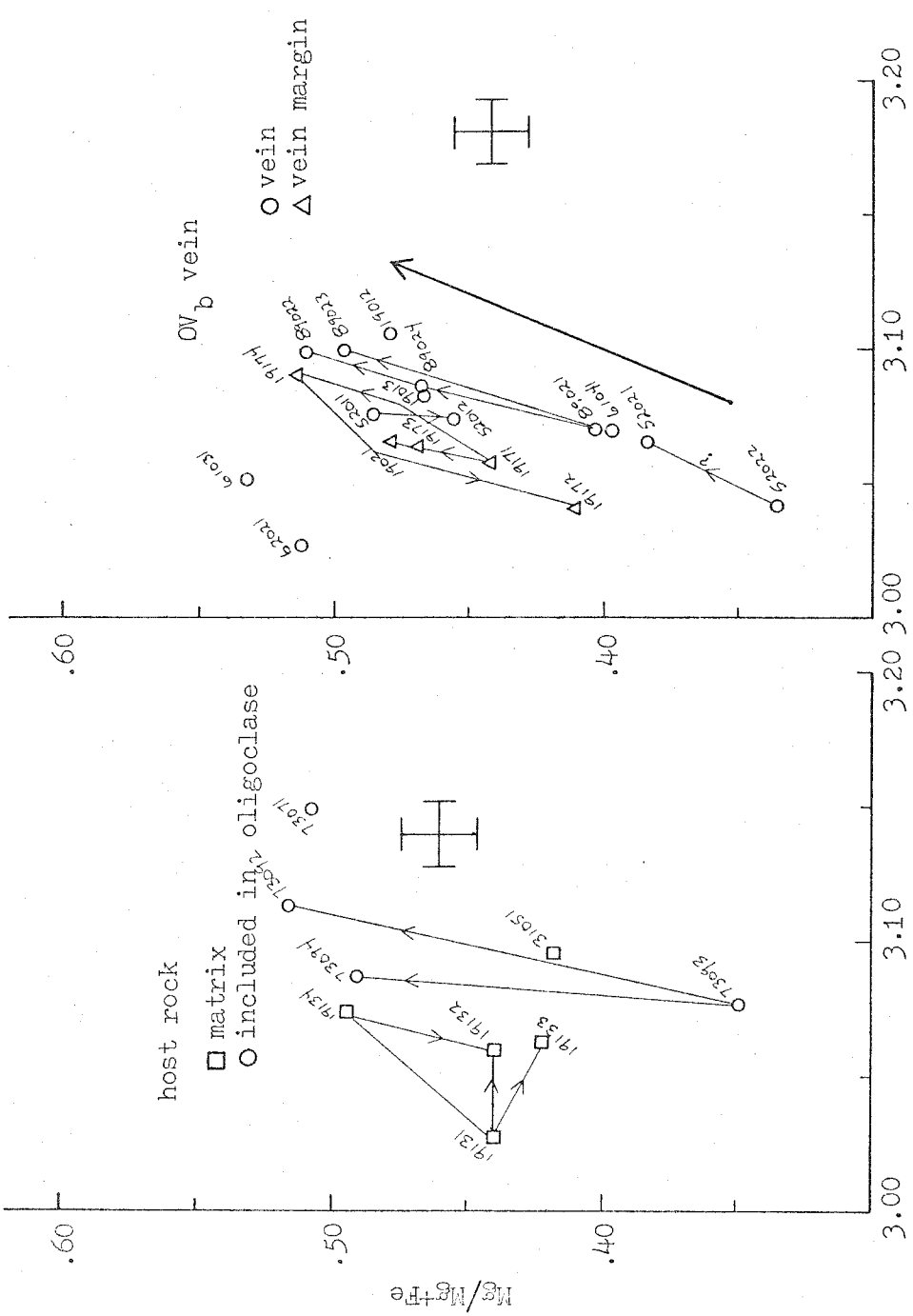

Figure 31a Plot of Si vs. Mg/Mg+Fe for muscovite in host rock of JR-5-A.

Figure 31b Plot of Si vs. Mg/Mg+Fe for muscovite in OV$_b$ vein of JR-5-A.

Compositions of OV_b vein muscovite in JR-5-B are shown in Figure 32. The range of these compositions and compositional variation trends are very similar to those of OV_b vein muscovite in JR-5-A. In fact, the coincidence of these two groups is perhaps important given that the two samples were at least 15 centimeters away from each other in the outcrop. This suggests that there was equilibrium among growing grains in the OV_b vein at least on the scale of 15 centimeters.

Also within JR-5-B are white mica grains which are texturally related to limited alteration of plagioclase. These grains have abnormally high Na and Ca contents indicating that they are intergrowths of muscovite, paragonite, and perhaps margarite. This type of late alteration is commonly observed in the more calcic plagioclase in both OV_b and DV_a veins in this part of the study area.

Much of the variation of Mg/Mg+Fe in the muscovite in these and other samples appears to be due to variations in the ferrimuscovite substitution, as Fe^{3+} is included in the total Fe. This is determined by considering the amount of excess Fe+Mg+Mn relative to the amount of phengite substitution (Si over 3.00 formula proportions). The analyses with the most excess Fe+Mg+Mn tend to be the most Fe-rich for a given value of Si. For some analyses, the calculated

Figure 32 Plot of Si vs. Mg/Mg+Fe for muscovite in OV_b vein of JR-5-B.

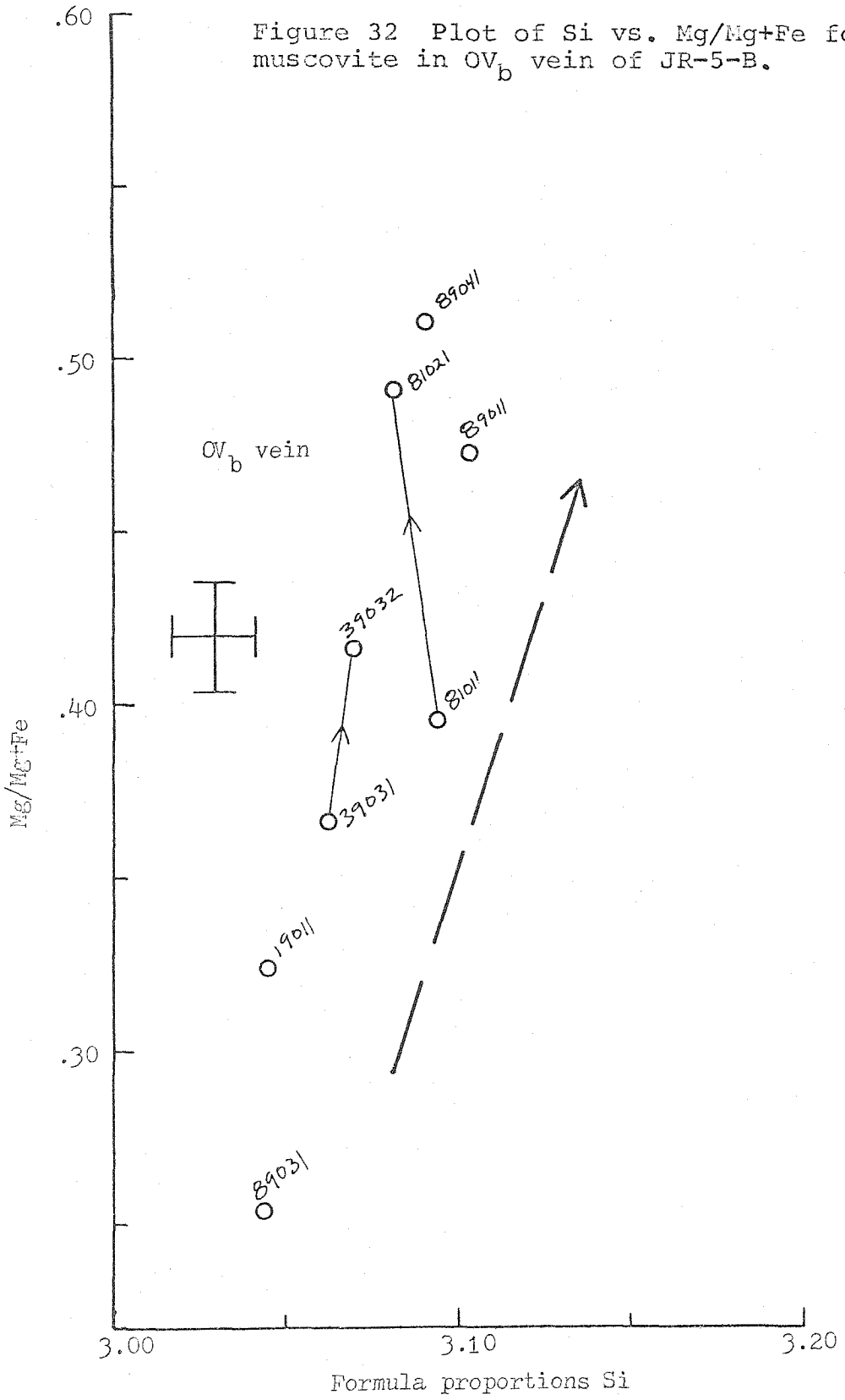

Fe^{3+} comprises all of the Fe present. Calculation of Fe^{3+} is, however, subject to considerable error in a mineral in which site vacancies can be present.

There is compositional variation in other minerals in these samples. OV_b vein calcite appears to have increasing Ca and decreasing Fe from core to rim. Mg and Mn are roughly constant. Host rock ilmenite is fairly constant in composition with virtually no Fe_2O_3 substitution and about 7% substitution of $MnTiO_3$ for $FeTiO_3$.

As mentioned, the vein plagioclase shows evidence of alteration to white mica and also calcite, so that there is an additional mineral growth generation. The alteration product calcite in these vein samples is nearly pure $CaCO_3$. Pyrrhotite in both the host rock and the vein is partly altered to pyrite. Some ilmenite grains are partly altered to rutile. It is not clear when these alteration reactions occurred except that they were either very late in the OM_b-forming event or in a subsequent event. Because similar effects are seen in the DV_a vein studied at this location, the alteration is thought to be post-DV_a.

The compositional and textural evidence in JR-5-A and JR-5-B seem to indicate that the first OM_b mineral growth occurred in the host rock and then the OV_b vein began to form. Host plagioclase growth stopped when the vein growth

started and this may be true for chlorite also. Host plagioclase zoning indicates that OM_b host rock mineral growth occurred as the grade was progressively increasing. The OV_b vein began to form at the peak of OM_b metamorphism and vein growth continued down grade. Strong deformation associated with the formation of OF_b folds and OS_b schistosity must have ended as the OV_b veins began to form because there appears to be no effect of OF_b and OS_b on the veins. OM_a chlorite and plagioclase appear to be preserved in the prerotation albite cores in host rock plagioclase grains. Some OM_a chlorite may be preserved in the cores of the larger chlorite grains in the host rock matrix. There is no evidence of DM_a growth and DS_a slip cleavage is not observed in either of these samples.

JR-5-G

In host rock a few meters away from samples JR-5-A and JR-5-B, DM_a mineral growth is very prominent. The difference between JR-5-A and samples where DM_a is observed is that DS_a slip cleavage is well developed in the latter. Parallel to the DS_a slip cleavage are a number of DV_a veins. JR-5-G is a sample of one of these veins and its adjacent schist. This vein is shown in Figure 31 in Chapter II.

The DV_a vein from which JR-5-G is taken is about 2

meters long and 15 centimeters wide in cross-section. An irregularly developed border zone of euhedral plagioclase and anhedral calcite is about 1 centimeter wide. The vein mineral assemblage is quartz-plagioclase-calcite-pyrrhotite plus small amounts of chlorite and apatite which occur at the vein margin on the host rock wall. Figure 33 is a photograph of the contact between the vein and the host rock. The contact is generally parallel to DS_a surfaces but there are discrete offsets nearly perpendicular to DS_a. DS_a is well developed in the host rock.

Figure 34a shows the compositions of plagioclase in the DV_a vein. The compositional variation trend appears to be increasing An content from An_{30} to An_{35}, then decreasing to perhaps An_{15} at the rims. By volume, most of the vein plagioclase lies along the portion of the trend involving decreasing An content. The compositional range and trend are remarkably similar to those of OV_b vein plagioclase in JR-5-A and JR-5-B.

DV_a vein plagioclase is partly altered to calcite, white mica (intergrown muscovite and paragonite), and perhaps albite. The three albite compositions shown in Figure 34a are from grains which texturally appear to be altered. It is not absolutely certain whether this albite is post-DM_a or perhaps late DM_a.

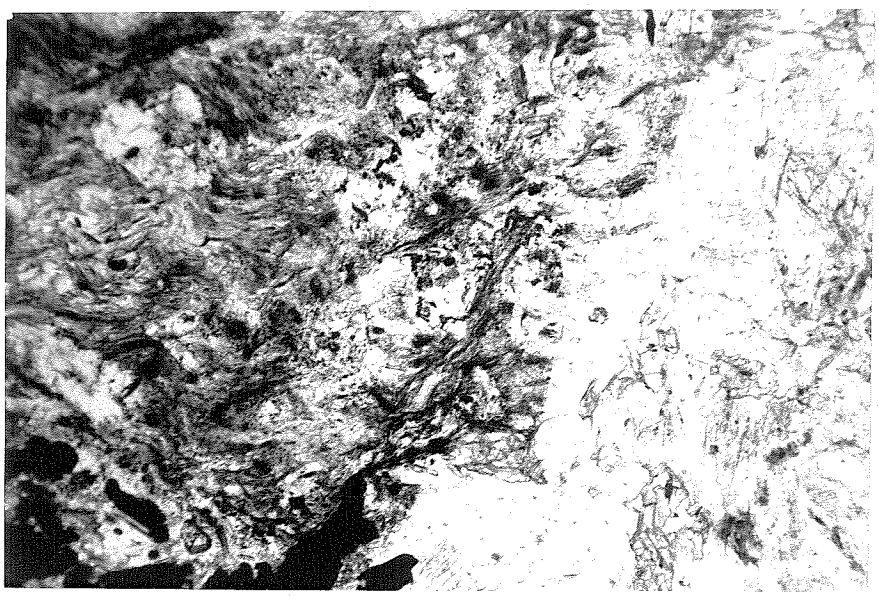

Figure 33 Contact between DV_a vein and host rock in JR-5-G. DS_a slip cleavage is parallel to contact and OS_a/OS_b schistosity is crosscut by vein. 3.2 mm field of view, plane polarized light.

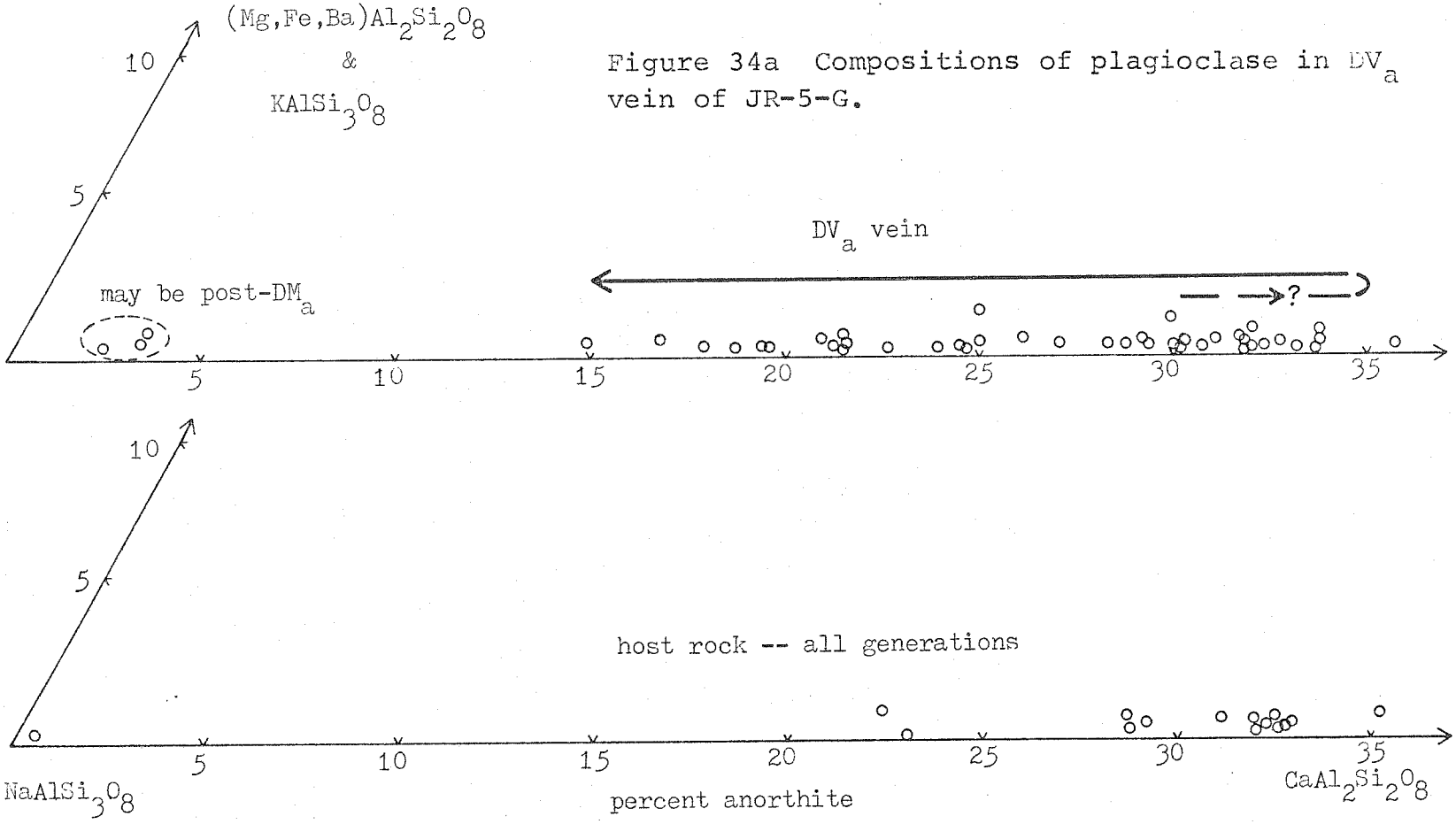

Figure 34a Compositions of plagioclase in DV_a vein of JR-5-G.

Figure 34b Compositions of plagioclase in host rock of JR-5-G.

In the host rock of JR-5-G there appear to be two generations of calcic plagioclase with compositions of oligoclase to andesine. The textural relationships of these two generations, OM_b and DM_a, are similar to those seen in JR-5-I and are discussed in detail for that sample. In JR-5-G much of the pre-DM_a inclusion trains have been destroyed. It is difficult to document rotated OM_b plagioclase and prerotation OM_a albite such as observed in JR-5-A. Figure 34b shows the compositions of analyzed host rock plagioclase points. These are not differentiated as to generation. They are probably a mixture of DM_a, OM_b, and perhaps OM_a albite. The zoning pattern for both DM_a and OM_b plagioclase in the host rock seems to be increasing An content from core to rim.

Host rock and vein chlorite analyses are shown on a plot of Al vs. Mg/Mg+Fe in Figure 35. Points shown as OM_b chlorite are from grains which have preferred orientation parallel to the highly deformed schistosity OS_a/OS_b. Host rock DM_a chlorite points are from grains with preferred orientation parallel to DS_a or without preferred orientation. Some of the host rock DM_a points are from thin rims around the OM_b chlorite. The only possible vein chlorite growth is at the vein margin. Some of the vein margin grains clearly grow out into the vein and are part of the

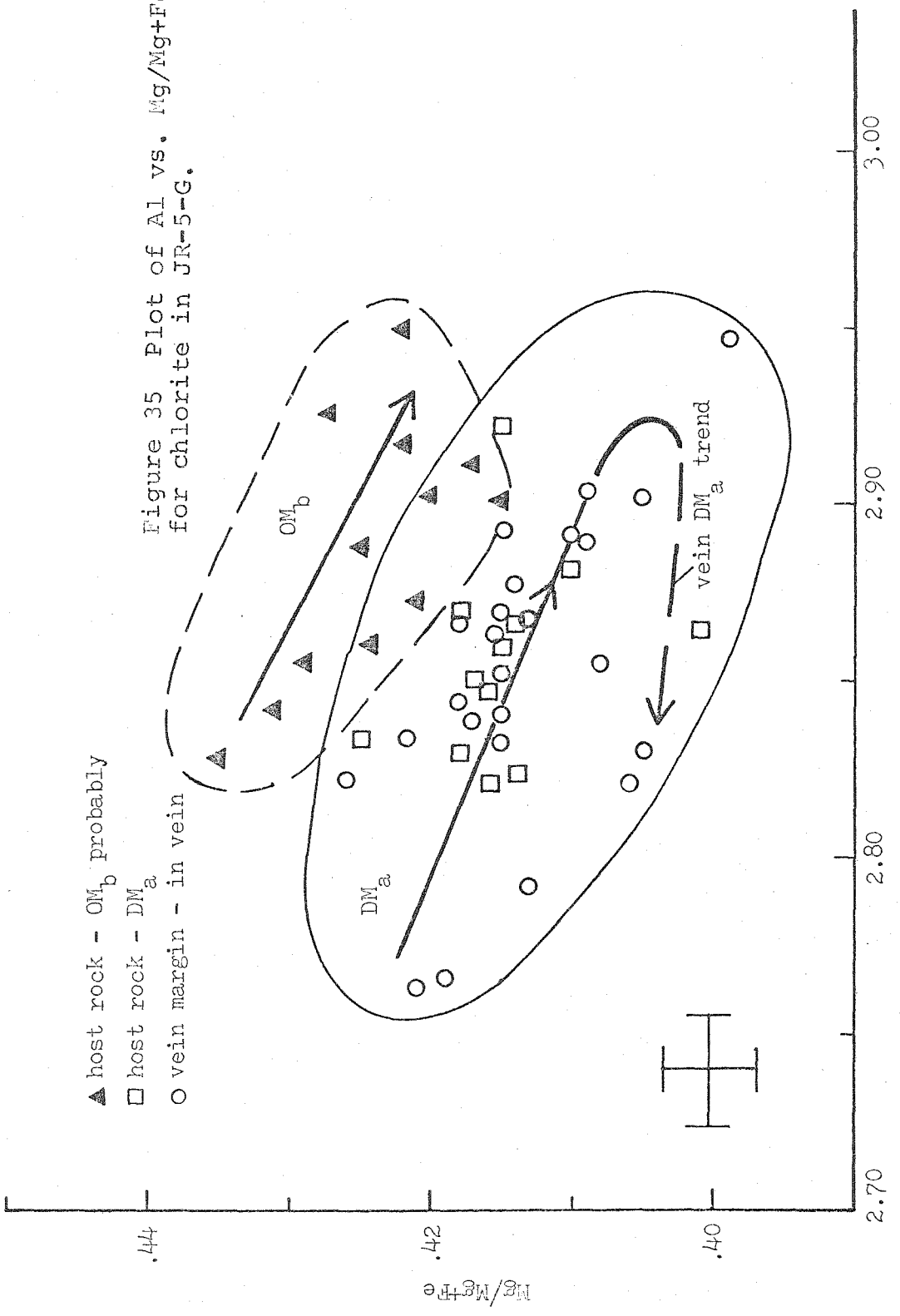

Figure 35 Plot of Al vs. Mg/Mg+Fe for chlorite in JR-5-G.

vein growth. Some of the vein margin chlorite may include pre-vein cores.

DM_a host rock chlorite is reasonably abundant. Many of the OM_b grains appear to be optically zoned with crossed nicols; the rims of these grains have compositions similar to grains which are clearly DM_a chlorite. The DM_a host rock chlorite and vein chlorite have very similar compositional ranges. A compositional trend has been defined for the DM_a vein margin chlorite and for the OM_b host rock chlorite as well. These trends are indicated on Figure 35. A trend was not defined for the host rock DM_a chlorite, but it may be different than the vein margin chlorite trend.

A small amount of garnet occurs in JR-5-G. Many of these grains appear to be extensively resorbed and replaced by various matrix minerals. There are single anhedral, rounded garnet grains and clusters of several irregular, rounded small grains, which are apparently fragments of a larger original grain. The remnant garnet grains seem to preserve their original zoning as indicated by the Mn content of various fragments of the original porphyroblasts. The Mn content depends upon the position of the fragment relative to the original outline of the grain. The Mn content decreases from core to rim. Apparently the garnet grains have been partially dissolved away without disturb-

ing the compositions of the remnant fragments. The compositions of analyzed garnet points are shown in Figure 36.

The garnet grains are probably all OM_b mineral growth. The resorption of these grains seems to have occurred during DM_a growth. The DM_a overprint on the garnet grains is not the type of retrograde texture which is observed in a number of other samples from nearby locations. Typically the retrograde products such as chlorite, muscovite, calcite, and/or biotite are pseudomorphous after the reacted garnet. There is no evidence of DM_a garnet growth at this outcrop.

The plagioclase zoning indicates that the DV_a vein began to form near the peak of D_a metamorphism, after extensive DM_a host rock mineral growth. The vein growth began as the grade was still increasing and then vein growth continued as the grade of the system decreased. DM_a host rock mineral growth has extensively overprinted the OM_b mineral growth in this sample. The relationship between the DV_a vein and the adjacent host mineral growth is very similar to that of the OV_b vein and adjacent host of JR-5-A.

JR-5-D and JR-5-I

Two samples of the Hazens Notch schist not adjacent to veins have been analyzed with the microprobe. JR-5-D is

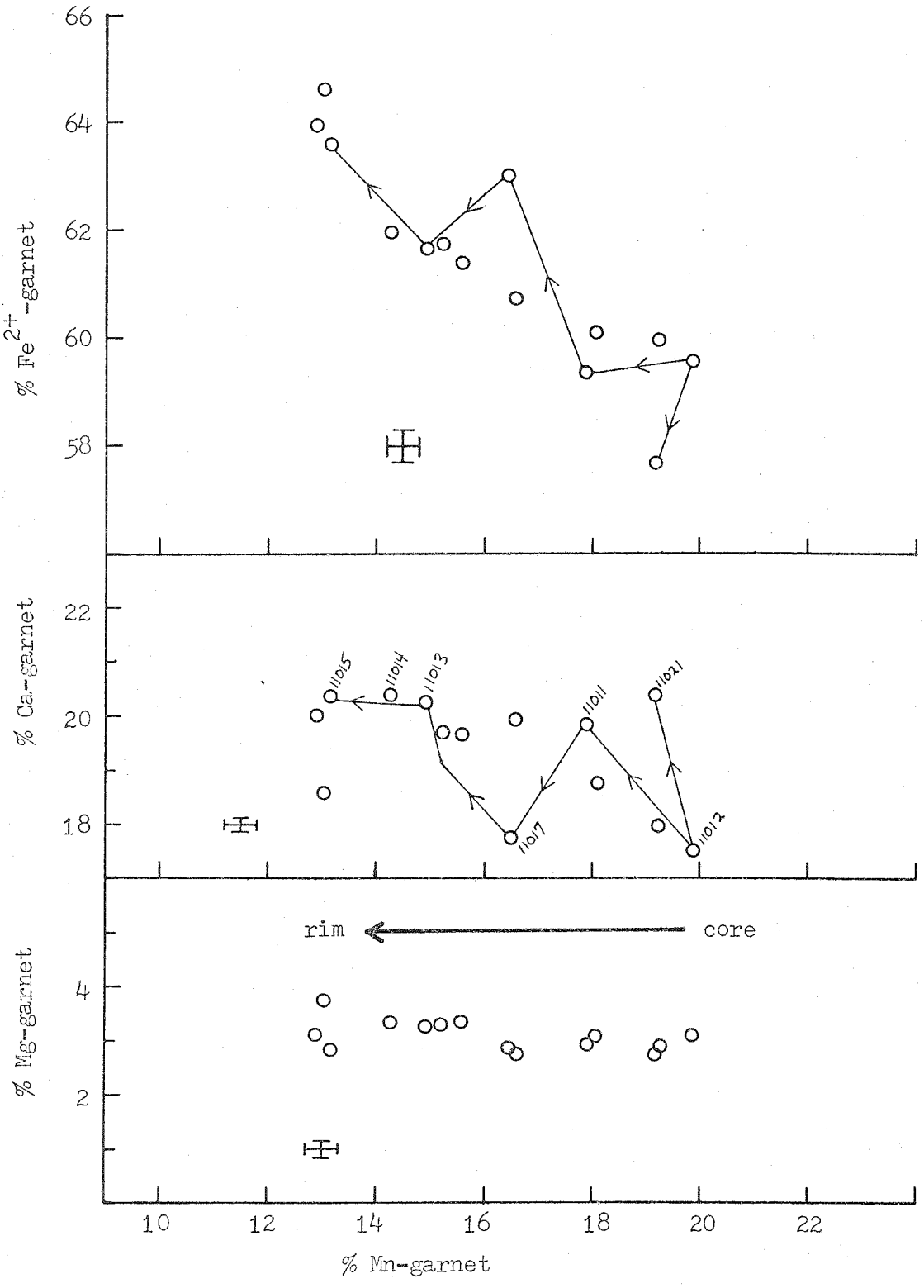

Figure 36 Compositions of garnet in host rock of JR-5-G.

from 15 centimeters away from the nearest OV_b vein and JR-5-I is from 30 centimeters away from the nearest DV_a vein. The assemblages in these two samples are nearly identical; both have quartz-muscovite-chlorite-garnet-plagioclase-epidote-apatite-ilmenite-pyrrhotite-pyrite (alteration of pyrrhotite)-zircon. There is also tourmaline and chalcopyrite in JR-5-I. Calcite is part of the assemblage in JR-5-D. DS_a slip cleavage is developed in both samples, with DS_a being somewhat more prominent in JR-5-I. DS_a seems to be largely defined by rotated pre-DS_a grains, but some new growth of chlorite and muscovite grains parallel to DS_a also seems to have occurred.

The textural relationships within plagioclase grains in these samples indicate multiple generations of mineral growth. This is best described using an example from JR-5-I shown in Figure 37a. Two grains, one large and one small, in this area were analyzed using electron beam scanning pictures of Na, Al, Si, and Ca. The EBS pictures were augmented with normal quantitative analyses of selected points. The data are compiled into the diagram shown in Figure 37b.

The large grain in Figure 37 has a cloudy core surrounded by a clear rim. The cloudy core has areas of both albite and oligoclase. The core is completely surrounded by clear albite and the clear albite is in turn surrounded

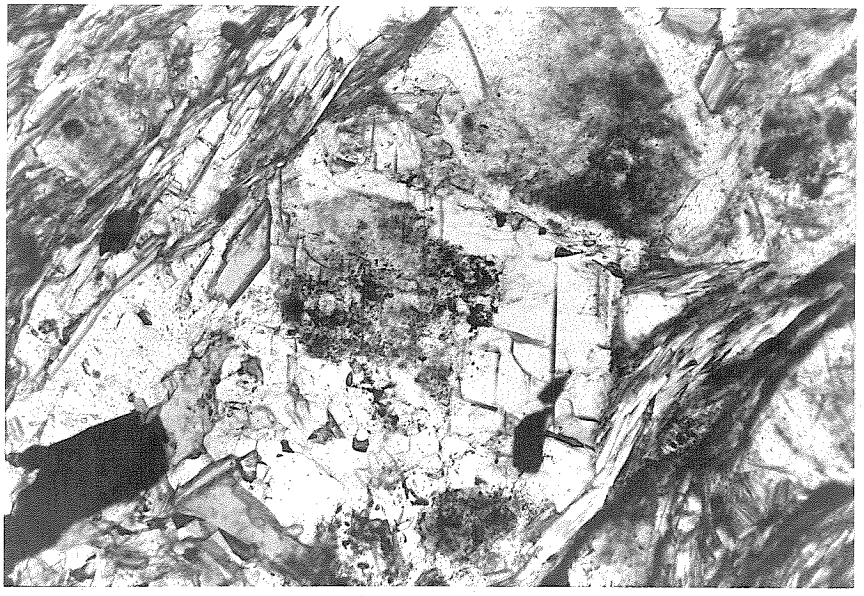

Figure 37a Plagioclase grain in JR-5-I. Cloudy core is OM_b (plus perhaps OM_a albite) and clear rim is DM_a. 1.6 mm field of view, plane polarized light.

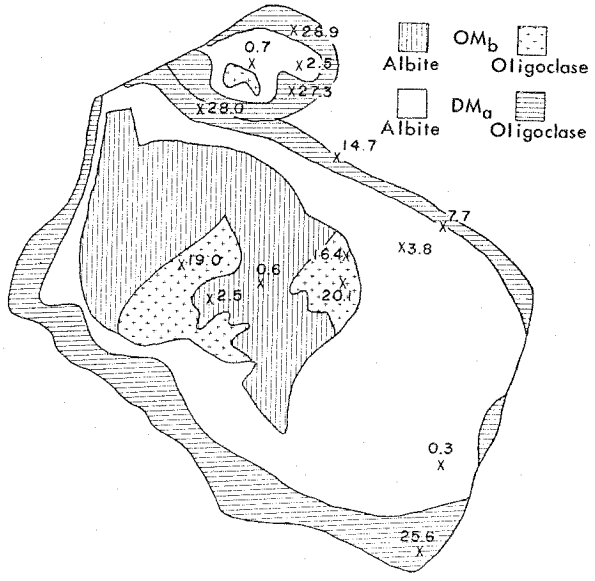

Figure 37b Distribution of plagioclase compositions in grain in Figure 37a. Data are from EBS pictures and quantitative analyses. Numbers on points indicate percent anorthite content.

by a rim of clear oligoclase. The small grain has three of these areas but not the cloudy albite zone. The boundary between albite and oligoclase is in all cases a sharp chemical discontinuity. The OV_b and DV_a veins present at this outcrop have established that there are two generations of plagioclase with oligoclase compositions, OM_b and DM_a. A reasonable interpretation of thegrains in Figure 37 is that the inner, cloudy oligoclase is OM_b and that the outer, clear oligoclase is DM_a. The cloudy albite is either OM_a or early OM_b or perhaps a combination of the two. The clear albite that rims the OM_b oligoclase is DM_a. The sharp discontinuity between DM_a albite and oligoclase is probably the peristerite gap which was encountered during progressive DM_a plagioclase growth. If any of the cloudy albite is OM_b, then the discontinuity between this albite and the cloudy OM_b oligoclase might also be the peristerite gap. The boundary between the cloudy plagioclase and the clear albite is either a growth or reaction boundary, but not the peristerite gap of a single growth generation.

Plagioclase grains similar to those in Figure 37 are common throughout JR-5-I and JR-5-D. Figures 38a and 38b show the compositions of analyzed plagioclase of all generations in the two samples. The points are distinguished as to generation by their textural relationships. The compo-

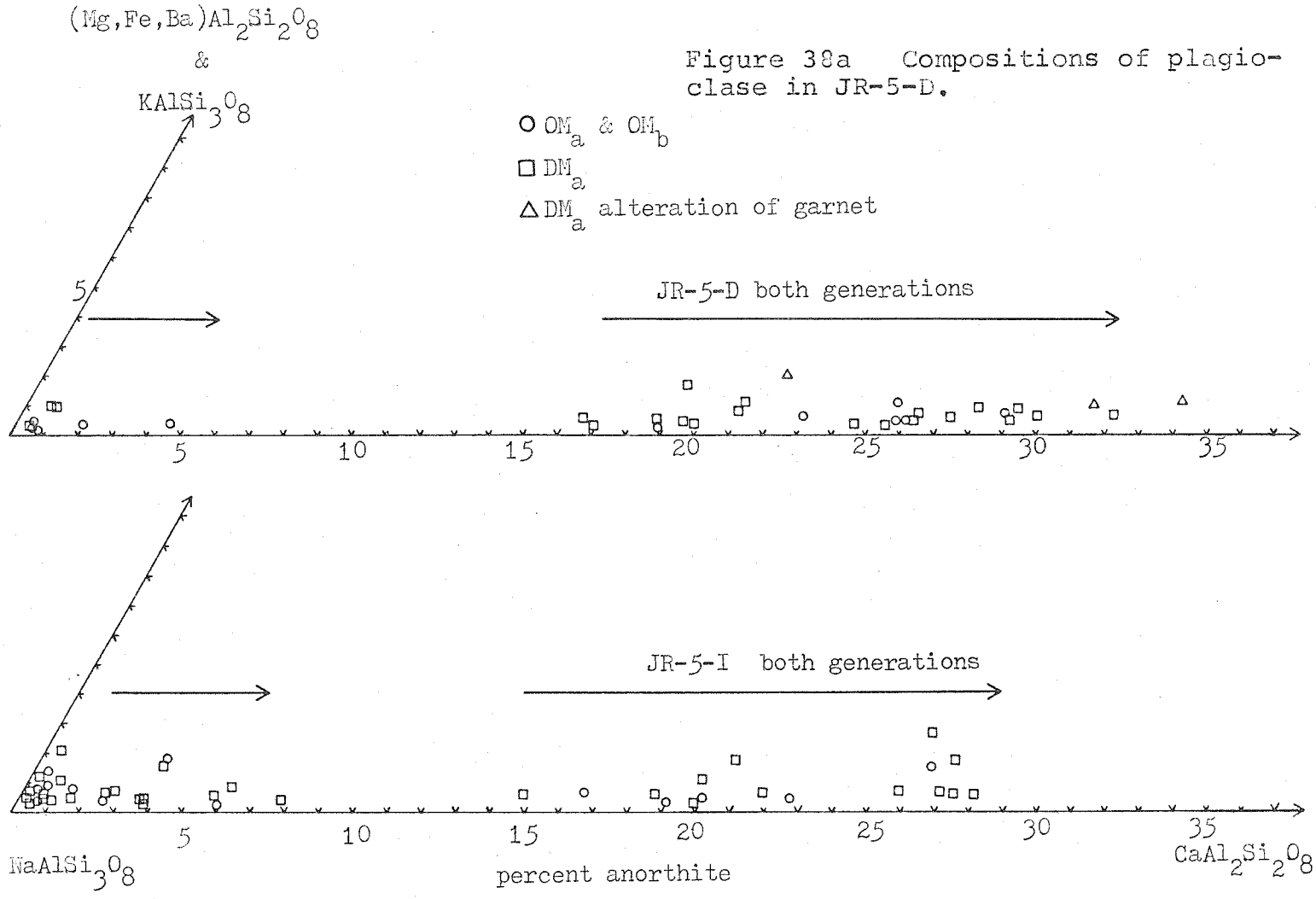

Figure 38a Compositions of plagioclase in JR-5-D.

Figure 38b Compositions of plagioclase in JR-5-I.

sitional trend for both OM_b and DM_a plagioclase in these samples is increasing An content from core to rim. The range of OM_b and DM_a plagioclase in each sample is roughly the same.

Chlorite grains are included in OM_b and DM_a plagioclase in both samples. The OM_b chlorite included in the cloudy cores is compositionally distinct from the DM_a chlorite included in the clear plagioclase rims. There is also chlorite in the matrix and chlorite which is spatially related to the retrograde of garnet. Most of the matrix chlorite appears to be compositionally related to the DM_a grains included in plagioclase. This is true even for matrix chlorite grains which appear to be parallel to OS_a/OS_b. Compositions of analyzed chlorite points are shown in Figures 39a and 39b. The points have been divided by compositions and textural relationships into three groups; OM_b, DM_a, and alteration of garnet. Most or all of the chlorite which is related to the retrogradation of OM_b garnet is probably DM_a. Some of the alteration could be DM_c; this chlorite is compositionally somewhat different from the chlorite which is clearly DM_a. A general trend has been established for the DM_a chlorite in JR-5-I and this is shown in Figure 39b. There are not enough analyses of the other groups to establish trends.

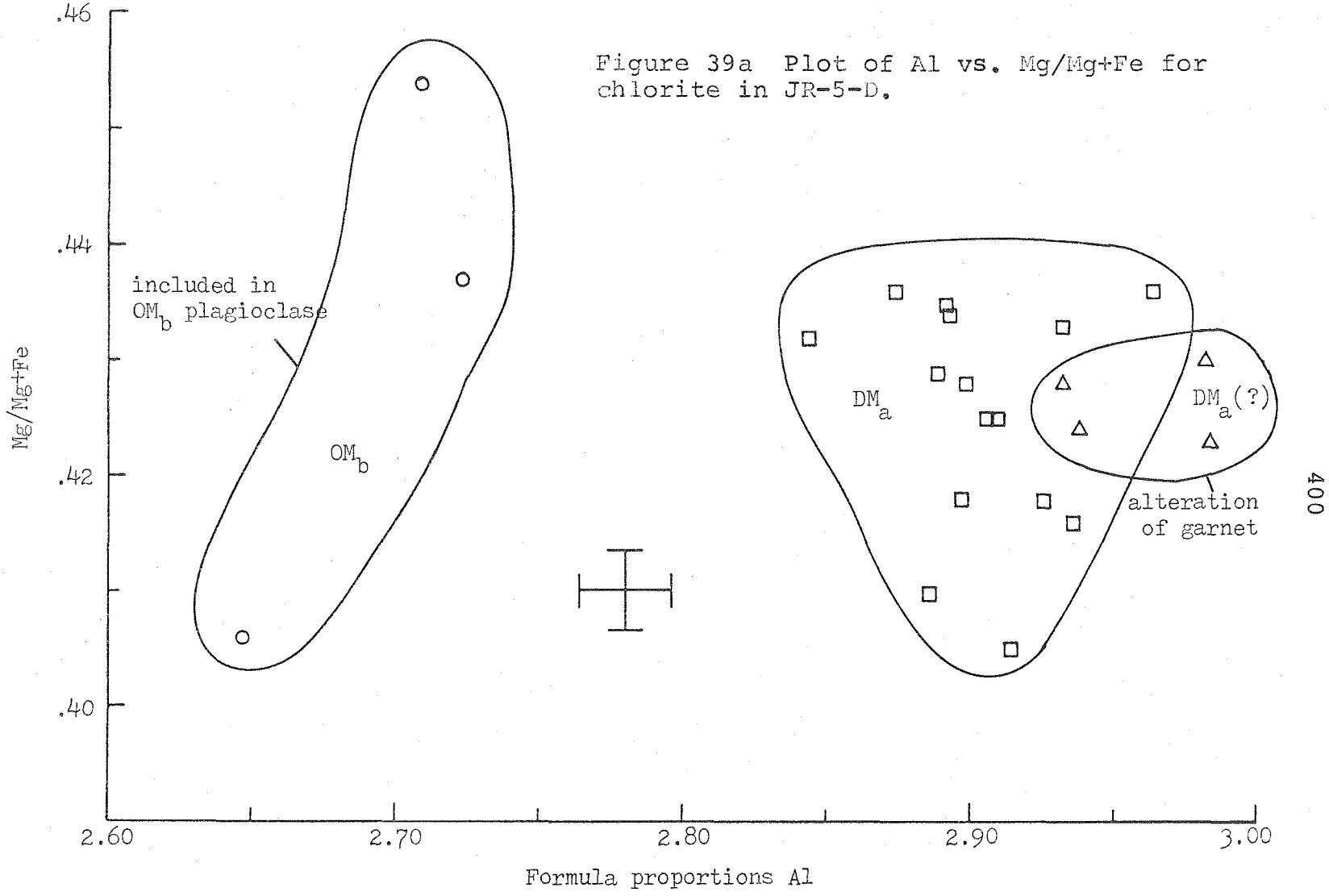

Figure 39a Plot of Al vs. Mg/Mg+Fe for chlorite in JR-5-D.

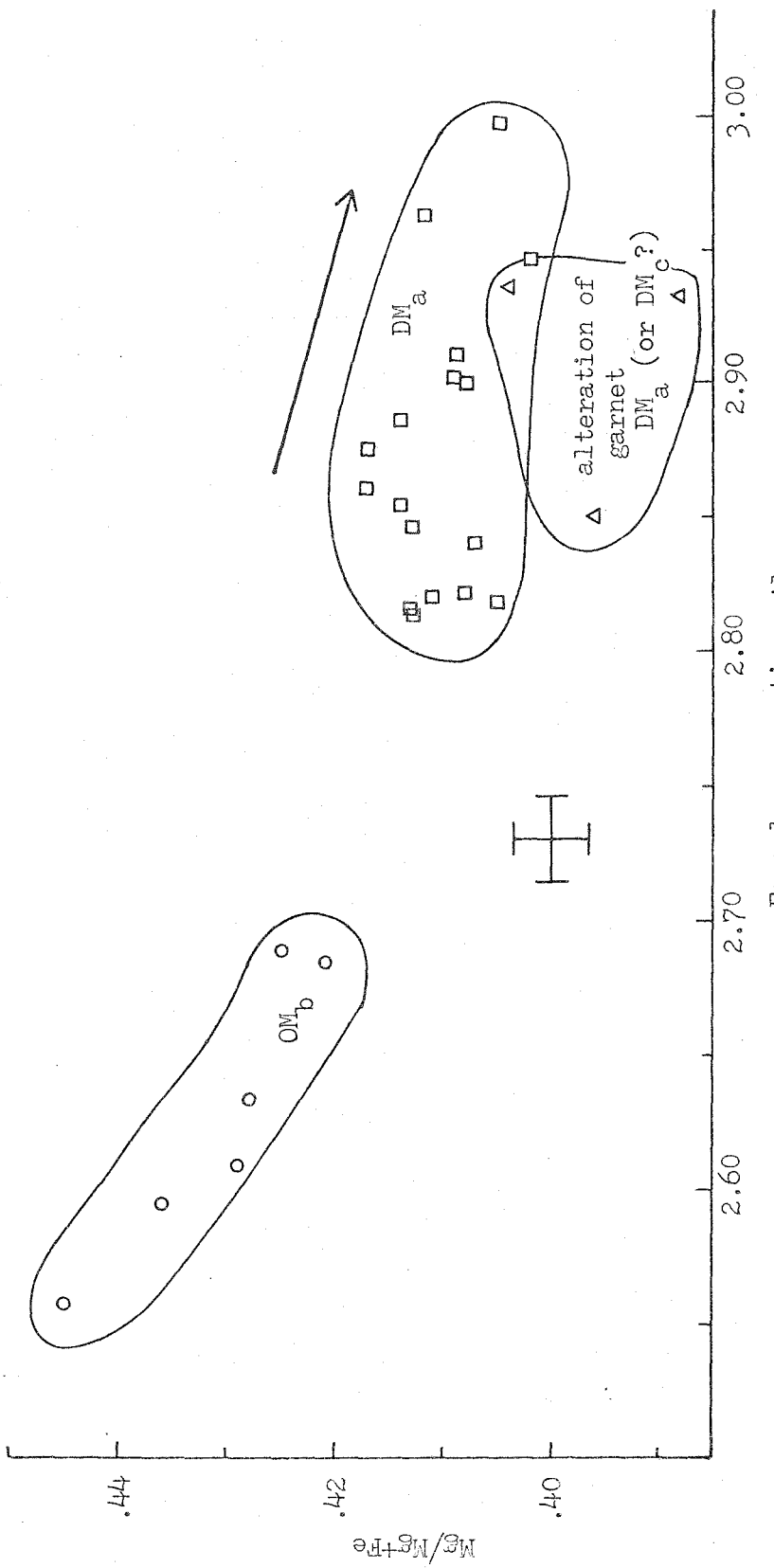

Figure 39b Plot of Al vs. Mg/Mg+Fe for chlorite in JR-5-I.

The included grains in the two generations of plagioclase and the distinct compositional ranges of the two groups of included chlorite is good evidence that two generations of chlorite are present and that these generations are DM_a and OM_b. None of the analyses come from chlorite grains included in plagioclase that might be OM_a so that the presence of OM_a chlorite has not been established. It appears that extensive recrystallization of matrix OM_b chlorite occurred during DM_a growth, more so than in sample JR-5-G. This recrystallization included grains parallel to OS_a/OS_b; only the core of one such grain in sample JR-5-D appeared to preserve a composition of the OM_b generation.

Garnet occurs in both samples, but is more abundant in JR-5-D. Much of the garnet has been altered or partially resorbed. Remnant fragments of garnet are surrounded by replacement minerals such as chlorite, plagioclase, quartz, and calcite. The reaction product plagioclase is free of inclusions and has a range of compositions identical to that of the DM_a plagioclase. The reaction product chlorite is similar, but not identical to DM_a chlorite. Most or all of the alteration of garnet is probably DM_a in generation. There is a limited amount of very fine-grained alteration product minerals that may be DM_c, similar to alteration products at location JR-4 which are thought to be DM_c.

Garnet grains in these two samples show consistent zoning trends of decreasing Mn content from core to rim. Compositions of analyzed garnet are shown in Figures 40a and 40b. There is significant variation in the Ca content of these garnet grains, even from point to point. This is similar to the compositional variation observed in the OM_b garnet in sample JR-73-A. There is a fairly smooth relationship between Mn and Mg which is also similar to the garnet in JR-73-A. Because the garnet grains in JR-5-D and JR-5-I are partially replaced by DM_a mineral growth, the garnet is interpreted to be OM_b.

The minerals which replace the garnet do not contain enough Mn to account for the Mn in the original garnet. In JR-5-D, the sample with the largest volume of retrograde garnet, the chlorite associated with the alteration does not have any more Mn in it than the other DM_a chlorite, DM_a chlorite in this sample has less Mn than the OM_b chlorite. Two minerals which could possibly take up the Mn are calcite and ilmenite. Calcite with about 1% by weight MnO is found in JR-5-D and is spatially associated with retrograded garnet grains.

Muscovite grains in the matrix of the two samples have been analyzed. These grains have been texturally assigned to OM_b and DM_a based upon whether or not they are parallel

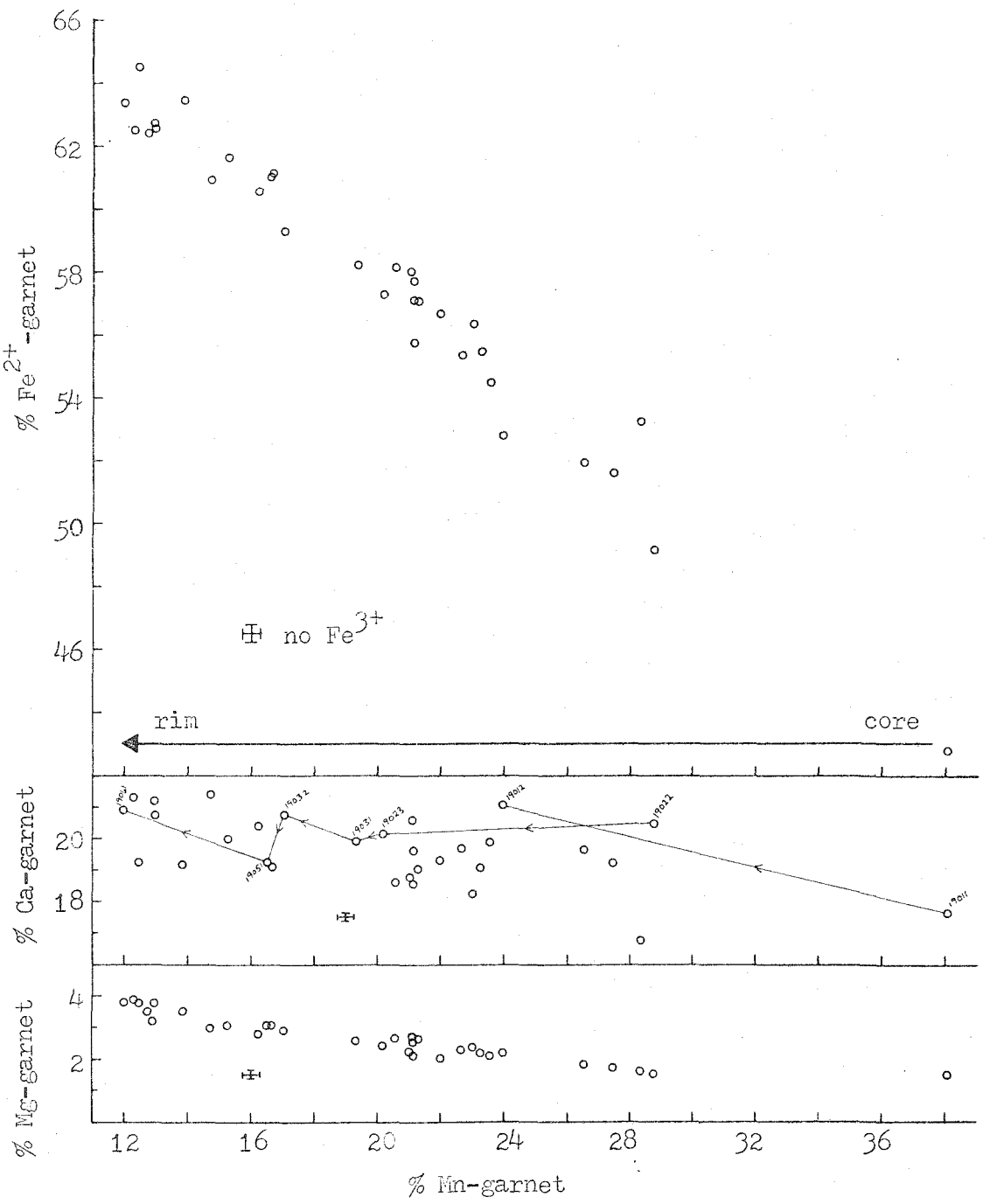

Figure 40a Compositions of garnet in JR-5-D.

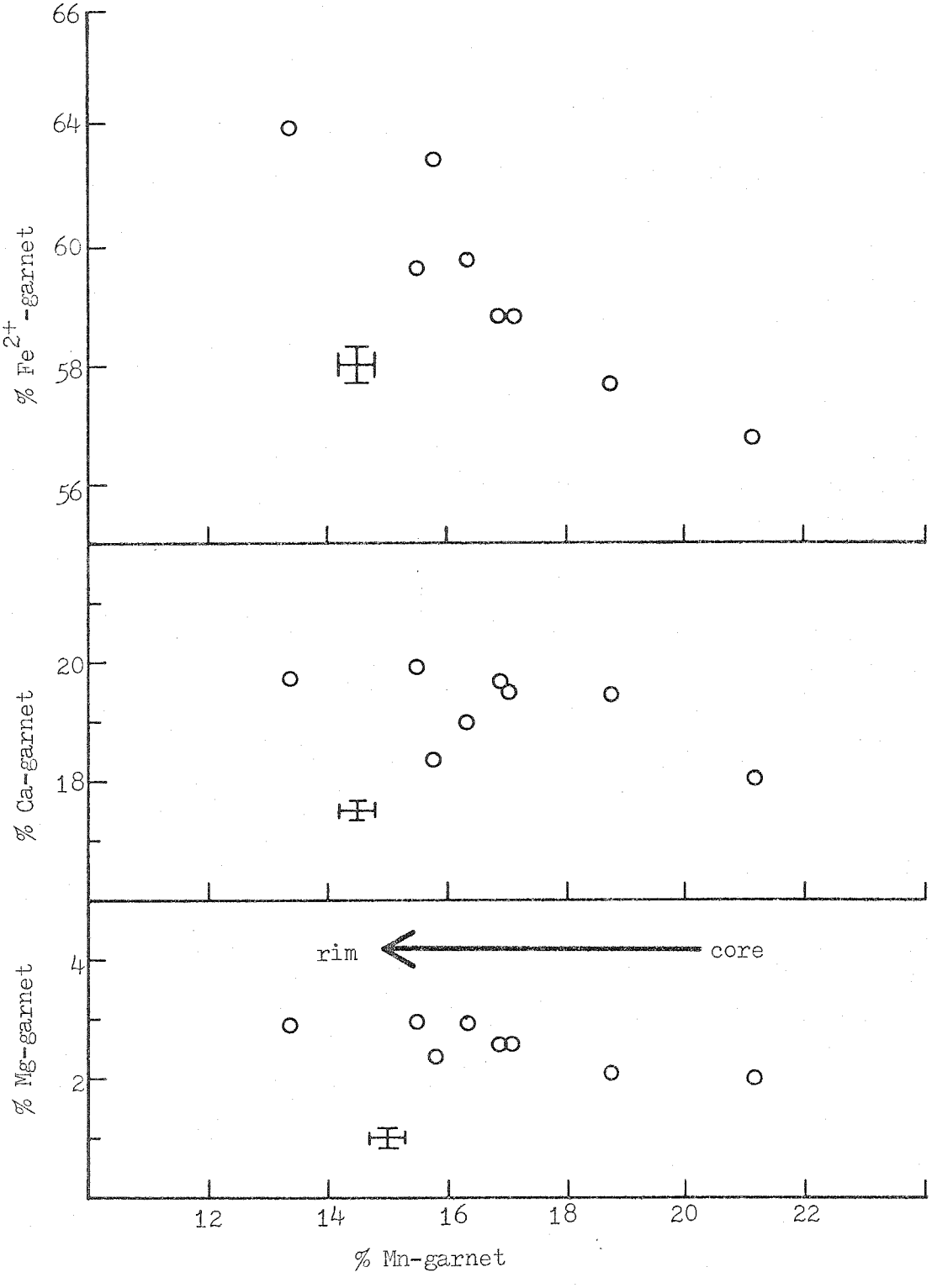

Figure 40b Compositions of garnet in JR-5-I.

to OS_a/OS_b, taking into consideration possible rotation by DF_a. Of course, the chlorite data seem to indicate extensive recrystallization of grains with preferred orientations parallel to OS_a/OS_b. In sample JR-5-I two of the points from grains identified as OM_b have compositions distinct from the DM_a muscovite and one OM_b point overlaps with the range of compositions of DM_a as shown in Figure 41. There are not enough analyses to establish compositional trends.

Ilmenite in JR-5-I and JR-5-D is zoned slightly with respect to Mn. The Mn content increases somewhat from core to rim. The average MnO content of ilmenite in these samples is 2.5-3.0 weight %. The ilmenite grains have preferred orientations parallel to OS_a/OS_b. At least the cores of these grains are probably OM_a and/or OM_b in generation.

Pyrrhotite in both samples is partly altered to pyrite. There is no evidence to suggest when this occurred. The presence of pyrrhotite in the DV_a vein of sample JR-5-G suggests that this occurred after DM_a. Except for garnet, none of the other minerals appear to be extensively altered.

General discussion of JR-5

The variation in the prominence of DM_a mineral growth from sample to sample at JR-5 is remarkable. There is

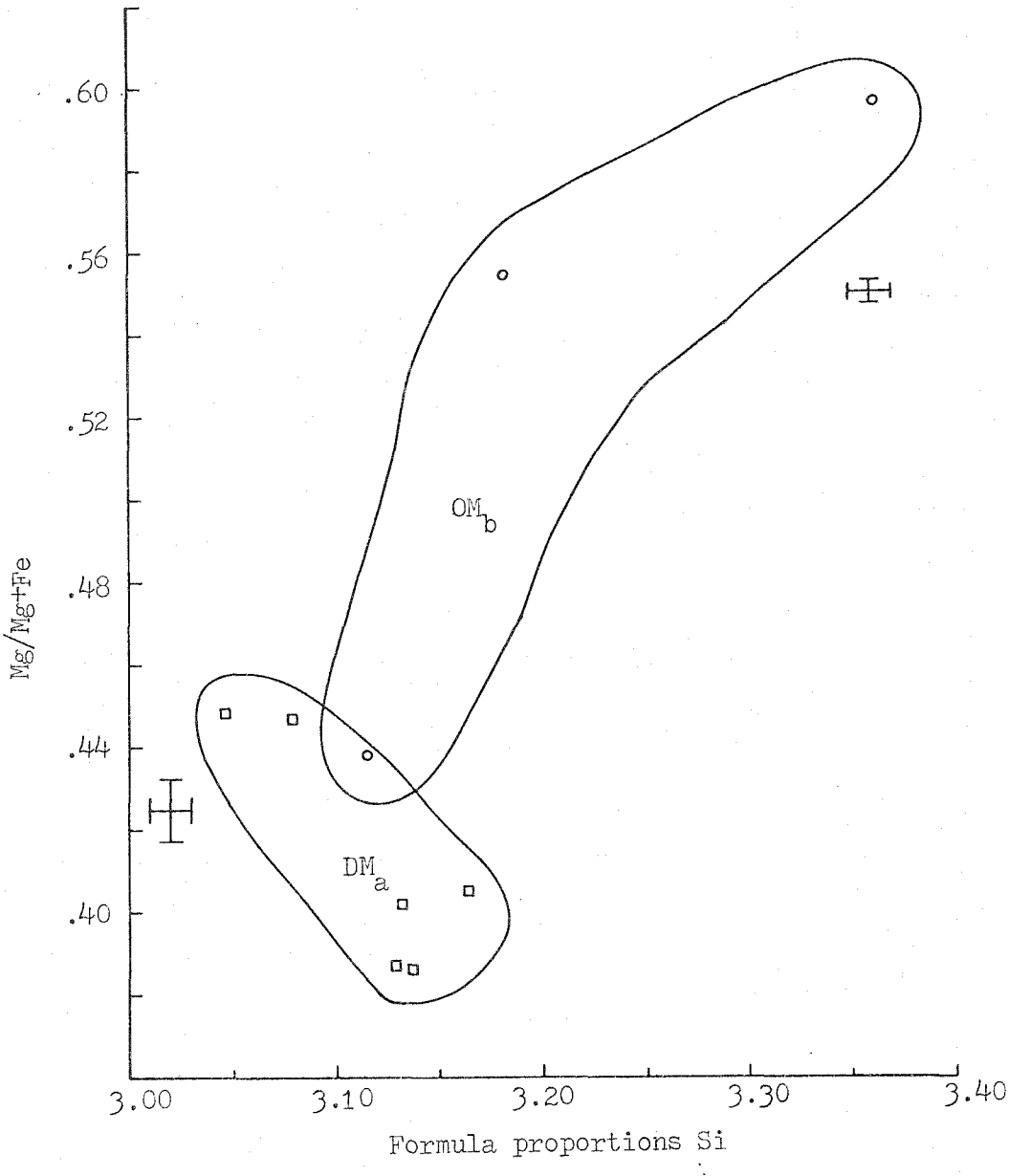

Figure 41 Plot of Si vs. Mg/Mg+Fe for muscovite in JR-5-I.

essentially no evidence of DM_a in JR-5-A, but DM_a is dominant in JR-5-D and JR-5-I. The only clear difference between these samples is the degree to which DS_a slip cleavage is developed. Apparently the strong mechanical action involved in the formation of the DF_a microfolds and DS_a slip cleavage greatly enhances the process of recrystallization during DM_a growth. The variation in DM_a prominence within a single outcrop is somewhat disturbing because it indicates that the relationships observed at a location can strongly depend upon the positions of the samples taken.

The presence of at least three generations of mineral growth at JR-5 is documented by the presence of the three generations of metamorphic veins, OV_a, OV_b, and DV_a. The mineral growth generation OM_a is really more of a structural entity than a mineral growth entity because it has been strongly overprinted by OM_b and DM_a. The structural aspect of OM_a is preserved as OV_a veins and OS_a schistosity at the noses of OF_b folds. OM_b and DM_a are the two dominant mineral growth generations at JR-5. OM_b mineral growth was garnet grade at the peak of metamorphism and DM_a mineral growth was biotite grade, as evidenced by the retrograde of OM_b garnet. Plagioclase with compositions in the range from oligoclase to andesine was produced during both mineral growth events.

There is also evidence of late alteration of vein plagioclase, host and vein pyrrhotite, and possibly minor alteration of OM_b garnet. This alteration must be either post-DM_a or very late DM_a. Because of the presence of DM_c growth at the next location to be discussed, JR-163, the late alteration is interpreted as probably being DM_c.

Location JR-163

Location JR-163 is about 1.5 miles west of location JR-5 and is an outcrop of the Underhill formation. The structural elements present at JR-5 are also present at JR-163 and are similar in character. In addition, there are other elements present at JR-163. OV_a veins and OS_a schistosity are folded by isoclinal OF_b folds. Parallel to the axial planes of OF_b are OV_b veins and OS_b schistosity. These are in turn folded by asymmetric DF_a folds and cut by DS_a slip cleavage and DV_a veins. Unlike the relationships at JR-5, DS_a and DV_a are clearly folded by open, gentle DF_b folds. The DF_b folds and all the older structures are crosscut by a discontinuous vein which is related to low grade mineral growth in the host rock and which is interpreted to be DV_c. The DV_c vein is gently warped by north-south trending folds, DF_d.

The effects of strong DM_c growth seem to be restricted

to the vein and the host rock immediately adjacent to the vein. This establishes a fourth generation of vein and host rock mineral growth in addition to the three generations already documented: OM_a, OM_b, and DM_a. These generations are also present at JR-163, but only one sample, from the DV_c vein and adjacent host, has been studied with the microprobe. DV_c veins are fairly rare in this part of northern Vermont. Another vein has been observed at location JR-76, which is close to JR-5. A DV_c vein from location JR-66 has already been described. DV_c veins are abundant in northeastern Vermont where DM_c mineral growth is higher grade.

The highest grade mineral growth at JR-163 appears to be OM_b in generation. OM_b assemblages include quartz-muscovite-garnet-chlorite-biotite-peristerite (albite + oligoclase in concentric growth relationship). DM_a assemblages include biotite, chlorite, and peristerite, but no garnet. Garnet seems to have been retrograded during DM_a growth. OM_a is again strongly overprinted, but probably included albite, chlorite, and biotite.

The DV_c vein is on the average about 1 centimeter wide and 6 meters long. The vein assemblage is albite-chlorite-apatite-rutile. More than 90% of the vein is albite. Some chlorite growth in the vein occurs at the host rock

wall, but no well-developed vein borders occur. Chlorite grains are found throughout the vein and tend to be in accordian-like books with no preferred orientation.

The host rock adjacent to the DV_c vein in the sample, JR-163-D, has the assemblage quartz-muscovite-chlorite-plagioclase-epidote-tourmaline-ilmenite-rutile-hematite-magnetite-zircon. Within 2 centimeters of the vein there is abundant evidence of overprint of chlorite and plagioclase. Host rock chlorite grains are optically zoned. The cores are optically negative and have an anomalous brown interference color. The rims are optically positive and have an anomalous purple interference color. The cores are most prominent in large grains and grains which are relatively isolated as inclsions in plagioclase or quartz. The host rock plagioclase has the typical optical zoning seen in zoned OM_b and DM_a grains, but superimposed on this is a mottled texture often observed where overprint has occurred.

The other reaction or overprint relationships in the host rock involve magnetite and hematite. Hematite appears to be replacing magnetite; this is seen in several host rock samples from this location. There are grains of hematite alone in a DV_a sample, so the hematite may be DM_a in generation. Ilmenite grains are partially replaced by rutile. This appears to be largely confined to the 2 centimeter wide zone around the DV_c vein and there is rutile in the

DV_c vein. The alteration of ilmenite to rutile may be DM_c. The overprint texture in the host plagioclase grains is strongest within the 2 centimeter wide band and this is therefore probably DM_c.

Compositions of plagioclase in the DV_c vein of JR-163-D are shown in Figure 42a. Grains with the most extensive zoning have core compositions of $An_{1.5}$ to $An_{2.0}$; from core to rim the An content increases to $An_{4.7}$; then there is a reversal and the An content decreases to $An_{2.0}$. There is some minor variation in the Fe content of the analyzed grains, but this variation does not seem to be systematic. Two grains which preserve the same zoning with respect to An content do not preserve the same zoning with respect to Fe.

Compositional variation in plagioclase in the host rock is much more complicated. Compositions of host rock plagioclase are shown in Figure 42b. The compositions have been divided into four groups based upon textural relationships. Equant plagioclase grains with concentric zoning, Group I, are zoned from $An_{13.5}$ in the cores to $An_{21.0}$-$An_{23.2}$ near, but not at, the rims. In one grain there is a zoning reversal or overgrowth that is zoned from $An_{19.3}$ to $An_{14.6}$ and this is shown as Group II. Both groups of oligoclase are overgrown by albite rims, Group III, which have zoning

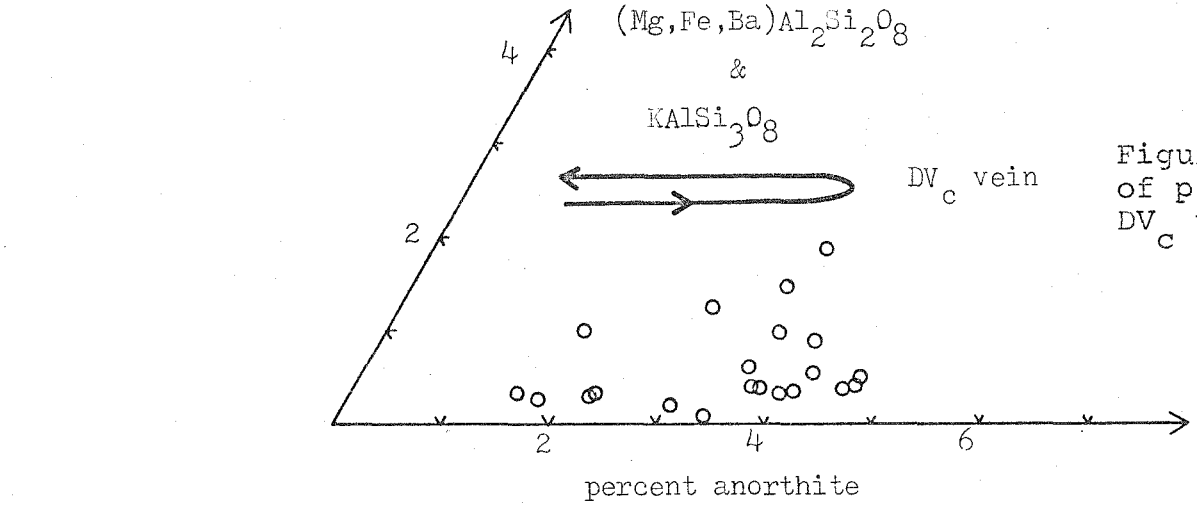

Figure 42a Compositions of plagioclase in the DV_c vein of JR-163-D.

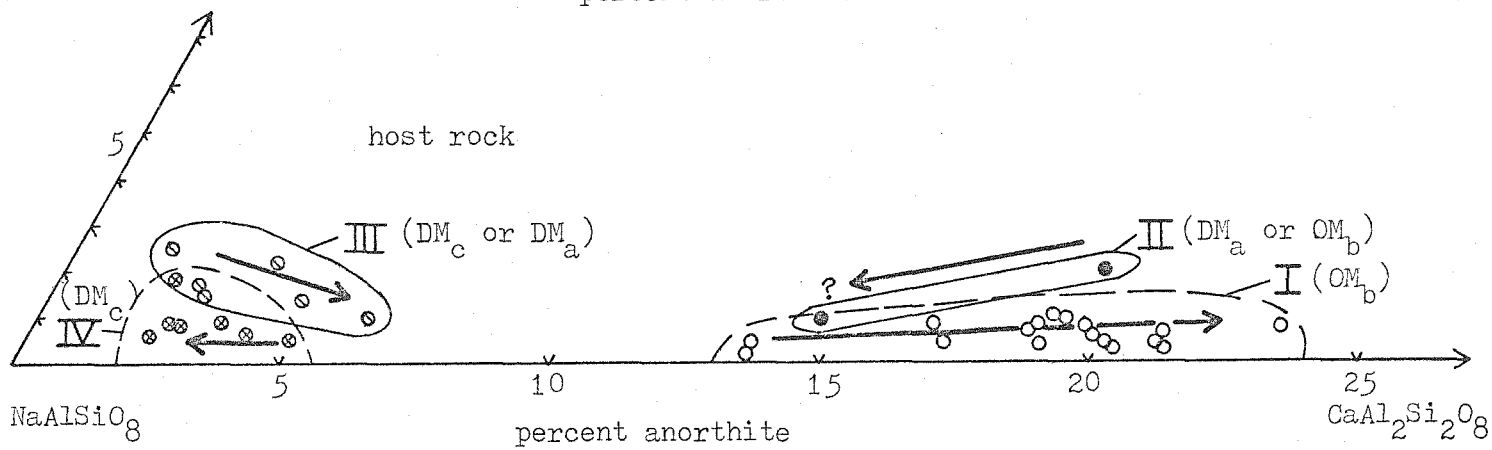

Figure 42b Compositions of plagioclase in the host rock of JR-163-D.

from $An_{1.8}$ to $An_{6.2}$ at the outer rim. One grain of albite alone was analyzed and this was zoned from $An_{5.0}$ in the core to $An_{2.2}$ at the rim. This is shown as Group IV. The albite grain is associated with chlorite which appears to be DM_c and is adjacent to the vein. The different generations of plagioclase are difficult to unambiguously determine, but an interpretation can be made based upon observations of the samples of OV_b and DV_a veins at this outcrop. The oligoclase cores, Group I, are probably OM_b growth. The reverse-zoned oligoclase, Group II, may be late OM_b of DM_a. The albite rims, Group III, may be DM_a or DM_c. The single albite grain is probably DM_c.

Figure 43a is a plot of Mg/Mg+Fe vs. Al for chlorite in the host rock and DV_c vein of JR-163-D. There is a very large compositional range of chlorite in this sample. Grains in the host rock which are optically zoned under crossed nicols are strongly zoned with respect to Mg/Mg+Fe. These grains have strongly decreasing Mg/Mg+Fe from core to rim. The change in optic sign occurs roughly at Mg/Mg+Fe = 0.45. Chlorite in the DV_c vein has a smaller range of Mg/Mg+Fe values and this range overlaps with the range of compositions of host rock grain rims. Optically unzoned chlorite grains in the host rock next to the vein have compositions similar to DV_c vein chlorite. It appears that DM_c

Figure 43a Plot of Al vs. Mg/Mg+Fe for chlorite in host rock and DV_c vein of JR-163-D.

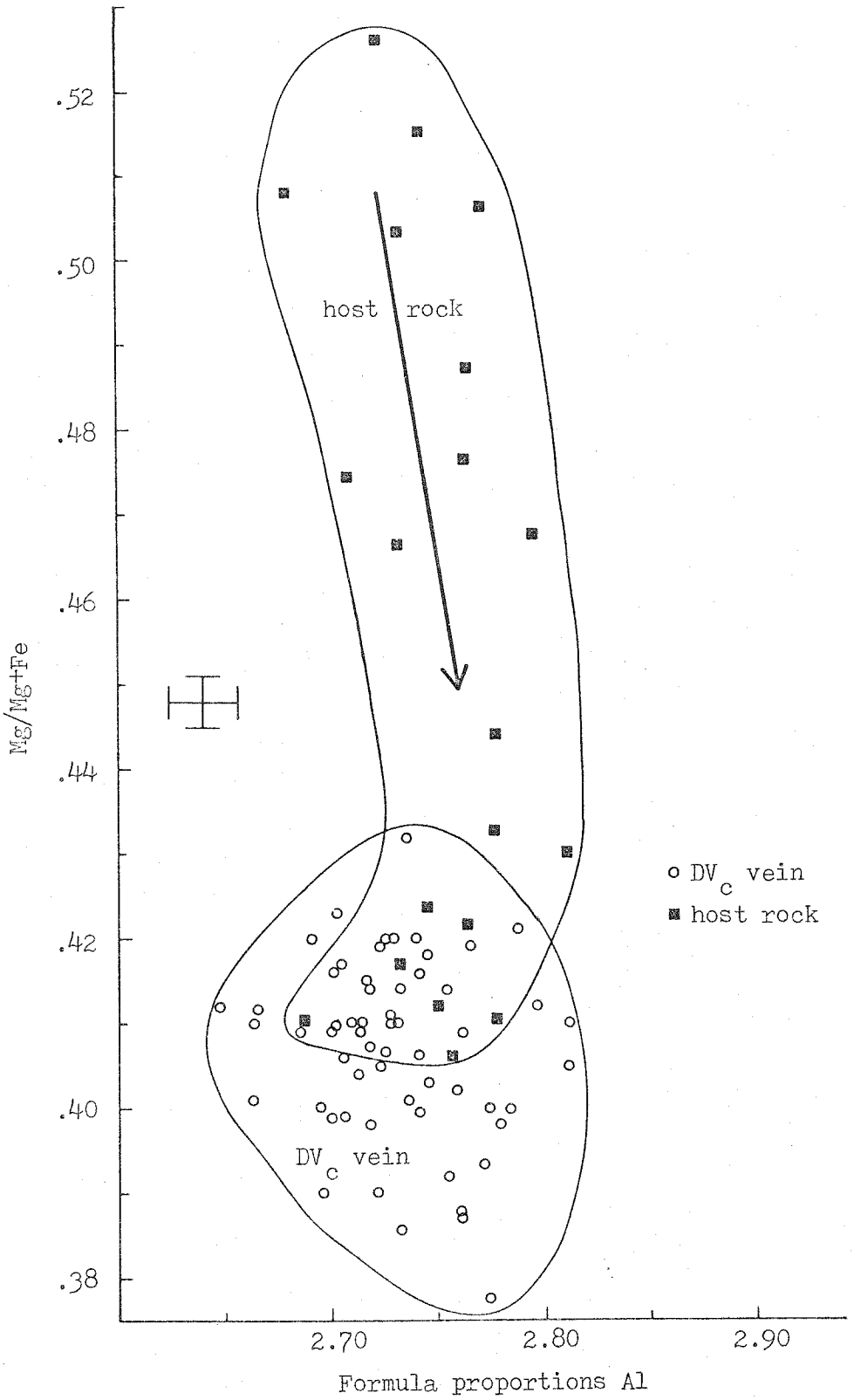
.52
.50
.48
.46
.44
.42
.40
.38
Mg/Mg+Fe
host rock
DV c vein
2.70
2.80
2.90
Formula proportions Al
o DV c vein
host rock

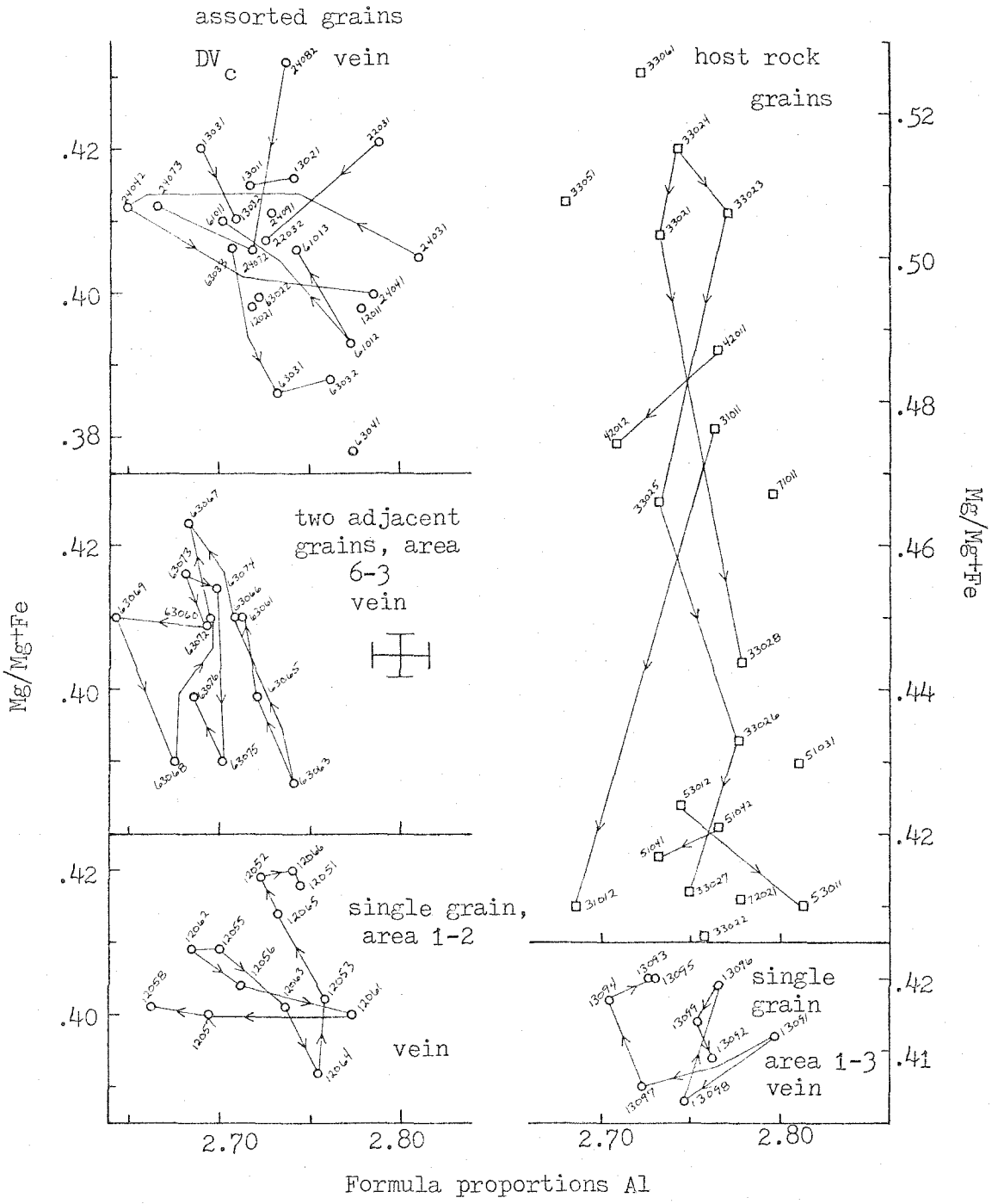

Figure 43b Plots of Al vs. Mg/Mg+Fe for chlorite grains in various areas of JR-163-D.

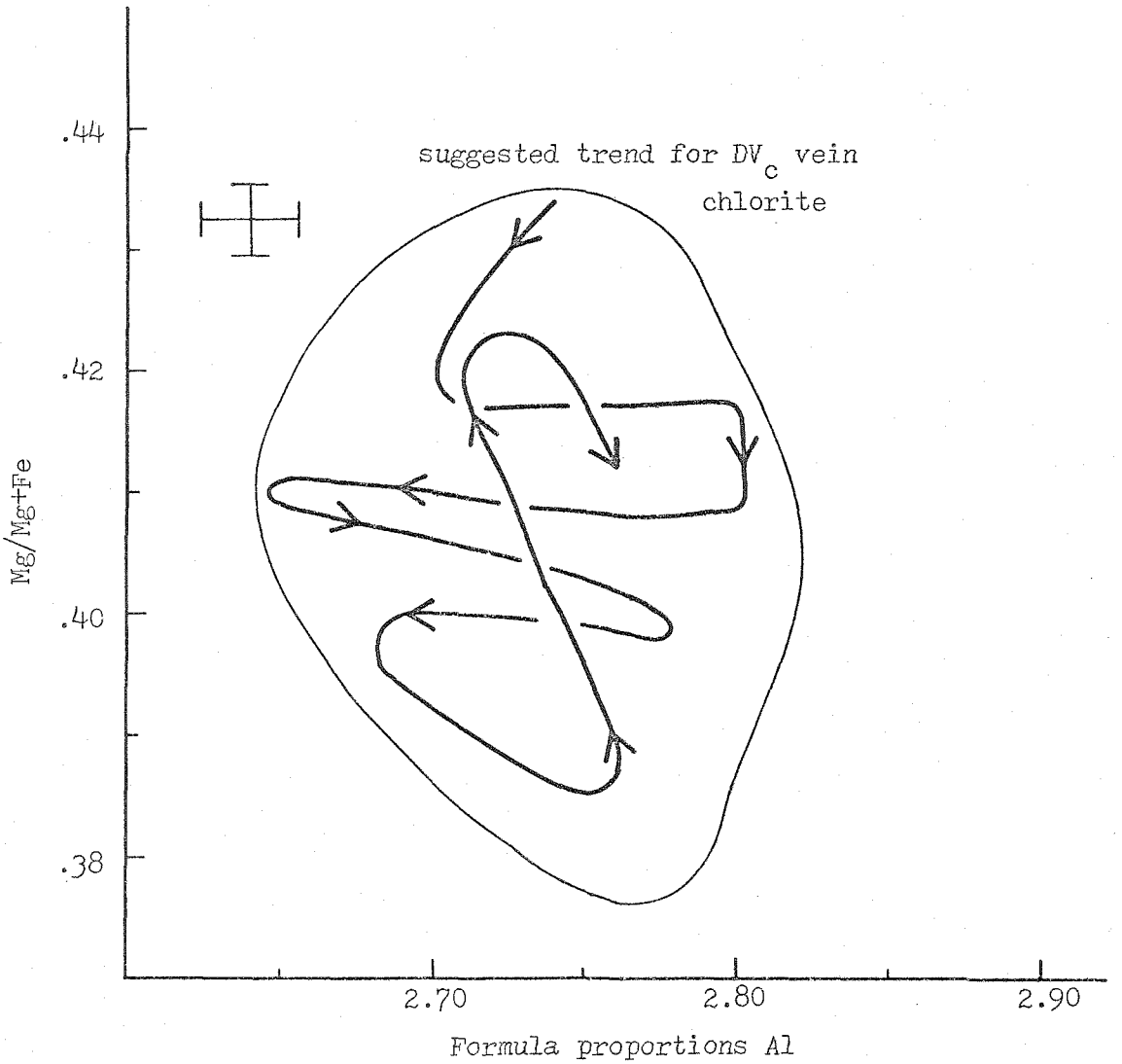

Figure 43c Suggested compositional trend for DV$_c$ vein chlorite in JR-163-D.

chlorite growth in the host rock has strongly overprinted pre-existing chlorite. The pre-existing chlorite has preferred orientation parallel to OS_a/OS_b and is included in OM_b plagioclase; it is therefore probably OM_b chlorite. The entire host rock chlorite compositional range can be observed in single zoned grains on the scale of 20-30 microns. The zoning is compatible with reconstitution of the OM_b chlorite by diffusion in the solid state, as the zoning pattern consists of compositions intermediate between host rock chlorite cores and DM_c chlorite. Strict growth zoning preserved within grains cannot be ruled out, however.

DV_c chlorite grains have very complicated zoning that probably is a primary growth feature. The zoning in vein and host rock chlorite grains is shown in Figure 43b. A very complicated trend that could account for the zoning observed in every DV_c vein chlorite grain is shown in Figure 43c. This is only a suggested trend; each of the zoning patterns in 43b might be confined to local domains in the thin section. Whether the DV_c vein chlorite has a single systematic compositional variation trend remains an open question.

In the host rock, optically zoned chlorite grains are prominent only within 2 centimeters of the DV_c vein and

beyond this the grains are generally unzoned. It is not clear why the strong DM_c effects are limited to this band. The DV_c vein is discontinuous in outcrop and could not have brought in material from outside the system. It may be that conditions in the vicinity of the forming vein were favorable in a kinetic sense for the DM_c recrystallization in the host rock.

There is evidence of limited DM_c overprint of muscovite in the host rock adjacent to the DV_c vein. Apparent remnant cores of medium-grained muscovite are surrounded by very fine-grained muscovite which has no preferred orientation. The unaffected muscovite grains have preferred orientations parallel to OS_a/OS_b and this schistosity is folded by DF_a microfolds. Therefore the unaltered muscovite is probably OM_b. There does not appear to be any growth of muscovite in the DV_c vein. Figure 44 shows the compositions of analyzed muscovite in the host rock. The OM_b muscovite has a consistent compositional trend from core to rim of decreasing Si and Mg/Mg+Fe. Two points from the very fine-grained muscovite, probably DM_c, are also shown.

There is not as much evidence about the timing of DM_c growth in host and vein as there is for the OV_b and DV_a veins at JR-5. The limited zoning in the DV_c vein albite suggests that growth occurred during initially increasing

Figure 44 Plot of Si vs. Mg/Mg+Fe for muscovite in host rock of JR-163-D.

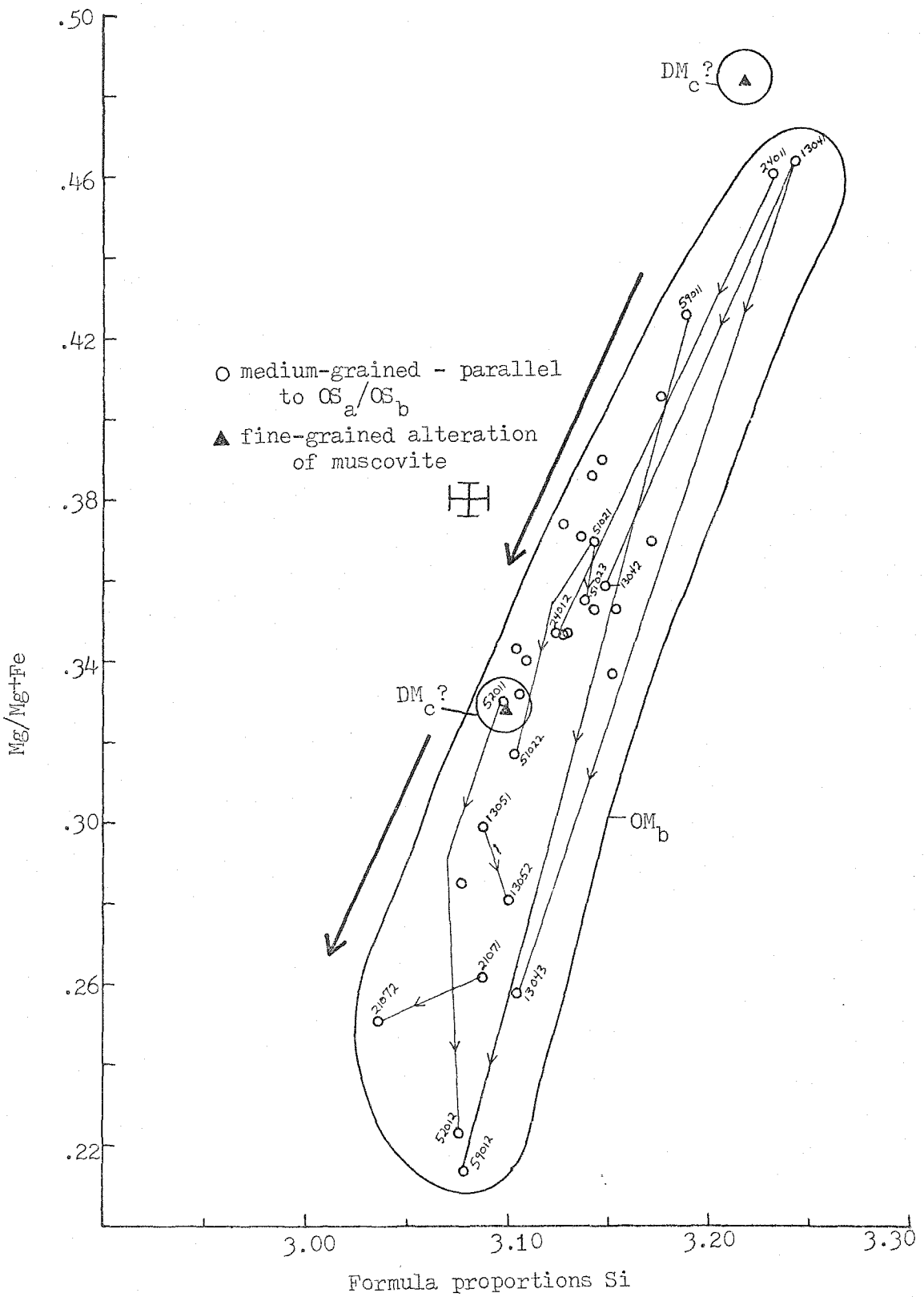
.50
.46
.42
.38
.34
.30
.26
.22
Mg/Mg+Fe
3.00
3.10
3.20
3.30
Formula proportions Si
DM c ?
DM c ?
OM b
o medium-grained - parallel to OS a/OS b
▲ fine-grained alteration of muscovite
2N011
13041
5P011
5I021
5I013
13042
5I012
5I011
5I012
13051
13052
21071
21072
13043
5J012
5P012

grade and then continued as the grade decreased from the "peak." This is perhaps using the plagioclase zoning beyond its reliability. Host albite grains, probably DM_c, are zoned with decreasing An content from core to rim. This corresponds to the latter part of the DV_c vein albite compositional trend. There may also be DM_c albite in the host rock which corresponds to the earlier part of the DV_c vein albite trend of increasing An content. In any event, evidence from the albite and also from the chlorite suggests that vein growth was occurring over the entire span of time in which DM_c growth in the host rock was occurring. This timing of vein and host growth is different than that observed for DV_a and OV_b veins at JR-5.

Although the strong effects of DM_c growth in the host rock seem to be confined to a narrow band around the DV_c vein, there is textural evidence of limited DM_c growth in other samples. Zoned chlorite similar to that just described and fine-grained alteration of muscovite can be observed but are not abundant. Much of the alteration of minerals in DV_a veins and other samples is probably DM_c. This includes perhaps the alteration of pyrrhotite to pyrite which is observed in DV_a veins, OV_b veins, and in the host rock.

Location JR-4

Location JR-4 is about 0.3 miles east of location JR-5. The structural elements described at JR-5 are also present at JR-4. This outcrop is the easternmost exposure along this traverse segment in which DS_a is not predominantly parallel to OS_a/OS_b. This structural transition coincides with the garnet isograd as mapped by Christman and Secor (1961). The mapped isograd defines the limits of good preservation of OM_b garnet rather than the limit of growth of garnet. Small amounts of garnet are preserved in samples from locations to the east of JR-4.

Three samples from JR-4 have been analyzed with the electron microprobe:

JR-4-M host schist 1 meter from nearest vein

JR-4-P DV_a vein and adjacent schist

JR-4-R OV_b vein and adjacent schist

The DV_a vein from which JR-4-P is taken is a relatively undeformed lense-shaped vein that is 20 centimeters in maximum width and 1.3 meters long. It has been very gently flexed by DF_b folds. JR-4-R is from a 15 centimeter wide OV_b vein that is folded by DF_a folds and pinches out due to this deformation; its present length of about 1 meter is much less than the original, predeformation length.

JR-4-R

The assemblage in the host rock adjacent to the OV_b vein in JR-4-R is quartz-muscovite-chlorite-plagioclase-epidote-calcite-apatite-ilmenite-sphene-zircon. Within the OV_b vein is quartz-muscovite-chlorite-plagioclase-calcite-zircon. The zircon in the vein is in a partly recrystallized host rock inclusion. Zircon which appears to have been formed by primary vein mineral growth is only found in veins within zircon-rich metagreywacke host rock. There is limited, irregular development of a border zone in JR-4-R. The border zone minerals are plagioclase, muscovite, and chlorite.

Figure 45 shows the compositions of analyzed plagioclase in the OV_b vein and host rock. Host rock plagioclase appears optically to be unzoned. All of the analyzed host rock plagioclase is albite with less than 1.5% anorthite component. In contrast, OV_b vein plagioclase is strongly zoned from albite cores to oligoclase rims. Within the zoned grains is a sharp optical break between albite and oligoclase. As in samples previously discussed, this optical and chemical discontinuity which is preserved within single grains seems to represent the peristerite gap. In one grain in the vein there is a reversal in trend from $An_{13.5}$ near the rim to $An_{10.8}$ at the rim. Except for this

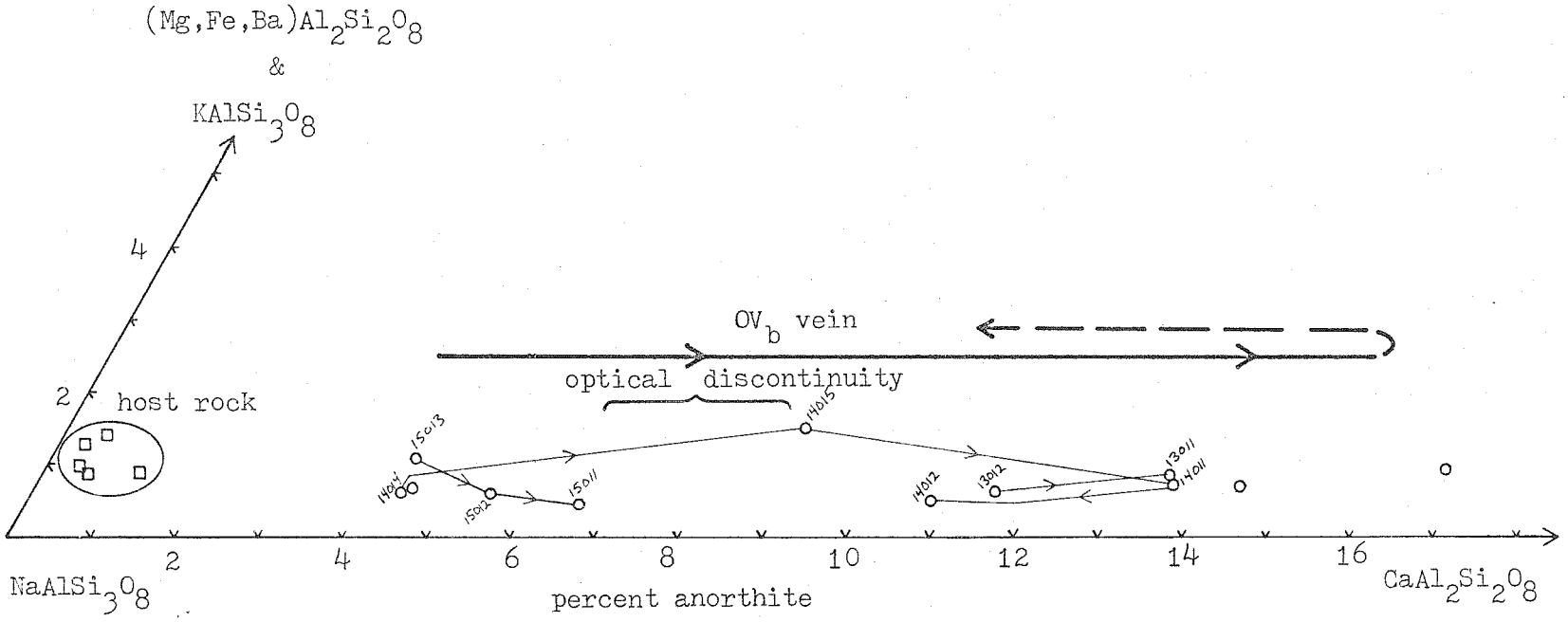

Figure 45 Compositions of plagioclase in host rock and OV_b vein of JR-4-R.

reversal, the compositional trend in this OV_b vein plagioclase is exactly opposite of that observed in sample JR-5-A; this suggests a difference in the timing of the initiation of OV_b formation. There does not seem to be any plagioclase in the host that corresponds to the vein plagioclase. The vein plagioclase trend indicates growth during increasing grade and then perhaps late growth during decreasing grade. At JR-5 the OM_b growth with increasing grade occurred only in the host rock. In the OV_b vein at JR-5 there was down-grade growth of plagioclase, but no such growth in the host rock. It appears that most OM_b growth of plagioclase in JR-4-R occurred in the vein. The albite in the host rock appears to be early OM_b or OM_a.

The compositions of analyzed chlorite from the host rock and vein are shown on a plot of Al vs. Mg/Mg+Fe in Figure 46a. The points are divided into three groups: host rock matrix, included grains in host rock albite, and OV_b vein chlorite. The groups are shown separately in Figures 46b, 46c, and 46d. Suggested general trends for host rock matrix chlorite and OV_b vein chlorite are shown.

In this sample, OS_a/OS_b is significantly deformed by DF_d microfolds. DS_a slip cleavage is developed due to rotation of pre-existing grains on the short limbs of microfolds. In other samples previously described in which DS_a

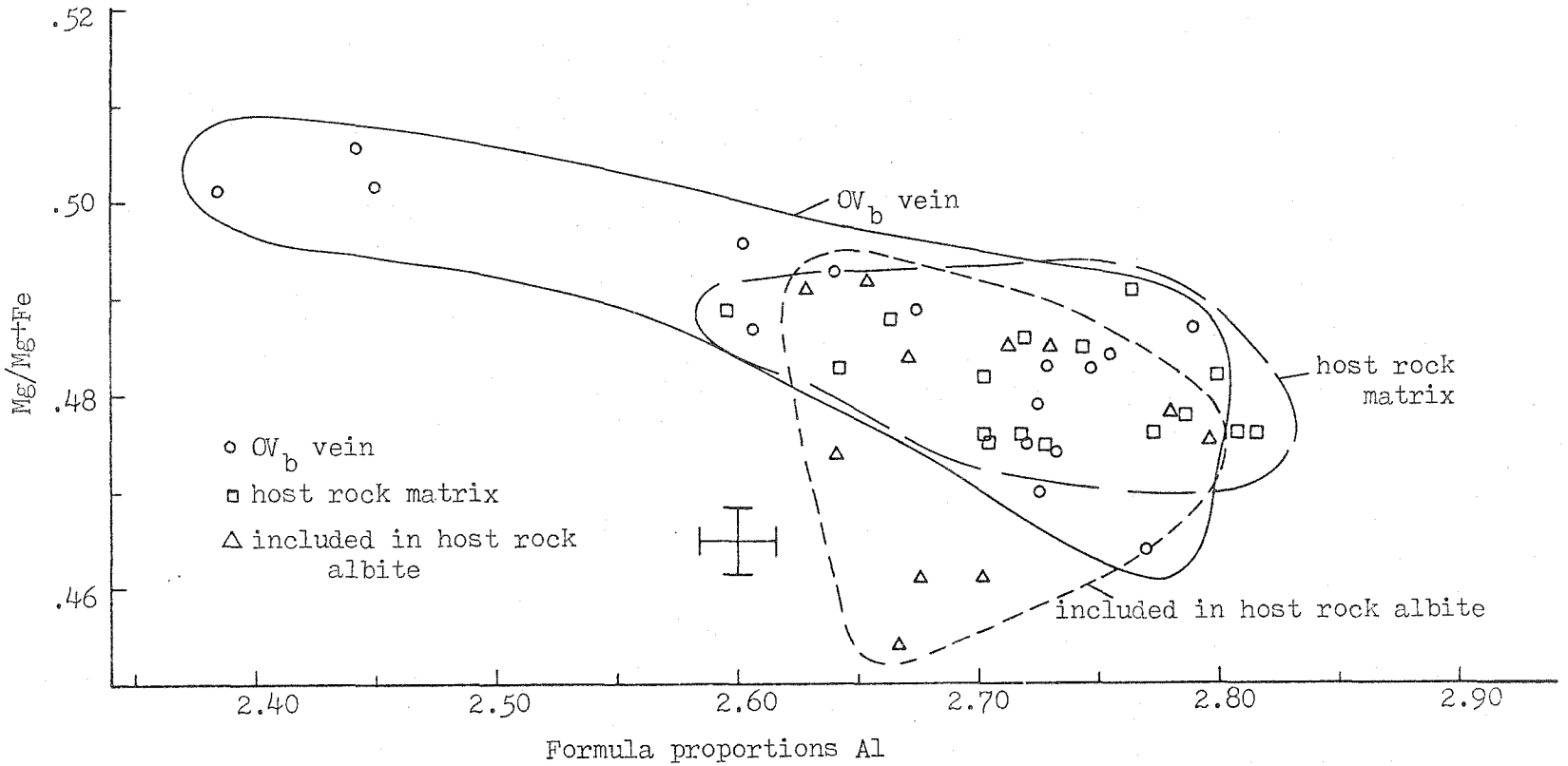

Figure 46a Plot of Al vs. Mg/Mg+Fe for chlorite in host rock and OV$_b$ vein of JR-4-R.

Figure 46b Plot of Al vs. Mg/Mg+Fe for chlorite included in host rock albite in JR-4-R.

Figure 46c Plot of Al vs. Mg/Mg+Fe for chlorite in host rock matrix of JR-4-R.

Figure 46d Plot of Al vs. Mg/Mg+Fe for chlorite in OV_b vein of JR-4-R.

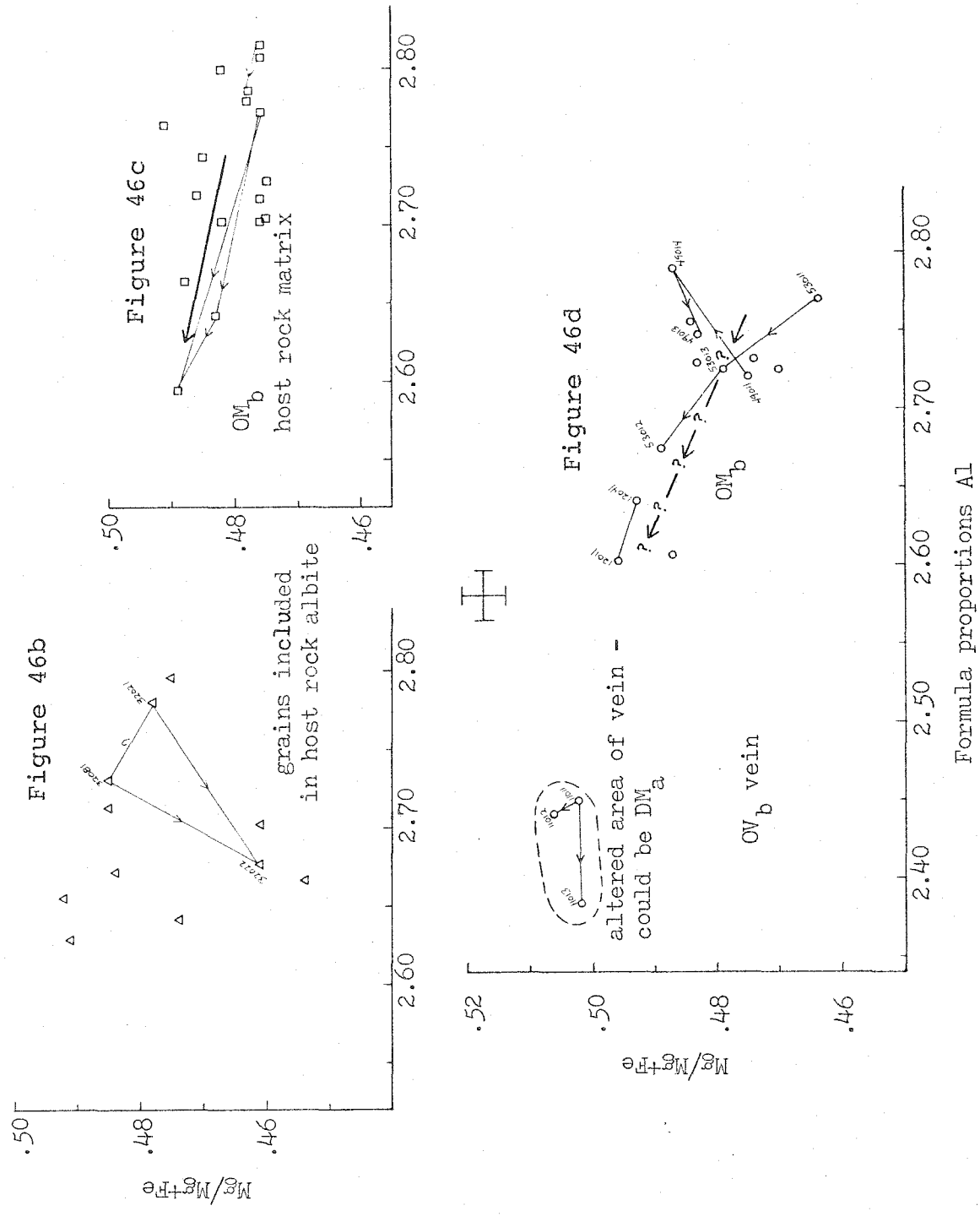
Figure 46b
grains included
in host rock albite
Figure 46c
OM$_b$
host rock matrix
Figure 46d
altered area of vein -
could be DM$_a$
OW$_b$ vein
OM$_b$
Mg/Mg+Fe
Formula proportions Al
.50
.48
.46
.52
2.40
2.50
2.60
2.70
2.80

was well developed, there was chemical evidence of DS_a growth. Although there does not appear to be any primary growth of DM_a chlorite or muscovite parallel to DS_a in JR-4-R, some DM_a chlorite growth might be expected.

Grains which are most likely to preserve OM_b chlorite compositions are those in the OV_b vein which are within coarse-grained quartz. Most of the analyses shown in Figure 46d are from such grains. Three OV_b vein chlorite analyses have significantly less Al than the others. They are from a grain in altered plagioclase and are less likely to preserve OM_b compositions; these might be DM_a. The other analyses are probably OM_b.

The compositional range and possible compositional variation trend of host rock matrix chlorite are essentially the same as those for OV_b vein chlorite as shown in Figure 46c and 46d. This strongly suggests that the matrix grains are also OM_b. These grains are parallel to OS_a/OS_b, but are clearly deformed by DF_a microfolds. It may be that the deformation occurred without any significant change to the OM_b compositions. Of course, it is possible that DM_a recrystallization occurred and that DM_a compositions are similar to OM_b compositions.

The compositional range of chlorite included in host rock albite grains is only partly coincident with the range

of the other two groups. The trend of this group has not been defined, but it appears that it must be different from the other two trends. The albite that encloses this chlorite does not correspond to plagioclase in the OV_b vein. It is to be expected that the included chlorite would not correspond to the vein chlorite as well. However, because of the great amount of overlap of all three groups, it is difficult to sort out the exact relationships.

There is no chemical evidence that establishes that there was any significant DM_a chlorite growth, but DM_a growth cannot be ruled out. It appears that chlorite in the host rock matrix corresponds to the OV_b vein chlorite and that both are OM_b. Evidence from the plagioclase in the vein and host rock suggests that during vein formation OM_b plagioclase grew only in the vein. It looks as if OM_b chlorite grew in the vein and in the host rock at the same time. The chlorite included in the host rock albite should be the oldest chlorite in the sample. The albite is probably pre-OV_b, so that the included chlorite is also pre-OV_b. This chlorite must then be either OM_a and/or early OM_b.

There is some significant alteration of plagioclase in the OV_b vein. This type of alteration, mostly sericitization, is also observed in the DV_a sample. The alteration may be DM_c in both, or the alteration in the OV_b vein may

be a combination of DM_a and DM_c.

JR-4-P

Present at JR-4 are DV_a veins which are very similar to the DV_a veins at JR-5. JR-4-P is from one of these veins and a limited amount of microprobe data have been obtained from this sample. The DV_a vein has the assemblage quartz-muscovite-chlorite-biotite-plagioclase-calcite. The adjacent host rock is quartz-muscovite-chlorite-biotite-garnet-plagioclase-epidote-calcite-apatite-ilmenite-tourmaline-zircon. Garnet is only seen as included grains in plagioclase. Chlorite is present in the host rock matrix and as inclusions in plagioclase. Biotite is abundant in the host rock matrix but rarely occurs as included grains in plagioclase.

Host rock plagioclase in JR-4-P optically appears to be unzoned. Two analyzed points are nearly pure albite ($An_{0.2}$ and $An_{0.6}$). This is probably OM_a or OM_b. DV_a vein plagioclase is optically and chemically zoned. Compositions of points from two vein plagioclase grains are shown in Figure 47. One of these grains has two closed optical and chemical discontinuities, representing the peristerite gap, preserved within it. This grain is zoned from albite in the core, across a discontinuity to oligoclase at mid-

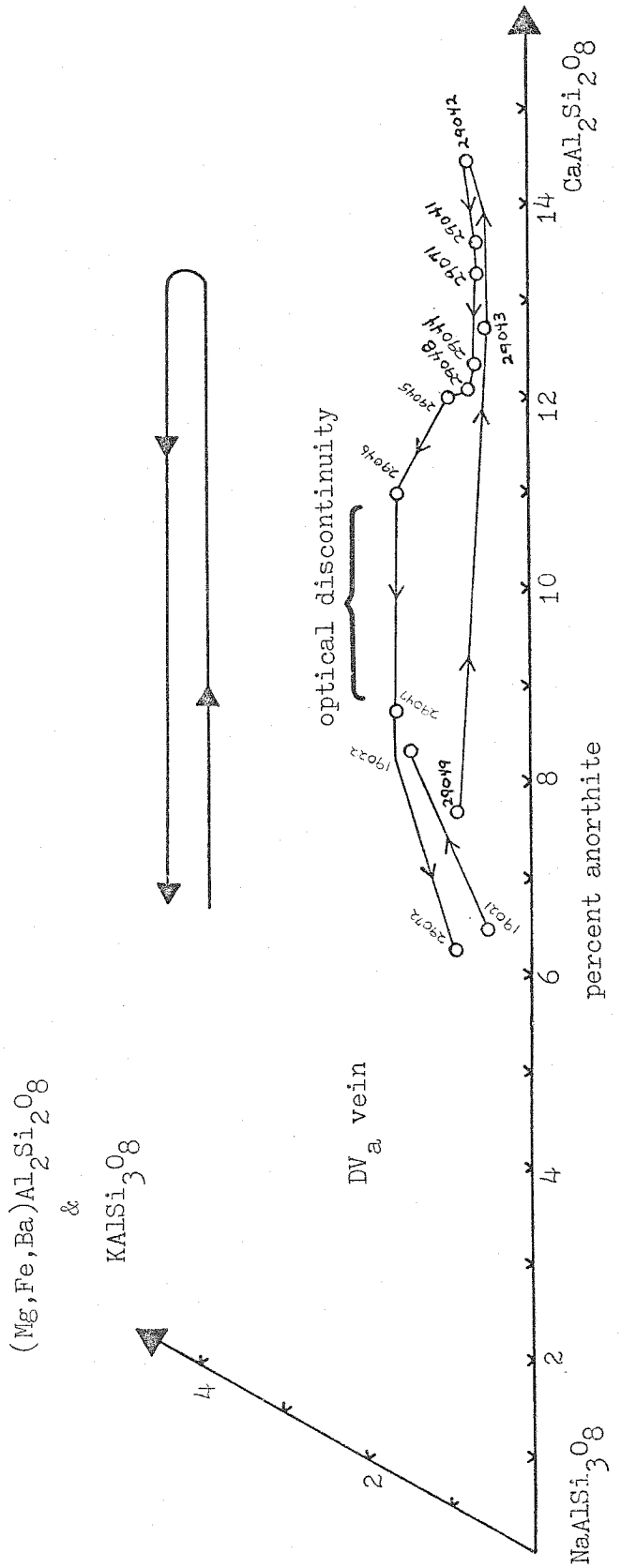

Figure 47 Compositions of plagioclase in DV_a vein of JR-4-P.

grain, and finally across another discontinuity to an albite rim. The zoning is concentric and seems to indicate a path of increasing grade, then decreasing grade. No corresponding plagioclase with optical zoning was observed in the host rock. The zoning and discontinuities in these vein plagioclase grains are more subtle than typically observed in peristerites. This may be due to the limited compositional range. There is no post-DM_a event displayed in this area which could have produced the observed zoning by overprinting DM_a plagioclase. The zoning must be a primary feature of DV_a vein growth.

Shown in Figure 48 is a plot of Al vs. Mg/Mg+Fe for analyzed chlorite in the host rock and DV_a vein. The host rock analyses come from one grain in the matrix, a grain included in the rim of an albite grain, and a grain included in the core of an albite grain. The matrix grain and the grain included in the albite rim have compositions very similar to DV_a vein chlorite. The grain in the albite core is much more Fe-rich than the others. The grain in the albite core is associated with included garnet; it is probably OM_b. The other host rock grains seem to be DM_a based on the similarity to vein chlorite. The evidence from the vein plagioclase suggests that the vein was forming throughout the growth of DM_a. Therefore, the host rock and vein

Figure 48 Plot of Al vs. Mg/Mg+Fe for chlorite in host rock and DV_a vein of JR-4-P.

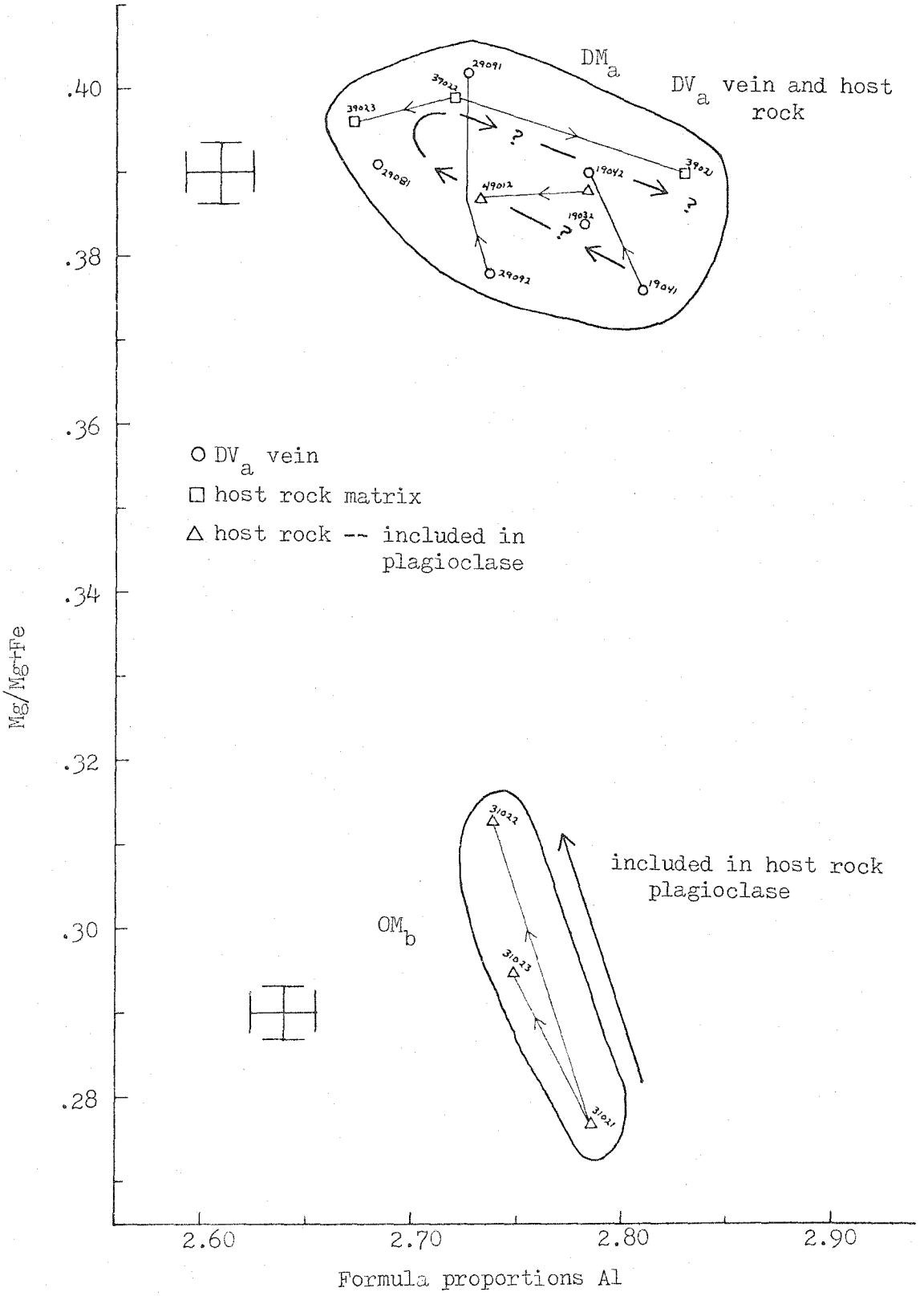
DM$_a$
DV$_a$ vein and host rock
O DV$_a$ vein
□ host rock matrix
△ host rock -- included in plagioclase
OM$_b$
included in host rock plagioclase
Mg/Mg+Fe
.40
.38
.36
.34
.32
.30
.28
2.60
2.70
2.80
2.90
Formula proportions Al

DM_a chlorite have been combined to define a very tentative trend.

Analyses from DV_a vein biotite are shown in Figures 49a and 49b. The points are from two grains and a compositional trend has been determined by the zoning in these grains. There are coincident reversals in these grains with respect to Al and Ti. Mg/Mg+Fe decreases somewhat from core to rim.

Figure 50 is a plot of Si v. Mg/Mg+Fe for DV_a vein muscovite. The general trend for the grains analyzed is increasing Si from core to rim, but there are not many analyses. The phengite substitution in the muscovite is buffered by the presence of quartz, biotite, and chlorite.

Chlorite, biotite, and muscovite compositions are shown on a plot of Si/Si+Al vs. Mg/Mg+Fe in Figure 51. The use of ratios eliminates most problems of normalization in comparing the different minerals. Chlorite and biotite seem to have opposite trends with respect to both Si/Si+Al and Mg/Mg+Fe. However, the apparent starting point for DM_a chlorite may not have formed at the time as the apparent starting point for biotite. Showing the correspondence in time between compositions of two minerals is always a problem. If this problem could be overcome, the data would be much more useful.

Figure 49a Plot of Al vs. Ti for biotite in DV_a vein of JR-4-P.

Figure 49b Plot of Al vs. Mg/Mg+Fe for biotite in DV_a vein of JR-4-P.

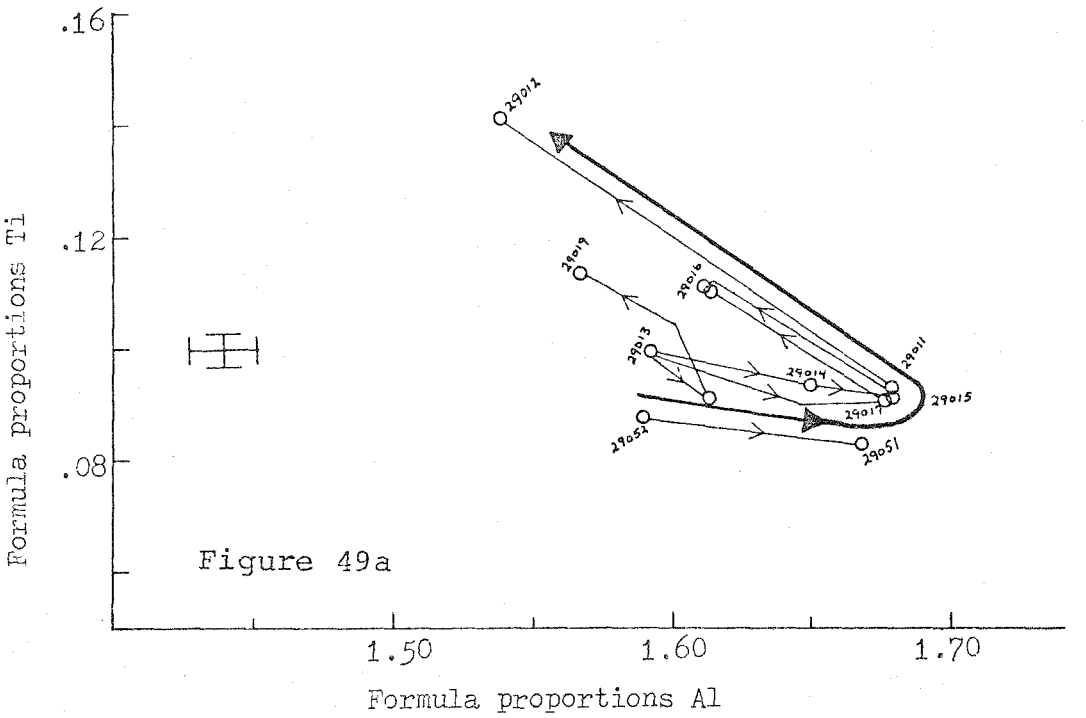

Figure 49a

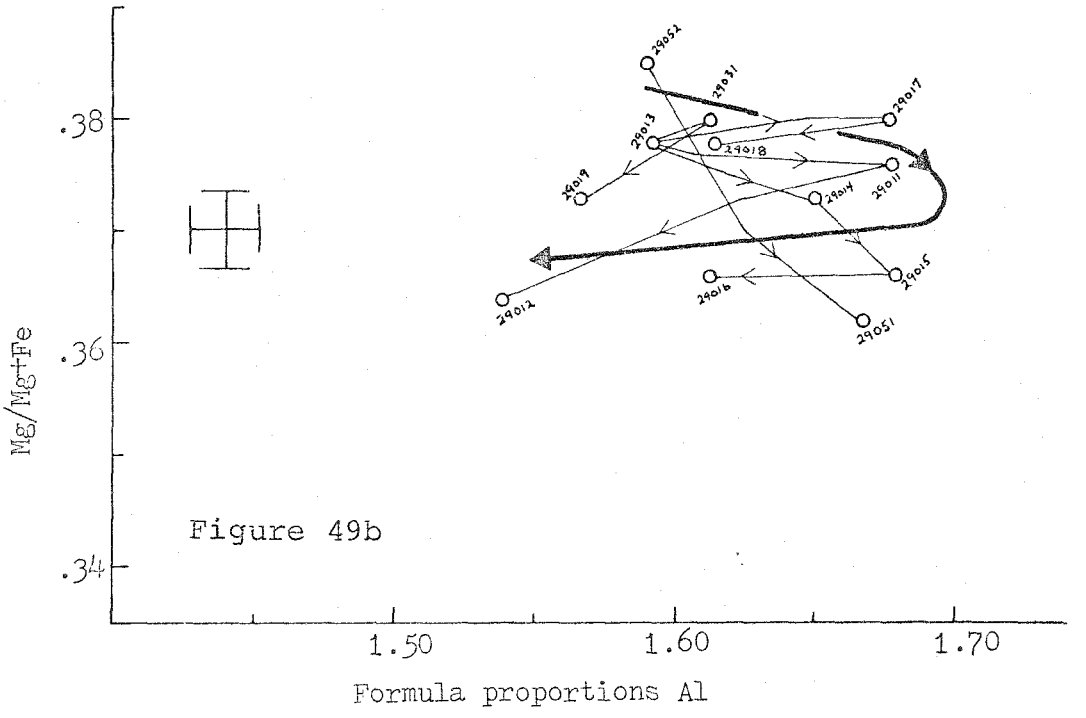

Figure 49b

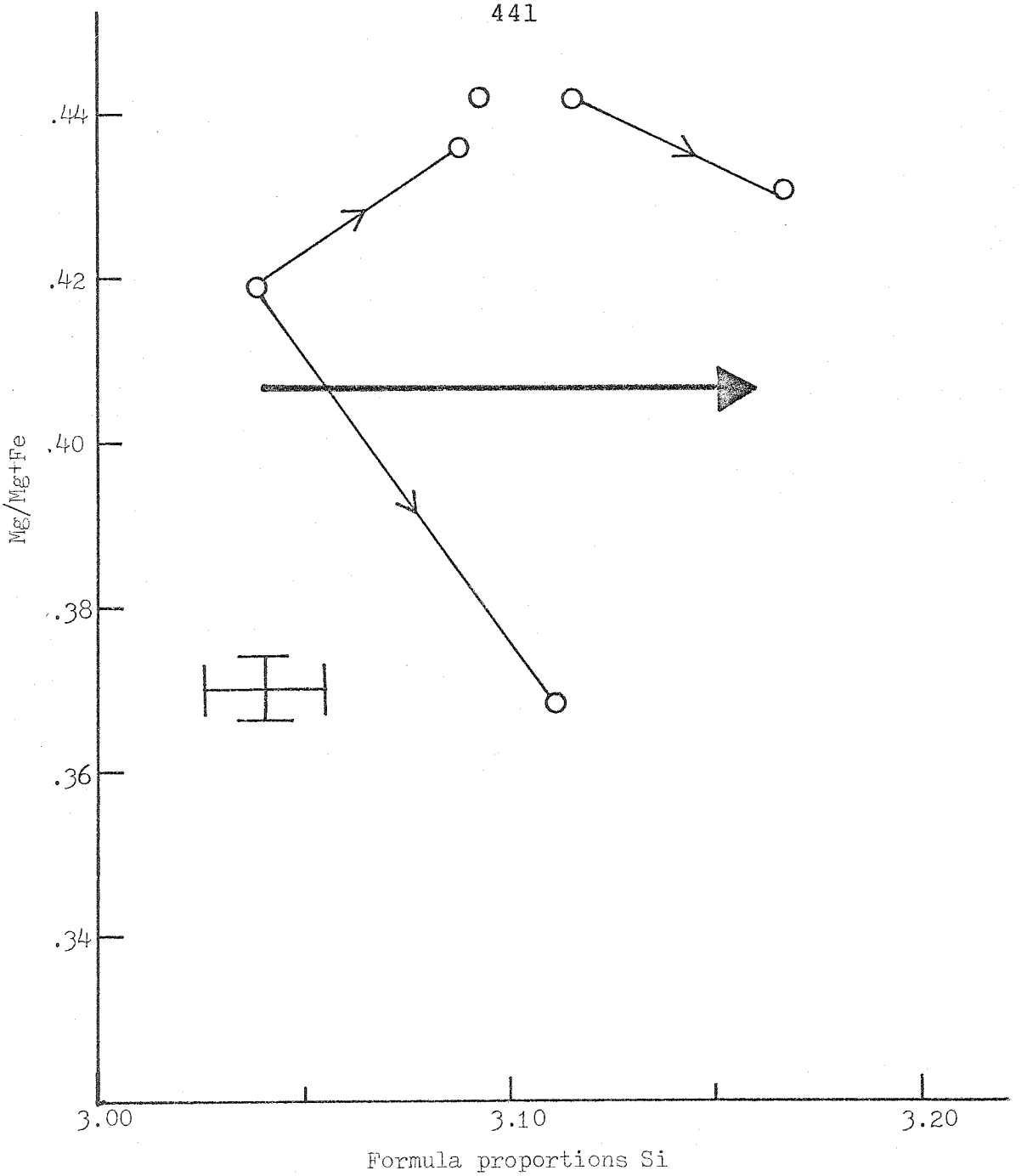

Figure 50 Plot of Si vs. Mg/Mg+Fe for muscovite in DV_a vein of JR-4-P.

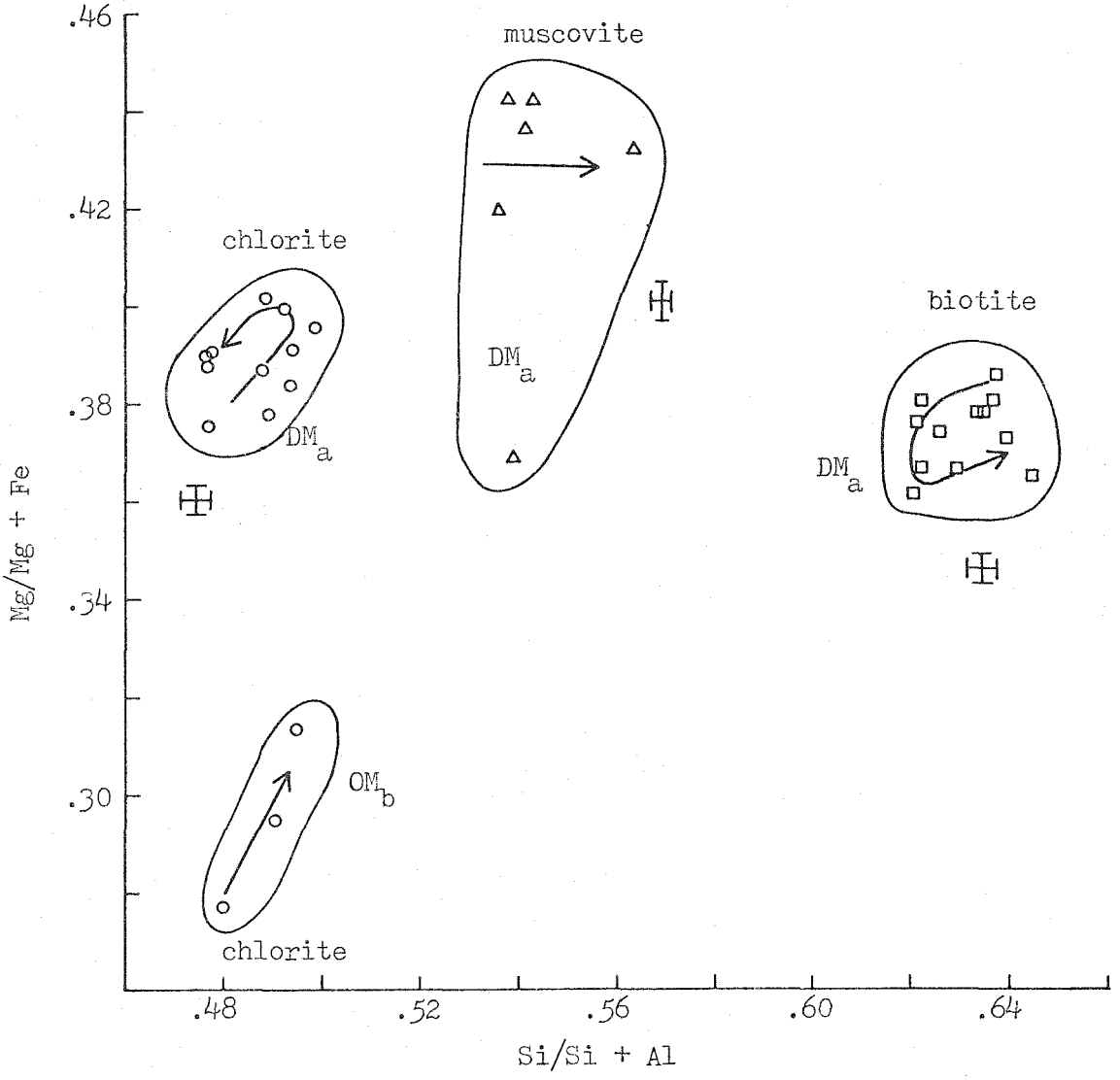

Figure 51 Plot of Si/Si+Al vs. Mg/Mg+Fe for chlorite, muscovite, and biotite in JR-4-P.

Plagioclase in the DV_a vein is partly altered to very fine-grained white mica. This is the only evidence of post-DM_a alteration in this sample. The alteration may be due to DM_c overprint.

JR-4-M

JR-4-M is a sample of schist 1 meter away from the nearest vein, a DV_a vein. DS_a slip cleavage is visible in hand sample, but not as noticeable in thin section. The rock is comprised of about 80% plagioclase and quartz. The assemblage is quartz-muscovite-chlorite-biotite-garnet-plagioclase-epidote-calcite-apatite-ilmenite-pyrite-chalcopyrite-sphene-tourmaline-zircon. Plagioclase is present as porphyroblasts 1-5 millimeters in diameter which have abundant inclusions of all of the other minerals. A typical plagioclase grain is shown in Figure 52.

Epidote-allanite grains are strongly zoned with respect to rare earth elements. Cores contain up to 12% by weight of combined Ce_2O_3, La_2O_3, and Nd_2O_3. Rims of such grains can have less than 1% total REE. This type of zoning in epidote is commonly observed in the pelitic schists of the Underhill and Hazens Notch formations. Epidote in this sample is not optically zoned, but in others there are distinct allanite cores and epidote rims. The presence of

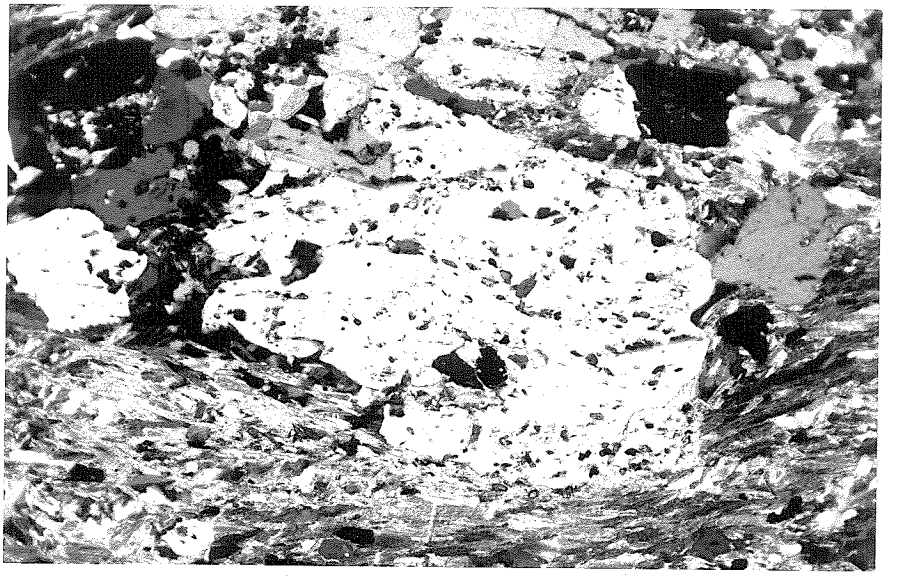

Figure 52a Plagioclase porphyroblast in JR-4-M. Included minerals are quartz, chlorite, biotite, garnet, muscovite, sphene, epidote, tourmaline, and ilmenite. 5 mm field of view, crossed nicols.

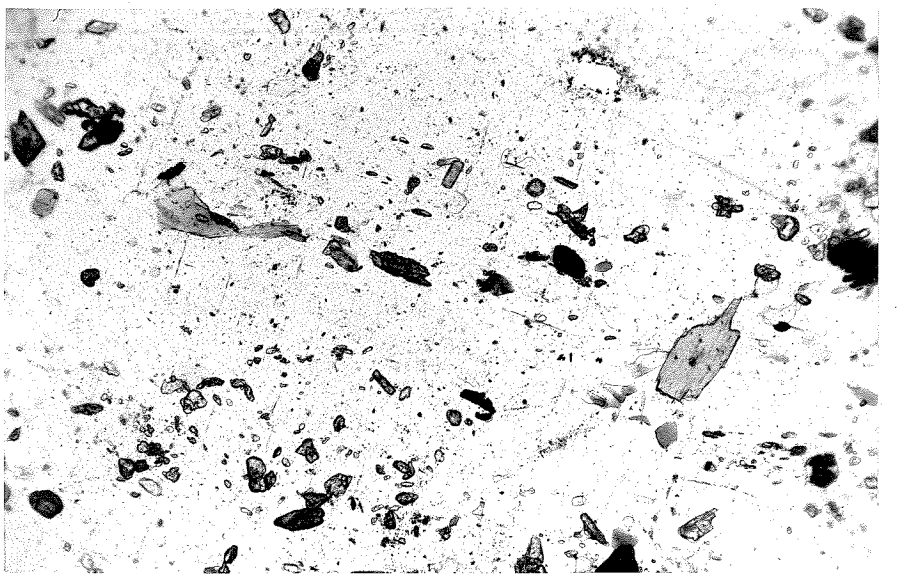

Figure 52b Enlarged view of central portion of porphyroblast in Figure 52a. 1.2 mm field of view, plane polarized light.

significant REE in epidote is somewhat of a problem when considering possible calcic plagioclase-producing reactions.

Plagioclase grains optically appear to be unzoned. All analyzed points have compositions between $An_{0.8}$ and $An_{0.0}$ except for one point on a rim which is $An_{2.0}$ in composition. There is no textural evidence of more than one generation of plagioclase growth. These plagioclase porphyroblasts are very similar in appearance to the host rock albite in JR-4-R and JR-4-P which is thought to be OM_b and/or OM_a. Inclusions trains within the albite preserve a sometimes ill-defined foliation which appears to be parallel to OS_a/OS_b. OS_a/OS_b is the only well developed s-surface which can be observed in thin section. There is no evidence of any appreciable rotation of the albite grains during or after formation.

Euhedral garnet grains occur only as inclusions in albite, but partly to wholly retrograded grains are in the matrix. Present are two texturally distinct types of garnet retrogradation. One type involves the apparent resorption of garnet and replacement of distinct grains of chlorite and biotite; these grains are up to 0.1 mm in largest dimension. The replacement grains do not preserve the original outline of the garnet. The second type of retrograde relationship involves very fine-grained, intergrown

chlorite, biotite, and calcite. Masses of these retrograde products are pseudomorphous after the original garnet grains.

Compositions of preserved garnet in this sample are shown in Figure 53. All grains are zoned with decreasing Mn from core to rim. Fe and Mg increase from core to rim and Ca is variable. The compositional extremes are $Fe^{2+}_{26}Mg_1Mn_{51}Ca_{22}$ and $Fe^{2+}_{57}Mg_2Mn_{17}Ca_{24}$. The cores are very rich in Mn and low in Fe^{2+} relative to samples from JR-5. The Ca content is also high compared to garnet from other samples along this traverse segment; there is up to 26% Ca-garnet component in JR-4-M garnet in contrast to a maximum of 21% in samples from JR-5. The only difference in assemblages between JR-4-M and the samples at JR-5 is that the plagioclase at JR-5 is more calcic. All of the OM_b and DM_a plagioclase in the host rocks analyzed at JR-5 included compositions in the range oligoclase to andesine. No plagioclase in the host rocks at JR-4 has been analyzed which is more calcic than $An_{2.0}$.

There is a smooth relationship between Mn and Mg for JR-4-M garnet. The Ca content is variable and sharp changes from point to point are not uncommon. The sharp changes in Ca are compensated by opposing changes in Fe^{2+}. However, the short range changes in Fe^{2+} are superimposed on the long range trend of increasing Fe^{2+} from core to rim; this

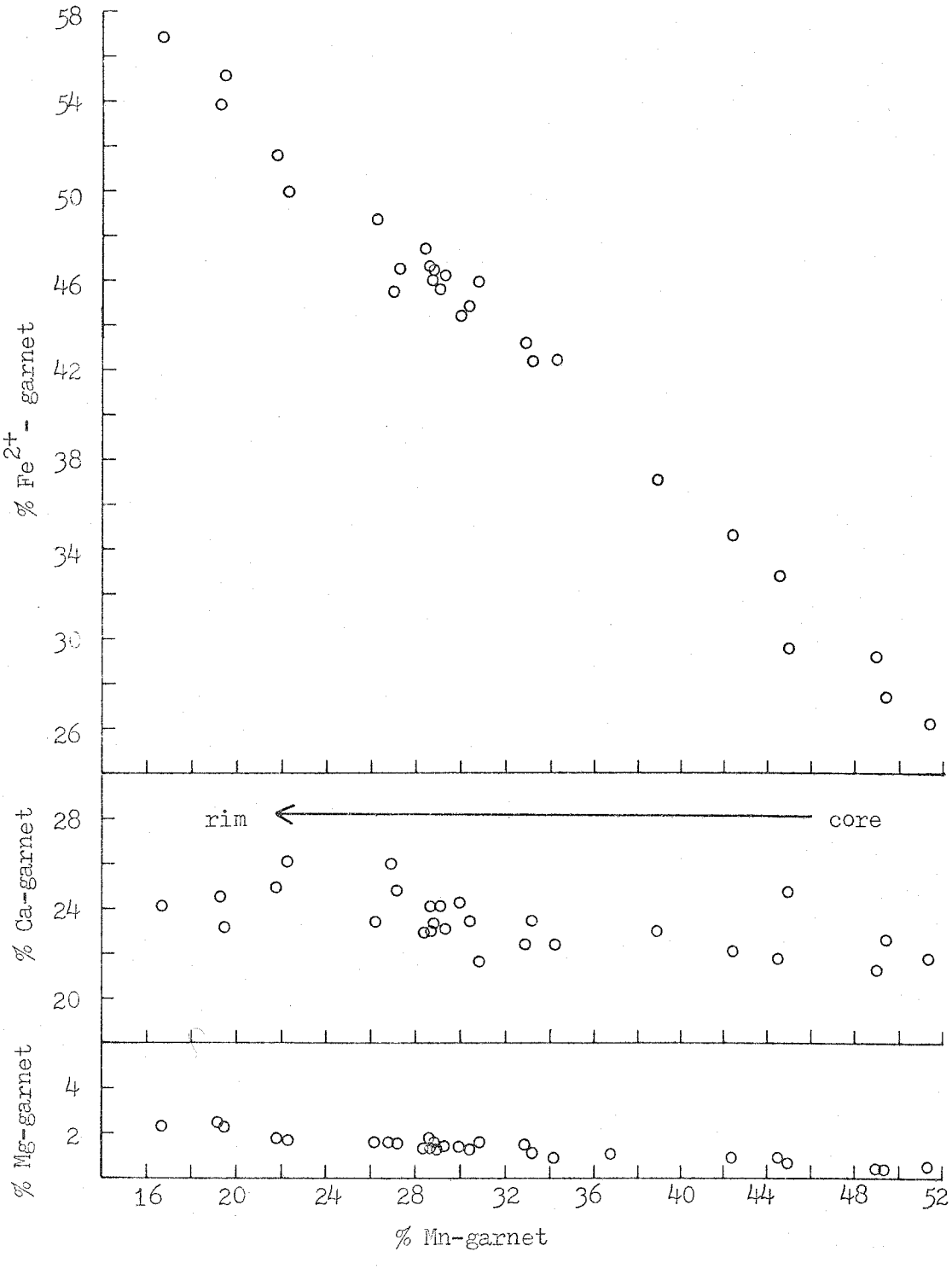

Figure 53 Compositions of garnet in JR-4-M. Standard deviation is about size of points.

tends to obscure the short range changes on the diagram. The irregular Ca zoning seems to be characteristic of OM_b growth in this local area. The garnet in JR-4-M is thought to be OM_b because of the inclusion relationships, the apparent DM_a alteration of garnet, and the presence of OM_b garnet at nearby JR-5.

Chlorite analyses are shown in Figure 54. These have been divided into four groups based upon textural relationships and composition. Group I chlorite is found as included grains in the cores of host albite and does not appear to be associated with included garnet. Group II chlorite is included grains in the rims of host albite and matrix grains which are parallel to OS_a/OS_b. These grains are associated with garnet. Group III chlorite analyses are from matrix grains which have no preferred orientation and also rims of grains which are parallel to OS_a/OS_b and have cores with Group II compositions. Group III grains also occur replacing partially resorbed garnet. Group IV chlorite analyses are from very fine-grained alteration of garnet.

Suggested compositional variation trends for Group I and Group II have been established using the position of small grains within the host albite. The innermost grains are assumed to be the oldest and the outermost the youngest.

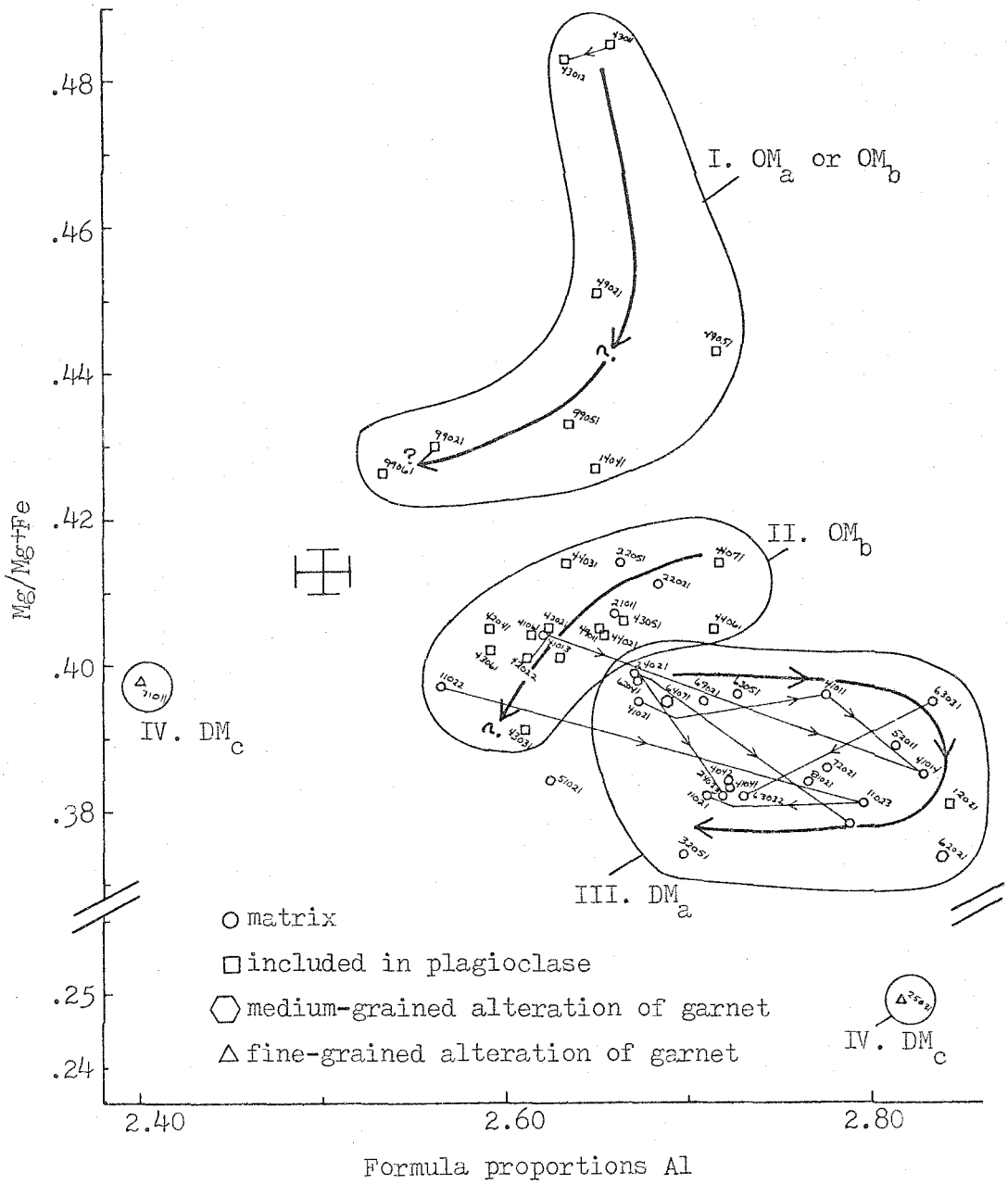

Figure 54 Plot of Al vs. Mg/Mg+Fe for chlorite in JR-4-M.

The compositional trend for Group III is defined by the zoning in matrix grains. There are only two analyses from Group IV.

Because there is no vein growth with which to directly compare mineral compositions, more interpretation is involved in assigning generations in this sample than in some of the others. However, using the relationships observed in the other samples, a reasonable interpretation is possible. The oldest chlorite is Group I chlorite. This is not associated with garnet, thought to be OM_b, and is not observed in the matrix. Group I chlorite is therefore probably OM_a or early OM_b. Group II chlorite is associated with OM_b garnet and predates the retrograde alteration of garnet. Cores of grains parallel to OS_a/OS_b have Group II compositions. Group II is probably OM_b. Overprinting OM_b growth is Group III; these grains generally have no preferred orientation and are associated with the resorption of OM_b garnet. This indicates that Group III is probably DM_a. Group IV chlorite is seen as a very fine-grained alteration product of OM_b garnet. There may also be some effect on DM_a minerals. In any event, Group IV appears to be younger than Group III and is therefore probably DM_c. All four of the mineral growth generations documented along this traverse segment may be present within a single thin section.

Two points which are very different from each other are shown as Group IV. Both are from texturally similar chlorite. The point with the lowest Mg/Mg+Fe has 1.4% by weight MnO, an abnormally large amount of Mn compared to the 0.3% in the other point, a more typical Mn content. It may be that during the low grade DM_c overprint some of the retrograde reactions occurred in relatively isolated environments so that the compositions of the products are close to the compositions of the reactant garnet. Such isolated environments might be able to maintain abnormally high activities of the components in which the reactants are rich. A similar situation may have existed during DM_c alteration of plagioclase in OV_b and DV_a veins. In OV_b vein plagioclase in JR-5-A and JR-5-B, intergrown muscovite, paragonite, and perhaps margarite appear to be alteration products. Paragonite and margarite are not found in either the host rock or veins as primary minerals in these samples.

The compositions of analyzed biotite points are shown in Figure 55a and are divided into four groups. These groups exactly correspond to the chlorite groups. Group I is OM_a or early OM_b, Group II is OM_b, Group III is DM_a, and Group IV is DM_c. The trends have been established in the same manner as for chlorite and are shown. Figure 55b is a plot of Mg/Mg+Fe vs. Ti for these four groups. There is no

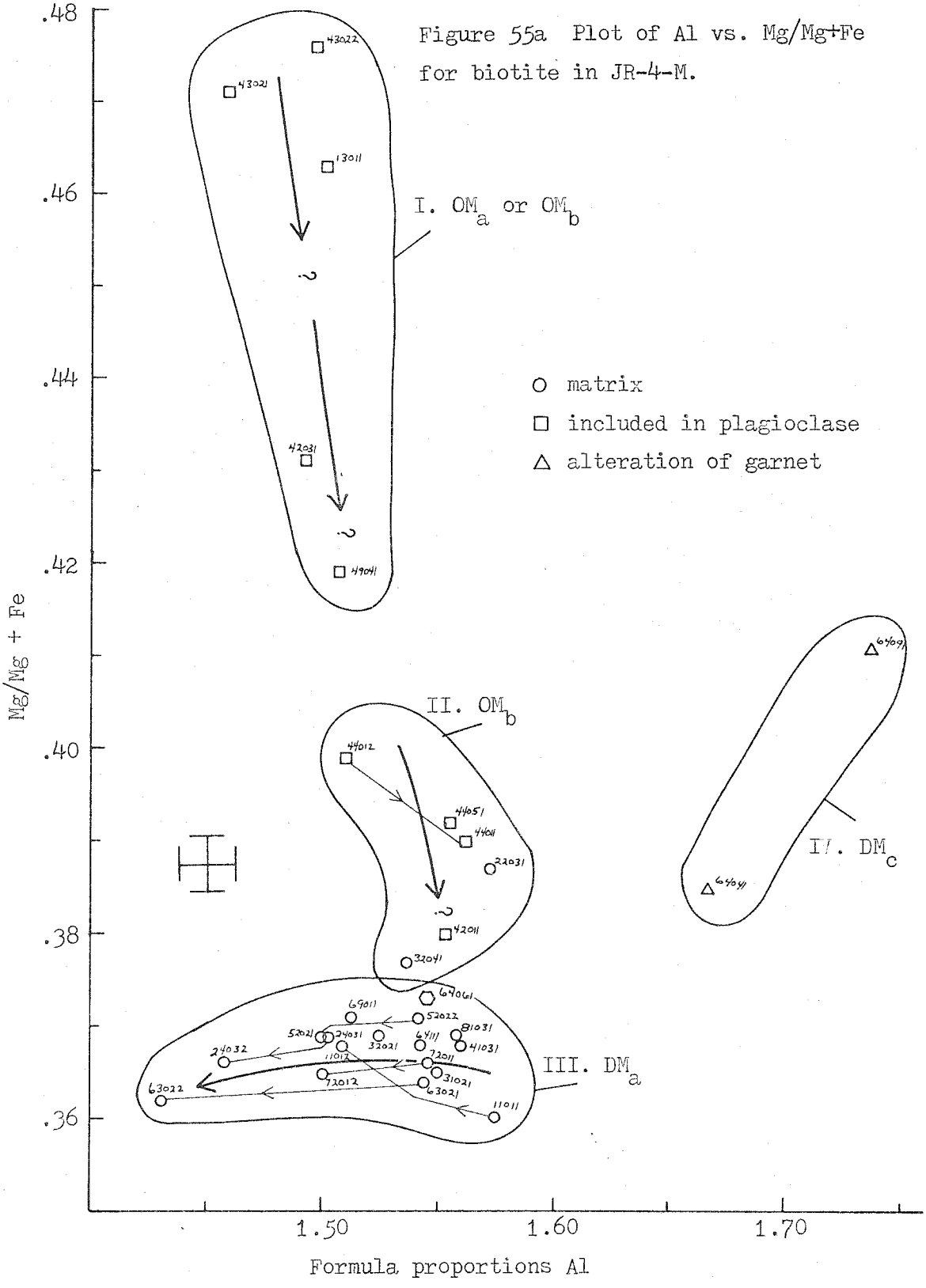

Figure 55a Plot of Al vs. Mg/Mg+Fe for biotite in JR-4-M.

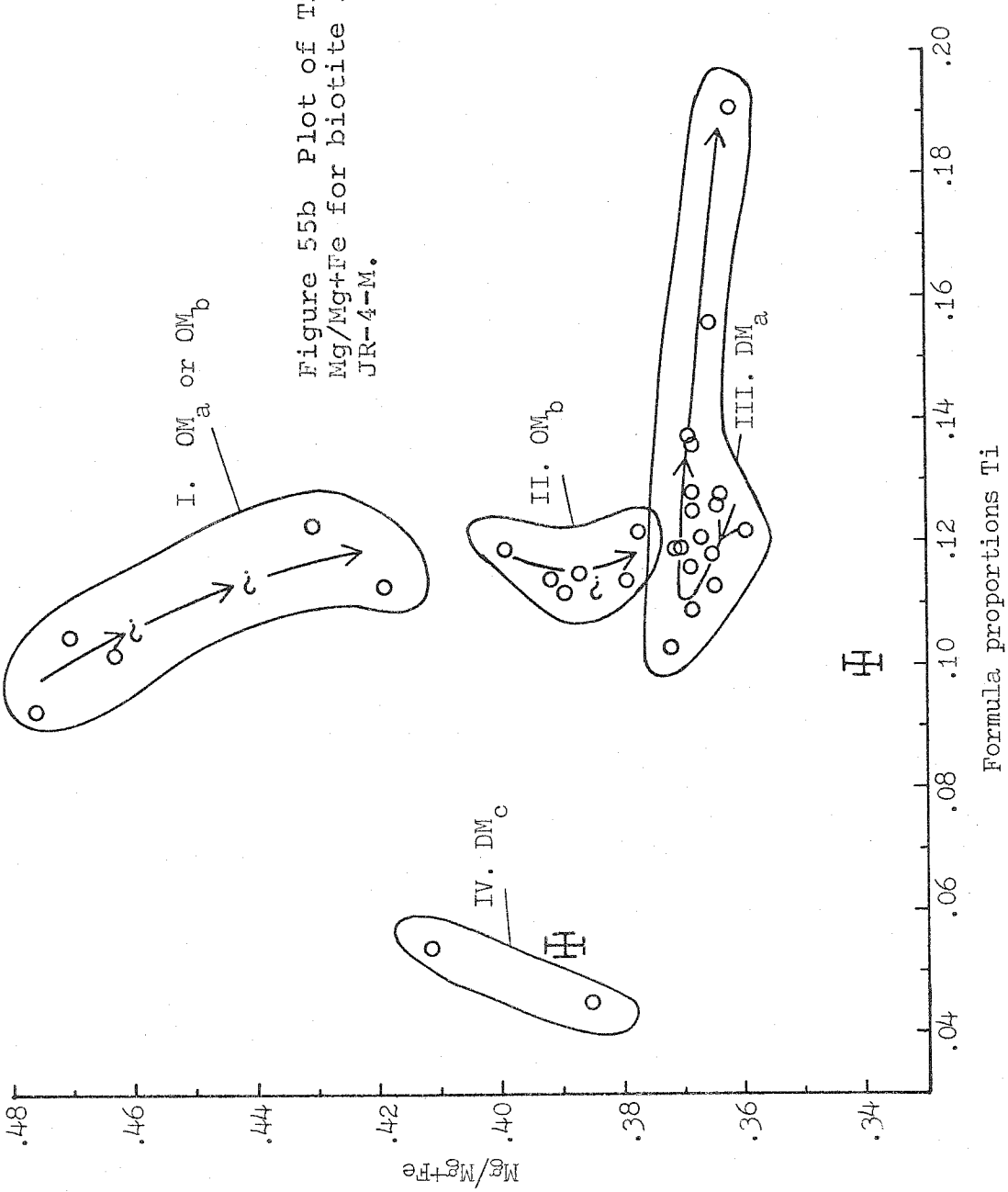

Figure 55b Plot of Ti vs. Mg/Mg+Fe for biotite in JR-4-M.

significant variation in Mn or Na/Na+K in JR-4-M biotite.

As has been discussed, it is difficult to determine the compositions of two or more minerals which formed simultaneously. For this sample, there is perhaps the best opportunity to successfully do this. The included grains of Group I and Group II chlorite and biotite are generally small and the grains of the two minerals are closely associated in the host albite. The compositional trends of Group III chlorite and biotite, DM_a, are fairly well established, so that these trends can be compared. Figure 56a shows all analyses of chlorite and biotite on a plot of Si/Si+Al vs. Mg/Mg+Fe. For each group, the compositional ranges of chlorite and biotite are similar in extent. The relationships from group to group are the same for biotite and chlorite. The apparent trends of Group I and Group II chlorite and biotite are very similar. The relationships are somewhat more complex for Group III.

Rim compositions of adjacent grains from Groups I, II, and III are shown in Figure 56b. Although it has been previously demonstrated that adjacent rim compositions do not necessarily represent material that grew simultaneously, this is the best approach available. Without exception the chlorite member of each pair has a slightly greater Mg/Mg+Fe value than the biotite. There is some cross-

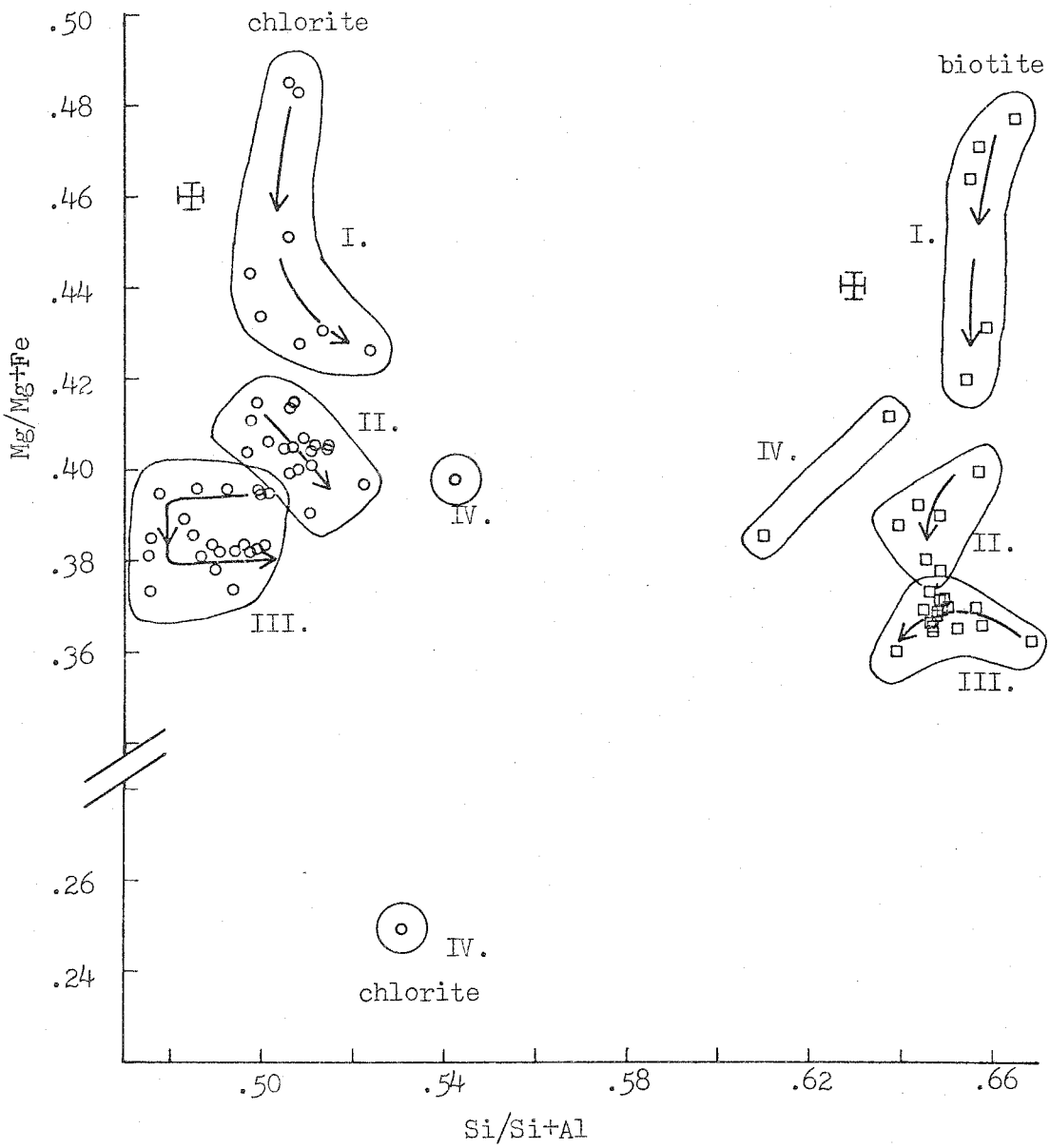

Figure 56a Plot of Si/Si+Al vs. Mg/Mg+Fe for chlorite and biotite in JR-4-M.

Figure 56b Plot of Si/Si+Al vs. Mg/Mg+Fe for rim compositions of adjacent chlorite and biotite grains in JR-4-M.

Figure 56c Logarithmic plot of Mg/Fe for chlorite-biotite pairs in JR-4-M. Also shown are K_D values. The relative standard deviation of the K_D's is about 2%.

Figure 56b

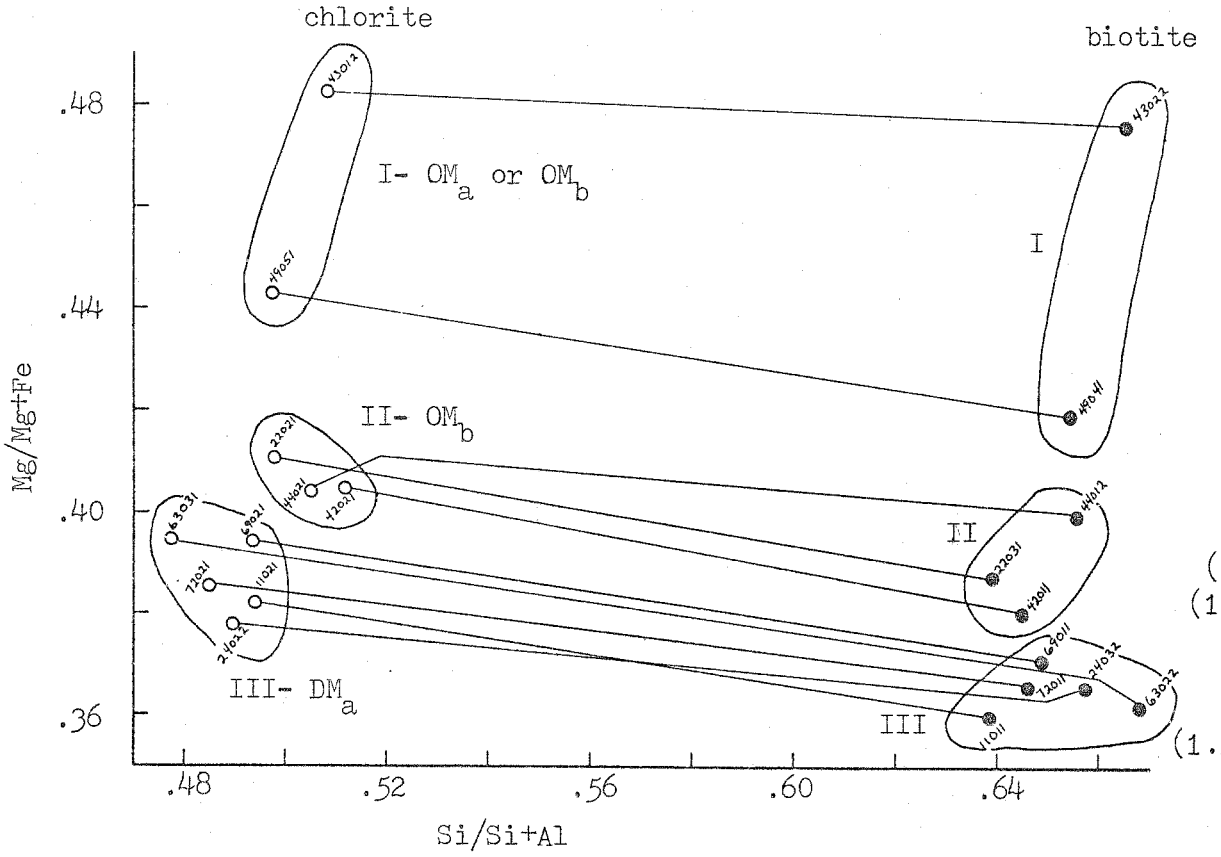

Figure 56c

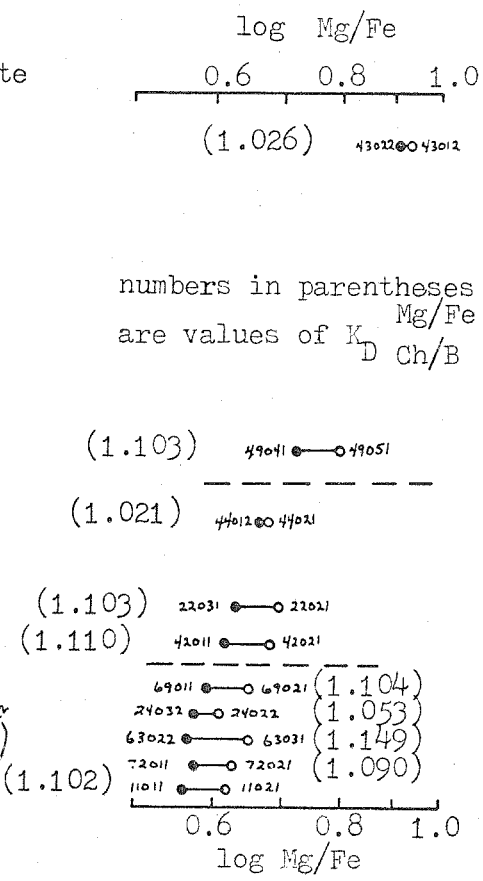

ing of tie-lines between pairs of DM_a chlorite and biotite. Figure 56c shows the pairs on a logarithmic plot of Mg/Fe. The apparent partition coefficients are shown by the length of the lines between the points of each pair. These apparent K_D's vary considerably within single groups, but there is no significant variation from group to group. This may be a fairly close approach to finding cogenetic pairs, but there is still considerable ambiguity and the results are on the whole unsatisfactory.

Chlorite in this sample has more Mn in absolute weight percent and Mn/total FM than biotite of the same generation. The Mn content in biotite is close to the limits of detection so that the analytical error is high. The counting statistics are better for Mn in chlorite, but within this error there is no significant variation in Mn within the groups. Groups II and III have essentially identical Mn contents. Group I, which represents chlorite growth before the first appearance of garnet, has somewhat less Mn than Groups II and III. Typical MnO contents of Group II and Group III chlorite are between 0.3 and 0.4 weight percent. Group I chlorite has between 0.2 and 0.3 weight percent MnO. Typical biotite analyses have between 0.1 and 0.2 weight percent MnO.

Compositional variation is also observed in ilmenite.

Grains are zoned with increasing Mn from core to rim. Most of the grains have preferred orientations parallel to OS_a/OS_b and therefore are perhaps OM_b in generation. The limits of MnO content are from 1.0 to 3.7 weight percent. It is interesting to note that the ilmenite might be co-genetic with garnet which is zoned with decreasing Mn from core to rim, the opposite of the ilmenite zoning. Another interpretation might be that the Mn-rich rims represent DM_a growth during the retrograde alteration of OM_b garnet. DM_a chlorite and biotite do not have any more Mn than their OM_b counterparts and the Mn from garnet retrograde must be taken up by some mineral. Stoichiometry indicates that substitution of Fe_2O_3 in the ilmenite is limited to 1% or less and does not vary significantly.

Only a few analyses were made of matrix muscovite. These are shown in Figure 57. Four of the points are from grains texturally similar to and associated with DM_a chlorite and biotite. These are therefore probably also DM_a. Two points are from grains parallel to OS_a/OS_b and may be OM_b growth. The OM_b analyses are from the cores of the two grains and have a significant amount of phengite substitution.

There is minor variation in the compositions of calcite in JR-4-M. Calcite is associated with chlorite and

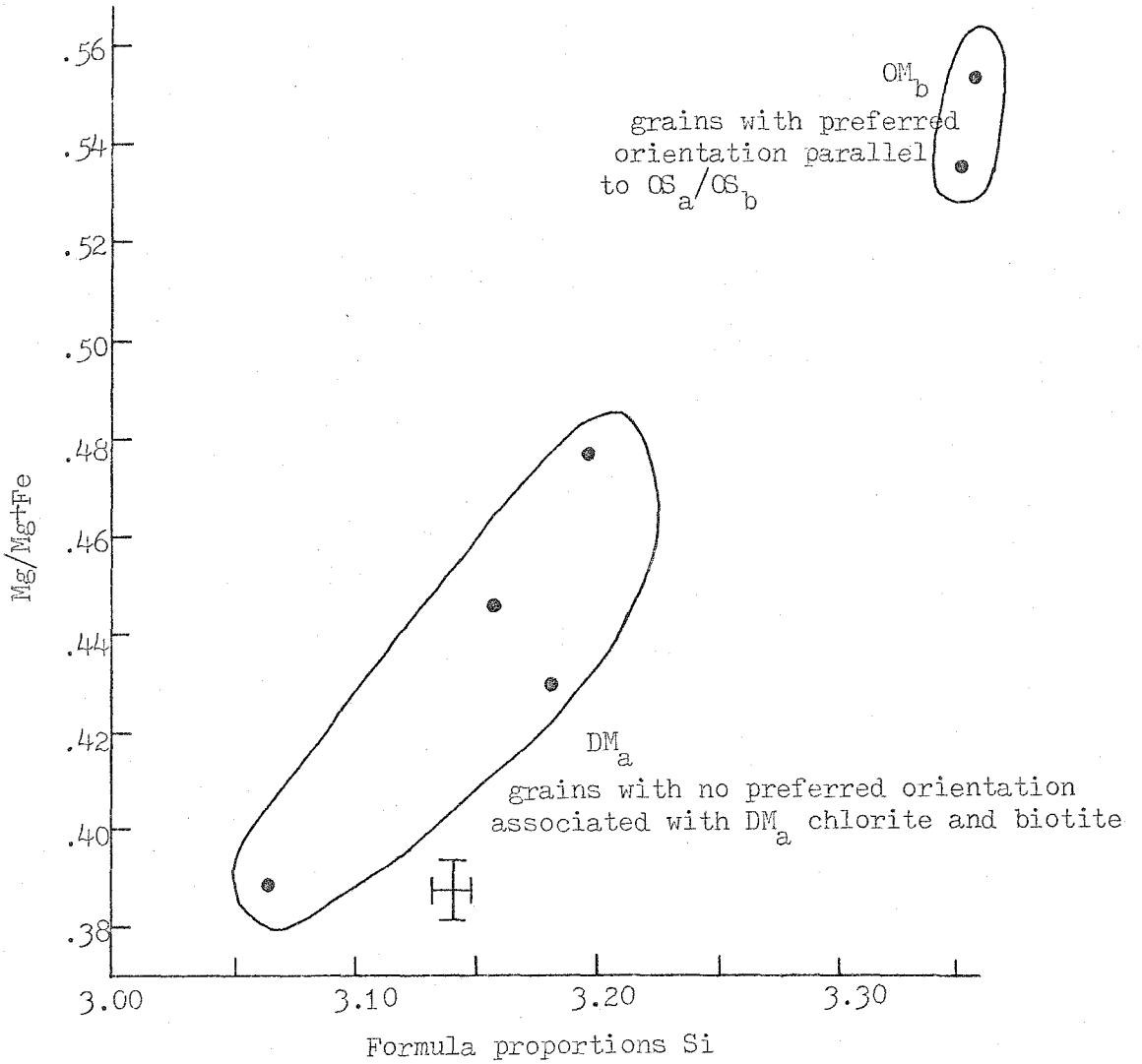

Figure 57 Plot of Si vs. Mg/Mg+Fe for muscovite in JR-4-M.

biotite thought to be OM_a, OM_b, and DM_a. There may be calcite of each of these generations, but the compositions of all of this calcite are similar. These contain 1.2-1.4 weight percent MnO. Calcite associated with Group IV chlorite and biotite, DM_c, has 2.2 weight percent MnO. As for chlorite and biotite, calcite which may have been cogenetic with OM_b garnet does not seem to have any significant variation in Mn, although small variations in Fe and Mg are preserved.

General discussion of JR-4

Several interesting features are observed in the rocks of JR-4 which are not observed elsewhere. The OV_b vein in JR-4-R appears to have had significant up-grade growth, unlike the OV_b vein in JR-5-A. There is no evidence of growth of oligoclase in any of the host rock samples, despite the presence of oligoclase in the OV_b vein. Oligoclase is also in the DV_a vein in JR-4-P and seems to record both up-grade and down-grade growth. There may also be down-grade growth recorded in the OV_b vein plagioclase. It does appear that there was significant growth of OM_b and DM_a chlorite during vein growth in the host rocks adjacent to the veins.

The lack of oligoclase in the host rock is perhaps in

contrast to the high Ca content of the OM_b garnet. It appears in JR-4-M that high-Ca garnet grew at the same time as albite. Oligoclase in the OV_b vein in sample JR-4-R was probably forming at about the same time. There is matrix oligoclase in host rocks from locations immediately both to the east and west. JR-5 is only 0.3 miles away and the assemblages in the rocks at JR-4 and JR-5 are essentially the same. No simple mechanism can explain these features. Given the presence of calcite and epidote, low Ca content in the plagioclase should also be reflected by low Ca content in the garnet compared to compositions observed at JR-5. Metamorphic conditions at JR-4 during OM_b growth could not have been that different from the conditions at JR-5. The only major difference between the two locations is the relatively early formation of veins in the events O_b and D_a.

The presence of OM_a, OM_b, and DM_a growth at JR-4 is documented by the presence of OV_a, OV_b, and DV_a veins. There is no such direct evidence of DM_c growth, but the evidence present in the samples does strongly suggest that there was limited DM_c growth. There is no evidence to suggest the presence of any other mineral growth generation at JR-4.

JR-78

Samples from three other locations along this traverse segment have been analyzed. One of these, JR-73-A, was described in the previous section. The other two samples are JR-78-C, from an OV_b vein and adjacent host rock, and JR-162-G, a sample of a DV_a vein and adjacent host. The structural sequence at these two locations is essentially the same as described for JR-5, with the exception that gentle DF_b folds are more noticeable than at JR-5. OV_a, OV_b, and DV_a veins are present at these locations as they are at most locations along the traverse segment.

Location JR-78 is on the west limb of the Green Mountain anticlinorium near the western limit of the area of garnet grade rocks mapped by Christman and Secor (1961). JR-78-C is a sample of an OV_b vein and the enclosing Underhill schist. No garnet occurs in JR-78-C, but other schist samples from JR-78 have assemblages that include quartz -muscovite-chlorite-biotite-garnet. Garnet appears to be OM_b in generation and is partly retrograded to chlorite and biotite, apparently DM_a in generation. DS_a slip cleavage is well developed in some parts of the outcrop, including where the retrograde alteration of garnet is most complete. DS_a is not well developed in JR-78-C. The only retrograde relationship in JR-78-C is the partial replace-

ment of pyrrhotite by pyrite.

The OV_b vein from which JR-78-C is taken is unusual in that it consists largely of calcite and ankerite. The almost ubiquitous OV_b vein plagioclase is not present. The vein assemblage is quartz-muscovite-calcite-ankerite-muscovite-pyrrhotite-pyrite (alteration of pyrrhotite)-chlorite-biotite. There is only one grain each of biotite and chlorite in the thin section of JR-78-C. Quartz, calcite and ankerite are very coarse-grained and ankerite grains tend to be euhedral. There is no border zone. The host rock assemblage is quartz-muscovite-chlorite-calcite-ankerite-plagioclase-ilmenite-pyrrhotite-pyrite (alteration of pyrrhotite)-chalcopyrite-apatite-tourmaline. The host rock is comprised largely of medium-grained quartz and plagioclase so that OS_a/OS_b is not prominent.

Muscovite in the vein and host rock has relatively little compositional variation with respect to phengite substitution. The analyzed points are plotted in Figures 58a, 58b, and 58c. The compositional variation trends for host rock and vein muscovite are shown on Figures 58b and 58c respectively. The compositional ranges of vein and host rock muscovite are similar. There are also similarities in the trends, but it is not clear that vein and host rock muscovite represent simultaneous growth. The host rock

Figure 58a Plot of Si vs. Mg/Mg+Fe for muscovite in JR-78-C.

Figure 58b Plot of Si vs. Mg/Mg+Fe for muscovite in host rock of JR-78-C.

Figure 58c Plot of Si vs. Mg/Mg+Fe for muscovite in OV_b vein of JR-78-C.

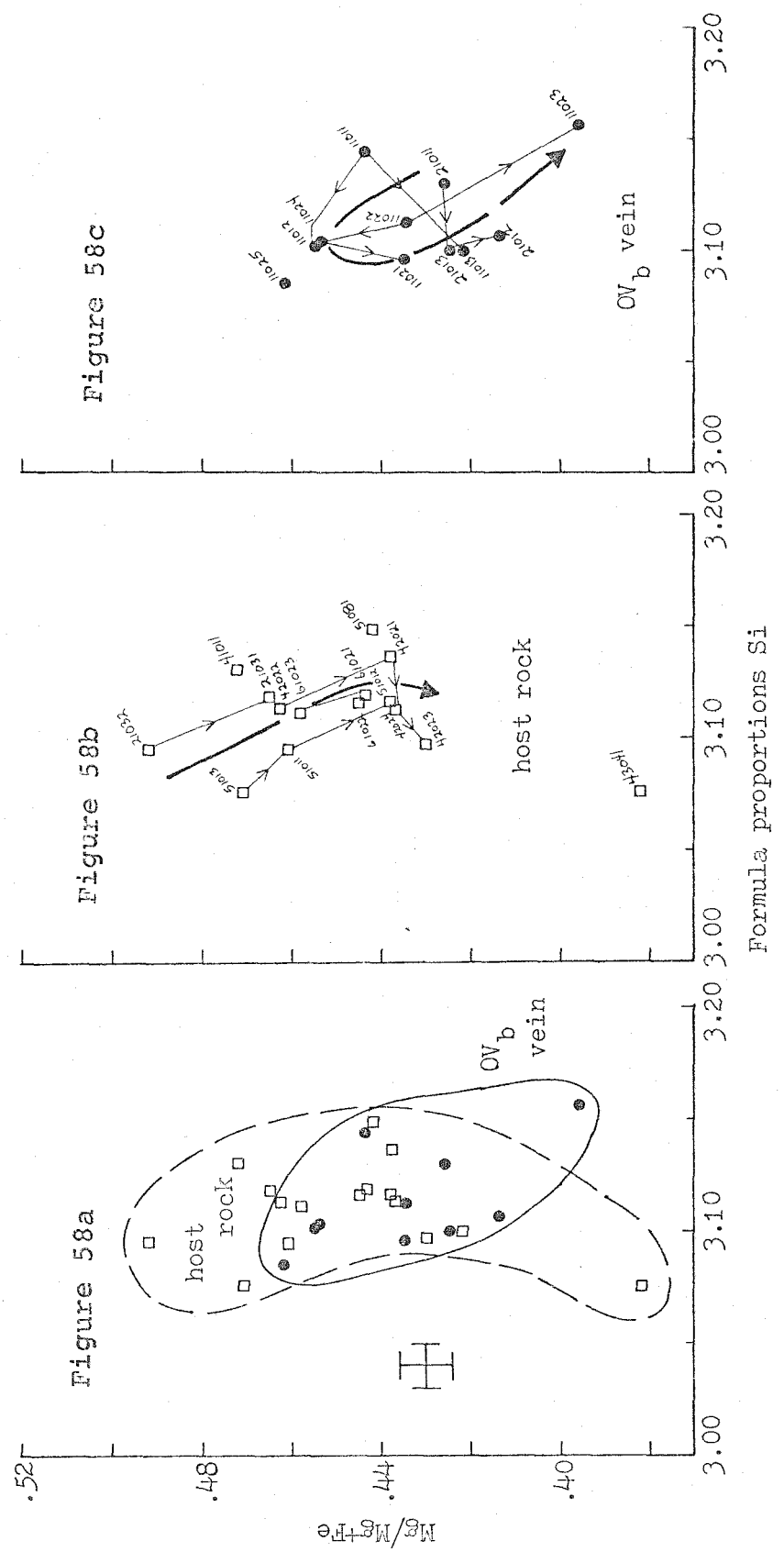
Figure 58a
host rock
OV$_b$ vein
Figure 58b
host rock
Figure 58c
OV$_b$ vein
Mg/Mg+Fe
.52
.48
.44
.40
3.00
3.10
3.20
Formula proportions Si

muscovite is probably all OM_b in generation, as it has preferred orientation parallel to OS_a/OS_b.

Compositional data for calcite and ankerite are shown in Figures 59a and 59b. Most of the analyses are from grains in the OV_b vein. Calcite in the vein has strong zoning with respect to the substitution of Fe and Mg for Ca. The amount of substitution decreases from core to rim. The Mn content of calcite is relatively constant. Ankerite in the vein has opposing trends of Mg and Fe. Fe decreases from core to rim and Mg increases. Mn also increases from core to rim, but to a lesser extent than Mg. There is also a decrease in excess Ca from core to rim. The simultaneous decreases in Fe+Mg+Mn substitution in calcite and Ca substitution in ankerite suggest that the system was gradually moving down temperature.

The compositions of plagioclase in the host rock are shown in Figure 60. All of the host rock plagioclase is albite. None of the grains appear to be optically zoned and there are no optical discontinuities. The range of compositions is from $An_{0.2}$ to $An_{4.4}$. All of the compositions more calcic than $An_{1.0}$ are from points within a few tens of microns from the grain rims. The bulk of the volume of host rock plagioclase grains, which average 1-3 millimeters in diameter, is nearly end-member albite. The

Figure 59a Compositions of calcite in OV_b vein of JR-78-C. Standard deviation is about size of points.

Figure 59b Compositions of ankerite in OV_b vein and host rock of JR-78-C.

Figure 59a

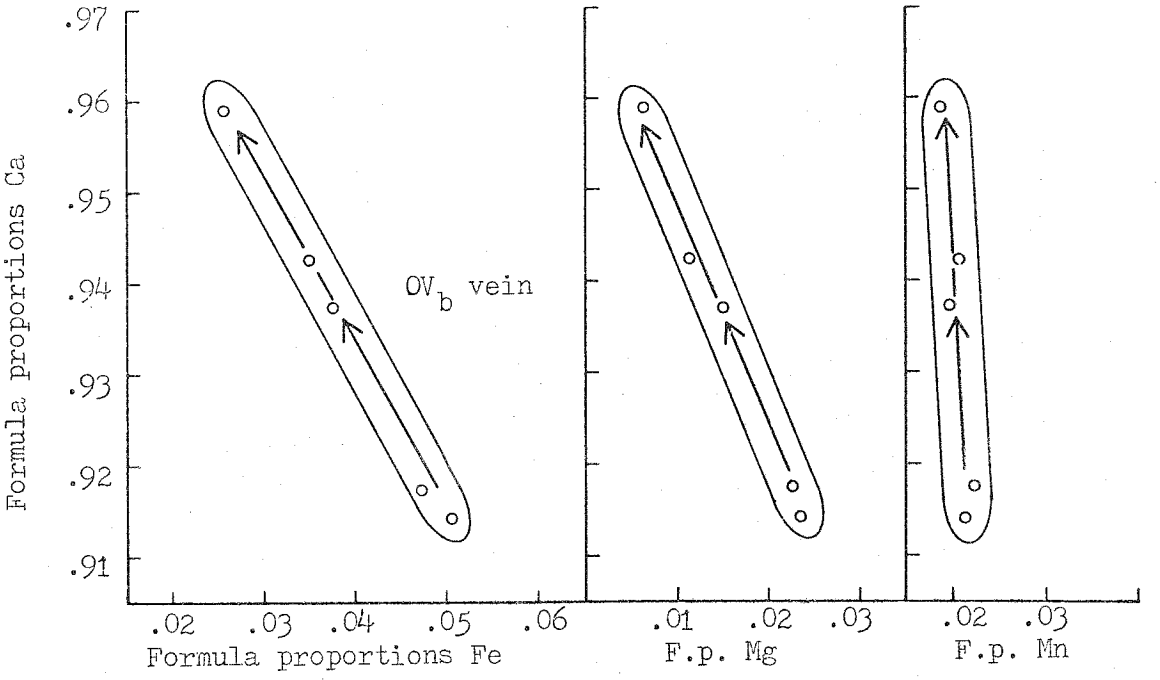

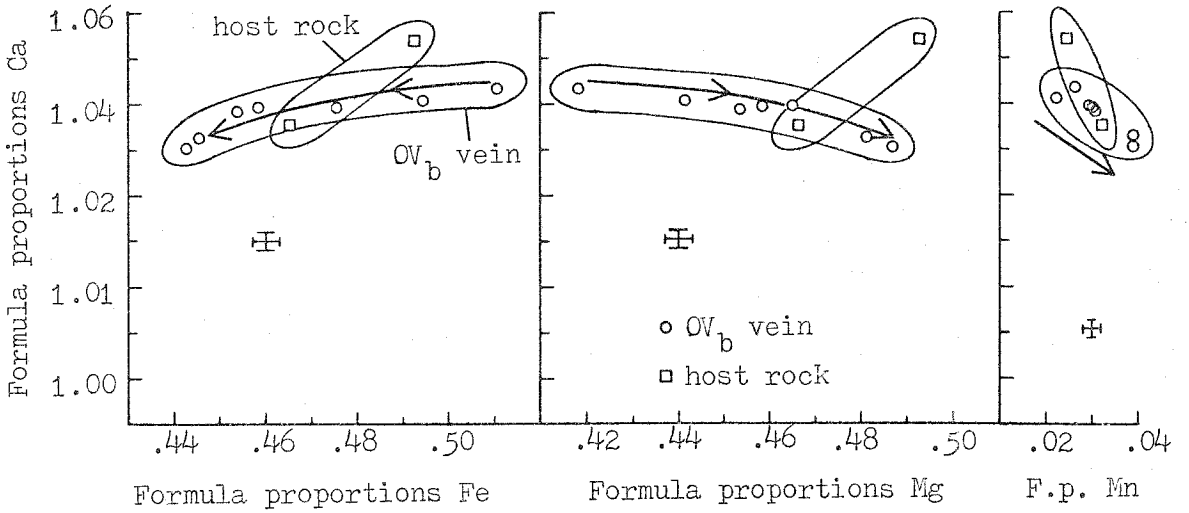

Figure 59b

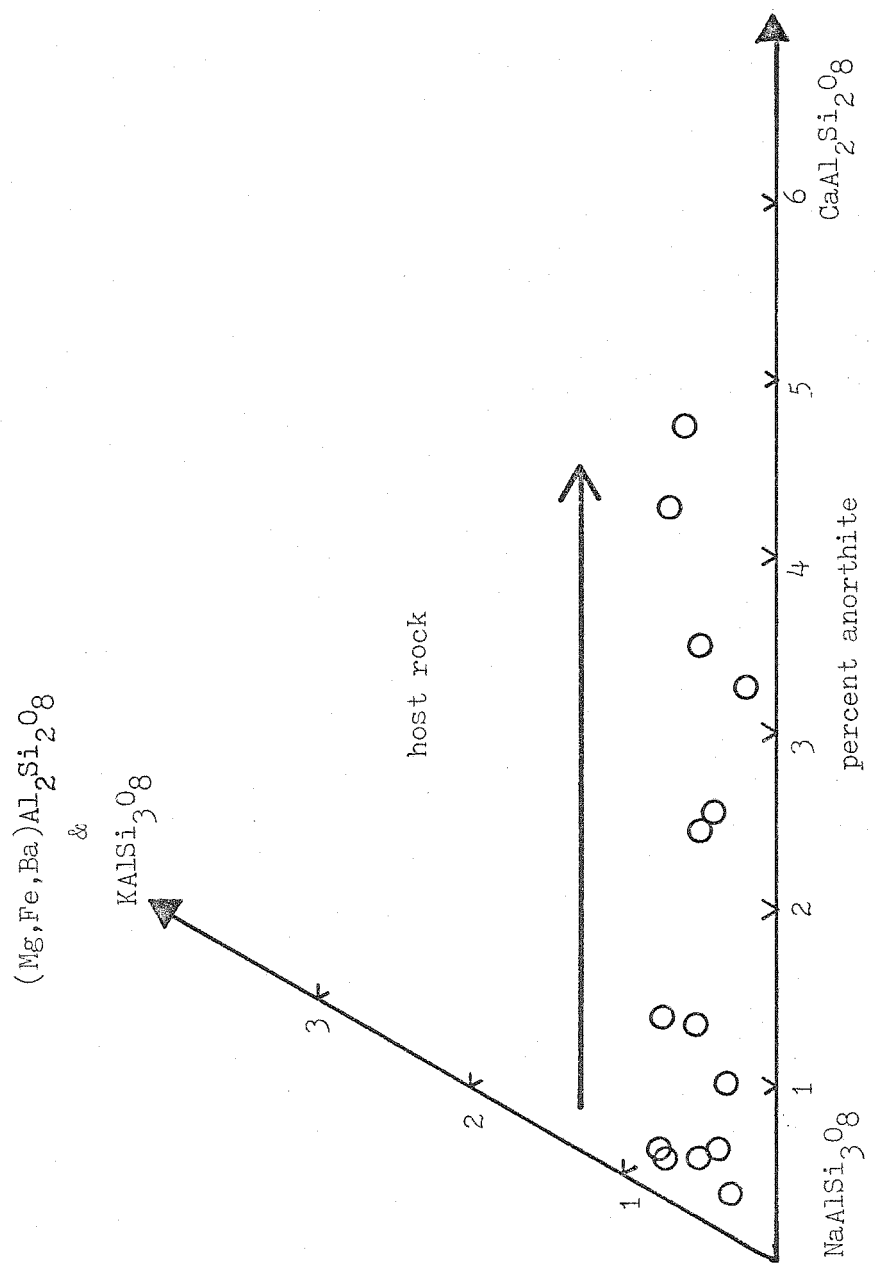

Figure 60 Compositions of plagioclase in host rock of JR-78-C.

zoning pattern in the outer portions of the grains involves strictly increasing An content toward the rims. The plagioclase is probably OM_b or OM_a and OM_b.

Two types of chlorite occur in the host rock. There are chlorite grains included in the albite grains and chlorite in the host rock matrix. Chlorite compositions are shown in Figure 61. There is an unusually large compositional range for chlorite which is included in albite. The general compositional trend for these is decreasing Mg/Mg+Fe, but the compositions tend to be in discrete groups. Matrix grains are generally parallel to OS_a/OS_b and are probably OM_b. Shown is a well defined compositional trend for host rock matrix chlorite. Vein chlorite was not analyzed as there was none in the microprobe section.

Some of the compositions of included chlorite are similar to compositions of matrix chlorite. These compositions seem to be younger than the included chlorite compositions which are more Mg-rich. Because the two groups of compositions seem to be distinctly separate, they may represent separate generations. The oldest, most Mg-rich included chlorite may be OM_a. The included chlorite which is compositionally similar to OM_b matrix chlorite may be OM_b. It is not clear what the three points from the most Mg-poor included chlorite represent. These three seem to

Figure 61 Plot of Al vs. Mg/Mg+Fe for chlorite in host rock of JR-78-C.

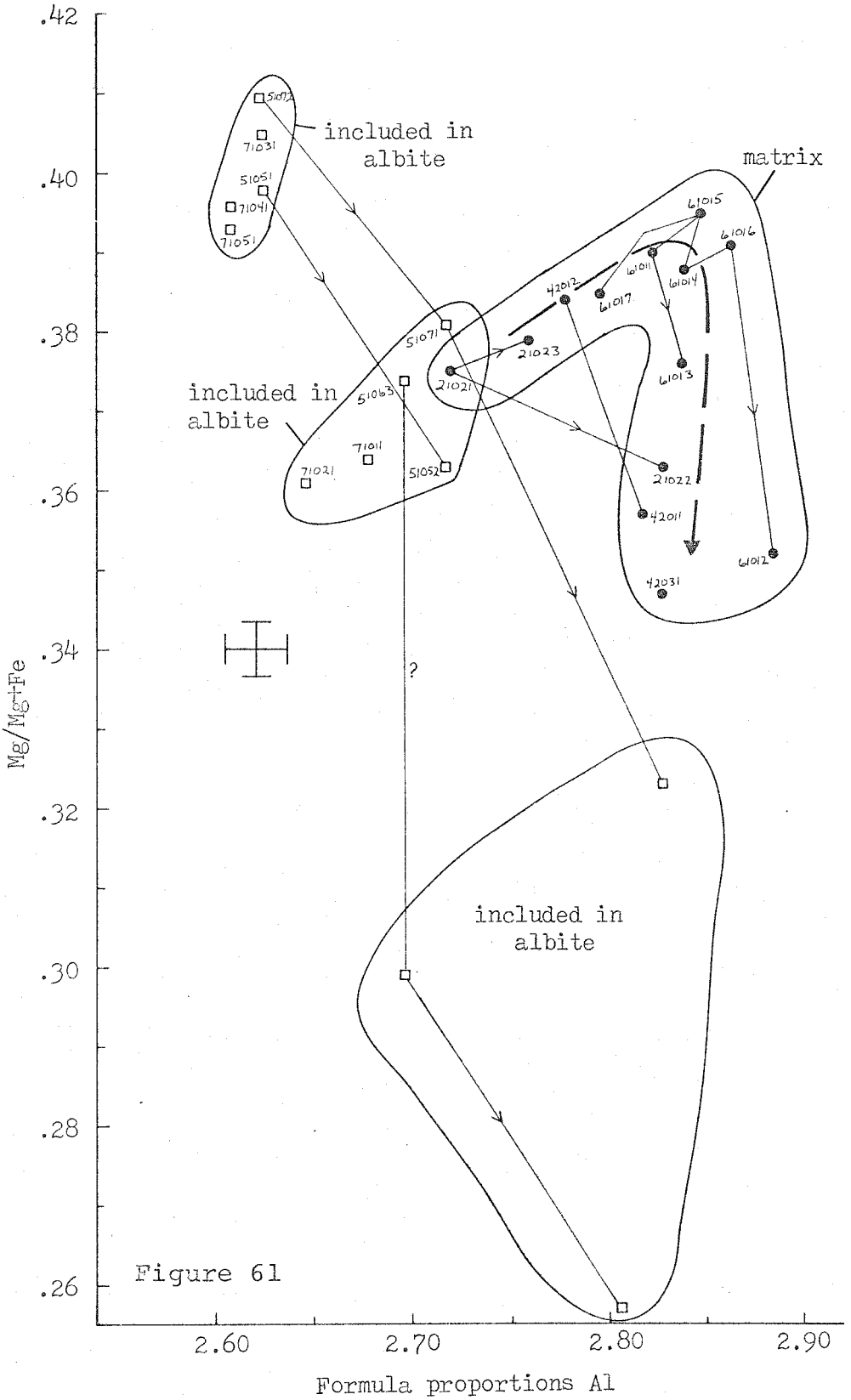
.42
.40
.38
.36
.34
.32
.30
.28
.26
Mg/Mg+Fe
2.60
2.70
2.80
2.90
Formula proportions Al
included in albite
matrix
included in albite
included in albite
?
51071
71031
51051
71041
71051
51071
51063
71011
71021
51052
21023
21021
21022
42012
61017
61011
61015
61016
61014
61013
42011
61012
42031

Figure 61

be the youngest compositions of the included chlorite and may be later OM_b growth. Although included grains in minerals such as albite generally seem to be relatively isolated, growth after inclusion might occur in some instances. Limited post-inclusion growth on the cores of included chlorite in albite seems to have occurred in sample JR-5-A. The Mg-poor chlorite growth on the inclusions may also represent late, post-inclusion growth, perhaps late OM_b in generation.

JR-78-C is the first sample described in which there may be some control on the relative path of temperature during vein growth. In other samples the path of grade can be described, but grade is the combined effects of P, T, and the partial pressures of volatile species. The zoning patterns in vein calcite and ankerite suggest that temperature was decreasing during vein growth in this case. The path of relative grade during vein growth seems to vary from vein to vein. There is no reason to suppose that temperature was decreasing during the growth of all veins or even all OV_b veins even if that is true for this vein.

JR-162-G

Location JR-162 is a roadcut in the Underhill formation about 1 mile east of JR-78 and 1.5 miles west of the

main axis of the Green Mountain anticlinorium. JR-162-G is a sample of a DV_a vein and adjacent schist. As DF_a microfolds are fairly open, DS_a is not developed by rotation of pre-existing grains. A fairly well developed DS_a set was produced by the growth of mica grains parallel to DS_a and crosscutting OS_a/OS_b. Because DS_a is mostly a growth feature, DS_a is more pervasive and approaches being an unspaced schistosity. Perhaps reflecting this, the contact between the host rock and the DV_a vein in sample JR-162-G is not sharp and well defined, but rather an irregular mixed zone of host rock mineral grains and vein growth. This zone averages 1-2 millimeters in width.

The DV_a vein assemblage is quartz-muscovite-chlorite-plagioclase-paragonite-calcite. In the host rock the assemblage is quartz-muscovite-chlorite-plagioclase-epidote-calcite-ilmenite-magnetite-tourmaline-zircon. In other schist samples from JR-162 chlorite-biotite-garnet-peristerite and chlorite-garnet-peristerite are observed. The garnet grade assemblages appear to be OM_b. In sample JR-162-I garnet grains are highly fractured. The fragments of what were apparently single garnet grains have been pulled apart and there is a quartz filling between fragments. A small volume of the garnet has been retrograded. The fragmentation of the garnet grains seems to be related

to DF_a microfolding. Here, as at the other locations along this traverse segment, OM_b garnet appears to have been retrograded and deformed during event D_a.

Only a limited amount of microprobe data was collected from JR-162-G. Most of these were analyses of chlorite and plagioclase. Analyses of chlorite are shown on a plot of Al vs. Mg/Mg+Fe in Figure 62. Significant compositional variation occurs in the three analyzed chlorite grains from the DV_a vein. A suggested compositional variation trend is shown for these. There are also analyses from two different types of chlorite grains in the host rock. Six analyses are from grains with preferred orientation parallel to OS_a/OS_b and five analyses are from grains without preferred orientation. The compositions of grains without preferred orientation have essentially the same range and compositional trend as the DV_a vein chlorite. These host rock grains appear to be younger than the grains parallel OS_a/OS_b. The compositional and textural evidence indicates that the grains without preferred orientation in the host rock are DM_a.

Texturally the host rock chlorite grains with preferred orientation would seem to be OM_b. The compositions of these grains essentially all fall within the compositional range of DM_a chlorite. There are two possible explanations.

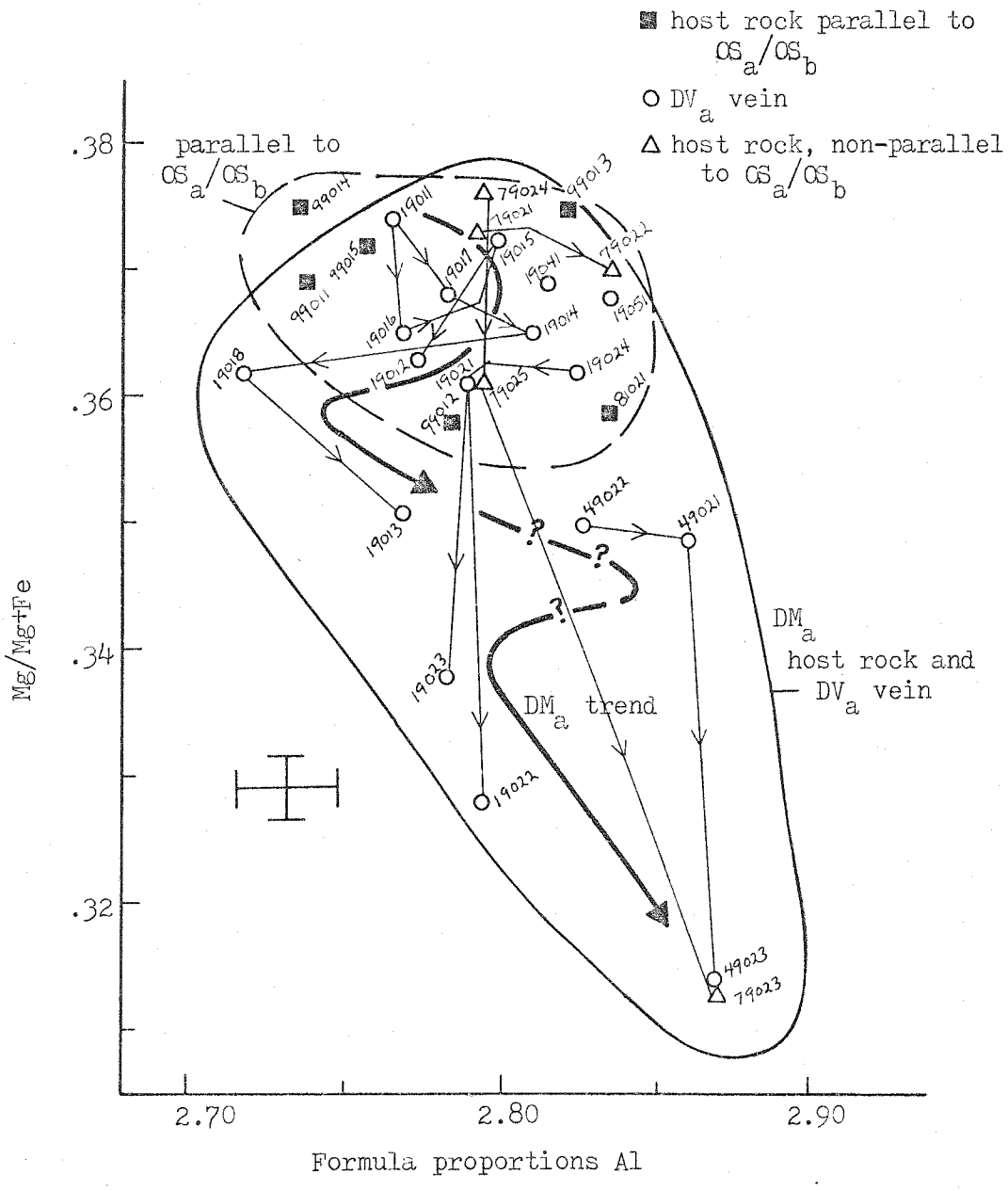

Figure 62 Plot of Al vs. Mg/Mg+Fe for chlorite in JR-162-G.

OM_b compositions may be by chance roughly the same as DM_a. The other possibility is that there was extensive chemical reconstitution of OM_b grains during DM_a growth. The evidence is such that neither of these possible explanations seems better than the other.

Plagioclase grains in the host rock do not show the sort of overprint texture observed in samples such as JR-5-I. The plagioclase may represent only one generation, probably OM_b. The compositions of analyzed points from three host rock plagioclase grains are shown in Figure 63a. One grain has an albite core ($An_{4.1}$) and a sodic oligoclase rim ($An_{10.2}$), with an optical discontinuity between. Neither of the other two grains has an optical discontinuity and the compositions of analyzed points from core and rim are all more calcic than $An_{9.0}$. The zoning pattern in all host rock grains is increasing An content from core to rim.

Analyses from DV_a vein plagioclase are shown in Figure 63b. The general zoning pattern seems to be decreasing An content from core to near the rim, then a reversal and an increase in An content, another reversal, and finally decreasing An content across an optical discontinuity. The core compositions are oligoclase and the outside rims are albite. The great bulk of the volume of vein plagioclase is oligoclase with the An content decreasing toward the rim. The discontinuity represents the peristerite gap and

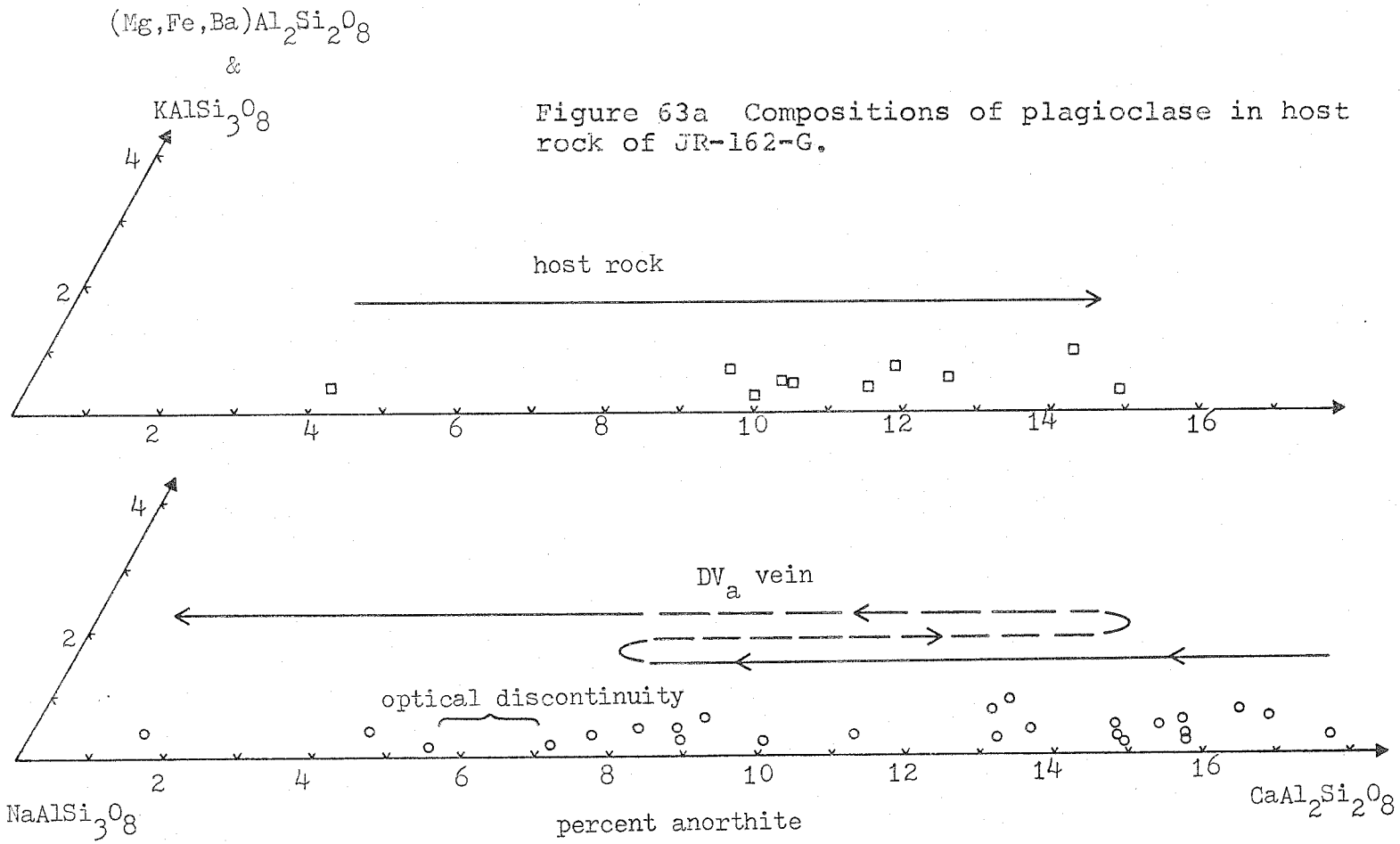

Figure 63a Compositions of plagioclase in host rock of JR-162-G.

Figure 63b Compositions of plagioclase in DV_a vein of JR-162-G.

is present in all grains with albite rims.

Paragonite occurs in the DV_a vein, but this is found within plagioclase grains that appear to be altered. The paragonite is probably an alteration product and it might be DM_c in generation. Also, some muscovite is intergrown with the paragonite and it is probably similar in origin.

There is no evidence of DM_a plagioclase growth in the host rock, but there has been extensive DM_a host rock chlorite growth. This DM_a chlorite appears to have been forming at the same time as chlorite in the DV_a vein. The general compositional trend of the vein plagioclase suggests downgrade growth, but the compositional reversal in thin, outer portions of grains indicates that perhaps plagioclase compositions are very sensitive to small changes in some parameter such as f_{CO_2}.

Discussion of the traverse samples

The metamorphic veins are very useful in establishing the presence and general grade of the various mineral growth generations. Reasonable interpretations of the mineral growth generations in the host rock can be made, but are always subject to a little more ambiguity than the veins. The metamorphic veins along this traverse segment have established that four mineral growth generations are

present: OM_a, OM_b, DM_a, and DM_c. There is no evidence of any other mineral growth generations.

Considerable compositional variation occurs in most of the minerals in these rocks. The mineral grains in general seem to preserve zoning due to changing conditions during growth. The conditions which were changing may only have been the activities of chemical species. There is also evidence that in some cases extensive chemical reconstitution of pre-existing grains during a mineral growth event can occur. The best example is JR-163-D, which is still a little ambiguous. Certainly reconstitution during overprint must occur to some extent. It is often difficult to sort out the effects of overgrowth and diffusion in the solid state. For a mineral in a sample which appears to have a fairly complicated, systematic compositional trend, it seems reasonable to suppose that this is a growth feature.

There is a great diversity in the apparent timing of vein and host mineral growth and the apparent trend of grade during vein growth. Some veins, such as the OV_b vein in JR-5-A, appear to have grown after mineral growth in the host rock stopped. This is at least true for the plagioclase growth. In some veins, such as the DV_a vein in sample JR-162-G just discussed, there is evidence that chlorite

growth in the vein and in the host rock occurred at the same time. Plagioclase growth may have simultaneously occurred in the host rock and DV_c vein of JR-163-D. Generally there is not an exact correspondence of plagioclase in the vein and in the host rock. In JR-5-A and JR-5-G it appears that host rock plagioclase growth occurred and then vein plagioclase growth occurred. In these cases the plagioclase zoning indicates increasing grade during host rock growth and decreasing grade during most of the vein growth. In samples such as JR-4-R and JR-4-P, the plagioclase zoning indicates vein growth during increasing then decreasing grade. In these samples no plagioclase in the host corresponds to the vein plagioclase. Generally plagioclase seems to grow in veins or in the host rock, but not in both at the same time. Chlorite growth may be very different as it may occur in the vein and host rock simultaneously. There are not enough data on muscovite and biotite to make generalizations.

Most host rock growth seems to have occurred as the grade of the system was increasing. Veins may grow during this period of increasing grade, but vein growth can also continue as the grade of the system decreases. Because of the diversity of timing of vein growth, it appears that the apparent down-grade growth recorded in the veins is not an

effect of vein growth itself. In only one sample, JR-78-C, was there any direct evidence that this decrease in grade also involved a decrease in temperature.

One of the most disturbing aspects of the samples studied is the variation in the effects of various events from sample to sample within single outcrops. What is observed at a location depends upon the sample sites within the outcrop. This variation within outcrops and the variation in the nature of vein and host mineral growth features and timing make one hesitant to make many generalizations. If fewer samples were studied, there might be many more "firm" conclusions.

General distribution of grade indicating minerals

It is useful to consider the distribution of mineral assemblages that give some indication of the metamorphic grade attained during each event. These outcrops are along a linear traverse so that there is not enough areal coverage to define isograds for the mineral growth generations. The data are useful in considering the nature of previously mapped isograds and can provide a basis for further study.

The host rock types at the locations along this traverse segment are generally pelitic in character and all have quartz and muscovite as part of their assemblages. Other

major minerals encountered in these rocks are various combinations of chlorite, biotite, garnet, chloritoid (included in garnet), plagioclase, and stilpnomelane. Also commonly occurring are calcite, epidote (often with REE-rich cores), apatite, tourmaline, zircon, and sphene. Ankerite is present in a few samples. Typically one to four of the following opaque minerals are present: pyrrhotite, pyrite, magnetite, ilmenite, hematite, rutile, and chalcopyrite.

Garnet is the highest grade mineral observed in this local area and is used as a grade indicator. The retrograde alteration of pre-existing garnet is also used as an indicator of sub-garnet grade conditions. The presence or absence of plagioclase with oligoclase compositions is another indicator of grade. The typical oligoclase in these rocks is seen in concentric growth relationships with albite which is apparently of the same generation. Between the albite and the oligoclase is an optical and chemical discontinuity representing the peristerite gap. In the diagrams that follow, such plagioclase is referred to as peristerite. In the veins, albite rims of the same generation are not always seen on the oligoclase cores, but these are still referred to as peristerite. The albite and oligoclase in a grain of peristerite are of the same generation. The isograd determined by the presence of or absence of per-

isterite could also be referred to as the oligoclase isograd. However, albite compositions can be on the calcic side of the peristerite gap in some instances, so that the feature of interest is the presence or absence of the peristerite gap in a single generation of plagioclase.

Pyrite and pyrrhotite might be useful as indicators of grade, but there were not enough polished thin sections of sulfide-bearing samples to have any control on this. None of the other minerals seem to be of much use in determining grade without extensive chemical data from every outcrop. More data on calcite-ankerite pairs would be useful and as would perhaps data from muscovite in samples in which the phengite substitution is buffered.

Figures 64a, 64b, and 64c show the distribution of the grade indicating assemblages by generation for OM_b, DM_a, and DM_c. These are shown for locations along the traverse segment and for a few other locations to the east and west. The data are comprised of petrographic observations of 122 thin sections from 24 locations plus the microprobe work already described. The generations are separated based upon the presence of the assemblages in veins of known generation and the textural relationships in the host rock samples. The use of the veins is of key importance, particularly with regard to the generations of

Figure 64a OM_b assemblages in pelitic rocks at locations along the Winooski River traverse in the Camels Hump quadrangle.

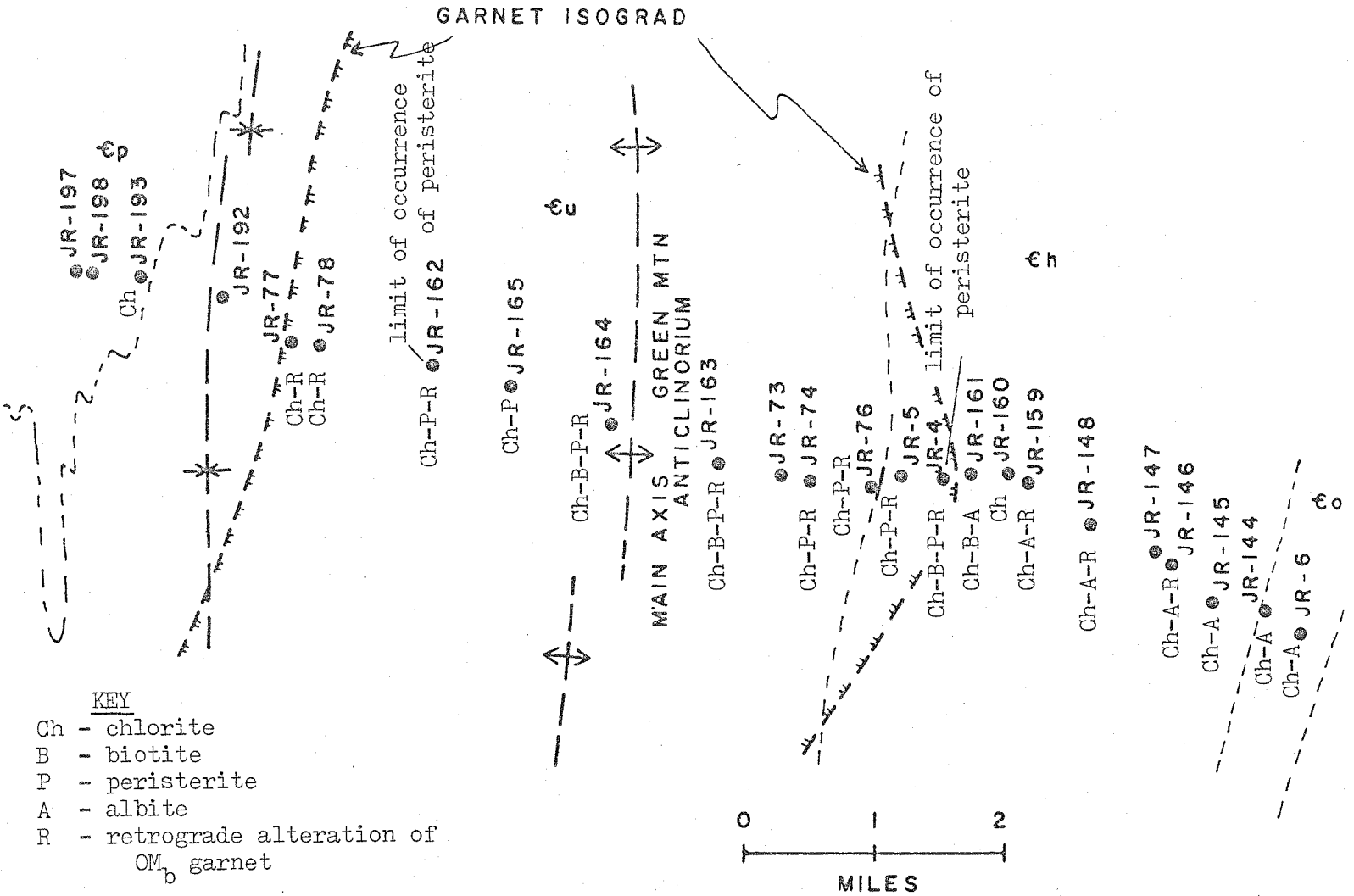

Figure 64b DM$_a$ assemblages in pelitic rocks at locations along the Winooski River traverse in the Camels Hump quadrangle.

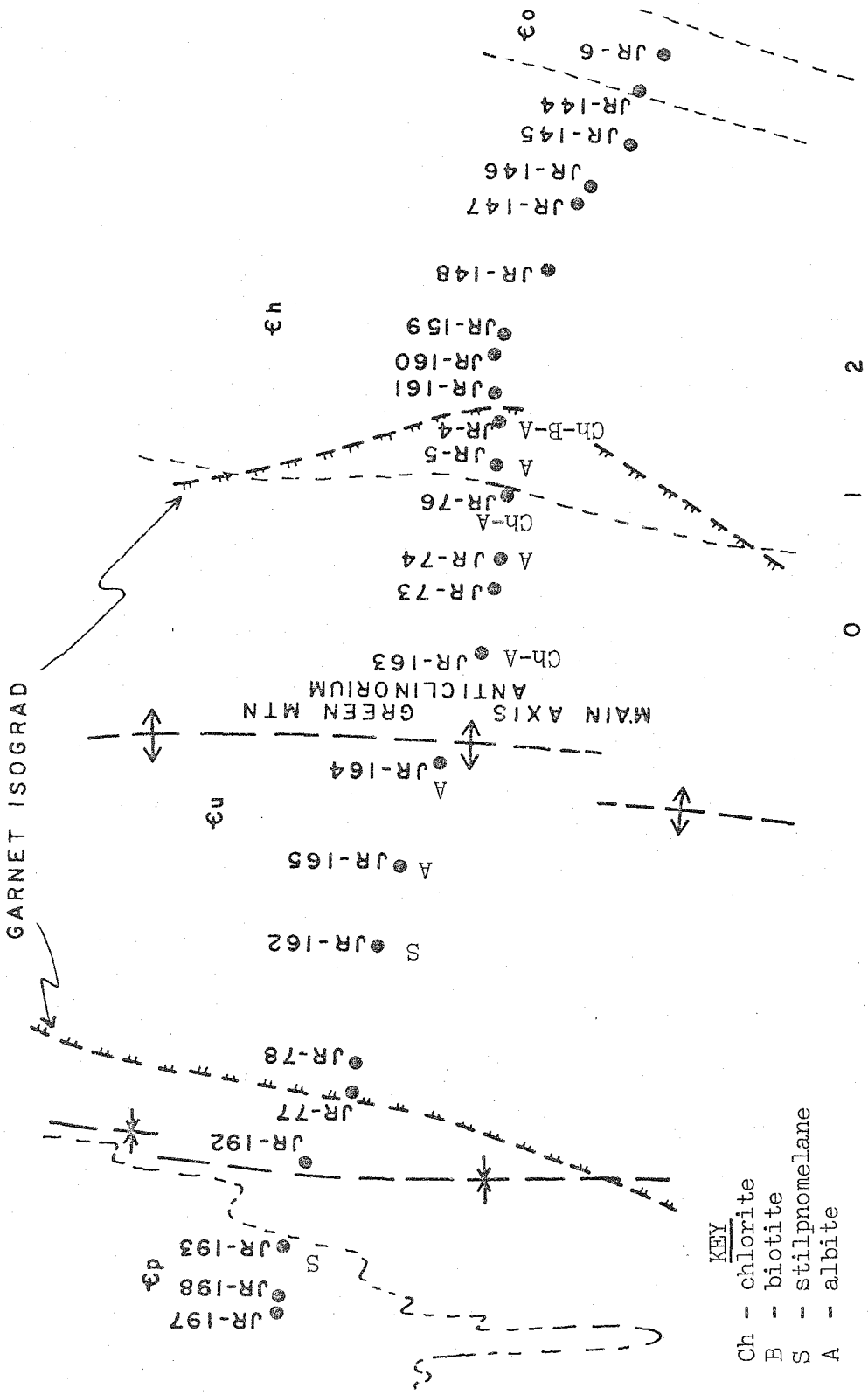

Figure 64c DM_c assemblages in pelitic rocks at locations along the Winooski River traverse in the Camels Hump quadrangle.

plagioclase growth and the identification of DM_c. DM_c can be identified with reasonable certainty as mineral growth overprinting DV_a vein minerals and as primary growth in DV_c veins.

No diagram is shown for OM_a growth because the OM_b overprint on this generation is so extensive. It is often difficult to know what is really OM_a growth and what is recrystallized OM_a. In general, OM_a mineral growth is thought to be biotite grade everywhere. OM_a plagioclase is probably all albite in composition. Assemblages in OV_a veins are typically very simple, more simple than in OV_b veins in the same host rock. Plagioclase is often absent. For the generations which are less severely overprinted and for which there is more control, such simplicity of vein assemblages correlates in a general way to sub-garnet grade conditions during vein formation.

Figure 64a shows the distribution of the assemblages of interest for OM_b mineral growth. Quartz and muscovite are part of the assemblage in every case. Going from east to west, the initial assemblages include chlorite and albite. The eastern limit of occurrence of garnet is at location JR-146 and this garnet seems to coexist with OM_b albite. Peristerite is first observed at location JR-148, so that the first occurrence of peristerite is within the

garnet grade rocks on the east side of the area. Biotite is not observed until location JR-161, presumably due to the composition of the host rock. In the central part of the area various combinations of chlorite, biotite and garnet are observed. The most complete assemblages are shown on the diagram. Going to the west, the last outcrop in which garnet is observed is JR-77. OM_b peristerite is observed in the outcrops to the west of JR-77, so that the limit of occurrence of peristerite is beyond the limit of garnet occurrence. Another mineral of interest is chloritoid. This is observed only as included grains in OM_b garnet in samples from the central part of the traverse segment.

The garnet isograd mapped by Christman and Secor (1961) is shown in Figure 64a. On the west side of the traverse segment, the mapped garnet isograd agrees exactly with the data of this study. On the east side, garnet is observed almost two miles to the east of the isograd. As already discussed, the mapped isograd appears to represent more of a limit of preservation than a limit of growth of garnet. Most of the garnet to the east of location JR-4 seems to have been destroyed by strong D_a deformation. To the east of JR-4, DS_a is commonly parallel to OS_a/OS_b and DF_a folds

are tighter than to the west. The strong deformation east of JR-4 makes that area difficult to interpret without extensive sampling. The sampling in this study seems adequate to define the mineral growth relationships here. However, there is not as much coverage in the corresponding area along the Lamoille River traverse where the interpretation becomes more ambiguous.

To the west of location JR-197 it appears that peristerite is absent from the assemblages and only OM_b albite is present. However, preservation becomes a problem here, too. Sampling is insufficient to show the relationships in detail. Poorly preserved grains of peristerite, which are probably OM_b, occur at location JR-152, two miles northwest of the town of Richmond.

Figure 64b shows the distribution of assemblages for DM_a mineral growth. Everywhere that OM_b garnet is present, DM_a involves the retrogradation of the garnet. Assemblages always include chlorite or chlorite-biotite. The only change in assemblage that may indicate a change in grade is the presence or absence of peristerite. Going east to west, the first occurrence of DM_a peristerite is at JR-4. DM_a peristerite can be observed in samples from locations JR-4 through JR-162. West of JR-162 only DM_a albite is observed. DM_a peristerite is sub-garnet grade everywhere

along this traverse segment. The high grade DM_a area marked by the presence of peristerite occurs entirely within the OM_b garnet grade area. The high grade areas of OM_b and DM_a are both nearly symmetric around the main axis of the Green Mountain anticlinorium. This strongly suggests that the isograd pattern is produced by post-DM_a folding, most likely DF_b. There is good structural evidence of the presence of open DF_b folds in this area. The data from the mineral assemblages suggest that the broad arch of the anticlinorium could be DF_b in generation.

Figure 64c shows the distribution of key assemblages for DM_c mineral growth. DM_c is difficult to pick out in many samples and only those samples in which mineral growth can reasonably be interpreted as DM_c are used. The best samples are DV_a veins with post-DV_a alteration and DV_c veins. All of the observed DM_c plagioclase in this area is albite. DM_c assemblages also can include chlorite, chlorite-albite, or stilpnomelane. Paragonite, usually with muscovite, is often observed as an alteration product of plagioclase in DV_a and OV_b veins and is interpreted as DM_c. Typically calcite accompanies the white mica alteration products. There may have been variations in the conditions during DM_c growth in the area, but the mineral assemblages are not sensitive to changing conditions at such low grade.

The dominant and highest grade mineral growth in the traverse segment is OV_b. This is a large area in which garnet grade was attained during the late Ordovician. The garnet grade area to the north of the Winooski River within the same mapped garnet isograd appears to be also the result of O_b metamorphism. There is not much coverage of the area to the south of the Winooski River, but high grade OM_b growth also occurs along the Green Mountain axis in the Lincoln Mountain quadrangle.

DM_a growth is only slightly lower in grade than OM_b. DM_a growth is very extensive and is dominant in places where D_a deformation is most intense. No garnet grade DM_a growth has been documented along the Green Mountain axis north of the Winooski River. DM_a seems to be a wide spread biotite grade mineral growth generation in northwestern Vermont.

K. Mineral growth along the I91 traverse in northeastern Vermont

The locations described in this section are from along the I91 traverse that goes from St. Johnsbury Center in the northeast corner of the St. Johnsbury quadrangle to the town of Orleans in the southwestern part of the Memphremagog quadrangle, as shown in Figure 65. Most of the locations are roadcuts along Highway I91 which provide the best avail-

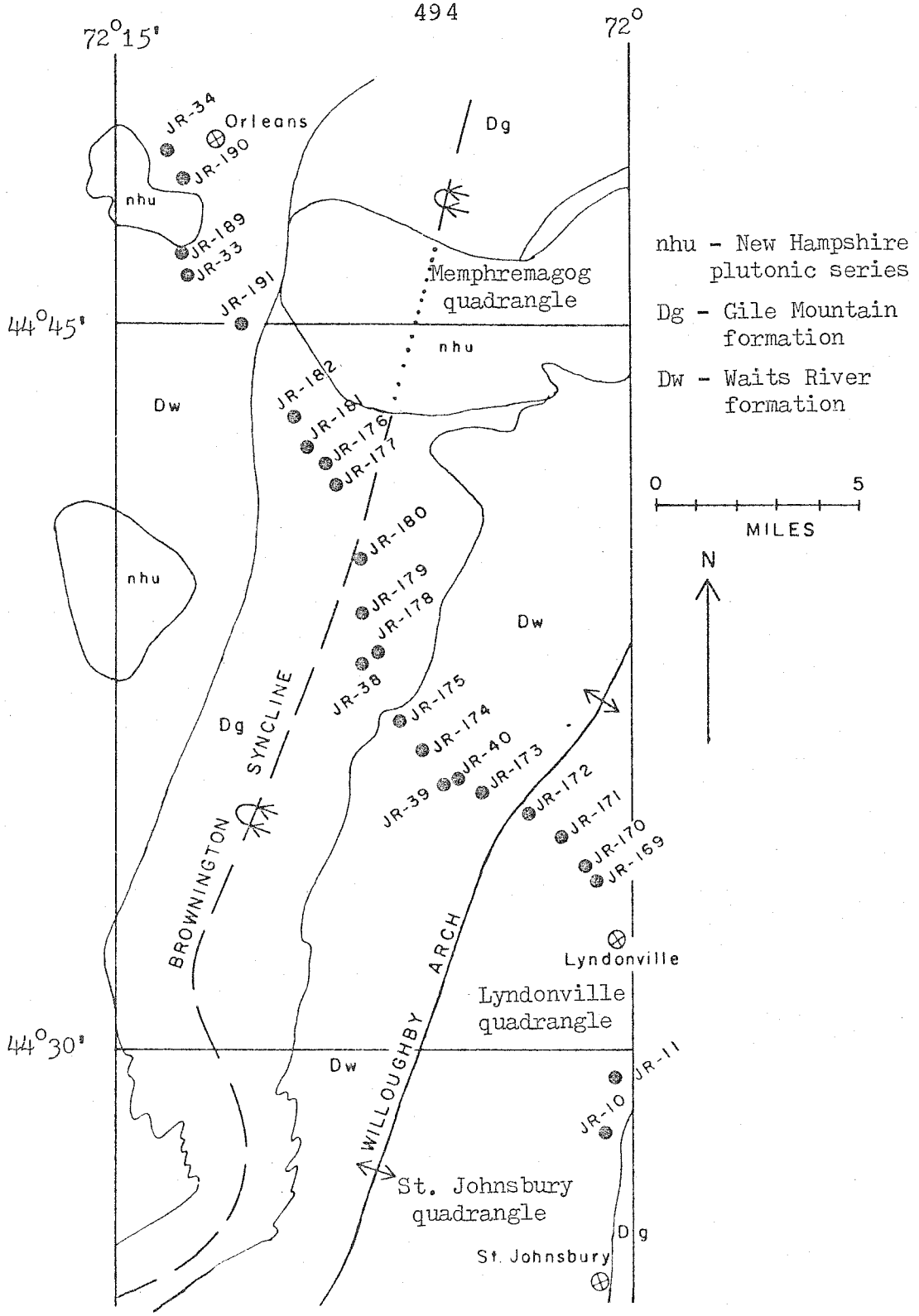

Figure 65 Map of locations along I91 traverse.

able exposures in the area.

The highest grade attained during all of the metamorphic events varies greatly in this area. In places, the transition from the lowest grade in the area, biotite grade, to the highest grade, sillimanite grade, occurs over an interval of only a few miles. The mapped isograds are shown in Figure 25-1 of Albee (1968), modified after Doll and others (1961). In many of the rocks from the traverse it is difficult to determine the maximum grade of metamorphism. The indicator minerals used are found in typical pelitic rocks. These minerals are not always developed in the calcareous rocks of the Waits River formation. Rocks of the Gile Mountain formation tend more often to have pelitic assemblages, but can also have fairly unusual compositions. Some of the Gile Mountain and Waits River rocks have 50% or more tourmaline and can also be highly graphitic. The most graphitic rocks are essentially opaque in thin section. Minerals such as cummingtonite, hornblende, idocrase, and so on were produced by progressive metamorphic reactions in the rocks along this traverse, but these minerals cannot be used within the framework of the grade indicating minerals of pelitic rocks.

As an aside, the common tourmaline-rich layers in the rocks exposed along the traverse are of some interest stra-

tigraphically. Such layers are found at locations JR-175, JR-176, JR-178, JR-190, and JR-191. The high boron content of these rocks suggests that there may have been evaporite layers interbedded with the parent rocks of the schists. Metamorphic veins in these rocks can be devoid of or have very little tourmaline in them so that it does not appear that the boron was brought in from elsewhere. The veins seem to be discontinuous in any event, which generally rules out the long-range transport of anything through the veins.

The traverse crosses two major structures, the Strafford-Willoughby arch and the Browning ton syncline. The Browning ton syncline is probably a DF_a fold which is deformed by the younger DF_b folds such as the Strafford-Willoughby arch. The area has been intruded by granitic bodies of the New Hampshire plutonic series. The traverse is essentially surrounded by such plutons. The larger plutons seem to have a strong effect on the isograd surfaces as the highest grade areas tend to be spatially related to these bodies.

There are various small scale structural features exposed at these locations. DF_a folds are often difficult to find, but are observed at some locations. In part the difficulty in observing DF_a folds rests in their large average wavelengths. Parallel to the axial planes of DF_a

folds are the well developed schistosity DS_a and abundant DV_a veins. Significant growth of minerals occurred during D_a. DM_a mineral growth can be observed everywhere except where obliterated by very strong D_b formation. DM_a assemblages are from biotite grade to garnet grade along the traverse.

The D_a structures have been deformed by the D_b elements, DF_b and DS_b. DF_b folds vary greatly in intensity from isoclinal to open folds. The style of DF_b folds can vary within single outcrops, but there is a significant regional variation. Going from the southeast to the northwest along the traverse, the typical style of DF_b changes from tight, isoclinal folds to open, asymmetric folds. Axial plane DS_b is generally a well developed schistosity where DF_b folds are isoclinal. DS_b associated with more open DF_b folds tends to be a spaced slip cleavage or may be absent. No veins are found which are parallel to DS_b. There is mineral growth parallel to DS_b in the host rocks where DS_b is well developed. All DM_b mineral growth seems to be biotite grade.

DF_b and DS_b are crosscut by DV_c veins. DV_c veins also crosscut semi-concordant granodiorite sheets apparently related to the New Hampshire plutonic series. The DV_c veins are apparently cogenetic with mineral growth in the host

rocks. DM_c mineral growth ranges from biotite grade to staurolite grade in the rocks along the traverse. DV_c veins are folded by open DF_d folds. A number of minor vein generations are also present in the area. The minor veins do not seem to be related to significant mineral growth in the host rocks and generally have very simple assemblages.

Five samples from four locations along this traverse have been analyzed with the electron microprobe. Three of the samples are from DV_a veins, one is from a DV_c vein, and the fifth sample is from host rock only. The analyzed rocks provide a reasonable sampling of the diversity of observed relationships.

JR-190

Location JR-190 is in the Waits River formation about 0.2 miles from the contact of a small pluton of the New Hampshire series. The location is near the northern end of the traverse. One sample, JR-190-A, has been analyzed; this is from a DV_c vein and the adjacent schist. The sampled vein is fairly typical of the DV_c veins in northeastern Vermont. Veins of this generation are much more abundant in northeastern Vermont than anywhere else in the study area. Here DV_c veins are associated with prograde metamorphism in the host rocks which can be as high as

sillimanite grade near the New Hampshire series plutons. This is in contrast to the western part of the study area where DV_c veins are scarce and are associated with sub-garnet grade alteration of the pre-exisiting host rock minerals. Despite the regional differences in DV_c veins, they occupy the same structural position everywhere.

JR-190-A is from a 4 centimeter wide DV_c vein which is very gently warped by DF_d folds. The vein is medium- to coarse-grained and consists largely of plagioclase, quartz, and muscovite. This and other DV_c veins in the area have an appearance in outcrop very similar to pegmatite veins of igneous origin. The bulk chemistry of the veins and the relationships between the vein mineral growth and the well-developed DM_c mineral growth in the host rocks shows that they are not pegmatites. The host rock in JR-190-A is a dark grey, very fine-grained biotite-rich schist. DS_a is fairly well developed and is sharply crosscut by the vein. There is a 1-3 millimeter zone in the host rock along the vein contact in which coarsening of quartz and plagioclase has occurred. DS_a is still preserved by biotite and muscovite grains with preferred orientation in this zone. There is no border zone developed within the vein.

The assemblage in the host rock is quartz-muscovite-biotite-staurolite-plagioclase-ilmenite-pyrrhotite-chal-

copyrite-tourmaline. In another host rock, JR-190-D, is the assemblage quartz-muscovite-biotite-staurolite-andalusite-plagioclase. Muscovite and biotite grains are of two textural types. Fine-grained muscovite and biotite have preferred orientations parallel to DS_a and are probably DM_a in generation. Somewhat coarser biotite and muscovite grains have no preferred orientations and crosscut DS_a; the grains are probably DM_c. DM_c biotite tends to form clusters of grains around ilmenite grains that are parallel to DS_a. DM_a ilmenite grains were the preferred nucleation site for DM_c biotite, and the ilmenite seems to have been resorbed at the expense of biotite growth. In hand sample, the biotite clusters appear to have preferred orientation parallel to DS_a. The individual grains in the clusters have no preferred orientation. The apparent orientation of the biotite clusters is inherited from the ilmenite.

Plagioclase grains in the host may also be of two textural types. Some grains are very fine-grained and tend to be elongate parallel to DS_a. Other grains, less abundant, are somewhat coarser and do not show preferred elongation. The first type are probably DM_a and the second are DM_c. DM_c plagioclase is associated with DM_c biotite. The staurolite grains in JR-190-A are euhedral and have no preferred orientation. These are probably DM_c. The staurolite is

unusual in that it is very fine-grained, much finer-grained than the associated DM_c biotite. The andalusite in JR-190-D also appears to be DM_c. There is no evidence of any DM_b growth in JR-190-A. DS_b slip cleavage is not developed in JR-190-A and is only poorly developed in some of the other samples from JR-190.

DM_a mineral growth in this sample has been very heavily overprinted by DM_c growth. It is very difficult to determine with certainty the complete DM_a assemblage. Preserved in the rock is the DM_a assemblage quartz-muscovite-biotite-plagioclase-tourmaline. Other DM_a minerals may have been eliminated by DM_c growth. This is a problem encountered in many samples in which DM_c growth is fairly high grade or in which D_b deformation was intense. However, DM_c growth in the samples from this traverse never completely obliterated the pre-existing features and assemblages.

One feature of DM_c overprint in the host rock is the apparent removal by reaction of what looks like very fine-grained graphite. Graphite is present throughout most of the host rock. Individual grains or clusters tend to have preferred orientation parallel to DS_a. In the coarsened zone next to the vein and associated with DM_c mineral growth elsewhere in the host rock are areas which are free of the fine-grained graphitic material.

The assemblage in the DV_c vein in JR-190-A is quartz-muscovite-garnet-plagioclase-pyrrhotite-tourmaline-apatite-chlorite (alteration of garnet). A few euhedral grains of garnet occur and these have been partly to wholly retrograded to chlorite and muscovite. Most of the muscovite in the vein is primary DM_c growth. The retrogradation of the garnet occurred after DV_c growth and may therefore be a later mineral growth generation. Minor retrograde effects on garnet and DV_c vein plagioclase are observed elsewhere which suggests that there is another mineral growth generation. This late, low grade growth has been tentatively assigned to a separate, post-DM_c generation which is called DM_e. There is no structural control on the age of DM_e other than it must be post-DV_c. Staurolite has not been observed in the vein, nor has garnet been observed in the host rock. However, the DM_c assemblages in the host rock and in the vein are compatible with each other.

The compositions of host and vein muscovite are shown in Figure 66. Analyzed DM_c host rock muscovite has a limited compositional range. There is a trend of perhaps slightly decreasing Si content. The compositional range for DV_c vein muscovite is much larger. Most of the variation in vein muscovite is with respect to Mg/Mg+Fe. There

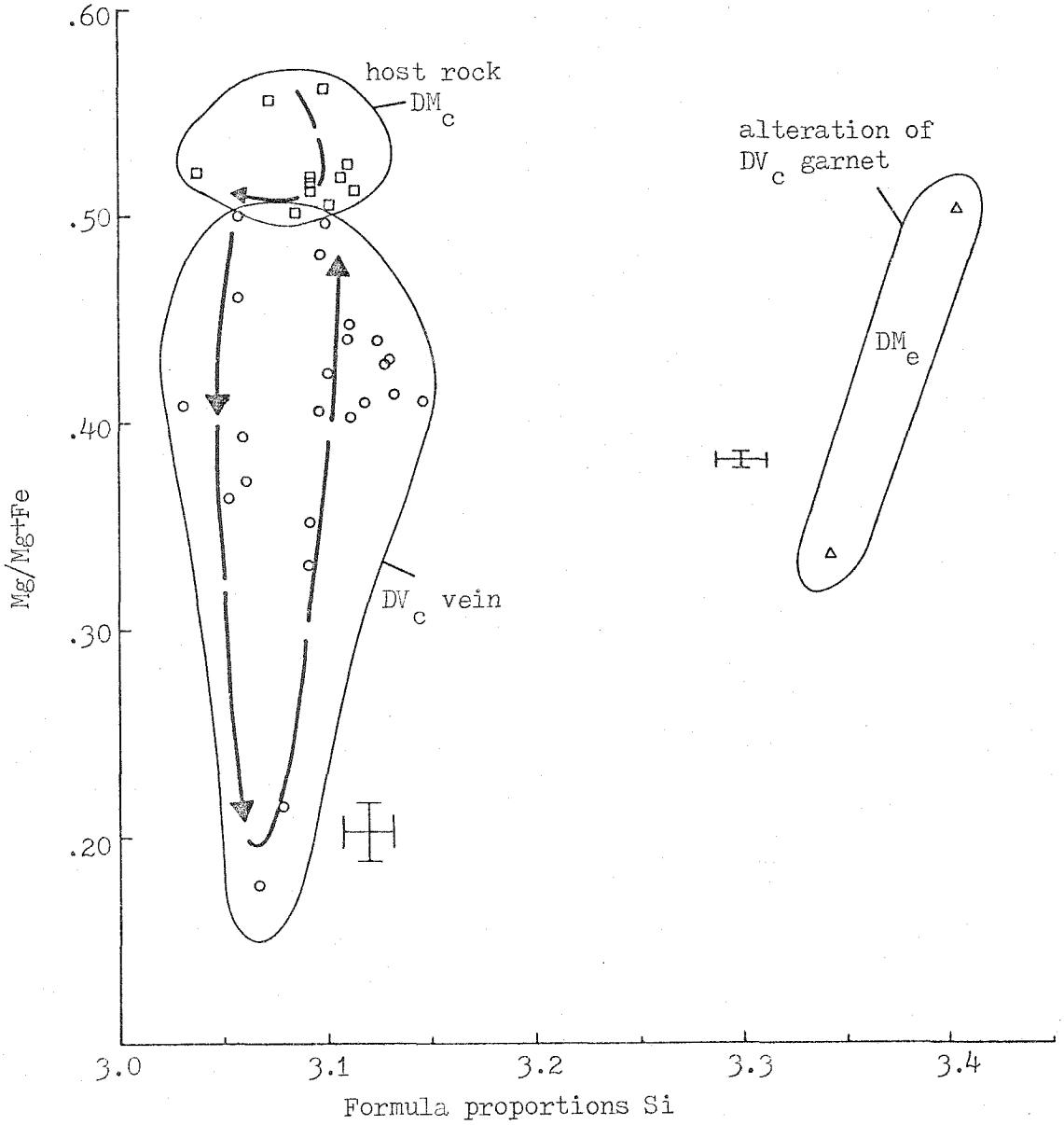

Figure 66 Plot of Si vs. Mg/Mg+Fe for muscovite in JR-190-A.

is an overall trend of slightly increasing Si from core to rim. A possible interpretation of this diagram is that host rock muscovite grew first, then the vein began to form. Host rock growth ceased as the vein growth began. Two points shown with high phengite contents are from muscovite formed by the retrograde alteration of garnet and are therefore DM_e.

DM_c plagioclase compositions are shown in Figure 67. The overall compositional range for vein and host rock plagioclase is from $An_{5.5}$ to $An_{28.3}$. The ranges of vein and host rock plagioclase are similar but the trends are exactly opposite. Host rock grains are zoned with increasing An content from core to rim and vein plagioclase grains have decreasing An content from core to rim. The timing of host rock and vein growth suggested by the plagioclase trends is the same as that suggested by muscovite. The host rock plagioclase grew first, then the host rock growth stopped and the vein growth began. The host rock growth was up-grade and the vein growth was down-grade. This is similar to the timing and path of grade observed in the OV_b vein of JR-5-A. Of course, the trends of muscovite and plagioclase could be interpreted as showing growth first in the vein and then in the host rock. This requires down-grade growth in the veins to be followed by up-grade growth

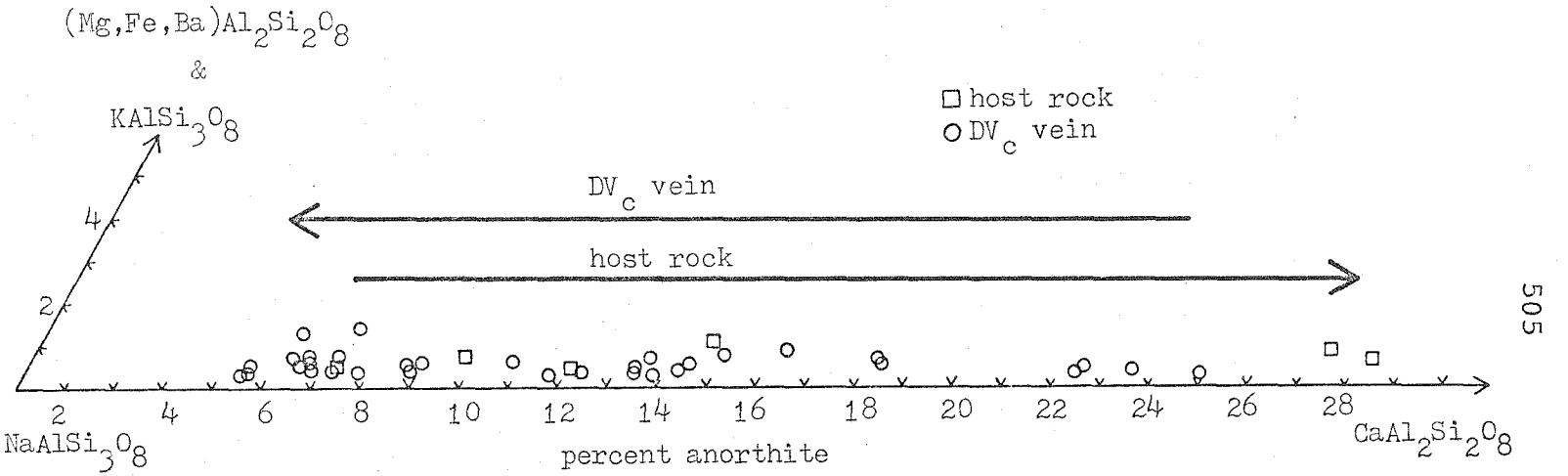

Figure 67 Compositions of plagioclase in JR-190-A.

in the host rock which seems less likely.

Analyses from two grains of garnet in the DV_c vein are shown in Figure 68. Two points from the rim on one side of a grain fall off the trend defined by the other points. The overall trend is consistently decreasing Mn and increasing Fe and Mg from core to rim. Zoning of Ca in this garnet contrasts sharply with the irregular, oscillatory Ca-zoning in the OM_b garnet described in the previous section. Ca tends to increase from core to rim, with a slight reversal near the rim. The Ca content is relatively low compared to garnet in other samples. The trend of Mn-zoning is the same in this garnet as for garnet in other samples which appears to have grown during progressively increasing grade. The similarity in the trend of Mn regardless of the relative path of the system with respect to grade strongly suggests that the observed Mn-zoning has resulted from depletion effects.

Compositions of host rock biotite are shown in Figure 69. Most of the points are from grains without preferred orientations and which appear to be DM_c. One analysis is from a grain with preferred orientation parallel to DS_a. Although it might be surprising if DM_a biotite preserved its original composition through DM_c overprint, this one analysis is compositionally different from the others. No

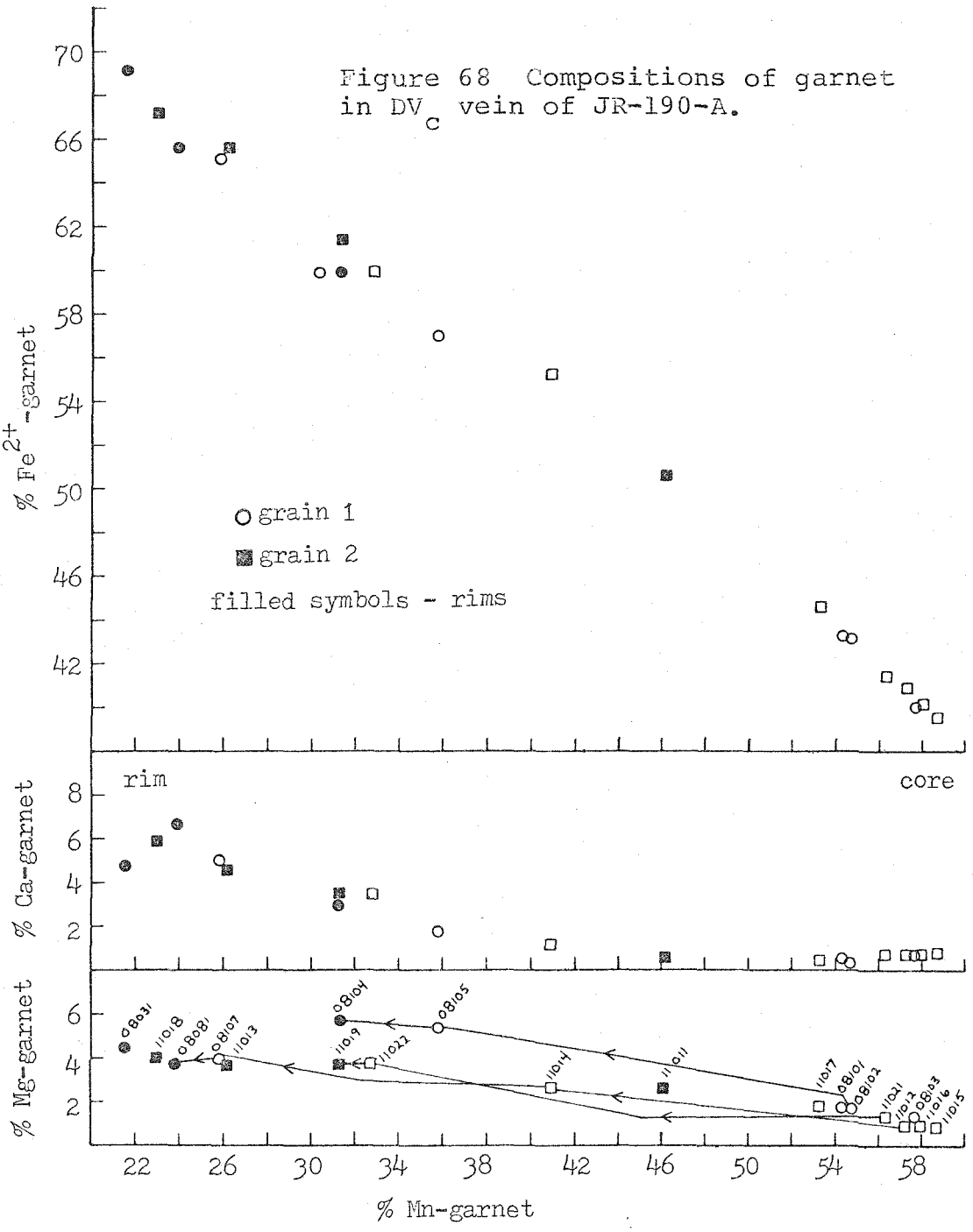

Figure 68 Compositions of garnet in DV_C vein of JR-190-A.

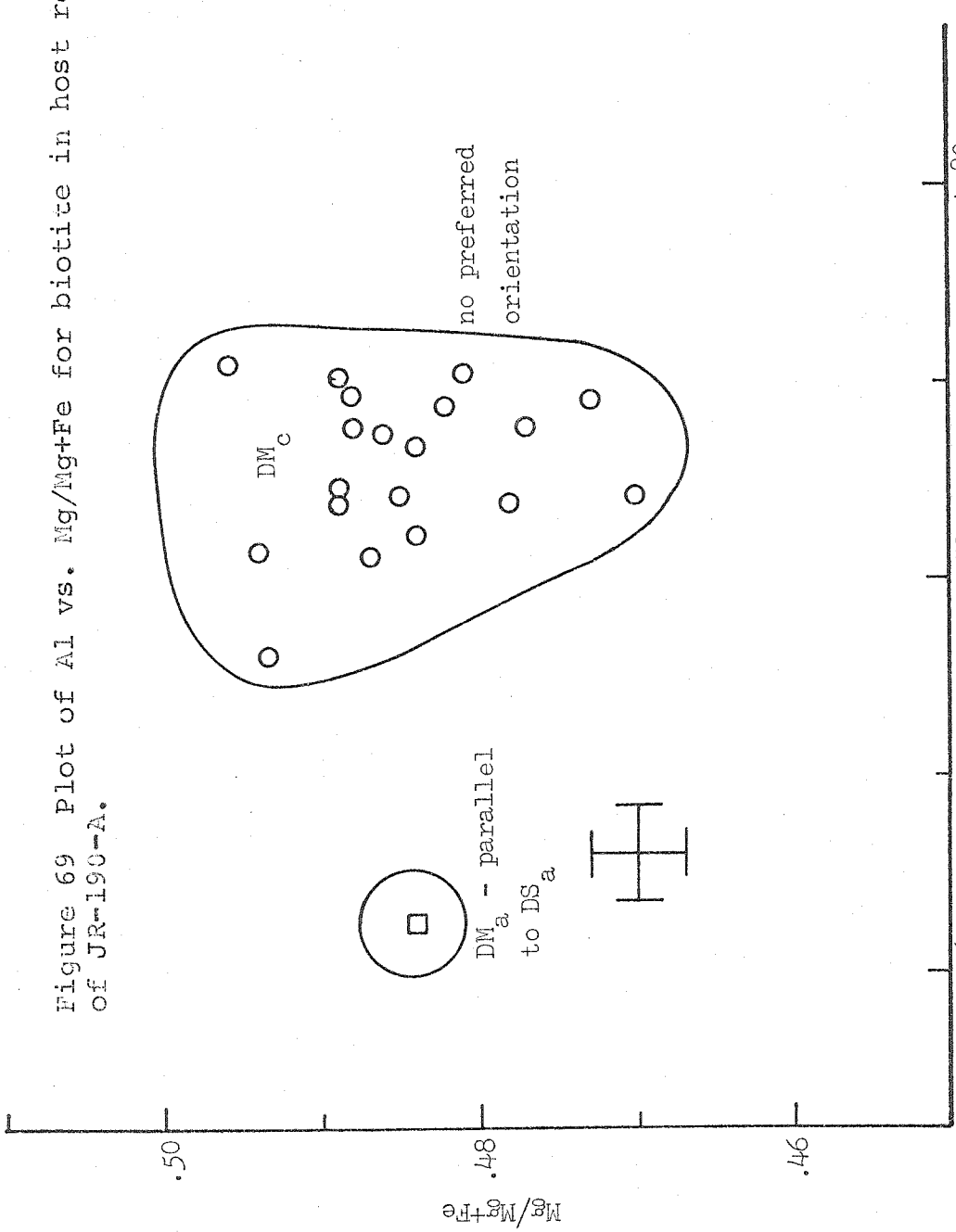

Figure 69 Plot of Al vs. Mg/Mg+Fe for biotite in host rock of JR-190-A.

trend has been defined for the DM_c biotite.

The evidence from JR-190 suggests that DM_c growth was staurolite-andalusite grade at its maximum. Host rock growth occurred during increasing grade. The DV_c vein began to form at about the metamorphic peak and vein growth continued as grade decreased. The overprint on DM_a growth was not so extensive that all DM_a mineral grains were completely destroyed or recrystallized. The available evidence suggests that DM_a growth was biotite grade here. Late alteration of DV_c vein garnet and plagioclase may be a separate mineral growth generation, DM_e.

JR-11

Location JR-11 is an exposure of amphibolite of the Standing Pond member of the Waits River formation interlayered with Waits River schist. It is near the southern end of the traverse. Within the host rocks are DV_a veins, some of which have suffered strong D_b deformation. The amphibolite host rock has fairly well preserved pillow structures in it and is not as strongly deformed as the veins. The two analyzed samples, JR-11-D and JR-11-F, are from a DV_a vein within pillow amphibolite.

The DV_a vein from which the two samples are taken is strongly deformed by DF_b folding and the associated forma-

tion of pinch-and-swell structures. Sample JR-11-F is from the center of a pod-shaped portion of the DV_a vein. JR-11-D is from 20 centimeters away at the contact between the host rock and the vein. The original dimensions of the vein are hard to determine due to the deformation. It was originally at least 3 meters long, probably longer, and perhaps 10 centimeters wide. The vein is now comprised of pods connected by thin, neck-out portions of the vein. The largest pod is roughly 50 centimeters wide.

The DV_a vein is generally coarse-grained in the center of the pods, but fine-grained and highly granulated at the vein margins. A "ground-up" zone extends from near the host rock wall into the vein a few centimeters or so. There are no obvious effects of the same nature on the host rock. Areas of granulated material also occur in other parts of the vein. Apparently much of the deformation was accomplished by translation and rotation of the small grains formed by granulation.

JR-11-D and JR-11-F are very complicated samples. Part of the complexity arises because of the high degree of deformation. There are also complex textural relationships and unusual mineral assemblages. The interpretation of these samples in part relies upon the observations of D_b deformation and mineral growth and DM_c mineral growth

at nearby locations. There is good evidence within the two samples, but ambiguities about the identification of mineral growth generations are resolved using the knowledge of the other samples.

The mineral assemblage in the DV_a vein is quartz-calcite-plagioclase-clinozoisite+epidote (continuously zoned between the two)-hornblende-muscovite-paragonite-biotite -chlorite-ilmenite-pyrrhotite-chalcopyrite. Chlorite is only in sample JR-11-F. Hornblende, biotite, pyrrhotite, and chalcopyrite are only in JR-11-D. Quartz and calcite are the dominant minerals, followed by plagioclase and clinozoisite. This is the only sample of the 40 samples studied with the microprobe that contains clinozoisite; epidote is found in the others which contain an epidote-family mineral. There are single crystals and bundles of elongate crystals of clinozoisite-epidote. The plagioclase ranges in composition from oligoclase to anorthite. In areas of JR-11-F, calcite, clinozoisite, anorthite, oligoclase, paragonite, muscovite, and quartz are all in close proximity to each other. This unusual assemblage by itself strongly suggests that there is more than one generation of mineral growth present. There is textural evidence that there are in fact three generations: DM_a, DM_b, and DM_c.

The assemblage in the host amphibolite is quartz-calcite-hornblende-clinozoisite+epidote (continuous zoning) -plagioclase-biotite-ilmenite-pyrrhotite-chalcopyrite. The amphibolite is not a typical mafic rock in bulk composition as up to 50% of it is calcite. DS_a is not well defined in this sample, although in another sample at the vein-host contact DS_a is clearly present. The contact is parallel to DS_a in this other sample, JR-11-G. The amphibolite surrounding this vein and elsewhere in the outcrop is very fine-grained.

Compositions of plagioclase in the DV_a vein and host amphibolite are shown in Figure 70a and 70b. Grains in the host rock are zoned from core to rim with increasing, then decreasing An content as shown in Figure 70b. These appear to be DM_a growth. Some grains in the adjacent vein have a similar compositional range and have compositional trends similar to the latter part of the host plagioclase trend. Within the ground-up zone in JR-11-D there are also grains which are zoned from core to rim with increasing An content and which have much more calcic compositions than the other plagioclase. In the middle of the vein in sample JR-11-F are two distict textural types of plagioclase. Euhedral grains have compositions in the range of DM_a host rock plagioclase and have the same trend as the less calcic vein

Figure 70a Compositions of plagioclase in DV_a vein of JR-11-F.

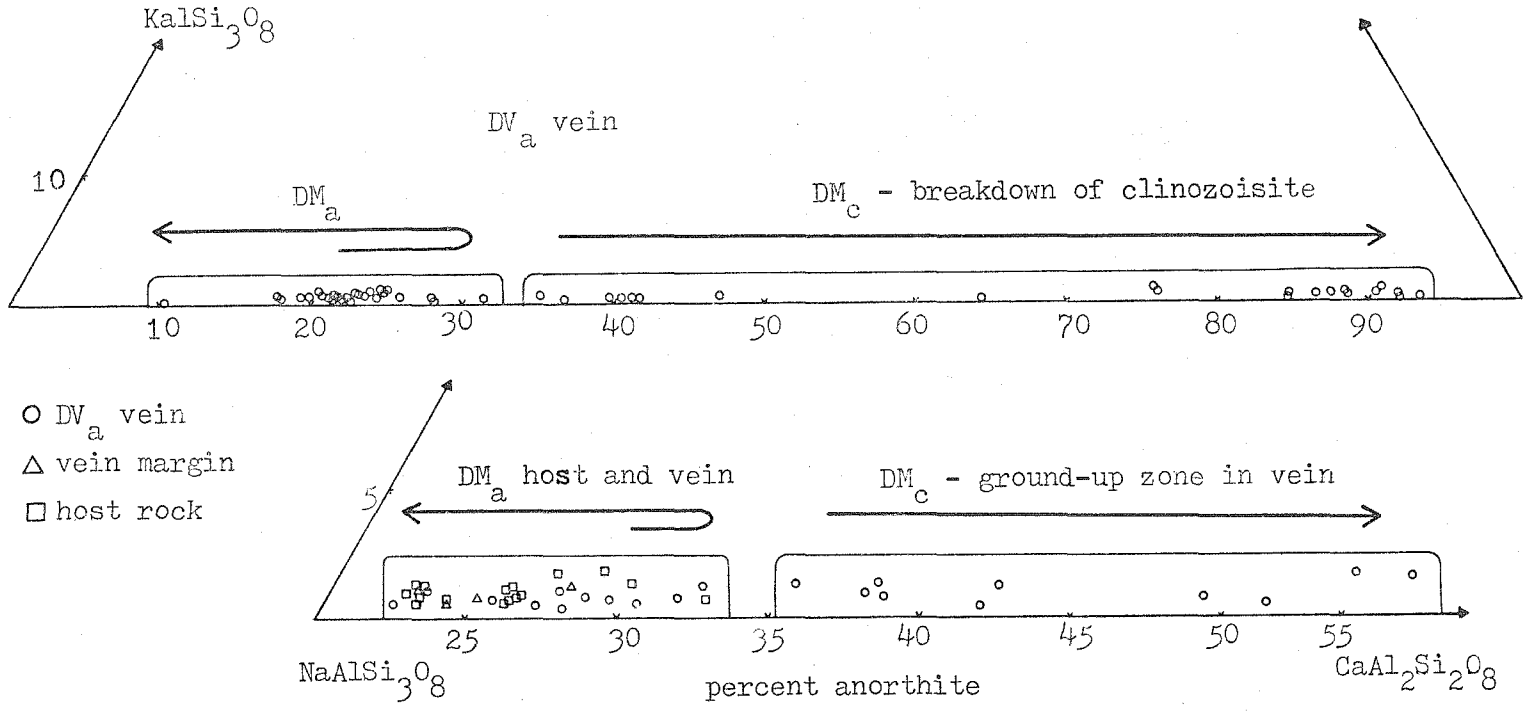

Fig 70b Compositions of plagioclase in DV_a vein and host rock of JR-11-D

plagioclase in JR-11-D. The euhedral grains seem to represent primary vein growth. All of the plagioclase with compositions less calcic then about An_{35} seems to be DM_a, both in the host rock and vein. The most calcic DM_a compositions might be as high as An_{40}. The other plagioclase in JR-11-F is associated with the breakdown of clinozoisite. Remnant cores of clinozoisite are within many of these grains. In areas where the clinozoisite was granulated by D_b deformation, there is also reaction product plagioclase, but the plagioclase appears to have not been affected by the granulation. The range of compositions for this plagioclase is from about An_{35} to An_{93}. The calcic plagioclase appears to be post-D_b and therefore is probably DM_c. This is in accord with the evidence from DV_c veins in the area that DM_c growth can be fairly high grade. The calcic plagioclase in the ground-up zone in JR-11-D appears to be of the same generation. It also is not affected by the granulation.

Optical discontinuities are preserved in plagioclase grains in the DV_a vein. The grains which were investigated turned out to have DM_a composition cores and DM_c rims. The discontinuity was between the two generations. For instance, the compositions on either side of optical discontinuity in one grain were An_{36} and An_{87}. A number of

analyses have compositions between these two and it seems unlikely that this represents a solvus. However, there may be grains which are entirely DM_c in generation that have discontinuities which do represent a solvus. Such a gap has not been demonstrated in this sample and further work is needed. The breaks in the compositions could represent incomplete sampling. A gap must be found in a single grain, such as was found for the peristerites in the last section.

There is no evidence of DM_b plagioclase, but there does appear to be some pre-DM_c alteration of DM_a plagioclase to calcite and paragonite. Within a ground-up area in JR-11-F is DM_a plagioclase which is altered partly to calcite and white mica. The DM_a plagioclase and alteration is overgrown by DM_c plagioclase. Paragonite is found as grains which are only within the ground-up areas. All of the pargonite and a little of the calcite in the vein appear to be DM_b.

Further evidence of DM_b being retrograde in nature is found in sample JR-11-H. There are fractures which seem to be DS_b in this amphibolite sample. Within the fractures are apparent retrograde products of the breakdown of DM_a hornblende. Grains of chlorite, biotite, quartz, and calcite occur in these fractures, which appear as thin microveinlets.

These are the closest thing to a DV_b vein that has been found. There is evidence in other samples from nearby locations that mineral growth in the host rocks parallel to DS_b is always sub-garnet grade.

Figure 71 shows the compositions of analyzed calcite points in sample JR-11-F. The calcite compositions fall into two groups. Most of the points are from coarse-grained calcite that seems to represent primary vein growth and is probably DM_a. The compositional trend of this calcite is increasing, then decreasing Fe+Mg+Mn solid solution from core to rim. No ankerite occurs in the sample, so the substitution is not buffered. There is also fine-grained calcite associated with paragonite and the breakdown of DM_a plagioclase. This calcite is probably DM_b and has compositions which are more nearly pure calcite. No calcite in JR-11-F appears to be DM_c, but there isn't any evidence of calcite breakdown during DM_c growth. There are no reaction products formed at the expense of the coarse DM_a calcite. *This calcite is seen to be in contact with all of the other* minerals. Apparently extensive breakdown of clinozoisite occurred without any effect on calcite, suggesting a high f_{CO_2} during DM_c overprint.

Compositions of analyzed amphibole are shown on various plots in Figures 72a, 72b, and 72c. All of the amphibole

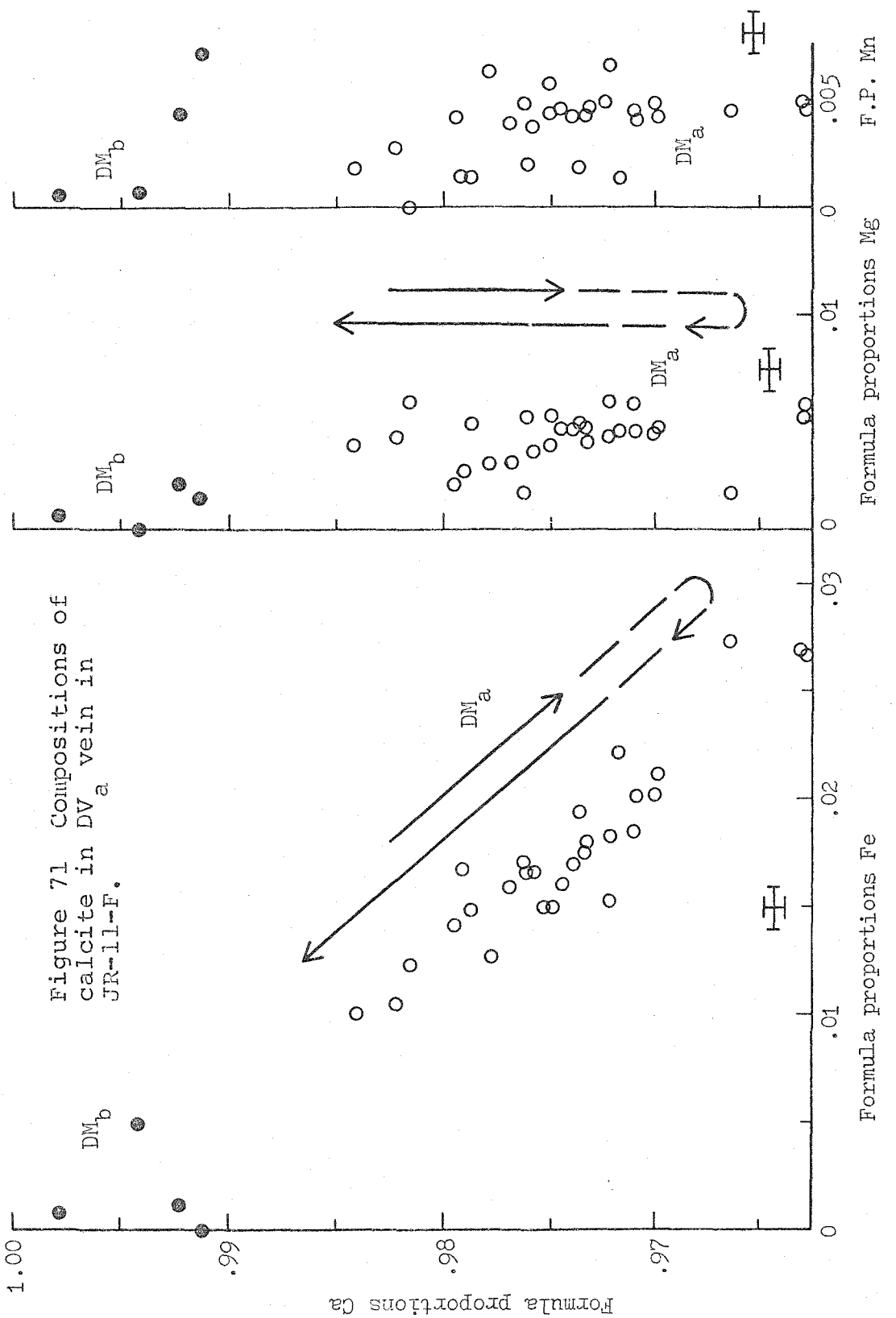

Figure 71 Compositions of calcite in DV_a vein in JR-11-F.

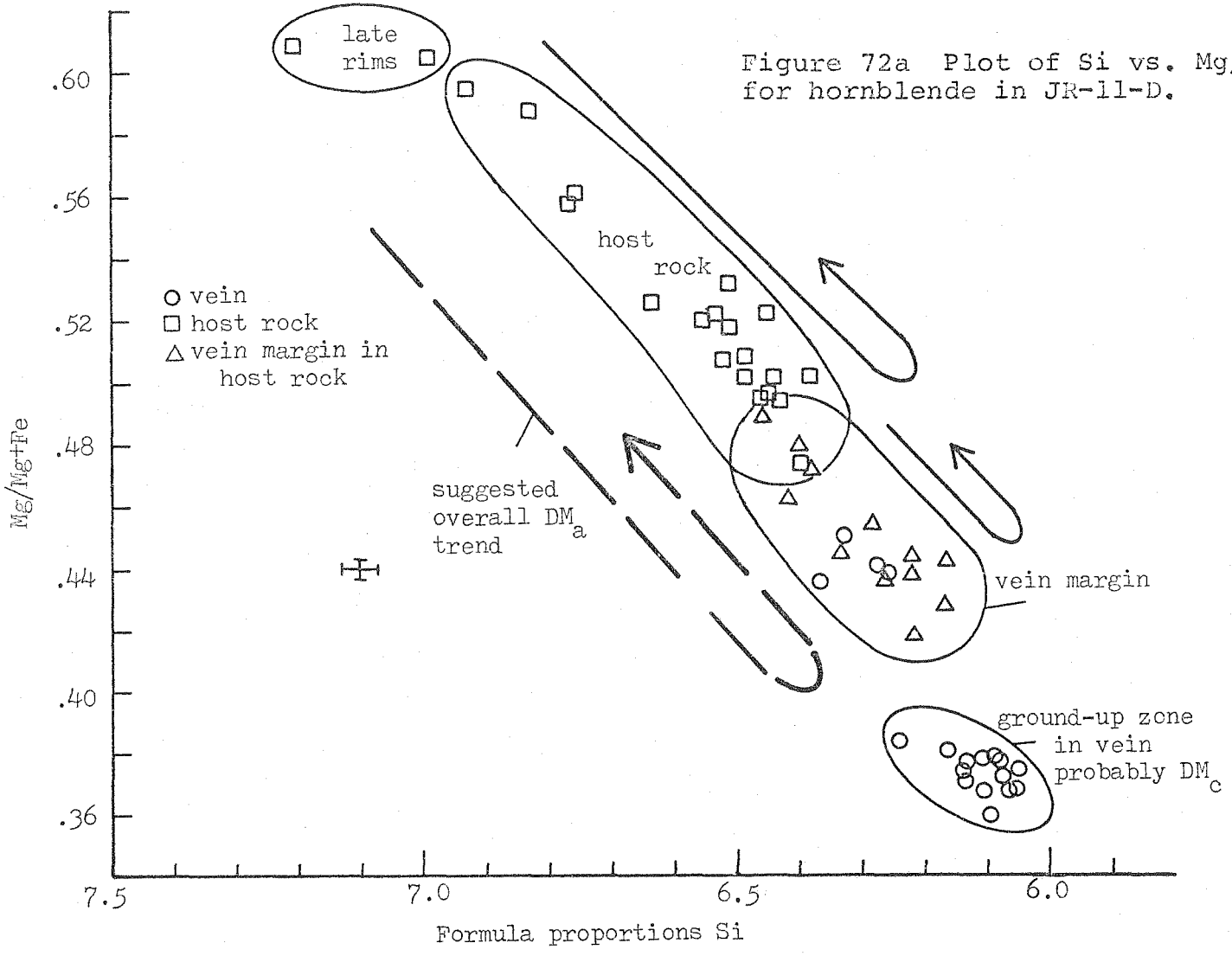

Figure 72a Plot of Si vs. Mg/Mg+Fe for hornblende in JR-11-D.

Figure 72b Plot of Si vs. $Al^{VI}+Fe^{3+}+Ti+Cr$ for hornblende in JR-11-D.

Figure 72c Plot of Si vs. Na+K for hornblende in JR-11-D.

Figure 72b

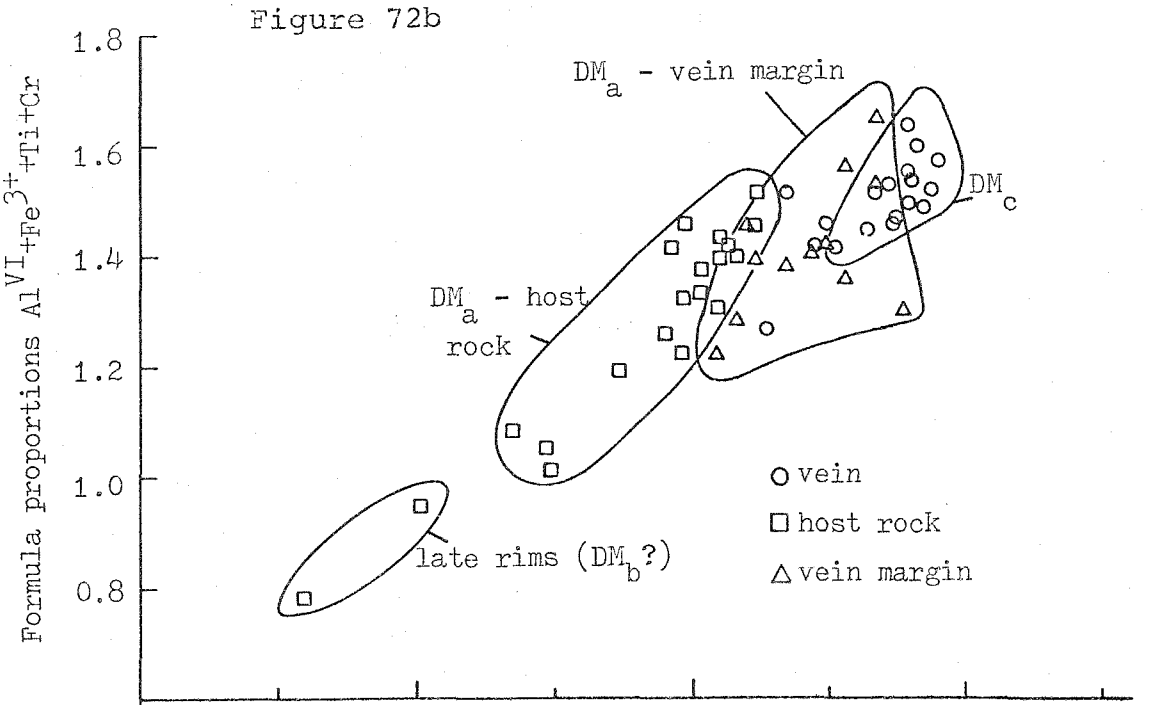

Figure 72c

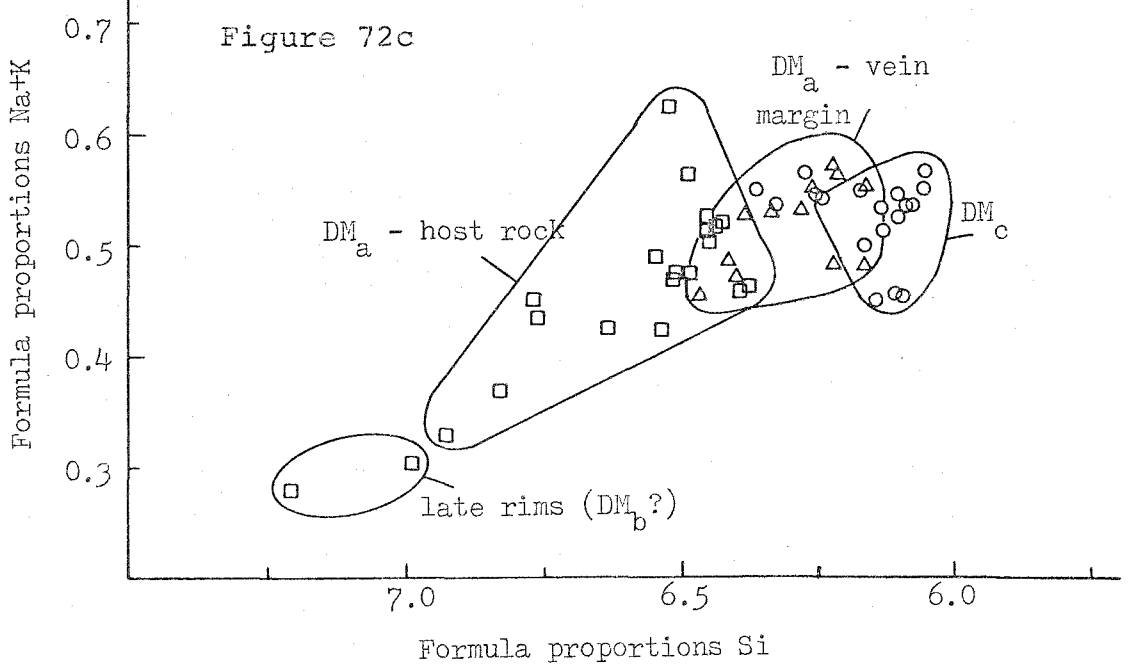

is green hornblende. Formula proportions Si vary from nearly 6.0 to about 7.2 and the compositions can be divided into four groups based upon textural relationships. Hornblende in the host rock which is at least 0.5 centimeters away from the contact with the vein has a fairly wide range of compositions as shown on the diagrams. The trend for these grains is decreasing Si and Mg/Mg+Fe from core to rim. There is a late reversal and a slight increase in Si and Mg/Mg+Fe. At the outer rim of the grains are fairly distinct zones of hornblende which is more actinolitic in composition and slightly lighter in color. Two analyses are shown from these late rims. A third group of analyses is from the DV_a vein where the material is not granulated and from the host rock immediately adjacent to the vein, shown as the vein margin in the diagrams. These analyses only partly overlap with the compositional range of the host rock grains. They have a similar trend in that there is decreasing Si and Mg/Mg+Fe and then a reversal. Distinctly different, as best shown in Figure 72a, is the hornblende in the ground-up zone of the DV_a vein in JR-11-D. These have the lowest values of Si and Mg/Mg+Fe. This last group is closely associated with plagioclase thought to be DM_c.

Most of the hornblende in the host rock is probably

DM_a. The only possible exceptions are the more actinolitic late rims. The rims appear to be fairly distinct optically and therefore may represent later growth. The most likely generation for the rims is DM_b, although they could be late DM_a. The hornblende grains at the vein margin and those in the vein with similar compositions also appear to be DM_a. The grains are euhedral and similar in form to other host rock grains. No actinolitic rims were found on the vein margin hornblende grains. This may be a sampling problem as optically such rims appear to be present. The last group of compositions, from anhedral, irregular grains in the ground-up zone, probably represent DM_c recrystallization of DM_a hornblende that was granulated by D_b deformation. The close association of DM_c plagioclase, formed by the breakdown of clinozoisite, and this chemically distinct hornblende is good evidence that this is the case. Without inventing another mineral growth generation, this seems to be the only reasonable explanation available. The very fine-grained nature of the hornblende makes the interpretation of all of these groups somewhat more difficult. For instance, the late rims are very thin and therefore difficult not only to analyze, but also to observe in many grains.

The DM_a hornblende preserves a compositional trend that seems to indicate increasing, then decreasing grade. It is

not clear that part of the reversal in DM_a is not due to effects from the overprinting that produced the more actinolitic rims. The vein hornblende probably started to form near the peak of DM_a metamorphism, similar to the history suggested by plagioclase zoning. DM_b overprinting, somewhat lower in grade than DM_a, may have produced the thin rims. Apparently the highest grade amphibole in these samples is the DM_c hornblende in the ground-up zone of the vein. Little compositional variation is present in this group so that the path of metamorphism is not suggested. Zoning in the plagioclase suggests increasing grade with time during DM_c growth. However, given the obvious evidence of nonequilibrium, such as the coexistence of DM_b paragonite and DM_c anorthite, the zoning patterns may not be very meaningful for DM_c growth.

There is a great deal of variation in the compositions of muscovite in the vein, as shown in Figure 73. The compositions fall into three textural groups. A few large grains seem to represent primary vein growth and the cores of these grains probably preserve DM_a compositions. This group has the lowest Mg/Mg+Fe values and generally has decreasing phengite substitution from core to rim. A second group of compositions are from separate grains associated with DM_c plagioclase and from the rims of DM_a grains.

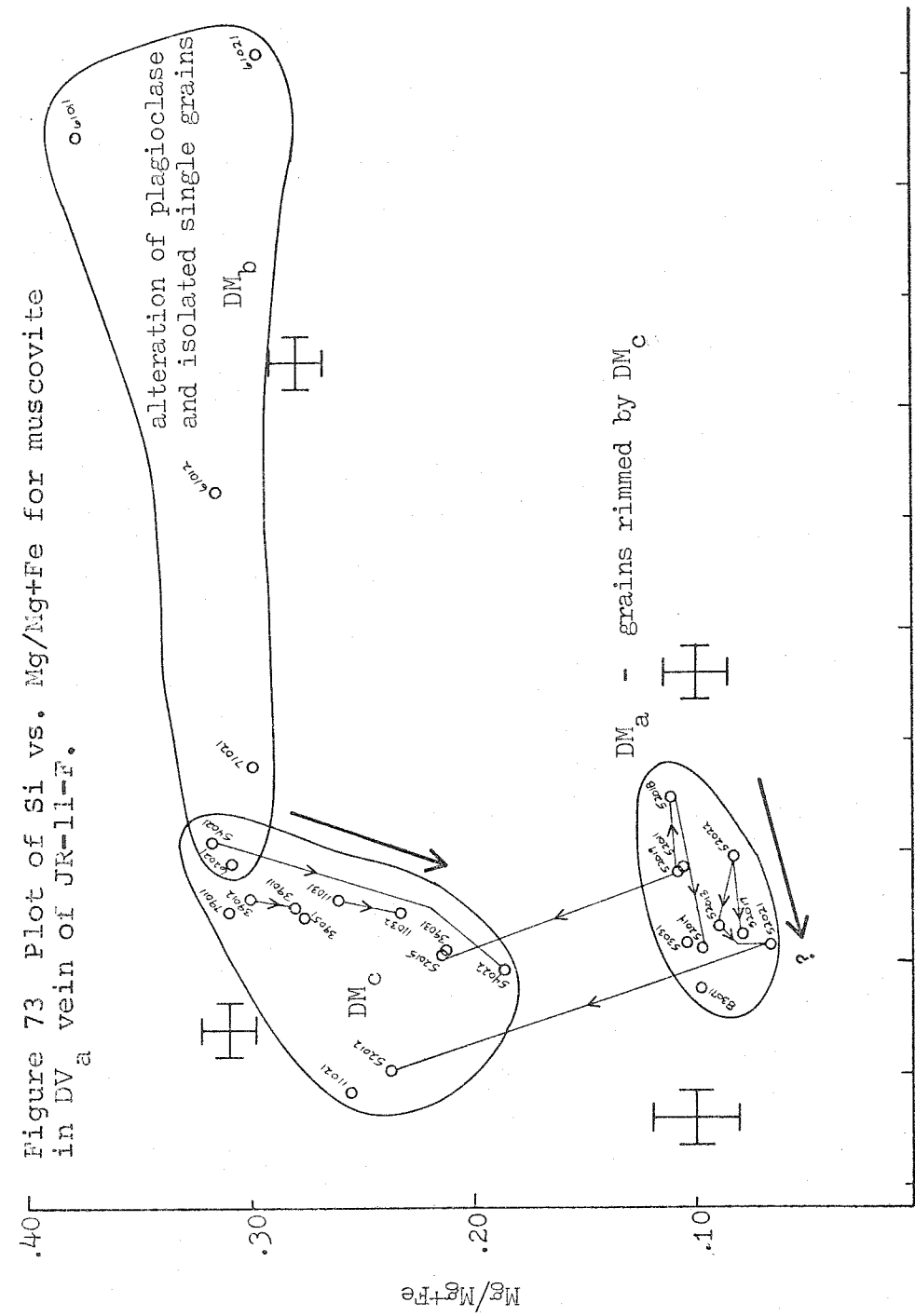

Figure 73 Plot of Si vs. Mg/Mg+Fe for muscovite in DV a vein of JR-11-F.

These appear to be DM_c. The general trend of most of the DM_c muscovite is decreasing phengite substitution and decreasing Mg/Mg+Fe. The third group consists of grains apparently associated with the alteration of DM_a plagioclase plus separate small grains in fractures within vein quartz. Two of the analyses are from grains associated with calcite which was tentatively identified as DM_b. This muscovite may be DM_b and/or DM_e. DM_a and DM_c muscovite are fairly straightforward, but this other muscovite cannot be unambiguously identified.

The evidence from the various minerals suggests that DM_a mineral growth was at least garnet grade. Garnet does not occur in any samples from the location, but the hornblende and plagioclase compositions are of some use in indicating the grade. Hornblende with similar Si contents from other samples is associated with at least garnet grade growth in nearby pelitic rocks. The apparent vein assemblage for DM_a growth was quartz-calcite-clinozoisite-plagioclase (oligoclase-andesine)-hornblende-muscovite-chlorite-biotite-pyrrhotite-ilmenite-chalcopyrite. The assemblage in the host rock was similar except that no muscovite or chlorite has been observed in the amphibolite host in JR-11-D.

The evidence of D_b deformation is clear, but the evi-

dence of DM_b growth is much more ambiguous. It appears likely that the paragonite, some of the calcite, and perhaps some of the muscovite is DM_b. The rims on host rock hornblende may also be DM_b. However, the suggested DM_b amphibole is hornblendic in composition. It seems unlikely that the hornblende could be associated with the alteration of plagioclase to paragonite and calcite. It may be that the compositions of DM_a plagioclase were unstable with the DM_b growth. Another possibility is that DM_b growth occurred over a range of conditions. Other mineral growth seems to have occurred over wide ranges of conditions both in these samples and in others. Some of the alteration of plagioclase might be DM_e. DM_e growth was seen as late retrogradation of DM_c mineral growth in sample JR-190-A. Some altered DM_a plagioclase is overgrown by unaltered DM_c plagioclase; this relationship offers good evidence of DM_b alteration. DM_b growth was lower grade than DM_a or DM_c.

Perhaps the highest grade mineral growth is DM_c. The DM_c minerals in the vein are plagioclase (andesine-anorthite), muscovite, and hornblende. Some DM_c biotite growth may or may not be present; there are not enough data. During DM_c growth, the breakdown of DM_a clinozoisite in the DV_a vein was extensive. The grade of DM_c cannot be established with certainty, but it surely must be garnet grade or higher.

DM_c growth and recrystallization were most effective in the areas of the vein that were highly granulated by D_b deformation. DM_c mineral grains were not affected by the deformation.

None of the overprinting events were intense enough or long enough in duration to completely reconstitute the vein or the host rock. There seems to be little effect of DM_c on the host rock and the possible DM_b mineral growth there is minor. The effects of overprinting are best developed where the kinetics of recrystallization were aided by large surface areas on small grains produced by granulation. The high grade character of DM_c growth coupled with the limited extent of its effects strongly suggest the DM_c growth occurred over a relatively short period of time. If DM_c growth had continued for as long as DM_a growth, surely rocks would have been largely reconstituted. In many samples in the area, DM_c growth is high grade but limited in extent. The high grade conditions during D_c were apparently maintained for only a short period of time throughout the area. It is not possible at present to determine the exact time scale involved in a single event. Certainly in these samples, the time was not long enough for the system to come to complete equilibrium.

The question of time scale for DM_b growth is a differ-

ent problem. Because DM_b growth is lower in grade, there may have been a relatively long time during which the highest grade DM_b conditions were maintained. Retrograde reactions may easily be impeded by low partial pressures of the needed volatile constituents. The general lack of DV_b veins may suggest that the total fluid pressure was low during D_b metamorphism.

There is one side issue of interest for which evidence is found in JR-11-F. Generally, concentrically zoned grains of a mineral are thought to have grown progressively from core to rim. Compositional trends are determined in most cases by finding core to rim zoning in grains, but some of the DM_c plagioclase probably violates this general principle. Because much of the DM_c plagioclase seems to be an in-place reaction product of the breakdown of clinozoisite, these grains tend to have the earliest growth near the rims and the youngest growth near the remnant clinozoisite in the cores. If further growth had occurred, it probably would have been in the core by reaction of this clinozoisite. One of the analyzed grains seemed to have grown both by in-place replacement of clinozoisite, with increasing An content from rim to core, and also by overgrowth, with the same zoning pattern preserved in the outer portion from core to rim. Some grains appear to be DM_a

plagioclase which is overgrown by DM_c plagioclase. These have optical discontinuities between the two generations and have no clinozoisite within the grains. Within the DM_c portion of such grains the zoning pattern is increasing An content from core to rim; this is normal concentric growth, probably the general growth mechanism in typical samples from the study area. However, wherever there is evidence that a reaction such as the breakdown of clinozoisite has occurred the possibility of a reverse zoning pattern must be considered. In this case both replacement and normal concentric growth seem to have occurred and this has allowed the general trend to be established. If a smaller number of analyses had been obtained, a different compositional trend may have been postulated. The trend shown for this sample may not really reflect the actual trend because of the complications, but it appears to be the best interpretation of the data.

JR-10

Location JR-10 is about 1.4 miles south of JR-11 and is an exposure of massive gray carbonate-rich rock interbedded with thin layers of biotite schist. There are abundant deformed DV_a veins within the schist. Sample JR-10-A is from such a DV_a vein and the adjacent schist. As at

JR-11, D_b deformation has been intense in these rocks. In contrast to the DV_a vein and host amphibolite at JR-11, the schist here is more strongly affected by D_b than the vein. This seems to be a function of the relative contrasts of the rock types involved in each case: massive amphibolite and a quartz-calcite vein versus mica-rich schist and a quartz-calcite vein.

Within the schist in sample JR-10-A, DS_b is a very well developed s-surface. DS_b is between a spaced slip cleavage and a pervasive schistosity in character. Some DS_b planes are clearly spaced 1 millimeter or less apart. In some areas of the sample, the spacings become so small that DS_b is essentially a pervasive, unspaced schistosity that has obliterated the earlier DS_a. Where DS_b is well spaced, DS_a can be observed. DS_b has been produced both by the rotation of DM_a grains along the long limbs of DF_b microfolds and by primary DM_b growth of micaceous minerals. Grains of DM_b chlorite, biotite, and muscovite have preferred orientations parallel to DS_b and crosscut DS_a. DS_b is both a transposition of DS_a and a primary growth feature.

DS_a is defined by the preferred orientation of fine-grained biotite, chlorite, and muscovite. DM_b grains of the same minerals are a little coarser than the DM_a grains. Superimposed on both DS_a and DS_b are porphyroblasts of biotite which have no preferred orientation. The largest

of the porphyroblasts have maximum dimensions of 1-2 millimeters. There is also some growth of chlorite grains without preferred orientation which seems to be related to the biotite porphyroblasts. Grains with preferred orientation parallel to DS_a are DM_a growth. Grains parallel to DS_b are DM_b growth. The post-DS_b biotite and chlorite are DM_c.

The assemblage in the host rock of JR-10-A is quartz-muscovite-biotite-chlorite-plagioclase-calcite-apatite-rutile-pyrrhotite-pyrite (alteration of pyrrhotite)-chalcopyrite. All of the pyrite in the host rock appears to be an alteration product in irregular cracks and elsewhere in pyrrhotite grains. Plagioclase grains have irregular optical zoning and some contain optical discontinuities. The microprobe data show that these discontinuities are reaction and/or overgrowth boundaries.

Within the DV_a vein is the assemblage quartz-muscovite-biotite-chlorite-plagioclase-calcite-ankerite-apatite-pyrrhotite-pyrite-chalcopyrite. Some of the pyrite is an alteration product of pyrrhotite with textural relationships similar to the pyrite in the host schist. There are also single grains of pyrite which appear to be primary vein growth. Vein pyrrhotite never encloses primary pyrite grains, but some of the apparently primary vein pyrite partially encloses vein pyrrhotite. The textural relation-

ships seem to indicate that some growth of DM_a pyrite occurred late in the formation of the vein. The alteration of vein and host rock pyrrhotite may have happened later in another event, such as D_b or D_e. The plagioclase in the DV_a vein has irregular optical zoning and irregular optical discontinuities occur in some grains; these appear to be reaction fronts between two generations of plagioclase. The microprobe data confirm this. Some plagioclase has been altered to white mica and calcite. It is possible that the alteration occurred in more than one event, but the textural relationships of the plagioclase alteration products are ambiguous. Also present is late alteration of pyrite and pyrrhotite to goethite.

Limited growth of a border zone has occurred along the host rock wall. Minerals in this zone are biotite, chlorite, plagioclase, and pyrrhotite. The border zone is not more than a few grains wide and is not present in places. It is hard to sort out the border zone growth from DM_c overprint in some areas of the sample. Most of the vein is comprised of coarse-grained quartz and calcite.

The compositions of analyzed chlorite are shown in Figure 74. Not much chlorite is in the host rock, so most of the analyses are from the vein. Isolated grains in DV_a vein quartz and other grains in the vein have compositions

Figure 74 Plot of Al vs. Mg/Mg+Fe for chlorite in JR-10-A

Figure 75 Plot of Al vs. Mg/Mg+Fe for biotite in JR-10-A

Figure 74

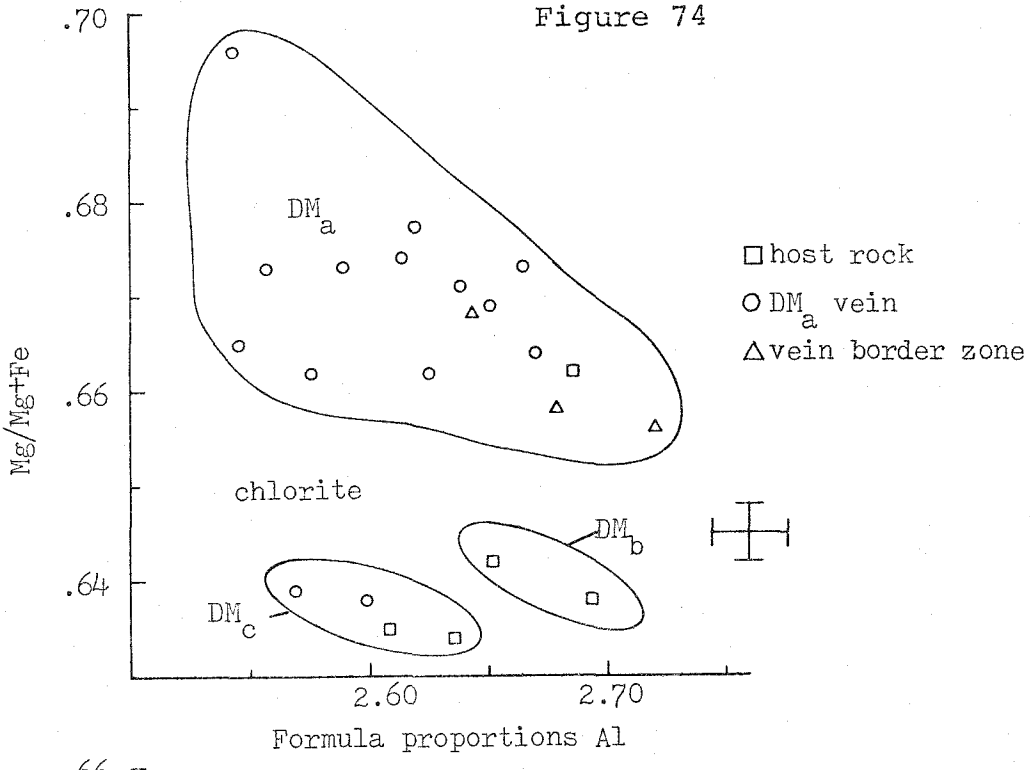

Figure 75

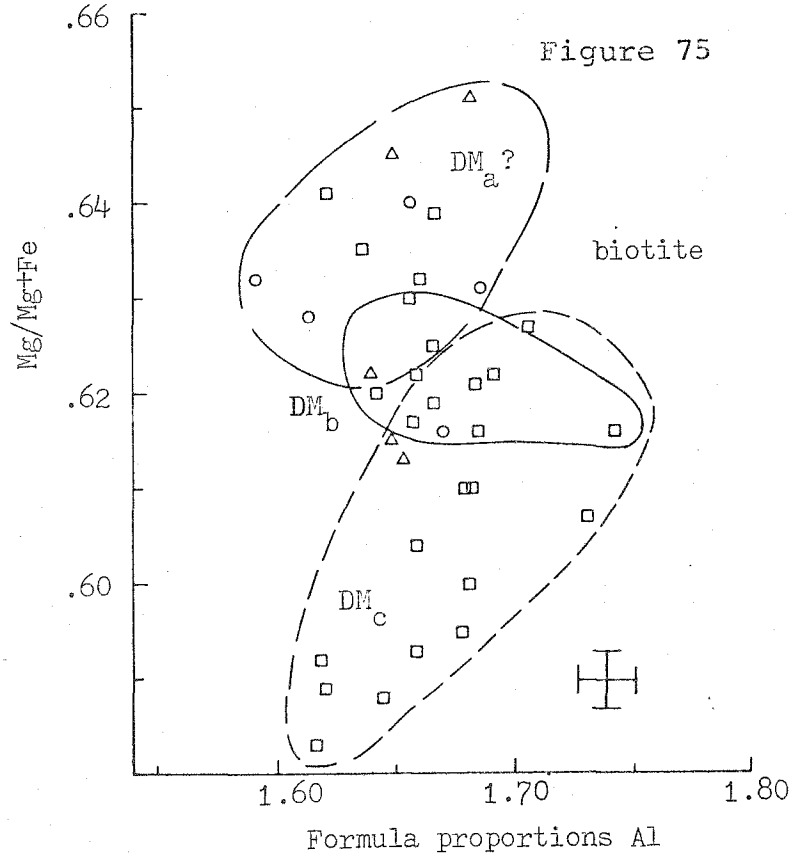

similar to that of a small grain in the host rock with preferred orientation parallel to DS_a. These may then preserve original DM_a compositions. One chlorite grain in the host rock with preferred orientation parallel to DS_b may preserve DM_b compositions. There are also analyses from a grain in the host rock and a grain in the vein which appear to represent DM_c overprint. Each of these three groups have separate, nonoverlapping compositional ranges. It appears that chlorite may preserve the original compositions of the three generations; however, there may also be diffusion or recrystallization effects of the DM_c overprint on the DM_a and DM_b chlorite. The evidence is ambiguous in this regard.

Three distinct textural types of biotite are also present: DM_a parallel to DS_a in the host rock and as isolated grains in the vein, DM_b parallel to DS_b in the host rock, and DM_c which overprints both DM_a and DM_b. The compositions of analyzed grains are shown in Figure 75. The compositional groups have the same general relationships as for chlorite; DM_a biotite is more Mg-rich than DM_b and DM_c. For biotite, there is extensive overlap of the compositional range of apparent DM_b points and the other two generations. Biotite may also tend to preserve the original compositions of DM_a and DM_b growth. Again, possible effects of DM_c overprint cannot be ruled out. The best way to test the degree of DM_c overprint would be to analyze DM_a and DM_b

grains which are included in plagioclase of the same generation. No such included grains occur in the sample.

There has been extensive DM_c overprint on plagioclase in the vein and host rock which appears to have originally been DM_a grains. A typical grain has an irregular core with compositions in the range An_{13} to An_{35} which is overgrown by much more calcic plagioclase. The plagioclase compositions are shown in Figure 76. The cores are probably DM_a and one isolated grain in the vein that appears to be primary DV_a vein growth has only compositions similar to the cores of the other grains. The overgrown rims are probably DM_c. In the host rock, DM_c plagioclase growth seems to postdate formation of DS_b. The compositional range of DM_c plagioclase is from about An_{37} to An_{64}. Although the upper limit of An content in DM_a and the lower limit in DM_c are close to each other, generally there is a sharp compositional discontinuity between the outer DM_a composition and the inner DM_c composition in any given grain. For instance, the adjacent DM_a and DM_c compositions in a grain in the host rock are An_{28} and An_{60} respectively. In such grains there is an optical discontinuity between the two generations. Many analyses are in the compositional range between these two, so the gap does not represent a solvus.

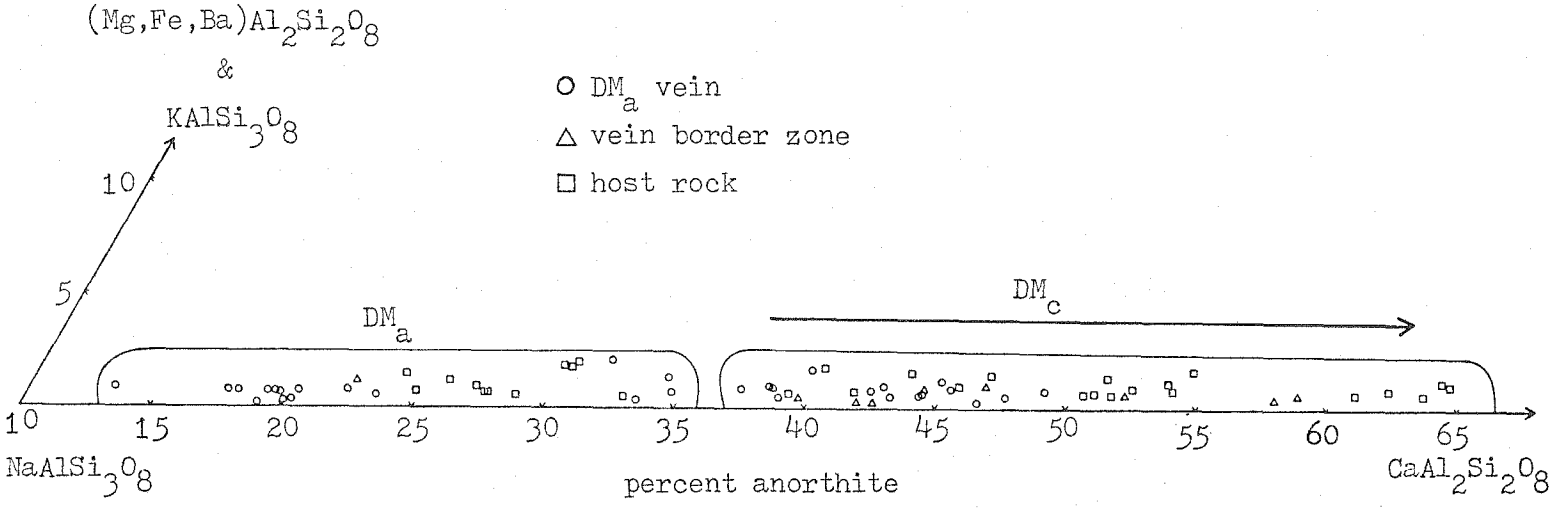

Figure 76 Compositions of plagioclase in JR-10-A.

Probably no solvus was encountered in either DM_a or DM_c plagioclase growth.

The border between DM_a plagioclase cores and DM_c rims in some grains is very irregular. There can also be apparently isolated patches of DM_c plagioclase in the DM_a cores. Of course, the isolation may be an effect of the two dimensional thin section. These relationships suggest that DM_c growth was at the expense of DM_a plagioclase. Some grains seem to have only simple DM_c overgrowth on DM_a cores. Only the compositional trend of DM_c plagioclase has been well established. The trend seems to be consistently increasing An content from core to rim. Trends of both increasing and decreasing An content are found in DV_a vein grains. A reversal has not been found in a single grain, so that the trend cannot be defined. In other DV_a veins, the pattern is generally increasing, then decreasing An content.

There is no evidence of DM_b growth of plagioclase. Some fairly coarse-grained white mica and calcite appear to be alteration products of DM_a plagioclase and may be DM_b. Somewhat finer-grained alteration of DM_c plagioclase also is present and is probably DM_e in generation. While DM_b alteration of DM_a plagioclase may have occurred, all of the alteration cannot be DM_b.

Most of the calcite and the small amount of ankerite

in the vein appear to be DM_a in generation. The calcite compositional trend has not been well established due to difficulties similar to those for DM_a plagioclase. There are grains with increasing Fe+Mg+Mn substitution from core to rim. A single grain with a reversal was not found. In any event, the presence of zoning in the calcite which coexisted with ankerite indicates that the temperature was changing during DM_a growth. The one analyzed ankerite grain does not have much compositional variation, but more analyses are needed to establish the ankerite compositional range. One calcite grain seems to have rim growth that is compositionally distinct from the rest of the grain and from the other grains. This rim material has 11% Fe+Mg+Mn solid solution as opposed to a maximum of 9% for the other analyses. This could possibly be DM_c calcite overgrowth.

As is often the case in this part of the study area, there is a lack of indicator minerals which could define the relative conditions of the three events. Biotite and chlorite are part of the assemblage for all three. The other samples from this outcrop do not help very much. Hall (1959) shows this area as garnet grade, but both DM_a and DM_c could be garnet grade. The plagioclase compositions indicate that the conditions during DM_a and DM_c growth probably were at least garnet grade. The possible retrograde

of plagioclase during DM_b and the lack of DM_b plagioclase growth suggest that DM_b conditions were not as high grade as for the other events. Whatever the conditions of their growth, all three mineral growth generations seem to be well preserved. The fourth generation, low grade DM_e alteration of plagioclase and perhaps pyrrhotite, also seems to be present.

JR-175

Location JR-175 is about in the middle of the traverse and is an exposure of the Waits River formation. Interlayered pelitic schist and carbonate schist are present and some layers have large amounts of tourmaline, up to 50% or more by volume. Other layers are highly graphitic, in some cases to the point of the rocks being essentially opaque in thin section. The structure is dominated by prominent DF_b folding. Two schistosities, DS_a and DS_b, are present in much of the rock, but DS_b is the dominant schistosity in places. DV_c veins crosscut the D_b structures.

Garnet is present locally in pelitic layers and the grains seem to be deformed by DS_b in some samples; the garnet is therefore DM_a. In some samples the garnet grains have been almost completely resorbed and replaced by biotite, chlorite, muscovite, quartz, and plagioclase grains

which are younger than the DS_b schistosity. These grains have no preferred orientation and appear to be DM_c. There is mineral growth of muscovite, biotite, and chlorite parallel to DS_b which is much finer-grained than the DM_c grains. Where DS_a is preserved muscovite and biotite grains which are parallel to DS_a also occur and are therefore DM_a. Where DF_b microfolds are isoclinal, DS_a and DS_b are parallel. In these cases DS_b seems to be generally dominant and most of the mineral growth is probably DM_b.

DM_c overprint is not limited to the resorption of DM_a garnet as porphyroblasts of biotite, plus some of chlorite, are also developed in the samples. In sample JR-175-A, from one of the DV_c veins, DM_c cordierite plus muscovite, quartz, calcite, and strongly zoned plagioclase occur. DM_c growth tends to be medium-grained in the host rocks and coarse-grained in the DV_c veins. This is much coarser than most of the mineral growth that appears to be DM_a and DM_b. The exception is the DM_a garnet porphyroblasts which tend to be 1-2 millimeters in diameter.

The mineral growth in the DV_c veins is heavily overprinted by low grade retrogradation. Present is a large amount of very fine-grained alteration product minerals such as white mica and calcite within altered plagioclase. Such alteration has been previously called DM_e. As in the

other samples in which this occurs, it is not absolutely clear that the alteration represents a distinctly separate event. It could have resulted from the late, low grade DM_c effects.

JR-175-H is a sample of pelitic schist that has been analyzed with the electron microprobe. DM_a garnet in this sample has only been slightly resorbed. DS_b seems to be a dominant transposition schistosity. The assemblage in JR-175 is quartz-muscovite-chlorite-biotite-garnet-plagioclase-calcite-sphene-rutile-pyrrhotite-chalcopyrite-tourmaline. Most of the fine-grained muscovite, biotite, and chlorite with preferred orientation parallel to DS_b (also DS_a) is probably DM_b growth because of the apparent intensity of D_b deformation. Deformed quartz- and sulfide-rich "veinlets" are parallel to the deformed DS_a and isoclinal DF_b microfolds are best shown by these thin layers, which may or may not be true veins. Probably the best chance of finding preserved DM_a mica would be within these veinlets. Porphyroblasts of biotite and lesser amounts of chlorite are superimposed on DS_b and appear to be DM_c. Some of the pyrrhotite and rutile are intergrown and appear to be pseudomorphous after ilmenite. Ilmenite may have been part of the original DM_a assemblage and the rutile and associated pyrrhotite is then either DM_b or DM_c. Most of

the pyrrhotite is not intergrown with rutile and may have been originally DM_a growth.

Generally the sample has abundant fine-grained graphitic material throughout, but there are areas which are distinctly devoid of this material. The quartz-sulfide veinlets, the DM_a garnet porphyroblasts, and the DM_c growth which replaces resorbed garnet is free of such fine-grained inclusions. In samples such as JR-175-G in which the garnet has been completely resorbed, there are areas of inclusion-free medium-grained DM_c growth that are pseudomorphous after garnet. The surrounding material in JR-175-G is essentially opaque in thin section because of the amount of graphitic material.

The only minerals for which the microprobe data are worth discussing in detail are muscovite and garnet. The compositional ranges of the apparently different generations of chlorite, biotite, and plagioclase extensively overlap. This may be a coincidence or there may have been extensive recrystallization during the last major event, D_c. The range of plagioclase is from An_{23} to An_{37}. Biotite and chlorite are Mg-rich with average Mg/Mg+Fe values of 0.63 and 0.67 respectively.

Compositions of analyzed muscovite points are shown in Figure 77. These have been divided into three textural

Figure 77 Plot of Si vs. Mg/Mg+Fe for muscovite in JR-175-H.

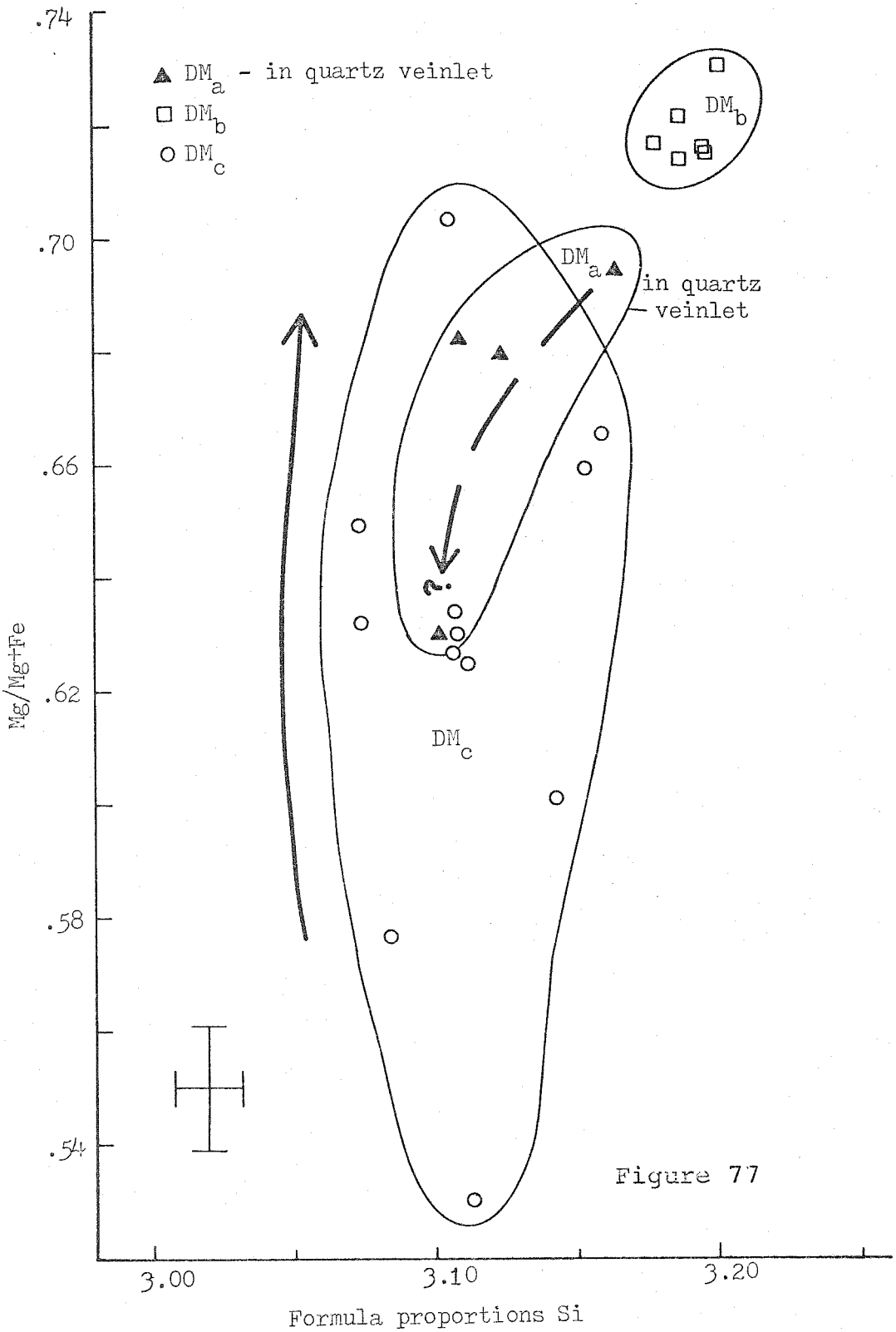
.74
.70
.66
.62
.58
.54
Mg/Mg+Fe
▲ DM$_a$ - in quartz veinlet
□ DM$_b$
○ DM$_c$
DM$_b$
DM$_a$
in quartz veinlet
DM$_c$
3.00
3.10
3.20
Formula proportions Si

Figure 77

groups. The group with the most phengite substitution are grains which have preferred orientation parallel to DS_b and are probably DM_b. Within the thin veinlets are grains of muscovite with preferred orientation parallel to DS_a (and DS_b) which could be DM_a. They are perhaps compositionally distinct from the DM_b muscovite. The other analyses are from grains which replace DM_a garnet or appear to be late grains superimposed upon DS_b. These are probably all DM_c in generation. The apparent trends for DM_a and DM_c muscovite are opposite each other, but DM_a compositions fall within the range of DM_c. The phengite substitution is buffered in this rock so that the relative Si values may have some meaning. DM_b growth seems to be the lowest grade, a situation which is also suggested by the apparent assemblages of the different generations in the samples at JR-175.

The compositional zoning in the garnet porphyroblasts in this sample is different than that in other samples previously described. Most importantly, there are reversals in the compositional trend with respect to Mn. Grains are generally zoned from core to rim with decreasing Mn over most of the grain, then there is a reversal near the edge and Mn sharply increases in some grains. Another difference is the relationship between Mn and Mg. For samples from the Green Mountain axis, plots of Mn vs. Mg in garnet define a smooth curve and the pyrope content

of an analysis could be predicted if the spessartine content was known. No such smooth relationship between Mn and Mg exists in the garnet from JR-175-H; in particular there is no systematic relationship between the two components in the portions of the grains with reversed Mn zoning.

Figure 78a shows all of the compositions from analyzed points. The rim compositions are all shown with a separate symbol. The variation in rim compositions is as great as the total variation of all points. The pyrope content of these grains is high, up to 10%. For the central portions of the grains with normal Mn zoning, the plots in Figure 78a define fairly smooth relationships. For the rims and zones with reversed Mn zoning, the Ca-garnet and Mg-garnet zoning is very irregular.

Figures 78b and 78c show the zoning profiles of two garnet grains. The grain in Figure 78b has a fairly symmetric profile. Mn decreases from core to rim, with the exception that there is a reversal in Mn zoning on one rim. The reversal occurs in the outermost 10 microns of the grain. In contrast to the symmetry of the zoning profile in this grain is the profile shown in Figure 78c. This second grain has Mn reversals on both rims, but the reversals occur at different compositions. The opposite sides of the grain have zoning which is similar in the

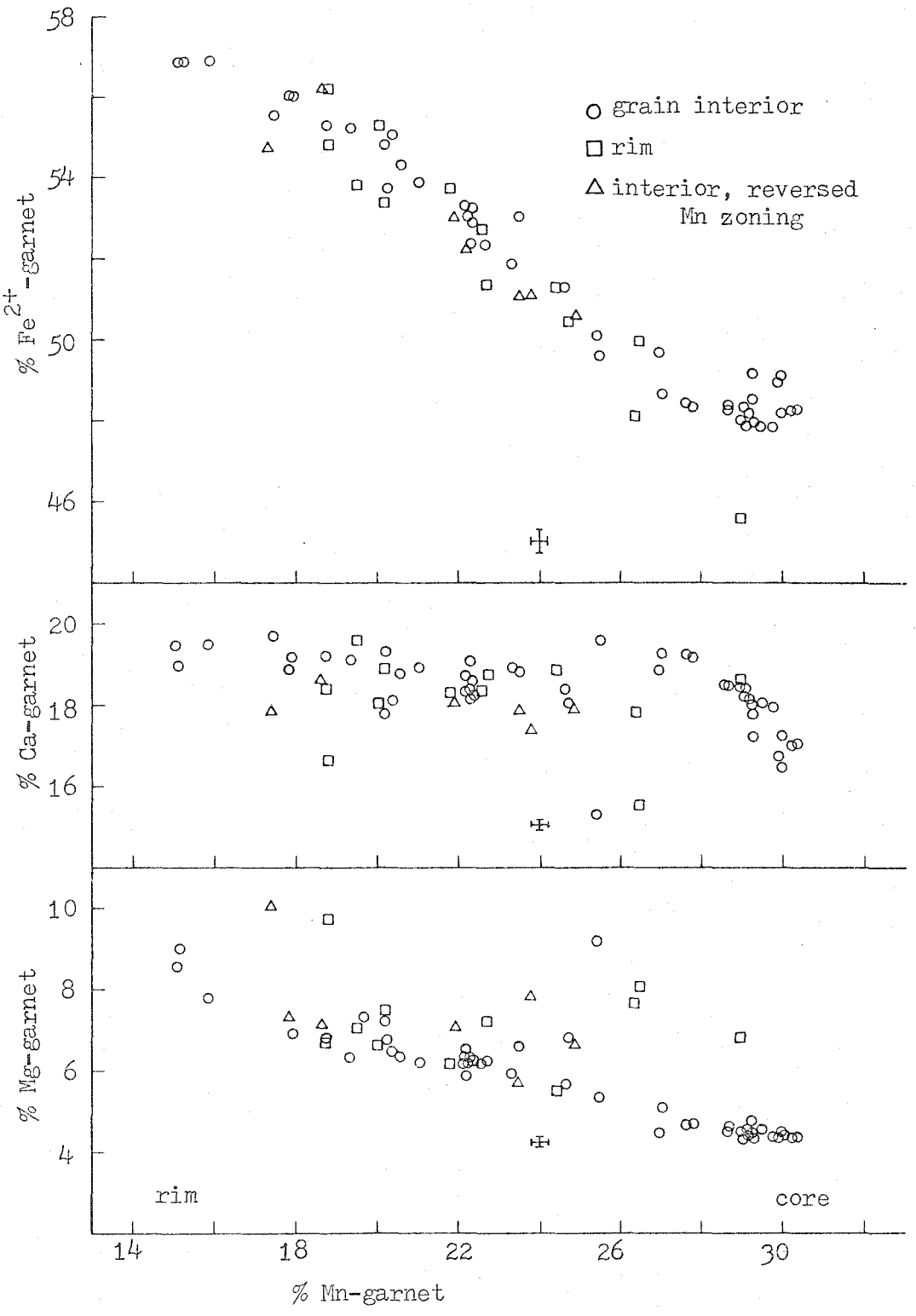

Figure 78a Compositions of garnet in JR-175-H.

Figure 78b Compositional profile of single garnet grain in JR-175-H.

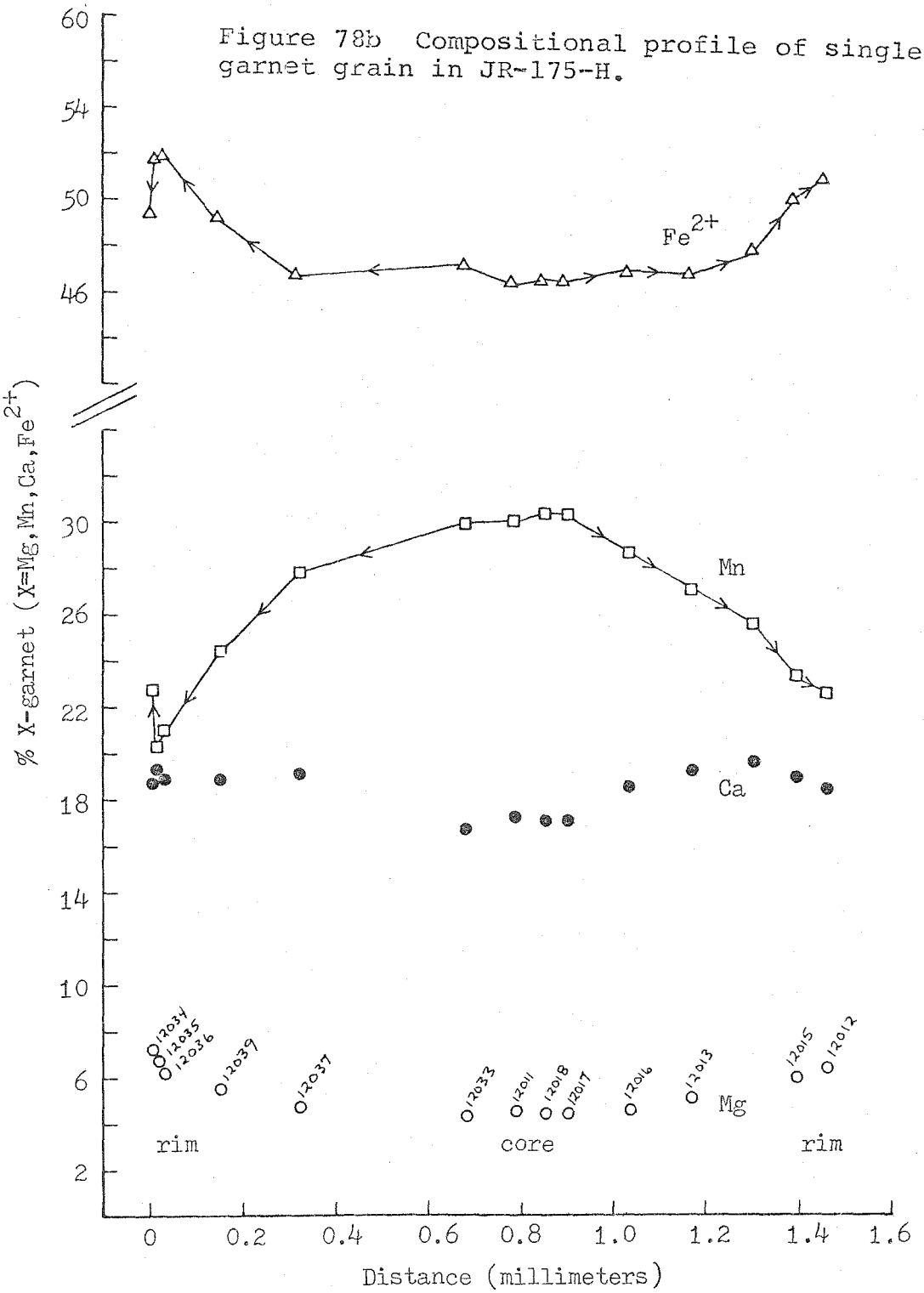

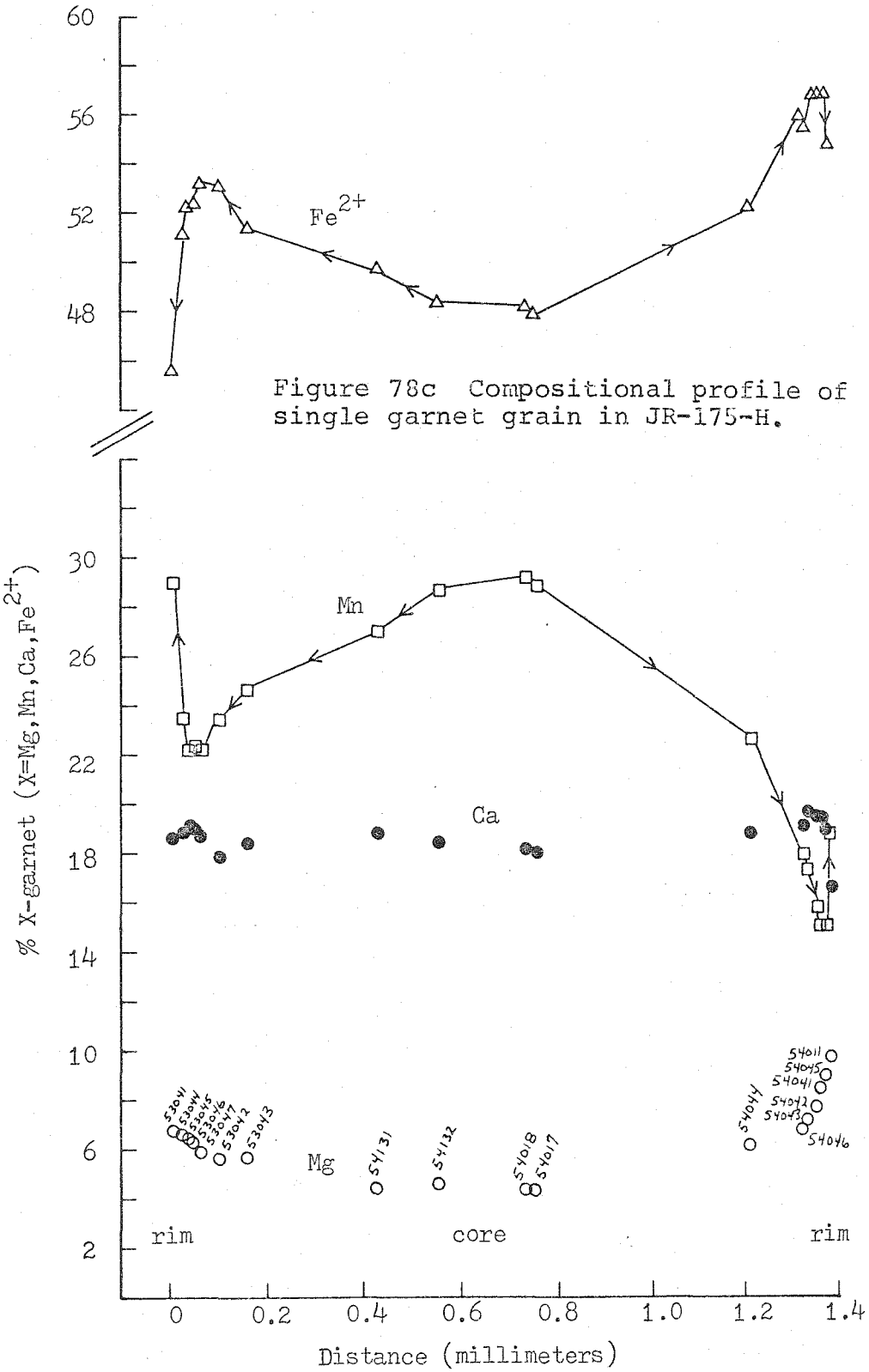

Figure 78c Compositional profile of single garnet grain in JR-175-H.

general trend direction, but the compositions are very different for corresponding positions on the trend. On one side of the grain there is an increase of 7% spessartine component over a distance of 40 microns. The opposite side has a sharp increase in the pyrope content. The zoning profile in Figure 78c and a comparison of the two profiles suggest that there is no single zoning trend for all of the garnet in this sample.

One notable textural feature of the garnet grains is occurrence of numerous tiny, euhedral crystal faces on the margins. Even those grains which have been extensively resorbed have this feature. This differs from the grain fragments with smooth margins of resorbed garnet in the samples from the Green Mountain axis. The complex zoning and textural relationships suggest a complicated history for the garnet in JR-175-H.

There is good evidence that the garnet was originally DM_a. Some grains in another thin section from the same hand specimen appear to have been fractured and deformed by DS_b. The minerals which replace the resorbed grains are not disturbed by DS_b. There may have been some minor retrograde alteration of garnet during D_b (there is no evidence of it), but the indication is that the resorption involved growth of DM_c minerals. The Mn-zoning reversal

is the hardest feature to explain. There must be a source of excess Mn that was not available during the growth of the core. It appears that ilmenite was originally in the rock and the breakdown of this ilmenite would have produced a large amount of Mn which could have then gone into the garnet. Two weight percent MnO is a typical content for the ilmenite of these rocks. The MnO content can be much higher. If the breakdown of the hypothesized ilmenite occurred during DM_a growth, then the garnet growth could have been entirely DM_a. Another possibility is that limited growth of garnet occurred during DM_c overprint and produced the reversed-zoned rims. There are two possible sources of Mn for DM_c garnet growth; the breakdown of ilmenite and the breakdown of DM_a garnet. It is difficult to imagine that resorption and growth of the same mineral can occur at the same time. Because physical conditions seem to have been changing during the various events, it is possible that resorption could have occurred first and then limited growth. Another possible explanation is that there was diffusion in the solid state. The outer rims would represent the areas that were partially reequilibrated by the diffusion. Garnet in other samples seems to be completely devoid of evidence of any such diffusion. Although it cannot be ruled out, diffusion in the solid state seems perhaps an unsatis-

factory explanation.

The grade of DM_a growth at this location is fairly clear; it is at least garnet grade. DM_b conditions were probably biotite grade as indicated by the abundant fine-grained chlorite and biotite that is parallel to DS_b and the lack of DM_b garnet growth. DM_c growth is somewhat of a problem. Cordierite occurs in a DV_c vein and there was perhaps some garnet growth. DM_c plagioclase is oligoclase to andesine in composition. DM_c conditions may have been garnet grade at the peak of metamorphism. Except for the survival of DM_a garnet, much of the evidence of DM_a growth has been obliterated by D_b deformation.

General distribution of grade indicating minerals

Eighty thin sections from the 24 locations along the traverse have been petrographically studied. Many of these rocks are not pelitic in composition and do not have pelitic-type assemblages. The samples which do have pelitic assemblages, including quartz and muscovite, can be used in an attempt to define the regional variation in grade for the three mineral growth generations, DM_a, DM_b, and DM_c. Also of some use is the presence of hornblende in the non-pelitic rocks. Generally hornblende seems to have formed under conditions of garnet grade or higher.

In many locations the pelitic-type assemblages are very simple, typically chlorite-biotite (plus quartz, muscovite, plagioclase, and accessories). Such simple assemblages may occur in higher grade areas given certain rock compositions. The rocks at locations along this traverse are typically very rich in biotite. Rocks with only biotite-quartz-muscovite are found in the same outcrops with garnet-chlorite-biotite-quartz-muscovite. Because of the problem of the typical rock compositions at locations along this traverse, the presence of grade indicating minerals is meaningful but the lack of such minerals does not necessarily indicate lower grade.

The distribution of grade indicating minerals in pelitic-type assemblages for DM_a mineral growth is shown in Figure 79a. Also shown are the locations at which hornblende is observed. DM_a mineral growth is recognized by its presence as primary mineral growth in DV_a veins, by deformation of grains by DF_b and DS_b, and by the preferred orientation of grains parallel to DS_a. Assemblages with garnet-chlorite-biotite are observed at five locations on the northern half of the traverse. Cordierite is observed as primary vein growth in DV_a veins from JR-175 and JR-176. The DM_a garnet is typically partially resorbed. Hornblende that appears to be DM_a is observed at locations JR-11,

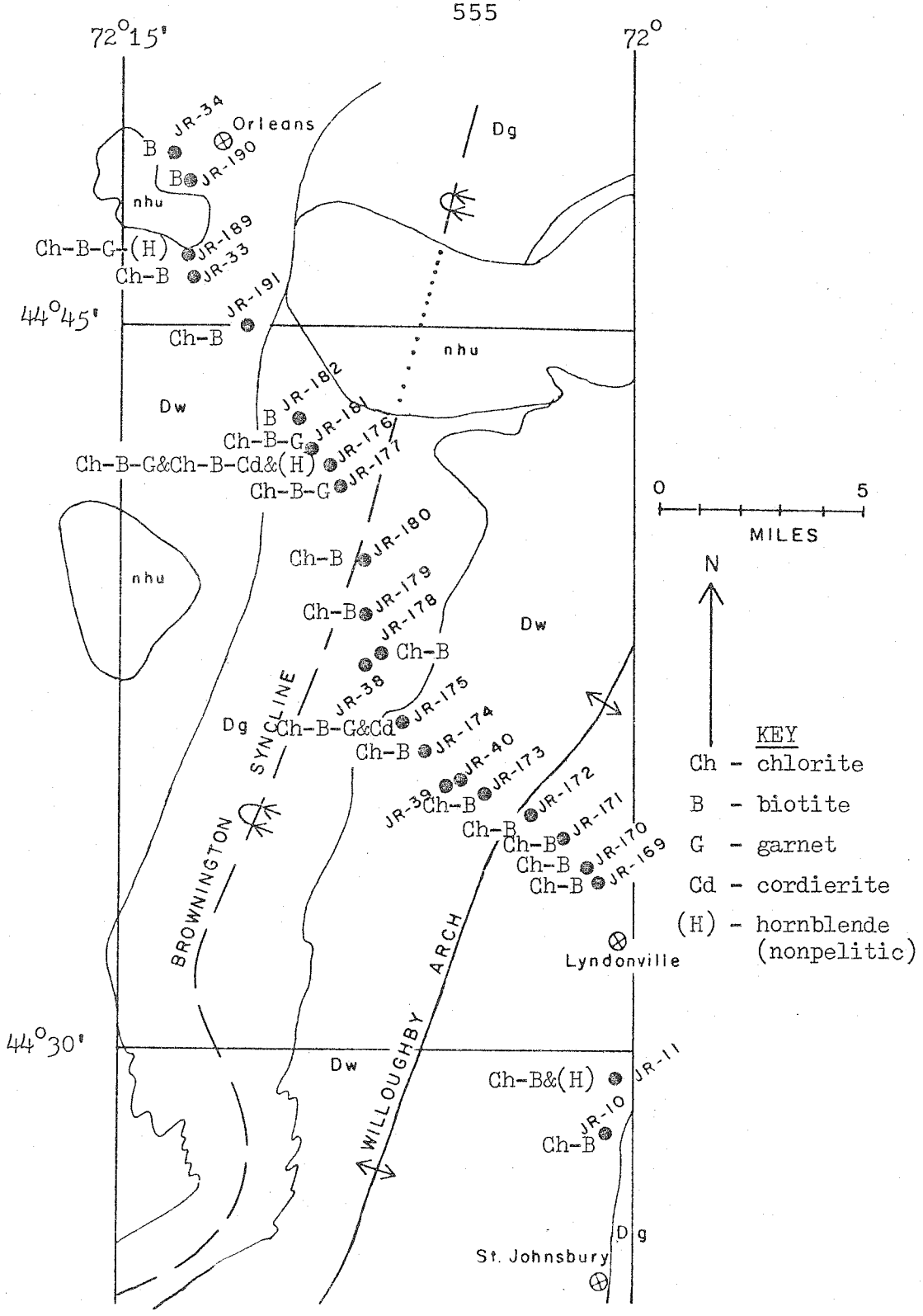

Figure 79a DM_a assemblages in pelitic rocks at locations along the I91 traverse. Also shown is the distribution of DM_a hornblende.

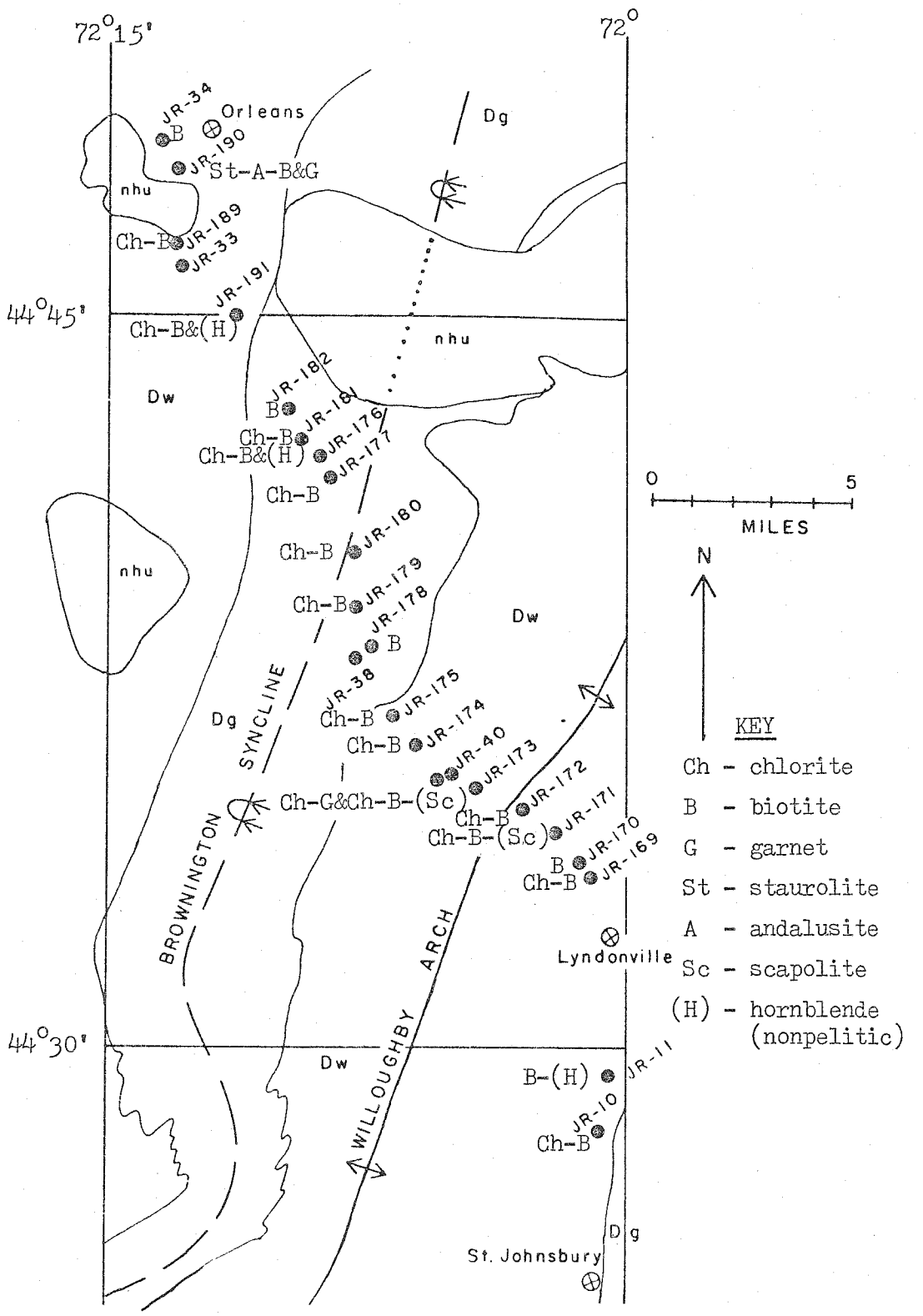

Figure 79b DM_c assemblages in pelitic rocks at locations along the I91 traverse. Also shown is the distribution of DM_c hornblende.

JR-176, and JR-189. At JR-176 and JR-189 there is DM_a garnet also present. There seems to be no systematic distribution of the higher grade DM_a assemblages. They are found in four small areas along the whole length of the traverse.

The lack of higher grade DM_a assemblages near the axis of the Willoughby arch may well be due to a lack of preservation rather than a feature of DM_a growth. The eastern exposure of the Waits River formation through which the axis of the Willoughby arch runs is the area of most intense D_b deformation. DS_a schistosity and DM_a mineral growth are largely obliterated in many of the rocks in this part of the traverse. The grade of DM_b growth seems to be biotite grade. Higher grade DM_a assemblages would not be expected to survive the deformation except in massive, competent rocks such as the amphibolite at JR-11. There are higher grade DM_a assemblages on the flanks of the DF_b Willoughby arch. One might expect that higher grade DM_a assemblages would also be exposed near the axis of the DF_b arch that must have warped the DM_a isograd surfaces. In the Green Mountain area to the west the highest grade DM_a and OM_b assemblages are exposed along the main axis of the anticlinorium. The lack of garnet grade assemblages near the axis of the arch and the presence of such assemblages on the flanks suggests that there may have been higher grade DM_a growth that was completely destroyed by D_b defor-

mation and mineral growth.

Extensive DM_b growth is apparent where DS_b is well developed. DM_b growth never seems to have been higher than biotite grade as no DM_b garnet has been observed. Biotite and chlorite are the typical minerals which are seen as DM_b growth. The degree of development of DM_b depends upon the character of DS_b, but the low grade conditions of DM_b growth are uniform throughout the area covered by the traverse. Because of this, no map is shown for DM_b.

The distribution of assemblages for DM_c growth is shown in Figure 79b. Garnet is observed at locations JR-173 and JR-190. The assemblage staurolite-andalusite-biotite-quartz-muscovite occurs at location JR-190, near a small plutonic body of the New Hampshire series. Hornblende that is DM_c in generation occurs at locations JR-191, JR-176, and JR-11. Scapolite occurs in DV_c veins at JR-173 and JR-171. At all of the locations, the plagioclase in DV_c veins is strongly zoned and is oligoclase or more calcic in composition. Most of the DM_c assemblages are very simple: biotite-chlorite-muscovite-quartz or biotite-muscovite-quartz. DM_c growth in the host rocks is generally as large porphyroblasts of the micaceous minerals and amphibole. These are superimposed on the older DS_b surfaces. DM_c growth does not obliterate the earlier growth, but it

is often observed to be well developed. The apparent low grade assemblages at many locations may be in part a function of rock composition. However, at the location where DM_a garnet is observed, much of that garnet has been apparently resorbed during DM_c growth. It appears that DM_c growth along the traverse ranges from biotite grade to staurolite grade. Most of the higher grade assemblages are found at the northwestern end of the traverse. These perhaps are spatially related to bodies of the New Hampshire series. Higher grade DM_c assemblages are found at locations in the Burke quadrangle which are also close to plutons.

The coverage is not sufficient to define the isograds for each of the mineral growth generations. This would require considerably more work. Near the axis of the Willoughby arch, it is important to find samples in which DS_b is not so well developed as to obliterate DM_a growth. It seems possible that the large area of mapped biotite grade rocks near the axis of the Willoughby arch may reflect a lack of preservation of DM_a assemblages through the strong overprint of D_b deformation and DM_b and DM_c mineral growth. Also it is important to find samples with more complicated DM_c assemblages if such samples exist. Microprobe work on the carbonate schists in the area might allow a better

definition of DM_c conditions as well. DM_c amphibole is developed in these rocks and perhaps also coexisting DM_c ankerite and calcite. The compositions of these minerals could provide useful information.

The presence of both DM_a and DM_c higher grade assemblages indicates that the previously mapped isograds are hybrids resulting from the superposition of the two generations. The mapped isograds are also perhaps in part preservation surfaces. Limited exposure, intense deformation, and nonideal rock compositions make the definition of isograds for each generation a difficult problem.

L. Mineral growth in the Worcester Mountains and Lowell Mountains

The last area to be discussed is the higher grade area of the Stowe formation in the Worcester Mountains. Also briefly discussed are the kyanite-bearing rocks of the Umbrella Hill member of the Missisquoi formation in the Lowell Mountains. The Lowell Mountains are essentially the northern extension of the Worcester Mountains. The locations discussed are shown in Figure 80. These are within the Montpelier, Hyde Park, Hardwick, and Irasburg quadrangles and are between the two areas previously discussed. To the west, OM_b mineral growth is the highest grade growth present. DM_a is biotite grade, but well

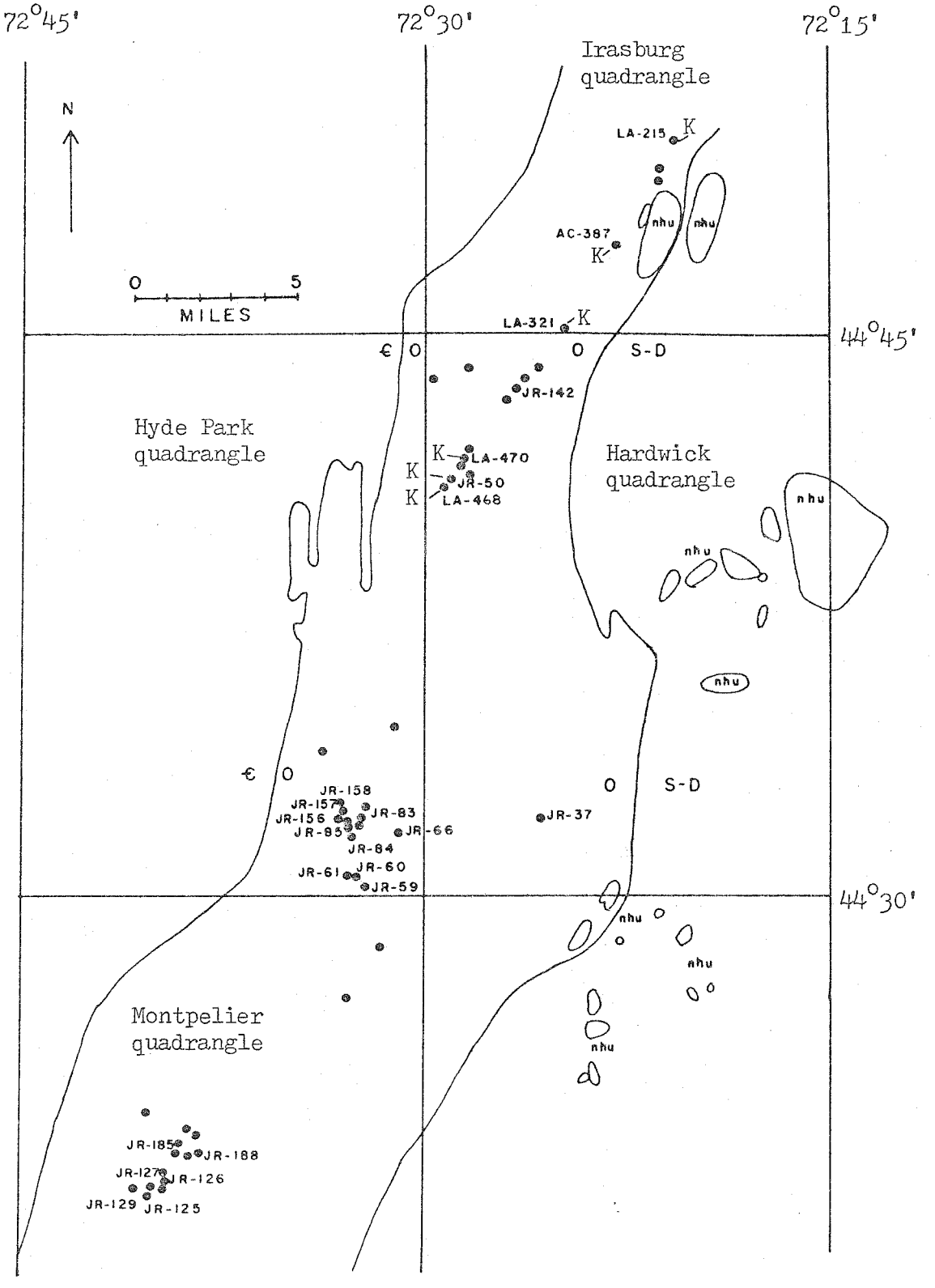

Figure 80 Map of locations in the Worcester and Lowell Mountains. Locations in the Lowell Mountains at which kyanite occurs are shown with a "K".

developed. DM_c is both low grade and poorly developed in general. To the east, both DM_a and DM_c are well developed and high grade in large areas.

The major structures of the Worcester and Lowell Mountains have been mapped by Cady (1956), Albee (1957a & b), and Cady, Albee, and Chidester (1963). The garnet grade and kyanite grade areas of the Worcester Mountains in the central part of the Montpelier quadrange are more or less symmetric about the axis of a northeast trending anticline. To the north in the Montpelier quadrangle and in the vicinity of Elmore Mountain in the Hyde Park quadrangle, the structure becomes more complicated. The kyanite isograd mapped by Albee (1957a & b) appears to be symmetric about the axis of a possible gentle syncline. The syncline may be superimposed upon a larger anticlinal structure.

The major north to northeast trending folds in the Worcester Mountains were thought by Albee (1957a & b) and Cady (1956) to be of the same generation as the small scale folds which are called DF_a in this study. DF_b folds have also been recognized in the Worcester Mountains in this study. It is conceivable that the complicated structure at Elmore Mountain and to the south is the product of interfering DF_a and DF_b folds. The presence of the later DF_b folds has not been previously considered in the Worcester Mountains.

All of the higher grade assemblages in the Stowe formation rocks in the Worcester Mountains are probably OM_b in generation. Both DF_a and DF_b folding could therefore produce the pattern of isograds observed. The isograds define elongate areas oriented with the trends of the folds. A major anticlinal structure is required to produce such an exposure of older high grade assemblages. A major syncline would be expected to produce a relatively low grade area due to the folding of the isograd surfaces. The dominant north to northeast trending structure in the Worcester Mountains is an anticline with subsidiary smaller anticlines and synclines of the same or a later generation. Whether the anticlinal structure is of sufficient magnitude to create the exposure of the high grade area is open to some question.

The Umbrella Hill member in the Lowell Mountains is on the east limb of a northeast trending anticline that may be the northward continuation of the Worcester Mountain anticline. This was mapped by Cady, Albee, and Chidester (1963). The structure in the Lowell Mountains is also complicated, although for different reasons. The Umbrella Hill member is a fairly thin unit of interlayered pebble conglomerate and phyllite. The unit occurs only on one limb of the Lowell Mountain anticline. Apparently the

Umbrella Hill member pinches out to the west.

Apparent higher grade assemblages in the Lowell Mountains are confined to the Umbrella Hill member rocks. These are richer in Al and Fe^{3+} than the surrounding rocks of the Stowe and Missisquoi formations and most of the other rocks in northern Vermont. The higher grade assemblage found is kyanite-chloritoid-chlorite-quartz-muscovite. Garnet is not observed in the Umbrella Hill rocks nor in the surrounding rocks. This assemblage is lower grade than the assemblages in the Worcester Mountains that include kyanite-garnet-biotite and kyanite-staurolite-garnet-biotite. The compositional control of the kyanite-bearing assemblages in the Lowell Mountains rules out finding any reasonable relationship between the structural features and an isograd surface.

The Worcester Mountains and Lowell Mountains are in fairly close proximity to bodies of the New Hampshire plutonic series, as close as many of the locations along the I91 traverse, just described. The plutons near the present area of discussion are the smaller bodies of the series. This close proximity is in contrast to the locations along the portion of the Winooski River traverse near the Green Mountain axis which are much farther removed from any Devonian intrusive rocks.

The sequence of small scale structural elements in the Worcester Mountains is similar to that in the Green Mountains to the west. In the pelitic rocks there are thin OV_a veins. These have been highly granulated and folded by tight, isoclinal OF_b folds with wavelengths that are generally only a few centimeters or less. Larger OF_b folds were only observed in interlayered amphibolite and pelitic schist on the west slope of Elmore Mountain. OS_a is essentially completely obliterated by the well developed, highly pervasive OS_b transposition schistosity. Parallel to OS_b are OV_b veins. These can have some of the higher grade minerals such as kyanite within them.

OS_b and OV_b have been highly deformed by asymmetric DF_a folds in the pelitic rocks and DS_a is generally a well developed slip cleavage. The amphibolite layers have not been so strongly deformed. OS_b is well preserved in amphibolite and DS_a is generally only a spaced fracture cleavage or absent. Although present at only a few outcrops, DV_a veins have been found which are parallel to DS_a. DV_a veins are most abundantly developed in the amphibolite layers. Part of the problem in finding DV_a veins rests in the nature of the exposed outcrops which are small, natural exposures rather than the extensive exposures of the roadcuts along the major highways.

DV_a and DS_a are seen to be gently folded by DF_b folds. DS_b is not present in the higher grade areas. DV_c veins were found only at location JR-66. However, there is apparent DM_c mineral growth which is superimposed upon mineral growth in the DV_a veins at other locations.

The small scale structures in the Umbrella Hill rocks are more difficult to observe in the quartz- and slate-pebble conglomerate layers. In many places there are no well defined s-surfaces that can be found in outcrop. Where structures can be observed, OS_a/OS_b is present as well as OV_a and OV_b veins. OF_b folds are only seen as small folds of OV_a veins. The OV_b veins locally contain kyanite and these veins are folded by asymmetric DF_a folds. DS_a is locally present as a slip cleavage. DV_a veins are fairly common and are folded by asymmetric DF_b folds which are somewhat more prominent than the DF_b folds in the Worcester Mountains. No DV_c veins were found.

In both the Worcester and Lowell Mountains, the only veins which contain the higher grade minerals are OV_b veins. DV_a veins always contain lower grade assemblages. In the Stowe amphibolite, the DV_a veins typically contain actinolite in contrast to the hornblende in the host rock. OV_b veins in the amphibolite contain hornblende (sometimes with actinolite rims). The relationships shown in the two

samples from JR-66, already described, seem to apply to the entire area. The higher grade assemblages are OM_b. DM_a and DM_c are both present and are difficult to separate in the host rock samples. Both events have involved the retrogradation of OM_b minerals. There is very little preserved evidence of OM_a growth as it apparently has been obliterated by the strong OM_b overprint. Some OM_a growth is preserved in the Green Mountain area, as already described, but OM_b growth in that part of the Green Mountain area is not as high grade in general. In many samples from the Worcester Mountains OM_b growth has been also nearly obliterated by the overprint of DM_a and DM_c.

Samples from the Worcester Mountains

Data from samples taken at JR-66 have already been described. The two samples are from a DV_a vein and DV_c vein and enclosing amphibolite. JR-66 is near Elmore Mountain at the northern end of the range. Microprobe data from two other samples are described in the following pages. These two are from the central part of the Montpelier quadrangle about 12 miles to the south to JR-66. One sample is from a DV_a vein and enclosing pelitic schist and the other is a sample of pelitic schist only.

JR-127

Location JR-127 is two small outcrops, one of pelitic schist and the other of amphibolite, which are in the saddle between Densmore Mountain and Burnt Mountain. Sample JR-127-B is from a DV_a quartz-albite vein in muscovite-rich pelitic schist. The vein is folded by open, but clearly present DF_b folds. In the adjacent host rock, OS_b is defined by muscovite grains with preferred orientation (because of the very strong O_b overprint on OS_a, the schistosity is called OS_b rather than OS_a/OS_b). OS_b is deformed by DF_a microfolds. DS_a is defined by the axial planes of microscopic DF_a kink bands and rotated OM_b muscovite grains. There is very little evidence ofprimary mineral growth of DM_a grains with preferred orientation parallel to DS_a.

Two of the host rock samples from JR-127 have evidence of OM_b garnet which has been completely retrograded. Areas of intergrown chlorite, epidote, and white mica are pseudomorphous after garnet. There also was apparently calcic plagioclase in the OM_b assemblage. At present there are areas of highly granulated albite with intergrown epidote, perhaps the reaction products of more calcic plagioclase. All of the epidote in the host rock appears to be post-OM_b, as does the chlorite. The original OM_b assemblage probably included quartz-muscovite-garnet-plagioclase-ilmenite-tour-

maline-apatite, plus perhaps magnetite. The post-OM_b assemblage includes muscovite-chlorite-albite-epidote-sphene -magnetite. The later muscovite is much finer-grained than the OM_b muscovite. Up to half or more of the OM_b muscovite can be altered to fine-grained muscovite in host rock samples. Similar fine-grained muscovite that is an alteration product of kyanite occurs in samples from nearby locations, but it is almost always associated with reaction product chloritoid. There is no evidence of kyanite in the samples from JR-127.

The amphibolite at location JR-127 does not show strong overprint effects. The rock is primarily hornblende and epidote. Only a small amount of the hornblende has been retrograded to actinolite and chlorite. At nearby location JR-126, about 200 meters to the south, an OV_b vein contains euhedral grains of hornblende. This establishes the hornblende as OM_b and the retrograde as post-OM_b.

The DV_a vein of sample JR-127-B has the assemblage quartz-muscovite-chlorite-albite-epidote-magnetite. Albite and epidote are seen as euhedral grains. Accordian-like books of chlorite are included in albite, quartz, and epidote. There are also chlorite masses which are at the boundaries of grains of the other minerals and are not isolated as are the included grains. The muscovite is

generally medium grained, but some has been altered to very fine-grained muscovite similar to the alteration of the host muscovite. This is a post-DV_a alteration feature. The vein minerals also show the effects of DF_b microfolding as inclusion bands in vein quartz are folded and some albite grains have been broken.

The compositions of the various textural types of muscovite are shown in Figure 81. Medium-grained muscovite in the host rock that appears to be OM_b is similar in composition to the primary growth muscovite in the DV_a vein. Perhaps there has been some reconstitution of the OM_b muscovite during DM_a overprint. The fine-grained muscovite in the host rock also has compositions similar to the medium-grained muscovite and is seen as masses of small grains without preferred orientations. The fine-grained muscovite that is an alteration product of DV_a vein muscovite is perhaps compositionally distinct from the other groups; this muscovite has more phengite substitution than the others.

The fine-grained muscovite in the vein is post-DV_a and therefore probably either DM_b or DM_c. The presence of DM_c growth has been established at JR-66. There is no documented evidence of DM_b growth in the area, but the possibility cannot be ruled out. It seems most likely

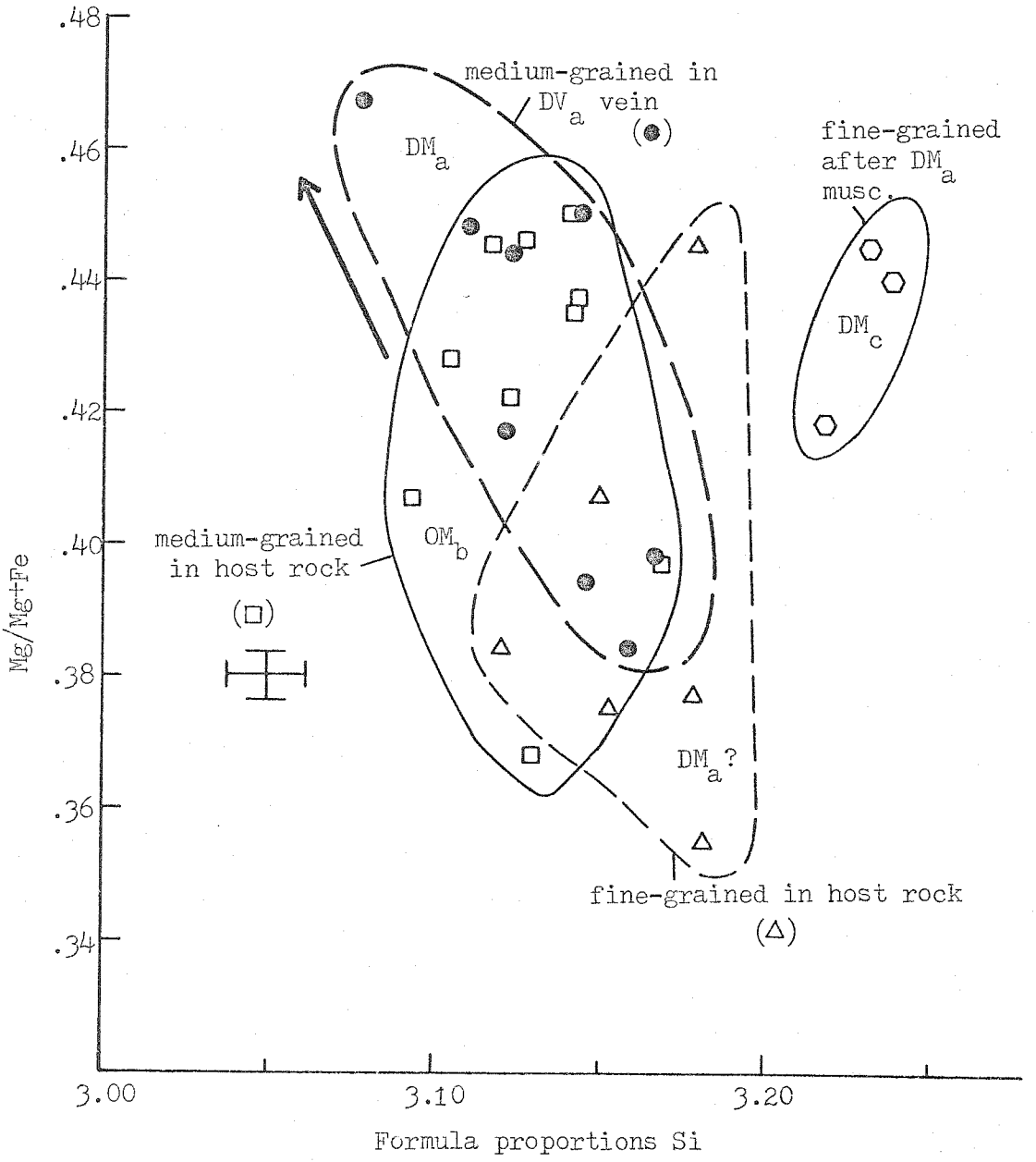

Figure 81 Plot of Si vs. Mg/Mg+Fe for muscovite in JR-127-B.

that this overprint is DM_c. The fine-grained muscovite in the host rock is similar in composition to the DM_a muscovite in the vein. Even though the textures are different, it appears likely that the fine-grained muscovite in the host rock is also DM_a. The compositional differences between the fine-grained muscovite in the host rock and in the vein suggests that these two groups are of different generations. There may well be fine-grained muscovite in the host rock which is equivalent to the apparent DM_c muscovite in the vein, but it was not found with the microprobe.

Based on textural evidence alone, the two types of fine-grained muscovite would be thought to be cogenetic. If the alteration product muscovite in the host rock is really DM_a and that in the vein DM_c, there is a possible explanation of the textures; the in-place alteration of medium-grained muscovite may generally result in fine-grained product muscovite. The medium-grained muscovite in the vein and in the host rock is the result of primary growth at different times. If this is correct, then the interpretation of muscovite textures in these rocks is difficult. It may not be possible to separate DM_a and DM_c muscovite growth in some of pelitic rocks.

It is impossible to determine whether there has been

some compositional reconstitution of the OM_b muscovite or not. The range of compositions of this muscovite might be reasonable for garnet to kyanite grade rocks, although one would expect perhaps that the minimum amount of phengite substitution for this group would be a little less than the 3.09 formula proportions Si observed.

The plagioclase in the DV_a vein is all albite in composition. Most of the albite has less than 1% anorthite substitution. Thin rims show a slight increase in An content up to $An_{2.0}$. There was no albite in the host rock portion of the sample, but plagioclase in other samples appears to also be albite.

Epidote is a major mineral in the DV_a vein. It appears that epidote was produced by the alteration of Ca-rich garnet and perhaps plagioclase in the host rock. There is some variation in the Al-Fe^{3+} substitution in the epidote, but as in all other samples analyzed, this variation does not appear to be really systematic. The possible general trend is increasing Fe^{3+} from core to rim. The vein epidote grains are large and euhedral. These might be expected to be most likely to preserve any compositional zoning. The grains apparently do not preserve the zoning well enough to define a compositional trend in any detail.

The compositions of chlorite in the DV_a vein of JR-

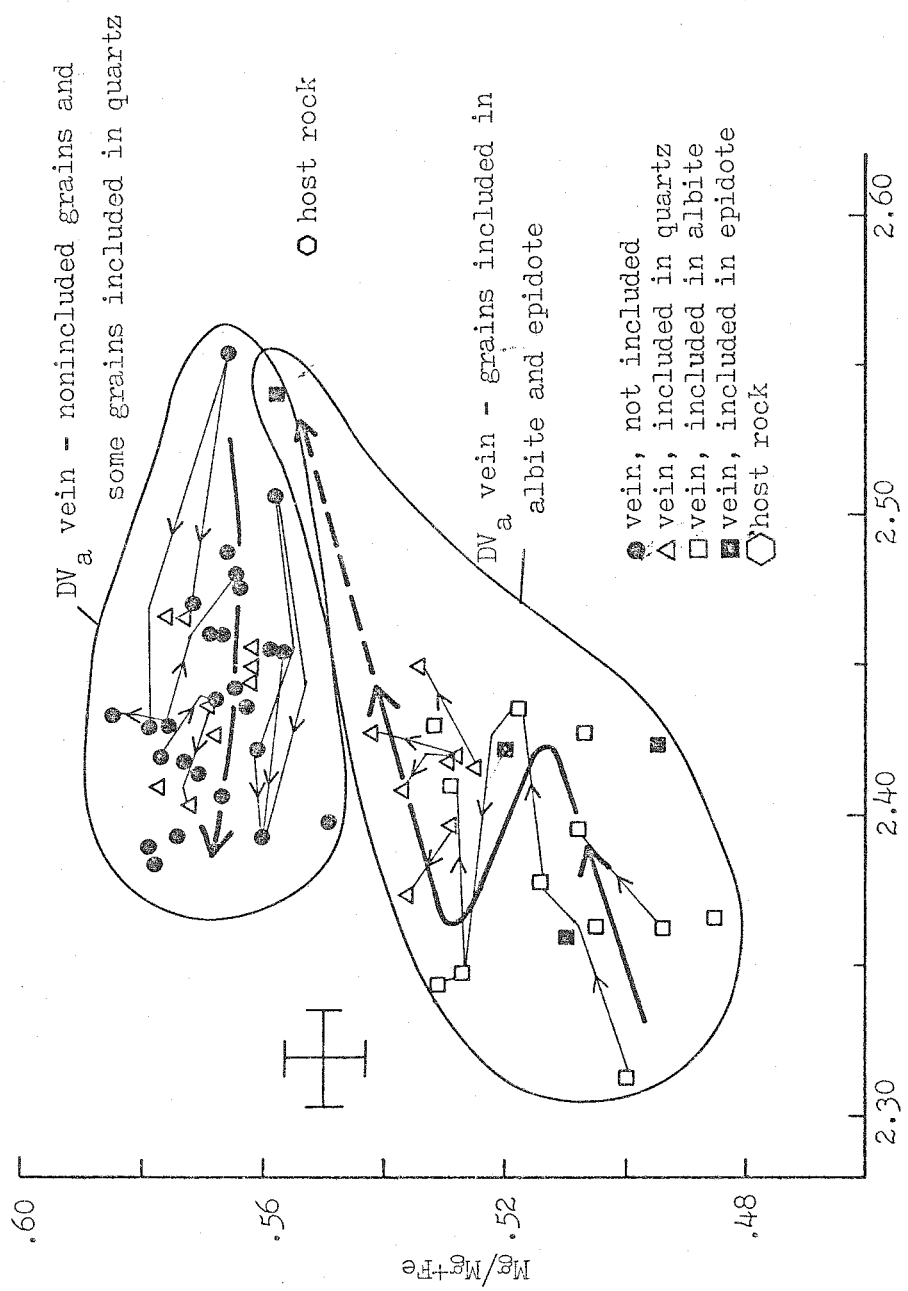

Figure 82 Plot of Al vs. Mg/Mg+Fe for chlorite in JR-127-B.

127-B are shown in Figure 82. Little chlorite is in the host rock part of this sample and only one uncontaminated analysis was obtained; this is also shown. More analyses are needed to make use of the chlorite in interpreting the generations. The chlorite in the vein does show an interesting compositional feature. Many chlorite grains are included in albite and a few are included in epidote. Analyses from these grains are different than analyses from grains which are not included in other minerals. Chlorite grains are also included in quartz and the compositions of these fall into both groups. There are many cracks in the quartz grains and the quartz may not be as isolated an environment for the chlorite as are the albite and epidote grains. The compositional trends for the included grains and for the nonincluded grains are shown.

There are two possible explanations for the relationships shown by chlorite. The first is that all of the chlorite is DM_a; the included grains grew first and then the other grains grew. The other explanation is that the included grains are DM_a and that the nonincluded grains are equivalent to the fine-grained muscovite alteration of DV_a vein muscovite. This would require extensive recrystallization of the DM_a chlorite as there are no nonincluded grains with compositions similar to the included

grains which are clearly DM_a. It seems perhaps most likely that all of the chlorite is DM_a. However, it is odd to find no compositions in the nonincluded grains which are equivalent to the compositions of the included grains. The one analysis from the host rock is similar to the vein chlorite compositions.

All of the chlorite in the host rock appears to be post-OM_b. The chlorite is associated with the retrograde of garnet and of what was probably ilmenite. There is evidence from nearby locations such as JR-129, discussed later, that kyanite and biotite were stable during OM_b metamorphism. This would rule out the coexistence of garnet and chlorite at JR-127 if the conditions were similar.

The DV_a vein establishes the presence of DM_a mineral growth. The DM_a conditions were lower in grade than the OM_b conditions. Garnet was retrograded during DM_a and nearly pure albite was the stable plagioclase composition. There is also evidence of another later event. This may be DM_c which has been documented at JR-66. This event was perhaps even lower grade than DM_a.

JR-185

Location JR-185 is a large exposure of Stowe formation pelitic schist near the summit of White Rock Mountain.

Sample JR-185-A is from the schist only. OV_b veins are abundant here, but no DV_a veins were observed. The OV_b veins are prominently folded by asymmetric DF_a folds.

The OM_b assemblage in the sample includes quartz-muscovite-paragonite-garnet-ilmenite-apatite-tourmaline-zircon. Also present are chlorite, albite, and pyrite. The chlorite appears to be all post-OM_b. There may have been Fe-sulfide in the OM_b assemblage, probably pyrrhotite, but the pyrite grains present appear to be post-OM_b growth. OM_b plagioclase might have been in the rock also, although one would expect it to have been more calcic. At JR-127, DM_a epidote is associated with albite in the host rock, suggesting that calcic OM_b plagioclase broke down. No such epidote occurs in JR-185-A, suggesting that there may have been no plagioclase in this OM_b assemblage. The later albite could be a reaction product of the breakdown of OM_b paragonite. Other than garnet and apatite, no Ca-rich minerals occur in the rock.

OS_b is defined by medium-grained muscovite and paragonite with preferred orientation. This has been folded by DS_a microfolds. DS_a is a slip cleavage and locally a schistosity defined by rotation of OM_b muscovite and primary growth of medium-grained DM_a muscovite and chlorite grains with preferred orientation. Also present are

medium-grained muscovite and chlorite with no preferred orientation, some of which is associated with the partial retrograde alteration of OM_b garnet. Another textural type of muscovite, fine-grained alteration of OM_b muscovite, is present.

Compositions of analyzed muscovite in JR-185-A are shown in Figure 83. Grains parallel to OS_b have the same compositions, as does the fine-grained muscovite. The only muscovite with substantially different compositions are the grains without preferred orientation that are associated with the retrogradation of garnet. Garnet, muscovite, and albite are the major retrograde products and are pseudomorphous after garnet. The grains of muscovite parallel to DS_a which crosscut OS_b are clearly DM_a. The grains without preferred orientation that have similar compositions are also probably DM_a, as is perhaps the fine-grained muscovite. The compositions of grains which are parallel to OS_b probably do not represent the original compositions, because there is more phengite substitution than would be expected for the higher grade conditions. These could only be preserved OM_b compositions if the total pressure during OM_b growth was very high relative to the OM_b conditions in the nearby Green Mountains. It seems probable that the OM_b compositions have been reconstituted by DM_a overprint.

Figure 83 Plot of Si vs. Mg/Mg+Fe for muscovite in JR-185-A.

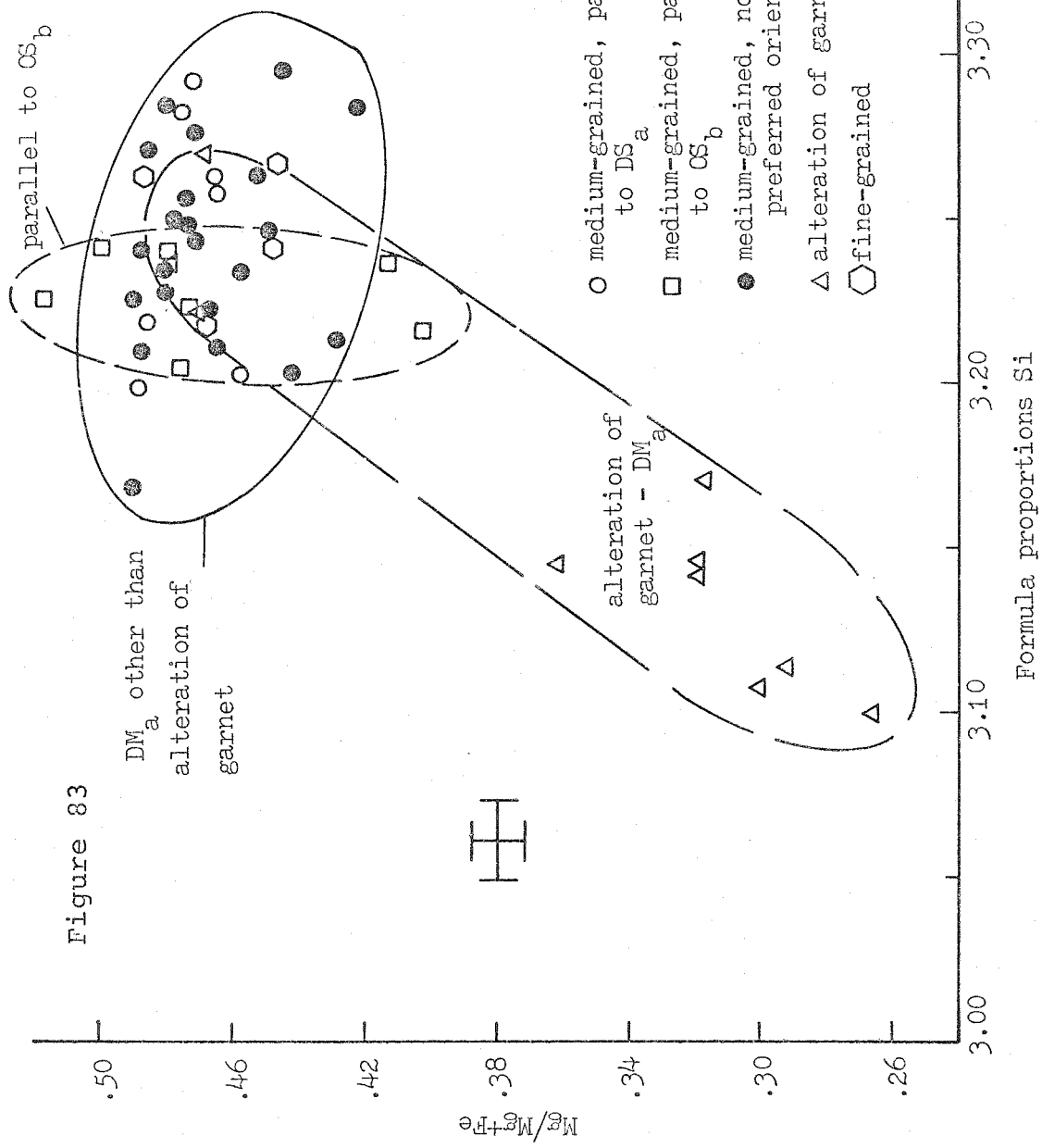
parallel to CS_b
DM_a other than alteration of garnet
alteration of garnet - DM_a
○ medium-grained, parallel to DS_a
□ medium-grained, parallel to CS_b
● medium-grained, no preferred orientation
△ alteration of garnet
⬡ fine-grained
$Mg/Mg+Fe$
.50
.46
.42
.38
.34
.30
.26
3.00
3.10
3.20
3.30
Formula proportions Si

Figure 83

This leaves the grains without preferred orientation which are associated with the retrograded garnet. These grains are intergrown with chlorite that appears to be DM_a and are not texturally different from grains without preferred orientation that have the more phengitic compositions. It appears that this muscovite is also DM_a although perhaps it did not grow at the same time as the other DM_a muscovite. One grain with a core of this distinct composition is rimmed by muscovite with compositions similar to that of the grains parallel to DS_a. The low-phengite compositions of the alteration product muscovite may represent the earliest DM_a growth. There is some evidence of pre-Silurian retrograde alteration in the amphibolite at JR-66. Possibly there could also have been some pre-Silurian alteration of the garnet. This must remain unresolved due to a lack of evidence.

A wide range of chlorite compositions is shown in Figure 84. None of the chlorite grains have preferred orientation parallel to OS_b. The chlorite in the sample is of three textural types; grains with no preferred orientation, grains with no preferred orientation associated with retrograded garnet, and grains with preferred orientation parallel to DS_a. Also, some grains are included in albite. The compositional ranges of these types all overlap each other,

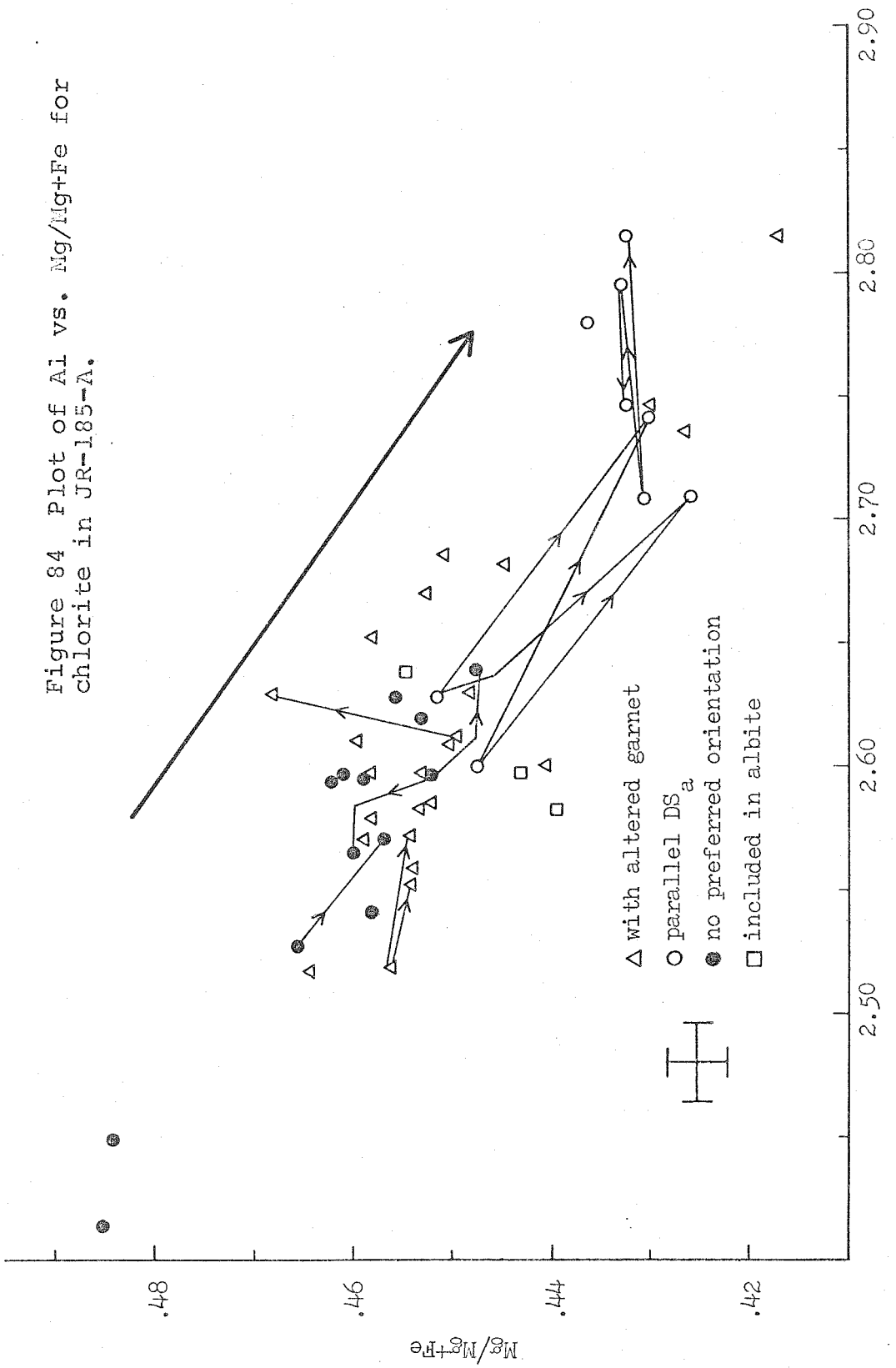

Figure 84 Plot of Al vs. Mg/Mg+Fe for chlorite in JR-185-A.

but there are three fairly distinct compositional groups. One grain which is included in a quartz grain has the most Mg-rich and Al-poor compositions. Other than the inclusion relationship, there is no textural difference between this grain and many of the other analyzed grains. Another group consists of chlorite which is more Al-rich and Mg-poor than most of the other points. These analyses come from the rims of grains with preferred orientations parallel to DS_a and grains without preferred orientation which are associated with retrograded garnet. They may be late DM_a growth or conceivably DM_c overgrowth. It seems likely that most or all of the chlorite is DM_a in generation and that DM_a had a wide compositional range. As for the muscovite, there is not enough evidence to firmly establish all of the post-OM_b relationships, but the chlorite is clearly post-OM_b.

Garnet seems to be the only OM_b mineral growth to survive the later overprint. These garnet grains show the typical OM_b zoning pattern. Mn decreases from core to rim and there are fluctuations in the Ca content. Changes in the order of 1-2% of the Ca-garnet content can occur within small intervals over which the Mn-garnet component changes 1% or less. The compositions are shown in Figure 85. For most of the volume of the garnet grains, the relationship

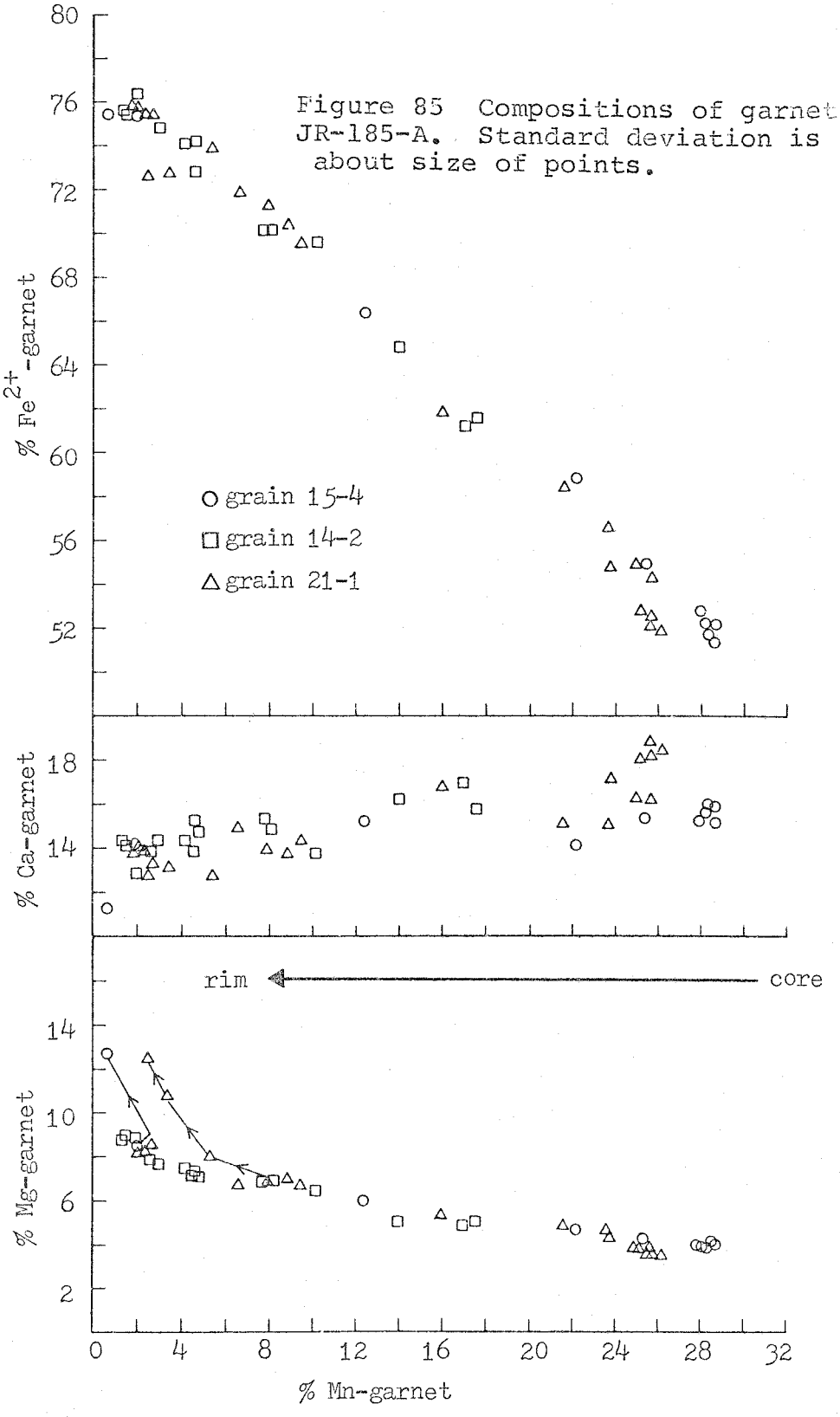

Figure 85 Compositions of garnet in JR-185-A. Standard deviation is about size of points.

between Mn and Mg is smooth for all of the grains combined. The pyrope content can be predicted for any point if the spessartine content is known. At the rims of two grains, however, are rather sharp rises in pyrope content from about 8% to over 12% and, for a given pyrope content, the spessartine contents are not the same for the two rims. It appears that there were local differences in the Mn activity as the two rims grew.

These two garnet rims are original rims that are next to quartz. The rims at other parts of the same grains and on other grains are surrounded by chlorite and muscovite that appear to be retrograde products. Therefore the outer parts of these other rims may have been stripped away by alteration. It is interesting to note that the spessartine content of the rims goes as low as 1%.

The plagioclase in the sample is all albite in composition. The most calcic composition is about $An_{3.5}$. All of the albite with compositions between $An_{2.0}$ and $An_{3.5}$ appear to be associated with the retrograde of OM_b garnet. Also, porphyroblasts of albite contain included chlorite grains with compositions similar to the retrograde product chlorite. There might have been some OM_b plagioclase, but it appears that all of the albite now present is post-OM_b, probably DM_a.

Sample JR-185-A establishes that the overprint on the OM_b assemblages has been severe. Most of the overprinting mineral growth appears to be DM_a. The relationships are not so clear as to rule out the effects of other overprinting events. There is quite a bit of ambiguity in the relationships of the low grade, post-OM_b events. These relationships are only clear in the appropriate vein generations. The scarcity of DV_a veins and particularly DV_c veins compounds the ambiguity.

The fine-grained muscovite alteration product of OM_b muscovite may be DM_a in this sample, as is apparently the case for the host rock in JR-127-B. The fine-grained muscovite in the DV_a vein at JR-127 is post-DM_a. The fine-grained muscovite is important because of the isotopic age data of Lanphere and Albee (1974) on fine-grained muscovite from Albee's location LA-384, equivalent to JR-129 of this study. There are some textural differences in the fine-grained muscovite from various samples. The post-DV_a muscovite in the vein in JR-127-B is somewhat finer-grained than the fine-grained muscovite in the host rock. The fine-grained muscovite in sample JR-185-A is somewhat coarser than the fine-grained muscovite in the host rock of JR-127-B. Some samples of host rock contain extensive amounts of very fine-grained muscovite that may be super-

imposed on DM_a growth, as will be discussed later. It is not entirely clear that these subtle textural differences can be used without microprobe data to aid the interpretation.

JR-129

No samples from JR-129 were analyzed with the electron microprobe in this study, but it is an important location because of the isotopic data of Lanphere and Albee (1974). A description of the relationships observed in thin sections from the location are of some use. JR-129 is a small outcrop of pelitic schist on the west slope of Densmore Mountain. Highly deformed OV_b veins, now seen as pods, have been strongly deformed by DF_a folds and DS_a slip cleavage. The OV_b veins are parallel to OS_b.

The OV_b veins consist primarily of highly granulated quartz with coarse books of essentially undeformed muscovite. In thin section, effects of the granulation of the quartz are less visible and the quartz appears to be coarse-grained rather than fine-grained. The muscovite does not show the alteration to fine-grained muscovite that is seen in some host rock samples. The muscovite appears to be primary OV_b vein growth. Surrounding the central portion of the pods in some instances are well developed

border zones. The border zones, primarily made up of large blades of kyanite which have no preferred orientation, can be up to 1.5 centimeters wide. The kyanite grains in the host rock have preferred orientations parallel to OS_b. The kyanite grains in the vein border zone and in the host schist have been completely retrograded to fine-grained white mica. Chloritoid is also a retrograde product of OM_b kyanite in the host rock.

There are several retrograde relationships within the host rock. Garnet porphyroblasts have been altered to mostly chlorite and white mica. There has been a limited amount of alteration of OM_b white mica to very fine-grained white mica. The kyanite is altered to fine-grained white mica and chloritoid; Lanphere and Albee (1974) have indentified the white mica as intergrown muscovite, paragonite, and margarite. Aggregates of chlorite, quartz, rutile needles, and minor white mica appear to be pseudomorphous after OM_b biotite as indicated by the grain outlines and the type of reaction products. The most convincing evidence is the preservation of similar grains with some of the biotite intact in the OV_b vein. The OM_b host rock assemblage apparently included quartz-muscovite-kyanite-garnet-biotite. There is no clear evidence whether the retrograde products are DM_a and/or DM_c. The retrograde

assemblage includes chlorite-chloritoid-rutile-muscovite -paragonite-margarite-epidote. The minor epidote is associated with retrograded garnet.

The OV_b assemblage is of major importance. The primary minerals were quartz-muscovite-kyanite-garnet-biotite. The muscovite is well preserved and there are small amounts of preserved biotite and garnet. The reaction products are nicely pseudomorphous after garnet, biotite, and kyanite. Only the kyanite is not preserved at all, but the white mica masses that are pseudomorphous after the kyanite blades make these easy to identify. Locally some preserved kyanite can be found. The primary vein minerals uniquely identify the high grade assemblage as OM_b in generation.

The reaction products after biotite in the vein are similar to those in the host rock. There are thin, long sheets of chlorite parallel to the original biotite sheets. The thin sheets are separated by fine-grained quartz, although the quartz is not present throughout all of the grains. Very fine needles of what is apparently rutile occur throughout the pseudomorphs. A minor amount of fine-grained white mica is also in some of the retrograded biotite. However, the retrogradation of biotite in these samples has resulted in the loss of K. The K produced in this reaction was then used in the kyanite retrograde

reaction, of which muscovite is a product. Apparent pseudomorphs after biotite are common in many samples in the Worcester Mountains. The assemblage quartz-muscovite-kyanite-garnet-biotite was apparently very common as a result of OM_b growth. The retrograde of kyanite in the Worcester Mountains has been facilitated by the breakdown of OM_b biotite, as suggested by Albee (1968). There is no reason to postulate that K was brought in from some external source. There is presently very little biotite in the Worcester Mountains.

All of the chloritoid in the samples from JR-129 is a retrograde product. In fact, all of the chloritoid observed in the samples collected in this study from the Worcester Mountains appears to be a post-OM_b retrograde product. Chlorite and chloritoid are common minerals of the retrograde assemblage.

It is unfortunate that there is no direct means of determining the mineral growth generation of the fine-grained white mica that is pseudomorphous after kyanite. This material was dated by Lanphere and Albee (1974) and gave an age of 358 ± 4 m.y. This appears to be a time near the end of Devonian plutonism, using the data of Naylor (1971). DM_a growth is clearly older than the intrusion of the various plutonic bodies in northern Vermont, so this

age is more appropriate for DM_c growth. Unpublished K-Ar ages determined by Lanphere on samples that Albee collected from the Green Mountain axial region in the Lincoln Mountain quadrangle give five consistent ages between 375 and 378 m.y. This is an area of strong DM_a overprint with probably little influence from DM_c. As shown, these are the relationships to the north along the Winooski River. Some work has been done in the Lincoln Mountain quadrangle in this study and the relationships seem to be consistent along the Green Mountain axis. It appears that the 358 m.y. age of the fine-grained white mica reflects the DM_c event, if only due to a loss of argon from DM_a white mica. Certainly the very fine-grained white mica would be more susceptible to argon loss than the coarser grains.

The coarse-grained muscovite in the OV_b vein was analyzed by Lanphere and Albee (1974) and gave an age of 439±9 m.y. The OM_b muscovite has preserved its radiogenic argon through the overprinting events. They also dated hornblende from an exposure of the Stowe amphibolite that is near JR-129; the hornblende gave a K-Ar age of 457±26 m.y. The retention of argon in this muscovite may make loss of argon from DM_a white mica seem unlikely. If so, the fine-grained white mica is probably DM_c.

Other samples from the Worcester Mountains

Relationships and assemblages similar to those seen at JR-129 are seen elsewhere in the Worcester Mountains. In the vicinity of Elmore Mountain at the northern end of the range, OM_b assemblages including quartz-muscovite-kyanite -garnet-biotite are observed at locations JR-83, JR-84, JR-85, and JR-156. A small amount of OM_b biotite with OM_b kyanite is preserved at locations JR-59 and JR-85. Chloritoid is abundant in these samples and is always a post-OM_b retrograde product often associated with fine-grained white mica pseudomorphous after kyanite. Cores of kyanite are fairly well preserved in the samples from Elmore Mountain. The three common retrograde products are chlorite, chloritoid, and white mica.

Sample JR-156-B is a pelitic schist sample that offers some evidence as to the timing of the retrograde reaction. Medium-grained white mica replacing kyanite appears to be related to the D_a deformation as similar white mica has preferred orientation parallel to DS_a. Apparently superimposed on the medium-grained DM_a white mica and the DF_a microfolds is very fine-grained white mica. This white mica is therefore post-DM_a and therefore probably DM_c. In most other samples such a textural distinction of DM_a and DM_c cannot be made.

Albee (1968) reported the occurrence of staurolite from his location LA-304 on the west slope of Mt. Hunger, which is fairly close to JR-185. At LA-304 OM_b minerals have barely been affected by the later retrograde reactions. This is in sharp contrast to the extensive retrogradation in most of the samples from this area. The OM_b assemblage includes quartz-muscovite-kyanite-garnet-biotite-staurolite. There is some chlorite as included grains in the garnet that may also be OM_b. However, the only chlorite in the matrix appears to be a retrograde product and not OM_b. The OM_b chlorite is presumably preserved in the garnet from an earlier stable assemblage. The major OM_b minerals, kyanite, garnet, biotite, and staurolite, are not in any obvious reaction relationships with each other and appear to be a stable assemblage. Garnet and sphene are the only minerals with significant Ca contents and sphene is the major Ti-bearing mineral. It may be that the four-phase assemblage kyanite-garnet-biotite-staurolite is not in violation of the general phase rule treatment of pelitic systems because of this. It seems less likely that the explanation of the four-phase assemblage is that only an infinitely small volume of the garnet is effectively in the system because of the garnet zoning and the apparent difficulty of solid state diffusion in garnet. All of the

minerals in these rocks tend to preserve zoning. Diffusion can perhaps occur in biotite, but staurolite and kyanite may behave like garnet. Staurolite in JR-190-A preserves significant zoning. Kyanite in the samples analyzed in this study is not zoned, but one would not expect significant compositional variation. There is no reason to suppose that kyanite should be more susceptible to diffusion in the solid state than any of the other minerals in these rocks.

The same assemblage, quartz-muscovite-kyanite-garnet-biotite-staurolite, also occurs in Albee's sample LA-477-E, from a location near the top of Mt. Worcester. Sphene is again the only other Ca-bearing mineral besides garnet. Extensive retrogradation has occurred in this sample, but some of each of the major OM_b minerals are preserved. Sample LA-477-K has textural relationships similar to those seen in JR-156-B. Medium-grained white mica is an alteration product of kyanite and appears to be DM_a. Superimposed on this is fine-grained white mica that is probably post-DM_a and therefore DM_c. Some of the samples from LA-477 have medium- to coarse-grained chloritoid that appears to be DM_a. In sample LA-477-D the chloritoid is roughly pseudomorphous after OM_b garnet and remnant garnet fragments are preserved in the cores of some of the chloritoid grains.

None of the chloritoid in the higher grade rocks in the Worcester Mountains appears to be OM_b. Much of it may be DM_a and some may also be DM_c. Except for the included chlorite in LA-477-E and perhaps chlorite included in garnet in other samples, there is no observed OM_b chlorite in the higher grade rocks. DM_a and DM_c chlorite is very abundant.

General discussion of the Worcester Mountains

All of the higher grade minerals, garnet, kyanite, and staurolite, are OM_b in generation. The isograds mapped by previous workers in this area (Albee, 1957 a & b; Cady, 1956) define the OM_b metamorphic grade, although these isograds may in part reflect the limit of preservation of OM_b high grade minerals, rather than the limit of growth. DM_a and DM_c mineral growth are both sub-garnet grade throughout this area. The closest location at which DM_a garnet growth has been observed is at JR-37 in the Hardwick quadrangle and is shown on Figure 80. The closest DM_c higher grade growth is probably a little farther in distance from the Worcester Mountains and to the south of JR-37 in the Plainfield quadrangle.

The highest grade isograd in the Worcester Mountains is shown by Doll and others (1961) and Albee (1968) as the

kyanite-chloritoid isograd. As the chloritoid and kyanite are of different generations, this designation for the isograd is incorrect. Staurolite is present and may have been stable over a larger area than has now been observed. The isograd might in fact be the kyanite-staurolite isograd. Because of the lack of preserved staurolite, it is best to simply call it the kyanite isograd, as originally designated by Albee (1957a & b).

It is very difficult to distinguish DM_a and DM_c in the host rocks. The best evidence of the two events is found in the veins at location JR-66. Other DV_a veins also demonstrate the presence of DM_a. The textural relationships in a few pelitic schist samples suggest that very fine-grained DM_c white mica is superimposed upon DM_a growth. DM_c alteration of DV_a vein muscovite occurs at location JR-127. Both DM_a and DM_c are probably biotite grade throughout the area. There is biotite, chlorite, and actinolite of both generations at JR-66. There may be chloritoid and chlorite of both generations throughout the Worcester Mountains.

Samples from the Lowell Mountains

A limited amount of microprobe data has been collected from five samples of OV_b veins and host rock from the

Umbrella Hill member in the Lowell Mountains. The microprobe data are augmented by petrographic and X-ray diffraction data from samples at 35 locations. The relationships in the Umbrella Hill rocks are fairly consistent over a large area and the data will be discussed in general terms. The locations at which kyanite occurs are shown in Figure 80.

One sample, LA-215-P, provides a good example of the general relationships. The sample is from an OV_b vein and adjacent host rock. The vein contains kyanite, quartz, chlorite, hematite, and apatite as primary OM_b minerals. The kyanite has been extensively altered to medium- to coarse-grained muscovite. This muscovite in turn has been extensively altered to very fine-grained muscovite and pyrophyllite. Very fine-grained muscovite also appears to be the product of the alteration of kyanite. No pyrophyllite appears to be the direct result of the alteration of kyanite; muscovite is always the intermediate mineral. This was established with the microprobe because it is not really possible to identify the different white mica minerals with the microscope only.

The same relationships are also seen in sample LA-321-C, from another apparent OV_b vein. Coarse-grained kyanite in the vein has been altered to medium- to fine-grained

muscovite and the muscovite in turn has been altered to fine-grained pyrophyllite. Between pyrophyllite and kyanite there is always muscovite.

In the OV_b veins in samples LA-470-A and LA-468-A, another alteration mineral occurs in the same position as pyrophyllite. Microprobe analyses and the X-ray diffraction pattern of this mineral suggest that it is the lithium chlorite cookeite. Four microprobe analyses give an average composition, in weight percent, of 0.1% Na_2O, 0.2% K_2O, 0.1% CaO, 0.4% MgO, 0.6% FeO, 0.3% ZnO, 0.1% F, 0.1% Cl, 44.1% Al_2O_3, 34.9% SiO_2, and no detectable amounts of MnO or TiO_2. The range of SiO_2 contents is from 34.8% to 35.1% and the Al_2O_3 range is from 43.3% to 45.1%. Semiquantitative optical emission spectrograph analyses of samples of this mineral intergrown with pyrophyllite show the presence of small amounts of Li_2O, up to 0.2%. Even considering that the samples are roughly 50% pyrophyllite, there is not enough Li for true cookeite. It is suggested that H_3O^+ is in the place of Li^+ and the mineral will be referred to as "hydrocookeite." The presence of H_3O^+ has not been verified.

The textural relationships in the veins suggest a two stage, perhaps two event alteration process. The first stage is the alteration of OM_b kyanite to muscovite which

requires the addition of SiO_2, H_2O, and K_2O. The SiO_2 is readily available in the form of vein quartz and the H_2O can come from the intergranular fluid which is thought to be present. The only problem is K_2O. There is no biotite in these samples and not a single grain of biotite has been observed in the Umbrella Hill rocks in this study. The source of K for the retrograde alteration of OM_b kyanite in the Worcester Mountains was the breakdown of biotite, but this cannot apply in the Lowell Mountains. There is one possible solution to the problem that does not involve transport of K^+ over any large distance. There is very little kyanite in these rocks if an outcrop sized volume is considered. The kyanite is concentrated in the veins and is very prominent here. However, if a reasonable outcrop sized volume is considered, the percentage of kyanite is very low, far less than 1% by volume. This is very different from the Stowe rocks in the Worcester Mountains; kyanite there is often a major consituent. Because of the low abundance of kyanite, sufficient K^+ could be derived from the dissoved K^+ in the intergranular fluid in such an outcrop sized volume of rock. Some diffusion of K^+ would have to have taken place, but perhaps only over distances on the order of a few meters or less.

The alteration of kyanite to muscovite may have occurred

in two events. The textural evidence for this is the presence of coarse-grained and fine-grained muscovite. The coarse-grained muscovite may be DM_a in generation and the fine-grained muscovite might be DM_c. The identifications are only suggested, but the muscovite is clearly post-OM_b and the textures are similar to those in the kyanite-bearing rocks in the Worcester Mountains. There are DV_a veins within the Umbrella Hill rocks and DM_c is clearly present just to the east of the Lowell Mountains in the Irasburg quadrangle.

The second stage of alteration involves the breakdown of muscovite to pyrophyllite or pyrophyllite and "hydrocookeite." K^+ is a product and it must have been returned to the fluid phase. The second stage alteration apparently only occurred in one event, interpreted to be DM_c. The hydrolysis reactions, including the suggested reaction that forms "hydrocookeite," are as follows:

stage 1:

kyanite quartz muscovite

$$3Al_2SiO_5 + 3SiO_2 + 3H_2O + 2K^+ \longrightarrow 2KAl_3Si_3O_{10}(OH)_2 + 2H^+ \quad (1)$$

stage 2:

muscovite quartz pyrophyllite

$$2KAl_3Si_3O_{10}(OH)_2 + 2H^+ + 6SiO_2 \rightarrow 3Al_2Si_4O_{10}(OH)_2 + 2K^+ \quad (2)$$

muscovite

$$5KAl_3Si_3O_{10}(OH)_2 + 9H_2O + 5H^+ + \text{minor } Li^+ \longrightarrow$$

"hydrocookeite" quartz

$$3(H_3O, Li)Al_4Si_3AlO_{10}(OH)_8 + 6SiO_2 + 5K^+ \qquad (3)$$

The textual evidence indicates that kyanite was breaking down to fine-grained muscovite at the same time that coarse-grained muscovite was breaking down to pyrophyllite. There is very little compositional difference between the fine-grained muscovite and the coarse-grained muscovite. Apparently kyanite did not react directly to form pyrophyllite because of a kinetic barrier. The reaction rate of kyanite going to muscovite must be much greater than the reaction rate of kyanite going to pyrophyllite. The apparent activiation energy barrier to the reaction of kyanite to pyrophyllite may explain the rarity of occurrence of pyrophyllite in metamorphic rocks as a retrograde mineral.

Chloritoid is a primary vein mineral with kyanite in OV_b veins at locations LA-321 and JR-50. The other vein minerals are quartz, hematite, rutile, and apatite. Chlorite appears to be a primary OV_b vein mineral in some samples. There may be a small amount of primary OV_b vein muscovite, but most of the white mica in the vein samples is a later alteration product. The complete basic assem-

blage in the OV_b veins is quartz-muscovite-kyanite-chloritoid-chlorite-rutile-hematite-apatite. Other assemblages are less complete subsets of the basic assemblage. Minor minerals found in a few samples are tourmaline and monazite.

Veins which appear to be DV_a in generation are found at a number of locations. The DV_a vein assemblages are all fairly simple, typically chlorite, hematite, and quartz. A small amount of white mica can also be present. DS_a slip cleavage is often difficult to find in these rocks, but it can be observed in places. At locations such as JR-142, the DV_a veins are clearly parallel to the slip cleavage. Also present in the area are highly deformed OV_a veins which have simple assemblages similar to those found in the DV_a veins.

The assemblages in the host rocks are similar to those in the veins. The typical apparent OM_b host rock assemblage is most or all of the basic assemblage quartz-muscovite-kyanite-chloritoid-chlorite-rutile-hematite-apatite. Kyanite is really quite rare in the Umbrella Hill host rocks, so that assemblages with chloritoid-chlorite are most common. Albite has been found at two locations, JR-49 and JR-72, but is not with kyanite. Tourmaline is found in some host rock samples. Calcite, epidote, and sphene are fairly rare minor minerals. No garnet, biotite, or sulfide

minerals have been found in the Umbrella Hill rocks. The only other possible OM_b minerals of importance are margarite and paragonite; OM_b mica in host rock samples from LA-321 and LA-468 appears to be intergrown muscovite and margarite and intergrown muscovite, margarite, and paragonite. No analyses of pure margarite were obtained, but some mica analyses have up to 20-30% margarite component in them. This is probably far more margarite than can be accommodated in muscovite as solid solution. Typical margarite contents in presumably pure muscovite are less than 1%. Muscovite and paragonite have been observed to be finely intergrown in other samples from the study area and such intergrowth is apparently the rule rather than the exception. This creates problems in determining the actual paragonite compositions.

The apparent lack of garnet in these kyanite-bearing rocks may be due to the high fugacity of oxygen that is indicated by the ubiquitous presence of hematite and absence of magnetite. Hsu (1968) has shown that almandine stability is strongly dependent upon f_{O_2}. The high oxygen fugacities in these rocks during OM_b growth did not favor the formation of garnet. The apparent highly aluminous bulk composition of these rocks is also in part due to the high oxygen fugacities. Much of the Fe is present as Fe^{3+}

in hematite, which effectively makes the bulk composition more Al-rich relative to Fe^{2+}. The rocks are fairly aluminous in any event, so that the effective bulk composition allowed the aluminous assemblage kyanite-chloritoid-chlorite to be stable. The surrounding rocks of the Stowe and Missisquoi formations are not so aluminous, nor do they have hematite. Garnet is not found in these rocks either. It appears that the assemblage quartz-muscovite-kyanite-chloritoid-chlorite may have formed in sub-garnet grade conditions. Unlike the DM_a chloritoid and OM_b kyanite in the Worcester Mountains, these are true kyanite-chloritoid assemblages.

Although chloritoid in many cases tends to be in radiating "crow's feet" clusters or as single grains without preferred orientation, in some samples there is some tendency for chloritoid grains to show preferred orientation. In a number of samples individual chloritoid grains have a general preferred orientation parallel to OS_a/OS_b. Kyanite in the host rocks shows a similar orientation. In some samples, such as those from LA-328 and LA-468, a portion of the chloritoid grains have preferred orientations parallel to DS_a. In a sample from AC-387, there are OM_b kyanite grains with preferred orientation parallel to OS_a/OS_b which appear to be altered to chloritoid and white mica. Kyanite

seems to be replaced by chloritoid in sample LA-468-E, so there may be DM_a chloritoid also. The basic DM_a assemblage seems to include muscovite-chloritoid-chlorite, but probably no DM_a kyanite growth occurred. It is likely that some or all of the coarse- to medium-grained muscovite in the OV_b veins that has resulted from the alteration of kyanite may be DM_a. DM_a growth is perhaps just slightly lower in grade than OM_b growth.

No DV_c veins have been found in the Umbrella Hill rocks. By analogy to the Worcester Mountains to the south, it seems reasonable that the fine-grained pyrophyllite and muscovite represent DM_c growth. Some DM_c chlorite may be associated with these other minerals, but apparently there was no DM_c chloritoid growth. Locally, OV_b vein chloritoid is altered to fine-grained white mica and chlorite. It was suggested earlier that there may be some relationship between DM_c growth and the emplacement of the New Hampshire series plutons. The Umbrella Hill rocks are in fairly close proximity to plutonic bodies of this series, especially to the north near location LA-215. Some of the most extensive alteration of kyanite and coarse-grained muscovite to fine-grained muscovite and pyrophyllite that has been observed is in samples from LA-215.

The history of mineral growth in the Umbrella Hill

rocks seems similar to that of the Stowe formation rocks in the Worcester Mountains. The first mineral growth was OM_a; the only real evidence of this growth is in the OV_a veins. The veins here are not as deformed as they are to the south in the Worcester range. OM_a growth was probably low grade, with chlorite and perhaps chloritoid growth, but no kyanite growth. The highest grade mineral growth is OM_b; the most complete OM_b assemblages include kyanite -chloritoid-chlorite. The kyanite-chloritoid assemblages have been overprinted by perhaps two events, D_a and D_c. Kyanite was altered to DM_a muscovite and there was also DM_a chlorite and chloritoid growth. The second overprint, DM_c, involved the alteration of kyanite to muscovite, the alteration of muscovite to pyrophyllite, and also perhaps the alteration of DM_a and OM_b chloritoid to chlorite and white mica.

CHAPTER IV. CONCLUDING STATEMENTS

Northern Vermont is a complicated metamorphic terrain. Five major events, involving significant deformation and/or mineral growth, have affected the area. During three of these events, mineral growth that was garnet grade or higher occurred in large areas. The regional changes in the character of a single generation of mineral growth can be profound. By themselves, the mineral growth generations cannot be followed in detail throughout the area, but the sequence of small scale structural elements can be followed. Metamorphic veins have provided the bridge between the structural sequence and the mineral growth sequence. The mineral growth generations probably could not have been delineated and followed through the area in this study without the use of metamorphic veins.

The oldest mineral growth generation in the pre-Silurian rocks is OM_a. The principal evidence of OM_a is the presence of highly deformed OV_a veins which are parallel to the secondary bedding schistosity OS_a. OM_a has been strongly overprinted by events O_b and D_a. In the areas of the pre-Silurian rocks that were discussed, OM_a is probably everywhere biotite grade.

The second event in the pre-Silurian rocks is O_b. OM_b

is the highest grade mineral growth in most of the western part of the study area. In the Worcester Mountains, rocks with kyanite-staurolite grade assemblages are exposed. Extensive garnet grade OM_b growth occurred in the Green Mountain area. OM_b mineral growth is associated with significant deformation that produced small and large scale east-west trending folds and the prominent schistosity OS_b. OV_b veins commonly occur and are parallel to OS_b. The structural correlation and the isotopic data establish the age of O_b as late Ordovician.

The oldest major event to have affected the Silurian and Devonian rocks is D_a. The effects of this event occur throughout the thesis area. In northeastern Vermont, DM_a mineral growth is garnet grade in much of the area. In the Worcester and Green Mountains, DM_a assemblages are biotite grade and the pre-Silurian mineral growth has been heavily overprinted by DM_a and associated D_a deformation. Many of the major north to northeast trending folds are probably DF_a folds. In the pre-Silurian rocks, small scale DF_a folds and associated DS_a slip cleavage are typically the most prominent structural elements. DS_a is the oldest prominent secondary schistosity in the Silurian and Devonian rocks. DV_a veins, parallel to DS_a, are a key element in the correlation of the structural sequence from east to

west across northern Vermont. The structural and isotopic data suggest an age for D_a of Middle to Late Devonian.

D_b is most prominent as a structural event. The Strafford-Willoughby arch and associated small folds are DF_b folds. The broad arch of the Green Mountain anticlinorium may be due to DF_b folding as suggested by the regional distributuion of OM_b and DM_a assemblages along the Winooski River traverse. However, many of the major folds within the anticlinorium are probably DF_a in generation. DM_b mineral growth is presentwhere DS_b is developed as schistosity or slip cleavage. All observed DM_b growth is biotite grade.

The D_c event is very different from the others. No obvious structural elements are associated with D_c other than DV_c veins. DM_c mineral growth is widespread in occurrence throughout northeastern Vermont. DM_c assemblages with staurolite-andalusite have been found in that part of the area and sillimanite grade mineral growth in northeastern Vermont is also probably DM_c. There is a striking spatial relationship between the character of DM_c mineral growth and the plutons of the New Hampshire series; the highest grade DM_c growth is close to the plutons and as the distance from the nearest pluton increases, DM_c decreases both in grade and in the degree of development.

DM_c is not, however, a local contact metamorphic feature. D_c is a widespread thermal event of regional significance which is probably late Devonian in age.

There is some evidence of a sixth, low grade mineral growth event in northeastern Vermont. This has been designated DM_e. The isotopic data of Zartman and others (1970) suggests the presence of a Permian thermal disturbance just to the east in northern New Hampshire. DM_e may be low grade mineral growth associated with this Permian event.

The data presented in this chapter also have several general implications of importance. It appears that each sample preserves the chemical history of mineral growth over a range of conditions for single events. The samples also preserve textural and chemical evidence of multiple generations of growth. The minerals in these rocks do not define some unique set of physical conditions. Attempting to find the unique P and T of formation for a sample is to some degree pointless; even if such determined conditions were actually experienced by the system, only a small portion of the mineral growth probably grew at the defined P and T. It is of more importance to attempt to define the path with respect to P, T, and other variables that the system experienced. This has not been accomplished in the

present study, but the data suggest it may be possible.

No samples were found in which there was homogeneous equilibrium. The only scale on which equilibrium might have been attained or closely approached seems to be surface equilibrium between simultaneously growing grains. In investigating metamorphic rocks such as these, average compositions of any sort cannot be used. In general, mineral grains are chemically zoned and the zoning trends may be very complicated. Aside from other objections, an average composition can be one that is not present in any grain.

Other than the aluminum silicate polymorphs, none of the minerals in the pelitic rocks seem to be very useful as indicators of total pressure. Compositions of Ca-amphibole in amphibolite may be good pressure indicators, as shown by the work of Laird (in preparation) in this area. Her work suggests that OM_b growth occurred at high to moderate pressure conditions, DM_a occurred at moderate pressure, and DM_c occurred at relatively low pressure conditions. In pelitic rocks, muscovite does not seem to be a particularly good indicator of relative pressure conditions; the range of phengite substitution in much of the OM_b muscovite is similar to that for DM_c muscovite. The amount of phengite substitution seems to be more a function of grade in general than of pressure alone. The pyrope content of

garnet does not seem to be very useful either because of the similarity in compositional ranges of the various generations.

The widespread occurrence of metamorphic veins establishes the presence of an intergranular fluid phase with a fluid pressure close to the confining pressure. The fluid is of obvious importance to the diffusion of materials for mineral growth and the attainment of grain surface equilibrium. The only major event in northern Vermont that does not have associated metamorphic veins is D_b.

The technique of using veins as the bridge between the structural sequence and the mineral growth sequence may be useful in other regional metamorphic terrains. Its usefulness depends upon the nature of the structural sequence. If veins are not associated with the major events, the technique is obviously of no use. If the structural sequence cannot be followed through the area, the mineral growth generations cannot be followed either. Northern Vermont is an ideal area for the use of metamorphic veins, but there are probably many other areas with similar structural sequences where metamorphic veins can be used to define and follow the mineral growth sequence.

APPENDIX I. LOCATIONS OF KEY OUTCROPS

A number of outcrops are described in detail in the text. The general locations of these are shown on Figure 3 in Chapter I. More detailed descriptions are given in this appendix so that other workers can find the outcrops. A number of outcrops are along Interstate Highways I89 and I91. Mile markers are placed along these roads, with the mile numbers increasing to the north for both, and there are also smaller markers every tenth of a mile. The location descriptions refer to these mile markers. Also, portions of U.S. Route 2 are immediately adjacent to I89 and some of the outcrops along Route 2 are described in terms of the markers on I89. It should be noted that I89 and I91 are limited access highways and it is illegal to park along them.

Barre quadrangle

JR-107: roadcut on the east side of I89 at mile 52.0.

JR-108: roadcut on the northeast side of I89 at mile 52.7, just south of the Montpelier exit, exit 8.

JR-112: roadcut on the east side of I89 at mile 51.2, which is 0.9 mile north of the exit 7 overpass.

Camels Hump quadrangle

JR-4: roadcut on the north side of U.S. Route 2, just west of an underpass of I89 and adjacent to mile 66.8 on I89.

JR-5: next roadcut west of JR-4 on north side of U.S. Route 2, adjacent to mile 67.1 on I89.

JR-6: a series of roadcuts on Vermont Route 100 just north of the Waterbury exit of I89, exit 10. Roadcuts are also along exit ramps.

JR-73: roadcut on the north side of U.S. Route 2, 2.5 miles east of the village of Bolton.

JR-78: roadcut of the north side of U.S. Route 2, 1.2 miles west of the village of Bolton.

JR-144: roadcut on the north side of I89 at mile 64.0.

JR-145: roadcut on the north side of I89 at mile 64.4.

JR-161: roadcut on the north side of I89 at mile 66.45.

JR-162: roadcut on the north side of I89 at mile 70.9.

JR-163: roadcut on the north side of U.S. Route 2, adjacent to mile 68.6 on I89.

Hyde Park quadrangle

JR-66: small roadcut on the east side of Vermont Route 12 at the southeast corner of Elmore Pond.

JR-113: roadcut on the northeast side of the road to Ithiel Falls, 0.55 mile west of the junction of this road with Vermont Route 15.

JR-114: roadcut on the northeast side of the road to Ithiel Falls, 0.6 mile west of JR-113.

JR-158: ledge on the west slope of Elmore Mountain at elevation 1780 feet and along an azimuth of 335° from the fire tower on Elmore Mountain.

Lyndonville quadrangle

JR-175: roadcut on the east side of I91 at mile 146.25.

JR-191: roadcut on the west side of I91 at mile 156.8.

Memphremagog quadrangle

JR-190: roadcut on the east side of I91 at mile 160.55.

Montpelier quadrangle

JR-127: small overgrown ledge on the southwest slope of Burnt Mountain at elevation 2580 feet and on an azimuth of 334° from bench mark 1590 at the southeast base of Densmore Mountain.

JR-129: small ledge in an old pasture on the west slope of Densmore Mountain at elevation 1800 feet and along an azimuth of 316° from bench mark 1590 at the southeast base of Densmore Mountain.

JR-139: roadcut on the south side of I89 at mile 63.45.

JR-185: flat outcrop about 300 feet northeast of the summit of White Rock Mountain near the orange dot trail to Mt. Hunger at elevation 3130 feet.

St. Johnsbury quadrangle

JR-10: roadcut on the west side of U.S. Route 5, 1.1 miles north of St. Johnsbury Center.

JR-11: roadcut on the west side of U.S. Route 5, 2.5 miles north of St. Johnsbury Center.

BIBLIOGRAPHY

Albee, A. L., 1957a, Geology of the Hyde Park quadrangle, Vermont: Ph.D. thesis, Harvard University, 139 p.

Albee, A. L., 1957b, Bedrock geology of the Hyde Park quadrangle, Vermont: U. S. Geological Survey Quadrangle Map GQ-102.

Albee, A. L., 1968, Metamorphic zones in northern Vermont, in Zen, E-an, White, W. S., Hadley, J. B., and Thompson, J. B., editors, Studies of Appalachian Geology: Northern and Maritime: Interscience, New York, p. 329-341.

Albee, A. L., and Ray, L., 1970, Correction factors for electron microprobe microanalysis of silicates, oxides, carbonates, phosphates, and sulfates: Analytical Chemistry, v. 42, p. 1408-1414.

Albee, A. L., 1972a, Stratigraphic and structural relationships across the Green Mountain anticlinorium in northcentral Vermont: Guidebook for Field Trips in Vermont, New England Intercollegiate Geological Conference, p. 179-194.

Albee, A. L., 1972b, Metamorphism of pelitic schists: reaction relationships of chloritoid and staurolite: Geological Society of America Bulletin, v. 83, p. 3249-3268.

Bence, A. E., and Albee, A. L., 1968, Empirical correction factors for the electron microanalysis of silicates and oxides: Journal of Geology, v. 76, p. 382-403.

Brace, W. F., 1968, The mechanical effects of pore pressure on fracturing in rocks: Geological Survey of Canada Paper 68-52, p. 113-124.

Cady, W. M., 1956, Bedrock geology of the Montpelier quadrangle, Vermont: U. S. Geological Survey Quadrangle Map GQ-79.

Cady, W. M., Albee, A. L. and Murphy, J. F., 1962, Bedrock geology of the Lincoln Mountain quadrangle, Vermont: U.S. Geological Survey Quadrangle Map GQ-164.

Cady, W. M., Albee, A. L., and Chidester, A. H., 1963, Bedrock geology and asbestos deposits of the upper Missisquoi valley and vicinity, Vermont: U. S. Geological Survey Bulletin 1122-B, 78 p.

Cady, W. M., 1969, Regional tectonic synthesis of northwestern New England and adjacent Quebec: Geological Society of America Memoir 120, 181 p.

Carpenter, R. H., 1974, Pyrrhotite isograd in southeastern Tennessee and southwestern North Carolina: Geological Society of America Bulletin, v. 85, p. 451-456.

Champion, D. E., Albee, A. L., and Chodos, A. A., 1975, Reproducibility and operator bias in a computer-controlled system for quantitative electron microprobe analysis: Proceedings, Tenth Annual Conference of the Microbeam Analysis Society, p. 55A-55F.

Chapman, C. A., 1950, Quartz veins formed by metamorphic differentiation of aluminous schists: American Mineralogist, v. 35, p. 693-710.

Chodos, A. A., Albee, A. L., Gancarz, A. J., and Laird, J., 1973, Optimization of computer-controlled quantitative analysis of minerals: Proceedings, Eighth Annual Conference on Electron Probe Analysis, p. 45A-45C.

Christman, R. A., 1959, Geology of the Mount Mansfield quadrangle, Vermont: Vermont Geological Survey Bulletin 12, 75 p.

Christman, R. A., and Secor, D. T., 1961, Geology of the Camels Hump quadrangle, Vermont: Vermont Geological Survey Bulletin 15, 70 p.

Dennis, J. G., 1956, the geology of the Lyndonville area, Vermont: Vermont Geological Survey Bulletin 8, 98 p.

Doll, C. G., 1951, Geology of the Memphremagog quadrangle and the southeastern portion of the Irasburg quadrangle, Vermont: Vermont Geological Survey Bulletin 3, 113 p.

Doll, C. G., Cady, W. M., Thompson, J. B., and Billings, M. P., compilers and editors, 1961, Centennial geologic map of Vermont: Vermont Geological Survey.

Donath, F. A., and Parker, R. B., 1964, Folds and folding: Geological Society of America Bulletin, v. 75, p. 45-62.

Ernst, W. G., 1963, Significance of phengitic micas from low-grade schists: American Mineralogist, v. 48, p. 1357-1371.

Ernst, W. G., 1968, Amphiboles: Springer-Verlag, New York, 125 p.

Eugster, H. P., Albee, A. L., Bence, A. E., Thompson, J. B., and Waldbaum, D. R., 1972, The two-phase region and excess mixing properties of paragonite-muscovite crystalline solutions: Journal of Petrology, v. 13, p. 147-179.

Goldsmith, J. R., and Newton, R. C., 1969, P-T-X relations in the system $CaCO_3$-$MgCO_3$ at high temperatures and pressures: American Journal of Schience, v. 267-A, p. 160-190.

Goodwin, B. K., 1963, Geology of the Island Pond area, Vermont: Vermont Geological Survey Bulletin 20, 111 p.

Hall, L. M., 1959, The geology of the St. Johnsbury quadrangle, Vermont and New Hampshire: Vermont Geological Survey Bulletin 13, 105 p.

Handin, J., 1966, Strength and ductility, in Handbook of physical constants: Geological Society of America Memoir 97, p. 223-290.

Harper, C. T., 1968, Isotopic ages from the Appalachians and their tectonic significance: Canadian Journal of Earth Sciences, v. 5, p. 49-59

Hsu, L. C., 1968, Selected phase relationships in the system Al-Mn-Fe-Si-O-H: a model for garnet equilibira: Journal of Petrology, v. 9, p. 40-83.

Konig, R. H., 1961, Geology of the Plainfield quadrangle, Vermont: Vermont Geological Survey Bulletin 16, 86 p.

Konig, R. H., and Dennis, J. G., 1964, The geology of the Hardwick area, Vermont: Vermont Geological Survey Bulletin 24, 57 p.

Laird, J., in preparation, Phase equilibria in interbedded amphibolitic and pelitic schists in the northern Appalachian Mountains and the polymetamorphic history of Vermont: Ph.D. thesis, California Institute of Technology.

Lanphere, M. A., and Albee, A. L., 1974, $^{40}Ar/^{39}Ar$ age measurements in the Worcester Mountains: evidence of Ordovician and Devonian metamorphic events in northern Vermont: American Journal of Science, v. 274, p. 545-555.

Longhi, J., Walker, D., and Hays, J. F., 1976, Fe, Mg, and silica in lunar plagioclase: Lunar Science VII, The Lunar Science Institute, Houston, p. 501-503.

Murthy, V. R., 1957, Bed rock geology of the East Barre area, Vermont: Vermont Geological Survey Bulletin 10, 121 p.

Naylor, N. S., 1971, Acadian orogeny: an abrupt and brief event: Science, v. 172, p. 558-560.

Orville, P. M., 1974, The "peristerite gap" as an equilibrium between ordered albite and disordered plagioclase solid solution: Société Francaise de Mineralogie Bulletin, v. 97. p. 386-392.

Phillips, W. J., 1972, Hydraulic fracturing and mineralization: Journal of the Geological Society of London, v. 128, p. 337-359.

Ramsay, J. G., 1967, Folding and fracturing of rocks: McGraw-Hill, New York, 568 p.

Reed, S. J. B., 1975, Electron Microprobe analysis: Cambridge University Press, Cambridge, 400 p.

Rich, R. A., 1973, A regional fluid inclusion study of Paleozoic metamorphic rocks in New England: Geological Society of America Abstracts with Programs, v. 5, p. 780-781.

Rich, R. A., 1975, Fluid inclusions in metamorphosed Paleozoic rocks of eastern Vermont: Ph.D. thesis, Harvard University, 299 p.

Rosenfeld, J. L., 1968, Garnet rotations due to the major Paleozoic deformations in southeast Vermont, in Zen, E-an, White, W. S., Hadley, J. B., and Thompson, J. B., editors, Studies of Appalachian Geology: Northern and Maritime: Interscience, New York, p. 185-202.

Stone, S. W., and Dennis, J. G., 1964, The geology of the Milton quadrangle, Vermont: Vermont Geological Survey Bulletin 26, 79 p.

Thompson, J. B., Jr., 1957, The graphical analysis of mineral assemblages in pelitic schists: American Mineralogist, v. 42, p. 842-858.

Thompson, J. B., Jr., 1972, Oxides and sulfides in regional metamorphism of pelitic schists: 24th IGC, Section 10, p. 27-35.

Thresher, J. E., 1972, Polymetamorphism in the Richmond area, Vermont: Guidebook for Field Trips in Vermont, New England Intercollegiate Geological Conference, p. 269.

Turner, F. J., and Weiss, L. E., 1963, Structural analysis of metamorphic tectonites: McGraw-Hill, New York, 545 p.

Velde, B., 1965, Phengite micas: synthesis, stability, and natural occurrence: American Journal of Science, v. 263, p. 886-913.

Velde, B., 1967, Si^{+4} content of natural phengites: Contributions to Mineralogy and Petrology, v. 14, p. 250-258.

Vidale, R. J., 1974, Vein assemblages and metamorphism in Dutchess County, New York: Geological Society of America Bulletin, v. 85, p. 303-306.

White, W. S., and Jahns, R. H., 1950, Structure of central and east-central Vermont: Journal of Geology, v. 58, p. 179-220.

White, W. S., and Billings, M. P., 1951, Geology of the Woodsville quadrangle, Vermont-New Hampshire: Geological Society of America Bulletin, v. 62, p. 647-696.

Woodland, B. G., 1965, The geology of the Burke quadrangle, Vermont: Vermont Geological Survey Bulletin 28, 151 p.

Woodland, B. G., in press, Structural analysis of the Siluro-Devonian rocks of the Royalton area, Vermont: Geological Society of America Bulletin.

Zartman, R. E., Hurley, P. M., Krueger, H. W., and Giletti, B. J., 1970, A Permian distrubance of K-Ar ages in New England: its occurrence and cause: Geological Society of America Bulletin, v. 81, p. 3359-3374.

Zen, E-an, 1969, Petrographic evidence for polymetamorphism in the western part of the northern Appalachians and a possible regional chronology: Geological Society of America Abstracts with Programs, v. 1, p. 297-299.

Zen, E-an, 1972, Some revisions in the interpretation of the Taconic allocthon in west-central Vermont: Geological Society of America Bulletin, v. 83, p. 2573-2588.

APPENDIX II. SOME GENERAL IMPLICATIONS OF THE STUDY

Much of the focus of this thesis has been on three aspects: 1) defining the sequence of metamorphic events; 2) developing the technique of using metamorphic veins in defining this sequence and; 3) attempting to show the chemical path experienced by the rock systems during the events. However, the data which were used for the above purposes have other implications as well. Many such implications are mentioned briefly in the text, but for emphasis it is useful to restate and discuss these in more detail in this appendix. Some of this discussion is highly speculative, particularly in cases for which the data are insufficient. Hence, the discussion is meant to suggest working hypotheses on a number of topics that merit further examination.

Compositional zoning in mineral grains

Compositional zoning of grains with respect to major elements was observed for most of the major mineral types. The extent and complexity of the zoning varies from one mineral type to another and from sample to sample. The significance of this compositional variation within grains depends upon the mechanism which produced the zoning. Two general mechanisms are possible: growth zoning and solid-state diffusion zoning. These mechanisms are not mutually exclusive, so that any given example may be some combination of both types of compositional zoning. Several tests for determining which of the mechanisms predominated in a sample are discussed in Chapter III.

Diffusion of elements through the lattice of a mineral grain could produce compositional zoning. As a hypothetical example, start with a homogeneous grain of chlorite with a uniform Mg/Mg+Fe value. Suppose that, subsequent to the formation of the grain, the relative activities of Mg^{2+} and Fe^{2+} in the rock have changed from the original conditions due to the breakdown of an Fe^{2+}-rich mineral such as ilmenite. The activity of Fe^{2+} would then be higher at the margin of the grain than in the homogeneous core and diffusion of Mg^{2+} and Fe^{2+} might occur. Along with suitable diffusion rates, there must not be a prohibitive activation energy barrier to the necessary exchange of cations in the lattice once diffusion has occurred. If the diffusion process went to completion, then the grain would be compositionally homogeneous. If the process did not go to completion, the zoning pattern produced should be quite simple; the Mg/Mg+Fe value should gradually increase in a simple manner from rim to core. An irregular zoning pattern, for instance an oscillatory pattern, would not result from such diffusion since nothing in this process can produce irregularities in the activity gradients.

Compositional zoning could also be produced by the growth of a mineral grain over a period of time in which the activities of some of the major chemical species were changing in the immediately surrounding volume of rock. For instance if the activity of Fe^{2+} increased steadily over time, as the grain grew, relative to the activity of Mg^{2+}, a chlorite grain with a zoning pattern such as that described above might be produced. However, if the variations in

activities over time involved reversals, a more complicated zoning pattern could result.

For most minerals in the samples described in the text, the compositional variation seems to be due to preserved growth zoning rather than to solid-state diffusion; a number of criteria can be used to establish this. Growth zoning is suggested by zoning patterns which are more complicated than can be produced by solid-state diffusion in an originally homogeneous grain. Preservation of an identical complicated zoning pattern in many grains suggests that the growth zoning has not been later modified by diffusion. Preservation of growth zoning is suggested if the zoning patterns in relatively isolated grains, such as grains included in porphyroblasts, are the same as the zoning patterns of grains in the matrix. Lattice structure and compositional discontinuities which are parallel to the compositional zoning pattern probably could only be formed by primary growth. Such a discontinuity might represent a solvus, the peristerite gap for example. It is doubtful that the peristerite gap could migrate by diffusion. Commonly within a sample the rims of two adjacent grains of the same mineral have different compositions and this suggests that diffusion in the lattice was not an important process; the common presence of zoning in itself also suggests this. Primary growth zoning in some instances may have been somewhat modified by latter solid-state diffusion; in such a case one might find a complicated zoning pattern which is not exactly the same from grain to grain. In any event, diffusion and exchange does not have

to involve all of the major species of a mineral. For example, primary growth zoning with respect to Si and Al may be preserved and the Fe and Mg growth zoning pattern may be highly modified. Establishing the zoning mechanism is also complicated by the problem of the scale of equilibrium during growth; over what scale in the rock were equal activities maintained in the pore fluid.

If the zoning pattern of a grain is simple, it can be difficult to differentiate between growth zoning and diffusion zoning. Ambiguity will always remain for cases which don't meet the tests for growth zoning. In samples such as JR-163-D, textural evidence supports the interpretation that extensive solid-state diffusion has occurred for a mineral, in this case chlorite. The textural evidence in the DV_c vein and host rock indicates to which generation the various mineral grains belong, OM_b or DM_c. OM_b chlorite grains with very strong Mg-Fe zoning have rims with compositions similar to DM_c chlorite, the Mg-Fe zoning patterns are simple, and relatively isolated OM_b chlorite grains seem to have preserved core material of compositions not found in nonisolated grains. The grains with strong compositional zoning are also optically zoned and such optically zoned grains are restricted to host rock adjacent to the DV_c vein. The evidence suggests OM_b chlorite grains may have been modified by diffusion and exchange of Fe and Mg during event D_c. Thus, in cases which don't meet the tests for growth zoning, other factors including textural evidence can be considered; these other factors are perhaps more subjective and therefore less reliable,

however.

An example of probable primary growth zoning is the zoned plagioclase in a number of samples, such as JR-5-A. The plagioclase grains are concentrically zoned with varying anorthite content. The patterns are not complex except that within many of the grains is a closed surface, parallel to the zoning pattern, which represents a compositional and structural doscontinuity and is interpreted as due to the peristerite gap. In sample JR-4-P, two such discontinuities occur within a single grain. From grain to grain, given the same mineral growth generation, the zoning patterns are the same. In JR-5-A the compositional zoning pattern for the host rock grains is exactly the opposite of that in the grains in the OV_b vein. This evidence further supports the interpretation that the zoning is a feature of growth; if the zoning in the vein plagioclase was produced by diffusion and exchange, then why wasn't the host rock plagioclase affected in the same way. If the host rock plagioclase formed after the vein plagioclase, as opposed to the interpretation given in the text that the vein formed last, then the argument can be applied equally well. If the two types of plagioclase formed at the same time, diffusion still cannot be invoked. The fact that some grains of host rock plagioclase and vein plagioclase are within a few millimeters proximity and the differences in the zoning patterns are still consistent suggests that only growth over two different, but probably contiguous, periods of time is responsible.

Evidence from samples such as JR-5-I (see Figure 37, Chapter

III) suggests that if plagioclase grains have been subjected to significant overprinting effects, sharp but irregular boundaries occur between older and newer material; these irregular boundaries seem to be influenced by any original zoning pattern. Thus overprinting may produce compositional discontinuities, but such discontinuities are not parallel to the compositional zoning (except perhaps by some rare coincidence, but surely not for all grains in a sample).

The common presence of compositionally zoned mineral grains, many of which seem to have resulted from primary growth, has a number of implications for the rocks of the study area and for metamorphic terrains similar to northern Vermont. First, the zoned minerals have no unique composition. Attempts to delimit unique physical conditions often rely upon the equilibrium partitioning of major or minor elements in coexisting phases. However, useful partition coefficients cannot be determined for zoned minerals unless there is some way to determine the compositions of simultaneously growing material. Even if this could be done, a range of physical conditions would be determined. These rocks did not form under a single set of physical conditions, but rather formed over a period of time in which some or all of the conditions may have been changing. The zoning patterns of grains of minerals such as plagioclase, muscovite, calcite, ankerite, and Ca-amphibole typically suggest that the grade was changing during the periods of mineral growth. Another

important implication is that the presence of zoned grains suggests that only the grain rims are really actively a part of the system; this is further discussed later in the appendix.

The electron microprobe data show that zoning occurs for both major and minor elements. Further, this compositional zoning suggests that homogeneity of these grains with respect to trace elements and isotopes cannot be assumed. For instance, if the temperature of the system varied significantly as grains were growing, the grains may be zoned with respect to their oxygen isotopic compositions. The significance of "temperatures" determined with oxygen isotopes for metamorphic rocks such as those in northern Vermont might then be in question.

Relative susceptibility of various minerals to solid-state diffusion

The data for some minerals in several of the samples described in Chapter III suggest that diffusion and exchange in the crystal lattice have occurred to varied extents. As discussed, such interpretations are necessarily ambiguous. However, using textural evidence as well as the chemical evidence of zoning, it appears that such diffusion probably occurred and was superimposed on primary growth zoning in these relatively few cases. An example already cited is the chlorite in JR-163-D, which is strongly zoned with respect to Mg and Fe and is probably the least ambiguous case. Zoning with respect to Al, Si and Ti may be more apt to be preserved, reflecting the difficulty in exchanging Al^{3+} and Si^{4+} because by necessity

another exchange must occur to maintain charge balance. On the other hand, exchange of Mg^{2+} for Fe^{2+} may be more likely because significant rearrangement of the lattice is not required. More data are needed in regard to this problem.

Based on general observations and somewhat subjective interpretations, an approximate ranking can be made for the various minerals with regard to susceptibility to diffusion and exchange in the solid-state. Those minerals which are considered to be least susceptible to this process are those for which the data suggest in every case that primary growth zoning is present. The minerals regarded as most susceptible are considered so because in one or more samples, the data were permissive for an interpretation of diffusion zoning. Of the susceptible minerals, the ranking is a relative order of the apparent magnitude of possible diffusion effects in the few samples in question.

Epidote may be highly susceptible to diffusion and exchange, at least with respect to Fe^{3+} and Al^{3+}. Epidote typically shows significant compositional variation within single grains, but almost never seems to have a systematic zoning pattern that meets the tests for growth zoning. The zoning patterns with respect to Fe^{3+} - Al^{3+} substitution are irregular, even in individual euhedral grains included in vein quartz (such as in sample JR-127-B). Zoning with respect to REE content seems to be more systematic in some samples and the zoning patterns suggest depletion zoning; the cores are always enriched in REE relative to the rims, if significant REE is present. In amphib-

olite samples from JR-66, Fe^{3+}-rich epidote is spatially associated with products of the retrograde alteration of hornblende and cores of epidote grains tend to be the most Al^{3+}-rich, but the sort of consistent, systematic zoning patterns found in other minerals are not present.

In some samples, biotite and chlorite may have been fairly susceptible to diffusion and exchange of Mg and Fe; chlorite in JR-163-D is an example already described. Chlorite grains in most samples seem to preserve growth zoning very well, however. Biotite may be slightly more susceptible to diffusion and exchange than chlorite, but this is not really clear. A number of other minerals seem perhaps more resistant than biotite and chlorite to compositional alteration by diffusion and exchange and it is difficult to rank the minerals in this group relative to each other; these minerals include calcite, ankerite, sphene, chloritoid, hematite, ilmenite, tourmaline, and perhaps rutile.

Muscovite and plagioclase typically seem to preserve primary growth zoning and are probably not very susceptible to diffusion and exchange. In samples that have a generation of muscovite and/or plagioclase grains that have been overprinted by a later mineral growth event, the grains seem to have been replaced in part by completely new, recrystallized material; the boundaries between older and newer material are sharp. This is not a feature of the diffusion and exchange process being discussed. Ca-amphibole grains commonly seem to preserve primary growth zoning and in some samples, grains

may have concentric zones which represent successive mineral growth generations. The mineral which is apparently the least susceptible to solid-state diffusion is garnet; evidence of this is the complicated Ca zoning in OM_b garnet in a number of samples such as JR-73-A.

Several of the mineral types analyzed generally show no significant compositional variation within single grains; this is apparently due to limited compositional ranges possible given the metamorphic conditions attained in the study area and the bulk rock compositions. This group of minerals includes magnetite, kyanite, and apatite. Zircon is probably also generally in this group, but in some samples zoning with respect to Hf is present and Hf was not determined in all zircon analyses. In some samples, apatite grains are zoned with respect to Ce and, to a lesser extent, Y and other REE. Ce_2O_3 concentrations in apatite are typically 0.5% or less and most zoned grains have decreasing concentration from core to rim. In rocks that have only experienced relatively low-grade conditions, essentially unzoned albite grains are also observed. As plagioclase which formed at higher grade preserves significant zoning, the unzoned albite seems to reflect the limited compositional range of low-grade plagioclase in these rocks rather than the effects of some re-equilibration process.

Preservation of multiple generations

Strong evidence for the presence of more than one mineral growth generation is found in most of the samples described in the

text. Four mineral growth generations may be present in sample JR-4-M, and other samples appear to have at least two generations. If the various generations in a rock can be separated and identified, the phase assemblage and chemical data for each generation can be used to construct a fairly detailed picture of the metamorphic history of the rock. A sample which has more than one mineral growth generation can present problems if it is difficult to separate the effects of the different generations; it may then be difficult to determine the assemblages of minerals that were actually cogenetic, rather than merely coexistent.

The formation of a new mineral growth generation requires that some older mineral growth be partly or wholly destroyed. In order to preserve evidence of the older generations, the destruction must in some way be selective. An example of such a selective process is the formation of a slip cleavage set during the growth of a new mineral growth generation. Old material along the slip cleavage planes may have been granulated preferentially relative to similar grains away from the planes. Such granulated material seems to have been the source for the growth of the new generation of grains in the slip cleavage zones, while at the same time the older generation grains between slip cleavage planes may have been virtually unaffected.

Another mechanism by which older material has been preserved through an overprinting event is by inclusion of grains within grains of other minerals that are relatively unreactive or resistant to diffusion, such as garnet or plagioclase. An example is the presence

of abundant inclusions of chloritoid in garnet porphyroblasts in sample JR-73-A; these included grains of chloritoid are the only chloritoid in the sample. Apparently all nonincluded chloritoid grains were destroyed sometime after the growth of the garnet grains.

Even if there isn't chemical preservation of overprinted mineral generations, textural evidence may be preserved. In the extreme case, new grains are pseudomorphous after grains of a different mineral formed before the overprinting event. On other cases grains of a mineral such as chlorite may texturally appear to be original growth of an old generation but at the same time have a compositional range that suggests complete reconstitution by recrystallization or by diffusion and exchange in the solid state. Such preservation is apparent for some minerals in several samples that have evidence of multiple preserved mineral growth generations.

Types of isograds in northern Vermont

Several complexities can arise in the mapping of isograds in a metamorphic terrain if the area has been subjected to several metamorphic events. Two such problems complicate the mapping of isograds in northern Vermont; the limit of occurrence of an index mineral may be due to the destruction of the index mineral by an overprinting event and the areal extents of two generations of the same index mineral may overlap. This results in two special types of isograds which are termed here "preservation isograds" and "hybrid isograds" respectively. Isograds which represent the areal limit of stability

or growth of an index mineral for a single generation are called "primary isograds" in the following discussion.

Primary isograds

The term "isograd" has historically implied that the limit of occurrence of an index mineral is related to the spatial distribution of metamorphic grade during a prograde metamorphic event. An isograd ideally marks the map expression of relatively equal grade conditions which separate product and reactant mineral assemblages of an index mineral-producing reaction. Whether or not the reaction occurred was also dependent upon kinetic factors and the bulk composition of the rock. However, such primary isograds are the best estimate of surfaces of equal grade available from assemblage data and are of great importance in making regional interpretations of the structure, estimates of physical conditions and gradients, and the tectonic history. An example of a primary isograd is the garnet isograd on the west limb of the Green Mountain anticlinorium along the Winooski River Traverse. On the east side of the Green Mountain anticlinorium, the garnet isograd is a preservation isograd so that the entire garnet isograd in that area is a hybrid isograd, a combination of a primary isograd and a preservation isograd.

Preservation isograds

Retrograde alteration of one generation of mineral growth by the overprint of another event has occurred over large areas of northern Vermont. As mentioned above, a good example is the retro-

gradation of OM_b garnet due mainly to the effects of event D_a along the east limb of the Green Mountain anticlinorium in the Camels Hump quadrangle. The garnet isograd mapped near location JR-4 by Christman and Secor (1961), as shown in Figure 24 of Chapter III, represents a structural boundary with regard to the style of D_a deformation. To the east of JR-4, very well developed DS_a slip cleavage is typically parallel to either the long or short limbs of small DF_a folds. To the west of JR-4, DS_a slip cleavage is not so pervasive and is generally not parallel to either limb of small DF_a folds. The change in style of D_a deformation is accompanied by a change in the degree of preservation of OM_b garnet. To the west of JR-4, OM_b garnet is commonly present and well preserved. To the east of JR-4, only a small amount of OM_b garnet is preserved and textural evidence suggests that most of the OM_b garnet was replaced by DM_a retrograde minerals. OM_b garnet was clearly stable on both sides of the mapped isograd, so that the apparent isograd is controlled by the style and intensity of the overprinting event rather than by the limit of OM_b garnet growth. At least two other examples of preservation isograds are in the study area: the kyanite isograd in the Worcester Mountains and the garnet isograd near the Willoughby arch in the Lyndonville and St. Johnsbury quadrangles as shown by Albee (1968).

Hybrid isograds

Any mapped isograd which is actually a combination of two or more generations of primary isograds or of primary isograds and

preservation isograds is considered to be a hybrid isograd. The term "hybrid" is used here to merely imply that the total isograd as mapped is not the result of a single event, whether prograde or retrograde in nature. Specific segments of a hybrid isograd are either primary or preservation isograds and it may be possible to identify such segments. It is possible that primary isograds of two separate mineral growth generations could roughly coincide, but this would be a highly unlikely special case.

As already mentioned, the garnet isograd which defines the "Green Mountain higher grade zone" in Figure 25-1 of Albee (1968) is a hybrid isograd consisting of at least a segment which is a primary isograd due to OM_b growth and a segment which is a preservation isograd due to D_a overprinting; this hybrid isograd could even turn out to be more complicated if it were studied in detail. Some of the mapped isograds in the St. Johnsbury and Lyndonville quadrangles may also be hybrid isograds produced by overlapping areas of higher grade DM_a and DM_c mineral growth with further complications due to D_b retrogradation. Much more detailed data are necessary to determine the nature of the various mapped isograds in northern Vermont.

One point of interest here is the use of the areal distribution of various mineral types to determine the physical conditions of metamorphism. An example is the distribution of the polymorphs of Al_2SiO_5. Attention must be paid to the mineral growth generations involved; isobaric surfaces cannot be constructed based upon the distribution of intermixed generations of the different polymorphs.

The presence of OM_b kyanite in the Lowell Mountains and, immediately to the east, DM_c andalusite and sillimanite in the Memphremagog quadrangle certainly does not indicate that somewhere conditions were attained corresponding to the triple point of the Al_2SiO_5 system. The possible coexistence of DM_a kyanite and DM_c andalusite and sillimanite within a very small area is also a possibility in northern Vermont. This is not unrelated to the problem of identifying generations within single samples; a number of proposed "geothermometers" and "geobarometers" utilize the compositions of coexisting minerals and if the coexisting minerals are not cogenetic, then such data cannot be used for that purpose.

Separation of events

A persistent problem in the study of polymetamorphic terrains has been the difficulty in establishing whether or not the metamorphic events which produced mineral growth and/or deformation were distinct periods of time separated by significant time intervals. This is mostly a problem with regard to the various events or stages that comprise a single orogenic episode. The major episodes typically can be shown to be separate using structural evidence such as unconformities and also radiometric age techniques.

Within the two major orogenic episodes in northern Vermont, the Taconic and Acadian episodes, consistent sequences of superimposed deformational and mineral growth features have been formed. The mineral growth generations may or may not be resolvable by radiometric techniques and even two "resolvable" events may be consecutive,

long events which had no distinct separation in time. If a correspondence between mineral growth generations and deformational elements has not been established, or if some of the deformational elements have no corresponding associated mineral growth, then demonstrating separations in time between deformational events can be even more of a problem. Without evidence to the contrary, events cannot be assumed to have been separated by any significant time period. However, one might intuitively expect that major shifts in the regional stress field, changes in the style of deformation, and/or changes in mineral growth conditions would indicate a separation of events if the changes appear to have been discontinuous.

In discussing the idea of separate events within an orogenic episode, some definitions are needed so as not to get lost in semantic problems. "Events" are discussed extensively in the text and imply a period of time during which a single association of mineral growth and deformational elements was formed. Each association is superimposed on older associations and has been affected by younger associations. These associations of metamorphic features which result from the various events that have occurred in northern Vermont are observed to be regionally uniform in that any single element, a specific fold generation for instance, belongs to only one specific association throughout the study area. A single element is not part of one association in one place and another association in another place.

Information about when an event "began" or "ended" depends upon

the definitions used for these terms and these definitions lead directly to a definition of "separate" events. In this discussion, an event began when the first mineral growth or observable deformation commenced and the event continued until all mineral growth and deformation had ceased. Two events are considered to be separate if some evidence indicates that a significant time interval probably occurred between the end of one event and the beginning of another event. One complication here is that the beginning or end of an event may vary in absolute age from one local area to another, but two such events may still be separated in time throughout the region.

Two types of evidence can be used to suggest that two sequential events were separated in time. Structural evidence may indicate that two events may be separate and petrologic evidence, in particular compositional evidence, may also be useful. In most cases the evidence is at best indirect and somewhat ambiguous. However, if all of the evidence is taken together, it suggests that each of the major events within the two episodes that have affected northern Vermont were separate in time from one another.

It is relatively easy to show that events O_b and D_a were distinctly separate in time. OM_b mineral growth had already formed in the Cambrian and Ordovician rocks before the uplift and erosion that produced the unconformity upon which Silurian strata were deposited. OM_b mineral growth in the Moretown member near the unconformity in the Montpelier quadrangle was at least biotite grade before the uplift and erosion. After the unconfirmity was produced, a great thickness

of Silurian and Devonian strata was deposited and then event D_a occurred. The time interval between O_b and D_a must have been on the order of tens of millions of years to accomplish all the intervening processes.

Another line of structural evidence can be found in the presence of minor vein generations which were formed between the major events. In general the veins of these minor generations have fairly simple assemblages, quartz, calcite, and perhaps chlorite and/or albite in some instances; these appear to have formed under lower grade conditions than the mineral growth associated with the major events. Table 1 on page 27 of Chapter II lists these minor vein generations. At least one minor vein generation was formed between events O_a and O_b, at least three generations were formed between D_a and D_b, at least one generation was formed between D_b and D_c, and three minor vein generations were formed between O_b and D_a. Each of the minor vein generations seems to have had a specific associated regional stress field and from one generation to another the stress field changed. The three generations between D_a and D_b must be separate in time. Furthermore, the minor vein assemblages may suggest that the rocks were at lower grade conditions than those prevalent during D_a and also perhaps D_b. This comparison can be made based upon DV_a assemblages and the minor vein assemblages. As no veins seem to be associated with D_b, a comparison cannot be made for these assemblages, but DM_b host rock assemblages seem higher grade than the minor vein

assemblages based upon observed relationships between host rock and vein assemblages for other generations. The occurrence of only at least one minor vein generation between two events is not as convincing as the occurrence of at least three generations, but still suggests a separation in time between events O_a and O_b and between D_b and D_c. However, for these last two cases, some other evidence is needed to establish time separation with any certainty.

Another line of structural evidence for the events being distinct, if not actually separated in time, are the apparently discontinuous changes in the style of deformation from one event to another. Each event also seems to have had its own distinct associated regional stress field, although for the Acadian events the regional stress field did not shift very much from one event to another. Furthermore, the elements of each successively younger event are clearly superimposed upon all of the older elements. The superposition suggests that some conditions changed and that perhaps these changes required an interval of time, and changes in the regional stress field also suggest that the events were distinct.

The petrologic evidence for events being separate in time is mainly from mineral compositions in the veins and host rocks. It is useful first to consider the various features of events O_b and D_a, which are clearly separate in time, and then see if similar features can be found and used to demonstrate the separation of other pairs of sequential events.

Consider as an example the petrologic features of events O_b

and D_a at locations along the Winooski River traverse in the Camels Hump quadrangle. The compositional zoning patterns in host rock OM_b muscovite and plagioclase generally indicate that grade was increasing with time. The zoning patterns of these minerals in OV_b veins suggest grade was generally decreasing during vein growth, so that the overall path for OM_b growth was first increasing grade, with growth starting at perhaps low biotite grade and then progressively up to garnet grade, then decreasing from garnet grade to low biotite grade before OM_b growth stopped. Evidence from DM_a mineral growth in the host rocks and DV_a veins suggests a similar path, although DM_a growth never quite reached garnet grade in the exposed rocks along this traverse segment. The two events appear to have been separated by a period of time during which no deformation occurred and no mineral growth occurred because the grade conditions were too low.

The presence of nonoverlapping compositional ranges for two generations of a single mineral type provides other evidence of separation of events. In samples JR-5-I and JR-5-D, both OM_b and DM_a chlorite occurs and the two generations of chlorite do not have overlapping compositional ranges. This suggests that some of the physical conditions must have changed between OM_b and DM_a growth; such changes probably must have required a period of time during which no mineral growth occurred.

Unfortunately, the compositional data for sequential pairs of events other than O_b - D_a are not so readily applied to demonstrating

time separation, with a few exceptions. First, DV_a vein mineral compositional zoning patterns indicate that grade decreased during the waning stages of event D_a. From the structural evidence, we know that at least three generations of minor veins formed under low-grade conditions before event D_b. No particular trend for the change in grade during D_b has been established, but within several samples are both DM_a and DM_b growth of a single mineral type for which there is no compositional overlap between the two generations. Examples are muscovite in JR-175-H and chlorite in JR-10-A. Nonoverlapping compositional ranges for OM_a and OM_b chlorite occur in sample JR-5-A, which suggests that O_a and O_b may be distinct. Other examples of nonoverlapping compositional ranges for two generations of a mineral in a sample are DM_e and DM_c muscovite in JR-190-A, and DM_b and DM_c muscovite in JR-175-H. Compositional trends for DM_c mineral growth indicate generally increasing grade in host rock samples and generally decreasing grade in DV_c veins. Such trends have not been established for DM_b or OM_a in any samples.

Of the two types of evidence, structural and petrologic, the structural evidence generally demonstrates more convincingly that two sequential events were separated in time. The evidence for the separation of O_b and D_a is clear and the three intervening minor vein generations indicate that D_a and D_b were separate in time. Not so strong is the demonstration that the pairs O_a - O_b and D_b - D_c involved a time separation, as the evidence for each is limited to the presence of one intervening minor vein generation and a small

amount of useful compositional data. No evidence at all suggests that any of these pairs were not separated in time.

Factors which affect the extent of mineral growth

Large differences in the extent of development of various mineral growth generations have been observed within small areas, such as single outcrops. This suggests that some factors affecting mineral growth rates varied over the area during the metamorphic events. Careful examination of a suite of samples from locations at which mineral growth of one or more generations is unevenly developed may provide evidence of these factors. Limiting each suite to a single outcrop insures that the conditions of grade for each event were the same for each of the samples. The factors which affect the extent of mineral growth are of at least three types: structural, chemical, and textural.

Mineral growth generations which are unevenly developed over a small area are typically generations which are superimposed upon one or more earlier generations. The oldest generation in a rock, representing the initial metamorphic mineral growth, is generally uniformly developed over an area. A good example of variation in the development of a superimposed mineral growth generation is DM_a growth in the various samples from location JR-5, an outcrop of Hazens Notch schist in the Camels Hump quadrangle. Within the schist, DM_a mineral growth is superimposed on OM_a and OM_b growth. There seems to be a positive correlation between the extent of development of DS_a slip cleavage

and the extent of DM_a mineral growth development; therefore the controlling factor is probably structural in nature. Textural factors include the degree to which older mineral generations are isolated within nonreactive minerals and the grain size distribution of various minerals within the rock as a mineral growth generation developed.

If a volume of rock was a relatively closed system with respect to most of the major chemical species over a period of time in which mineral growth occurred, some older mineral growth must have been destroyed in order for the new growth to occur. Generally, the newer growth would have a composition different from that of the older growth and the new growth would represent a state of lower free energy given the prevailing conditions. Given no kinetic barriers, the older mineral growth should be completely destroyed because it represents a higher free energy state. However, the older mineral growth generations have commonly survived to a significant extent during superimposed events. Over a large area, differences in time and metamorphic grade conditions will affect the extent of the newer mineral growth. Over a small area where time and grade are relatively uniform, other factors which have a direct kinetic effect must be responsible for varying mineral growth development.

Structural factors

Deformation of the rocks in northern Vermont has resulted in a variety of small scale features, among which are folds, various types of secondary foliation, and general granulation of mineral grains. Granulation also appears to have accompanied the formation of second-

ary foliation planes, but for spaced secondary foliations such as slip cleavage sets, granulation is localized in the vicinity of the planes rather than pervasive throughout the rock. Pervasive granulation is present in rocks from a portion of the study area and this granulation is not necessarily associated with well-defined secondary foliation planes. The best demonstration of generalized granulation is within very fine-grained quartz veins which were almost certainly much coarser-grained when originally formed. Large volumes of rock were extensively granulated during events O_b and D_a.

The granulation of mineral grains has at least two effects. The surface area of a given volume of rock is increased and therefore the total surface energy of the system is increased; in particular, extremely small grains with consequent high relative free energy may be produced. Secondly, granulation may expose the cores of compositionally zoned grains; the core material may have a higher free energy than the rim material but without the granulation the core material would be relatively isolated. Also, grains included in other minerals may be exposed to the effective system of the rock.(1) Deformation may also produce strain within grains which adds to the free energy of the system, but such a contribution does not require granulation.

---

(1) "Effective system" is used to denote those portions of the system which are not isolated by being enclosed in nonreactive material through which the diffusion of the various chemical species is significantly restricted. The interior portion of a garnet grain would not be considered to be part of the effective system.

Increasing the free energy of the reactants decreases the activation energy for a reaction and therefore increases the rate of reaction. If a reaction is possible within a system, then higher energy granulated material would be more likely to participate in the reaction than the nongranulated material in the system. Given a mineral growth generation which is overprinted by an event which produces both significant deformation and mineral growth, the destruction of the older mineral growth can be a selective process. New mineral growth may be most extensively developed where a new secondary foliation is being formed. If the new secondary foliation is a spaced slip cleavage, then the new mineral growth may be relatively localized within the volume bery close to the slip cleavage planes where the older material has been granulated. Regardless of the type of secondary foliation, the degree to which the foliation is developed and therefore the extent of granulation of older material should affect the degree to which the new mineral growth is developed. Competent rock units like massive amphibolite are apt to be less affected by deformation than pelitic schists and are therefore more apt to preserve older mineral growth generations through overprinting events, everything else being equal.

Textural factors

Differences in the average grain size from one rock volume to another may have been present before an overprinting event occurred. This would result in differences in surface energy from rock to rock, although a very large contrast in grain size would be necessary for

the surface energy difference to be significant. One factor that might be important and which is indirectly related to grain size is the degree to which grains of possible reactant minerals are included within grains of nonreactive minerals or otherwise isolated. For instance, most of the reasonably well-preserved OM_b biotite in the Worcester Mountains is within coarse-grained quartz veins; the biotite was relatively isolated in the nonreactive quartz.

Another possible textural factor controlling mineral growth may have been the size and extent of interconnection of the pore space in which the postulated pore fluid acted as a diffusion medium. This factor is perhaps impossible to assess in practice as the present pore space probably bears no relationship to the pore space during the various events. If the pore space was poorly interconnected, diffusion would have been limited and consequently the extent to which the reactions proceeded would have been hindered.

Chemical factors

Overprinting events commonly produced grains of a mineral type with a certain compositional range at the expense of older grains of the same mineral with different compositions. The physical conditions of the overprinting event, the bulk chemistry of the effective systems, and the older minerals present determined to what extent the older mineral growth was unstable. If the free energy difference between the material of new and old mineral growth generations was relatively small, then the reactions destroying old mineral growth and producing

new mineral growth were probably less likely to proceed than if the free energy difference was great, everything else being equal. Another chemical factor is the magnitude of the activation energy barriers that were present during the mineral growth. Therefore the mineral types and compositions of reactants and products, the magnitude of the prevalent activation energy barriers, and the physical conditions, including the activities of volatiles and dissolved species in the pore fluid are factors which would be expected to have influenced the extent to which mineral growth was developed in an overprinting event.

Overall effect

Many variables which might affect the extent of mineral growth development are listed above and the list is certainly not exhaustive. The various factors may have acted separately or in combination with each other to different degrees from one rock volume to another. The observed result is that an overprinting mineral growth generation may be well developed in one small rock volume and in another small rock volume in the same outcrop there may be little evidence of the generation. The destruction of older grains has been a selective process by which some grains were completely destroyed and other grains of the same generation and composition were essentially undisturbed. The common observation that mineral growth of a single generation is not uniformly developed within single outcrops is important to consider; the observation suggests that "grab" sampling in an area like northern Vermont can lead to problems in the interpretation of polymetamorphism.

Size of the effective system

If a system is at homogeneous equilibrium, then the mineral grains should all be compositionally unzoned and grains of the same mineral type should have identical compositions. As none of the rocks studied even approach this state, the systems clearly did not come close to homogeneous equilibrium during metamorphism; compositional zoning is nearly ubiquitous. However, within these rocks are indications of some approach to equilibrium on a limited scale; simultaneous growth of grains of a single mineral type within a sample seems to have resulted in identical or closely similar compositions. Furthermore, the phase rule is rarely violated except in cases where more than one mineral growth generation is present within a rock. Incompatible phases are typically separated by reaction rims or unreactive material. A contrast exists between the lack of homogeneous equilibrium and the apparent close approach to equilibrium with respect to actively forming mineral growth at any given time. This suggests that some part of the total system was actively participating in the chemical processes and some part of the system was relatively nonreactive. That part of the system which was not inert has been previously referred to as the "effective system" in this appendix.

The presence of a fluid phase through which diffusion of chemical species could have occurred has been assumed for these rocks and a fair amount of evidence substantiates the assumption. In the rocks studied with the electron microprobe, mineral growth seems to have

almost always occurred at grain boundaries in contact with the assumed fluid phase. As the rates of diffusion through a fluid would have been fairly rapid on the scale of a thin section, then it is not surprising that simultaneously growing mineral material was in relative equilibrium. The grain boundaries and the fluid phase are the most important parts of the effective system. For the purpose of discussion, any cracks within grains in which the pore fluid could exist and through which diffusion could occur are considered also to be grain boundaries.

The next question is how far into the grains from the grain boundaries did the effective system extend. The common presence of compositional differences between the grain "rim" and an area within 10 or 20 microns of the "rim" indicates that the typical effective system included only a small portion of the total volume of the grains in a rock. This is true for almost all minerals in almost all samples studied. The typical effective system was so small that it is beyond the spatial resolution capability of the electron microprobe. In a few samples, grains of some mineral types like chlorite and biotite are relatively homogeneous in composition; in such a case the effective system may have been somewhat larger than that described above.

The size of the effective system is a function of solid-state diffusion, a process with a finite rate, and therefore the time scale must play a determining role also. Over a long time scale, the effective system would be larger than for a short time scale. The

interiors of grains can participate in the effective system only if a significant amount of solid-state diffusion can occur over the time scale involved. As a result, there are perhaps three different parts of any system: one part is always in the effective system, one part is always inert, and one part may be inert or in the effective system, depending upon the time scale and the diffusion rates.

The limited size of the effective system during any of the events of the typical rocks from the study area has resulted in the presence of zoned grains and several mineral growth generations in single samples. The size of the effective system could have varied from one event to another and within single events. Many different parameters may play a role in determining the effective system size; among these parameters are time, temperature, and anything else that affects both the diffusion and reaction rates involved. It may be impossible to quantitatively evaluate the actual size of the effective system for any given period of time, but the concept is useful in its general application to explain the observed features in the rocks of northern Vermont.

Time scale of the events

Preserved within the rocks of the study area is evidence of a sequence of time periods ("events") during which significant mineral growth and/or deformation occurred. From beginning to end, each event had some absolute duration and it would be very useful to know the length of time involved. Determining the absolute duration of an

event may be complicated by variations in the times at which an event began and ended.

The available information on the structural (relative ages), stratigraphic, and isotopic ages is given in Table 4 of Chapter II, page 211. As the isotopic ages were all done by either the K/Ar method or the $^{40}Ar/^{39}Ar$ method, they represent Ar retention ages, but the mineral zoning data indicate that during the last stages of each event the grade decreased so that the retention ages should represent some point in time within an event. The exception would be if a rock lost Ar by some later disturbance. In any event, each isotopic age gives a single point in time and doesn't give information about the duration of the event. At present the best one can do with the isotopic data is to look at the differences between the ages of the different events and put upper limits on the duration of a single event.

A suggested, tentative age for event D_a is about 375 m.y. One age for possible DM_c growth is 358 m.y. and the isotopic ages for the New Hampshire plutons range from 380 to 344 m.y. Event D_a affected Lower Devonian sediments, so a conservative estimate of the time span involved for all three of the events D_a, D_b, and D_c might be from about 390 m.y. to 340 m.y., 50 m.y. in total duration. Some investigators such as Naylor (1971) suggest that the total length of the Acadian episode, which encompasses D_a, D_b, and D_c, was much shorter than 50 m.y. The present evidence from any source is not very strong one way or the other.

During this estimated 50 m.y. time interval, the following

occurred:

(1) event D_a -- a large volume of sediments and previously metamorphosed rocks were highly deformed and subjected to moderate pressure regional metamorphism which reached at least biotite to garnet grade over the entire study area;

(2) as event D_a ended, the metamorphic grade of the rocks decreased, perhaps due to uplift and erosion;

(3) at least three generations of minor veins were formed, DV_{a+1}, DV_{a+2}, and DV_{a+3}, at fairly low grade conditions;

(4) event D_b -- significant deformation and widespread chlorite to biotite grade metamorphic mineral growth occurred;

(5) DF_{b+1} folds and DS_{b+1} slip cleavage were formed;

(6) another set of minor veins, DV_{b+2}, was formed;

(7) event D_c -- relatively low pressure mineral growth occurred over a large area and locally reached sillimanite grade.

If the major events were roughly equal in duration (there is no reason to suppose that they were) then each would have been about 15 m.y. in maximum duration. If some significant part of the 50 m.y. involved no active metamorphism, then the events would have been accordingly shorter. It is really very difficult to put a lower limit on the duration of the events.

A fairly accurate determination of the duration of each event would clearly be useful; each major metamorphic event must reflect some significant tectonic event. The present data at least indicate that the individual events were certainly not more than 50 m.y. in

duration and probably more like 10-15 m.y. as a practical average upper limit. Purely as a guess, a lower limit of about 1 m.y. might be reasonable.

The question of the duration of an event may be a solvable problem in the future. Most of the chemical variation in the analyzed mineral grains seems to be the result of primary growth; physical conditions and/or chemical conditions were changing as the grains grew. If a microanalysis method could be used for a radiometric technique (given a technique that could resolve the time scales involved), then the zoning pattern of appropriate trace elements or isotopes might be used to determine the period of time over which mineral growth occurred. Obviously, if any diffusion of the trace elements within the grain had occurred, the results would not be accurate.